

JOURNAL OF

CHROMATOGRAPHY A

INCLUDING ELECTROPHORESIS AND OTHER SEPARATION METHODS

EDITORS

U.A.Th. Brinkman (Amsterdam)

R.W. Giese (Boston, MA)

J.K. Haken (Kensington, N.S.W.)

L.R. Snyder (Orinda, CA)

EDITORS, SYMPOSIUM VOLUMES.

E. Heftmann (Orinda, CA), Z. Deyl (Prague)

EDITORIAL BOARD

D.W. Armstrong (Rolla, MO)

W.A. Aue (Halifax)

P. Boček (Brno)

A.A. Boulton (Saskatoon)

P.W. Carr (Minneapolis, MN)

N.H.C. Cooke (San Ramon, CA)

V.A. Davankov (Moscow)

G.J. de Jong (Weesp)

Z. Deyl (Prague)

S. Dilli (Kensington, N.S.W.)

Z. El Rassi (Stillwater, OK)

H. Engelhardt (Saarbrücken)

F. Erni (Basle)

M.B. Evans (Hatfield)

J.L. Glajch (N. Billerica, MA)

G.A. Guiochon (Knoxville, TN)

P.R. Haddad (Hobart, Tasmania)

I.M. Hais (Hradec Králové)

W.S. Hancock (Palo Alto, CA)

S. Hjertén (Uppsala)

S. Honda (Higashi-Osaka)

Cs. Horváth (New Haven, CT)

J.F.K. Huber (Vienna)

K.-P. Hupe (Waldbronn)

J. Janák (Brno)

P. Jandera (Pardubice)

B.L. Karger (Boston, MA)

J.J. Kirkland (Newport, DE)

E. sz. Kováts (Lausanne)

K. Macek (Prague)

A.J.P. Martin (Cambridge)

L.W. McLaughlin (Chestnut Hill, MA)

E.D. Morgan (Keele)

J.D. Pearson (Kalamazoo, MI)

H. Poppe (Amsterdam)

F.E. Regnier (West Lafayette, IN)

P.G. Righetti (Milan)

P. Schoenmakers (Amsterdam)

R. Schwarzenbach (Dübendorf)

R.E. Shoup (West Lafayette, IN)

R.P. Singhal (Wichita, KS)

A.M. Siouffi (Marseille)

D.J. Strydom (Boston, MA)

N. Tanaka (Kyoto)

S. Terabe (Hyogo)

K.K. Unger (Mainz)

R. Verpoorte (Leiden)

Gy. Vigh (College Station, TX)

J.T. Watson (East Lansing, MI)

B.D. Westerlund (Uppsala)

EDITORS, BIBLIOGRAPHY SECTION

Z. Deyl (Prague), J. Janák (Brno), V. Schwarz (Prague)

ELSEVIER

JOURNAL OF CHROMATOGRAPHY A

INCLUDING ELECTROPHORESIS AND OTHER SEPARATION METHODS

Scope. The *Journal of Chromatography A* publishes papers on all aspects of **chromatography, electrophoresis** and related methods. Contributions consist mainly of research papers dealing with chromatographic theory, instrumental developments and their applications. In the *Symposium volumes*, which are under separate editorship, proceedings of symposia on chromatography, electrophoresis and related methods are published. *Journal of Chromatography B: Biomedical Applications*—This journal, which is under separate editorship, deals with the following aspects: developments in and applications of chromatographic and electrophoretic techniques related to clinical diagnosis or alterations during medical treatment; screening and profiling of body fluids or tissues related to the analysis of active substances and to metabolic disorders; drug level monitoring and pharmacokinetic studies; clinical toxicology; forensic medicine; veterinary medicine; occupational medicine; results from basic medical research with direct consequences in clinical practice.

Submission of Papers. The preferred medium of submission is on disk with accompanying manuscript (see *Electronic manuscripts* in the Instructions to Authors, which can be obtained from the publisher, Elsevier Science B.V., P.O. Box 330, 1000 AH Amsterdam, Netherlands). Manuscripts (in English; four copies are required) should be submitted to: Editorial Office of *Journal of Chromatography A*, P.O. Box 681, 1000 AR Amsterdam, Netherlands, Telefax (+31-20) 5862 304, or to: The Editor of *Journal of Chromatography B: Biomedical Applications*, P.O. Box 681, 1000 AR Amsterdam, Netherlands. Review articles are invited or proposed in writing to the Editors who welcome suggestions for subjects. An outline of the proposed review should first be forwarded to the Editors for preliminary discussion prior to preparation. Submission of an article is understood to imply that the article is original and unpublished and is not being considered for publication elsewhere. For copyright regulations, see below.

Publication information. *Journal of Chromatography A* (ISSN 0021-9673): for 1994 Vols. 652–682 are scheduled for publication. *Journal of Chromatography B: Biomedical Applications* (ISSN 0378-4347): for 1994 Vols. 652–662 are scheduled for publication. Subscription prices for *Journal of Chromatography A*, *Journal of Chromatography B: Biomedical Applications* or a combined subscription are available upon request from the publisher. Subscriptions are accepted on a prepaid basis only and are entered on a calendar year basis. Issues are sent by surface mail except to the following countries where air delivery via SAL is ensured: Argentina, Australia, Brazil, Canada, China, Hong Kong, India, Israel, Japan, Malaysia, Mexico, New Zealand, Pakistan, Singapore, South Africa, South Korea, Taiwan, Thailand, USA. For all other countries airmail rates are available upon request. Claims for missing issues must be made within six months of our publication (mailing) date. Please address all your requests regarding orders and subscription queries to: Elsevier Science B.V., Journal Department, P.O. Box 211, 1000 AE Amsterdam, Netherlands. Tel.: (+31-20) 5803 642; Fax: (+31-20) 5803 598. Customers in the USA and Canada wishing information on this and other Elsevier journals, please contact Journal Information Center, Elsevier Science Inc., 655 Avenue of the Americas, New York, NY 10010, USA, Tel. (+1-212) 633 3750, Telefax (+1-212) 633 3764.

Abstracts/Contents Lists published in Analytical Abstracts, Biochemical Abstracts, Biological Abstracts, Chemical Abstracts, Chemical Titles, Chromatography Abstracts, Current Awareness in Biological Sciences (CABS), Current Contents/Life Sciences, Current Contents/Physical, Chemical & Earth Sciences, Deep-Sea Research/Part B: Oceanographic Literature Review, Excerpta Medica, Index Medicus, Mass Spectrometry Bulletin, PASCAL-CNRS, Referativnyi Zhurnal, Research Alert and Science Citation Index.

US Mailing Notice. *Journal of Chromatography A* (ISSN 0021-9673) is published weekly (total 52 issues) by Elsevier Science B.V., (Sara Burgerhartstraat 25, P.O. Box 211, 1000 AE Amsterdam, Netherlands). Annual subscription price in the USA US\$ 4994.00 (US\$ price valid in North, Central and South America only) including air speed delivery. Second class postage paid at Jamaica, NY 11431. **USA POSTMASTERS:** Send address changes to *Journal of Chromatography A*, Publications Expediting, Inc., 200 Meacham Avenue, Elmont, NY 11003. Airfreight and mailing in the USA by Publications Expediting.

See inside back cover for Publication Schedule, Information for Authors and information on Advertisements.

© 1994 ELSEVIER SCIENCE B.V. All rights reserved.

0021-9673/94/\$07.00

No part of this publication may be reproduced, stored in a retrieval system or transmitted in any form or by any means, electronic, mechanical, photocopying, recording or otherwise, without the prior written permission of the publisher. Elsevier Science B.V., Copyright and Permissions Department, P.O. Box 521, 1000 AM Amsterdam, Netherlands.

Upon acceptance of an article by the journal, the author(s) will be asked to transfer copyright of the article to the publisher. The transfer will ensure the widest possible dissemination of information.

Special regulations for readers in the USA – This journal has been registered with the Copyright Clearance Center, Inc. Consent is given for copying of articles for personal or internal use, or for the personal use of specific clients. This consent is given on the condition that the copier pays through the Center the per-copy fee stated in the code on the first page of each article for copying beyond that permitted by Sections 107 or 108 of the US Copyright Law. The appropriate fee should be forwarded with a copy of the first page of the article to the Copyright Clearance Center, Inc., 27 Congress Street, Salem, MA 01970, USA. If no code appears in an article, the author has not given broad consent to copy and permission to copy must be obtained directly from the author. The fee indicated on the first page of an article in this issue will apply retroactively to all articles published in the journal, regardless of the year of publication. This consent does not extend to other kinds of copying, such as for general distribution, resale, advertising and promotion purposes, or for creating new collective works. Special written permission must be obtained from the publisher for such copying.

No responsibility is assumed by the Publisher for any injury and/or damage to persons or property as a matter of products liability, negligence or otherwise, or from any use or operation of any methods, products, instructions or ideas contained in the materials herein. Because of rapid advances in the medical sciences, the Publisher recommends that independent verification of diagnoses and drug dosages should be made.

Although all advertising material is expected to conform to ethical (medical) standards, inclusion in this publication does not constitute a guarantee or endorsement of the quality or value of such product or of the claims made of it by its manufacturer.

This issue is printed on acid-free paper.

Printed in the Netherlands

CONTENTS

(Abstracts/Contents Lists published in *Analytical Abstracts*, *Biochemical Abstracts*, *Biological Abstracts*, *Chemical Abstracts*, *Chemical Titles*, *Chromatography Abstracts*, *Current Awareness in Biological Sciences (CABS)*, *Current Contents/Life Sciences*, *Current Contents/Physical, Chemical & Earth Sciences*, *Deep-Sea Research/Part B: Oceanographic Literature Review*, *Excerpta Medica*, *Index Medicus*, *Mass Spectrometry Bulletin*, *PASCAL-CNRS*, *Referativnyi Zhurnal*, *Research Alert* and *Science Citation Index*)

REGULAR PAPERS

Column Liquid Chromatography

- Comparative evaluation of adsorption energy distribution functions obtained by analytical and numerical methods
by S. Golshan-Shirazi and G. Guiochon (Knoxville and Oak Ridge, TN, USA) (Received December 31st, 1993) 1
- Electrochromatography and micro high-performance liquid chromatography with 320 μm I.D. packed columns
by C. Yan, D. Schaufelberger and F. Erni (Basle, Switzerland) (Received February 15th, 1994) 15
- Preparation and evaluation of polyacrylate-coated fused-silica capillaries for reversed-phase open-tubular liquid chromatography
by R. Swart, J.C. Kraak and H. Poppe (Amsterdam, Netherlands) (Received January 26th, 1994) 25
- Chloromethylphenylcarbamate derivatives of cellulose as chiral stationary phases for high-performance liquid chromatography
by B. Chankvetadze, E. Yashima and Y. Okamoto (Nagoya, Japan) (Received January 25th, 1994) 39
- Factor analysis in ion chromatography of carboxylate ions
by U. Haldna (Tallinn, Estonia), J. Pentchuk (Tartu, Estonia), M. Righezza (Orléans, France) and J.R. Chrétien (Orléans and Paris, France) (Received February 9th, 1994) 51
- Determination of amino acids by precolumn derivatization with 6-aminoquinolyl-N-hydroxysuccinimidyl carbamate and high-performance liquid chromatography with ultraviolet detection
by H.J. Liu (Beijing, China) (Received January 31st, 1994) 59
- Separations of tocopherols and methylated tocots on cyclodextrin-bonded silica
by S.L. Abidi and T.L. Mounts (Peoria, IL, USA) (Received February 23rd, 1994) 67
- High-performance liquid chromatographic analysis of Romet-30 in Chinook salmon (*Oncorhynchus tshawytscha*): wash-out time, tissue distribution in muscle, liver and skin, and metabolism of sulfadimethoxine
by M. Zheng, H.-Y. Liu, S.F. Hall, D.D. Kitts and K.M. McErlane (Vancouver, Canada) (Received February 17th, 1994) 77
- ✓ Analysis of colloidal particles. V. Size-exclusion chromatography of colloidal semiconductor particles
by C.-H. Fischer, M. Giersig and T. Siebrands (Berlin, Germany) (Received February 17th, 1994) 89
- Ion chromatographic separation of alkali metal and ammonium cations on a C_{18} reversed-phase column
by K. Ito, H. Shimazu, E. Shoto, M. Okada, T. Hirokawa and H. Sunahara (Higashi-Hiroshima, Japan) (Received February 1st, 1994) 99
- Gas Chromatography*
- Extra-thermodynamic relationships in chromatography. Enthalpy-entropy compensation in gas chromatography
by J. Li and P.W. Carr (Minneapolis, MN, USA) (Received January 18th, 1994) 105
- Selective chemiluminescence detection of sulfur-containing compounds coupled with nitrogen-phosphorus detection for gas chromatography
by T.B. Ryerson, R.M. Barkley and R.E. Sievers (Boulder, CO, USA) (Received February 23rd, 1994) 117
- Capillary column gas chromatographic-tandem mass spectrometric analysis of phosphate esters in the presence of interfering hydrocarbons
by P.A. D'Agostino and L.R. Provost (Medicine Hat, Canada) (Received February 15th, 1994) 127
- Determination of various pesticides using membrane extraction discs and gas chromatography-mass spectrometry
by C. Crespo, R.M. Marcé and F. Borrull (Tarragona, Spain) (Received January 20th, 1994) 135
- Detection of alcohols in gas chromatographic effluent by laser-light scattering
by B.L. Wittkamp and D.C. Tilotta (Grand Forks, ND, USA) (Received February 14th, 1994) 145

Contents (continued)

- Toxic aldehydes formed by lipid peroxidation. I. Sensitive, gas chromatography-based stereoanalysis of 4-hydroxyalkenals, toxic products of lipid peroxidation
by G. Bringmann, M. Gassen and S. Schneider (Würzburg, Germany) (Received February 8th, 1994) 153

Supercritical Fluid Chromatography

- Effect of the sample solvent and instrument design on the reproducibility of retention times and peak shapes in packed-column supercritical fluid chromatography
by R.M. Smith and D.A. Briggs (Loughborough, UK) (Received February 18th, 1994) 161
- Experimental study of band broadening and solute interferences in preparative supercritical fluid chromatography
by G. Cretier, J. Neffati and J.L. Rocca (Villeurbanne, France) (Received February 3rd, 1994) 173

Planar Chromatography

- Chromatographic behaviour of diastereoisomers. XII. Effects of alumina on separations of esters of maleic and fumaric acids
by M. Palamareva, I. Kozekov and I. Jurova (Sofia, Bulgaria) (Received February 1st, 1994) 181
- Overpressured layer chromatography in comparison with thin-layer and high-performance liquid chromatography for the determination of coumarins with reference to the composition of the mobile phase
by P. Vuorela, E.-L. Rahko, R. Hiltunen and H. Vuorela (Helsinki, Finland) (Received February 9th, 1994) 191

Electrophoresis

- Factors affecting the capillary electrophoresis of ricin, a toxic glycoprotein
by H.B. Hines and E.E. Brueggemann (Frederick, MD, USA) (Received January 25th, 1994) 199
- Use of capillary electrophoresis for the determination of vitamins of the B group in pharmaceutical preparations
by S. Boonkerd, M.R. Detaevernier and Y. Michotte (Jette, Belgium) (Received December 15th, 1993) 209
- Capillary electrophoresis of nicotinamide-adenine dinucleotide and nicotinamide-adenine dinucleotide phosphate derivatives in coated tubular columns
by M. Nesi, M. Chiari, G. Carrea, G. Ottolina and P.G. Righetti (Milan, Italy) (Received January 28th, 1994) 215
- Determination of fluoride in feed mixtures by capillary isotachophoresis
by P. Blatný and F. Kvasnička (Prague, Czech Republic) (Received January 24th, 1994) 223

SHORT COMMUNICATIONS

Column Liquid Chromatography

- Purification of bacilli ribonucleases by reversed-phase high-performance liquid chromatography
by K.I. Panov (Moscow, Russian Federation) (Received February 15th, 1994) 229
- High-performance liquid chromatographic determination of mitoxantrone in liposome preparations using solid-phase extraction and its application in stability studies
by S.-L. Law and T.-F. Jang (Taipei, Taiwan) (Received February 17th, 1994) 234

Supercritical Fluid Chromatography

- Determination of enantiomeric purity of (*S*)-carboranylalanine using capillary column supercritical fluid chromatography
by P. Petersson, J. Malmquist, K.E. Markides and S. Sjöberg (Uppsala, Sweden) (Received March 4th, 1994) 239

BOOK REVIEWS

- Environmental analysis —Techniques, applications and quality assurance (edited by D. Barceló), reviewed by A.P. Bianchi (Southampton, UK) 243
- Statistical methods in analytical chemistry (by P.C. Meier and R.E. Zünd), reviewed by H.C. Smit (Amsterdam, Netherlands) 245

- AUTHOR INDEX 247

- Announcement of Special Issue on Chromatographic and Electrophoretic Analyses of Carbohydrates 249

JOURNAL OF CHROMATOGRAPHY A

VOL. 670 (1994)

JOURNAL OF CHROMATOGRAPHY A

INCLUDING ELECTROPHORESIS AND OTHER SEPARATION METHODS

EDITORS

U.A.Th. BRINKMAN (Amsterdam), R.W. GIESE (Boston, MA), J.K. HAKEN (Kensington, N.S.W.),
L.R. SNYDER (Orinda, CA)

EDITORS, SYMPOSIUM VOLUMES

E. HEFTMANN (Orinda, CA), Z. DEYL (Prague)

EDITORIAL BOARD

D.W. Armstrong (Rolla, MO), W.A. Aue (Halifax), P. Boček (Brno), A.A. Boulton (Saskatoon), P.W. Carr (Minneapolis, MN), N.H.C. Cooke (San Ramon, CA), V.A. Davankov (Moscow), G.J. de Jong (Weesp), Z. Deyl (Prague), S. Dilli (Kensington, N.S.W.), Z. El Rassi (Stillwater, OK), H. Engelhardt (Saarbrücken), F. Erni (Basle), M.B. Evans (Hatfield), J.L. Glajch (N. Billerica, MA), G.A. Guiochon (Knoxville, TN), P.R. Haddad (Hobart, Tasmania), I.M. Hais (Hradec Králové), W.S. Hancock (Palo Alto, CA), S. Hjertén (Uppsala), S. Honda (Higashi-Osaka), Cs. Horváth (New Haven, CT), J.F.K. Huber (Vienna), K.-P. Hupe (Waldbronn), J. Janák (Brno), P. Jandera (Pardubice), B.L. Karger (Boston, MA), J.J. Kirkland (Newport, DE), E. sz. Kováts (Lausanne), K. Macek (Prague), A.J.P. Martin (Cambridge), L.W. McLaughlin (Chestnut Hill, MA), E.D. Morgan (Keele), J.D. Pearson (Kalamazoo, MI), H. Poppe (Amsterdam), F.E. Regnier (West Lafayette, IN), P.G. Righetti (Milan), P. Schoenmakers (Amsterdam), R. Schwarzenbach (Dübendorf), R.E. Shoup (West Lafayette, IN), R.P. Singhal (Wichita, KS), A.M. Siouffi (Marseille), D.J. Strydom (Boston, MA), N. Tanaka (Kyoto), S. Terabe (Hyogo), K.K. Unger (Mainz), R. Verpoorte (Leiden), Gy. Vigh (College Station, TX), J.T. Watson (East Lansing, MI), B.D. Westerlund (Uppsala)

EDITORS, BIBLIOGRAPHY SECTION

Z. Deyl (Prague), J. Janák (Brno), V. Schwarz (Prague)



ELSEVIER

Amsterdam – Lausanne – New York – Oxford – Shannon – Tokyo

J. Chromatogr. A, Vol. 670 (1994)

No part of this publication may be reproduced, stored in a retrieval system or transmitted in any form or by any means, electronic, mechanical, photocopying, recording or otherwise, without the prior written permission of the publisher, Elsevier Science B.V., Copyright and Permissions Department, P.O. Box 521, 1000 AM Amsterdam, Netherlands.

Upon acceptance of an article by the journal, the author(s) will be asked to transfer copyright of the article to the publisher. The transfer will ensure the widest possible dissemination of information.

Special regulations for readers in the USA – This journal has been registered with the Copyright Clearance Center, Inc. Consent is given for copying of articles for personal or internal use, or for the personal use of specific clients. This consent is given on the condition that the copier pays through the Center the per-copy fee stated in the code on the first page of each article for copying beyond that permitted by Sections 107 or 108 of the US Copyright Law. The appropriate fee should be forwarded with a copy of the first page of the article to the Copyright Clearance Center, Inc., 27 Congress Street, Salem, MA 01970, USA. If no code appears in an article, the author has not given broad consent to copy and permission to copy must be obtained directly from the author. The fee indicated on the first page of an article in this issue will apply retroactively to all articles published in the journal, regardless of the year of publication. This consent does not extend to other kinds of copying, such as for general distribution, resale, advertising and promotion purposes, or for creating new collective works. Special written permission must be obtained from the publisher for such copying.

No responsibility is assumed by the Publisher for any injury and/or damage to persons or property as a matter of products liability, negligence or otherwise, or from any use or operation of any methods, products, instructions or ideas contained in the materials herein. Because of rapid advances in the medical sciences, the Publisher recommends that independent verification of diagnoses and drug dosages should be made.

Although all advertising material is expected to conform to ethical (medical) standards, inclusion in this publication does not constitute a guarantee or endorsement of the quality or value of such product or of the claims made of it by its manufacturer.

This issue is printed on acid-free paper.

Printed in the Netherlands

Comparative evaluation of adsorption energy distribution functions obtained by analytical and numerical methods

Sadroddin Golshan-Shirazi^{*}, Georges Guiochon^{*}

*Department of Chemistry, University of Tennessee, Knoxville, TN 37996-1503, USA and
Division of Analytical Chemistry, Oak Ridge National Laboratory, Oak Ridge, TN 37831-6120, USA*

(First received April 21st, 1993; revised manuscript received December 31st, 1993)

Abstract

The adsorption energy distributions derived from the Adamson and Ling (AL), and the House and Jaycock HILDA numerical methods are compared with the Sips analytical solution, which is used as a benchmark for these numerical methods. Excellent agreement between the analytical and numerical methods is achieved provided that the isotherm data are measured over a wide range of adsorbate partial pressures, extending to near the saturation capacity. While a lack of accurate low-pressure data will merely result in an inaccurate energy distribution in the high-energy range, a lack of these high-pressure data may result in an entirely wrong energy distribution.

1. Introduction

Almost all solid surfaces are heterogeneous [1,2]. A quantitative description of adsorption on a real, heterogeneous adsorbent requires the use of the adsorption energy distribution function [1]. Two widely different models of the adsorbent surface have been discussed in the literature [3,4]. The random distribution site model introduced by Hill [3] assumes that sites with different adsorption energy are randomly distributed over the surface, and the adsorption system must be considered as a single thermodynamic entity. The homotattic model [4] assumes that the surface is made of patches randomly distributed

on the surface, but that each patch is covered with adsorption sites having the same adsorption energy, *i.e.*, is homogeneous. These patches are large enough to permit the application of statistical thermodynamics to every one of them, so the whole system can be considered as a collection of independent subsystems.

In this work, we consider the latter, patch-wise heterogeneity model in which the average degree of surface coverage at constant temperature, $q^d(p)$, is related to the partial pressure, p , of the adsorbate vapor by

$$q^d(p) = \frac{q(p)}{q_s} = \int_{\epsilon_{\min}}^{\epsilon_{\max}} \theta(\epsilon, p) f(\epsilon) d\epsilon \quad (1)$$

where $q(p)$ is the experimental adsorption isotherm, q_s the monolayer saturation capacity of the adsorbent, $\theta(\epsilon, p)$ the local isotherm on the homogeneous patch having an adsorption energy

^{*} Corresponding author. Address for correspondence: Department of Chemistry, University of Tennessee, Knoxville, TN 37996-1503, USA.

^{*} Present address: AAI, Wilmington, NC, USA.

ϵ and $f(\epsilon)$ the energy distribution function, so $f(\epsilon) d\epsilon$ is the fraction of the surface on which the binding energy is between ϵ and $\epsilon + d\epsilon$. ϵ_{\min} and ϵ_{\max} are the lowest and the highest values of the adsorption energy on the heterogeneous surface considered, respectively.

The aim of this approach is the derivation of the energy distribution function, $f(\epsilon)$, from the experimental isotherm, $q(p)$ (which is the only parameter in Eq. 1 which can be determined experimentally), and assuming a model for the local isotherm, $\theta(\epsilon, p)$. It has been extensively used in the past 20 years to investigate real surfaces [1,2,5]. A number of different solutions of Eq. 1 have been suggested. However, few comparisons, if any, have been made between the results obtained when applying these different solutions to the same set of data.

There are two general types of solutions for such a problem, analytical and numerical. Analytical solutions can be derived only if further assumptions are made regarding both the local and the experimental isotherm models. These assumptions are too restrictive to be of practical value, so attention has mainly focused on numerical solutions. This approach requires less restrictive assumptions, regarding only the local isotherm model. However, it suffers from a considerable drawback. Numerical methods are essentially empirical, using computing power to derive the energy distribution function which permits the calculation of the isotherm that best approximates the experimental isotherm. The mathematical problem is ill-posed, however, and does not have a unique solution [1,2,5–9], so restrictions are necessary. Because there are no independent methods for the determination of the adsorption energy distribution function, and there are no adsorbents available with a known adsorption energy distribution function, we have no way of knowing whether the result of the calculation is correct. Therefore, the reliability of any procedure for the experimental determination of the adsorption energy distribution function is in doubt.

In this paper, we consider the analytical solutions of Eq. 1 and compare them with the numerical solutions available for the evaluation

of the adsorption energy distribution function from experimental isotherms. This work will provide further information on the sensitivity of the distribution function to the choice of a model for the experimental isotherm, to the accuracy of the experimental data and to the numerical errors.

2. Theory

From a mathematical point of view, Eq. 1 is a Fredholm integral equation of the first kind, for which there is no general analytical solution. The problem is ill-posed and does not have a unique solution, so further restrictions are necessary to obtain the solution of the physical problem. Two types of methods have been investigated in attempts to derive a solution, numerical methods based on iterative procedures and direct analytical methods, which require some further assumptions and simplifications. In all instances, an isotherm model must be assumed for the local adsorption isotherm. We discuss first analytical and then numerical solutions.

2.1. Analytical solution of the Sips method

Three different methods for the determination of an analytical solution of Eq. 1 have been suggested, the Sips [10], Hobson [11] and condensation approximation [12] methods. These methods differ mainly in the local isotherm model assumed. In the Sips method, the local isotherm is the Langmuir model: the adsorption is localized, the adsorbate does not move on the surface, there are no adsorbate–adsorbate interactions and the gas phase is ideal. As this method uses the least simplistic local model, it is the only method considered here.

The local isotherm is given by

$$\theta(\epsilon, P) = \frac{P}{P + K e^{-\epsilon/RT}} \quad (2)$$

where K is a constant independent of ϵ , of the column temperature T and of the location on the surface. The following equations have been

suggested in the literature to provide an estimate of the value of K :

$$K = \frac{\sqrt{MT}\sigma_m}{3.5 \cdot 10^{22}t_0} \quad (3a)$$

$$K = 1.76 \cdot 10^4 \sqrt{MT} \quad (3b)$$

$$K = P_s e^{\Lambda_v/RT} \quad (3c)$$

where M is the molecular mass of the adsorbate, σ_m the monolayer coverage (number of molecules per unit surface area of adsorbent), t_0 the vibration time of the adsorbed molecules (s); P_s the vapor pressure, Λ_v the molar heat of vaporization of the adsorbate studied and R the ideal gas constant (1.987 cal/K · mol) (1 cal = 4.186 J). With the numbers used, K in Eqs. 3a and 3b is given in Torr (1 Torr = 133.322 Pa).

The first equation is based on the kinetic derivation of the Langmuir isotherm, which equates at equilibrium the adsorption and desorption flux, assuming the condensation coefficient to be unity [11,13]. The second was suggested by Hobson [11] for nitrogen and the third by Dormant and Adamson [14]. In this work, we used Eq. 3c.

Eq. 1 is reformulated as a Stieltjes transform of the distribution function, which is inverted using standard mathematical techniques [15]. Inserting Eq. 2 into Eq. 1, and letting

$$y = \frac{K}{P} + 1 \quad (4a)$$

$$x = \exp(\epsilon/RT) \quad (4b)$$

$$g(x) = f[RT \ln(1+x)] = f(\epsilon) \quad (4c)$$

$$h(y) = \frac{1}{RT} q^d\left(\frac{K}{y-1}\right) \quad (4d)$$

we obtain for Eq. 1

$$h(y) = \int_0^\infty \frac{g(x)}{x+y} \quad (4)$$

Thus, $h(y)$ is the Stieltjes transform of $g(x)$, and the solution is [15]

$$f(\epsilon) = g(x) = \frac{h(x e^{-i\pi}) - h(x e^{i\pi})}{2i\pi} \quad (5)$$

For obvious physical reasons, the limits of $q^d(P)$ have following values:

$$q^d(0) = 0 \quad \text{and} \quad \lim_{P \rightarrow \infty} q^d = 1 \quad (6)$$

The first condition is always satisfied; the second one is also, provided that the function $f(\epsilon)$ is normalized, i.e., if

$$\int_0^\infty f(\epsilon) d\epsilon = 1 \quad (7)$$

To go further and determine $f(\epsilon)$, we need an analytical expression for the experimental isotherm. This equation must satisfy Eq. 6. Thus, for example, we can use the Langmuir model but not the Freundlich model, which does not satisfy the second limit condition. Usually, the Langmuir model does not fit well the experimental data measured with heterogeneous surfaces [1,2]. It is possible to derive an adsorption energy distribution function with the Sips method for only few local isotherm models.

Generalized Freundlich isotherm

This isotherm is given by

$$q^d(P) = \left(\frac{P}{P+K}\right)^c \quad (8)$$

where c is a numerical parameter and K is the same as in Eq. 2. Unlike the Freundlich isotherm, the generalized Freundlich isotherm satisfies the second condition in Eq. 6, if $0 < c < 1$. In this case, the adsorption energy distribution function is given by

$$f(\epsilon) = \frac{1}{RT} \cdot \frac{\sin \pi c}{\pi} (e^{\epsilon/RT} - 1)^{-c} \quad (9)$$

This result is easily extended to the generalized form of the isotherm in Eq. 8:

$$q^d(P) = \left(\frac{P}{P+A}\right)^c \quad (10)$$

with $A < K$. The adsorption energy distribution function for the isotherm in Eq. 10 is given by [10]

$$f(\epsilon) = 0 \quad 0 < \epsilon < \epsilon_0 \quad (11a)$$

$$f(\epsilon) = \frac{1}{RT} \cdot \frac{\sin \pi c}{\pi} [e^{(\epsilon - \epsilon_0)/RT} - 1]^{-c} \quad \epsilon_0 < \epsilon \quad (11b)$$

where $\epsilon_0 = RT \ln(K/A)$. Thus, the replacement of K by A merely shifts the adsorption energy distribution by the amount ϵ_0 .

Langmuir isotherm

In this case, $c = 1$ in Eqs. 10 and 11, and the latter reduces to a δ function, the distribution being zero everywhere, except for $\epsilon = \epsilon_0$, where it is infinite. This result is consistent with the Langmuir isotherm model which assumes a homogeneous surface, all the adsorption sites having the same adsorption energy, ϵ_0 .

Multi-Langmuir isotherm

Many experimental data can be fitted to a bi-Langmuir or a multi-Langmuir isotherm equation [16,17]:

$$q^d(P) = \frac{1}{q_s} \sum_i q_{s,i} \frac{P}{P + A_i} \quad (12)$$

Applying the same calculation procedure as above, we obtain that the adsorption energy distribution is zero everywhere, except at the energies

$$\epsilon_i = RT \ln \frac{K}{A_i} \quad (13)$$

where it is infinite. In practice, the adsorption energy distribution for a multi-Langmuir isotherm consists of a series of very sharp lines. The surface is made of homogeneous patches of a few different types. The number of lines is equal to the number of patch types, their energy to the adsorption energy on the corresponding adsorption site and the relative intensity of the impulse is $q_{s,i}/q_{s,\text{tot}}$, where $q_{s,i}$ is the saturation capacity of the corresponding Langmuir term and $q_{s,\text{tot}}$ is the total saturation capacity. This result is consistent with the multi-Langmuir isotherm model.

Misra isotherm

This isotherm is given by [18]

$$q^d(P) = \frac{np}{(K - np) \ln(1 + n)} \cdot \ln \left(\frac{1 + \frac{K}{P}}{1 + n} \right) \quad (14)$$

and the corresponding adsorption energy distribution is [18]

$$f(\epsilon) = \frac{n}{RT \ln(1 + n)} (n + e^{\epsilon/RT})^{-1} \quad (15)$$

If ϵ_0 is the lower limit of the adsorption energy distribution, the isotherm and the adsorption energy distributions become, respectively [18],

$$q^d(P) = \frac{np}{(K - np) \ln \left(1 + \frac{n}{r} \right)} \cdot \ln \left(\frac{r + \frac{K}{P}}{r + n} \right) \quad (16)$$

$$f(\epsilon) = \frac{n}{RT \ln(r + n) - \epsilon_0} (n + e^{\epsilon/RT})^{-1} \quad (17)$$

with $r = e^{\epsilon_0/RT}$. According to Eq. 11, $f(\epsilon)$ tends towards zero when ϵ increases indefinitely, it increases with decreasing ϵ and increases indefinitely when ϵ tends towards ϵ_0 . The adsorption energy distribution is zero at values of ϵ below ϵ_0 .

Dubinin–Radushkevich isotherm

The empirical Dubinin–Radushkevich isotherm [19] is given by

$$q^d(P) = \exp \left[-B' \left(RT \ln \frac{P_s}{P} \right)^2 \right] \quad (18)$$

where B' is a numerical constant and P_s is the vapor pressure of the pure liquid adsorbate at the temperature of the experiment. Like the Freundlich isotherm, the Dubinin–Radushkevich isotherm does not satisfy Eq. 6, as required for the Stieltjes transform, and is not physically compatible with the Sips method. Misra modified the Dubinin–Radushkevich isotherm and proposed a “generalized” equation that satisfies the requirements of the Stieltjes transform. This new isotherm equation is [20]

$$q^d(P) = \exp \left\{ -B \left[RT \ln \left(1 + \frac{c}{P} \right) \right]^2 \right\} \quad (19)$$

where B and c are numerical constants. With the addition of 1 in the expression under the logarithm operator, Eq. 6 is satisfied, and the replacement of P_s by an adjustable constant gives some flexibility to an empirical equation; c is obtained by fitting the experimental data to

Eq. 19. The adsorption energy distribution function is

$$f(\epsilon) = \frac{\exp(\pi^2 B R^2 T^2)}{\pi R T} \cdot \sin(2\pi R T B \epsilon) e^{-B \epsilon^2} \quad (20a)$$

The shape of the adsorption energy distribution obtained is very different from that given in Eq. 11. $f(\epsilon)$ tends towards 0 when ϵ tends towards either 0 or ∞ . The profile is a skewed Gaussian reaching its maximum value for

$$\epsilon = \epsilon_M = \frac{1}{\sqrt{2B}} \quad (20b)$$

2.2. Numerical solutions

With all numerical methods, a local isotherm model needs to be assumed for each patch. This means that a general model of the local isotherm (e.g., Langmuir) must be assumed, in addition to a functional relationship between the coefficients of this isotherm and the adsorption energy. Because of the ill-posed nature of the mathematical problem and the non-unicity of its general solution [6–9], two approaches have been used to calculate numerical solutions of Eq. 1. In the first approach, a particular form of the adsorption energy distribution function is assumed. Its coefficients are determined by matching the isotherm calculated with Eq. 1 to the experimental isotherm, and minimizing the residue with a conventional fitting procedure. In the second approach, no assumptions are made regarding the nature or shape of the adsorption energy distribution function, and this function is derived directly from the experimental isotherm. This type of computation is extremely difficult, however, because of the constraints imposed by the requirement of a realistic solution and the influence of experimental errors.

Methods based on the assumption of an analytical function for the adsorption energy distribution

Several groups have investigated this approach in the past. Ross and Oliver [4] assumed a Gaussian distribution function for the adsorption

energy distribution. Their method can also be used with the sum of a few Gaussian distributions. Hoory and Prausnitz [21] used a long-tail function, skewed and defined only for positive values of ϵ . Kindel [22] assumed a Maxwell function, Jaroniec *et al.* [23] a gamma function and Sparnaay [24] a surface covered by a few patches only.

In general, any kind of analytical expression can be assumed for the energy distribution, and the coefficients of this expression can be obtained by optimization, using any of a variety of curve-fitting algorithms. For example, Van Dongen [25] assumed an analytical expression for the energy distribution of the form

$$\ln f(\epsilon) = b_0 + b_1 \epsilon + b_2 \epsilon^2 + \dots + b_n \epsilon^n \quad (21)$$

The optimum values of the parameters b_i are obtained by minimizing the sum of the squares of the differences between calculated and experimental isotherm points with respect to the b_i .

The major disadvantage of this approach is that there are no methods available for the direct determination of the adsorption energy distribution, or any fundamental or even compelling reasons to choose any one of the many possible distribution functions available. The use of this approach was a practical necessity when the computing power available was low, and it has become obsolete with the advent of modern computers that permit the much more complex calculations required when no energy distributions are assumed.

Direct methods of calculation of the adsorption energy distribution

Three different, important procedures have been described in the literature, the Adamson and Ling (AL) method [26], the HILDA algorithm of House and Jaycock [27] and the CAEDMON algorithm of Ross and Morrison [28]. None of them makes any *a priori* assumption regarding the shape of the adsorption energy distribution, except that $f(0) = 0$, $f(\epsilon)$ tends towards zero when ϵ tends towards infinity and that the integral over the whole energy range is finite. We discuss these methods successively.

Adamson–Ling method. In this method [26], Eq. 1 is rewritten as

$$q^d(p) = \int_0^1 \theta(\epsilon, p) dF \quad (22a)$$

with

$$F(\epsilon) = \int_{\epsilon_{\min}}^{\epsilon_{\max}} f(\epsilon) d\epsilon \quad (22b)$$

where $F(\epsilon)$ is the integral site energy distribution, *i.e.*, the fraction of the surface covered by sites on which the adsorption energy exceeds ϵ . Eq. 22a can be approximated by the sum

$$q_{dj} = \sum_{i=1}^{i=n} \theta_{ji}(F_i - F_{i-1}) \quad j = 1, 2, \dots, m \quad (23)$$

where m is the number of data points acquired and n is the number of intervals used to represent the adsorption energy distribution. An iterative calculation procedure is used. The first approximation of the integral of the adsorption energy distribution for this iterative procedure is obtained by using the condensation approximation for the local isotherm:

$$q_{dj} = \int_0^{F(\epsilon_j)} 1 \times dF(\epsilon) + \int_{F(\epsilon_j)}^1 0 \times dF(\epsilon) \quad (24)$$

Hence, the first approximation of the energy integral is given by

$$F(\epsilon_j) = q_{dj_{\text{exp}}} \quad (25)$$

These values of the integral of the adsorption energy distribution are used in Eq. 22, together with a realistic model of the local isotherm, to evaluate the total isotherm, $q_{dj_{\text{cal}}}$. The monolayer capacity should be evaluated independently, for example from the results of the BET method.

In their original work, performed in 1961, Adamson and Ling [26] had to use a graphical procedure to judge the deviations between the calculated and the experimental isotherms, make the decisions regarding the extent of the disagreement and the nature of the adjustments best needed for the next iteration step. Difficulties arose because the distribution resulting from

successive approximations may not differ much from one step to the next, the changes may not be systematic and no continuous trend towards convergence was apparent. The graphical method showed also a tendency for ripples to appear in the energy distribution function, and to propagate. These ripples have to be damped and suppressed, so the final distribution function is not oscillating. Later, a computer program was developed to carry out the method, and the computation was ended when the root mean square of the deviation between the experimental and the calculated isotherms became smaller than a certain threshold.

HILDA algorithm. House and Jaycock [27] proposed a numerical method based on the iterative scheme of Adamson and Ling [26]. This method was presented under the acronym HILDA, for Heterogeneity Investigated at Loughborough by a Distribution Analysis. Instead of directly evaluating the Eq. 22, House and Jaycock rewrote it as

$$q^d(p_j) = \int_0^1 F(\epsilon) d\theta(\epsilon, p_j) \quad (26)$$

They assumed that the energy distribution has a finite width, determined by the lowest and highest partial pressures at which adsorbed amounts have been determined experimentally, that any surface patch which has an integral adsorption energy greater than ϵ_{\max} is fully covered with a monolayer of adsorbate, while any surface patch for which the integral adsorption energy is lower than ϵ_{\min} is empty. Then, Eq. 26 can be rewritten as

$$q^d(p_j) = \int_{\theta_l(p_j)}^{\theta_h(p_j)} F(\epsilon) d\theta(\epsilon, p_j) + F(\epsilon_{\min})\theta_l p_j + F(\epsilon_{\max})[1 - \theta_h(p_j)] \quad (27)$$

where θ_h and θ_l are the fractional coverages at the pressure p_j of the surface patches with the highest and lowest adsorption energies, respectively. As in the AL method, the condensation approximation is used for obtaining the initial value of the integral energy, F , and the value of F in the k th iteration is calculated according to

$$F^k(\epsilon_j) = \frac{q_{j\text{exp}}^d}{q_{j\text{cal}}^d} \cdot F^{k-1}(\epsilon_j) \quad (28)$$

The solution is reached when the root mean square deviation between the experimental and the calculated isotherms becomes lower than a given threshold.

The algorithm includes also a quadratic smoothing function for the isotherm data. This function can also be used to smooth the energy distribution function obtained, if necessary. In order to ensure that an evenly spaced adsorption energy distribution function will be obtained, the program does not use the experimental adsorption isotherm, under its classical representation, but with the adsorbate partial pressure expressed in a logarithmic scale. The HILDA program offers four choices for the local isotherm, the Langmuir, the Fowler–Guggenheim, the Hill–de Boer or the virial isotherms. Independent, prior knowledge of the monolayer capacity of the adsorbent is not a prerequisite for the calculation. The value of the monolayer capacity can be adjusted and eventually determined from the normalization factor, since $F(\epsilon_{\min}) = \int_{\epsilon_{\min}}^{\epsilon_{\max}} f(\epsilon) d\epsilon$ has to be equal to 1. The HILDA algorithm has been used extensively for the investigation of the surface heterogeneity of various solids [29].

CAEDMON algorithm. Ross and Morrison [28] developed another algorithm for the same purpose, the Computer Adsorptive Energy Distribution in the MONolayer (CAEDMON). This algorithm uses only the two-dimensional virial isotherm to represent the local isotherm. This algorithm was later modified by Sacher and Morrison [30], who used more reliable and effective procedures to ensure convergence and uniqueness of the solution.

Quasi-Adamson method. Roles and Guiochon [17] used a combination of two approaches developed previously. In a first part, they used a modification of the AL method, with computerized numerical iterations. The experimental isotherm is replaced by a multi-Langmuir isotherm. In most cases, a bi-Langmuir isotherm was found

to fit the experimental data excellently. As we have shown in the previous section, this algorithm is not necessary since for a multi-Langmuir experimental isotherm there is an analytical solution of Eq. 1, a series of impulses, one for each Langmuir term of the isotherm, at energies related to the coefficients of the Langmuir term. Although in a second, confirmation stage the method [17,31,32] replaces the multi-Langmuir isotherm by an Akima spline [33] representation of the experimental data to verify the number of modes of the energy distribution, it cannot divorce itself from the multi-Langmuir representation used in the first stage. Because isotherm measurements can be made only in a limited range of partial pressures, a multi-Langmuir isotherm still has to be used for the extrapolation of the experimental data at high pressures. As a consequence, the method may generate spurious peaks.

The second part of this procedure, called the Distribution Function Substitution, is similar to the method developed by Ross and Oliver [4]. Each peak of the energy distribution function derived in the first part of the procedure is replaced by an analytical function. If the peak obtained from the quasi-Adamson method is symmetrical, it is replaced by a Gaussian distribution; if slightly skewed, by an exponentially modified Gaussian distribution; and if highly unsymmetrical, by a Γ function. The parameters of these functions are adjusted and optimized by a simplex optimization pursued until the best fit is obtained between the experimental and calculated isotherms, using a test based on the value of the root mean square of the difference between measured and calculated isotherms.

In practice, this method suffers the same drawbacks as the Ross and Oliver approach [4]. It involves the replacement of the unknown adsorption energy distribution by the sum of a number of analytical functions, and the optimization of their parameters. Admittedly, the selected distributions are somewhat less arbitrarily chosen than those elected by Ross and Oliver [4], and by those following the same approach [21–25], but that still does not make the method realistic, since there are no reasons at this stage

to select any model for the adsorption energy distribution.

Algorithms selected for the calculation of the adsorption energy distribution

For further numerical calculations, we decided to select the Adamson and Ling [26] and the House and Jaycock [27] approaches, which make no arbitrary choices of either an isotherm model for the experimental isotherm or a distribution model for the adsorption energy distribution. We used slightly modified algorithms implementing the essential principles of the AL [26] and HILDA [27] original methods, and wrote computer programs to implement them. As the computers available to us are considerably more powerful than those available to these authors, numerical procedures can be more sophisticated and calculations pursued for orders of magnitude larger numbers of iterations. This contributes to considerable improvements in the quality of the results available and permits detailed comparisons between results of the two methods. Further, as there are isotherms for which an analytical solution does exist, we can design a quality benchmark for numerical solutions by calculating them in cases when the analytical solution exists and comparing both solutions.

In both algorithms, we assumed the local isotherm to be given by the Langmuir model (Eq. 2). This assumption is not a restriction; both programs could be used with any local isotherm model making physical sense. The Langmuir model is appropriate for a comparison between the results of various calculation methods.

Algorithm based on the AL method. This first algorithm is similar to the one designed by Roles and Guiochon [17], with the following differences:

- (i) The experimental isotherm is used directly, and not replaced by a model.
- (ii) We introduce q_s in Eq. 1, which provides the distribution $f(\epsilon)$, while they ignored it [17], with the result that this earlier algorithm gives $q_s f(\epsilon)$.
- (iii) Instead of using Eq. 1 directly in the

calculation [17], we replaced it by Eq. 22, as did Adamson and Ling [26]. The advantage is that the method requires only the use of the integral distribution, $F(\epsilon)$, in the calculation. As $F^k(\epsilon)$ is calculated from $F^{k-1}(\epsilon)$, there is no need to calculate $f(\epsilon)$, except once, at the very end of the program. In contrast, procedures using Eq. 1 require $f(\epsilon)$ to calculate q_{cal}^d at each iteration. This in turn requires the fitting of $F^{k-1}(\epsilon)$ with an Akima cubic spline [33], and differentiation of the spline. This change results into faster calculations and the possibility to carry out longer iterations.

(iv) As $F(\epsilon)$ must obviously be found within the interval 0–1, we introduce this condition in the program, by replacing systematically any negative value by 0, and any value larger than 1 by 1 at each iteration. This latter restriction has a profound positive influence on the shape of the adsorption energy distribution when the number of iterations is small or moderate and it hastens convergence (see Fig. 1).

(v) We found that a very large number of iterations has to be carried out. Some calculations reported below include up to 20 000 such iterations, whereas earlier results included no more than 200 [17]. The width of the energy distribution decreases slowly with increasing numbers of iterations (see below), especially when the energy distribution has sharp peaks. Hence the number of iterations needed for accurate results becomes very large when almost homogeneous surfaces are studied.

Algorithm based on the HILDA method. The algorithm developed includes only two modifications to the original HILDA algorithm:

- (i) Since, as mentioned in the previous section, $F(\epsilon)$ must be found within the interval 0–1, we included this restriction in this program also. At the end of each iteration, any negative value is replaced by 0, any value larger than 1 by 1.
- (ii) Since in any iteration, k , $F^k(\epsilon)_{j+1}$ must be larger than $F^k(\epsilon)_j$, for any data point j , the following statement is included in the program:

$$\begin{aligned} &\text{if } F^c(\epsilon)_{j+1} < F^c(\epsilon)_j \\ &\text{then } F^c(\epsilon)_{j+1} = F^c(\epsilon)_j \end{aligned} \quad (29)$$

instead of $F^c(\epsilon)_{j+1} = F^c(\epsilon)_j + 1 \cdot 10^{-6}$ as used by House and Jaycock [26]. The number $1 \cdot 10^{-6}$ is arbitrary. We found that when the number of iterations is small, the shape of the distribution changes somewhat with the value chosen for that small number, and we preferred to replace it by zero.

3. Results and discussion

We compared the adsorption energy distributions obtained with the two numerical solutions and the Sips analytical solution in the cases when the experimental isotherm is a Langmuir and a Misra isotherm.

3.1. The experimental isotherm is a Langmuir isotherm

In this case the analytical solution is a single impulse, or Dirac δ function at the energy $\epsilon = RT \ln(K/A)$. The comparison between this solution and the numerical solutions will be instructive regarding the ability of the program to handle discontinuities. Numerical solutions always include some dispersion of numerical origin, related to the computer need to round-up numbers, and programs experience great difficulties in accounting for discontinuities or impulses. To perform the comparison, we selected a value $A = 0.0013$ atm, and $K = 36\,450$ atm, which gives as solution an impulse at $\epsilon = 10.66$ kcal/mol.

Fig. 1 shows the results obtained with different algorithms, all run for the same number of iterations (2000). The vertical solid line gives the analytical solution. The dotted line is the numerical solution given by the HILDA method, while the dashed line results from the AL method. Note that both algorithms include the condition that $F(\epsilon)$ cannot exceed 1. The AL and HILDA solutions are almost exactly overlaid, and cannot be distinguished, except at the very top. Note that the energy range used for the figure is only 1 kcal/mol. Two other solutions are shown in Fig. 1, the solution given by the HILDA algorithm without the added restrictions regarding the value of $F(\epsilon)$ which cannot exceed

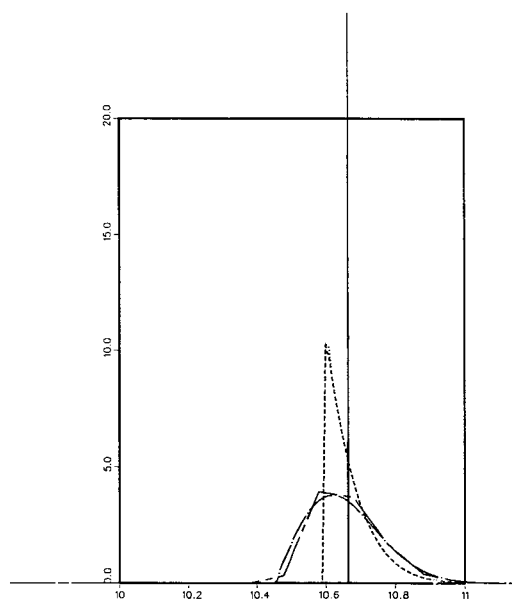


Fig. 1. Comparison of the analytical and several numerical solutions obtained for the adsorption energy distribution in the case when the experimental isotherm follows the Langmuir model. Abscissa, adsorption energy (kcal/mol). Ordinate, energy distribution (mol/kcal). Solid line, analytical solution, a δ -function at $\epsilon = RT \ln(K/A)$ (Eq. 13); dotted line, numerical solution calculated with our implementation of the HILDA algorithm [26]; dashed line, numerical solution calculated with our implementation of the Adamson and Ling [25] algorithm; dot-chain line (---), numerical solution calculated with the original HILDA algorithm [26], without the restriction added by us [if $F(\epsilon) > 1$, then $F(\epsilon) = 1.0$]; dashed-chain line (---), numerical solution calculated with the “quasi-Adamson” algorithm of Roles and Guiochon [16]. In all the numerical calculations, the number of iterations is equal to 2000.

1 (--- line), and the Roles–Guiochon algorithm (--- line). These last two lines are very close.

These results demonstrate the profound similarity between the AL [26] and HILDA [27] methods. They also show the significant improvement brought by our simple correction to these methods [If $F(\epsilon) < 0$, $F(\epsilon) = 0$; if $F(\epsilon) > 1$, $F(\epsilon) = 1$], resulting in a numerical solution which is much sharper on the low-energy side, and closer to the analytical solution, although still significantly different on the high-energy side. The results obtained with the quasi-Adamson method [17,31] are slightly different from those given by the AL method or the HILDA algo-

rithm, probably because in this calculation procedure $f(\epsilon)$ is calculated at each iteration step, by fitting the values of $F(\epsilon)$ to an Akima cubic spline and differentiating the spline. This procedure causes errors of numerical origin which remain significant as long as the number of iterations is not very large.

A further improvement could be made by increasing the number of iterations. We compare in Fig. 2 the analytical solution (solid line) and the numerical solution derived from the HILDA algorithm (dotted line) after 20 000 iterations.

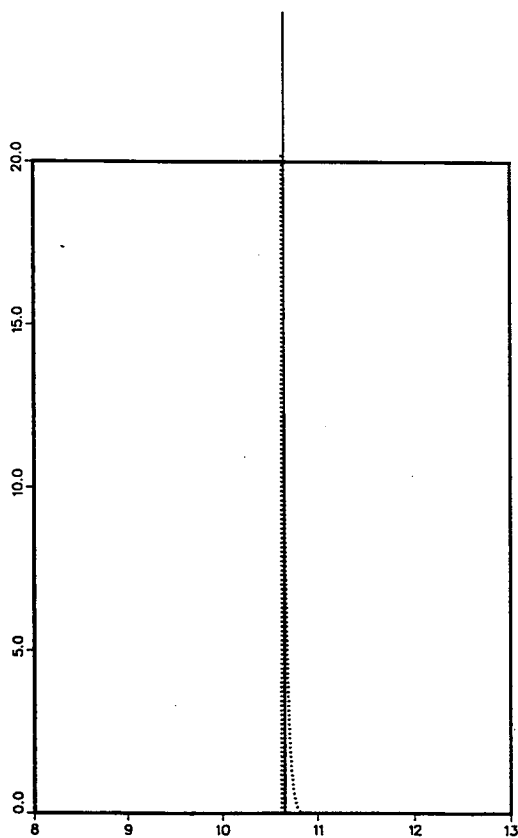


Fig. 2. Comparison of the analytical and numerical solutions obtained for the adsorption energy distribution in the case when the experimental isotherm follows the Langmuir model. Abscissa, adsorption energy (kcal/mol). Ordinate, energy distribution (mol/kcal). Solid line, adsorption energy distribution calculated from the analytical solution (Eq. 13); dotted line, adsorption energy distribution calculated with our implementation of the HILDA algorithm [26]. The number of iterations for this numerical solution is 20 000.

The numerical solution has become much narrower, and is now very close to the analytical solution.

Finally, in Fig. 3, we compare the analytical solution obtained for a bi-Langmuir isotherm (solid lines) and the numerical solution calculated with the HILDA algorithm, and 20 000 iterations (dotted line). For a multi-Langmuir isotherm, the solution is a series of impulses. The number of impulses is the number of terms in the isotherm model; their location is given by Eq. 13. The numerical solution has two narrow peaks. The numerical dispersion is more im-

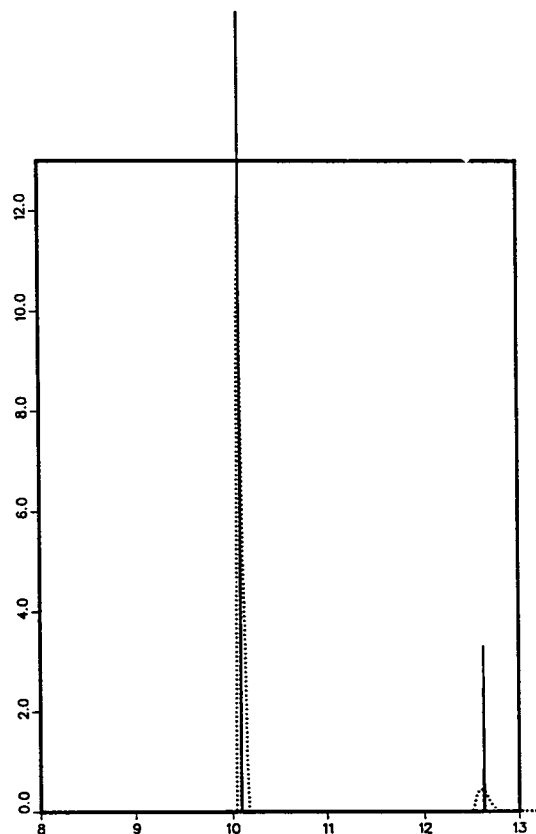


Fig. 3. Comparison of the analytical and numerical solutions obtained for the adsorption energy distribution in the case when the experimental isotherm follows a bi-Langmuir model. Abscissa, adsorption energy (kcal/mol). Ordinate, energy distribution (mol/kcal). Solid line, adsorption energy distribution obtained from the analytical solution (Eq. 13); dotted line, energy distribution calculated with our implementation of the HILDA algorithm [26]. The number of iterations is 20 000.

portant for the higher energy than for the lower energy impulse.

3.2. The experimental isotherm is a Misra isotherm

With the Misra isotherm [18] also, the adsorption energy distribution can be derived as an analytical solution to Eq. 1. This solution is a broad distribution which provides a different test of the validity of the numerical algorithms. The Misra isotherm is given by Eq. 16 and the corresponding adsorption energy distribution by Eq. 17. In the calculations, we assumed that $n = 5$, $\epsilon_0 = 1$ kcal/mol, and $K = 36\,450$ atm. Using the isotherm given by Eq. 16 as an experimental isotherm, we also calculated the adsorption energy distributions using the AL and the HILDA algorithm.

The adsorption energy distributions calculated with the AL and the HILDA algorithms are compared in Fig. 4. They are nearly identical. In Fig. 5, we compare these two distributions, represented by the solution of the HILDA algorithm (dotted line), and the analytical solution given by Eq. 17 (solid line). The two results are in very good agreement, in spite of a slight smoothing of the energy discontinuity at ϵ_0 which is replaced by a steep decay, and a rounding up of the energy maximum. This completes the demonstration that if the AL and HILDA algorithms are carried out with a sufficiently large number of iterations, they give an accurate solution of Eq. 1, and can provide the correct energy distribution, provided that the isotherm data made available to the programs contain all the required information, *i.e.*, cover a sufficiently broad range of partial pressures, and extend close enough to the saturation limit.

3.3. Required range of isotherm data

In principle, the isotherm data should be measured over a range of partial pressures that extends to the monolayer saturation. It is important to find out what error can be caused by the truncation of the isotherm data. In Fig. 6, we compare the numerical solution of Eq. 1 with the

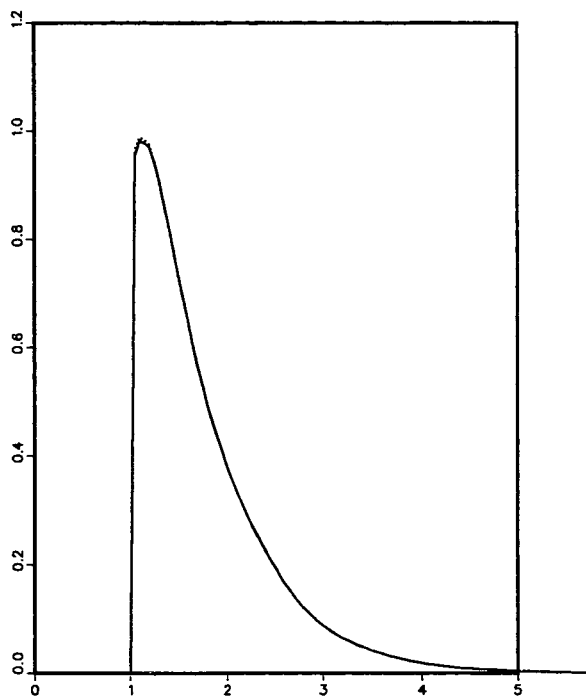


Fig. 4. Comparison of two numerical solutions obtained for the adsorption energy distribution in the case when the experimental isotherm follows a Misra model (Eq. 16). Abscissa, adsorption energy (kcal/mol). Ordinate, energy distribution (mol/kcal). Solid line, adsorption energy distribution calculated with our implementation of the algorithm based on the Adamson and Ling method [25]; dotted line, adsorption energy distribution calculated with our implementation of the HILDA algorithm [26]. The number of iterations in both calculations is 20 000. As expected, there is no difference between the two results.

“experimental” isotherm given by Eq. 16, in three different cases. In the first (solid line), the isotherm data used cover the whole isotherm range. This figure shows that the isotherm data should be acquired from pressures as low as that corresponding to $\epsilon_{\max} = 5$ kcal/mol, an up to pressures as high as that corresponding to $\epsilon_{\min} = 1$ kcal/mol. In order to investigate the consequences of a truncation of the isotherm data, we carried out two other calculations, using the same isotherm data, but truncated at either low or high pressures.

The energy distribution given by the dotted line was calculated with the same isotherm data, after truncation of the low-pressure isotherm data, the cut point corresponding to $\epsilon = 4$. The

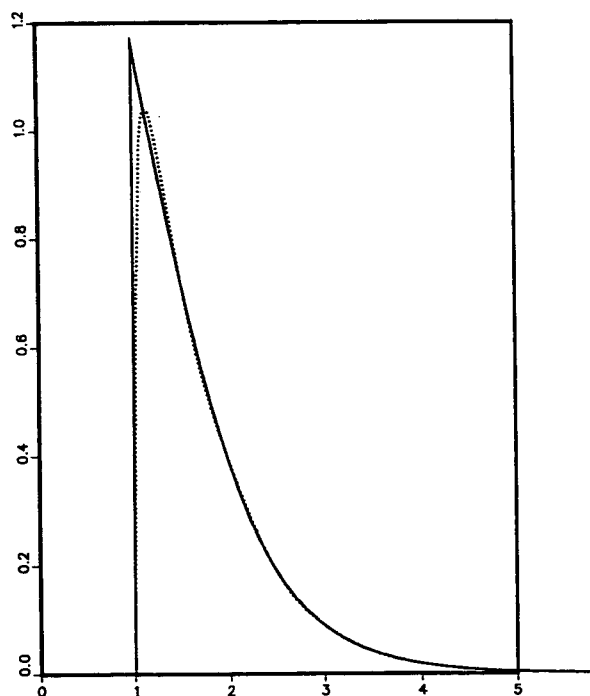


Fig. 5. Comparison of the analytical and numerical solutions obtained for the adsorption energy distribution in the case when the experimental isotherm follows a Misra model (Eq. 16). Abscissa, adsorption energy (kcal/mol). Ordinate, energy distribution (mol/kcal). Solid line, adsorption energy distribution calculated with the analytical solution (Eq. 17); dotted line, adsorption energy distribution calculated with our implementation of the HILDA algorithm [26]. The number of iterations is 20 000.

energy distribution obtained is nearly correct below $\epsilon = 3$, but in serious error above, and even making no sense for energies exceeding 4 kcal/mol. Missing the data corresponding to the high-energy sites has relatively little effect on the energy distribution for the low-energy sites. Conversely, the dashed line shows the energy distribution calculated using the same isotherm data, after truncation of the high-pressure part, corresponding to adsorption energies lower than $\epsilon_{\min} = 2$. The energy distribution obtained in this case is made of three sharp peaks, and could be mistaken for a distribution corresponding to a tri-Langmuir isotherm. It has nothing in common with the "true" energy distribution (solid line).

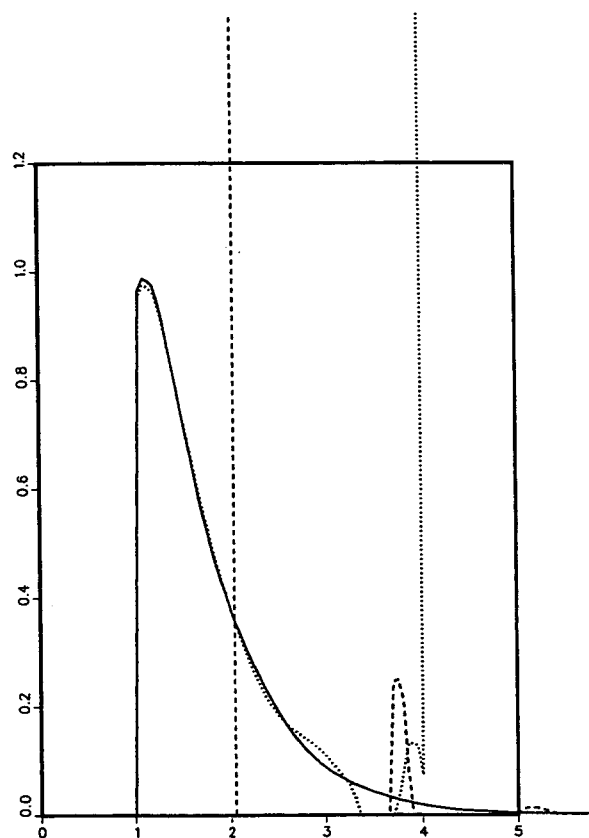


Fig. 6. Effect of the range of isotherm data acquired for the calculation of the adsorption energy distribution. Abscissa, adsorption energy (kcal/mol). Ordinate, energy distribution (mol/kcal). Comparison of numerical solutions obtained for the adsorption energy distribution in the case when the experimental isotherm follows a Misra model (Eq. 16). In this instance, the isotherm data used in the program include the whole range of partial pressures up to the saturation capacity. Dotted line, adsorption energy distribution calculated with isotherm data truncated at low pressures and complete at high pressures, so the data include all those corresponding to an adsorption energy lower than $\epsilon_{\max} = 4.0$ kcal/mol; dashed line, adsorption energy distribution calculated with isotherm data truncated at high pressures but complete at low pressures, so the isotherm data include those corresponding to an energy higher than $\epsilon_{\min} = 2$ kcal/mol.

These results show how important it is to acquire isotherm data up to very high values of the adsorbate partial pressure. The lack of measurements carried out in a sufficiently wide

partial pressure range results in erroneous adsorption energy distributions, and leads to incorrect conclusions.

4. Conclusions

The Sips method gives the only analytical solution that corresponds to a Langmuir model for the local isotherm, but it requires that we use one of the few isotherm models for which it can be solved to account for the experimental adsorption data and it cannot be applied directly to the experimental adsorption isotherm. For that, a numerical solution is necessary [1,2]. Such a solution does not require any model for the experimental isotherm data, but uses directly the experimental data, and has the further advantage of being able, at least in principle, to accommodate any local isotherm model.

The availability of an analytical solution in a non-trivial case, however, is extremely helpful as a benchmark for the numerical solutions. The implementation of these solutions requires a large number of iterations. Such calculations introduce numerical errors, usually in the form of dispersive contributions. The comparison between the energy distributions resulting from a numerical solution and from the corresponding analytical solution, when it exists, gives a useful performance index of the numerical procedure used. From this point of view, both the Adamson–Ling and the HILDA algorithms are satisfactory.

Finally, the computer simulation of an entire experiment performing the determination of the adsorption energy distribution on a surface with an assumed distribution permits the determination of the specifications regarding the experimental parameters selected and the study of the systematic errors introduced by experimental procedures (e.g., temperature or flow-rate). Both numerical methods studied here require the determination of isotherm data up to unrealistically high values of the partial pressure of the adsorbate.

5. Acknowledgements

This work was supported in part by Grant DE-FG05-88ER13859 of the US Department of Energy and by the cooperative agreement between the University of Tennessee and the Oak Ridge National Laboratory. We acknowledge support of our computational effort by the University of Tennessee Computing Center.

6. References

- [1] W. Rudzinski, D.H. Everett, *Adsorption of Gases on Heterogeneous Surfaces*, Academic Press, New York, 1992.
- [2] M. Jaroniec and R. Madley, *Physical Adsorption on Heterogeneous Solids*, Elsevier, Amsterdam, 1988, Ch. 2 and 3.
- [3] T.L. Hill, *J. Chem. Phys.*, 17 (1949) 762.
- [4] S. Ross and J.P. Oliver, *On Physical Adsorption*, Interscience, New York, 1964.
- [5] R.R. Zolandz and A.L. Myers, *Prog. Filtr. Sep. Sci.*, 1 (1979) 1.
- [6] L.M. Dormant and A.W. Adamson, *Surf. Sci.*, 62 (1977) 337.
- [7] W.A. House, *J. Colloid Interface Sci.*, 67 (1978) 166.
- [8] P.H. Merz, *J. Comput. Phys.*, 38 (1980) 64.
- [9] G.F. Miller, in J. Walsh and L.M. Delves (Editors), *Numerical Solutions of Integral Equations*, Clarendon Press, Oxford, 1974, Ch. 13, p. 175.
- [10] R. Sips, *J. Chem. Phys.*, 18 (1958) 1024.
- [11] J.P. Hobson, *Can. J. Phys.*, 43 (1965) 1934.
- [12] L.B. Harris, *Surf. Sci.*, 10 (1968) 129.
- [13] J.H. De Boer, *The Dynamic Character of Adsorption*, Clarendon Press, Oxford, 1953, Ch. IV.
- [14] L.M. Dormant and A.W. Adamson, *J. Colloid Interface Sci.*, 38 (1972) 285.
- [15] D.W. Widder, *The Laplace Transform*, Princeton University Press, Princeton, NJ, 1946, p. 340.
- [16] D. Graham, *J. Phys. Chem.*, 57 (1953) 665.
- [17] J. Roles and G. Guiochon, *J. Phys. Chem.*, 95 (1991) 4098.
- [18] D.N. Misra, *J. Chem. Phys.*, 52 (1970) 5499.
- [19] M.M. Dubinin and L.V. Radushkevich, *Dokl. Akad. Nauk SSSR*, 55 (1947) 331.
- [20] D.N. Misra, *J. Surf. Sci.*, 18 (1969) 367.
- [21] S.E. Hoory and J.M. Prausnitz, *Surf. Sci.*, 6 (1967) 337.
- [22] B. Kindel, R.A. Pachovsky, B.A. Spencer and B.W. Wojciechowski, *J. Chem. Soc., Faraday Trans. 1*, 69 (1973) 1162.
- [23] M. Jaroniec, X. Lu and R. Madey, *J. Phys. Chem.*, 94 (1990) 5917.

- [24] M.J. Sparnaay, *Surf. Sci.*, 9 (1968) 100
- [25] R.H. Van Dongen, *Surf Sci.*, 39 (1973) 341.
- [26] A.W. Adamson and I. Ling, *Adv. Chem. Ser.*, 33 (1961) 51.
- [27] W.A. House and M.J. Jaycock, *J. Colloid Polym. Sci.*, 256 (1978) 52.
- [28] S. Ross and I.D. Morrison, *Surf. Sci.*, 52 (1975) 103.
- [29] A.T. Hope, C.A. Leng and C.R.A. Catlow, *Proc. R. Soc. London, Ser. A*, 424 (1989) 57.
- [30] R.S. Sacher and I.D. Morrison, *Surf. Sci.*, 70 (1979) 153.
- [31] J. Roles, M. Kevin and G. Guiochon, *Anal. Chem.*, 64 (1992) 25.
- [32] J. Roles and G. Guiochon, *Anal. Chem.*, 64 (1992) 32.
- [33] H. Akima, *J. Am. Ceram. Soc.*, 17 (1970) 589.

Electrochromatography and micro high-performance liquid chromatography with 320 μm I.D. packed columns

Chao Yan[☆], Daniel Schauffelberger, Fritz Erni^{*}

Analytical Research and Development, Sandoz Pharma Ltd., CH-4002 Basle, Switzerland

(First received August 9th, 1993; revised manuscript received February 15th, 1994)

Abstract

Electrochromatography is a chromatographic method in which the mobile phase (liquid or supercritical fluid) is “pumped” through a stationary phase in a microbore or capillary column by electroosmosis using an electric field. The technique permits separation of charged and uncharged compounds with higher resolution and superior efficiency when compared with micro-HPLC with an identical column. It is desirable to work with packed capillary columns with wide diameter in electrochromatography in order to improve detectability and column loadability. This study shows that we have moved a step forward towards this goal in spite of problems and difficulties, due to Joule heating, frit making and column packing in using wide-diameter columns. The paper demonstrates that the pressure pump of micro-HPLC with a commercially available 320 μm I.D. column can be replaced by the electroosmotic “pump” of capillary zone electrophoresis. Experiments were carried out in a chromatographic system under both electroosmosis and pressure-driven flow with 320 and 50 μm I.D. columns packed with 3- and 5- μm ODS. The advantage of electrochromatography over conventional micro-HPLC is shown.

1. Introduction

Electrochromatography (EC) is a developing analytical technique in which the mobile phase fluid is driven through a stationary phase in a microbore or capillary column by electroosmosis using an electric field. Retention in EC is governed both by the electrophoretic mobility of the solutes and their partitioning between the stationary and mobile phases. Micellar electrokinetic capillary chromatography (MECC) with pseudostationary phase also depends on electroosmosis as the driving force and it has been

used successfully for separation and analysis [1]. However, we prefer to exclude MECC from EC since it may have its own definition.

Microbore and capillary column high-performance liquid chromatography (micro-HPLC) have undergone moderate development since the pioneering work of Scott and Kucera [2]. This technique provides good selectivity in a wide range of applications [3–6]. The mobile phase in micro-HPLC is driven through the column by applying high pressure and this induces laminar flow which causes a parabolic velocity profile of the mobile phase and thus reduces the plate number.

In contrast to micro-HPLC, capillary zone electrophoresis (CZE) [7] provides excellent efficiency in addition to its characteristics of

^{*} Corresponding author.

[☆] Present address: Department of Chemistry, Stanford University, Stanford, CA 94305-5080, USA.

relatively simple instrumentation. Although this powerful technique enjoys the reputation of high resolution and superior efficiency in separation of charged molecules, its power diminishes in case of uncharged molecules and charged molecules with identical electrophoretic mobility.

EC has the potential to serve as an ideal bridge connecting micro-HPLC and CZE and, therefore, to allow the combination of the high efficiency in CZE with the wide range of application and selectivity in micro-HPLC.

As early as in 1952, Mould and Synge [8] applied electroosmotic flow (EOF) in thin-layer chromatography for the separation of substances according to their molecular masses. Twelve years later, Pretorius *et al.* [9] demonstrated, with unretained solute, the improvement of efficiency by using electroosmosis in both thin-layer and column chromatographic systems. An electroosmotic pump for isotachopheresis was described by Ryšlavý *et al.* [10]. In 1981 [7], Jorgenson and Lukacs reported the results of the performance of electroosmotic pumping in a chromatographic system. Tsuda [11,12] separated compounds with similar capacity factors but different charges using combined pressure and voltage. A systematic study on EC with packed columns was reported by Knox and Grant [13]. Their results of higher plate efficiency in EC over HPLC are quite convincing. However, they pointed out that the big obstacle lies in the effect of Joule (self) heating which limits the useful column inner diameter to 75 μm . The possibility and limitation of applying electroosmosis in a capillary packed with reversed phase were also investigated by Yamamoto *et al.* [14] and others [15,16]. Packed capillary columns with 50, 75 and 100 μm I.D. were successfully used in EC.

One of the major challenges to the future development of EC, as in micro-HPLC and CZE, is the detector sensitivity. With the use of small-I.D. columns, the sensitivity of on-column detection is restricted by the limited optical path length although several approaches have been developed to overcome this obstacle. The main objective of this investigation is to explore the possibility and limitation of using wide-diameter columns, such as 320 μm I.D. columns which are routinely used in micro-HPLC, in order to ex-

tend the applicable range of EC by improving the detectability and column loadability.

In this article, we report the results of our investigations on EC with 320 μm I.D. columns packed with 3- μm ODS. In addition, a new concept of column arrangement with a 50 μm I.D. column packed with 3- μm ODS in EC will be described.

2. Experimental

2.1. Apparatus

The outline of the chromatographic system used for both EC and micro-HPLC in this study was described previously [14]. A schematic diagram is shown in Fig. 1. The stainless-steel six-port rotary valve including an injection port (Model 7010; Rheodyne, Cotati, CA, USA) serves as a injection manifold. A high-pressure pump (Model 100 solvent metering system; Altex, Berkeley, CA, USA) connected to the injection manifold for HPLC operation was also used for filling the column with mobile phase and eliminating gas bubbles from the column for EC. A carbon electrode connected to the power supply (Alpha MKII, Model 2907 P, 0–60 kV; Brandenberg, Surry, UK) was dipped into the anode chamber filled with mobile phase. The chamber was connected to the injection manifold by a stainless-steel tube. So, the high voltage was

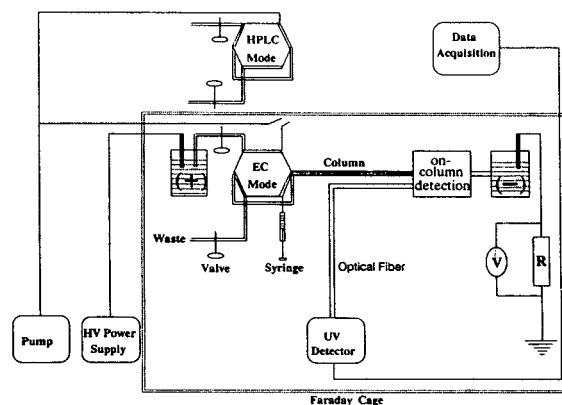


Fig. 1. A schematic diagram of the equipment used for both electrochromatography and micro-HPLC. HV = High-voltage.

applied to the stainless-steel six-port valve through the anode chamber (see Fig. 1). The outlet of the column was inserted into a capped cathode vial containing an electrode led to earth via an electrical resistor which was connected to an electrometer (168 Autorang DMM; Keithley Instruments, Cleveland, OH, USA) to measure the current. On-column detection was carried out with a modified UV detector (Model 783A; Applied Biosystems, Foster City, CA, USA) connected to a pair of optical fibres (about 60 cm long, 600 μm I.D., 1 mm O.D.; Laaber, Rüsselsheim, Germany). The equipment was partially housed within a Faraday cage which ensured the automatic disconnection of the high-voltage power supply whenever the cage was opened.

2.2. Columns

The 320 μm I.D. (450 μm O.D.) column packed with 5- μm Spherisorb ODS was obtained from LC Packings (Amsterdam, Netherlands). The original frit (a piece of PTFE filter) had to be removed after several runs because leaking was observed in the joint (glued) area between the column end and a piece of empty capillary. The new outlet frit was made as follows. First, a frit was sintered [14] at the end of a piece of empty capillary (ca. 15 cm \times 50 μm I.D. \times 280 μm O.D.) on which a detection window was created by burning off about 3 mm of the polyimide coating. The capillary with the sintered frit was then inserted into the 320 μm I.D. column and glued. The inlet frit was made in the same way but without detection window (see Fig. 2a).

The 50 μm I.D. (280 μm O.D.) column was packed with 3- μm Hypersil ODS (Shandon Southern Products, Runcorn, UK) similarly to the way described by Yamamoto *et al.* [14], but with the following simplification: the outlet of the packed column with a sintered frit was connected to a piece of empty capillary (on which a window was created) by means of a PTFE sleeve connector (250 μm I.D., LC Packings) (see Fig. 2b). In doing so, we were able to avoid the tedious and time-consuming procedure of packing and depacking the column with silica gel prior to packing with reversed phase [14].

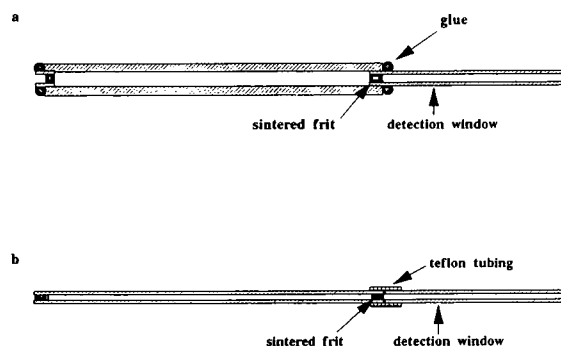


Fig. 2. Schematic presentation of the cross-section of the columns: (a) 320 μm I.D. packed column; (b) 50 μm I.D. packed column.

2.3. Chemicals

Sodium tetraborate, acetonitrile, thiourea, benzylalcohol, benzaldehyde, benzene and naphthalene were obtained from Merck (Darmstadt, Germany). The mobile phase was prepared by mixing 4 mM sodium tetraborate buffer (pH 9.1) with acetonitrile followed by filtration through a nylon-66 membrane (0.22 μm pore size) and by degassing (ultrasonic bath and helium).

2.4. Procedures

EC experiments were carried out as follows. First the column was connected to the injection manifold (set at HPLC mode, see Fig. 1) and flushed with pure buffer. The pump was switched off but not disconnected until the pressure reading dropped to zero. Then the above procedure was repeated, but this time using selected mobile phase instead of pure buffer. The column was then mounted as shown in Fig. 1. The outlet was inserted into the capped cathode chamber filled with mobile phase. After the pressure reading dropped to zero, the pump was disconnected and the injection manifold was switched to EC mode. Electrokinetic injection was carried out by filling the injection manifold with sample solution and then applying a low voltage (5 kV) across the column for about 5 s. The sample solution in the injection manifold was then thoroughly washed out with the mobile phase and the outlet valve

was closed. Finally, high voltage was applied and elution proceeded to start EC.

Micro-HPLC was carried out using the same chromatographic system with both hydrodynamic and electrokinetic injections. The hydrodynamic injection was carried out as follows. The injection manifold in the EC mode was filled with the sample solution. It was then switched to HPLC mode and low pressure (*ca.* 10 bar) was applied for *ca.* 3 s. The injection manifold was switched to the EC mode and flushed with mobile phase and the outlet valve was closed. The injection valve was switched back to HPLC mode and pressure was applied and elution proceeded.

The UV detector output was collected and analyzed by means of a chromatography laboratory automation system (CLAS; Perkin-Elmer, Norwalk, CT, USA). The experimental system was not thermostated or cooled except (when the ventilation system was off) a fan was used to blow air onto the column to encourage heat dissipation. Sample concentration of test mixture was estimated to be in the range of 0.5 to 1.0 mg/ml.

3. Results and discussion

3.1. EC with 320 μm I.D. column

Fig. 3 shows the EC separation of a test mixture of four neutral compounds on a commercially available 490 mm \times 320 μm column packed with 5- μm Spherisorb ODS. The elution was carried out with acetonitrile–4 mM sodium tetraborate buffer (pH 9.1) (90:10, v/v) at an applied voltage of 50 kV. Taking thiourea as an “unretained” solute marker, an electroosmotic velocity of 0.35 mm/s was calculated. Reduced plate heights were 3.1 for thiourea and 3.2 for benzaldehyde. In another experiment, using a mobile phase with 80% organic modifier, the influence of applied voltage on column efficiency was studied. EC parameters for benzaldehyde are listed in Table 1. Note that the plate height decreases with increasing applied voltage, indicating that a better column efficiency is attain-

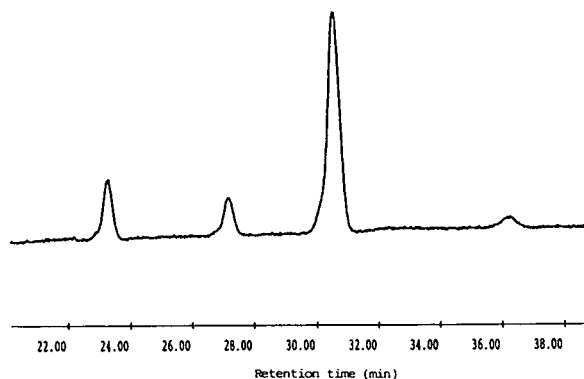


Fig. 3. Electrochromatographic separation of test mixture with 490 mm \times 320 μm I.D. column packed with 5- μm Spherisorb ODS. Mobile phase: CH_3CN –4 mM sodium tetraborate (pH 9.1) (90:10, v/v). Solutes in order of elution: thiourea, benzylalcohol, benzaldehyde, benzene.

able at even higher voltage (higher electroosmotic velocity). However, plots of applied voltage vs. measured current (Fig. 4) indicate, at least for 80% acetonitrile, a non-linear relationship, suggesting that Joule heating occurs within the column. In fact, attempts to increase the EOF in this particular column by applying higher voltages (56 kV) did not succeed because of the formation of bubbles inside the column.

In addition, the original frit of the 490 mm \times 320 μm I.D. column did not withstand repeated operation and we therefore shortened the column and inserted, at both ends, empty 50 μm I.D. capillaries, carrying each a sintered frit (see Fig. 2a). The following experiments were all carried out with columns modified in this way.

A plot of EOF vs. applied voltage (V) and

Table 1
Electrochromatographic parameters for benzaldehyde on the 490 mm \times 320 μm I.D. packed column

V (kV)	t_R (min)	N	H (μm)	h
30	54	20 000	25	5.0
35	41	26 000	19	3.8
40	36	35 000	14	2.8
45	32	41 000	12	2.4
50	29	46 000	11	2.2

Mobile phase: CH_3CN –4 mM sodium tetraborate (pH 9.1) (80:20, v/v).

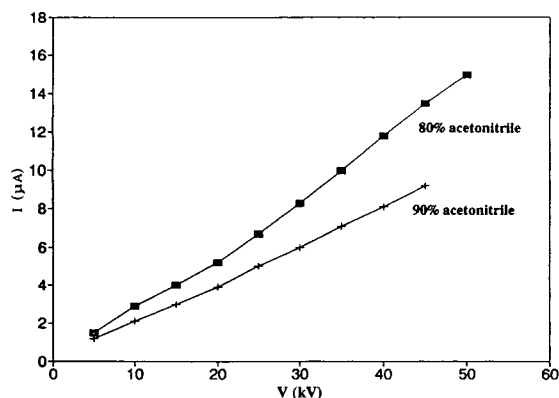


Fig. 4. Ohm's law plots for the 490 mm \times 320 μ m column.

current (I) from data obtained with a 250 mm \times 320 μ m I.D. column is shown in Fig. 5. The relationship between EOF and I is linear, as commonly observed in CZE [7] and MECC [17], and suggests that there was no significant effect of Joule heating in the column under these experimental conditions. However, this could be misleading since we were working in a relatively narrow range of voltage (see also Fig. 4).

By applying 40 kV voltage across the column, we were able to generate a EOF of 0.43 mm/s, which was still lower than one would like to have. The dependence of linear velocity on the concentration of organic modifier in the mobile phase is shown in Fig. 6. Results indicate that, at

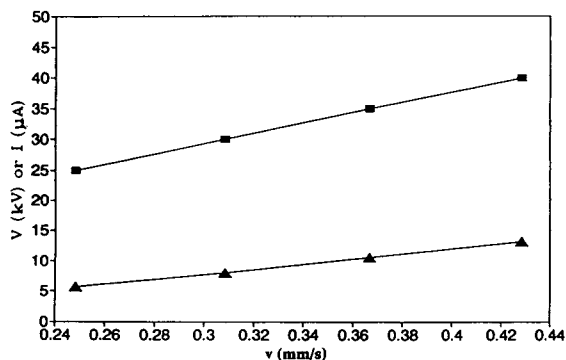


Fig. 5. Dependence of electroosmotic velocity (v) on applied voltage (V , \square) and current (I , \blacktriangle) for 250 mm \times 320 μ m I.D. column packed with 5- μ m Spherisorb ODS. Mobile phase: CH₃CN–4 mM sodium tetraborate (pH 9.1) (80:20, v/v). Thiourea was used as unretained solute marker.

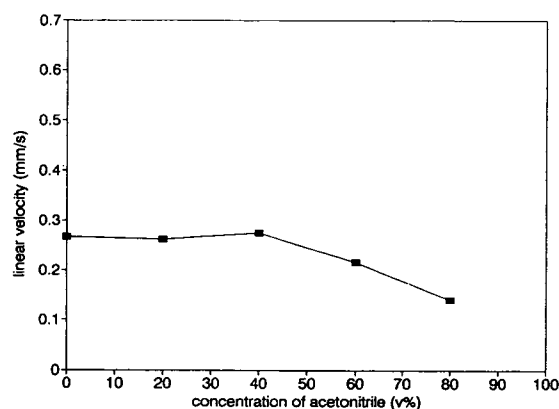


Fig. 6. Effect of organic modifier (CH₃CN) on electroosmotic velocity for 150 mm \times 320 μ m I.D. packed column at constant voltage of 25 kV.

concentrations of organic modifier higher than 40%, the EOF significantly decreases.

In order to compare the performance of EC with that of micro-HPLC, separations were carried out on the same column with both electroosmosis- and pressure-driven flow under otherwise the same conditions. Fig. 7 shows the plots of reduced plate height vs. linear velocities (Van Deemter plot) generated with both electroosmosis- and pressure-driven flow. The direct comparison shows that, in the range of 0.2 to 0.5 mm/s linear velocity, EC is more efficient than micro-HPLC. Higher velocities could not be achieved by EOF (see above) but one would

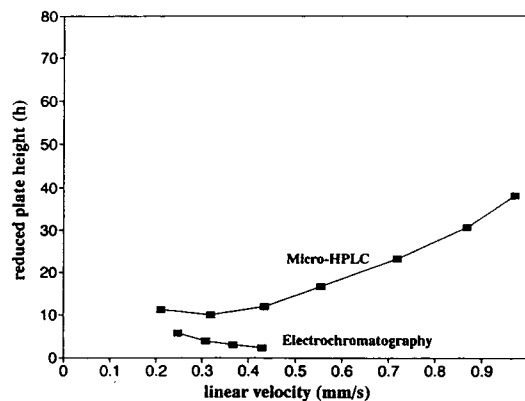


Fig. 7. Dependence of reduced plate height on mobile phase velocity obtained from both electroosmosis- and pressure-driven flow. Conditions as in Fig. 5.

predict that the efficiency might even be improved with flows higher than those achieved under the present experimental conditions. Micro-HPLC, on the other hand, is characterized by a decrease in efficiency at higher linear velocities.

The higher efficiency of EC is convincingly demonstrated in Fig. 8 showing the expanded peaks for thiourea on the same column using, respectively, electroosmosis-driven and pressure-driven flow under otherwise identical conditions.

3.2. EC with 50 μm I.D. column

At the current state of the development of EC, the best results are obtained with 50 μm I.D. capillaries. Similar to the concept introduced recently by Van Soest *et al.* [15], we used a new method for column arrangement: a packed capillary column with sintered frits at both ends was connected to a piece of empty capillary carrying a window for on-column detection. The connection was made by a PTFE sleeve with an inner diameter barely smaller than the outer diameter of the capillary. A schematic drawing of this two-stage column is given in Fig. 2b. Note that, instead of using a piece of filter as an outlet frit [15], we sintered the frit by gentle heating of the column end (*ca.* 2 mm) filled with 4- μm silica

wetted with sodium silicate solution [14]. With the sintered frit we were able to make a firm and direct column–capillary connection (without using any filter in between). In our experience, this arrangement significantly reduces the chance of bubble formation in the joint area. Following this design, we packed a 230 mm \times 50 μm I.D. column with 3- μm Hypersil ODS and used it for the separations of a test mixture in both EC and micro-HPLC. For comparison purposes, the applied voltage in EC was adjusted to yield the same linear flow (0.8 mm/s) as obtained with micro-HPLC. The chromatograms from the two non-optimized separations are shown in Fig. 9 and prove that the efficiency of electroosmosis-driven chromatography is higher than the efficiency of pressure-driven chromatography. The columns of the type described in Fig. 2b are particularly convenient and their preparation is less time-consuming compared with the previously used method with the outlet frit located several centimetres from the end of the capillary [14]. Another advantage of the column arrangement is that the empty capillary carrying the detection window can be retained so that there is no need to replace it if a new packed column is mounted.

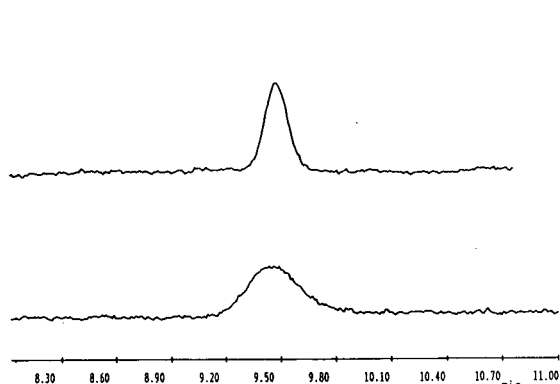


Fig. 8. Comparison of peak broadening between EC (upper; $h = 4.4$, applied voltage 40 kV) and HPLC (lower; $h = 19.1$, pressure 20 bar) on a 250 mm \times 320 μm I.D. packed column. Conditions as in Fig. 5 except for applied voltage and pressure.

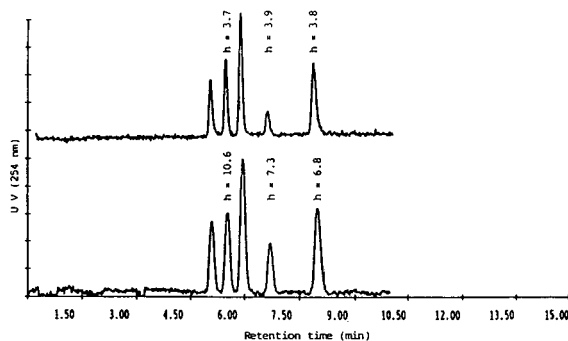


Fig. 9. Electrochromatographic separation of test mixture on a 230 mm \times 50 μm I.D. column packed with 3- μm Hypersil ODS. Mobile phase: CH_3CN –4 mM sodium tetraborate (pH 9.1) (80:20, v/v). Solutes in the order of elution: thiourea, benzylalcohol, benzaldehyde, benzene, naphthalene. (Top) EC, applied voltage 23 kV; (bottom) micro-HPLC, pressure 130 bar.

3.3. Major problems and difficulties in EC

Joule heating

Although it is believed that EC is indeed a promising separation technique, there are practical problems and difficulties, especially when wide-diameter columns are used. The major obstacle is Joule heating [13,18]. Joule heating of an EC system results in a temperature gradient in the column which consequently causes band broadening. What makes things worse is that the temperature increase in the packed column, where the particles and frits act as “boiling chips”, can assist in the formation of bubbles which generate baseline noises and dried-out sections in the column and eventually break the current and thus stop the EOF. Shown in Fig. 4 are Ohm's law plots for the 490 mm × 320 μm I.D. column packed with 5-μm Spherisorb ODS, where the Joule heating is clearly indicated by the deviations of the plots from linearity. According to Knox and Grant [18] and Poppe and co-workers [19,20], the temperature difference between the centre of a cylinder and its wall is given by

$$\Delta T = \frac{Qd^2}{16K} = \frac{EI}{4\pi K} \quad (1)$$

where Q is the rate of heat generation per unit volume within the cylinder, d is the column diameter, K is the thermal conductivity of the medium, E is the field strength and I is the current. The self heating is much greater in a wider-bore column since it is proportional to the square of the column diameter.

While the theoretical calculations led to the speculations that the use of a packed capillary column in EC may be limited to columns with I.D. < 100 μm, this experimental investigation shows that 320 μm I.D. columns can be used in EC in practice. This is probably due to the following reasons. (a) The amount of heat generated in EC with a packed column, as compared to CZE with an empty tube with the same diameter, is severely reduced because of the relatively low electric current (0–20 μA, see Fig.

4) due to the high resistance of the mobile phase (e.g., with 80% acetonitrile) plus the packing material. (b) The Joule heating effect on peak dispersion in EC is mainly caused by the changes of partition of the solutes (usually neutral) due to the temperature gradient in the column, in contrast to CZE where, in addition to the migration changes caused by the parabolic flow profile of the mobile phase due to the temperature gradient, the electrophoretic mobility of the solutes (usually charged) depends on the mobile phase viscosity. (c) The parabolic flow profile generated by the self-heating may be counterbalanced to some extent by the opposite parabolic profile caused by the relatively lower EOF in the centre of the column due to the partial coverage of the silica surface of the packing particles (ODS). To summarize, the influence of inhomogeneity of temperature on peak broadening due to Joule heating is much less in EC than in CZE.

Nevertheless, the formation of bubbles in the column is still a major problem in EC performance. Therefore, thorough degassing of the mobile phase is extremely important and efficient cooling system for further development of EC with wide-diameter columns may be necessary.

Frit

Frit is the key to the success of using electro-osmotic pumping in a chromatographic system. If fluorescence detector (on-column detection) is used, a window can be created within the packed section of the column [13] and this makes the outlet frit-making easier and also preserves the integrity of the migrating zone of the solutes. This sensitive device, however, is limited to detect only fluorescent solutes and there are many cases where other type of detector are desirable. The more commonly utilized UV detector requires a window created on a piece of empty capillary after the frit. While sintering a frit on a narrow-diameter column has been done without problems [7,13,14, and this paper], it becomes increasingly difficult when dealing with columns with wider diameter (say, 320 μm or up). Therefore, some sort of arrangement has to

be made (see, e.g., Fig. 2) to construct a frit and create a window. A good frit should possess at least the following characteristics: (a) it must be sufficiently mechanically strong to stand high pressure in the process of column packing; (b) it should be sufficiently chemically inert to bear the environment formed by the organic modifier and running buffer with certain range of pH value; (c) it must be sufficiently porous to allow the mobile phase and the solutes pass through (without significant back pressure) but, at the same time, not too porous to prevent the stationary phase bleeding; (d) it should not introduce significant dead volume to cause extra peak broadening.

Column packing

Column packing is crucial for the improvement of the performance of EC, as well as for the future commercialization of this technique. Knox and Grant [18] have predicted theoretically and proven experimentally [13] that the EOF is essentially unaffected by particle size at least down to 1.5 μm . As the particle size is reduced below 1 μm the plate height will be dominated by the B term (axial diffusion) in the Van Deemter equation ($H = A + B/u + Cu$). Should this theoretical prediction be substantiated, an efficiency of a million theoretical plates in less than 30 min could be achievable in EC. However, to pack such a column efficiently with fine particles will be a real challenge since, conventionally, extremely high pressure is required. Especially when coming to wide-diameter columns, application of such high pressure could be disastrous. Therefore, alternative ways have to be found out to pack micron and submicron particles in stable and uniform beds in order to take the full advantages of EC. Further investigation in this direction is underway.

4. Conclusions

EC is an unique separation technique which combines the high efficiency of CZE and the good selectivity of micro-HPLC. It can be used

to separate both neutral and ionized molecules because retention is governed by the electrophoretic mobility of the solutes, as in CZE, as well as by their partitioning equilibrium, as in HPLC. The use of commercially available 320 μm I.D. packed columns in EC has been demonstrated and the advantages of EC compared to micro-HPLC are obvious. It is anticipated that even wider-bore columns could be used and that this would further improve the detectability and column loadability.

The new arrangement for EC proposed by Van Soest *et al.* [15] represents an important step towards a wider use of EC and together with the method presented here, further emphasizes its potential. As a matter of fact, packed columns with narrow diameter (such as 50 μm I.D.) might be routinely used in commercially available CZE instruments. Further investigation in this direction is already in progress.

5. References

- [1] J. Vindevogel and P. Sandra, *Introduction to Micellar Electrokinetic Chromatography*, Hüthig, Heidelberg, 1992.
- [2] R.P.W. Scott and P. Kucera, *J. Chromatogr.*, 125 (1976) 251.
- [3] D. Ishii and T. Takeuchi, in M. Novotny and D. Ishii (Editors), *Microcolumn Separations*, Elsevier, Amsterdam, Oxford, New York, Tokyo, 1985, pp. 3–17.
- [4] R.T. Kennedy and J.W. Jorgenson, *Anal. Chem.*, 61 (1989) 436.
- [5] K.E. Karlsson and M. Novotny, *Anal. Chem.*, 60 (1988) 1662.
- [6] T. Tsuda, I. Tanaka and G. Nakagawa, *Anal. Chem.*, 56 (1984) 1249.
- [7] J.W. Jorgenson and K.D. Lukacs, *J. Chromatogr.*, 218 (1981) 209.
- [8] D.L. Mould and R.L.M. Synge, *Analyst (London)*, 77 (1952) 964.
- [9] V. Pretorius, B.J. Hopkins and J.D. Schieke, *J. Chromatogr.*, 99 (1974) 23.
- [10] Z. Ryšlavý, P. Boček, M. Deml and J. Janák, *J. Chromatogr.*, 147 (1978) 446.
- [11] T. Tsuda, *Anal. Chem.*, 59 (1987) 521.
- [12] T. Tsuda, *LC·GC*, 5, No.9 (1992) 26.
- [13] J.H. Knox and I.H. Grant, *Chromatographia*, 32 (1991) 317.
- [14] H. Yamamoto, J. Baumann and F. Erni, *J. Chromatogr.*, 593 (1992) 313.

- [15] R.E.J. van Soest, J.P. Chervet, M. Ursem and J.P. Salzmänn, presented at the *4th International Symposium on High Performance Capillary Electrophoresis, Amsterdam, February 9–13, 1992*, poster.
- [16] T. Eimer, B. Eray and K.K. Unger, presented at the *4th International Symposium on High Performance Capillary Electrophoresis, Amsterdam, February 9–13, 1992*, poster.
- [17] S. Terabe, K. Otsuka and T. Ando, *Anal. Chem.*, 57 (1985) 834.
- [18] J.H. Knox and I.H. Grant, *Chromatographia*, 24 (1987) 135.
- [19] H. Poppe and J.C. Kraak, *J. Chromatogr.*, 282 (1983) 399.
- [20] H. Poppe, J.C. Kraak, J.F.K. Huber and J.H.M. van den Berg, *Chromatographia*, 9 (1981) 515.

Preparation and evaluation of polyacrylate-coated fused-silica capillaries for reversed-phase open-tubular liquid chromatography

Remco Swart, Johan C. Kraak*, Hans Poppe

Laboratory for Analytical Chemistry, University of Amsterdam, Nieuwe Achtergracht 166, 1018 WV Amsterdam, Netherlands

(First received November 30th, 1993; revised manuscript received January 26th, 1994)

Abstract

By *in situ* photopolymerization of acrylates, thick polyacrylate films can be immobilized in 10- μm fused-silica capillaries. Up to 1.9- μm thick films can be produced in 0.3–1.2 m long capillaries, resulting in phase ratios >1.0 and leading to columns with high mass loadability. Owing to the high mass loadability, application of “on-column” UV detection is possible. The effect of incorporating alkyl acrylates in the film on retention behaviour and efficiency was extensively investigated. The success rate of the preparation of silicone–ethylhexyl acrylate films is almost 100%. The polyacrylate films are stable towards basic solutions up to pH 12. The column efficiency is demonstrated with separations of anthracene derivatives. A fast separation of methyl-substituted benzenes with on-column UV detection is shown.

1. Introduction

Chromatographic theory predicts that liquid chromatography can be performed best in tubes in order to produce large plate numbers in an acceptable time, owing to the favourable flow resistance [1]. However, to compete with liquid chromatography in packed columns in that respect, the internal diameter of the tubes must be about the same as the particle size as commonly used in HPLC or preferably smaller (*e.g.*, $<5\ \mu\text{m}$) [1]. This means that the separation system in addition to the detection and injection system has to be miniaturized. Moreover, a uniform retentive layer with sufficient sample capacity has to be immobilized on the inside wall of the

capillary. This last aspect is of paramount importance for two reasons: first for avoiding a decrease in efficiency due to overloading and second for allowing larger injected solute amounts, simplifying detection. Several research groups have recognized this bottleneck in the exploration of open-tubular LC (OT-LC) and have therefore put large efforts into the immobilization of retentive layers in glass and fused-silica capillaries. Efforts have so far been focused on two approaches: the realization of a porous silica layer that can be chemically modified [2–4] and the immobilization of polymeric phases such as cross-linked silicones [5] and acrylates [6,7]. Although some interesting results have been reported with porous silica layers, the retentivity and sample capacity of these layers are still small; as a result, these columns can only

* Corresponding author.

be used satisfactorily in combination with an extremely sensitive detection technique such as laser-induced fluorescence. More promising are the polymeric phases because thick layers with good sample capacity can be immobilized. A drawback of these polymeric phases is the poorer column efficiency due to small diffusion coefficients of solutes in these retentive layers [5,6].

In this paper, we report the results of an investigation to immobilize thick polyacrylate films in 10 μm I.D. fused-silica capillaries for reversed-phase OT-LC. The study involved the effect of the type of incorporated alkyl chain on the retentive properties, column efficiency, sample capacity and stability of the columns. The favourable properties of thick polyacrylate films for OT-LC is demonstrated with test solutes using laser-induced fluorescence (LIF) and UV detection.

2. Experimental

2.1. Materials

The applied fused-silica capillaries with an acrylate outside protective coating were a kind gift from Philips Research Labs. (Eindhoven, Netherlands). The outside acrylate coating possesses sufficient UV transparency for *in situ* photopolymerization.

HPLC-grade acetone, methanol and acetonitrile were obtained from Janssen (Beerse, Belgium) and 3-(methacryloxy)propyltrimethoxysilane (γ -MPS), butyl acrylate (BA) and ethylhexyl acrylate (EHA) from Fluka (Buchs, Switzerland). Silicone acrylate (SiA) (Tegomer V-Si2150) was a kind gift from Goldsmidt (Essen, Germany). Lauryl acrylate (LA) was purchased from Merck (Darmstadt, Germany).

α,α -Dimethoxy- α -phenylacetophenone (DM-PA) (Irgacure 651; Ciba-Geigy, Basle, Switzerland) was used to initiate the polymerization reaction. The capillaries were tested with various anthracene derivatives from Janssen. Solutions of these compounds were prepared in methanol.

2.2. Apparatus

The experimental set-up of the OT-LC system has been described previously [7]. The mobile phase delivery system consists of a solvent reservoir, which can be pressurized by means of helium. Injections were made with a laboratory-made splitting device connected to a 0.2- μl injection valve (Model 7525; Rheodyne, Cotati, CA, USA). On-column detection was performed by either fluorescence or UV absorption. A helium-cadmium laser, $\lambda_{\text{ex}} = 325 \text{ nm}$ (Model 356XM; Omnichrome, Chino, CA, USA) was used as a light source for fluorescence detection; the emission wavelength was set at 380 nm. The fluorescence yield was measured with a photomultiplier tube (Type 6225 S; EMI, Hayes, UK).

UV detection was performed with a Model 757 UV detector, Applied Biosystems, Foster City, CA, USA) adapted for on-column detection using a laboratory-made capillary cell with an adjustable aperture [8].

The reservoir for filling the capillaries with coating solutions has been described previously [9]. The silylation reaction and curing of the capillaries were carried out at elevated temperatures in an oven. Irradiation was effected with a UV lamp (Philips, TLD 40W/90N, $L = 120 \text{ cm}$). The light intensity during the polymerization experiments was measured with a laboratory-built UV curing radiometer.

Solvent evaporation from the capillaries was performed with a vacuum pump combined with a thermostated water-bath. Kinematic viscosities of the mobile phase were measured in a water-bath (Model 45; Tamson, Zoetermeer, Netherlands) with a viscometer (Tamson Model, 88233). The densities of the mobile phases, needed to calculate dynamic viscosities, were measured with a digital density meter. Pressures were determined with a digital pressure sensor.

2.3. Column preparation

All solutions were filtered through a 0.45- μm filter (Type HV; Millipore, Yonezawa, Japan) prior to use.

The preparation of the polyacrylate-coated capillaries consisted of four consecutive steps: etching of the bare silica capillary, silylation of the etched surface, *in situ* photopolymerization of acrylates and evaporation of the solvent.

Etching

A 1 mol/l NaOH solution was pumped through the capillary for 3 h at a pressure of 15 bar. The capillary was then flushed consecutively with distilled water for 1 h, 0.03 mol/l HCl for 1 h and distilled water for 1 h. Next the capillaries were dried overnight at 120°C under a stream of helium.

Silylation

The etched capillaries were silylated by pumping through a 5% (v/v) solution of γ -MPS in dried toluene at 120°C for 1 h at 15 bar. The capillary was then flushed successively with toluene for 0.5 h and helium for 4 h at ambient temperature.

Photopolymerization

The coating solutions were always prepared just before use by adding the silicone acrylate, alkyl acrylate and photoinitiator (DMPA) to the solvent and vibrationally mixing the solution. The capillary was then filled with this solution and sealed at both ends with grease to fix the solution during the irradiation step. The irradiation of the capillary was carried out by pulling the capillary through a quartz tube along the UV lamp at a constant velocity. By this means, each part of the capillary was exposed to the same curing dose. The light intensity was varied by changing the distance between the lamp and the quartz tube through which the capillary was pulled. The exposure time was set by adjusting the velocity at which the capillary was pulled over the lamp. The curing conditions and capillary dimensions are given in Table 1.

Evaporation

After the irradiation, the seal at one of the ends of the capillary was removed and this side was connected to a vacuum pump by means of a

Swagelok fitting with a PTFE ferrule. In order to remove the solvent and possible non-reacted monomers, the capillary was placed in a water-bath and vacuum applied. Then the temperature was raised slowly (in 5–10 min) from ambient to 30°C. The removal of the solvent from the capillary and the acrylate film obtained were checked under a microscope. The capillary was then thermally cured at 120°C for at least 12 h. Finally, the capillary was equilibrated with the mobile phase for 30 min.

2.4. Inner diameter and film thickness

The average inner diameter of the capillaries was measured by a hydrodynamic method, based on a rearrangement of the Poiseuille relationship:

$$r = \sqrt{\frac{8u\eta L}{\Delta p}}$$

where u is the mobile phase velocity, p is the pressure drop, r is the capillary radius, η is the viscosity of the mobile phase and L is the total length of the capillary.

By measuring the linear velocity of the mobile phase via a non-retarded solute (salicylate) at a given pressure, the diameter of the capillary can be calculated provided that the viscosity of the mobile phase is known. In order to verify that salicylate is unretained in coated capillaries, several other compounds such as trihydroxybenzoic acid, anthranilic acid and several ions (chromate and nitrite) were tested for their retention. Salicylate elutes together with trihydroxybenzoic acid, earlier than any of the other compounds.

The viscosity of the mobile phase was measured at various temperatures between 19.0 and 22.5°C. At least five measurements were carried out over a wide pressure range. The R.S.D. of the determination of the column diameter ranged between 0.1 and 0.5%. The polymer layer thickness was calculated by subtracting the column radius before and after the coating procedure.

Table 1
Experimental coating conditions for the prepared fused-silica columns

Capillary No.	<i>L</i> (cm)	Monomer (% v/v) (DMPA) ^a	Solvent ^b	Intensity (mW)	Time (s)	<i>d</i> _c ^c (μm)	<i>d</i> _t ^d (μm)	<i>V</i> _s / <i>V</i> _m
1	36.8	30% SiA	A/P	0.13	214	8.50	1.44	0.80
2	88.0	25% SiA	A/P	0.13	302	8.34	1.52	0.86
3	59.3	2.6% LA–30% SiA	A	0.14	400	8.50	1.44	0.79
4	93.0	2.6% LA–30% SiA	A	0.19	480	8.22	1.42	0.81
5	52.2	2.6% LA–30% SiA	A	0.15	522	8.14	1.46	0.85
6	34.1	2.6% LA–30% SiA	A	0.19	390	8.24	1.57	0.91
7	61.2	2.6% LA–30% SiA	A	0.14	285	7.58	1.90	1.25
8	63.0	15% BA–15% SiA	A	0.15	355	8.24	1.43	0.81
9	43.0	15% BA–15% SiA	A	0.15	420	8.02	1.68	1.01
10	52.1	15% BA–15% SiA	A	0.15	458	8.02	1.69	1.01
11	25.2	15% BA–15% SiA	A/P	0.15	304	7.72	1.70	1.07
12	74.5	7.5% EHA–7.5% SiA	A/P	0.13	700	10.44	0.51	0.20
13	79.6	10% EHA–10% SiA	A/P	0.14	345	9.66	0.86	0.39
14	77.1	12.5% EHA–12.5% SiA	A/P	0.13	350	9.72	0.87	0.39
15	115.1	15% EHA–15% SiA	A/P	0.14	385	8.88	1.27	0.65
16	81.3	15% EHA–15% SiA	A/P	0.14	385	8.64	1.39	0.75
17	121.0	15% EHA–15% SiA	A/P	0.15	390	8.32	1.39	0.78
18	56.4	15% EHA–15% SiA	A	0.14	390	8.20	1.43	0.82

^a DMPA concentration: 3.0 mg/ml for all solutions.

^b A = Acetone; P = pentane.

^c *d*_c = Diameter of the column after coating.

^d *d*_t = Thickness of acrylate film.

2.5. Chromatography

The chromatographic properties of the coated capillaries were measured using an OT-LC system, as described by Ruan *et al.* [7]. Pure methanol, acetonitrile or aqueous mixtures were used as mobile phases. Detection was carried out either by “on-column” UV detection using a cell with an adjustable slit width or by LIF. For both detection techniques it was necessary to remove the outside coating of the capillary for increased sensitivity. This was done by immersing the detection side of the capillary in methanol and stripping off the protective layer mechanically. All test solutions were prepared in pure methanol.

Experimental plate heights of test solutes were calculated according to $H = L\sigma^2/t_r^2$, where *L* is the column length and σ is the peak half-width at 0.61 of the peak height. Asymmetry of the peaks was measured at 10% of the peak height according to Snyder and Kirkland [10].

The column efficiency was evaluated by comparing the experimental and theoretical plate heights *versus* the linear velocity of the mobile phase. Theoretical values of the plate heights were calculated with the Golay equation.

3. Results and discussion

3.1. Preparation of polyacrylate films

Of the four main steps in the preparation of polyacrylate layers, the photopolymerization and evaporation of the solvent appear to be the critical steps for obtaining uniform films. During these steps serious problems can occur when no precautions are taken to control the experimental conditions carefully.

Photopolymerization

The reaction rate of the polymerization is affected by many variables, *e.g.*, monomer con-

centration, photoinitiator concentration, type of solvent and UV intensity. With given values for these parameters, the exposure time is in principle the sole parameter controlling the conversion and consequently the extent of cross-linking. In order to terminate the polymerization it is therefore not only necessary to stop the irradiation but also to shield the capillary from other light sources by which radicals can be formed. The necessity of shielding the capillary from light after the photopolymerization up to the complete removal of the solvent was experienced when evaporation of the solvent was carried out in daylight. It appears that in the first part of the capillary a regular film is obtained but when the evaporation proceeds a more wavy film arises. The formation of a wavy film is attributed to stress in the gel which occurs at higher percentages of cross-linking [11]. The change in film shape due to increasing cross-linking could be visualized by successively irradiating the same capillary and partly evaporating the solvent: with increasing irradiation time the film shape changes from a “pearl chain” shape to a regular shape into a wavy film. In ref. 7 an illustration of the different film shapes can be found. The formation of a “pearl chain” film is attributed to the Rayleigh instability [12] and occurs when the viscosity of the polymer (related to the extent of cross-linking) is relatively small, as is the case when the irradiation time is short.

The exclusion of light after the irradiation is therefore necessary to avoid undesirable progression of the polymerization during the evaporation of the solvent. However, in a separate experiment an indication was found that even in the dark the reaction is not completely terminated. Capillaries 15 and 16 were initially polymerized as a 2 m long capillary. During evaporation of the solvent in the dark a blockage occurred in about half of the capillary. Therefore, the remaining part of the capillary was cut off and the evaporation was continued. It appears that the second part (capillary 16) had a significantly thicker film (about 10%) than the first part (capillary 15). The reason why the polymerization proceeds in the dark is not clear and therefore additional experiments are being

undertaken to clarify this phenomenon. When this problem cannot be solved satisfactorily, serious problems will occur with the preparation of uniform layers in long capillaries.

Removal of the solvent

The choice of the coating solvent is very important because after the polymerization the solvent and unreacted monomers have to be removed from the capillary by evaporation under reduced pressure and elevated temperatures. Emptying of the capillary must be achieved in a reasonable time, also to avoid the polymerization reaction progressing as mentioned above. In order to select a suitable coating solvent with favourable evaporation characteristics, tetrahydrofuran (THF), acetone, *n*-pentane and acetone–*n*-pentane mixtures were tested. From these experiments it appeared that with all solvents at 40°C bubbles are formed, which finally leads to irregular films. When keeping the temperature below 30°C no bubble formation was observed. However, at this temperature blockages still frequently occurred with THF and *n*-pentane. Good results were obtained with acetone and particularly with acetone–*n*-pentane (1:1, v/v). With this mixture the speed of evaporation is about four times faster than with the pure solvents. The favourable properties of acetone–*n*-pentane mixtures in the free release coating technique have been reported previously [13]. It is known that the conversion of the polymerization reaction is dependent on the type of solvent and therefore may influence the thickness of the layer [11].

Incorporation of alkyl acrylates

In order to obtain retentive layers for reversed-phase OT-LC, various alkyl acrylate monomers were incorporated in the acrylate films. The addition of alkyl acrylate monomers on the one hand increases the hydrophobicity of the layer, and on the other it might decrease the cross-link density, because only the silicon diacrylate is responsible for cross-linking. In this study we investigated three reactive diluents: lauryl acrylate (LA), butyl acrylate (BA) and ethylhexyl acrylate (EHA).

In a previous paper [7], we reported the use of polyacrylate films containing a lauryl moiety. In that study a 30% solution of a 1:1 mixture of silicon acrylate and lauryl acrylate was used as coating solution. With this mixture relatively thick layers could be prepared, showing considerable retention with methanol as mobile phase. However, the success rate of the preparation of thick layers was small. For unknown reasons, on several occasions no gel was formed after irradiation. Therefore, this aspect was first studied in more detail. It appeared that by decreasing the lauryl acrylate concentration in the coating solution by a factor of 6 this problem could be satisfactorily solved. However, with butyl and ethylhexylacrylate monomers the aforementioned problems did not occur; SiA–BA and SiA–EHA mixtures could be used up to a ratio of 1:1 without problems.

From the experimental conditions under which the columns were prepared as listed in Table 1, some preliminary conclusions can be drawn. There is no clear relationship between the phase ratio and the irradiation time and intensity. The phase ratio can be changed by varying the monomer concentration in the coating solution as demonstrated with SiA–EHA. For a low monomer concentration it was found necessary to increase the irradiation time to obtain a good film. So far a fair prediction of the layer thickness is not yet possible.

From Table 1, it can also be seen that the repeatability of the coating procedure, with respect to the phase ratio obtained, decreases in

the order SiA–BA > SiA–EHA > SiA–LA. However, the success rate in preparing good films appears to be different and the order SiA/EHA (100%) > SiA–BA (80%) > SiA–LA (50%) was found.

3.2. Chromatography

Retention and selectivity

In order to characterize the specific nature of the layers, the capacity factors and selectivity factors of some test solutes on the columns were measured with methanol as mobile phase. From the capacity factors, k' , and the phase ratio, V_s/V_m , the distribution coefficient K was calculated according $K = k'V_m/V_s$. To determine the effect of the incorporation of an alkyl moiety in the layer, the retention behaviour of films prepared with only SiA were included in the study. The results are given in Table 2. It is evident that, with a selected coating mixture, polyacrylate layers with similar retentive properties can be immobilized irrespective of the film thickness. Moreover, only small differences in selectivity are found between different types of phases. From the large retention of the solutes on columns 1 and 2, it can be concluded that the silicon acrylate matrix itself is hydrophobic. However, incorporation of an alkyl moiety in the films causes an additional increase in retention, as can be seen with the SiA/BA and SiA/EHA columns. The increase in retention is about a factor of two larger with EHA compared to BA. In HPLC it is known that hydrophobic inter-

Table 2
Distribution coefficients (K) and selectivity factors ($\alpha_{j,i} = K_j/K_i$) of anthracene derivatives on acrylate-coated columns

Compound	SiA ($n = 2$)		SiA–LA ($n = 3$)		SiA–BA ($n = 4$)		SiA–EHA ($n = 7$)	
	K (R.S.D.)	$\alpha_{j,i}$ (R.S.D.)	K (R.S.D.)	$\alpha_{j,i}$ (R.S.D.)	K (R.S.D.)	$\alpha_{j,i}$ (R.S.D.)	K (R.S.D.)	$\alpha_{j,i}$ (R.S.D.)
Anthracenemethanol	0.28 (0.04)		0.21 (0.05)		0.38 (0.03)		0.39 (0.03)	
Anthracenecarbonitrile	0.57 (0.04)	2.11 (0.21)	0.56 (0.03)	2.76 (0.49)	0.82 (0.02)	2.21 (0.16)	1.02 (0.06)	2.67 (0.09)
Anthracene	0.68 (0.04)	1.20 (0.02)	0.68 (0.02)	1.20 (0.04)	0.90 (0.01)	1.11 (0.01)	1.19 (0.05)	1.17 (0.02)
Fluoranthene	0.80 (0.03)	1.18 (0.01)	0.83 (0.01)	1.23 (0.01)	1.13 (0.01)	1.25 (0.02)	1.51 (0.07)	1.26 (0.01)
9-Phenylanthracene	0.84 (0.03)	1.06 (0.01)	0.90 (0.02)	1.08 (0.01)	1.29 (0.02)	1.14 (0.01)	1.76 (0.08)	1.17 (0.01)
1,2-Benzanthracene	0.91 (0.04)	1.07 (0.01)	1.00 (0.02)	1.11 (0.01)	1.42 (0.02)	1.10 (0.01)	1.88 (0.09)	1.06 (0.01)

Mobile phase, methanol. R.S.D. = relative standard deviation (%).

action increases with increasing alkyl chain length of the stationary phase [14]. The alkyl chain of EHA is longer than that of BA and therefore the interaction of solutes with EHA will be larger, which results in a larger distribution coefficient. From Table 2 it can be seen that the effect of LA on the retention is marginal. This is as expected, because the amount of LA added to SiA is small (about 3%).

The relationship between the phase ratio and retention was studied by measuring the capacity factors of test solutes on a number of EHA–SiA columns with different film thicknesses. As shown in Fig. 1, a linear relationship between the capacity factor and phase ratio is found. This behaviour again confirms that the specific nature of the polyacrylate layers is independent of the layer thickness.

The retention can also be changed by varying the composition of the mobile phase. Fig. 2 shows the effect of the methanol content on the retention of the test solutes. A linear relationship between $\log k'$ and the percentage of

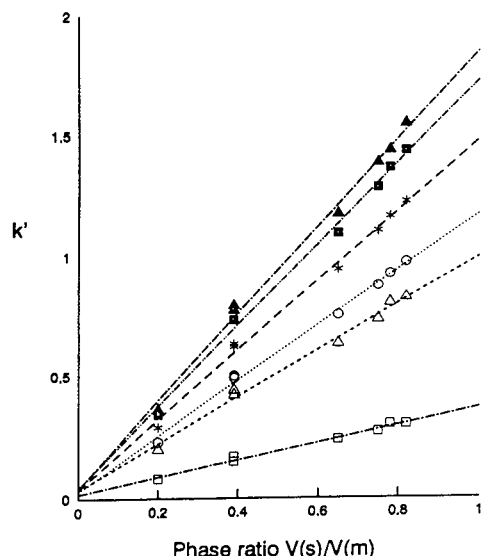


Fig. 1. Capacity factors of anthracene derivatives versus phase ratio on SiA–EHA-coated columns. Mobile phase, 100% methanol. \square = Anthracenemethanol; \triangle = anthracenecarbonitrile; \circ = anthracene; $*$ = fluoranthene; \blacksquare = 9-phenylanthracene; \blacklozenge = 1,2-benzanthracene.

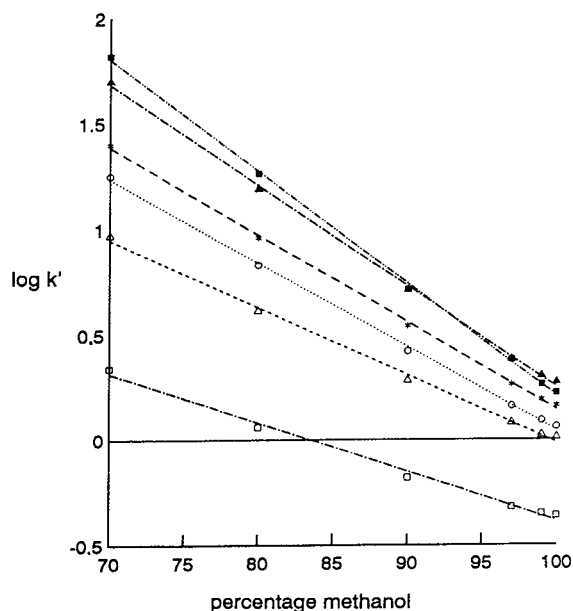


Fig. 2. Dependence of k' on the mobile phase composition for six anthracene derivatives on capillary 11. Detection, LIF. Symbols and compounds as in Fig. 1.

methanol is found, in agreement with findings in reversed-phase HPLC. This behaviour confirms the hydrophobic nature of the polyacrylate layers. Fig. 3 shows a representative chromatogram of some anthracene derivatives using pure methanol and methanol–water (4:1, v/v) as the mobile phase. From Figs. 2 and 3 it can be noted that the elution order of 1,2-benzanthracene and 9-phenylanthracene reverses on increasing the water content in the mobile phase. Such selectivity changes with the mobile phase composition also occur frequently in reversed-phase HPLC. From Fig. 3, it can be seen that the peak shapes remain very symmetrical on increasing the retention by adding water to the mobile phase.

Apart from methanol, acetonitrile was also tested as a mobile phase. The elution behaviour with both mobile phases on the same column and same linear velocity is illustrated in Fig. 4. It can be seen that the elution strength of acetonitrile on the polyacrylate column is significantly larger than that of methanol. This is in agreement with the retention theory in RP-HPLC, based on the solubility parameter of the mobile phase [15].

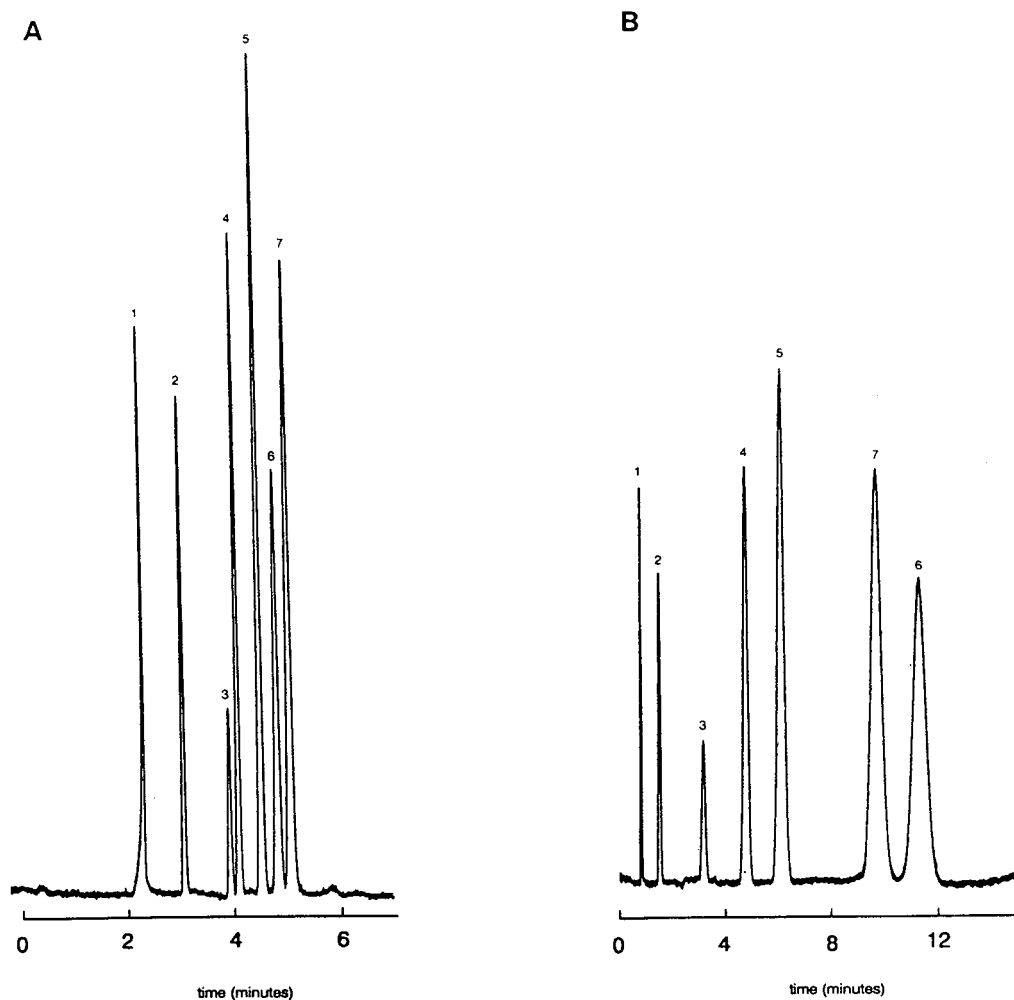


Fig. 3. Chromatograms of anthracene derivatives on column 8. Length, 61.1 cm; stationary phase, SiA-BA; $V_s/V_m = 0.81$. Peaks: 1 = salicylate; 2 = anthracenemethanol; 3 = anthracenecarbonitrile; 4 = anthracene; 5 = fluoranthene; 6 = phenylanthracene; 7 = 1,2-benzanthracene. (A) Mobile phase, methanol; pressure, 7.0 bar. (B) Mobile phase, methanol–water (80:20, v/v); pressure, 25.7 bar.

Further, the viscosity of acetonitrile is smaller than that of methanol, so that a smaller pressure drop is required to realize a desired separation speed.

Column performance

The theoretical plate height (H) in OT-LC can be calculated with the extended Golay equation according to

$$H = \frac{2D_m}{u} + \frac{(1 + 6k' + 11k'^2)d_c^2 u}{96D_m(1 + k')^2} + \frac{2k'd_f^2 u}{3D_s(1 + k')^2}$$

where

u = linear velocity of the mobile phase;

d_c = inner diameter;

d_f = film thickness;

D_m = diffusion coefficient in the mobile phase;

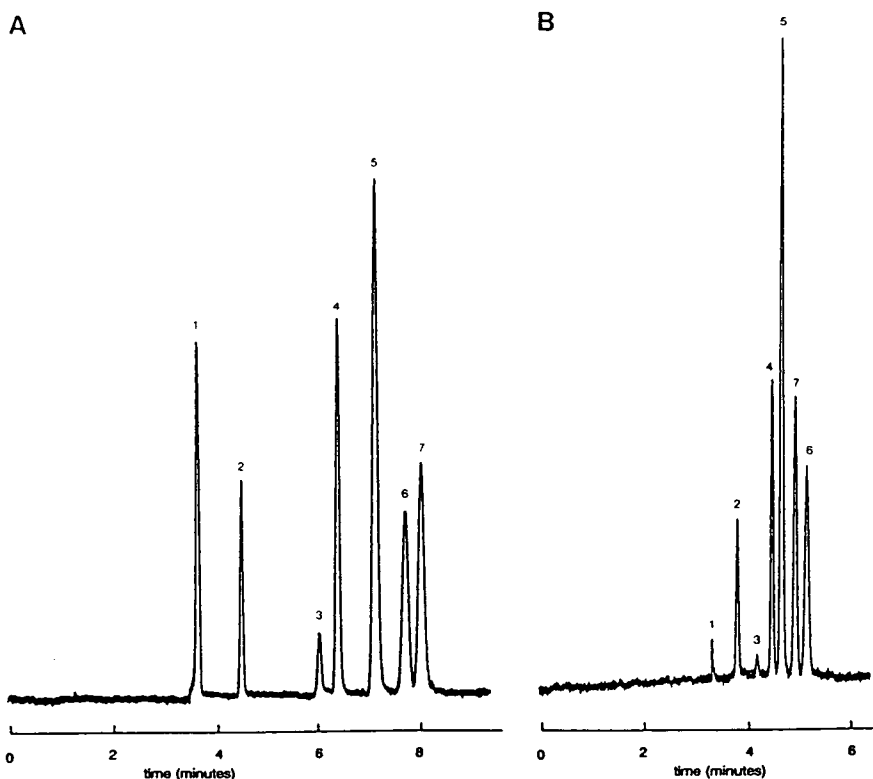


Fig. 4. Chromatograms of anthracene derivatives on column 15. Length, 115.1 cm; stationary phase, SiA-EHA; $V_s/V_m = 0.65$, LIF detection; peaks as in Fig. 3. (A) Mobile phase, methanol; pressure, 13.05 bar. (B) Mobile phase, acetonitrile; pressure, 7.5 bar.

D_s = diffusion coefficient in the stationary phase;

k' = capacity factor.

At higher linear velocities the contribution of the first term to the plate height can be neglected in OT-LC. For a given column with known inner diameter, film thickness and capacity factor, the plate height can be calculated provided that the diffusion coefficients in the mobile and stationary phase are known. Diffusion coefficients of solutes in the mobile phase can be calculated reasonably well with the Wilke–Chang equation. However, the diffusion coefficients in the stationary phase, in particular in polymeric layers, are little known. From previous studies with polymer coatings it is apparent that D_s plays

a decisive role in the selection of polymeric retentive layers for OT-LC.

The efficiencies of the polyacrylate columns were investigated by constructing H versus u curves with 1,2-benzanthracene as solute and methanol as mobile phase. Fig. 5 shows the H – u curves for three different types of columns with approximately the same phase ratio but different capacity factors. As an illustration, the H – u curve for an SiA-LA (1:1) polyacrylate film taken from a previous paper [7] is included. As can be seen, the experimental curves for columns 4, 8 and 16 are similar, but differ significantly from that for column 4 from ref. 7. The coincidence of the experimental data points is fortuitous and arises from the cancellation of the

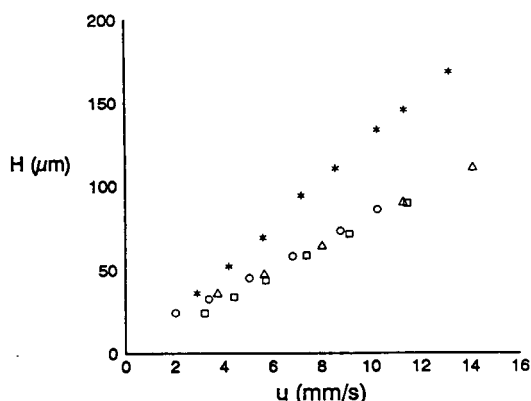


Fig. 5. Experimental plate heights of 1,2-benzanthracene versus mobile phase velocity. □ = Column 4, SiA-LA ($k' = 0.83$, $V_s/V_m = 0.81$); Δ = column 8, SiA-BA ($k' = 1.23$, $V_s/V_m = 0.81$); ○ = column 16, SiA-EHA ($k' = 1.38$, $V_s/V_m = 0.75$); * = column 4 from ref. 7 ($k' = 1.86$, $V_s/V_m = 0.22$).

effect of the magnitude of the diffusion coefficients in the layers (D_s) and the value of the capacity factors. By neglecting the peak broadening due to extra-column effects, the D_s values of 1,2-benzanthracene on several columns were calculated by fitting the experimental curves with the extended Golay equation. Inspection under a microscope showed that all the selected columns had visually a uniform layer. The results of the calculations are given in Table 3. Although the value of D_s within a set of columns varies considerably, some trends are clearly visible. The diffusivity in the SiA-LA (7:1) layer, which is almost a bare SiA layer, is the largest. Incorporation of alkyl chains in the

polymer network decreases the diffusivity and the decrease is larger the longer is the alkyl chain. From the point of view of column performance, OT-LC columns with bare SiA layers or SiA layers mixed with a short alkyl chain are to be preferred. This last option has our preference because the success rate with the mixed SiA/alkyl acrylate layers is considerably higher than with bare SiA layers.

Detection

So far, on-column LIF detection has been applied with OT-LC columns using highly fluorescent anthracene derivatives as test solutes. This detection mode is very convenient for studying OT-LC because it combines an extremely small detection volume with sufficient sensitivity needed to avoid mass overloading. However, to explore OT-LC further a more universal detection principle, such as UV detection, is preferable. On-column UV detection has been applied successfully in capillary electrophoresis and also recently by Crego *et al.* [4] in OT-LC. In OT-LC, the capillary inner diameters are about 5–10 μm , which means that the cell length with on-column detection is very small. This will adversely affect the concentration sensitivity. As a consequence, higher solute concentrations have to be injected with the risk of overloading the column. Therefore, the application of on-column UV detection in OT-LC only becomes attractive when the columns have sufficient sample capacity. As demonstrated in this study, thick retentive layers can be fabricated,

Table 3
Estimated diffusion coefficients of 1,2-benzanthracene in polyacrylate stationary phases

Capillary No.	Monomer	$D_s (\times 10^{-10} \text{ m}^2/\text{s})$	Mean $D_s (\times 10^{-10} \text{ m}^2/\text{s})$
3	LA	0.95	} 0.88
4	LA	0.65	
6	LA	1.05	
8	BA	0.75	} 0.77
9	BA	0.70	
10	BA	0.85	
13	EHA	0.43	} 0.53
14	EHA	0.51	
16	EHA	0.65	

which should give good sample capacities. Therefore, we investigated the application of on-column UV detection with the prepared polyacrylate columns. For this purpose we adapted the adjustable aperture used by Bruin *et al.* [8] for on-column UV detection in capillary electrophoresis. With this aperture the slit width can easily be adjusted under a microscope. The best signal-to-noise ratio was found when the slit width was the same as the inner diameter of the capillary. The length of the detection window was adjusted to 1 mm. In order to determine the extra peak broadening of the UV cell, the plate height of anthracene on column 17 was measured with LIF and UV detection (see Fig. 6). From previous studies it has been found that the extra peak broadening with on-column LIF detection is negligibly small. It can be seen that the plate heights with UV detection are about 10% larger than with LIF detection. On decreasing the width of the window, the plate heights with LIF and UV detection coincide but the signal-to-noise ratio decreases dramatically. As a decrease

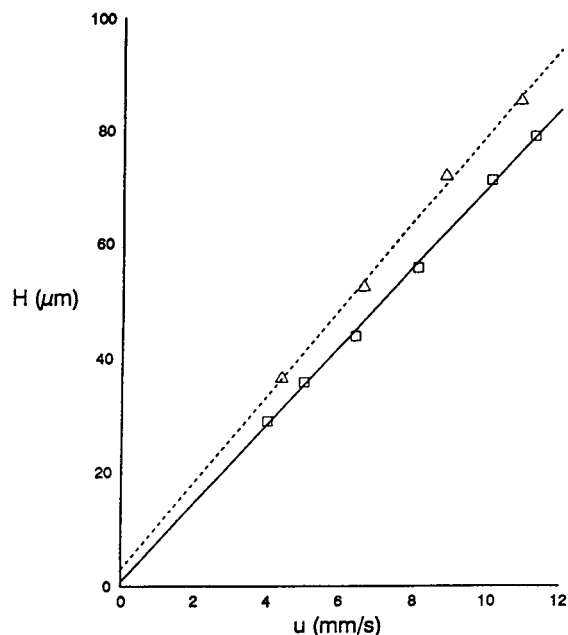


Fig. 6. Experimental H versus u plot for anthracene on column 17. Mobile phase, methanol; detection, □ = LIF and Δ = UV.

in efficiency of 10% is acceptable, a 1 mm window is a good compromise. Fig. 7 shows the chromatograms of anthracene derivatives with the same column and conditions using LIF and UV detection. The applicability of on-column UV detection in OT-LC is well demonstrated in Fig. 8, showing a rapid separation of alkylbenzenes.

Mass loadability

The mass loadability of polyacrylate columns was investigated by calculating the plate number and peak asymmetry from chromatograms obtained with different solute concentrations and methanol as the mobile phase. Toluene was

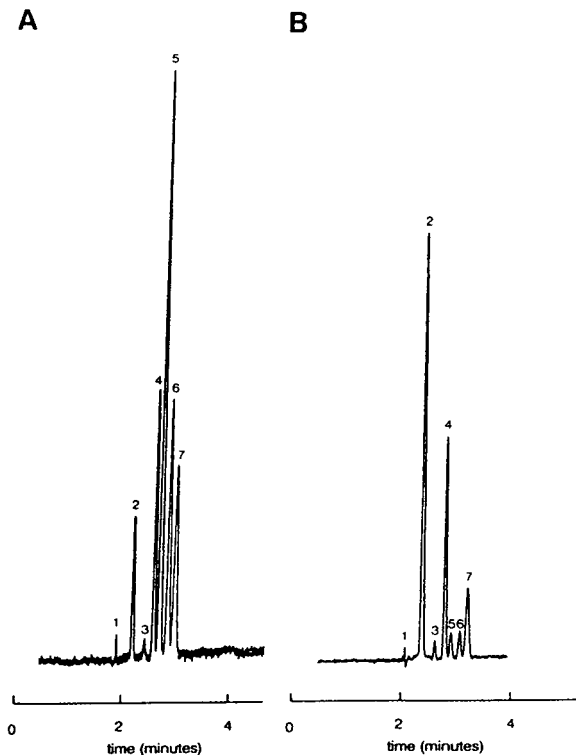


Fig. 7. Chromatograms of anthracene derivatives on column 15. Length, 115.1 cm; stationary phase, SiA-EHA; $V_s/V_m = 0.65$; mobile phase, acetonitrile. Peaks: 1 = salicylate; 2 = anthracenemethanol; 3 = anthracenecarbonitrile; 4 = anthracene; 5 = fluoranthene; 6 = 1,2-benzanthracene; 7 = 9-phenylanthracene. (A) Detection, LIF; pressure, 13.8 bar. (B) Detection, UV (258 nm); pressure, 13.0 bar.

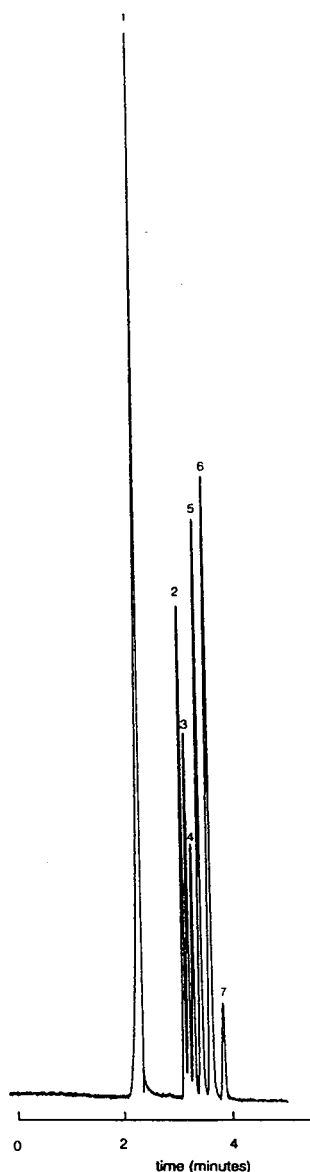


Fig. 8. Rapid separation of methyl-substituted benzenes on column 8. Detection, UV (210 nm); mobile phase, methanol. Peaks: 1 = salicylate; 2 = benzene (0.16 mol/l); 3 = toluene (0.14 mol/l); 4 = dimethylbenzene; 5 = trimethylbenzene; 6 = tetramethylbenzene; 7 = pentamethylbenzene.

selected as the test solute and on-column UV detection at 210 nm was applied. The change in plate number and peak asymmetry with increas-

ing solute concentration is shown in Fig. 9. The plate number is almost constant up to a concentration of 0.1 mol/l toluene. With an injection volume of 133 μ l this corresponds to an injected amount of about 13 ng. Surprisingly, the peak symmetry is still well preserved up to 1 mol/l toluene. From this mass loadability study,

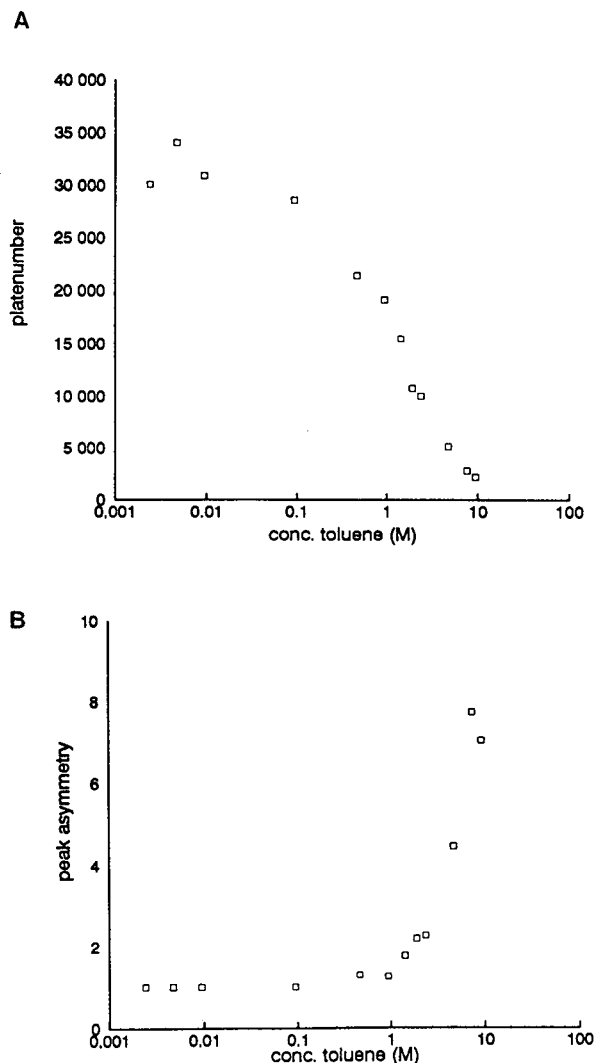


Fig. 9. (A) Plate number and (B) peak asymmetry versus injected toluene concentration on capillary 8. Mobile phase, methanol; detection, UV (220 nm); phase ratio, 0.81; injection volume, 133 μ l. Asymmetry of the peaks was calculated as described under Experimental.

it can be concluded that the thick polyacrylate layers have sufficient sample capacity to avoid decrease in efficiency by overloading and for on-column UV detection to be applied.

Long-term stability of the columns

The long-term stability of the various types of polyacrylate columns was investigated by measuring the efficiency and retention as a function of time with anthracene and 1,2-benzanthracene. With methanol and methanol–water mixtures as mobile phase no significant changes were observed over several months. In order to test the stability under more aggressive conditions, column 16 was flushed with 0.01 mol/l KOH for 3 h with methanol for 12 h. The capacity factors before and after the flushing with potassium hydroxide did not alter. Surprisingly, the plate height of anthracene was about 20% smaller after the flushing whereas that of 1,2-benzanthracene did not change.

As the columns appeared to be very stable with 0.01 mol/l KOH, the effect of a still higher potassium hydroxide concentration was investigated. For that purpose column 17 was flushed with 0.1 mol/l KOH for 1 h and then with methanol. In order to follow the equilibration of the column with methanol after the KOH flush, the capacity factors of the test solutes were measured at fixed time intervals. After 3 h of flushing the capacity factors of anthracene and 1,2-benzanthracene became constant; however, they were 15 and 19% smaller, respectively, than on the original column. By that time the film thickness appeared to have been reduced by 15%. This reduction results in a 20% decrease in the phase ratio, and this largely explains the decrease in the capacity factors. Further, the plate heights of the test solutes after the KOH flushing were found to be smaller (*ca.* 20%) than on the original column. The reason why the film thickness decreases is not yet clear, but probably some loosely bound constituents in the layer are extracted into the strong alkaline solution. No further deterioration of the layer was observed after flushing for an additional 4 h with 0.1 mol/l KOH.

4. Conclusions

Polyacrylate layers 1–2 μm thick can easily be prepared in 10 μm I.D. fused-silica capillaries. The layers appear to be very suitable for reversed-phase OT-LC. By using acetone–pentane as the coating solvent, the duration of the evaporation of the solvent is considerably decreased. With this solvent mixture the success rate of the preparation of SiA–EHA-coated capillaries was almost 100%.

The columns show a high mass loadability, which allows “on-column” UV detection. The possibility of using UV detection substantially increases the applicability of OT-LC. Extra peak broadening can be kept reasonably small by using a UV cell with an adjustable aperture. The polyacrylate films are extremely stable and can even withstand basic solutions of pH 12.

Current research is focused on the immobilization of thick polyacrylate layers in 5- μm capillaries. Other acrylates will be used in order to change the selectivity of the stationary phases.

5. References

- [1] P.A. Bristow and J.H. Knox, *Chromatographia*, 10 (1977) 279.
- [2] P.P.H. Tock, G. Stegeman, R. Peerboom, H. Poppe, J.C. Kraak and K.K. Unger, *Chromatographia*, 24 (1987) 617.
- [3] P.P.H. Tock, C. Boshoven, H. Poppe, J.C. Kraak and K.K. Unger, *J. Chromatogr.*, 477 (1989) 95.
- [4] A.L. Crego, J.C. Díez-Masa and M.V. Dabrio, *Anal. Chem.*, 65 (1993) 1615.
- [5] K. Göhlin and M. Larsson, *J. Chromatogr.*, 645 (1993) 41.
- [6] S. Eguchi, P.P.H. Tock, J.G. Kloosterboer, C.P.G. Zegers, P.J. Schoenmakers, J.C. Kraak and H. Poppe, *J. Chromatogr.*, 516 (1990) 301.
- [7] Y. Ruan, G. Feenstra, J.C. Kraak and H. Poppe, *Chromatographia*, 35 (1993) 597.
- [8] G.J.M. Bruin, G. Stegeman, A.C. van Asten, X. Xu, J.C. Kraak and H. Poppe, *J. Chromatogr.*, 559 (1991) 163.
- [9] O. van Berkel-Geldof, J.C. Kraak and H. Poppe, *J. Chromatogr.*, 499 (1990) 345.
- [10] L.R. Snyder and J.J. Kirkland, *Introduction to Modern Liquid Chromatography*, Wiley, New York, 1979.
- [11] S. Eguchi, *Philips Report No. 6318*, Philips Research Laboratory, Eindhoven, 1988.

- [12] K.D. Bartle, C.L. Woolley, K.E. Markides, M.L. Lee and R.S. Hansen, *J. High Resolut. Chromatogr. Chromatogr. Commun.*, 10 (1987) 128.
- [13] B. Xu and N.P.E. Vermeulen, *Chromatographia*, 18 (1984) 520.
- [14] G.E. Berendsen and L. de Galan, *J. Chromatogr.*, 196 (1980) 21.
- [15] P.J. Schoenmakers, *Optimization of Chromatographic Selectivity*, Elsevier, Amsterdam, 1986.

Chloromethylphenylcarbamate derivatives of cellulose as chiral stationary phases for high-performance liquid chromatography

Bezhan Chankvetadze[☆], Eiji Yashima, Yoshio Okamoto*

Department of Applied Chemistry, Faculty of Engineering, Nagoya University, Chikusa-ku, Nagoya 464-01, Japan

(First received November 9th, 1993; revised manuscript received January 25th, 1994)

Abstract

A new class of eight chloromethylphenylcarbamate derivatives of cellulose was prepared by introducing both an electron-donating methyl group and an electron-withdrawing chloro group on to the phenyl moieties and their chiral recognition abilities were evaluated as chiral stationary phases (CSPs) for high-performance liquid chromatography. The superiority of these derivatives over dichloro- and dimethylphenylcarbamates of cellulose as CSPs was demonstrated for some racemic compounds. The elution order and enantioselectivity were greatly dependent on the positions of the substituents. *Meta*- and *para*-disubstituted derivatives showed higher chiral recognition than *ortho*- and *meta*- or *para*-disubstituted derivatives. The correlation between the chemical shifts of the N–H protons of the carbamate moieties and the enantiomer-resolving abilities of the derivatives is discussed. Some of the derivatives were effective CSPs in both normal- and reversed-phase conditions and could efficiently separate some chiral drug enantiomers.

1. Introduction

In recent years, the separation of enantiomers of various biologically active compounds such as pharmaceuticals, agrochemicals and food additives has become one of the most developing areas of separation science owing to its importance in structure–activity relationship studies, metabolism and chiral pharmacokinetic studies and even in dating some archaeological materials. Direct HPLC enantioseparation, parallel to capillary electrophoresis (CE) and supercritical fluid chromatography (SFC), provides a more promising technique for the analysis of chiral

biologically active substances [1–3]. Among many commercially available chiral stationary phases (CSPs) for HPLC enantioseparation, polysaccharide derivative phases are among the most widely used for practical applications. The important advantages of polysaccharides in addition to their availability as natural sources are the ease of substitution and functionalization of the hydroxy groups of the glucose unit and the potential for application in large-scale separations [4,5].

Intensive studies of various polysaccharides, especially those of cellulose derivatives, reveal some correlations between their chiral recognition abilities and electronic and structural properties [4–10]. For benzoate and phenylcarbamate derivatives of cellulose, it has been established that their chiral recognition depends greatly on

* Corresponding author.

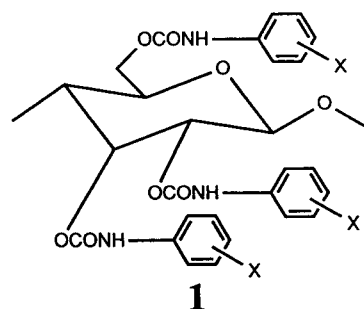
[☆] Permanent address: Department of Chemistry, Tbilisi State University, Chavchavadze Ave. 1, 380028 Tbilisi, Georgia.

the type and position of the substituents introduced on to the phenyl group [6,7]. The benzoate derivatives having electron-donating substituents such as methyl groups at *meta* and/or *para* positions showed better chiral resolving abilities than those having electron-withdrawing substituents such as chloro groups [6]. On the other hand, the introduction of either electron-donating or electron-withdrawing substituents tends to improve the optical resolution abilities of phenylcarbamate derivatives CSPs [7,8]. Substitution at a *meta* or *para* position on the phenyl moiety is considered to be more preferable than substitution at an *ortho* position for benzoate and phenylcarbamate derivatives of cellulose to prepare CSPs with a higher chiral recognition ability [6,7].

The tris(3,5-dimethylphenylcarbamate) of cellulose is one of the most powerful CSPs and can be used for both normal- and reversed-phase HPLC enantioseparations [11]. Cellulose tris(3,5-dichlorophenylcarbamate) also shows high chiral recognition, but its practical application is limited because of its exceptionally high solubility in most of chromatographic eluents [7]. In spite of the fact that the above-mentioned and some other polysaccharide derivatives [2,3] are intensively used for the separation of enantiomers of many types of chiral compounds, their chiral recognition mechanism remains obscure.

This work was carried out in order to improve the chiral recognition abilities and enhance the stability of chloro-substituted phenylcarbamates of cellulose by introducing a methyl group as a second substituent. Chloromethylphenylcarbamates of cellulose are versatile systems for studying the relationship between the electronic and structural properties of polysaccharides and their chiral recognition ability [12].

In this study, eight chloromethylphenylcarbamate derivatives of cellulose (Fig. 1) were prepared and their chiral recognition abilities were evaluated as CSPs. The effects of the position of the substituents on the elution order and chiral recognition abilities were studied. Correlations between the chemical shifts of N–H protons of the carbamate moieties of these derivatives and their enantiomer-resolving



a: 4-Cl-3-CH ₃	e: 2-Cl-4-CH ₃	i: 4-CH ₃
X= b: 3-Cl-4-CH ₃	f: 2-Cl-5-CH ₃	j: 4-Cl
c: 3-Cl-2-CH ₃	g: 2-Cl-6-CH ₃	k: 3,4-(CH ₃) ₂
d: 5-Cl-2-CH ₃	h: 4-Cl-2-CH ₃	l: 3,4-Cl ₂

Fig. 1. Structures of CSPs.

abilities were examined. The potential of use of these derivatives for reversed-phase HPLC and for the separation of some chiral drug enantiomers was also tested.

2. Experimental

2.1. Chemicals

Microcrystalline cellulose (Avicel) was purchased from Merck (Darmstadt, Germany). (3-Aminopropyl)triethoxysilane, 3-chloro-4-methylaniline and 3-chloro-2-methylaniline were of guaranteed reagent grade from Tokyo Kasei (Tokyo, Japan). 2-Chloro-6-methylaniline was obtained from Janssen Chimica (Beerse, Belgium) and triphosgene, pyridine-*d*₅, 2-chloro-4-methylaniline, 4-chloro-2-methylaniline, 5-chloro-2-methylaniline and 2-chloro-5-methylaniline from Aldrich (Milwaukee, WI, USA). All isocyanates were prepared from the corresponding amines by the conventional method using triphosgene. Wide-pore silica gel (Daiso gel SP-1000, pore size 100 nm, particle size 7 μ m) was obtained from Daiso (Osaka, Japan) and was silanized using (3-aminopropyl)triethoxysilane in benzene at 80°C before use. Hexane, 2-propanol and acetonitrile used as components of the eluents were of analytical-reagent grade.

Racemic compounds were obtained from different sources.

2.2. Preparation of tris(chloromethylphenylcarbamate) derivatives of cellulose

Cellulose tris(chloromethylphenylcarbamate) derivatives (**1a–h**) were prepared as described previously [7] by the reaction of cellulose with an excess of corresponding isocyanates in dry pyridine at *ca.* 100°C and isolated as methanol-insoluble fractions. Elemental analyses (Table 1) and IR and ¹H NMR spectra showed that hydroxy groups of cellulose were almost completely converted into the carbamate moieties.

2.3. Preparation of stationary phase

Column packing materials were prepared as described previously [7] using macroporous silica gel (Daiso gel SP-1000) and packed into 25 cm × 0.46 cm I.D. stainless-steel tubes by the conventional high-pressure slurry packing technique using a CCP-085 Econo packer pump (Chemco, Osaka, Japan). The plate numbers of the columns were 2000–4000 for benzene with hexane–2-propanol (90:10) at a flow-rate of 0.5 ml/min as the eluent at 20°C. The dead time (*t*₀) of the columns was determined using 1,3,5-tri-*tert*-butylbenzene as a non-retained compound.

2.4. Apparatus

All chromatographic experiments were performed on a Jasco Trirotar-II liquid chromatograph equipped with UV (Jasco 875-UV) and polarimetric (Jasco 181-C) detectors. A Model 7125 injector with a 100-μl loop (Rheodyne, Cotati, CA, USA) was used for injection of samples. All column evaluations were carried out at ambient temperature. IR analyses were carried out using a Jasco Fourier transform infrared spectrometer with a Jasco PTL-396 data processor. UV spectra were measured in tetrahydrofuran (THF) solutions using a Jasco Ubest-55 spectrophotometer. Circular dichroism (CD) spectra were measured in THF solutions in a 0.01 cm cell using a Jasco J-720 L spectropolarimeter. ¹H NMR spectra were taken in pyridine-*d*₅ solution at 80°C using a Varian VXR-500 NMR spectrometer operating at 500 MHz. Tetramethylsilane (TMS) was used as the internal standard.

3. Results and discussion

The results of the enantioseparation of fourteen racemic compounds (Fig. 2) on the chloromethylphenylcarbamate derivatives of cellulose are given in Table 2 together with those on 4-methyl-, 4-chloro-, 3,4-dimethyl- and 3,4-dichlorophenylcarbamates of cellulose [7]. As can

Table 1
Elemental analysis and N–H chemical shifts of **1a–h**

Compound	C (%)	H (%)	N (%)	Cl (%)	NH-proton, δ (ppm)		
					I	II	III
1a	53.10	4.23	6.22	15.96	10.51	9.88	9.64
1b	53.27	4.24	6.28	15.65	10.57	10.00	9.82
1c	54.15	4.32	6.39	16.13	9.76	9.17	8.85
1d	52.90	4.20	6.31	16.05	9.46	8.85	8.46
1e	54.10	4.22	6.29	16.20	8.95	8.73	8.25
1f	54.06	4.31	6.26	16.09	9.00	8.20	7.96
1g	53.90	4.32	6.36	16.12	9.12	8.90	8.44
1h	54.44	4.39	6.80		9.33	8.80	8.44
Calculated	54.33	3.92	6.34	16.08			

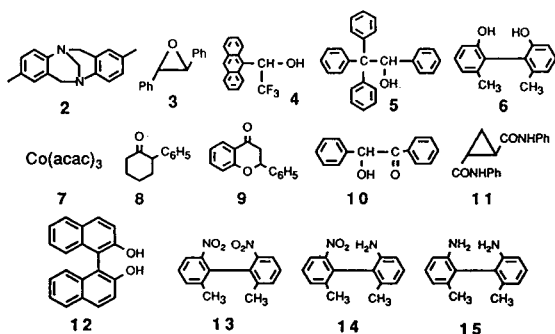


Fig. 2. Structures of racemic compounds.

be seen, more efficient chiral recognition abilities are exhibited by CSPs **1a** and **1b**, which can separate all fourteen racemic compounds with reasonable selectivity, and some racemic compounds were separated better than on dimethyl- (**1k**) and dichloro- (**1l**) phenylcarbamate derivatives of cellulose [7]. It seems noteworthy that these cellulose phenylcarbamate derivatives do not contain a substituent at the *ortho* position on the phenyl moiety. Cellulose tris(3,5-dimethylphenylcarbamate), which is one of the most powerful and widely used columns, could not separate the racemic compound **7**, which was completely separated on **1a** and **1b**. An interesting "synergistic" effect can be observed for some racemic compounds; for example, neither **1k** nor **1l** could separate the compound **5**, which was separated both on **1a** and **1b** with high selectivity ($\alpha = 3.05$ and 1.95 , respectively).

The resolving power of the derivatives possessing a substituent at the *ortho* position was relatively low compared with those of **1a** and **1b**. However, these derivatives, particularly **1c** and **1d**, showed characteristic chiral recognition for biphenyl and binaphthyl derivatives (**6** and **12–15**). Analogous low chiral recognition was previously found for *ortho*-substituted chloro-, methyl-, dimethyl- and dichlorophenylcarbamates of cellulose [7].

All disubstituted derivatives prepared in this study are scarcely soluble in hexane containing 10–20% of 2-propanol in which cellulose tris(3,5-dichlorophenylcarbamate) is swollen or dissolved.

As can be seen from Table 2, the chiral

recognition power of **1l** was almost the same as that of cellulose tris(4-chlorophenylcarbamate) (**1j**) [7], whereas introducing an electron-donating methyl group at the *meta* position to **1j** leads to a substantial increase in the enantiomer resolving ability. However, introduction of methyl group at the *ortho* position (**1h**) lowered the chiral recognition abilities towards most of the racemic compounds used in this study. Introduction of a methyl group at the *meta* position (**1k**) of tris(4-methylphenylcarbamate) (**1i**) of cellulose led to a slight increase in enantioselectivity, but the CSP lost enantioselectivity to the racemic compound **5**, whereas introduction of chloro group at the same *meta* position led to almost the same enantioselectivity without losing enantioselectivity for the racemic compound **5**.

These results clearly demonstrate that the introduction of an electron-donating group at a *meta* or *para* position as a second substituent on the phenyl moiety of cellulose phenylcarbamate derivatives containing one electron-withdrawing substituent at a *meta* or *para* position is much more preferable and *vice versa*. At present it is not clear if this finding can be generalized for all electron-donating and electron-withdrawing groups or whether it may be due to some steric effect.

Some interesting data were obtained from the results of enantioseparation on **1c**, **1d**, **1g** and **1h**, all of which possess a methyl group at the *ortho* position and a chloro group at different positions. The chiral recognition abilities of these derivatives depended on the position of the chloro group and were slightly higher than that of cellulose tris(2-methylphenylcarbamate) [7]. The elution orders of some racemic compounds were reversed depending on the position of the chloro group. In **1h**, the chloro group is far from the carbamate moiety than in other derivatives and the steric hindrance for racemic compounds interacting with the carbamate moiety must be lowest in this instance. Despite this fact, **1c**, **1d** and even **1g** separated most of the racemic compounds **11–15**, whereas only **15** could be partially separated on **1h**.

No reverse elution order of any racemic compounds was observed on changing the position of

Table 2

Optical resolution of 2–15 on cellulose phenylcarbamate derivatives 1a–h^a

Compound	1a			1b			1c			1d		
	k'_1	α	R_s	k'_1	α	R_s	k'_1	α	R_s	k'_1	α	R_s
2	1.10(+)	1.13	0.6	0.77(+)	1.25	3.8	0.67(–)	~1		0.80(+)	~1	
3	0.43(+)	3.25	5.0	0.45(+)	2.09	1.6	0.63(+)	~1		0.67(+)	1.30	1.0
4	0.80(–)	1.25	0.9	0.79(–)	1.20	1.3	0.60	1.00		1.53(–)	~1	
5	0.73(+)	3.05	5.0	0.65(+)	1.95	3.8	0.97(+)	1.17	0.7	1.00	1.00	
6	1.80(–)	1.35	1.1	1.45(–)	1.24	0.8	1.47(+)	1.25	0.8	1.90(+)	1.19	
7	5.86(+) ^b	1.44	3.0	2.50(+) ^b	1.67	3.0	3.93(–) ^b	~1		2.87(+) ^b	1.05	
8	1.27(–)	1.26	2.0	1.05(–)	1.19	1.3	1.58(+)	1.08		2.20(–)	~1	
9	1.73(–)	1.06		1.36(–)	1.09	0.8	1.77(+)	~1		1.90(–)	1.08	
10	4.70(–)	1.23	2.7	3.36(–)	1.27	3.5	3.67(+)	1.30	1.3	4.76(+)	1.10	0.9
11	2.13(–)	1.54	1.4	1.10(–)	2.06	3.5	1.50(+)	1.24	1.0	1.30(–)	1.20	
12	4.60(–)	1.54	0.9	3.77(–)	1.22	0.9	3.60(+)	1.50	1.4	4.30(+)	2.28	1.5
13	2.66(–)	1.19	1.5	1.86(–)	1.08	0.8	4.87(+)	1.05		7.66(+)	1.16	0.8
14	2.57(–)	1.56	4.5	1.87(–)	1.82	3.0	3.17(–)	1.24	1.3	4.67(–)	1.33	1.1
15	1.63(–)	1.31	2.0	1.33(–)	1.13		1.37(–)	1.27	0.9	1.33(–)	1.25	0.8
	1e			1f			1g			1h		
	k'_1	α	R_s	k'_1	α	R_s	k'_1	α	R_s	k'_1	α	R_s
2	1.37(+)	1.09		1.03(+)	~1		1.00(+)	~1		1.08(+)	~1	
3	0.83(+)	1.16	0.7	0.70(+)	1.71	0.8	0.80(+)	~1		0.97(+)	1.07	
4	2.80	1.00		1.67(–)	1.34	0.8	1.50(–)	~1		3.47(–)	~1	
5	2.13	1.00		1.28(+)	1.40		1.07(+)	~1		1.20	1.00	
6	3.67(+)	1.45	0.6	1.87(+)	1.23		2.36(+)	1.20	0.8	3.46(–)	1.11	
7	0.47(+)	~1		0.58(+)	~1		1.33(–)	~1		1.67	1.00	
8	1.10(–)	~1		1.18(–)	~1		0.60(–)	~1		1.43	1.00	
9	2.47(–)	1.04		2.08	1.00		2.40(+)	~1		2.60	1.00	
10	4.08(–)	1.08		3.23	1.00		4.40(+)	1.15	1.3	5.30(–)	1.08	
11	1.67	1.00		0.93	1.00		1.20(+)	1.61	1.1	3.00	1.00	
12	16.33	1.41	1.0	6.07(–)	1.38		7.27	1.56		8.67	1.00	
13	5.40(–)	1.05		4.00(–)	~1		6.80	1.00		8.37	1.00	
14	3.97(–)	1.22	1.0	3.00(–)	1.22		7.40(–)	1.21	1.0	9.40	1.00	
15	1.77(–)	1.26	1.0	1.33(–)	1.30	0.7	6.70(–)	~1		2.63(–)	1.09	
	1i ^c			1j ^c			1k ^c			1l ^c		
	k'_1	α	R_s	k'_1	α	R_s	k'_1	α	R_s	k'_1	α	R_s
2	0.75(+)	1.48	2.6	0.89(+)	1.16	0.8	0.87(+)	1.49	2.1	0.79(+)	1.47	1.7
3	0.51(+)	1.55	2.4	0.38(+)	1.68	2.3	0.61(+)	1.13	0.6	0.38(+)	1.93	2.9
4	1.54(–)	1.52	3.8	0.48(–)	1.29	1.1	1.76(–)	2.13	4.8	0.33(–)	1.21	
5	1.33(+)	1.37	2.5	0.81(+)	1.95	3.3	1.55(+)	~1		0.48	1.00	
6	2.48(–)	1.30	0.9	0.90(–)	1.20	0.8	1.86(–)	1.87	2.6	1.34(–)	~1	
7	0.90(+)	1.75	3.4	3.16(+)	1.46	2.8	0.57(+)	1.32	1.1	1.21(+)	1.63	2.1
8	1.14(–)	1.20	1.4	1.63(–)	1.16	1.3	0.95(–)	1.20	0.8	1.92(–)	1.31	
9	1.57(+)	1.16	1.5	1.85(+)	1.12	1.1	1.53(–)	1.42	2.6	1.29(+)	1.04	
10	3.00(–)	1.12	1.1	4.00(–)	1.20	2.0	3.24(–)	1.10	0.6	2.77(+)	1.31	1.9
11	1.83(–)	1.35	1.8	1.45(–)	1.44	1.3	1.27(+)	2.39	3.6	0.81(+)	1.15	
12												
13	2.50	1.00		3.95(–)	1.12	1.1				2.18(–)	1.24	1.5
14	2.37(+)	1.34	3.2	2.78(–)	1.30	2.4				2.24(–)	1.20	
15												

^a The sign in parentheses represents the optical rotation of the first-eluted enantiomer. Eluent, hexane–2-propanol (90:10, v/v); flow-rate, 0.5 ml/min.^b Eluent, hexane–2-propanol (98:2, v/v).^c Data are taken from ref. 7.

the methyl group in the derivatives bearing a chloro group at position 4 (**1a** and **1h**), whereas the elution order of some racemic compounds was reversed depending on the position of the methyl group in *m*-chlorophenylcarbamates of cellulose (**1b**, **1c** and **1d**). As will be shown below from IR data, intramolecular hydrogen bonding, which probably contributes to maintaining a higher ordered secondary structure of polysaccharide derivatives, is weaker in *ortho*-substituted phenylcarbamate derivatives of cellulose, and probably this is the reason for the dramatic changes in the chiral resolving power and elution order of some racemates. The elution orders of the racemic compounds (**2–15**) were identical on **1a** and **1b**, which may indicate that these two derivatives form the same regular structures, probably owing to strong intramolecular hydrogen bonding.

Comparison of the retention times and enantioselectivities of four biphenyl derivatives (**6**, **13**, **14** and **15**) having a similar structure but different functional groups on the CSPs is of interest. The racemic compounds **13** and **14** possess a nitro group capable of hydrogen bonding with the N–H of the carbamate moiety of cellulose phenylcarbamate derivatives, and they are characterized with longer retention times than the other two derivatives (**6**, **15**). Although a longer retention time does not always lead to a better separation of enantiomers [13], compound **13** with the longest retention time exhibited the lowest enantioselectivity among all the above-mentioned biphenyl derivatives.

Fig. 3 shows the ^1H NMR spectra of the NH region of the chloromethylphenylcarbamate derivatives and trisphenylcarbamate (CTPC) of cellulose. The N–H proton chemical shifts of cellulose phenylcarbamate derivatives depended greatly on the position of the substituents, and three resonances corresponding to the N–H protons of carbamate groups at positions 2, 3 and 6 of the glucose units were observed in the N–H regions. The N–H resonance at the lowest field may be assigned to the N–H proton at position 6 [14]. The chemical shifts of the N–H resonances reflect the acidity of N–H protons and shift downfield with increase in acidity of

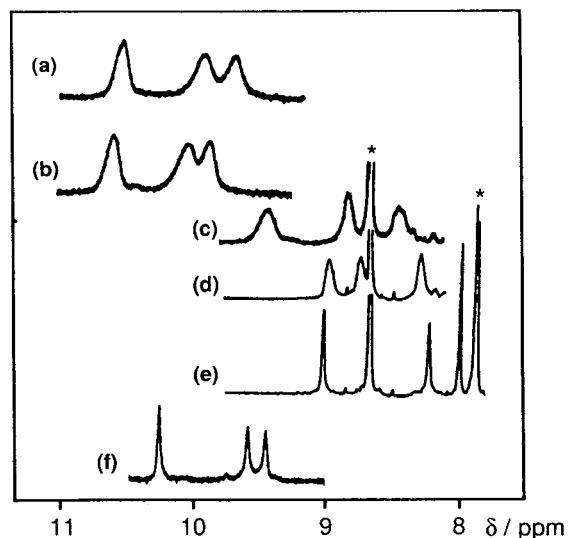


Fig. 3. ^1H NMR spectra of cellulose phenylcarbamate derivatives (a) **1a**, (b) **1b**, (c) **1d**, (d) **1e** and (e) **1f** and (f) cellulose trisphenylcarbamate. Pyridine- d_5 , 80°C, 500 MHz. Asterisks denote the solvent.

N–H [7]. The N–H protons of **1a** and **1b** resonate slightly downfield of those of CTPC, but upfield of those of cellulose tris(3,5-dichlorophenylcarbamate) [14]. This indicates that the N–H protons of **1a** and **1b** were more acidic than those of CTPC, whereas with *ortho*-substituted derivatives, the N–H resonances dramatically shift upfield, probably owing to steric hindrance of the substituents at the *ortho* position which may disturb the planar structure of the phenylcarbamate residues. The more acidic N–H will interact with appropriate racemic compounds more strongly via hydrogen bonding and if this occurs, the retention times of **13** and **14** on 3,4-disubstituted derivatives will be longer than on *ortho*-substituted derivatives. However, the reverse order was observed (Table 2).

This apparent contradiction can be solved by using the IR spectral data for the above-mentioned phenylcarbamate derivatives of cellulose (Fig. 4). There are at least two N–H peaks in the IR spectra of some derivatives (e.g., **1a**). The peak in the range $3400\text{--}3435\text{ cm}^{-1}$ may be assigned to a free N–H residue and that in the range $3330\text{--}3350\text{ cm}^{-1}$ to N–H involved in intramolecular hydrogen bonding [7]. Most of

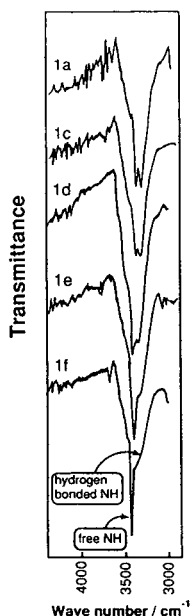


Fig. 4. IR spectra of N–H of chloromethylphenylcarbamate derivatives of cellulose (**1a**, **1c**, **1d**, **1e** and **1f**).

the N–H appears to be free in the case of *ortho*-substituted derivatives, especially 2-chloro-substituted derivatives, and the free N–H will interact strongly with appropriate racemic compounds (in this instance **13** and **14**). This will result in longer retention. However, in 3,4-disubstituted derivatives, the N–H groups are markedly involved in intramolecular hydrogen bonding (Fig. 4) and this part will not contribute to retention if we assume that intramolecularly hydrogen-bonded N–H loses the capability of interacting with appropriate solutes. The racemate **14** possesses both nitro and amino groups and is capable of interacting with both N–H and C=O groups of the carbamate moieties, which may be the reason for the long retention time and high enantioselectivity of this compound. The racemates **6** and **15** will probably interact with the carbonyl fragment of the carbamate moieties which are close to chiral glucose units and this may be the reason for the high enantioselectivity for these compounds.

To demonstrate the importance of hydrogen bonding in chiral recognition on cellulose phenylcarbamate derivatives, separation factors

(α) of the racemic compounds **10** and **11** were plotted against N–H chemical shifts of the 6-position of phenylcarbamate derivatives (lowest field resonance) (Fig. 5). As can be seen, reasonable correlations exist between separation factors of the racemic compounds **10** and **11** and N–H chemical shifts. The separation factors generally increased as the N–H chemical shift increased. Other reliable correlations such as this can be found in Table 2 not only for compounds capable of interacting with N–H groups of carbamate moieties (**7–11**, **13**, **14**) but also for other racemic compounds. These results indicate that N–H groups of the carbamate moieties contribute significantly to chiral recognition not only as a local chiral adsorptive site, but also by forming intramolecular hydrogen bonds to maintain a regular structure. The latter will affect both enantioselectivity and column efficiency, in this instance the resolution factor (R_s).

To examine more closely the effect of intramolecular hydrogen bonding on the resolution factor, the R_s value of **15** was divided by the plate numbers (N) of the columns and the resulting R_s/N values were plotted against the N–H chemical shifts of some cellulose phenylcarbamate derivatives (Fig. 6). This plot was constructed in order to exclude the effect of the different efficiencies of the columns, and the racemic compound **15** was chosen because it most probably could not interact with the N–H

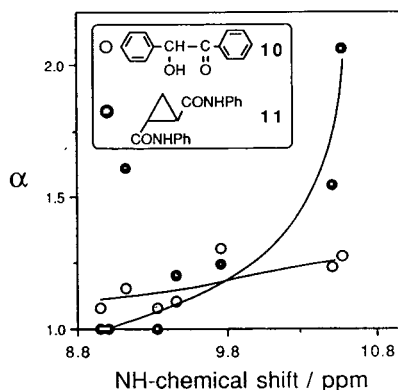


Fig. 5. Dependence of separation factor (α) of benzoine (**10**) and *trans*-cyclopropanedicarboxylic acid dianilide (**11**) on the N–H chemical shift of cellulose phenylcarbamate derivatives (**1a–h**).

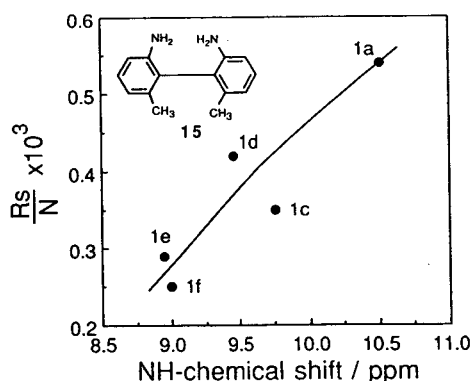


Fig. 6. Dependence of R_s/N for 2,2'-diamino-6,6'-dimethylbiphenyl (**15**) on the N–H chemical shift of cellulose phenylcarbamate derivatives (**1a**, **1c**, **1d**, **1e** and **1f**).

groups of the carbamate moieties as a local chiral adsorptive site and it shows almost the same capacity factor ($k'_1 = 1.33$ – 1.77) and the same separation factor ($\alpha = 1.25$ – 1.31) on most of the cellulose phenylcarbamate derivatives in this study (**1a**, **1c**, **1d**, **1e** and **1f**). As can be seen from Fig. 6, R_s/N decreases with decrease in N–H chemical shift. This suggests that **1c**, **1d** and especially **1e** and **1f** possess other kinds of adsorbing sites than **1a**, probably owing to their irregular structures and **1a** has a limited number of adsorbing sites owing to its regular structure. IR spectra of the same cellulose phenylcarbamate derivatives (Fig. 4) show that part of the N–H forms intramolecular hydrogen bonds, and the ratio decreased in the same order as that in Fig. 6.

Further evidence for the regular structure of **1a** can be seen in the CD spectra of the above-mentioned cellulose phenylcarbamate derivatives (Fig. 7). The CD spectra showed differences in the patterns, wavelengths of the peak tops and intensities of the peaks, depending on the position of the substituents. The column of **1a** with a high enantiomer resolving ability shows the most intense peak in the region of 210–220 nm (C=O region), which suggests that the structure of **1a** may be highly regular. These results suggest that the position and type of substituents may vary the conformation of the main chain and/or side-

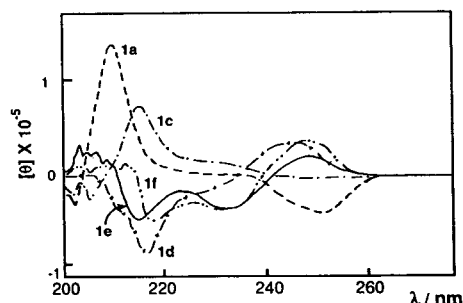


Fig. 7. CD spectra of cellulose phenylcarbamate derivatives (**1a**, **1c**, **1d**, **1e** and **1f**) in THF.

chains. This will influence the chiral recognition powers of CSPs.

Hence we can conclude that N–H groups of phenylcarbamate moieties can contribute to chiral recognition by direct interaction with some racemic compounds as a local chiral adsorptive site and also by maintaining a higher ordered secondary structure of CSPs via intramolecular hydrogen bonding, and the latter contribution is more universal and may not depend on the type of a solute and will affect the resolution factor to a considerable extent.

The above-proposed mechanism for the role of intramolecular hydrogen bonding and free N–H groups can explain not only the chiral recognition mechanism of polysaccharide phenylcarbamate derivatives, but also some general physical and chemical properties of these derivatives. For example, the high solubility of cellulose tris(3,5-dichlorophenylcarbamate) may be attributed to a large fraction of free N–H groups with high acidity [7]. Cellulose tris(2-methylphenylcarbamate) shows lyotropic liquid crystallinity, but cellulose tris(2-chlorophenylcarbamate) does not. This may be ascribed to the fact that an *ortho*-substituted chloro group tends to disturb intramolecular hydrogen bonding substantially, whereas a methyl group in the same position does not disturb it, as it can be seen from the IR spectra of these carbamates. Therefore, it is suggested that liquid crystallinity may be closely related to the intramolecular hydrogen bonding abilities of the derivatives.

In the early stages of the development of

cellulose tribenzoate as a CSP, the successful resolution of enantiomers with water-containing eluents was considered to be due to hydrophobic interactions between the CSPs and enantiomers, which plays an important role in chiral recognition [15]. Recently, an attempt was made to improve the chiral recognition abilities of cellulose tris(3,5-dimethylphenylcarbamate) to some hydroperoxides and alcohols by saturation of water in hexane–2-propanol eluent [16] and tris(3,5-dimethylphenylcarbamate) of cellulose was proposed as a successful CSP for the reversed-phase separation of enantiomers [11]. All these data substantially extend the universality of cellulose phenylcarbamate derivatives as CSPs and show that in the absence of interaction of racemic compounds with carbamate fragments via hydrogen bonding in water-containing eluents, alternative chiral sites can contribute to enantioseparation. An example of the enantioseparation of the racemic compound **3** in both normal- and reversed-phase conditions on **1a** is shown in Fig. 8. Better separation was achieved in the former than in the latter instance. Probably the chiral resolving power in reversed-phase systems will be markedly improved by optimizing the separation conditions (buffer system, pH, additives, temperature, etc.), but this is outside the scope of this work. Both normal- (hexane–2-propanol) and reversed-phase (water–acetonitrile, water–ethanol, water–methanol mixtures)

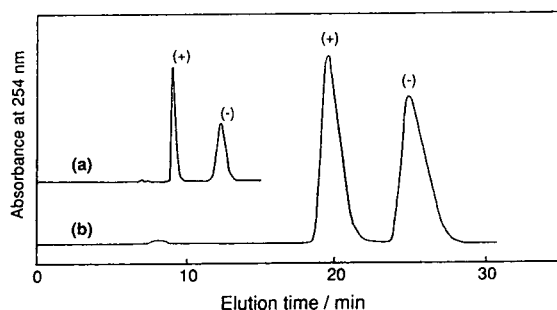


Fig. 8. Separation of enantiomers of *trans*-2,3-diphenyloxirane (**3**) under (a) normal- and (b) reversed-phase conditions on cellulose tris(3-chloro-4-methylphenylcarbamate) (**1b**). Eluent, (a) hexane–2-propanol (90:10), flow-rate 0.5 ml/min; (b) water–acetonitrile (50:50), flow-rate 1.0 ml/min.

enantioseparations were possible on a single column at least for the present separations.

The high chiral recognition abilities exhibited by chloromethylphenylcarbamates of cellulose, especially **1a** and **1b**, were also demonstrated in the separation of enantiomers of some pharmacologically important compounds used in the treatment of various cardio- and cerebrovascular disorders, such as hypertension, angina pectoris and cardiac arrhythmia (Fig. 9). It must be noted that some of these compounds were not separated using cellulose tris(3,5-dimethylphenylcarbamate), which shows high resolving abilities for many racemic compounds including drugs [1,4,7]. Recently, Ching *et al.* [17] reported the separation of acebutolol enantiomers using cellulose tris(3,5-dimethylphenylcarbamate), but the separation factor was low ($\alpha = 1.12$).

4-Aryl-1,4-dihydropyridine calcium antagonists are important peripheral vasodilators and are widely used in the treatment of cerebrocirculatory disorders and hypertension [18]. It has been established that in many instances chiral dihydropyridines such as nitrendipine and nicardipine are superior to the corresponding symmetrically substituted derivatives such as nifedipine [19,20]. Detailed pharmacological studies revealed that enantiomers of chiral dihydropyridines have different, in some instances even opposite, vasodi-

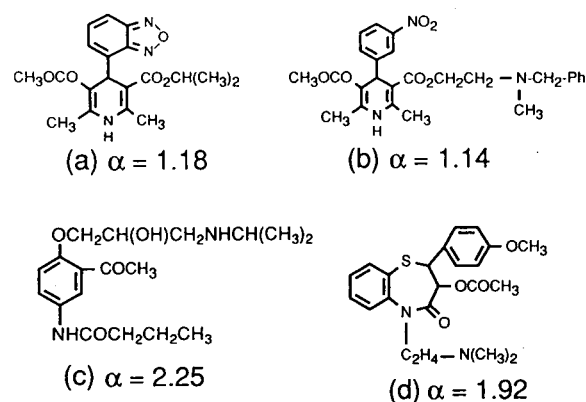


Fig. 9. Racemic drugs resolved on cellulose tris(4-chloro-3-methylphenylcarbamate) (**1a**). (a) Isradipine; (b) nicardipine; (c) acebutolol; (d) *cis*-diltiazem. Eluent, (a–c) hexane–2-propanol (90:10); (d) hexane–2-propanol (80:20).

lating and hypotensive activities and toxicities [21]. In most instances, the 4*S*-enantiomer is more active than the 4*R*-enantiomer [21–23]. The chiral dihydropyridines nitrendipine, nicardipine and isradipine cannot be separated using cellulose tris(3,5-dimethylphenylcarbamate) [4,9]. Enantiomers of these drugs were separated using cellulose tris(4-*tert*-butylphenylcarbamate) with very long retention times, especially for nicardipine [9].

A chiral thiazepine derivative with the same calcium channel-blocking activity, *cis*-diltiazem, can also be separated using other cellulose [4] and amylose derivatives, but the separation factor on **1a** was much higher, and this will permit the use of this CSP for large-scale separations.

Some other chiral drugs, *e.g.*, the β -blockers propranolol ($k'_1 = 0.53$, $\alpha = 2.00$), oxprenolol ($k'_1 = 1.18$, $\alpha = 1.14$) and alprenolol ($k'_1 = 1.40$, $\alpha = 1.10$) and the antihistaminic carbinoxamine ($k'_1 = 7.71$, $\alpha = 1.21$) and doxylamine ($k'_1 = 0.93$, $\alpha = 1.85$), can be successfully separated using **1a** and/or **1b**.

4. Conclusions

The chiral recognition abilities of eight chloromethylphenylcarbamate derivatives of cellulose were evaluated as CSPs for HPLC and it was established that 3,4-chloromethylphenylcarbamates of cellulose show higher resolving powers for some racemic compounds than dimethyl- and dichlorophenylcarbamates of cellulose. However, *ortho*-substituted derivatives showed low chiral recognition. Some correlations were established between ^1H NMR chemical shifts of the N–H groups of the carbamate moieties and the enantiomer resolving abilities of the above-mentioned cellulose derivatives. It is suggested that the N–H groups of the carbamate moieties will contribute to the chiral recognition as local chiral adsorbing sites and also by maintaining a higher ordered secondary structure of polysaccharide CSPs via intramolecular hydrogen bonding, and the latter is more universal and does not depend on the nature of the solute. The

potential of use of these CSPs in reversed-phase conditions and for the separation of some practically important drug enantiomers has also been demonstrated.

5. Acknowledgements

B. Chankvetadze thanks the Japan Cultural Association for financial support during his stay at Nagoya University. The authors are grateful to Professor Emeritus H. Suda of Kanazawa University for providing chiral biphenyl derivatives. This work was partially supported by Grant-in-Aids for Scientific Research Nos. 02555184 and 05559009 from the Ministry of Education, Science and Culture, Japan.

6. References

- [1] S. Ahuja, *Chiral Separation by Liquid Chromatography* (ACS Symposium Series, No. 471), American Chemical Society, Washington, DC, 1991.
- [2] Y. Okamoto and Y. Kaida, *J. Synth. Org. Chem. Jpn.*, 51 (1993) 41.
- [3] Y. Okamoto, R. Aburatani, K. Hatano and K. Hatada, *J. Liq. Chromatogr.*, 11 (1988) 2147.
- [4] M. Negawa and F. Shoji, *J. Chromatogr.*, 590 (1992) 113.
- [5] E. Francotte and R.M. Wolf, *J. Chromatogr.*, 595 (1992) 63.
- [6] Y. Okamoto, R. Aburatani and K. Hatada, *J. Chromatogr.*, 389 (1987) 95.
- [7] Y. Okamoto, M. Kawashima and K. Hatada, *J. Chromatogr.*, 363 (1986) 173.
- [8] Y. Okamoto, M. Kawashima, R. Aburatani, K. Hatada, T. Nishiyama and M. Masuda, *Chem. Lett.*, (1986) 1237.
- [9] Y. Okamoto, R. Aburatani, K. Hatada, M. Honda, N. Inotsume and M. Nakano, *J. Chromatogr.*, 513 (1990) 375.
- [10] Y. Kaida and Y. Okamoto, *J. Chromatogr.*, 641 (1993) 267.
- [11] K. Ikeda, T. Hamasaki, H. Kohno, T. Ogawa, T. Matsumoto and J. Sakai, *Chem. Lett.*, (1989) 1089.
- [12] B. Chankvetadze, E. Yashima and Y. Okamoto, *Chem. Lett.*, (1992) 617.
- [13] D.T. Witte, J.P. Franke, F.J. Bruggeman, D. Dijkstra and R.A. De Zeeuw, *Chirality*, 4 (1992) 389.
- [14] Y. Kaida and Y. Okamoto, *Bull. Chem. Soc. Jpn.*, 66 (1993) 2225.

- [15] Y. Okamoto, M. Kawashima, K. Yamamoto and K. Hatada, *Chem. Lett.*, (1984) 739.
- [16] A. Kunath, E. Hofst and H. Hamann, *J. Chromatogr.*, 588 (1991) 352.
- [17] C.B. Ching, B.G. Lim, E.J.D. Lee and S.C. Ng, *Chirality*, 4 (1992) 174.
- [18] F. Bossert and W. Vater, *Med. Res. Rev.*, 9 (1989) 291.
- [19] L. Dagnino, K.K. Li, M.W. Wolowyk, H. Wynn, C.R. Triggle and E.E. Kraus, *J. Med. Chem.*, 29 (1986) 2525.
- [20] M. Iwanami, T. Shibata, M. Fujimoto, R. Kawai, K. Tamazawa, K. Takenata, K. Takahashi and M. Murakami, *Chem. Pharm. Bull.*, 27 (1979) 1426.
- [21] S. Goldmann and J. Stoltefuss, *Angew. Chem., Int. Ed. Engl.*, 30 (1991) 1559.
- [22] M. Kajino, Y. Wada, Y. Nagai, A. Nagaoka and K. Meguro, *Chem. Pharm. Bull.*, 37 (1989) 2225.
- [23] G. Marziniak, A. Delgado, G. Leclerc, J. Velly, N. Decker and J. Schwartz, *J. Med. Chem.*, 32 (1989) 1402.

Factor analysis in ion chromatography of carboxylate ions

Ulo Haldna^a, Jaan Pentchuk^b, Michel Righezza^c, Jacques R. Chrétien^{*,d}

^a*Institute of Chemistry, Estonian Academy of Sciences, Akadeemia tee 15, EE-0103 Tallinn, Estonia*

^b*Tartu University, Ulrikool Street 18, EE-2404 Tartu, Estonia*

^c*Laboratoire de Chimimétrie, Université d'Orléans, B.P. 6759, 45067 Orléans Cedex 2, France*

^d*Laboratoire de Chimimétrie, Université d'Orléans, B.P. 6759, 45067 Orléans Cedex 2, France, and Institut de Topologie et de Dynamique des Systèmes, Associé au CNRS, Université de Paris VII, 1 Rue Guy de la Brosse, 75005 Paris, France*

(First received May 25th, 1993; revised manuscript received February 9th, 1994)

Abstract

The retention times of five carboxylate ions (formate, acetate, propionate, *n*-butanoate and *n*-pentanoate) in ion chromatography were determined using 25 eluents prepared from NaHCO₃ and Na₂CO₃. Principal component analysis (PCA) and correspondence factor analysis (CFA) were applied to describe the behaviour of the carboxylate anions and the influence of the carbonate concentration of the eluents. With PCA, only one factor is necessary to model the retention times of each ion studied. CFA offers an analysis of second-order effects and shows how the selectivities of the chromatographic systems are modified with either the carbonate concentration or the concentration ratio of NaHCO₃ and Na₂CO₃.

1. Introduction

There is great interest in the chemometric analysis of large sets of chromatographic data [1,2]. The process and applications of factor analysis [3] to gas chromatography (GC) [4–9] and liquid chromatography (LC) [10–14] have been particularly developed in the last two decades. Chemometric analysis of chromatographic retention data can be useful at two levels: for an overall view, through the variation of retention indices in GC or capacity factors in LC, and for an in-depth analysis of the behaviour of compounds through the selectivity parameters of the chromatographic systems.

Principal component analysis (PCA) is appropriate to give an overall view of chromatographic data [4,5,10,11,14], *e.g.*, to show independence of the mechanism between normal-phase and reversed-phase liquid chromatography [14]. A more in-depth analysis is possible with correspondence factor analysis (CFA) [6–9,12–14], which is particularly appropriate for studying second-order effects, responsible for the selectivity in a given retention mechanism.

The ion chromatography (IC) of organic ions with a hydrophilic polar group and a hydrophobic part or chain involves a mechanism that is not easy to understand and to handle in order to optimize the selectivity [15,16]. Hence, the extension of the application of factor analysis in GC or LC retention data processing to IC became desirable. The need was simultaneously to delineate the potential interest in factor analy-

* Corresponding author. Address for correspondence:
Laboratoire de Chimimétrie, Université d'Orléans, B.P.
6759, 45067 Orléans Cedex 2, France.

sis for data processing of IC retention data and to gain a deeper insight into the behaviour of organic ions in IC. This was confirmed recently with a systematic study of parameters that could influence the retention of peptides and proteins in IC [17].

In this work, the retention times (t_R) of a model series of five carboxylate anions (HCOO^- , CH_3COO^- , $\text{C}_2\text{H}_5\text{COO}^-$, $\text{C}_3\text{H}_7\text{COO}^-$ and $\text{C}_4\text{H}_9\text{COO}^-$) using 25 carbonate eluents were determined. The corresponding data matrix was submitted to factor analysis by using PCA and CFA successively in order to evaluate the complexity of the retention mechanism and search for optimization. With PCA, the stress is placed on modelling the retention times of anions, and with CFA, the stress is placed on the relative behaviour of the anions and on the delineation of all the tenuous factors that govern it.

2. Experimental

The ion chromatograph used was an Eesti TASK Model IVK-21 equipped with a conductivity detector, an HIKS-1 separation column (150×3 mm I.D.) and a KU-2 suppressor column (250×4 mm I.D.). The eluents were NaHCO_3 (0–0.9 mM)– Na_2CO_3 (0.2–1.2 mM) solutions delivered at 1.6 ml/min. The HIKS-1 resin is based on a methacrylic matrix, a copolymer of 2-hydroxyethyl methacrylate and ethylene dimethacrylate, and has a pellicular coated surface consisting of an ion exchanger: $-\{\text{CH}_2\text{CH}[\text{C}_6\text{H}_4\text{CH}_2\text{N}^+(\text{CH}_3)_3]\}_m$.

The general formula of the studied anions is $\text{H}(\text{CH}_2)_n\text{COO}^-$, with values of n ranging from 0 to 4. The aqueous solutions of the corresponding organic acids injected contained $1\text{--}10 \cdot 10^{-3} \text{ g l}^{-1}$ of the compounds HCOOH , CH_3COOH , $\text{C}_2\text{H}_5\text{COOH}$, $n\text{-C}_3\text{H}_7\text{COOH}$ or $n\text{-C}_4\text{H}_9\text{COOH}$. The sample volume was 0.1 ml. Analytical-reagent grade reagents and doubly distilled water were used. The retention times measured are presented in Table 1. The void time of the system used was 94 s.

Table 1

Retention times (s) of carboxylate ions on the HIKS-1 resin for various carbonate eluents with different concentrations C and ratios Z

$Z = \frac{C_{\text{NaHCO}_3}}{C_{\text{Na}_2\text{CO}_3}}$	Anion	$C = C_{\text{Na}_2\text{CO}_3} + C_{\text{NaHCO}_3}$ (mM)				
		0.2	0.4	0.6	0.8	1.2
3.0	HCOO^-	374	258	218	202	179
	CH_3COO^-	354	245	204	188	172
	$\text{C}_2\text{H}_5\text{COO}^-$	432	280	231	208	183
	$\text{C}_3\text{H}_7\text{COO}^-$	450	305	250	226	197
	$\text{C}_4\text{H}_9\text{COO}^-$	588	405	322	295	247
1.0	HCOO^-	340	222	197	180	162
	CH_3COO^-	294	212	192	176	156
	$\text{C}_2\text{H}_5\text{COO}^-$	326	250	212	185	168
	$\text{C}_3\text{H}_7\text{COO}^-$	370	261	245	203	185
	$\text{C}_4\text{H}_9\text{COO}^-$	496	335	298	260	236
0.5	HCOO^-	280	210	185	171	157
	CH_3COO^-	264	202	179	161	150
	$\text{C}_2\text{H}_5\text{COO}^-$	286	222	192	176	160
	$\text{C}_3\text{H}_7\text{COO}^-$	315	254	215	194	176
	$\text{C}_4\text{H}_9\text{COO}^-$	442	322	284	256	228
0.33	HCOO^-	273	203	181	168	155
	CH_3COO^-	250	196	170	161	148
	$\text{C}_2\text{H}_5\text{COO}^-$	274	217	185	171	158
	$\text{C}_3\text{H}_7\text{COO}^-$	304	250	204	192	172
	$\text{C}_4\text{H}_9\text{COO}^-$	422	310	275	245	226
0.0	HCOO^-	235	194	174	159	147
	CH_3COO^-	230	172	166	155	144
	$\text{C}_2\text{H}_5\text{COO}^-$	250	200	180	168	156
	$\text{C}_3\text{H}_7\text{COO}^-$	279	218	202	181	171
	$\text{C}_4\text{H}_9\text{COO}^-$	385	302	268	241	223

3. Data processing

3.1. Principal component analysis

The retention times $t_{i,j}$ for every ion (i) studied with j eluents vary by a factor of 2–3 (Table 1).

The matrix of the normalized retention times $[D]$ was submitted to PCA [3] to calculate the row and column vectors, R_k and C_k , respectively, in order to recalculate $[D]$ as

$$[D] = \sum_1^k R_k C_k$$

where k is the number of abstract factors in the new and reduced hyperspace.

3.2. Correspondence factor analysis

With the original data matrix, a new matrix X_{ij} was constructed which was formed with the elements $x_{i,j}$ [7,18,19]:

$$x_{i,j} = \frac{t_{i,j} - t_{i.}t_{.j}}{\sqrt{(t_{i.}t_{.j})}}$$

where

$$t_{i.} = \sum_{j=1}^{j=p} t_{i,j} \quad \text{and} \quad t_{.j} = \sum_{i=1}^{i=n} t_{i,j}$$

Then the variance data matrix was calculated in order to determine the set of eigenvalues and the related eigenvectors.

The symmetrical role of the variables i and j must be emphasized [7]. It allows the superposition on the same graph of the projections of the row-points in the reduced hyperspace of the columns and, reciprocally, the projections of the column-points in the reduced hyperspace of the rows.

4. Results and discussion

The retention times of the five carboxylate ions, given in Table 1, follow regular trends:

(i) For the same ionic strength, the retention time of the carboxylate ions increases with R varying from Me to n -Bu.

(ii) The retention time of the formate ion is between those for acetate and propionate ions. It is outside the relatively regular deviation of the retention time as is often seen with the first member of a series.

(iii) With increase in the concentration of carbonate eluents C , all the carboxylate ions follow a classical trend, *i.e.*, a decrease in their retention time. This is accompanied simultaneously by a decrease in the amplitude of the variation between the less retained acetate ion and the more retained ion, pentanoate. A simultaneous decrease in the selectivity between any pair of given compounds is also observed.

(iv) For a given value of C , a decrease in the ratio Z of the carbonate eluents, which corre-

sponds to a relative increase in the concentration of the Na_2CO_3 eluent, induces a decrease in all the retention times. This decrease is similar to the preceding one, but with a lower sensitivity. With the previous decrease in Z , which induces a decrease in the retention times, the selectivity between given pairs of the carboxylate ion, with $R = \text{Me}$ up to n -Bu, remains relatively constant in most instances, but not all.

(v) Variations of selectivity between pairs of carboxylate ions are more sensitive to variations of the C term than to the Z term.

(vi) Nevertheless, when looking at relative decreases in retention data when C increases for the same Z value and the same ion, or when comparing the evolution of selectivity for a given ion pair when Z decreases for the same C value, more subtle variations are seen outside the above general trends. This motivated a more quantitative examination of the experimental results, on a statistical basis, *i.e.*, with multivariate analysis.

4.1. Principal component analysis

To obtain an overall view of the main trends governing the retention, the data set was configured as the data matrix presented in Table 2, and submitted to PCA. This second matrix has i rows corresponding to the combination of the C and Z terms and j columns corresponding to the carboxylate ions. Within the estimated experimental errors ($\pm 2\%$), only one main factor is necessary to calculate the retention times. This simple relationship suggests that only a major retention mechanism is responsible for the observed retention times. This is in agreement with the relatively regular trends mentioned previously when considering the retention times, *i.e.*, the fairly good proportionality between the behaviour of the different carboxylate ions.

4.2. Correspondence factor analysis

In a second step, to analyse the secondary-order effects on retention, which are hidden by the above classical effect of the carbonate eluent concentrations, a CFA was undertaken. The

Table 2

First reorganization of the original IC retention data matrix of the carboxylate ion for the CFA study

Label	Z	C	HCOO ⁻	CH ₃ COO ⁻	C ₂ H ₅ COO ⁻	C ₃ H ₇ COO ⁻	C ₄ H ₉ COO ⁻
1	3.0	0.2	Retention times as in Table 1				
2	3.0	0.4					
3	3.0	0.6					
4	3.0	0.8					
5	3.0	1.2					
6	1.0	0.2					
7	1.0	0.4					
8	1.0	0.6					
9	1.0	0.8					
10	1.0	1.2					
11	0.5	0.2					
12	0.5	0.4					
13	0.5	0.6					
14	0.5	0.8					
15	0.5	1.2					
16	0.33	0.2					
17	0.33	0.4					
18	0.33	0.6					
19	0.33	0.8					
20	0.33	1.2					
21	0.00	0.2					
22	0.00	0.4					
23	0.00	0.6					
24	0.00	0.8					
25	0.00	1.2					

The carboxylate ions correspond to the column of this new matrix. The rows of this matrix correspond to the combination of the Z and C terms.

original experimental data matrix (Table 1) was modified in the form of a second matrix, given in Table 2, to make a better distinction between the variables corresponding to the composition of the eluent and the variables corresponding to the considered carboxylate ions.

This modified matrix was submitted to CFA. The row-points (the C and Z combinations) and the column-points (the studied anions) are projected simultaneously on the first factorial plane, defined by the axes 1 and 2 in Fig. 1, and which represents 78% of the information content. These axes 1 and 2 correspond to 44% and 34%, respectively, of the total information content. The relative behaviour of the carboxylate ions and the relative influences of the eluents are clearly taken into account by this first factorial plane.

On this map, we have drawn five clusters

where the projected row-points correspond to the same value of the eluent concentration C. The five clusters are ordered along the second bisector with a progressive increase from C = 0.2, in the left corner of the graph, up to C = 1.2, in the right corner. The dispersion of the row-points inside these clusters also shows the simultaneous and different contributions of the Z ratio according to the considered C values. A higher dispersion of the row-points for clusters C = 0.2 and 0.4 is observed. This is related to the higher selectivity at these lower C values, *i.e.*, at this lower ionic strength.

The projections of the five anions according to axis 1 go from the right side, with CH₃COO⁻, up to the left side, with C₄H₉COO⁻. Even if the behaviour of the carboxylate ions, for example, through modification of the selectivity of the chromatographic system, could be dependent on

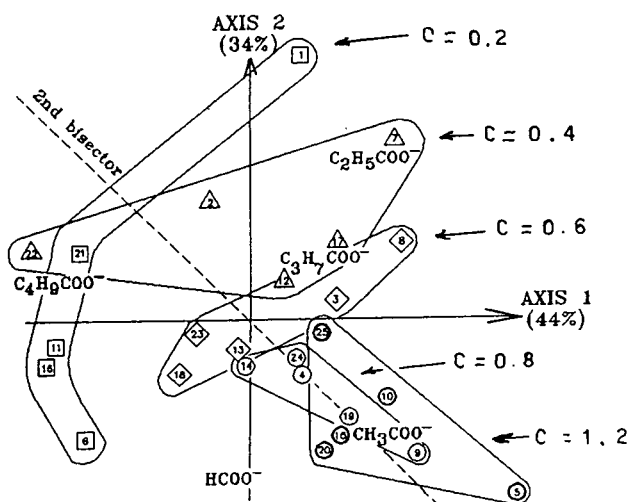


Fig. 1. CFA map of the five carboxylate ions studied with 25 chromatographic systems. The carboxylate ions correspond to the columns and the chromatographic systems to the rows of the considered data matrix (cf., Table 2). Simultaneous projection of the carboxylate ions and chromatographic systems on the first factorial plane defined by axes 1 and 2. The clusters delineate the different concentrations C of the eluents. The points inside these clusters correspond to the different Z values, from $Z=0$ up to 3.0.

the length of the alkyl chain, no special regularities can be seen according to axis 1 or 2. This suggests that the contribution of the alkyl chain to the retention mechanism is not simple.

The original data matrix was reorganized according to Table 3 to give a third matrix, with an organization only slightly different, from Table 1, for the row-points. Now, the columns correspond to the concentrations of the eluent, from $C=0.2$ up to 1.2. The rows correspond to the different carboxylate ions with their various values of the Z ratio, from 0 up to 3.

The simultaneous projections of the column-points and row-points are given in Fig. 2. Axes 1 and 2 represent 88% and 8% of the information content, respectively. The first factorial plane now represents 96% of the total information content. (This time, axis 1 corresponds to a more evident main axis of inertia.)

All the column-points and row-points are ordered regularly according to axis 1. Five clusters can also be delineated but for similar Z

Table 3
Second reorganization of the original IC retention data matrix of the carboxylate ion for the CFA study

Label	Ion	Z	C				
			0.2	0.4	0.6	0.8	1.2
1	HCOO ⁻	3.0	} Retention times as in Table 1				
2		1.0					
3		0.5					
4		0.33					
5		0.00					
6	CH ₃ COO ⁻	3.0					
7		1.0					
8		0.5					
9		0.33					
10		0.00					
11	C ₂ H ₅ COO ⁻	3.0					
12		1.0					
13		0.5					
14		0.33					
15		0.00					
16	C ₃ H ₇ COO ⁻	3.0					
17		1.0					
18		0.5					
19		0.33					
20		0.00					
21	C ₄ H ₉ COO ⁻	3.0					
22		1.0					
23		0.5					
24		0.33					
25		0.00					

The rows correspond to the carboxylate ions, from HCOO⁻ up to C₄H₉COO⁻, eluted with different Z ratios, from $Z=3.0$ to $Z=0$. The columns of this new matrix correspond to the C terms.

values, from $Z=3$ on the left of the graph up to $Z=0$ on the right. Simultaneously, the column-points are ordered also according to axis 1, but in the opposite increasing order, from $C=0.2$ on the left up to $C=1.2$ on the right of the graph. Each sub-series of row-points corresponding to the same carboxylate ion, with its different Z values, is stretched all along axis 1.

4.3. Selectivity of eluents

The selectivity of eluents appears when the projection of the row-points is examined through

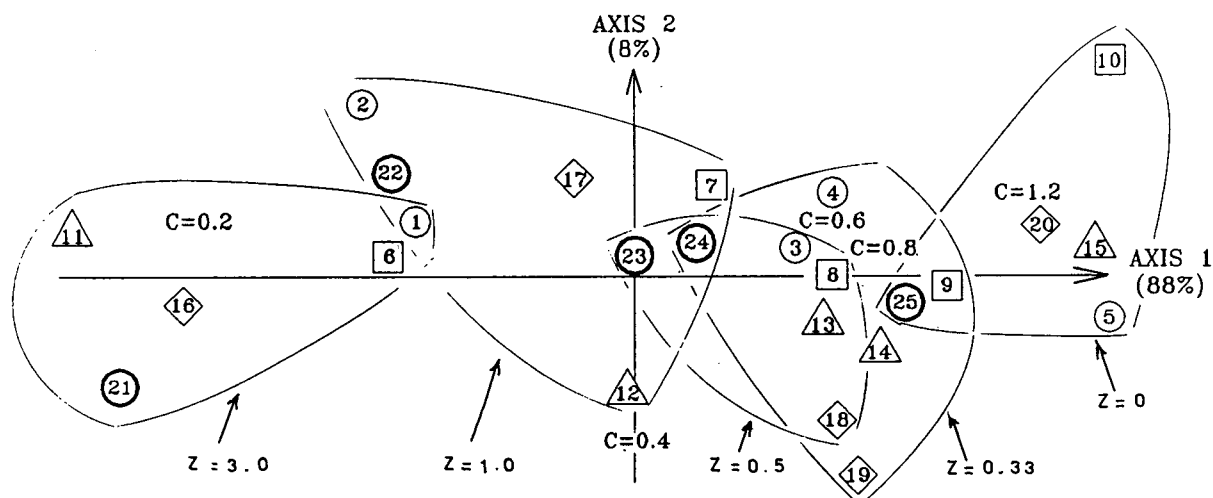


Fig. 2. CFA map of the data matrix where the columns are the concentrations of the eluents (C) and the rows are the five carboxylate ions studied with five different Z values of the ratio of carbonated species. Labels are given in Table 3. Each series of carboxylate ions constitutes HCOO^- (\circ), CH_3COO^- (\square), $\text{C}_2\text{H}_5\text{COO}^-$ (\triangle), $\text{C}_3\text{H}_7\text{COO}^-$ (\diamond) and $\text{C}_4\text{H}_9\text{COO}^-$ (\circ). The clusters delineate the different Z values. The points inside these clusters correspond to the behaviour of the five anions studied at this Z value (cf., Table 3).

the projection of the concentration of the eluents.

To explain the specific selectivity of the eluents, we selected two carboxylate ions, HCOO^- and $\text{C}_3\text{H}_7\text{COO}^-$, and the selectivity was calculated as the ratio of the capacity factors of these two ions. To clarify the projections, we hide all row-points corresponding to the other three carboxylate ions, CH_3COO^- , $\text{C}_2\text{H}_5\text{COO}^-$ and $\text{C}_4\text{H}_9\text{COO}^-$. Then the selectivity between the pairs of points 1–16, 2–17, 3–18, 4–19 and 5–20 corresponding to the values of $Z = 3.0$, 1.0, 0.5, 0.33 and 0.0, respectively, at five levels of concentration, are calculated. The results are given Fig. 3. It has been demonstrated [14] that the selectivity can be estimated on CFA maps. The selectivity is measured as the distance between the projection of the row-points considered on the axis defined by a chromatographic system and the origin of the axes. A consequence of this method is that the best chromatographic system, able to separate two compounds, is the one which is projected near the two compounds. This consequence is shown in Fig. 3. For example, points 5 and 20 are separated with the best selectivity, equal to 1.45, when the

concentration of the eluent is high, equal to 1.2. Effectively, both points are projected near the column-point $C = 1.2$. In the same manner, the highest selectivities between the points 2–17 and 3–18 are obtained with low concentrations of the eluent, $C = 0.2$ and 0.4, respectively. These points are projected near column-points $C = 0.2$ and 0.4, respectively.

With the pairs 1–16 and 4–19, the analysis of the selectivity is more complex. Compounds 1 and 4 are far from compounds 16 and 19. Each pair defines a direction that has two components, one along axis 1 and the other along axis 2. The column-point $C = 0.4$ projected on axis 2 defines a direction along axis 2. Hence the column-point gives a good selectivity for the separation of the pairs 1–16 and 4–19. The first conclusion is that pair 1–16 is separated with an equal selectivity with eluents projected along axes 1 and 2. Second, for the pair 4–19, the best selectivity is obtained with a concentration of the eluent $C = 0.4$. The selectivity is a function of both C and Z terms. With a high value of the Z terms the selectivity is better when the concentration is kept to a low value, and *vice versa*.

The CFA maps (Figs. 2 and 3) give simulta-

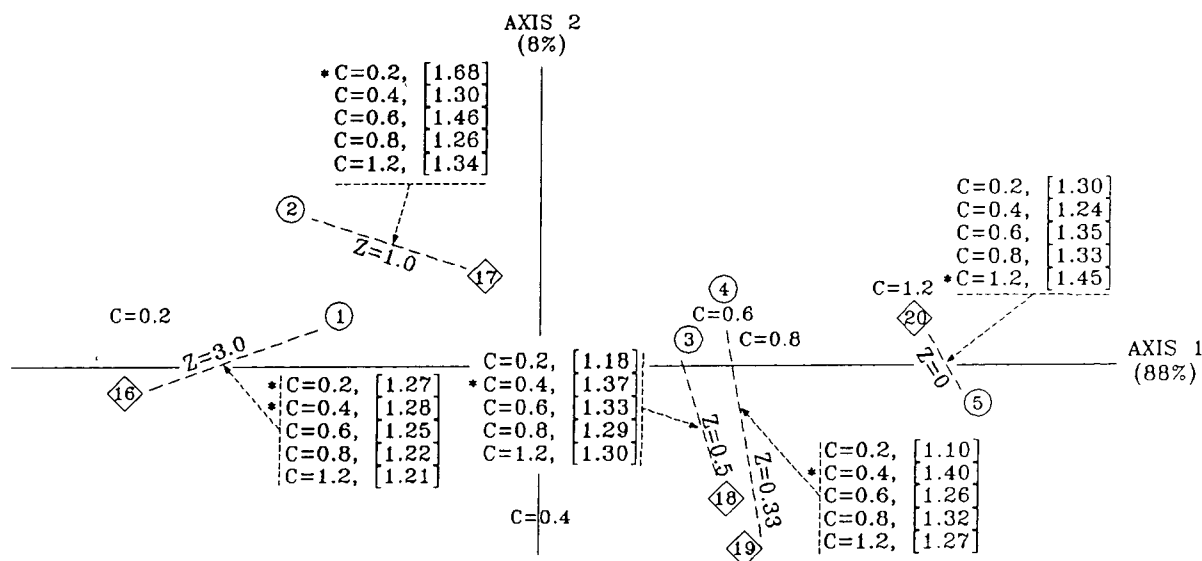


Fig. 3. Partial CFA map used for optimization. The complete CFA map is given in Fig. 2. The carboxylate ions are limited to HCOO^- (○) and $\text{C}_3\text{H}_7\text{COO}^-$ (◇). The projections of the other carboxylate ions are hidden. The values of the selectivity obtained with different values of the concentration of the eluent (C) are given in brackets. The asterisks indicate the C terms that induce the best selectivity.

neous representations of the variation of the retention times and the selectivity *versus* the concentration of the eluent.

5. Conclusions

In a general way, factor analysis applied to the study of large matrices of retention data can be a valuable tool for the chromatographer. Evidently, it is only a means of revealing the information content nested in the data matrix. Part of this information content can be evident to a well trained chromatographer. However, the main interest is in offering a quantitative analysis of the information content on a statistical basis. Further, it could be a valuable method to reveal hidden factors that can be important from a mechanistic or optimization point of view.

PCA helps to model the retention times. The fact that only one PCA factor is necessary for calculating the retention time of each carboxylate ion, with its mean retention time, suggests that only one main retention mechanism is responsible for the measured retention times.

This mechanism is most probably an ion-exchange equilibrium.

Keeping this in mind, one should ask why anions with a higher n value in $\text{H}(\text{CH}_2)_n\text{COO}^-$ are more retained. It should be noted that all the carboxylic acids studied have pK values in the range 3.75–4.86, *i.e.*, they are all completely ionized in the carbonate eluents applied. If only one main retention mechanism is taking place, it does not mean that it is a simple one. Further, it rules out, with a high probability, the possibility of the anions having a longer aliphatic chain being retained, on the chromatographic column, by a specific mechanism, independent of the main mechanism. The hydrophobic effect of the aliphatic group in the anions studied could certainly be involved [20]. This hydrophobic effect increases with increasing chain length. This “structure-making” effect causes an additional stabilization for the resin-linked anions $\text{H}(\text{CH}_2)_n\text{COO}^-$ because the resin surface itself is probably also a “structure maker”. The result of such stabilization is an increase in the concentration of resin-linked anions, which in turn leads to longer retention times for the anions

with a more pronounced “fatty” character, *i.e.*, with higher values of n . The HCOO^- ions are not “structure makers” but “structure breakers”; therefore, they are outside a regular evolution of the retention with increasing value of n .

An analysis of trends of effects acting, at a second-order level, on this main mechanism are delineated by CFA. This method gives a more in-depth data analysis of the experimental data matrix [21]. This analysis shows how the concentrations of carbonate eluents modify, relatively, both the retention times and the selectivity of the chromatographic system. The selectivity is a function of the C and Z terms. Even if the mechanism of retention, *i.e.*, the roles of NaHCO_3 and Na_2CO_3 and of the alkyl chain on the modification of the selectivity, is explained only qualitatively, such approaches could be useful for optimizing the separation of various mixtures of carboxylate ions by IC.

6. References

- [1] R. Kalizsan, *Quantitative Structure–Chromatographic Retention Relationships* (Chemical Analysis, Vol. 93), Wiley, New York, 1987.
- [2] J.R. Chrétien, *Trends Anal. Chem.*, 6 (1987) 275–278.
- [3] E.R. Malinowski and D.G. Howery, *Factor Analysis in Chemistry*, Wiley, New York, Chichester, 1980, pp. 50–99.
- [4] P.H. Weiner, J. Dack and G. Howery, *J. Chromatogr.*, 69 (1972) 249–260.
- [5] D.G. Howery, *Anal. Chem.*, 46 (1974) 829.
- [6] M. Chastrette, *J. Chromatogr. Sci.*, 14 (1976) 357–359.
- [7] R.F. Hirsch, R.J. Gaydosh and J.R. Chrétien, *Anal. Chem.*, 52 (1980) 723–728.
- [8] K. Szymoniak and J.R. Chrétien, *J. Chromatogr.*, 404 (1987) 11–12.
- [9] J.R. Chrétien, M. Righezza, A. Hassani and B.Y. Meklati, *J. Chromatogr.*, 609 (1992) 261–267.
- [10] R.M. Smith, *Anal. Chem.*, 56 (1984) 256–262.
- [11] T. Cserhati, *J. Chromatogr. Sci.*, 29 (1991) 210–216.
- [12] B. Walczak, L. Morin-Allory, M. Lafosse, M. Dreux and J.R. Chrétien, *J. Chromatogr.*, 395 (1987) 183–202.
- [13] M. Righezza and J.R. Chrétien, *J. Chromatogr.*, 544 (1991) 393–411.
- [14] M. Righezza and J.R. Chrétien, *J. Chromatogr.*, 556 (1991) 169–180.
- [15] J.S. Fritz, D.T. Gjerde and C. Pohlandt, *Ion Chromatography*, Hüthig, Heidelberg, 1982, pp. 84–143.
- [16] U. Haldna, R. Palvadre, J. Pentshuk and T. Kleemeier, *J. Chromatogr.*, 350 (1985) 296–298.
- [17] G. Malmquist and N. Lundell, *J. Chromatogr.*, 627 (1992) 107–124.
- [18] J.P. Benzécri, *L'Analyse des Données*, Vol. 2, Dunod, Paris, 1973.
- [19] L. Lebart and J.P. Fenelon, *Statistique et Informatique Appliquées*, Dunod, Paris, 1975.
- [20] T. Erdey-Gruz, *Transport Phenomena in Aqueous Solution*, Akadémiai Kiadó, Budapest, 1974, p. 74.
- [21] M. Righezza and J.R. Chrétien, *Chromatographia*, 36 (1993) 125–129.



ELSEVIER

Journal of Chromatography A, 670 (1994) 59–66

JOURNAL OF
CHROMATOGRAPHY A

Determination of amino acids by precolumn derivatization with 6-aminoquinolyl-N-hydroxysuccinimidyl carbamate and high-performance liquid chromatography with ultraviolet detection

Hong Ji Liu

Waters Division of Millipore China Ltd., 1101-6 Asia Pacific Building, No. 8, Ya Bao Road, Chao Yong District, Beijing, China

(First received November 17th, 1993; revised manuscript received January 31st, 1994)

Abstract

A precolumn derivatization method for the determination of amino acids using 6-aminoquinolyl-N-hydroxysuccinimidyl carbamate (AQC) followed by high-performance liquid chromatography is described. Ultraviolet detection was used for the assay of AQC derivatives of amino acids with the detection wavelength set at 248 nm. The reagent peak interference was minimized by optimizing the pH of the eluent and the gradient elution profile to improve the resolution between the reagent peak and amino acid derivatives. All nineteen amino acids were separated in 35 min with resolutions ≥ 1.6 . The correlation coefficients of the calibration graphs for seventeen amino acids were fairly good ($r \geq 0.9999$) at concentrations of 25–500 μM . The detection limits for all common amino acids including cystine and tryptophan were at the range 0.07–0.3 pmol. Good reproducibility and accuracy of the method were demonstrated by the determination of amino acids in three typical kinds of samples (protein, peptide and feed). The average relative standard deviations for bovine serum albumin (BSA) and neuromedin were 0.86% and 1.36, respectively, and the average relative errors were 3.2% and 2.3%, respectively. The results of the analysis of feed hydrolysates agreed with those obtained by an ion-exchange method and the average recovery of the method for feed hydrolysates was 98%.

1. Introduction

Since it was found that amino acids are basic elements of proteins, the separation and determination of amino acids has become very important to those interested in protein studies. Liquid chromatography (LC) is now the most widely used technique for such determinations. The two types of LC systems used are the postcolumn and precolumn derivatization methods, respectively. The former is characterized by

an ion-exchange separation mechanism and post-column derivatization with ninhydrin. Since it was developed by Spackman *et al.* [1] in 1958, this method has been used for amino acid determinations in a wide variety of samples and has become a classical method because of its accuracy, reproducibility and automation. However, some disadvantages such as long run times, low sensitivity and high instrument expense make this postcolumn derivatization method unsuitable in many instances.

Since the 1970s, reversed-phase high-performance liquid chromatography has been used for the isolation of precolumn-derivatized amino acids and many reagents [2–5] have been used for derivatization. Speed, sensitivity and flexibility are the main advantages of the precolumn strategy over the postcolumn one approach. However, all the precolumn derivatization reagents have various weaknesses which make precolumn methods labour-intensive or the reproducibility and accuracy are not good enough for amino acid analyses.

Recently, Cohen and Michaud [6] developed a precolumn derivatization method in which a novel reagent, 6-aminoquinolyl-N-hydroxysuccinimidyl carbamate (AQC), was used for amino acid derivatization. AQC can react quantitatively with all primary and secondary amino acids in a few seconds with little matrix interference and single and very stable derivatives are formed. Fluorescence detection was applied with excitation at 250 nm and emission at 395 nm, which allowed for direct injection of the reaction mixture because of the 60-nm blue shift of the wavelength of amino acid derivatives compared with 6-aminoquinoline (AMQ), the hydrolysate of AQC [6]. As the 6-aminoquinolyl derivatives of amino acids have very strong ultraviolet (UV) absorbance, UV detection can also be used for the determination of AQC-derivatized amino acids provided that the huge reagent peak does not interfere with the isolation of the amino acid derivatives. The purpose of this study was to develop a UV detection method for AQC-derivatized amino acids by modifying the chromatographic conditions described by Cohen and Michaud [6].

2. Experimental

2.1. Materials

Analytical-reagent grade chemicals were used unless indicated otherwise and ultrapure water was generated using a Milli-Q water purification system (Millipore, Milford, MA, USA).

The derivatization reagent kit (AQC, 0.2 M

borate buffer and DNA-grade acetonitrile) was obtained from Millipore. Phosphoric acid, hydrochloric acid and phenol were purchased from Wako (Osaka, Japan). Amino acid standard was purchased from Pierce (Rockford, IL, USA). Bovine serum albumin (BSA) was purchased from Pharmacia (Uppsala, Sweden). Neuromedin was supplied by Millipore. Sodium acetate, Triethylamine, Acetonitrile (HPLC grade) and ethylenediaminetetraacetic acid disodium salt (EDTA) were all local products. Sodium azide was obtained from Farco Chemical Supplies (Hong Kong).

2.2. Apparatus

Two HPLC systems from Millipore were used. System 1 consists of two Model 510 pumps, a Model M717 autosampler, a Waters Model 486 tunable absorbance detector or a Waters Model 996 photodiode-array detector and a temperature control module. System 2 was a Waters LC Module 1 system with a column heater option. Millennium 2010 Chromatography Manager was connected with the systems for data acquisition and management.

2.3. Sample hydrolysis and derivatization

Approximately 14.3 μg of BSA and 2 μg of neuromedin (a synthesized basic peptide containing eight amino acid residues) were hydrolysed using the following standard gas-phase hydrolysis procedure. An aliquot of sample was pipetted into the bottom of a 6 \times 50 mm tube and dried under vacuum. A 200- μl volume of 6 M HCl containing 0.5% phenol was placed in the bottom of a vacuum vial and then the tube was inserted into the vial. The vial was sealed under vacuum after three alternate vacuum–nitrogen flushing steps. Hydrolysis was then carried out at 115°C for 24 or 42 h. Feed samples were hydrolysed using the liquid-phase hydrolysis protocol as follows. A 59-mg amount of feed powder was added to 10 ml of 6 M HCl and hydrolysed for 24 h. After filtration through a 0.45- μm Millex-HV filter (Millipore), the hydrolysate was diluted with ultrapure water to a

concentration of approximately 1.5 mg/ml of amino acids and 10 μ l of the diluted solution were pipetted into a 6 \times 50 mm tube. After drying under vacuum, all these protein, peptide and feed hydrolysates were reacted with AQC using the procedure optimized by Cohen and Michaud [6].

2.4. Chromatographic conditions

Both systems were operated under the same chromatographic conditions: eluent A concentrate was prepared as described by Cohen and Michaud [6] except that the pH was lowered to 4.95 from 5.05 and that 0.01% of sodium azide was present in the concentrate to protect the buffer from bacterial growth. The working eluent A was prepared by mixing 100 ml of the concentrate with 900 ml of water. Eluent B was acetonitrile–water (60:40, v/v) containing 0.01% acetone. A 4- μ m AccQ-Tag C₁₈ column (150 mm \times 3.9 mm I.D.) was connected to the systems with the temperature controlled at 37°C. The gradient condition were as follows: initial, 100% A; 17 min, 93% A; 21 min, 90% A; 32 min, 66% A (all linear). After a 1-min hold, the column was washed with 100% eluent B for 3 min and then re-equilibrated with 100% A for 7 min. The run time (injection-to-injection) was 45 min. The flow-rate was maintained at 1 ml/min over the whole gradient.

3. Results and discussion

3.1. Improvement of the separation of amino acid derivatives and reagent peak

Many previous precolumn derivatization methods for amino acid determinations suffered from interference from excess of reagent because it has similar absorbance or fluorescence emission properties to those of the derivatives, so extra steps, *e.g.*, vacuum or extraction, had to be taken to remove the excess of reagent after derivatization. With AQC using fluorescence detection [6], the reagent interference was minimal because the resolution between the reagent

peak (AMQ) and Asp, the fastest eluted amino acid, was sufficient for accurate determination of Asp as the AMQ peak was small and 1.8 min from that of Asp. A 1.8-min separation was not sufficient, however, if the fluorescence detector was replaced with a UV detector under the same chromatographic conditions because AMQ and its amino acid derivatives gave very similar UV absorbances so the reagent peak was huge one compared with those of the amino acid derivatives and the Asp peak would be eluted before the AMQ peak had returned to the baseline. This problem was especially serious when highly sensitive analysis was required: the small Asp peak was eluted on the tail of the reagent peak, which made accurate integration of the Asp peak difficult. Hence the resolution between these two peaks had to be increased before UV detection method could be applied. In this study, the separation between the AMQ and Asp peaks was improved in two ways: by lowering the pH of buffer A or by making the gradient shallower.

As AMQ is basic and Asp is acidic, AMQ would be eluted faster and Asp more slowly as the pH of mobile phase A decreased. Fig. 1 shows that when the pH of eluent A was lowered to 4.90 from 5.05, the distance between the two peaks increased sharply from 1.8 to 3.3 min. Considering that lowering the pH could worsen the resolution of the Asp–Ser and Glu–Gly pairs

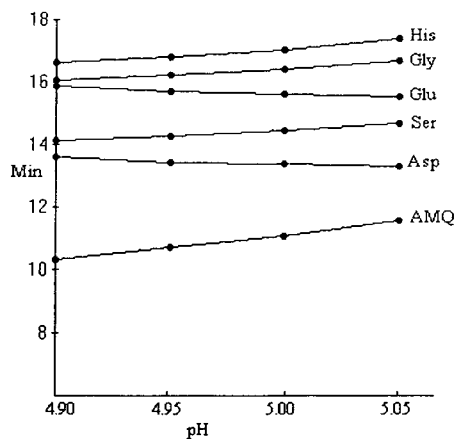


Fig. 1. Effect of pH of mobile phase A on retention time of AMQ and other early-eluted amino acids. Gradient conditions as described in ref. 6.

and that the separation between Glu and Gly would become unacceptable if the pH was lowered to 4.90, 4.95 was chosen as the final pH of mobile phase A. Another approach, namely making the elution gradient shallower, was also tried as the 2.7 min distance between the AMQ and Asp peaks was still unsatisfactory for the analysis of samples with low Asp concentrations. Under the final gradient conditions adopted, AMQ was isolated 3.4 min away from Asp on both systems and all other amino acids were separated from each other with a resolution larger than 1.6 (Fig. 2). It could be expected that as little as 10 pmol or less of Asp could still be determined accurately (Fig. 2b) because of the lack of reagent interference, which apparently was impossible when UV detection was applied

under the fluorescence chromatographic conditions [6]. The purpose of adding acetone to eluent B was to eliminate the baseline drift of the chromatogram caused by eluent A having a stronger UV absorbance than eluent B.

The reproducibility of the responses of seven replicate analyses of derivatives of amino acid standards is shown in Fig. 3. Among all eighteen amino acids, methonine, one of the most unstable amino acids, displayed the highest relative standard derivation (R.S.D.) of 2.3%; for Asp, because of its distance from the reagent peak, the R.S.D. was 0.99%, below the average value for all the amino acids.

3.2. UV absorbance properties of AQC-amino acid derivatives

The maximum absorbance wavelengths (λ_{\max}) of all the AQC-derivatized amino acids were 248 nm with the exception of cystine and Lys, the two disubstituted derivatives with AQC, with λ_{\max} 243 nm. The λ_{\max} of AMQ was 257 nm, so 248 nm was chosen as the detection wavelength to increase the detection sensitivity of the method and to decrease the response of the reagent peak.

3.3. Compositional analysis of BSA and neuromedin

Some data have been reported [6] to demonstrate the accuracy of the AQC derivatization method with fluorescence detection for the determination of amino acids. However, this is the

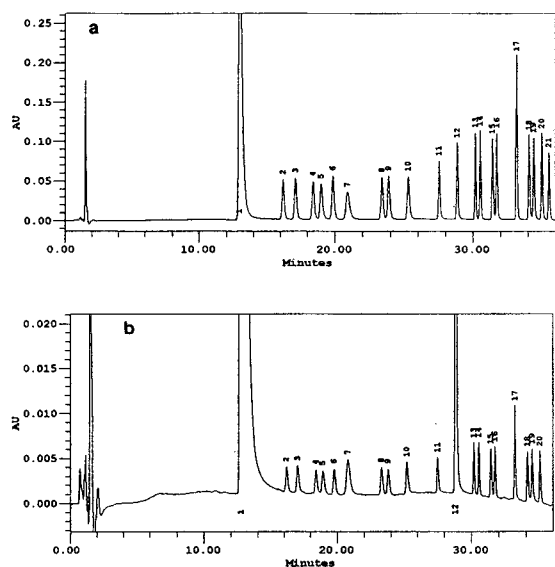


Fig. 2. Chromatogram of AQC derivatives with amino acid standard containing nineteen amino acids. Derivatization procedure: (1) 70 μ l of 0.2 M borate buffer added to 10 μ l of amino acid solution and vortex mixed; (2), 20 μ l of 3 mg/ml AQC solution in acetonitrile added and vortex mixed immediately for 2 s; (3) derivatized sample transferred into an autosampler vial; (4) vial heated for 10 min at 55°C. Volumes of 5 μ l of the derivatized samples were injected. Amount injected: (a) 250 and (b) 12.5 pmol. Peaks: 1 = AMQ; 2 = Asp; 3 = Ser; 4 = Glu; 5 = Gly; 6 = His; 7 = NH₃; 8 = Arg; 9 = Thr; 10 = Ala; 11 = Pro; 12 = α -aminobutyric acid (AABA); 13 = cystine (Cys2); 14 = Tyr; 15 = Val; 16 = Met; 17 = Lys; 18 = Ile; 19 = Leu; 20 = Phe; 21 = Trp.

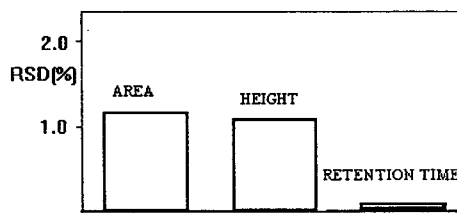


Fig. 3. Average R.S.D. bar plot for seven replicate analyses of derivatized amino acid standard. Seven aliquots of amino acid standards containing 5 nmol of each amino acid were derivatized and analysed under the same conditions. A 250 pmol amount of each sample was injected.

first report in which AQC-derivatized amino acids were determined with UV absorbance detection, so it was necessary to conduct more experiments to investigate the accuracy of the method with UV detection as it is less selective than fluorescence detection. Fig. 4 shows the chromatograms of BSA and neuromedin hydrolysates. It is interesting that the two minor reagent-related interference peaks mentioned in ref. 6 were not found in the chromatograms with UV detection even on a very sensitive scale (Fig. 4c), which suggests that negligible interference from these two peaks could be expected in the UV detection method.

Table 1 summarizes the composition of BSA

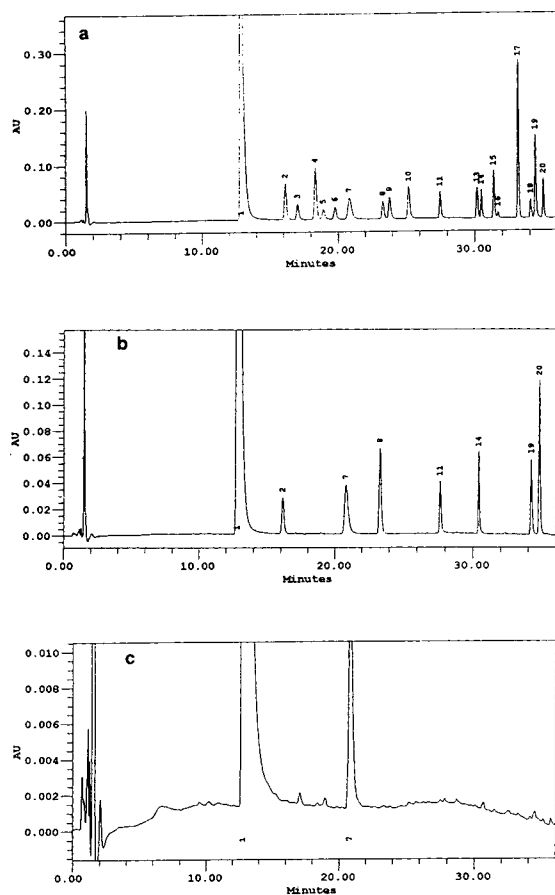


Fig. 4. Chromatograms of derivatives of amino acids in (a) BSA and (b) neuromedin hydrolysates and (c) hydrolysis blank. One twentieth of the derivatized amount was injected. Injection volume, 5 μ l. Peaks as in Fig. 1.

samples and Table 2 gives the results for neuromedin. The average R.S.D. for five replicate analyses of BSA and neuromedin samples were 0.86% and 1.36%, respectively, which, resulting from the stability of the derivatized amino acids, are comparable to those for any techniques for amino acid determination including the post-column method. The average relative errors of the results were also good. The two largest errors in BSA sample analysis were for Met and Gly, a possible reason for which is background contamination. Another reason for the error for Met is its relative smaller residue number in BSA as compared with other amino acids. Ser and Thr are degraded during hydrolysis. Because of the easy dehydration, the recovery of Ser was 70–90% and that of Thr was 85–95%. Correction of the data for these two amino acids for the losses during hydrolysis were made by hydrolysing the protein for different times and extrapolating to zero time. Because the compositional results for BSA after hydrolysis for 42 h were 19.44 for Ser and 27.81 for Thr (normalized to Val), the corrected results were 27.35 for Ser and 34.58 for Thr, which were comparable to the sequence of BSA. After correction the average relative error of the calculated composition was 3.2%.

3.4. Determination of amino acids in feed hydrolysates

The chromatographic profile of AQC-derivatized amino acids in feed hydrolysates is shown in Fig. 5. Table 3 summarizes the results obtained with the proposed method and also for the

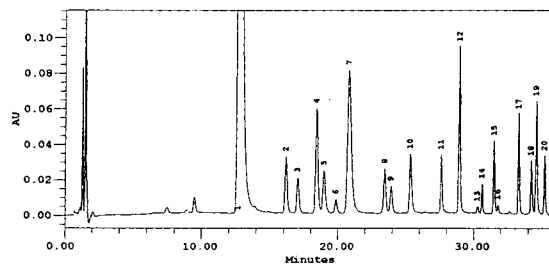


Fig. 5. Chromatogram of amino acids in feed hydrolysate. One twentieth of the derivatized amount was injected. Injection volume, 5 μ l. Peaks as in Fig. 1.

Table 1
Determination of composition of five replicated BSA samples

Amino acid	Sequence of BSA	Calculated composition ^a (average, <i>n</i> = 5)	R.S.D. (%)	Error (%)
Ala	46	45.66	0.9	−0.74
Arg	23	22.95	0.53	−0.22
Asp	54	54.41	1.45	0.75
Glu	79	79.78	0.81	0.99
Gly	16	18.13	2.52	13.31
His	17	16.85	0.53	−0.86
Ile	14	14.00	0.46	0.00
Leu	61	59.64	0.29	−2.23
Lys	59	57.93	1.29	−1.81
Met	4	4.75	0.64	−1.81
Phe	27	27.23	0.56	0.84
Pro	28	28.47	0.53	1.53
Ser	28	22.83	1.6	−18.46
Thr	34	30.71	0.41	−9.68
Tyr	19	19.98	1.31	5.16
Val	36	36	0.00	0.00

Five aliquots of BSA samples were hydrolysed for 24 h and then analysed under the same conditions.

^a All data were normalized to Val without correction for losses during hydrolysis.

Table 2
Determination of composition of five replicate neuromedin samples

Amino acid	Sequence	Calculated composition ^a (average, <i>n</i> = 5)	R.S.D. (%)	Error (%)
Asp	1	1.041	1.40	4
Arg	2	2.062	1.40	3.1
Pro	1	1.051	2.10	5.1
Tyr	1	0.998	2.20	−0.2
Leu	1	1	0.00	0
Phe	2	2.026	1.10	1.3

Five aliquots of neuromedin sample were hydrolysed for 24 h and then analysed under the same conditions.

^a All data were normalized to Leu without correction for losses during hydrolysis.

analysis of the same vial of sample with an ion-exchange method performed on a Hitachi 835 amino acid analysis system. The two sets of data agree fairly well. The precolumn method data (Data 1) were calculated by internal calibration method with AABA as internal standard. External calibration was also tested for the analysis of the same sample and the two sets of data were almost identical (not shown), which suggested that the complex matrix of the feed

hydrolysate had a minimal effect on the yield of the derivatization reaction. The reproducibility of the results with the internal calibration method, however, was generally better than that with external calibration (Table 4).

Another validation test for the accuracy of the method was done by measuring a known amount of amino acid standard added to the feed hydrolysate. The average recovery was about 98% (Table 5).

Table 3

Comparison of results for feed hydrolysate obtained using the proposed method (Data 1) and an ion-exchange method (Data 2)

Amino acid	Data 1 (mg per 100 mg feed)	Data 2 (mg per 100 mg feed)	Data 1/Data 2
Ala	1.85	1.76	1.05
Arg	2.65	2.25	1.17
Asp	2.92	2.74	1.07
Glu	6.09	5.9	1.03
Gly	1.38	1.27	1.09
His	0.746	0.75	0.99
Ile	1.28	1.38	0.93
Leu	2.63	2.69	0.98
Lys	1.36	1.37	0.99
Pro	1.74	1.58	1.1
Ser	1.41	1.36	1.04
Thr	0.95	1.12	0.85
Tyr	0.9	0.97	0.93
Val	1.61	1.73	0.93

Table 4

Comparison of reproducibilities of results for feed hydrolysates ($n = 5$)

Amino acid	R.S.D. (%)	
	Internal calibration	External calibration
Asp	0.66	2.3
Ser	1.7	2.8
Glu	0.68	1.8
Gly	1.6	2.6
His	1.4	2.5
Arg	0.4	2.1
Thr	0.29	1.5
Ala	0.64	1.6
Pro	0.34	1.8
Cys ₂	0.51	1.5
Tyr	0.33	2.2
Val	0.32	1.8
Met	4.1	2.9
Lys	0.1	2
Ile	0.17	1.9
Leu	0.1	1.9
Phe	0.73	1.5

Five aliquots of the same feed hydrolysate were derivatized and analysed. The raw data were processed with the internal and external calibration methods.

3.5. Linearity of calibration graphs and detection limits of the method

The UV detection method was not as insensitive as the fluorescence method. The detection limits for UV detection of all amino acids including cystine and Trp were in the range 0.07–0.30 pmol, as shown in Table 6, whereas for the fluorescence method they were 0.04–0.32 pmol except for cystine (0.8 pmol) and Trp (unknown) [6]. Table 6 also shows the linearity of the calibration graphs for seventeen amino acids which were obtained by analysing a series of dilutions of the standard mixture ranging from 25 to 500 μM . Most of the correlation coefficients were greater than 0.9999, which demonstrates excellent linearity of the calibrations.

4. Conclusions

Although UV detection is not as sensitive and selective as fluorescence detection, the results for BSA, neuromedin and feed samples described in this paper demonstrate that the accuracy and reproducibility of the method with AQC pre-

Table 5
Recovery of standards added to feed hydrolysate

Amino acid	Amount added (nmol)	Amount found (nmol)	Recovery (%)
Ala	1.00	1.01	101
Arg	1.00	1.12	112
Asp	1.00	0.94	94
Glu	1.00	0.93	93
Gly	1.00	1.03	103
His	1.00	0.92	92
Ile	1.00	0.97	97
Leu	1.00	0.95	95
Lys	1.00	0.97	97
Pro	1.00	1.01	101
Ser	1.00	0.94	94
Thr	1.00	0.98	98
Tyr	1.00	0.99	99
Val	1.00	0.98	98
Average			98

Table 6
Linearity of calibration graphs and detection limits of the UV method with AQC derivatization

Amino acid	Correlation coefficient	Detection limit (pmol) ^a
Asp	0.99997	0.26
Ser	0.999926	0.24
Glu	0.999976	0.29
Gly	0.999875	0.29
His	0.999941	0.26
Arg	0.999997	0.24
Thr	0.999991	0.26
Ala	0.999981	0.21
Pro	0.99998	0.19
Cys ₂	0.999965	0.06
Tyr	0.999974	0.13
Val	0.999995	0.15
Met	0.999907	0.14
Lys	0.999977	0.071
Ile	0.999986	0.13
Leu	0.999958	0.13
Phe	0.9990951	0.13
Trp	N.D. ^b	0.16

^a The detection limits were calculated from a 12.5-pmol injection and based on signal-to-noise ratio of 3 (noise level: $\pm 2 \cdot 10^{-5}$ absorbance, estimated from the baseline at 26.2–27.2 min).

^b Not determined.

column derivatization of amino acids and UV detection are similar to those with fluorescence detection and sensitive enough for the routine analysis of most kinds of amino acid samples.

5. Acknowledgements

The author thanks Dr. Liang Dong Sheng of the China National Centre for Quality Supervision and Testing of Feed for providing the feed hydrolysate and analytical results for the samples using the ion-exchange method.

6. References

- [1] D.H. Spackman, W.H. Stein and S. Moore, *Anal. Chem.*, 30 (1958) 1190–1205.
- [2] P. Lindroth and K. Mopper, *Anal. Chem.*, 51 (1979) 1667–1674.
- [3] B.A. Bidlingmeyer, S.A. Cohen and T.L. Tarvin, *J. Chromatogr.*, 336 (1984) 93–104.
- [4] S. Einarsson, B. Josefsson and S. Lagerkvist, *J. Chromatogr.*, 282 (1983) 609–618.
- [5] J.Y. Chang, R. Knecht and G. Branu, *Biochem. J.*, 199 (1981) 547–555.
- [6] S.A. Cohen and D.P. Michaud, *Anal. Biochem.*, 211 (1993) 279–287.

Separations of tocopherols and methylated tocols on cyclodextrin-bonded silica

S.L. Abidi *, T.L. Mounts

*Food Quality and Safety Research, National Center for Agricultural Utilization Research, Agricultural Research Service,
US Department of Agriculture, 1815 North University Street, Peoria, IL 61604, USA*

(First received January 11th, 1994; revised manuscript received February 23rd, 1994)

Abstract

α -, β -, γ -, and δ -tocopherols (methyl-substituted tocols) and 5,7-dimethyltolcol were separated by normal-phase HPLC on β - or γ -cyclodextrin-bonded silica (CDS) with fluorescence detection. The HPLC behavior of the tocol components was studied under various mobile phase conditions. Hexane or cyclohexane was used in combination with oxygen-containing solvents (alcohol, ether, and esters) in binary and ternary mobile phases. Capacity factors (k') and separation factors (α) for adjacent tocol components were determined. Incorporation of non-polar ethers in the hydrocarbon (hexane or cyclohexane) mobile phases favored the separation of β - and γ -tocopherols with improved α values, which enabled trace analysis of the β -isomer present in soybean oil. Analyte solutes tended to be more strongly adsorbed in mobile phases containing branched-chain alcohols and ethers than in those containing the corresponding straight-chain solvents. Generally, the k' values obtained with hexane mobile phases or with the β -CDS phase were greater than those observed in HPLC with cyclohexane mobile phases or with the γ -CDS phase.

1. Introduction

During the course of another study on the HPLC evaluation of minor non-triglyceride constituents in genetically modified soybean oil, it was necessary to solve analytical problems associated with the separation of tocopherol components in the oil samples. In HPLC with hexane–2-propanol mobile phases, β -tocopherol eluted first from a commercial amino column (Waters μ Bondapak NH₂, 10 μ m) followed very closely by the γ -isomer. Separation factors (α) for these β - and γ -isomers were much lower than

those for adjacent α – β - and γ – δ -pairs of tocopherol isomers. An efficient separation of the β – γ pair was highly desirable because of small amounts of the β -isomer normally present in soybean oil. Therefore, a comprehensive HPLC study was undertaken to achieve adequate separations of all isomeric components and to obtain accurate analytical results.

Earlier attempts at separating α -, β -, γ -, and δ -isomers of both the parent and methyl ether derivatives of tocopherols in soybean oil by reversed-phase HPLC were unsuccessful because the β - and γ -tocopherols remained unresolved under all HPLC conditions employed [1]. An extensive literature search indicated that little

* Corresponding author.

progress had been made for the past decade in the reversed-phase HPLC separation of all four soybean tocopherols. However, the first report of the separation of β -, and γ -homologues by normal-phase HPLC appeared in 1973 [2].

Since the normal-phase HPLC technique has proven to give better separations of tocopherol components than the reversed-phase method, many researchers have used the normal-phase technique for their tocopherol analyses with various sample matrices [3–14]. Most reported studies employed silica columns of various particle sizes and dimensions. There are only two publications in the literature describing the use of amino and cyano polar phases in tocopherol analyses [15,16]. Despite the vast volume of published work on tocopherol analyses, HPLC methods for the separation of the title compounds on cyclodextrin-bonded silica (CDS) columns have remained unexplored.

β - and γ -cyclodextrins (CD) are macrocyclic molecules containing several glucopyranose units arranged in the shape of hollow truncated cones with relatively hydrophobic interior cavities of 7.5 and 9.5 Å in diameter, respectively. Because of the presence of hydroxy groups, the CD exterior surfaces are hydrophilic. When commercially available β - and γ -CDS columns are used in the normal-phase mode, the chromatographic characteristics of analytes resemble those obtained with other silica-based polar phases. Normal-phase HPLC studies of a variety of compounds on CDS phases have been reported [17–21]. In view of the scarcity of published information concerning HPLC of tocopherols on polar phases, we report the results of a systematic HPLC study of the chromatographic behavior of tocopherol isomers including the 5,7-dimethyltolcol analogue on the β - and γ -CDS phases under various HPLC solvent conditions.

2. Experimental

2.1. Chemicals and reagents

Analytical reference standard compounds α -tocopherol (5,7,8-trimethyltolcol) (TMT), β -

tocopherol (5,8-dimethyltolcol) (DBT), γ -tocopherol (7,8-dimethyltolcol) (DGT) and 5,7-dimethyltolcol (DMT) were obtained from Matreya (Pleasant Gap, PA, USA). Analytical reference standard samples of δ -tocopherol (8-methyltolcol) (MDT) were obtained from Eastman Kodak (Rochester, NY, USA). Chromatography-grade HPLC solvents hexane (HX), cyclohexane (CHX), dioxane (DIOX), tetrahydrofuran (THF), and ethyl acetate (EtOAc) were purchased from Fisher (Fair Lawn, NJ, USA). Other HPLC solvents, including diisopropyl ether (IPIP), *tert*-butyl methyl ether (TBM), *n*-butyl methyl ether (NBM), tetrahydropyran (THP), ethanol (EtOH), 1-propanol (1-PR), 2-propanol (2-PR), *n*-butanol (*n*-BU), and *tert*-butanol (*t*-BU) were high-purity products of Aldrich (Milwaukee, WI, USA).

2.2. High-performance liquid chromatography

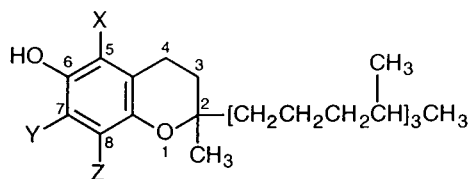
A Spectra-Physics (San Jose, CA, USA) Model SP8700 liquid chromatograph interfaced with an Applied Biosystems (Foster City, CA, USA) Model 980 programmable fluorescence detector was used throughout the HPLC studies. Tocopherols and 5,7-dimethyltolcol were detected at an excitation wavelength of 298 nm and an emission wavelength of 345 nm. Mobile phases employed binary solvent systems each consisting of a non-polar hydrocarbon solvent (hexane or cyclohexane) and a slightly polar oxygen-containing solvent such as an alcohol, ether, or ester. In some HPLC experiments, ternary solvent systems were also used. Mobile phase eluents were prepared by mixing binary of ternary solvents at various proportions.

Two different CDS stationary phases were obtained from Advanced Separation Technologies (Whippany, NJ, USA). These columns included (1) Cyclobond I (β -CDS), 5- μ m spherical particles, 250 \times 4.6 mm I.D., and (2) Cyclobond II (γ -CDS), 5- μ m spherical particles, 250 \times 4.6 mm I.D. The mobile phase eluents were degassed with helium sparge, filtered through a 0.02- μ m filter, and pumped at a flow-rate of 1 ml/min. Aliquots (5–10 μ l) of analyte samples in hexane (50–100 μ g/ml) were injected

onto the column via a Rheodyne (Cotati, CA, USA) Model 7125 injector equipped with a 10- μ l loop. Samples were stored in amber vials at -30°C for protection from light. Throughout the HPLC analyses, three replicate injections were made for each analysis of a tocol mixture under well-equilibrated HPLC conditions. Normally it required about 2–3 h between mobile phase variations for the HPLC column to reach equilibrium. Retention times (t) were mean values of three determinations with coefficients of variation ranging 2–5%. Capacity factors (k') were computed as $k' = t - t_0/t_0$ where t and t_0 represent retention times for an analyte and an unretained solute, respectively. Separation factors (α) were determined for adjacent tocopherol components as $\alpha = k'_{c+1}/k'_c$ where subscript “c” represents an analyte component.

3. Results and discussion

Structures of the five methyl-substituted tocols (four tocopherols and 5,7-dimethyltol) are shown in Fig. 1. These isomeric compounds were found to elute from a CDS column in the following sequence: 5,7,8-trimethyltol (TMT) < 5,7-dimethyltol (DMT) < 5,8-dimethyltol (DBT) < 7,8-dimethyltol (DGT) < 8-methyltol (MDT). As expected, the elution order parallels the decreasing number of



- (A) X = CH₃, Y = CH₃, Z = CH₃
 (B) X = CH₃, Y = CH₃, Z = H
 (C) X = CH₃, Y = H, Z = CH₃
 (D) X = H, Y = CH₃, Z = CH₃
 (E) X = H, Y = H, Z = CH₃

Fig. 1. Structures of investigated tocol compounds. (A) 5,7,8-trimethyltol (TMT) (α -tocopherol), (B) 5,7-dimethyltol (DMT), (C) 5,8-dimethyltol (DBT) (β -tocopherol), (D) 7,8-dimethyltol (DGT) (γ -tocopherol), and (E) 8-methyltol (MDT) (δ -tocopherol).

methyl substituents on the tocol molecules which is also indicative of an increasing order of polarity of the compounds. In normal-phase HPLC of the tocol compounds on CDS, analyte solute retention is believed to be due to solute adsorption to the outside of the CD molecule, while the CD cavity is occupied by a non-polar hydrocarbonaceous solvent [22]. The elution–polarity relationship observed in this normal-phase HPLC study can be interpreted in terms of the adsorption rationale described.

Figs. 2 and 3 show the effect of mobile phase compositions of hexane binary systems on the retention of tocol components on γ -CDS. HPLC with a small amount of alcohol in hexane produced a typical k' vs. % hexane profile in which

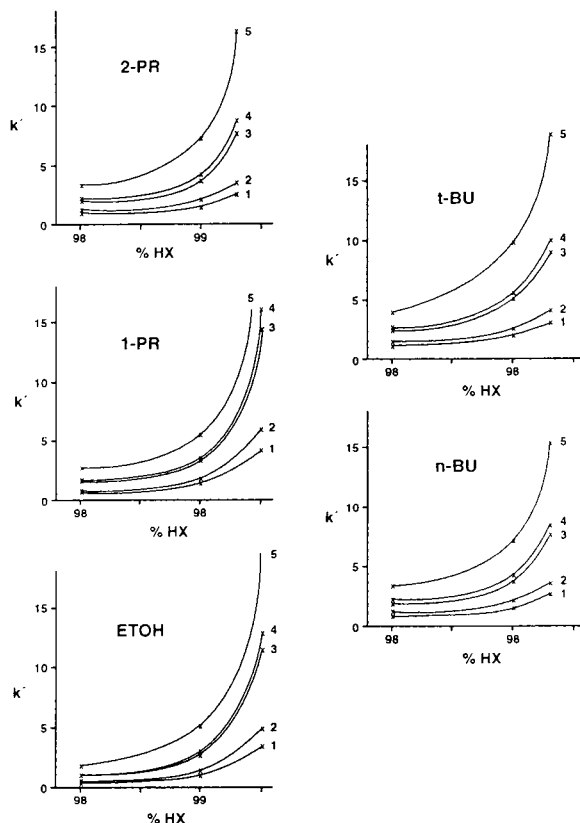


Fig. 2. Variation of capacity factor, k' , with alcohol composition in hexane binary mobile phase. Stationary phase: γ -CDS. Component identification: (1) TMT, (2) DMT, (3) DBT, (4) DGT, and (5) MDT. For component abbreviations, see Fig. 1.

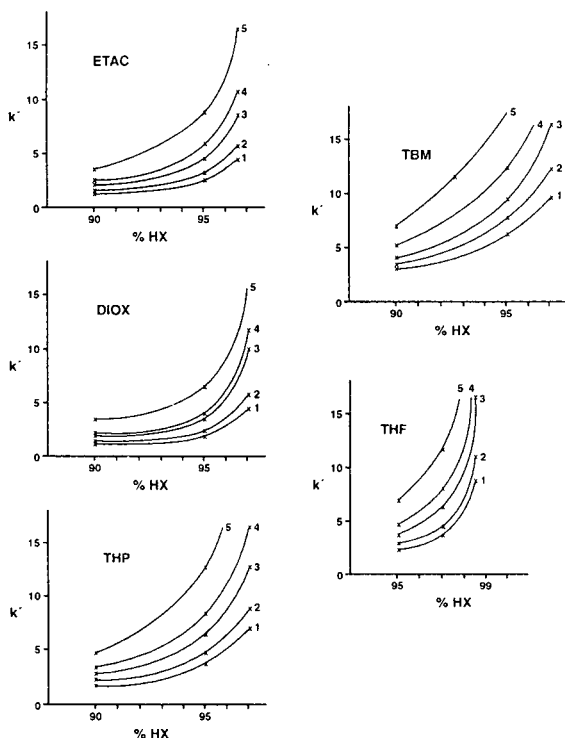


Fig. 3. Variation of capacity factor, k' , with ether or ester composition in hexane binary mobile phase. Stationary phase: γ -CDS. For component identification, see Fig. 2.

the differences in k' values between components 1 and 2 or components 3 and 4 were much smaller in comparison with those between components 2 and 3 or components 4 and 5 (Fig. 2). On the other hand, inspection of the k' vs. % hexane plots in Fig. 3 indicated that differential k' values among adjacent pairs [$\Delta k'$ (1–2), $\Delta k'$ (2–3), $\Delta k'$ (3–4), and $\Delta k'$ (4–5)] observed in HPLC with mobile phases containing ethers (or esters) became close in magnitude, particularly in analyses where ethers of low polarity were used. In other words, the five tocols tended to be more equally dispersed among the components in the latter solvent systems than in hexane–alcohol mobile phases.

In addition to the hexane binary mobile phases used in the study, the corresponding cyclohexane binary solvent systems were also used to ascertain the effect of the cyclic hydrocarbon structure

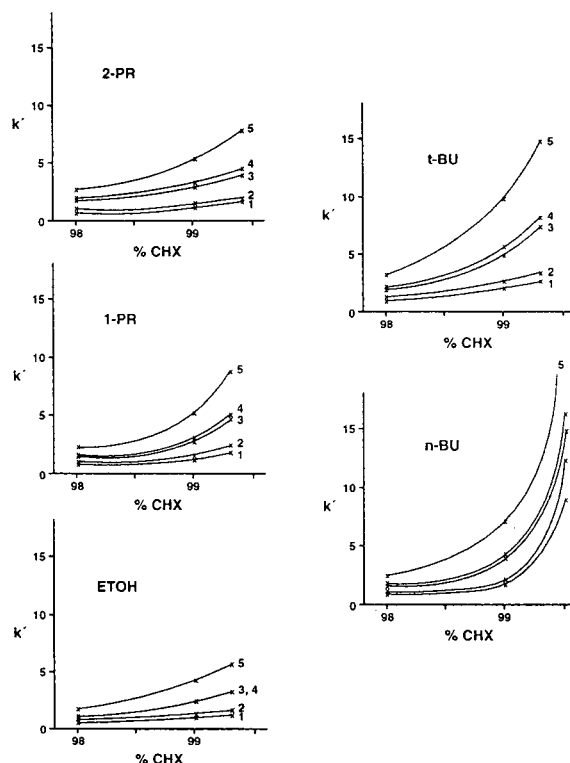


Fig. 4. Variation of capacity factor, k' , with alcohol composition in cyclohexane binary mobile phase. Stationary phase: γ -CDS. For component identification, see Fig. 2.

of cyclohexane on the HPLC separation of the compounds of interest. As shown in Figs. 4 and 5, the k' vs. % cyclohexane profiles are strikingly similar to the corresponding k' vs. % hexane profiles in Fig. 2 and 3. Generally the curvature of k' vs. % hexane curves appeared to be somewhat greater than that of the cyclohexane counterparts, especially in the region of higher hydrocarbon contents. These results suggest that adsorptions of tocol solutes in HPLC with hexane binary solvents are more susceptible to solvent effects than with cyclohexane mobile phases. Further, differential k' values [$\Delta k'$ (1–2) and $\Delta k'$ (3–4)] for the two pairs of tocol components observed in experiments using cyclohexane–ethers (or esters) (Fig. 5) seemed to be slightly smaller than those found in HPLC with hexane containing the same ether or ester solvents (Fig. 3).

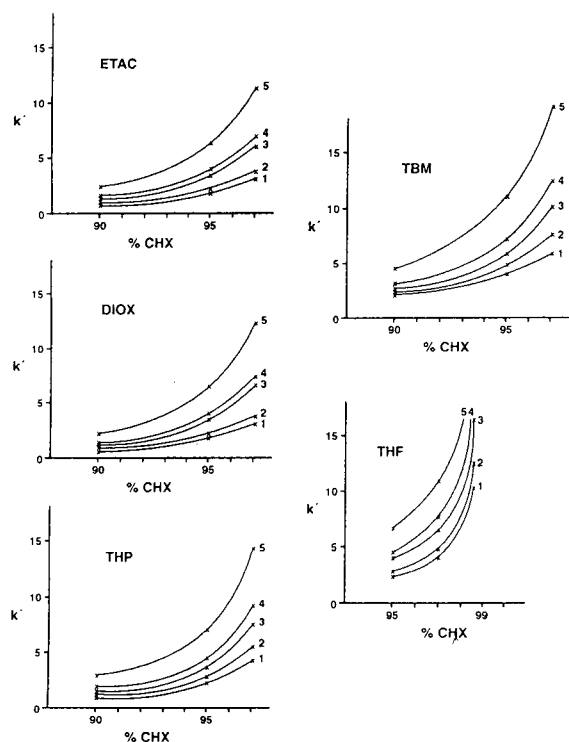


Fig. 5. Variation of capacity factor, k' , with ether or ester composition in cyclohexane binary mobile phase. Stationary phase: γ -CDS. For component identification, see Fig. 2.

Typical examples of chromatograms showing normal-phase separations of the five tocols on β -CDS are given in Fig. 6. Regardless of the type of oxygen-containing solvents used, solvent polarity plays an important role in controlling the separation of components 1 and 2 from components 3 and 4. Thus, in relation to separations of other adjacent pairs, the separation between components 1 and 2 or between components 3 and 4 is apparently smaller when relatively more polar solvents were used, as demonstrated in Fig. 6D (ether), Fig. 6F (alcohol) and Fig. 6G (ester). With ethyl acetate in the mobile phase (Fig. 6G), components 3, 4, and 5 emerged as weak peaks on the chromatogram probably due to solubility problems of the analyte components in the solvent systems employed.

Normal-phase retention and separation characteristics of the methylated tocols examined

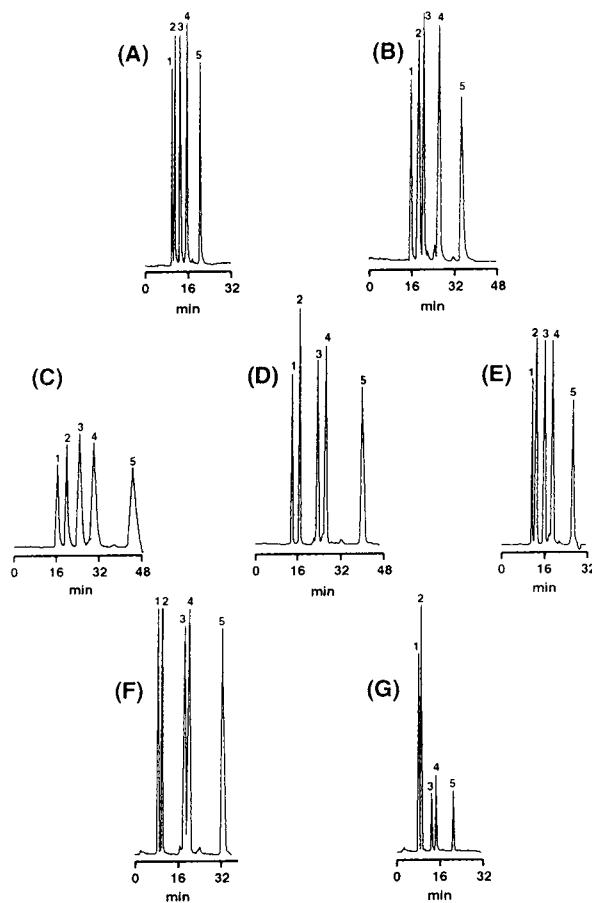


Fig. 6. Typical chromatograms showing normal-phase separations of tocol components on β -CDS. Mobile phases (A) hexane–tetrahydropyran (90:10), (B) hexane–*tert*-butyl methyl ether (90:10), (C) cyclohexane–*tert*-butyl methyl ether (95:5), (D) cyclohexane–diisopropyl ether (95:5), (E) cyclohexane–tetrahydropyran (95:5), (F) cyclohexane–*tert*-butanol (99:1), and (G) cyclohexane–ethyl acetate (95:5). For component identification, see Fig. 2.

under various HPLC conditions are compiled in Tables 1–5. Of the four different HPLC systems studied, highest k' values of tocols were invariably obtained from HPLC experiments where hexane binary mobile phases and a β -CDS stationary phase were used (Table 1). The analyte k' values normally decreased with the increasing polar nature of given HPLC solvent systems including stationary phases. If the mobile phase and stationary phase variables specified in Tables 1, 2, 3, and 4 are designated

Table 1

Normal-phase HPLC of methyl-substituted tocols on β -cyclodextrin-bonded silica with hexane binary mobile phases

Mobile phase	k' TMT	α	k' DMT	α	k' DBT	α	k' DGT	α	k' MDT
HX-2-PR (99:1)	1.70	1.34	2.28	1.80	4.11	1.17	4.81	1.58	7.60
HX-1-PR (99:1)	1.48	1.34	1.99	1.73	3.44	1.15	3.96	1.54	6.10
HX- <i>t</i> -BU (99:1)	2.93	1.23	3.62	1.82	6.60	1.16	7.67	1.54	11.8
HX- <i>n</i> -BU (99:1)	2.61	1.20	3.14	1.63	5.11	1.13	5.77	1.42	8.20
HX-EtOH (99:1)	1.38	1.36	1.88	1.80	3.38	1.12	3.79	1.42	5.84
HX-THF (95:5)	3.09	1.20	3.71	1.31	4.86	1.30	6.32	1.37	8.66
HX-DIOX (95:5)	2.33	1.23	2.87	1.50	4.32	1.16	5.00	1.53	7.65
HX-EtAc (95:5)	3.30	1.23	4.06	1.38	5.60	1.30	7.29	1.40	10.2
HX-THP (95:5)	5.20	1.22	6.34	1.31	8.32	1.31	10.9	1.44	15.7
HX-TBM (95:5)	8.60	1.28	11.0	1.25	13.8	1.35	18.6	1.51	28.0

For abbreviations see Experimental.

as (A), (B), (C), and (D), respectively, the general trends for the variation of k' values with polarity of HPLC systems are observed as follows: $k'(A) > k'(B) > k'(D)$; $k'(A) > k'(C) > k'(D)$. Since β - and γ -CD have respective seven and eight glucopyranose units in the molecules, the γ -CDS phase would be expected to be more polar than the β -CDS phase. However, comparisons of retention data obtained with the β -CDS phase (Tables 1 and 2) to those obtained with the γ -CDS phase (Table 3 and 4) indicate otherwise. The relatively less polar nature of the γ -CDS phase indicated by the observed lower k' values is presumably due to its lower CD load-

ing. Although retention of analyte solutes on CDS appears to proceed largely by adsorption, the exact nature of interactions between tocol solutes and the CDS phase is not clear at the present time.

Structural effects of oxygen-containing solvents in hexane or cyclohexane binary mobile phases on retention of tocols on β - or γ -CDS are demonstrated in Tables 1–4. Evidently, tocol compounds tended to be adsorbed more strongly on CDS in mobile phases containing branched-chain alcohols or ethers than those containing the straight-chain analogues: for example, (1) in the alcohol series, $k'(t\text{-BU}) > k'(n\text{-BU}) > k'(2\text{-}$

Table 2

Normal-phase HPLC of methyl-substituted tocols on β -cyclodextrin-bonded silica with cyclohexane binary mobile phases

Mobile phase	k' TMT	α	k' DMT	α	k' DBT	α	k' DGT	α	k' MDT
CHX-2-PR (99:1)	1.46	1.25	1.82	1.79	3.26	1.12	3.65	1.63	5.95
CHX-1-PR (99:1)	1.40	1.29	1.80	1.81	3.26	1.08	3.53	1.64	5.80
CHX- <i>t</i> -BU (99:1)	2.33	1.23	2.86	1.98	5.65	1.10	6.20	1.71	10.6
CHX- <i>n</i> -BU (99:1)	1.52	1.27	1.93	1.90	3.67	1.06	3.89	1.68	6.53
CHX-EtOH (99:1)	1.38	1.27	1.76	1.81	3.19	1.09	3.48	1.60	5.56
CHX-THF (95:5)	2.79	1.18	3.29	1.31	4.31	1.21	5.22	1.44	7.51
CHX-DIOX (95:5)	1.96	1.25	2.45	1.57	3.85	1.10	4.24	1.57	6.66
CHX-EtAc (95:5)	2.13	1.22	2.60	1.46	3.80	1.16	4.40	1.50	6.60
CHX-THP (95:5)	3.00	1.15	3.46	1.31	4.53	1.22	5.54	1.45	8.06
CHX-TBM (95:5)	5.40	1.22	6.60	1.25	8.26	1.22	10.1	1.50	15.1
CHX-IPIP (95:5)	3.73	1.27	4.73	1.48	7.00	1.15	8.06	1.58	12.7

Table 3

Normal-phase HPLC of methyl-substituted tocols on γ -cyclodextrin-bonded silica with hexane binary mobile phases

Mobile phase	k' TMT	α	k' DMT	α	k' DBT	α	k' DGT	α	k' MDT
HX-2-PR (99:1)	1.31	1.35	1.77	1.84	3.26	1.11	3.62	1.75	6.33
HX-1-PR (99:1)	1.20	1.38	1.66	1.91	3.00	1.09	3.26	1.67	5.46
HX- <i>t</i> -BU (99:1)	2.06	1.29	2.66	1.92	5.10	1.13	5.76	1.70	9.80
HX- <i>n</i> -BU (99:1)	1.73	1.27	2.20	1.75	3.86	1.10	4.26	1.69	7.20
HX-EtOH (99:1)	1.01	1.42	1.42	1.96	2.78	1.11	3.09	1.73	5.34
HX-THF (95:5)	2.46	1.22	3.00	1.29	3.86	1.26	4.86	1.44	7.00
HX-DIOX (95:5)	1.97	1.23	2.42	1.51	3.66	1.16	4.24	1.54	6.53
HX-EtAc (95:5)	2.67	1.21	3.23	1.45	4.68	1.27	5.95	1.49	8.86
HX-THP (95:5)	3.86	1.26	4.87	1.47	6.65	1.28	8.53	1.49	12.7
HX-TBM (95:5)	6.26	1.23	7.67	1.24	9.53	1.30	12.4	1.42	17.6
HX-NBM (95:5)	3.98	1.25	4.98	1.49	7.42	1.20	8.90	1.55	13.8
HX-NBM (90:10)	2.80	1.21	3.40	1.27	4.32	1.24	5.34	1.47	7.86

PR) $> k'(1\text{-PR}) > k'(\text{EtOH})$, (2) in the ether series, $k'(\text{TBM}) > k'(\text{NBM}) > k'(\text{THP}) > k'(\text{THF}) > k'(\text{DIOX})$. It is apparent that such structural effects on tocol retention seem to contradict, in part, conventional observations on the solvent polarity-retention relationship. A similar structural effect of alcohols on solute retention has been reported previously in reversed-phase HPLC of aromatic compounds on CDS [23].

Examination of the methyl substitution pattern in tocol molecules (Fig. 1) reveals that the 6-

hydroxy group is flanked by two methyls at the 5- and 7-positions in TMT and DMT molecules, but there is only one methyl adjacent to the hydroxy group in DBT and DGT structures. Correlation of the effect of methyl substitution in the three dimethyltocols DMT, DBT, and DGT with their k' values obtained in HPLC with polar solvents enabled us to understand why the k' values of DMT are very close to those of TMT and are much farther apart from those of DBT or DGT. The 6-hydroxy group in the latter pair of dimethyltocols appears to be more easily

Table 4

Normal-phase HPLC of methyl-substituted tocols on γ -cyclodextrin-bonded silica with cyclohexane binary mobile phases

Mobile phase	k' TMT	α	k' DMT	α	k' DBT	α	k' DGT	α	k' MDT
CHX-2-PR (99:1)	1.39	1.25	1.74	1.77	3.08	1.12	3.45	1.61	5.55
CHX-1-PR (99:1)	1.20	1.26	1.51	1.91	2.89	1.05	3.03	1.65	5.00
CHX- <i>t</i> -BU (99:1)	2.04	1.29	2.64	1.89	4.99	1.13	5.64	1.71	9.65
CHX-1-BU (99:1)	1.65	1.25	2.06	1.87	3.86	1.09	4.20	1.67	7.00
CHX-EtOH (99:1)	1.00	1.40	1.40	1.86	2.60	1.00	2.60	1.63	4.25
CHX-THF (95:5)	2.51	1.20	3.01	1.33	4.01	1.17	4.69	1.42	6.66
CHX-DIOX (95:5)	1.93	1.21	2.33	1.57	3.66	1.09	4.00	1.62	6.46
CHX-EtAc (95:5)	1.86	1.25	2.33	1.52	3.53	1.15	4.06	1.56	6.33
CHX-THP (95:5)	2.46	1.22	3.00	1.31	3.93	1.22	4.80	1.50	7.20
CHX-TBM (95:5)	4.00	1.25	5.00	1.20	6.00	1.22	7.32	1.50	11.0
CHX-NBM (95:5)	3.29	1.25	4.12	1.30	5.35	1.14	6.10	1.59	9.70
CHX-NBM (90:10)	2.00	1.23	2.46	1.27	3.13	1.17	3.66	1.55	5.67

Table 5
Normal-phase HPLC of methyl-substituted tocols on β -cyclodextrin-bonded silica with hexane ternary mobile phases

Mobile phase	k' TMT	α	k' DBT	α	k' DGT	α	k' MDT
HX–2-PR–DIOX (99:0.5:0.5)	3.13	2.28	7.13	1.19	8.46	1.74	14.7
HX–2-PR–DIOX (99:0.7:0.3)	3.15	1.63	5.13	1.11	5.67	1.52	8.60
HX–2-PR–DIOX (98:1:1)	1.00	1.67	1.67	1.08	1.80	1.52	2.73
HX–2-PR–DIOX (98.2:0.9:0.9)	2.33	2.03	4.73	1.15	5.46	1.60	8.73
HX–2-PR–DIOX (98.7:0.3:1)	5.34	2.51	13.4	1.17	15.7	1.77	27.8
HX–EtOH–DIOX (98:0.5:1.5)	3.73	2.20	8.20	1.28	10.5	1.46	15.3
HX–2-PR–THF (99:0.5:0.5)	9.00	1.07	9.67	1.10	10.6	1.44	15.3
HX–2-PR–THF (98.5:0.5:1)	1.66	2.05	3.40	1.19	4.06	1.63	6.53
HX–2-PR–THF (98.7:0.5:0.8)	2.06	1.97	4.06	1.15	4.66	1.59	7.40
HX–2-PR–THF (98.6:0.7:0.7)	1.86	2.00	3.73	1.19	4.45	1.47	6.53
HX–2-PR–THF (96.7:0.3:3)	3.06	1.59	4.86	1.25	6.06	1.40	8.46
HX–2-PR–EtAc (96.1:0.4:3.5)	0.86	1.47	1.26	1.31	1.65	1.41	2.32
HX–2-PR–EtAc (96.3:0.2:3.5)	1.93	1.79	3.46	1.17	4.06	1.49	6.06

accessible for interactions with the CDS phase than that in the TMT–DMT pair. Strong interactions of the polar mobile phase solvents (*e.g.* alcohol or polar ether) with the CDS phase had adverse effects on column selectivity for component separation. This rationalization can be used to account for the following elution sequences observed in experiments with polar mobile phases: k' DBT (or DGT) $>$ k' TMT (or DMT); $\Delta k'$ (MDT–DGT) or $\Delta k'$ (DBT–DMT) \gg $\Delta k'$ (DGT–DBT) or $\Delta k'$ (DMT–TMT). Because—of weak interactions of mobile phase solvents with the CDS stationary phase, HPLC with non-polar ether mobile phases provided superior selectivity for components yielding uniformly separated component peaks on individual chromatograms of tocol samples analyzed (Fig. 6).

Separation factors, α , for adjacent tocol component peaks on individual chromatograms were measured from normal-phase HPLC retention data (Tables 1–5). These α values were found to vary with the type and polarity of the oxygen-containing solvents in hexane (Tables 1 and 2) or in cyclohexane (Tables 3 and 4). In HPLC experiments with alcohols and polar ethers (*e.g.* dioxane) in hexane or cyclohexane mobile phases, the α values for DBT and DGT are lower than those observed for other adjacent pairs of tocols. The same observations were also

true in experiments conducted under similar conditions with ethyl acetate in cyclohexane mobile phases. The specific solvent effects described above are apparently independent of the type of CDS phases used. Separations of the DBT–DGT pair improved considerably with increased α -values (1.21–1.35) by the use of non-polar ethers (*e.g.* *tert.*-butyl methyl ether, tetrahydropyran, tetrahydrofuran) in hexane as mobile phases and a β -CDS column as the stationary phase.

Normal-phase HPLC data for the separation of soybean tocopherols on β -CDS with hexane–2-propanol-based ternary mobile phases are presented in Table 5. As demonstrated in Table 5, manipulation of solvent ratios in the hexane–2-propanol ternary systems brought about variable degrees of separations (variable α values) for the DBT–DGT pair. Thus, fairly small changes in the α values (1.08–1.19) were noted by adjusting the ratios of hexane–2-propanol–dioxane solvents. With THF in the hexane–2-propanol ternary systems, the α values were between 1.10–1.25, whereas with EtOAc they were between 1.17–1.31 in response to the change in the ratio of the three solvent components in the mobile phases. HPLC with a combination of hexane–ethanol–dioxane led to a favorable separation of the DBT–DGT pair ($\alpha = 1.28$). In the ternary

mobile phase systems studied, k' values obtained with tetrahydrofuran were higher than those with dioxane, in agreement with the earlier findings in HPLC with binary mobile phases.

In connection with another study on the HPLC analysis of soybean tocopherols using hexane–2-propanol mobile phases, problems associated with the separation of β - and γ -tocopherols (DBT and DGT) were often encountered during the analysis of samples with low levels of the β -isomer. Under the routine HPLC conditions (hexane–2-propanol) used, separations of β - and γ -isomers (DBT–DGT pair) were too close to reveal any interfering peaks for the precise quantitation of the β -tocopherol in soybean oil samples. To solve such analytical problems, ethers are highly recommended for use as co-solvents in hexane or cyclohexane mobile phases for practical tocopherol analysis. This is one of the reasons why discussion has focused on the separation of the DBT–DGT pair of tocopherol isomers throughout this study. Since a tocopherol-specific fluorescence detector was used in this study, the HPLC method developed can be applied to the direct analysis of tocopherols in soybean oil samples without sample cleanup.

In conclusion, the results of the present study represent the first report on the use of CDS columns for the separation of tocol compounds. Excellent separations of five methylated tocol compounds were achieved in most cases and can be extended to other tocols of similar structures by optimization of normal-phase HPLC conditions. The comprehensive approach taken to delineate the chromatographic behavior of the tocols of interest led to a better understanding of the mode of interactions between analyte solutes and CDS phases. HPLC data from comparative studies of mobile phase effects on retention and separation characteristics of tocols provide useful information regarding solvent selection to obtain

optimal separations of the analyte components within reasonable retention times.

4. References

- [1] S.L. Abidi, *unpublished results*, 1990.
- [2] P.J. Van Niekerk, *Anal. Biochem.*, 52 (1973) 533.
- [3] C.D. Carr, *Anal. Chem.*, 46 (1974) 743.
- [4] M. Matsuo and Y. Tahara, *Chem. Pharm. Bull.*, 25 (1977) 3381.
- [5] G.T. Vatassery and D.F. Hagen, *Anal. Biochem.*, 79 (1977) 129.
- [6] G.T. Vatassery, V.R. Maynard and D.F. Hagen, *J. Chromatogr.*, 161 (1978) 299.
- [7] B. Nilsson, B. Johansson, L. Jansson and L. Holmberg, *J. Chromatogr.*, 145 (1978) 169.
- [8] C.C. Tangney, J.A. Driskell and H.M. McNair, *J. Chromatogr.*, 172 (1979) 513.
- [9] A.P. Carpenter, *J. Am. Oil Chem. Soc.*, 56 (1979) 668.
- [10] J.N. Thompson and G. Hatina, *J. Liq. Chromatogr.*, 2 (1979) 327.
- [11] P.J. Vanker and A.E.C. Burger, *J. Am. Oil Chem. Soc.*, 62 (1985) 531.
- [12] A. Gapor, A. Kato and A.S.H. Ong, *J. Am. Oil Chem. Soc.*, 63 (1986) 330.
- [13] Y.L. Ha and A.S. Csallany, *Lipids*, 23 (1988) 359.
- [14] W.D. Pocklington and A. Dieffenbacher, *Pure App. Chem.*, 60 (1988) 877.
- [15] B.A. Ruggeri, T.R. Watkins, R.J.H. Gray and R.I. Tomlins, *J. Chromatogr.*, 291 (1984) 377.
- [16] W. Feldheim, H. Schulz and R. Katerberg, *Z. Lebensm.-Unters. Forsch.*, 178 (1984) 115.
- [17] D.W. Armstrong, A. Alak, W. DeMond, W.L. Hinze and T.E. Riehl, *J. Liq. Chromatogr.*, 8 (1985) 261.
- [18] C.A. Chang, Q. Wu and L. Tan, *J. Chromatogr.*, 361 (1986) 199.
- [19] C.A. Chang and Q. Wu, *Anal. Chim. Acta*, 189 (1986) 293.
- [20] C.A. Chang and Q. Wu, *J. Liq. Chromatogr.*, 10 (1987) 1359.
- [21] D.W. Armstrong, A.M. Stalcup, H.L. Jin, P. Mazur, F. Derguini and K. Nakanishi, *J. Chromatogr.*, 499 (1990) 627.
- [22] D.W. Armstrong, W. DeMond and B.P. Czech, *Anal. Chem.*, 57 (1985) 481.
- [23] I.Z. Atamna, G.M. Muschik and H.J. Issaq, *J. Chromatogr.*, 499 (1990) 477.

High-performance liquid chromatographic analysis of Romet-30 in Chinook salmon (*Oncorhynchus tshawytscha*): wash-out time, tissue distribution in muscle, liver and skin, and metabolism of sulfadimethoxine

Ming Zheng^a, He-Yi Liu^{☆,a}, Scott F. Hall^a, David D. Kitts^b,
Keith M. McErlane^{*,a}

^aFaculty of Pharmaceutical Sciences, University of British Columbia, Vancouver, B.C. V6T 1Z3, Canada

^bDepartment of Food Sciences, University of British Columbia, Vancouver, B.C. V6T 1W5, Canada

(First received November 12th, 1993; revised manuscript received February 17th, 1994)

Abstract

A high-performance liquid chromatographic (HPLC) assay was developed for the determination of Romet-30 residue levels in Chinook salmon muscle and liver tissues. The extraction recoveries averaged 66, 78 and 83% for ormetoprim (OMP), sulfadimethoxine (SDM) and N⁴-acetyl-SDM (N⁴-Ac-SDM), respectively, in muscle tissue; 61 and 72% for SDM and N⁴-Ac-SDM, respectively, in liver tissue. The HPLC assay had a lower detection limit of 0.05 µg/g for OMP, SDM and N⁴-Ac-SDM in muscle tissue, and a lower detection limit of 0.20 µg/g for SDM and N⁴-Ac-SDM in liver tissue. OMP could not be quantified in liver due to the presence of substantial amounts of co-extracted endogenous substances. The HPLC assay was applied to the analysis of Romet-30 residues in Chinook salmon after gastric intubation with Romet-30 at water temperatures between 8.0 and 9.0°C. Different disposition characteristics were found in muscle and liver tissues. The presence of N⁴-Ac-SDM in liver tissue was confirmed by MS and MS–MS analyses. An estimation of SDM and N⁴-Ac-SDM residue levels in skin tissue was obtained and the disposition of these two compounds was similar to the disposition in muscle tissue.

1. Introduction

Intensive aquaculture and occasional poor fish husbandry practices predispose fish to various infectious diseases due to a variety of stress factors [1]. These adverse conditions enhance the opportunities of introduction, transfer and rapid

dissemination of fish infections in the aquaculture industry [2]. Antimicrobial compounds are thus commonly used for the treatment and prevention of disease outbreaks.

Romet-30 (trademark of Hoffmann-La Roche, Mississauga, Ontario, Canada) is a potentiated sulfonamide consisting of a sulfadimethoxime (SDM)–ormetoprim (OMP) (5:1) mixture. It has been approved in the USA and Canada for the control of furunculosis in salmonids and enteric septicemia in channel catfish [3–5]. This antimicrobial is also effective in controlling en-

* Corresponding author.

[☆] Present address: Lilly Analytical Research Laboratory, Reichmann Research Building, 2075 Bayview Avenue, North York, Ont. M4N 3M5, Canada.

teric redmouth disease [6] and vibriosis [7] in salmonids. Romet-30 is administered in medicated feed at a dosage of 50 mg/kg of fish per day for five consecutive days followed by a 42-day withdrawal period required for salmonids [3] and a 3-day withdrawal period required for catfish [4]. The tolerance levels for SDM and OMP in edible fish tissues are 0.1 $\mu\text{g/g}$ [3,4].

Analytical assays are required for monitoring drug residue levels in edible fish tissue, as well as for drug disposition studies. Due to their sensitivity and selectivity, chromatographic methods are most suitable for the analysis of sulfonamide residues in fish tissues [8–17]. More recently, a capillary electrophoresis–mass spectrometric method was reported for analysis of various antimicrobials, including SDM and OMP, in shellfish tissue [18]. Radioisotope-labelled SDM and OMP have also been used to study the disposition of these two drugs in lobster (*Homarus americanus*) [19,20], channel catfish (*Ictalurus punctatus*) [21–23] and rainbow trout (*Salmo gairdneri* and *Oncorhynchus mykiss*) [24–27]. However, the radioisotope assays reported lacked specificity in that the parent drugs were not separated from their metabolites.

The objective of the present study was to develop an HPLC assay for the determination of wash-out time of Romet-30 in Chinook salmon and its tissue distribution in muscle, liver and skin tissues following gastric intubation. N^4 -Acetyl-SDM (N^4 -Ac-SDM), a metabolite of SDM, was also determined in these three tissues.

2. Experimental

2.1. Materials

Romet-30 was obtained through Syndel Labs. (Vancouver, Canada) (lot No. 4106). OMP and SDM were obtained from Hoffmann–La Roche (Nutley, NJ, USA). Tricaine methanesulfonate (MS-222) was obtained from Syndel Labs. The internal standard, sulfisoxazole, was obtained from Sigma (St. Louis, MO, USA). Tetra-butylammonium hydroxide (TBAH) (40%) and sodium carbonate were obtained from Aldrich (Milwaukee, WI, USA). Phosphoric acid (85%)

was obtained from Fisher Scientific (Fair Lawn, NJ, USA). Sodium sulfate anhydrous granular, sodium hydrogencarbonate, disodium hydrogenorthophosphate heptahydrate ($\text{Na}_2\text{HPO}_4 \cdot 7\text{H}_2\text{O}$) and acetic anhydride were obtained from BDH (Toronto, Canada). HPLC-grade methanol, acetonitrile and dichloromethane were obtained from BDH. Purified water was produced using a Milli-Q water purification system (Mississauga, Canada).

2.2. HPLC system

The HPLC system consisted of a Beckman Model 100A pump (Fullerton, CA, USA), a Shimadzu SIL-9A auto injector, a Shimadzu SPD-6A UV spectrophotometric detector and a Shimadzu C-R6A Chromatopac data processor (Kyoto, Japan), a Beckman Ultrasphere ion-pair column (5 μm , 250×4.6 mm I.D.) (San Ramon, CA, USA), and a guard column with a Brownlee RP-18 cartridge (15 \times 3.2 mm I.D.) (Santa Clara, CA, USA). The flow-rate of the mobile phase was 1.0 ml/min. The detection wavelength was at 280 nm. The absorbance range of the detector was at 0.01 AUFS.

2.3. Tandem mass spectrometric (MS–MS) system

The MS–MS experiments were performed on a Sciex API III triple quadrupole mass spectrometer (Thornhill, Canada), equipped with an ionspray interface and an atmospheric-pressure chemical ionization (APCI) source. The samples were delivered by flow injection with 10 $\mu\text{l/min}$ aqueous 50% methanol. A dwell time of 6 ms/u was used for full-scan MS analyses. APCI mass spectra were acquired in the first quadrupole Q1, and selected precursor ions were fragmented in the radio frequency (rf) only quadrupole Q2 at a collision energy of 36 eV. Argon was used as the target gas at a thickness of $5.48 \cdot 10^{14}$ molecules/ cm^2 . Product ions were examined in the third quadrupole Q3.

2.4. Stock solutions

A mixture of SDM and OMP was prepared by dissolving SDM and OMP in 50 ml of acetonitrile.

trile to give a concentration of 200 $\mu\text{g/ml}$ for both standards. This stock solution was further diluted to give a series of standard solutions with concentrations of 100, 20 and 2 $\mu\text{g/ml}$. Sulfoxazole internal standard solution was prepared in 100 ml of acetonitrile to give a final concentration of approximately 60 $\mu\text{g/ml}$.

The sodium carbonate–sodium hydrogencarbonate buffer (pH 10) was prepared according to Delory and King [28]. Sodium carbonate stock solution (0.2 M) was prepared by dissolving 21.2 g of sodium carbonate in 1000 ml of purified water. Sodium hydrogencarbonate stock solution (0.2 M) was prepared by dissolving 16.8 g of sodium hydrogencarbonate in 1000 ml of purified water. The buffer was prepared by mixing 27.5 ml of the above sodium carbonate solution and 22.5 ml of the above sodium hydrogencarbonate solution and further dilution to 200 ml with purified water.

2.5. Synthesis of N^4 -Ac-SDM

An excess of 5 ml of acetic anhydride (approximately 53 mmol) was added to 2 g of SDM (approximately 6 mmol) and the mixture was heated on a Thermolyne Dry-bath (Dubuque, IA, USA) at 70°C for 20 min with occasional manual shaking. The excess acetic anhydride was evaporated under nitrogen in a 40°C water bath. The resulting crystals were filtered and washed with water. The product was recrystallized from acetonitrile. Its melting point was determined to be 219–222°C on a capillary melting point apparatus (Arthur H. Thomas Co., Philadelphia, PA, USA), while the Merck Index value is 220–223°C [29]. The purity was determined to be greater than 99.5% by HPLC. A stock solution was then prepared in 25 ml of acetonitrile to give a concentration of 400 $\mu\text{g/ml}$. This stock solution was further diluted to give concentrations of 200, 100, 20 and 2 $\mu\text{g/ml}$.

2.6. Extraction procedures

A 5-g sample of muscle or liver tissue, or a 2-g sample of skin tissue, was dissected and placed in a 50-ml centrifuge tube. An aliquot of 200 μl of

sulfoxazole internal standard solution (approximately 12 μg sulfoxazole) was added along with 300 μl of 0.5 M TBAH, 1 ml of pH 10 Na_2CO_3 – NaHCO_3 buffer and 1 ml of 1 M NaOH. After brief manual mixing with a Pasteur pipette, 15 ml of dichloromethane were added and the sample was homogenized at medium speed using a Brinkmann Polytron Model PT 10/35 homogenizer (Rexdale, Canada) for 20–30 s. Granular sodium sulfate anhydrous (2 g) was added to the homogenate and the sample was vortex-mixed for 2 min. The mixture was then centrifuged at 2000 g for 15 min. After centrifugation, the top aqueous layer was removed to a test tube, the interfacial solid tissue plug was pushed aside, and the dichloromethane layer was removed. The aqueous layer was returned to the tube containing the tissue plug and an additional 10 ml of dichloromethane were added. The sample was vortex-mixed for 2 min and centrifuged. The dichloromethane layer was removed, combined with the initial dichloromethane extract and evaporated under a nitrogen stream in a 40°C water bath. The residue was reconstituted in 1 ml of HPLC mobile phase. After centrifugation for 5 min at 1450 g, the bottom layer was removed and filtered through a 0.45- μm Nylaflo membrane filter (Gelman Sciences, Ann Arbor, MI, USA). An aliquot of 20 μl of the filtrate was injected onto the HPLC system.

2.7. Calibration curves

The calibration curves in muscle tissue were determined in a series of 5-g muscle samples to which were added 200 μl of internal standard solution (60 $\mu\text{g/ml}$) and appropriate volumes of SDM–OMP and N^4 -Ac-SDM standard solutions to give final concentrations of 0.05, 0.10, 0.20, 0.50, 2.00, 5.00 and 10.0 $\mu\text{g/g}$ for each of the standards. The samples were stored at 4°C for 1 h, followed by extraction as described before. The calibration curves were constructed by plotting the peak area ratios of SDM, OMP and N^4 -Ac-SDM to the internal standard against the concentrations of SDM, OMP and N^4 -Ac-SDM added.

In a similar fashion, the calibration curves of SDM and N⁴-Ac-SDM in liver tissue were determined in a range of 0.20 to 25.0 µg/g.

2.8. Assay precision

The intra-assay variability in muscle tissue was determined by the analysis of six muscle samples to which SDM-OMP and N⁴-Ac-SDM were added at 0.50 µg/g, and six muscle samples to which SDM-OMP and N⁴-Ac-SDM were added at 5.00 µg/g. The analysis of the six muscle samples was completed in one day. The inter-assay variability in muscle tissue was determined at 0.50 and 5.00 µg/g at consecutive daily intervals over a six-day period. Similarly, the intra- and inter-assay variabilities for SDM and N⁴-Ac-SDM in liver tissue were determined at 0.50, 5.00 and 15.0 µg/g.

2.9. Extraction recoveries

To six muscle samples were added SDM-OMP and N⁴-Ac-SDM to give final concentrations of 0.50 µg/g for each analyte. An additional six muscle samples were prepared at concentrations of 5.00 µg/g for each of SDM-OMP and N⁴-Ac-SDM. The samples were extracted as described before, except that the internal standard was added just before the combined dichloromethane extract was evaporated to dryness. Two HPLC mobile phase solutions containing SDM-OMP and N⁴-Ac-SDM standards at 0.50 and 5.00 µg/ml along with the internal standard were prepared in parallel, but without undergoing extraction. The recoveries for SDM, OMP and N⁴-Ac-SDM were determined by comparison of the peak area ratios of SDM, OMP and N⁴-Ac-SDM to the internal standard (sulfisoxazole) from extracted tissue samples with those of SDM, OMP and N⁴-Ac-SDM to the internal standard from unextracted standard solutions of identical quantities. In a similar fashion, the recoveries of SDM and N⁴-Ac-SDM in liver tissue were determined at 0.50, 5.00 and 20.0 µg/g.

2.10. Confirmation of the presence of N⁴-Ac-SDM in liver tissue by MS–MS

A 10-g amount of liver sample from the intubation study was extracted as previously described. After reconstitution, the samples were injected onto the HPLC system. The fraction of the effluent corresponding to the synthetic N⁴-Ac-SDM standard was collected. The collected fraction was evaporated to dryness at 37°C in a SpeedVac concentrator (Savant Instruments, Farmingdale, NY, USA). The residues were re-extracted with dichloromethane and evaporated to dryness under a nitrogen stream. The residues were reconstituted with 100 µl of acetonitrile and an aliquot of 1 µl was injected onto the Sciex API III mass system for MS and MS–MS analyses by flow injection.

2.11. Intubation study

Forty-one Chinook salmon were obtained from Salt Spring Aquafarms (Salt Spring Island, Canada). Due to the relatively high mortality rate, probably due to the stress caused by transportation, only 26 fish were available for final analysis. The fish weighed from 615 to 1800 g (1094 ± 57 ; mean \pm S.E.M.). The seawater temperatures ranged from 8.0 to 9.0°C throughout the 20-day study.

The fish were maintained in flowing seawater tanks. After one week of acclimatization, the fish were gastrically intubated with a freshly prepared suspension of Romet-30 in water (25 mg/ml) for 10 days at a dosage of 40 mg/kg per day (standard protocol in British Columbia salmon aquaculture). Before intubation, the fish were lightly anesthetized in a MS-222 bath at a concentration of 43 mg/ml. Sodium hydrogencarbonate (43 mg/ml) was also added to the anesthetic solution in order to buffer the change in pH caused by the addition of MS-222 which otherwise would be irritant to the fish. No obvious regurgitation of the drug was observed after intubation.

Six fish were sampled on each of days 11 (*i.e.*, the first day after the cessation of the intubation) and 14. An additional 7 fish were sampled on

each of days 17 and 20. The fish were sacrificed by a blow to the cranium. Blood, skin, muscle, liver and kidney sampled were collected and kept frozen at -20°C until required for analysis.

2.12. Statistics

All statistical comparisons were performed with analysis of variance (ANOVA) using software NCSS (Kaysville, UT, USA).

3. Results and discussion

3.1. Chromatographic conditions

For the analysis of OMP, SDM and N^4 -Ac-SDM in muscle tissue, two different mobile phases were necessary to obtain the optimal separation of analytes from the endogenous substances. One mobile phase consisted of acetonitrile–methanol–0.1 M phosphate buffer pH 4.0 (12:13:75, v/v/v) and was used for the analysis of OMP. This mobile phase allowed the separation of OMP from the co-extracted endogenous substances eluting early on the chromatograms (Fig. 1). However, N^4 -Ac-SDM could not be separated from the late co-eluting endogenous substances with this mobile phase. A second mobile phase consisting of acetonitrile–methanol–0.1 M phosphate buffer pH 2.5 (11:23.4:75, v/v/v) was therefore used for the analysis of SDM and N^4 -Ac-SDM (Fig. 2).

Sulfisoxazole was chosen as an internal standard because it has a similar structure to SDM and eluted between OMP and SDM with a retention time of approximately 13 min (Figs. 1 and 2). Other sulfonamides were found to elute either too early or too late, or co-elute with endogenous substances.

Preliminary extraction studies with liver samples indicated that substantial amounts of co-extracted endogenous substances were present in the early portion of the chromatograms which coincided with the elution of OMP (Fig. 3). Despite numerous alternations of the extraction protocol and HPLC mobile phases, OMP could not be resolved from co-eluting endogenous

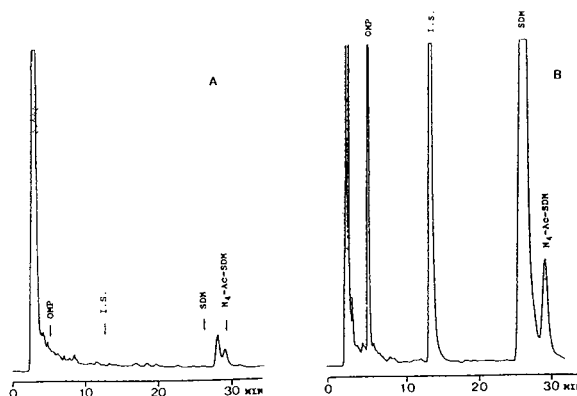


Fig. 1. Chromatograms of (A) a blank Chinook salmon muscle tissue extract and (B) a Chinook salmon muscle tissue extract from the intubation study. Chromatographic conditions: column, Ultrasphere ion pair 5 μm (250×4.6 mm I.D.); mobile phase, acetonitrile–methanol–0.1 M phosphate buffer pH 4.0 (12:13:75, v/v/v); flow-rate, 1.0 ml/min; ultraviolet detection wavelength, 280 nm; 0.01 AUFS. Peaks: OMP = ormetoprim; I.S. = internal standard; SDM = sulfadimethoxine; N^4 -Ac-SDM = N^4 -acetylsulfadimethoxine.

substances, thus precluding accurate measurement of OMP in liver tissue. Based on the analytical results in muscle tissue from the intubation study showing that SDM generally exhibited higher residue levels, it was concluded

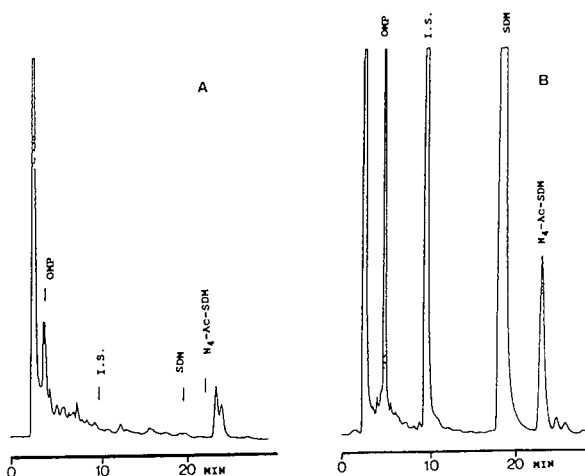


Fig. 2. Chromatograms of (A) a blank Chinook salmon muscle tissue extract and (B) a Chinook salmon muscle tissue extract from the intubation study. HPLC conditions as in Fig. 1, except for the mobile phase: acetonitrile–methanol–0.1 M phosphate buffer pH 2.5 (11:23.4:75, v/v/v). Peaks as in Fig. 1.

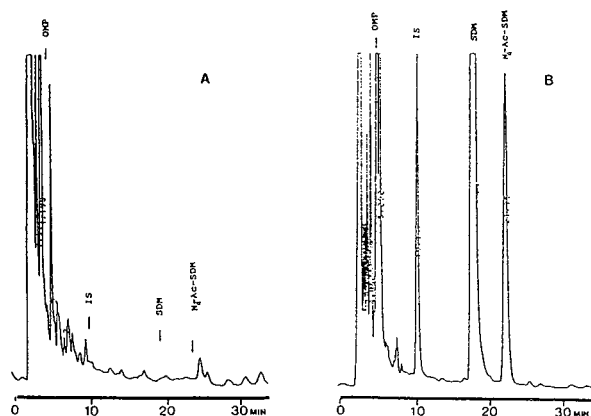


Fig. 3. Chromatograms of (A) a blank Chinook salmon liver tissue extract and (B) a Chinook salmon liver tissue extract from the intubation study. Peaks as in Fig. 1 and HPLC conditions as in Fig. 2.

that SDM represented a more important xenobiotic for the purpose of drug residue detection. For these reasons, only SDM and N^4 -Ac-SDM were analyzed in the liver tissue, using the second mobile phase mentioned above.

3.2. Confirmation of N^4 -Ac-SDM

During the analysis of liver samples from the intubation study, a significant peak was found to elute after SDM (Fig. 3). Since SDM is extensively metabolized to N^4 -Ac-SDM in channel catfish and rainbow trout [22,25], this peak was speculated to be N^4 -Ac-SDM. Synthetic N^4 -Ac-SDM was found to have the same retention time as the unknown peak. HPLC analysis of an admixture of the synthetic N^4 -Ac-SDM and a liver extract from an intubated salmon did not show any evidence of skewing of this peak.

The identity of N^4 -Ac-SDM was further confirmed by MS and MS–MS analyses. The dominant protonated molecular ion $[M + H]^+$ (m/z 353) of N^4 -Ac-SDM was observed by MS analysis from both the synthetic standard and the collected fraction from the liver samples (Fig. 4). Background ions present in the collected fraction (Fig. 4B) were apparently caused by the co-collected endogenous compounds. Further structural information was acquired by the use of the MS–MS technique. The precursor ion m/z 353

was fragmented in the second quadrupole Q2, and the product ions were analyzed in the third quadrupole Q3. The resulting product ion spectra from both samples showed very similar fragmentation patterns (Fig. 5).

The concentration of N^4 -Ac-SDM in muscle tissue was insufficient for detection by MS and MS–MS. However, the chromatographic behavior of the peak in muscle tissue (Fig. 2), and the above described HPLC, MS and MS–MS characteristics obtained in liver tissue confirmed the presence of N^4 -Ac-SDM in both liver and muscle tissues.

3.3. Calibration curves, assay precision and recovery studies

The calibration curves for OMP, SDM and N^4 -Ac-SDM in muscle tissue were linear ($r^2 > 0.999$) over the concentration range of 0.05 to 10.0 $\mu\text{g/g}$. Similarly, the calibration curves for SDM and N^4 -Ac-SDM in liver tissue were linear ($r^2 > 0.999$) over the concentration range of 0.20 to 25.0 $\mu\text{g/g}$. The lower detection limits of the assay were determined to be 0.05 $\mu\text{g/g}$ in muscle tissue and 0.20 $\mu\text{g/g}$ in liver tissue at a signal-to-noise ratio of 5. The minimum quantification limits were about 3.5 ng in muscle tissue and 14 ng in liver tissue.

The intra-assay variabilities were less than 5% in muscle tissue for all three compounds, and less than 10% in liver tissue for SDM and N^4 -Ac-SDM (Table 1). The inter-assay variabilities were less than 10% in both tissues (Table 2).

The extraction recoveries in muscle and liver tissues ranged from 58 to 84% (Table 3). During extraction, TBAH was added to form a tetrabutylammonium ion-pair with SDM which allowed simultaneous extraction of SDM and OMP into dichloromethane at pH 10 [10]. The addition of granular sodium sulfate anhydrous improved the extraction recoveries.

3.4. Intubation study

The concentration–time curves of OMP, SDM and N^4 -Ac-SDM residues in muscle and liver tissues after gastric intubation are presented in

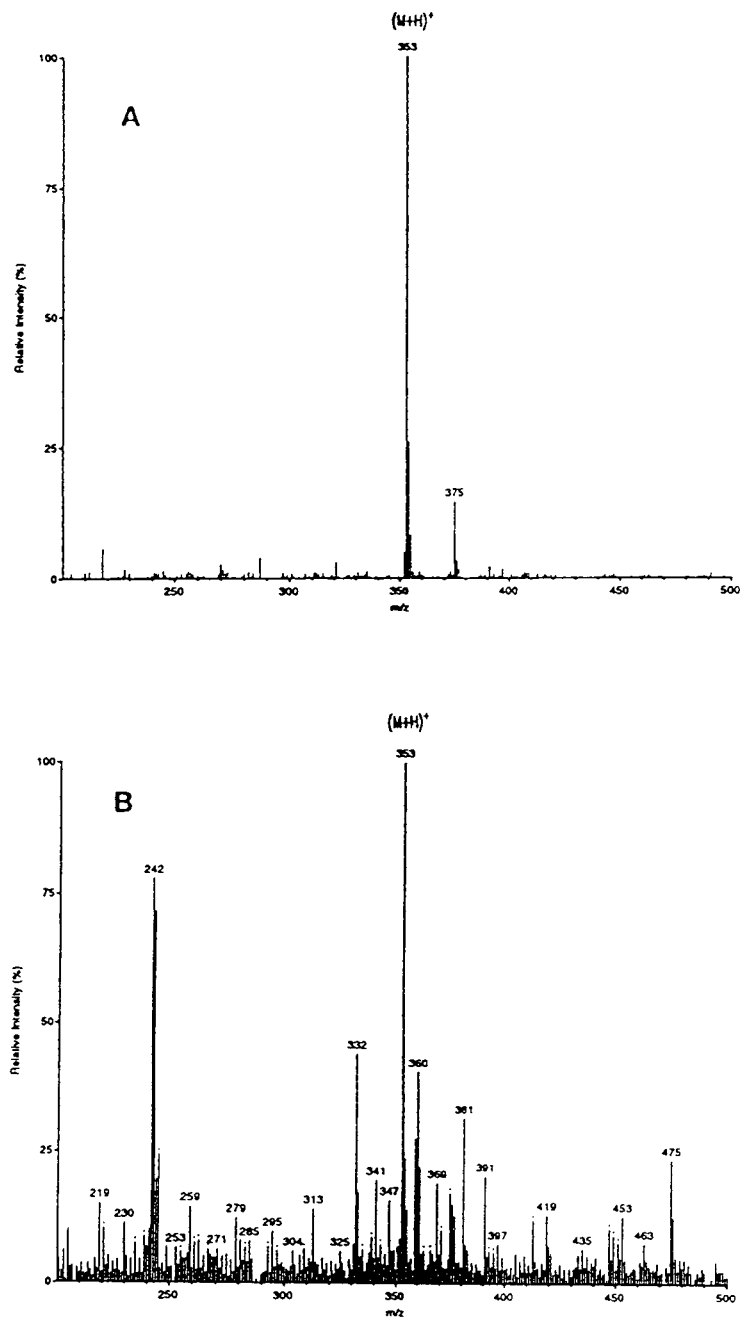


Fig. 4. Flow injection MS analysis of N^4 -Ac-SDM: (A) from N^4 -Ac-SDM synthetic standard and (B) from HPLC fraction containing N^4 -Ac-SDM from liver extract.

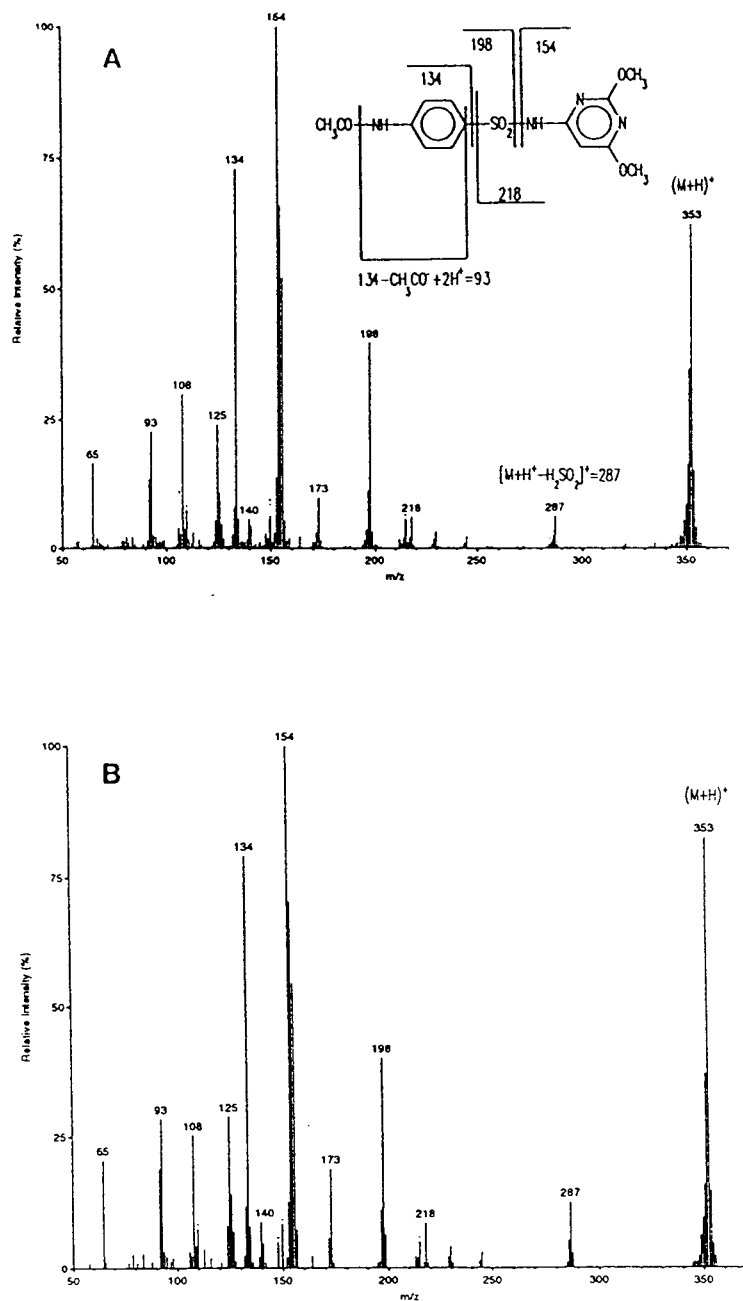


Fig. 5. MS–MS product ion spectra of the protonated molecular ion $[\text{M} + \text{H}]^+$ of N^4 -Ac-SDM obtained by flow injection: (A) from N^4 -Ac-SDM synthetic standard and (B) from HPLC fraction containing N^4 -Ac-SDM from liver extract. The formation of $[\text{M} + \text{H} - \text{H}_2\text{SO}_4]^+$ was confirmed by Pleasance *et al.* [17].

Table 1
Results of intra-assay variability study in muscle and liver tissues

Concentration ($\mu\text{g/g}$)	Variability of OMP (R.S.D., %)	Variability of SDM (R.S.D., %)	Variability of N ⁴ -Ac-SDM (R.S.D., %)
<i>Muscle tissue^a</i>			
0.50	3.6	2.8	1.2
5.00	4.8	0.89	0.19
<i>Liver tissue^a</i>			
0.50	N.D.	4.8	7.2
5.00	N.D.	4.6	3.5
15.0	N.D.	5.1	7.2

^a Six samples containing OMP, SDM and N⁴-Ac-SDM were analyzed at each concentration. N.D. = Not determined.

Figs. 6 and 7. Although OMP and SDM existed in a 1:5 ratio in the drug substances administered, this ratio was not observed from OMP and SDM residue levels in muscle tissue of fish intubated with Romet-30. This observation suggests a difference in the rate of absorption and/or elimination between the two compounds. OMP and SDM were both detectable up to day 20 in muscle tissue. Sulfonamides have been found to be rapidly eliminated initially, but a small persistent residue may remain for a longer period [30]. This finding is also true for the present study where the residue levels of SDM in muscle and liver tissues on days 14, 17 and 20

were not significantly different from one another ($P < 0.05$) (Figs. 6 and 7). SDM was also detectable up to day 20 in liver tissue, however, the overall residue level of SDM in liver tissue was higher than the residue level of SDM in muscle tissue (Figs. 6 and 7).

N⁴-Ac-SDM, a metabolite of SDM, was found to have the lowest residue level among the three analytes studied in muscle tissue and was not detected after day 11. We conclude that the distribution of N⁴-Ac-SDM into muscle tissue was limited and/or the elimination from muscle tissue was rapid. In contrast, the residue levels of SDM and N⁴-Ac-SDM in liver tissue were not

Table 2
Results of inter-assay variability study in muscle and liver tissues

Concentration ($\mu\text{g/g}$)	Variability of OMP (R.S.D., %)	Variability of SDM (R.S.D., %)	Variability of N ⁴ -Ac-SDM (R.S.D., %)
<i>Muscle tissue^a</i>			
0.50	7.9	5.4	3.5
5.00	6.7	5.8	3.0
<i>Liver tissue^a</i>			
0.50	N.D.	9.7	7.8
5.00	N.D.	7.5	5.6
15.0	N.D.	6.7	5.9

^a Six samples containing OMP, SDM and N⁴-Ac-SDM were analyzed at each concentration. N.D. = Not determined.

Table 3
Extraction recoveries from muscle and liver tissues

Concentration of each standard ($\mu\text{g/g}$)	Recovery of OMP (%)	Recovery of SDM (%)	Recovery of $\text{N}^4\text{-Ac-SDM}$ (%)
<i>Muscle tissue</i>			
0.50	65 ± 2^a	76 ± 0.7^a	82 ± 1^a
5.00	68 ± 2^a	79 ± 0.7^a	84 ± 0.6^a
<i>Liver tissue</i>			
0.50	N.D.	58^b	69^b
5.00	N.D.	64^b	74^b
20.0	N.D.	62^b	74^b

^a Presented as mean \pm S.E.M. ($n = 6$).

^b Presented as average values ($n = 2$). N.D. = Not determined.

significantly different from each other ($P < 0.05$) on the same sampling day. This observation suggests that the liver is the major site for the metabolism of SDM, which confirms previous conclusions made in both rainbow trout and channel catfish [22,24,25]. It has also been reported that $\text{N}^4\text{-Ac-SDM}$ predominated in bile of rainbow trout and channel catfish [22,24,25], thereby further indicating that hepatic metabolism and biliary excretion are important elimination pathways for SDM in fish. The extensive enterohepatic recirculation of SDM, and particularly $\text{N}^4\text{-Ac-SDM}$, reported by Kleinow *et al.*

[25] further explains the longer duration of $\text{N}^4\text{-Ac-SDM}$ residue detected in liver tissue up to day 20, as compared with $\text{N}^4\text{-Ac-SDM}$ residue in muscle tissue which was not detectable after day 11. $\text{N}^4\text{-Ac-SDM}$ was also found to be eliminated rapidly at the initial stage but persisted in liver tissue at lower concentrations during the latter sampling periods.

Although gastric intubation was employed to minimize the variations in drug residue levels between individual fish as noted in a previous feeding study [12], significant variations were still

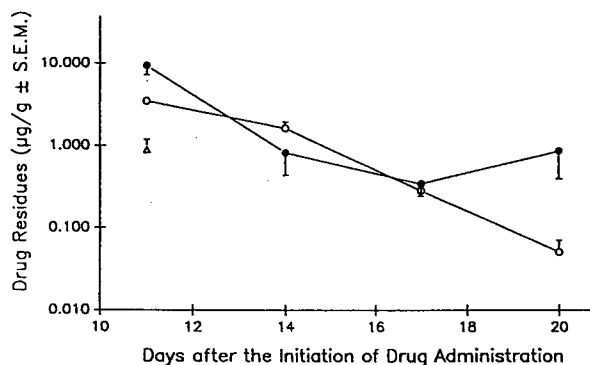


Fig. 6. OMP (○), SDM (●) and $\text{N}^4\text{-Ac-SDM}$ (△) residue profiles in Chinook salmon muscle tissue after intubation with Romet-30. Data points are presented as mean \pm standard error of the mean (S.E.M.).

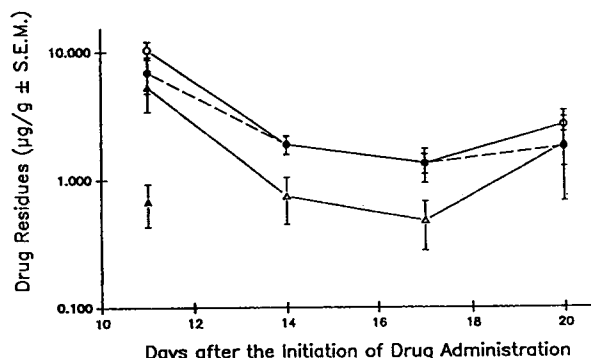


Fig. 7. SDM and $\text{N}^4\text{-Ac-SDM}$ residue profiles in Chinook salmon liver and skin tissues after intubation with Romet-30. Data points are presented as mean \pm standard error of the mean (S.E.M.). ○ = SDM in liver tissue; ● = $\text{N}^4\text{-Ac-SDM}$ in liver tissue; △ = SDM in skin tissue; ▲ = $\text{N}^4\text{-Ac-SDM}$ in skin tissue.

observed. These variations in drug residue levels were most likely attributed to biological variations, such as physical and health conditions of the fish, and to differences associated with absorption, distribution and/or elimination of the drug. Due to considerable inter-fish variations in SDM residue level, the wash-out time for Romet-30 could not be reliably determined from the present study. However, the data shows that the absorption and the elimination of sulfonamide antimicrobials in salmon are highly variable processes and depend on a number of factors beyond the control of the producer.

Although salmon skin tissue was more difficult to analyze because of the presence of high levels of endogenous interfering substances in the tissue extract, an estimation of the residue levels of SDM and N⁴-Ac-SDM was made. The data (Fig. 7) show that the residue profiles of SDM and N⁴-Ac-SDM in skin tissue are very similar to those found in muscle tissue. The overall residue level of SDM was also lower than the residue level of SDM in liver tissue.

The current HPLC assay could not be applied for the analysis in kidney tissue due to the presence of high amounts of endogenous substances, a phenomenon which was also reported by Reimer and Suarez [14].

In conclusion, a sensitive and selective HPLC assay has been developed for the analysis of OMP, SDM and N⁴-Ac-SDM in Chinook salmon muscle tissue and for the analysis of SDM and N⁴-Ac-SDM in Chinook salmon liver tissue. An *in vivo* intubation study revealed considerable variations in Romet-30 residue levels between individual fish. Since the developed HPLC assay in muscle tissue had a higher sensitivity (0.05 µg/g) than the tolerance level for Romet-30 (0.1 µg/g) [3,4], the muscle tissue appears to be a good target tissue for SDM and OMP residue analyses. The developed HPLC assay can also be used for disposition study of N⁴-Ac-SDM.

4. Acknowledgements

This research project was funded by the Science Council of British Columbia. The technical

assistance of Mr. Ron Aoyama, Mr. Michael Gentleman and Ms. Jacqueline Walisser during the intubation study are highly acknowledged. The authors wish to thank Dr. Frank Abbott and Mr. Anthony Borel for the MS–MS experiments. The authors also wish to thank Dr. Ed Donaldson of Department of Fisheries and Oceans for providing the tank space.

5. References

- [1] R.L. Herman and G.L. Bullock, *Vet. Hum. Toxicol.*, 28, Suppl. 1 (1986) 11–17.
- [2] J.S. Rohovec, *Food Rev. Int.*, 6 (1990) 389–397.
- [3] Food and Drug Administration, *Fed. Reg.*, 49 (1984) 46 371.
- [4] Food and Drug Administration, *Fed. Reg.*, 51 (1986) 18 883–18 884.
- [5] T. Bunn, personal communication, 1992.
- [6] G.L. Bullock, G. Maestrone, C. Starliper and B. Schill, *Can. J. Fish. Aquat. Sci.*, 40 (1983) 101–102.
- [7] B. Austin, *Aquaculture International Congress Proceedings*, B.C. Pavilion Corp., Vancouver, 1988, 595–602.
- [8] G.J. Reimer and A. Suarez, *J. Chromatogr.*, 555 (1991) 315–320.
- [9] N. Nose, Y. Hoshino, Y. Kikuchi, M. Horie, K. Saitoh, T. Kawachi and H. Nakazawa, *J. Assoc. Off. Anal. Chem.*, 70 (1987) 714–717.
- [10] G. Weiss, P.D. Duke and L. Gonzales, *J. Agric. Food Chem.*, 35 (1987) 905–909.
- [11] A.R. Long, L.C. Hsieh, M.S. Malbrough, C.R. Short and S.A. Barker, *J. Assoc. Off. Anal. Chem.*, 73 (1990) 868–871.
- [12] J.A. Walisser, H.M. Burt, T.A. Valg, D.D. Kitts and K.M. McErlane, *J. Chromatogr.*, 518 (1990) 179–188.
- [13] M. Horie, K. Saito, Y. Hoshino, N. Nose, H. Nakazawa and Y. Yamane, *J. Chromatogr.*, 538 (1991) 484–491.
- [14] G.J. Reimer and A. Suarez, *J. Assoc. Off. Anal. Chem.*, 75 (1992) 979–981.
- [15] V. Hormazabal and A. Rogstad, *J. Chromatogr.*, 583 (1992) 201–207.
- [16] M.S. Gentleman, H.M. Burt, D.D. Kitts and K.M. McErlane, *J. Chromatogr.*, 633 (1993) 105–110.
- [17] S. Pleasance, P. Blay, M.A. Quilliam and G. O'Hara, *J. Chromatogr.*, 558 (1991) 155–173.
- [18] S. Pleasance, P. Thibault and J. Kelly, *J. Chromatogr.*, 591 (1992) 325–339.
- [19] M.G. Barron and M.O. James, *Mar. Environ. Res.*, 24 (1988) 85–88.
- [20] M.G. Barron, C. Gedutis and M.O. James, *Xenobiotica*, 18 (1988) 269–276.
- [21] C.M.F. Michel, K.S. Squibb and J.M. O'Connor, *Xenobiotica*, 20 (1990) 1299–1309.

- [22] K.S. Squibb, C.M.F. Michel, J.T. Zelikoff and J.M. O'Connor, *Vet. Hum. Toxicol.*, 30, Suppl. 1 (1988) 31–35.
- [23] S.M. Plakas, R.W. Dickey, M.G. Barron and A.M. Guarino, *Can. J. Fish. Aquat. Sci.*, 47 (1990) 766–771.
- [24] K.M. Kleinow and J.J. Lech, *Vet. Hum. Toxicol.*, 30, Suppl. 1 (1988) 26–30.
- [25] K.M. Kleinow, W.L. Beilfuss, H.H. Jarboe, B.F. Droy and J.J. Lech, *Can. J. Fish. Aquat. Sci.*, 49 (1992) 1070–1077.
- [26] B.F. Droy, M.S. Goodrich, J.J. Lech and K.M. Kleinow, *Xenobiotica*, 20 (1990) 147–157.
- [27] B.F. Droy, T. Tate, J.J. Lech and K.M. Kleinow, *Comp. Biochem. Physiol.*, 94C (1989) 303–307.
- [28] G.E. Delory and E.J. King, *Biochem. J.*, 39 (1945) 245.
- [29] P.M. Windholz, S. Budavari, L.Y. Stroumstos and M.N. Fertig, *The Merck Index of Chemicals and Drugs*, Merck & Co., Rahway, NJ, 1976, p. 1152.
- [30] D.J. Alderman, in J.F. Muir and R.J. Roberts (Editors), *Recent Advances in Aquaculture*, Vol. 3, Croom Helm, London, Sydney, 1988, p. 18.

Analysis of colloidal particles

V[☆]. Size-exclusion chromatography of colloidal semiconductor particles

Christian-Herbert Fischer*, Michael Giersig, Thore Siebrands

Hahn-Meitner-Institut Berlin, Abt. Photochemie, Glienicker Strasse 100, D-14109 Berlin, Germany

(First received December 8th, 1993; revised manuscript received February 17th, 1994)

Abstract

An HPLC technique for the size determination of colloidal cadmium sulphide and zinc sulphide in a diameter range from 20 down to 2 nm using silica with pore sizes from 30 to 100 nm is described. The growth of the particles during the run was suppressed by the addition of stabilizers to the eluent and by the use of reversed-phase silica as the stationary phase for inorganic stabilizers. The calibration of the column sets by electron microscopy resulted in a linear relationship between the logarithm of the particle diameter and the elution time. The analysis was carried out within 4–10 min. The lateral resolution lay between 1.3% for larger particles and 1.9% for smaller particles. Below a diameter of 13 nm these values were better than those found from electron microscopy. From the comparison of the calibration lines for various colloidal materials, the differences in their electrical double layers could be estimated. The limitations of the method are discussed and the size-exclusion chromatographic and electron microscopic methods are compared.

1. Introduction

A new branch of colloid chemistry has arisen during the last 10 years resulting from numerous investigations of the photochemistry, radiation chemistry and electrochemistry of nanometre-sized semiconductor and metal particles [5,6]. In the presence of suitable stabilizers, such as polyphosphate and poly(vinyl alcohol), and under optimized conditions, aqueous sols could be prepared with particle diameters down to 1.3 nm [3]. When long-chain alkane thiols were used for the stabilization, the thiol groups were strongly bound to the surface of the inorganic

particles, and as a result they are soluble in organic solvents such as tetrahydrofuran and cyclohexane [7]. These nanoparticles show many interesting phenomena, *e.g.*, size quantization effects (*Q*-effects) in optical absorption and fluorescence spectra.

Colloidal semiconductors are of interest for their possible use of solar energy and in micro-electronic devices. Because of their extraordinary properties, nanoparticles are a very important topic for basic physico-chemical research. For these studies, a knowledge of the size and size distribution of the colloidal particles is very important. Electron microscopy (ELMI) is a good but time-consuming method with respect to particle instability and tedious evaluation [8]. Because many colloidal particles grow in spite of

* Corresponding author.

☆ For Parts I–IV, see refs. 1–4, respectively.

being stabilized, it was necessary to find a more rapid method.

Size-exclusion chromatography (SEC) seemed to be a promising alternative. It is widely used for the molar mass determination of organic polymers. In the past also many papers have been published dealing with the analysis of latexes [9], but only a very few on suspensions of solid inorganic particles, *e.g.*, silica and aluminosilicate, which are generally stable colloids [10,11]. This might be due to the fact that many nanometre-sized materials were developed only recently and with SEC they often cause severe problems with stability and absorption. Very recently gold sols have been proposed for the characterization of low-pressure LC columns [12].

Our studies on the SEC of inorganic nanoparticles began with low-pressure chromatography on Sephacryl gels [1]. The work continued with HPLC because of higher resolution and shorter analysis times [2,3]. The latter is extremely important for rapidly growing colloidal species. Previous papers published in physico-chemical journals have described the applications of SEC for colloidal chemists, such as studies of growth mechanisms, of the size-dependent optical spectra in metal sols [4], in semiconductor sols, of magic agglomeration numbers [2] and the preparation of colloids inside an HPLC column [3]. This paper deals with chromatographic aspects of the separation of unstable semiconductor particles by SEC. The method development was carried out with colloidal cadmium sulphide, as it is one of the best known semiconducting materials. The method also was applied to zinc sulphide. In the future, the rigid, non-swelling, non-shrinking, solid particles might also assist in understanding by comparison phenomena of the SEC of organic polymer coils.

2. Experimental

2.1. HPLC conditions

The equipment consisted of a Merck–Hitachi L 6000 pump and a Merck–Hitachi L4200 UV–

Vis detector operating at 250 nm or a Waters Model 990 diode-array detector and a Knauer electrically driven injection valve with a 20- μ l sample loop. For aqueous colloids a set of two 125 mm \times 4 mm I.D. Knauer columns were used in most instances, the first packed with Nucleosil 500 C₄ (7 μ m) and the second with Nucleosil 1000 C₄ (7 μ m) from Macherey–Nagel, and in some instances a set of two 250-mm columns containing Nucleosil 300 C₁₈ (5 μ m, 5.6 mm I.D.) and Nucleosil 500 C₁₈ (5 μ m, 4 mm I.D.). The mobile phase was an aqueous solution of 1 mM sodium polyphosphate [based on the formula Na₆(PO₃)₆; Riedel-de Haën] and 1 mM Cd(ClO₄)₂ (Ventron) for CdS colloids and Zn(ClO₄)₂ (Ventron) for ZnS colloids. CdS colloids stabilized with dodecanethiol were analysed on Nucleosil 500 (7 μ m) and Nucleosil 1000 (7 μ m) columns, the eluent being 1 mM Cd(ClO₄)₂–1 mM C₁₂H₂₅SH in tetrahydrofuran. The flow-rate was 0.5 ml/min under all conditions. Data collection was carried out with either a Bruker Chromstar system or a Waters Model 990 system.

2.2. Preparation of colloidal metal sulphides

Hydrogen sulphide gas or aqueous sodium hydrogensulphide solution was injected through a septum into an aqueous Cd(ClO₄)₂ or Zn(ClO₄)₂ and sodium polyphosphate solution (1 mM each), through which nitrogen had been bubbled for 10 min. After shaking, the solution was used. The particle size was controlled by the amount of sulphide and by the pH value [6]. CdS sols with an organic stabilizer were prepared as follows: Cd(ClO₄)₂ (1 mM) and C₁₂H₂₅SH (0.1 mM–1 M) were dissolved in tetrahydrofuran, and after evacuation and bubbling with nitrogen, hydrogen gas was injected (0.2 mM).

2.3. Electron microscopy

A small drop of sample was adsorbed on the copper grids coated with a 50-Å thick carbon support film. After a contact time of 10 s the fluid was blotted off. The grids were dried under argon and examined in a Philips CM 12 transmission electron microscope with an acceleration

voltage of 120 kV. The microscope was equipped with a supertwin lens and an EDAX detector. For imaging, axial illumination was used in addition to the “nanoprobe mode” with a beam spot size of 1.5 nm, to permit the diffraction of the individual clusters. All images were made under conditions of minimum phase contrast artefacts with magnifications of 120 000 and 430 000 \times .

3. Results and discussion

3.1. Stationary phase

Colloids cannot exist in the presence of high salt concentrations in the eluent as a means of reducing adsorption. Increasing ionic strength would lead to adsorption of ions on the charged surface of the particles. This diminishes the stabilizing net charge and thereby the repelling forces. Coagulation and finally precipitation can occur. Therefore, stationary phases with low

adsorption power had to be applied. In fact, the C₄-modified silica gave better resolution than the unmodified silica because the silanol groups which cause polar interactions were substantially shielded. For particles with diameters between 2 and 20 nm two columns in series with pore sizes of 50 and 100 nm, respectively, were used. These large pores were essential. Obviously the effective size of the particles was much larger. It included the electrical double layer, which was formed at the solid–liquid interface, when particles were charged, and opposite ions were localized at a certain distance from the surface. Also electrical interactions between colloidal particles and the surface of the stationary phase have to be considered. When both carried charges of the same sign, the resulting repulsion reduced the accessible pore volume.

The results for four aqueous cadmium sulphide sols stabilized with polyphosphate are shown in Fig. 1: on the left-hand side the electron micrographs and the corresponding size

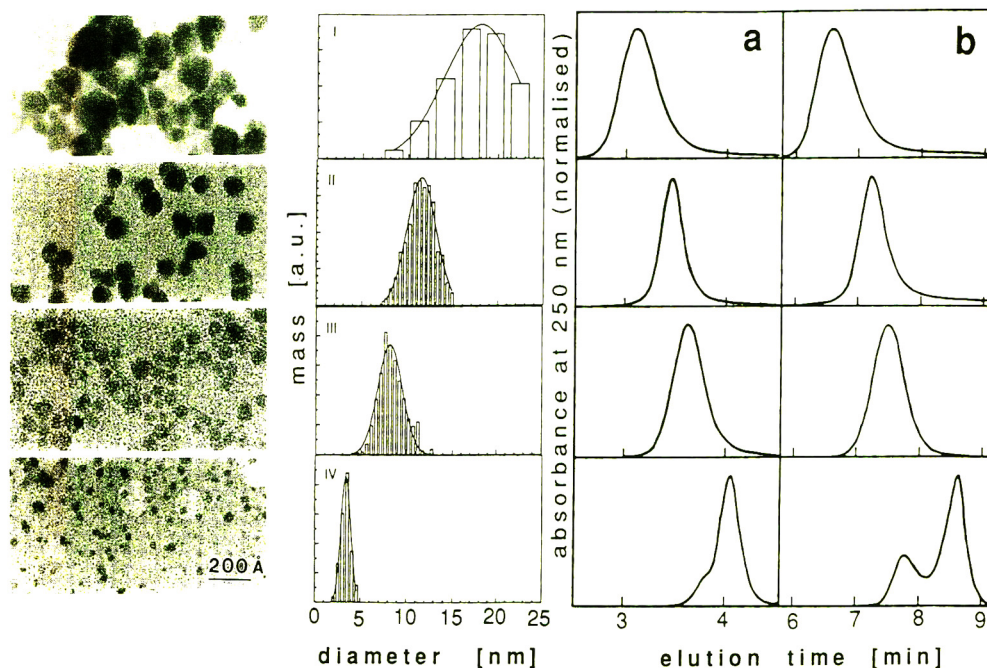


Fig. 1. Four aqueous CdS sols of different particle sizes (stabilizer polyphosphate). Left, electron micrographs and corresponding mass-based size distributions from ELMI; right, SEC separations (a) on Nucleosil 500 C₄ + Nucleosil 1000 C₄ (length each 120 mm) and (b) on Nucleosil 300 C₁₈ + Nucleosil 500 C₁₈ (length each 250 mm). Eluent for both series, 1 mM Cd(ClO₄)₂–1 mM polyphosphate; for further details, see Experimental.

distributions from ELMI and in the middle part the chromatograms obtained on two C_4 -modified silica columns as described under Experimental. The shift of the retention time was inversely related to the change in particle size. Later it was revealed that very small particles (below 2 nm), which do not absorb light in the visible range, grew during the run through the column, whereas no change took place within the same material when it was not injected on to the column. This growth was evident on inspection of the optical absorption spectra before and after the run (Fig. 2). The maximum at 275 nm had shifted to 305 nm after the passage through the column. The onset of absorption shifted towards longer wavelengths. According to the Q -effect, such a red shift takes place when the particle size increases. It is due to the decreasing energy gap between the valence band and the conductivity band. Therefore, in the actual case of the surface of the stationary phase, probably the remaining active silanol groups catalysed the growth of the particles. C_{18} -modified silica, where the silanol groups are better shielded by the larger hydrophilic layer, did not show this undesirable catalytic effect

The best results were obtained with two col-

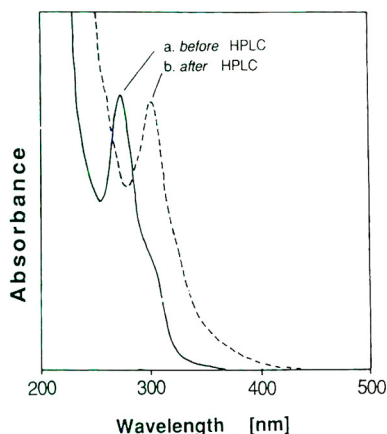


Fig. 2. Normalized optical absorption spectra of an aqueous CdS sol (stabilizer polyphosphate), containing very small particles (mean diameter of the original sample 1.3 nm). (a) Original sample; (b) collected effluent from Nucleosil 500 C_4 + Nucleosil 1000 C_4 .

umns (length of each 250 mm) with 30 and 50 nm pore size (Fig. 1, right). Further, the resolution was enhanced especially in the smaller diameter range so that the two populations in sample IV were better separated. The minor population of larger particles was invisible in the electron microscope (see below). When cadmium sulphide stabilized with organic substances such as long-chain alkanethiols was to be analysed, unmodified silica was preferred, in order to avoid a mixed SEC-reversed-phase mechanism. The surface of these particles is very hydrophobic so that adsorption does not play the same role as in the previous cases. It is worth mentioning that alterations of the colloids by the chromatographic process were also ruled out by reinjection experiments where no changes in the elution times were observed.

3.2. Mobile phase

Four normalized chromatograms of the same aqueous CdS sol stabilized with polyphosphate are shown in Fig. 3. It was injected on to the

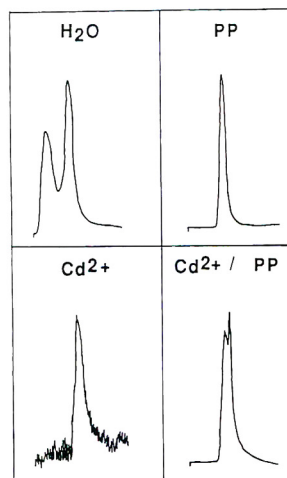


Fig. 3. Optimization of the eluent. Chromatograms of the same aqueous CdS sol (stabilizer polyphosphate) on Nucleosil 500 C_4 + Nucleosil 1000 C_4 with four different eluent compositions: water, water–1 mM polyphosphate (PP), water–1 mM $Cd(ClO_4)_2$ and water–1 mM $Cd(ClO_4)_2$ –1 mM polyphosphate. Only the time range between 2.5 and 4.7 min is shown.

same C_4 -modified silica columns (pore size 50 and 100 nm) but utilizing different eluents: pure water, water containing polyphosphate or cadmium perchlorate or polyphosphate plus cadmium perchlorate. The cadmium salt alone led to irreversible and almost complete adsorption of the colloidal material (evident from the high noise level). As already mentioned, electrolytes in the solution lower the stability of a sol, especially in the absence of a stabilizer. Not only are the repelling forces between the particles themselves reduced, but also between them and all kinds of other surfaces with the same charge. When water without stabilizer was used as the eluent, the weakly bound stabilizer molecules separated from the particles by SEC, because they were smaller. As a result of this loss of stabilizer, many particles had grown, as indicated by the second peak in the chromatogram at earlier elution times. The stabilizer did not appear in the chromatogram, because polyphosphate does not absorb substantially at 250 nm.

The best results with respect to particle stability and resolution were obtained with an eluent containing a 1 mM aqueous solution of both polyphosphate [1 mM based on the formula $Na_6(PO_3)_6$] and cadmium perchlorate. Under these conditions the particles are always surrounded by the stabilizer and by the cations of the colloid. From sol preparation it is well known that an excess of the metal cations over the precipitating anions (here sulphide) generates smaller particles as opposed to a deficiency, which forms larger particles [6,13]. It seemed to be possible to generalize this eluent composition: solvent of the colloid with 1 mM stabiliser + 1 mM of the cation, from which the sol was generated. This rule worked very well not only for aqueous sulphides of zinc and cadmium stabilized with polyphosphates, but also for cadmium sulphide stabilized with alkanethiols (Fig. 4). In the latter case tetrahydrofuran was chosen, for two reasons: it is an excellent organic solvent for inorganic salts and also its ether group has complex-forming and stabilizing properties as known from the Grignard reactions of metal organic compounds. It should be mentioned that a negative system peak appeared whenever the

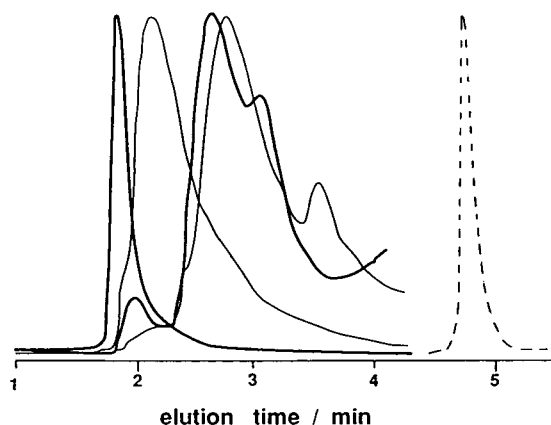


Fig. 4. Chromatograms of four CdS sols (solid lines) of various particle sizes in tetrahydrofuran with dodecanethiol as stabilizer. Columns, Nucleosil 500 + Nucleosil 1000; eluent, 1 mM $CdClO_4$ –1 mM dodecanethiol–tetrahydrofuran. Dashed line, dodecanethiol.

thiol concentration in the sample was lower than in the eluent. This offers a way to calculate the amount of stabilizer bound to the particles.

In another series of experiments, the influence of the stabilizer in SEC was investigated. Cadmium sulphide sols of various sizes prepared in the presence of polyphosphate were injected in both eluents, containing cadmium perchlorate with either polyphosphate or triphosphate. The concentration of the latter was 2 mM so that the content of phosphate units was the same in both mixtures. In all instances the elution time with the triphosphate eluent was significantly shorter (by 10–15%) than the corresponding value with polyphosphate. Growth of particles in the triphosphate eluent, because of its minor stabilizing power, could be ruled out by reinjection of the collected colloid from the triphosphate run in the polyphosphate eluent. No change in elution time was observed in comparison with the original sample also injected in polyphosphate eluent (Fig. 5). Only a large second peak appeared due to triphosphate, which became visible even at 250 nm, because the colloid was very highly diluted after two chromatographic runs and high sensitivity had to be applied.

The reason for the shift in elution time was the change in the electrical double layer when the

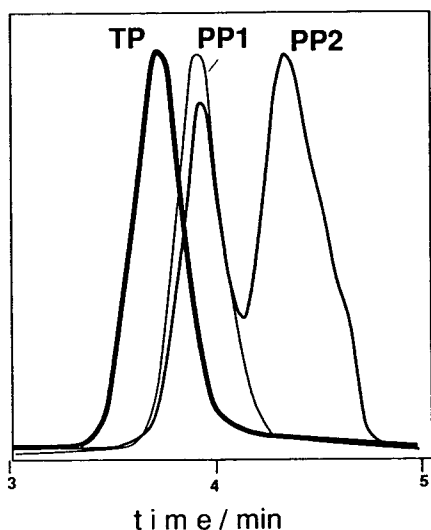


Fig. 5. SEC of an aqueous CdS sol (stabilizer polyphosphate) on Nucleosil 500 C₄ + Nucleosil 1000 C₄. The chromatograms are normalized. PP1: original sample; eluent, 1 mM Cd(ClO₄)₂–1 mM polyphosphate. TP: original sample; eluent, 1 mM Cd(ClO₄)₂–2 mM triphosphate. PP2: collected effluent from TP; eluent, 1 mM Cd(ClO₄)₂–1 mM polyphosphate.

electrolyte, which surrounded the particles, was varied. The used polyphosphate is a polyelectrolyte with a high content of hexamers and higher phosphates. The average negative charge per molecule is at least two times higher than for triphosphate. Therefore, the SEC result is in accordance with the Debye–Hückel model: the double layer thickness decreased exponentially with increasing charge of the electrolyte [14]. This effect can be illustrated by means of Fig. 5 and the calibration of the column discussed in the next section (Fig. 6). A CdS sol with an average size of 2.6 nm has an elution time of 3.93 min in a polyphosphate-containing eluent whereas in triphosphate it is only 3.73 min. This latter value corresponds to 3.9 nm according to the calibration in polyphosphate eluent (see below), *i.e.*, just by exchanging the stabilizer it allowed the particles to appear larger by 1.3 nm or 50%! The order of magnitude seemed reasonable for a change from an 1-6-electrolyte to an 1-3-electrolyte [14].

3.3. Calibration

For the calibration of a column set, relatively monodisperse sols of different particle sizes were prepared. These samples were investigated by transmission electron microscopy. The diameters of a statistically sufficient number of particles (whenever possible more than 300) were measured on the micrographs and the mass distributions of the diameters were constructed (Eq. 1 and Fig. 1):

$$nd^3 = f(d) \quad (1)$$

where n is the number of particles and d the particle diameter.

The mass-based instead of number-based distribution is necessary, because the spectrophotometric detector gives a response proportional to the concentration and therefore also to the mass of material. For the calibration, the logarithm of the diameter is plotted as a function of the elution time as colloidal chemists prefer the more descriptive diameter instead of the molar mass used in polymer chemistry.

Calibration plots are shown in Fig. 6 for the sulphides of cadmium and zinc, respectively, both stabilized with polyphosphate. The experiments of Fig. 6a were obtained on C₄-modified silica with a column length of 2 × 120 mm. The data points for zinc sulphide showed more scattering. The reason is the existence of two different crystal shapes, spherical and brick-like. Form factors would be necessary for a better linear fit. The side ratio of the bricks was about 1:3. For a first approach, two thirds of the long side was used as the size for these crystals when the histograms were constructed for the determination of the average size.

Large differences between the two materials are shown in Fig. 6a: cadmium sulphide particles eluted in cadmium perchlorate–polyphosphate much earlier than zinc sulphide of the same size in zinc perchlorate–polyphosphate. The delay of zinc sulphide was longer for smaller than for larger particles, *e.g.*, 8-nm ZnS corresponded to 3.8-nm CdS and 5-nm ZnS to 0.9-nm CdS, respectively. As described above the electrical

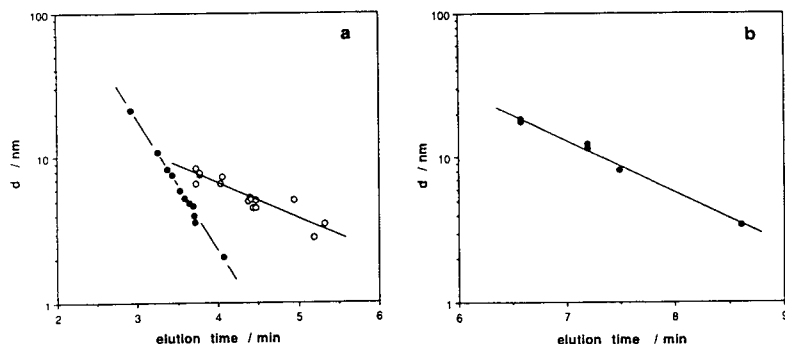


Fig. 6. SEC calibration on Nucleosil. (a) CdS (●) and ZnS (○) on Nucleosil 500 C₄ + Nucleosil 1000 C₄; (b) CdS on Nucleosil 300 C₁₈ + Nucleosil 500 C₁₈. For details, see Experimental part. Eluent, water–1 mM polyphosphate and 1 mM Cd(ClO₄)₂ or Zn(ClO₄)₂, respectively.

double layer is responsible for the differences between size of the solid particle and its effective size. The thickness of this double layer is dependent on the ions in the solution and of course also on the properties of the solid. With data from more materials it might be possible to estimate the relative thickness of the double layers. The effects of eluent components adsorbed on the stationary phase and their possible interactions with the colloids (repulsion or attraction) need further investigation. Consequently, one calibration is valid only for one kind of colloid under well defined conditions including the eluent composition (see above).

In Fig. 6b, the calibration on C₁₈-modified silica with longer columns (2 × 250 mm) is given. As already mentioned, under these conditions much better results were obtained even if in double the time. Nevertheless, the analysis times of 5 and 10 min, respectively, were remarkably short.

3.4. Comparison of SEC and ELMI

Resolution

Two kinds of resolutions have to be considered, as follows.

(1) Lateral resolution or scale resolution: lateral resolution is the term used in electron microscopy, meaning the smallest detectable difference in size, *i.e.*, actually between two

particles in ELMI. It corresponds to the smallest detectable difference in size between two strongly monodisperse sols in SEC. The lateral resolution of the Philips microscope utilized for these experiments is 0.18 nm. In SEC, the standard deviation of the measured size has to be considered. It can be assumed that it is mainly controlled by the uncertainty of the elution time as long as monodisperse samples are taken into account. The standard deviations of the elution time, σ_t , of eight injections of potassium iodide were found to be 0.0099 min (0.22%) for the combination of short 500 C₄ + 1000 C₄ columns and 0.018 min (0.17%) for that of long 300 C₁₈ + 500 C₁₈ columns. In contrast to electron microscopy, the lateral resolution in SEC is a function of the absolute size because of the logarithmic relationship between diameter and elution time. This function is determined from the calibration function in its exponential form (Eq. 2) with the determined relative standard deviation of elution time $\sigma_{t,rel}$. For a range of times t_i and diameters d_i , respectively, the diameters $d_{i+\sigma}$ are calculated. They correspond to the times t_i plus the standard deviation of time σ_{t_i} , which is the product of the time t_i multiplied by the relative standard deviation in % over 100 (Eq. 3).

$$d_i = 8890.3 \cdot 10^{-0.89856t_i} \quad (2)$$

(with d_i in nm and t_i in min);

$$d_{i+\sigma} = 8890.3 \cdot 10^{-0.89856t_i(1+\sigma_{t_{re}}/100)} \quad (3)$$

$$\sigma_{d_i} = d_i - d_{i+\sigma} \quad (4)$$

The difference between d_i and $d_{i+\sigma}$ is the standard deviation of the diameter σ_{d_i} at the particular diameter d_i (Eq. 4). Values between 0.07 and 0.24 nm were obtained for SEC in the size range between 2 and 20 nm, corresponding to relative standard deviations between 1.9% and 1.3%. As can be seen from Fig. 7 (top), the values for ELMI were better for larger particles,

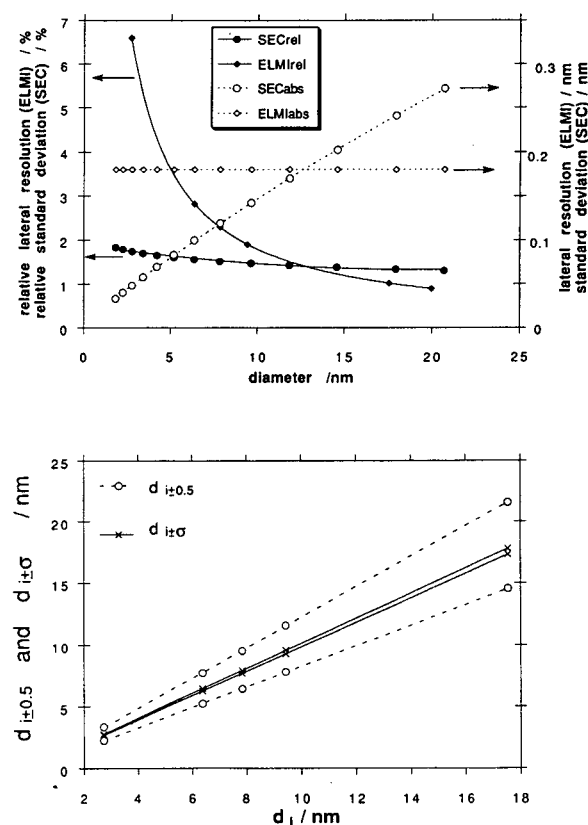


Fig. 7. Resolution of ELMI and SEC as a function of particle diameter. Aqueous CdS sols (stabilizer polyphosphate) on Nucleosil 500 C₄ + Nucleosil 1000 C₄. Top: absolute and relative lateral resolution in ELMI and absolute and relative standard deviation of the measured diameter in SEC as a function of the diameter. Bottom: lateral and separation resolution in SEC as a function of d_i . The full lines enclose the area between $d_{i+\sigma}$ and $d_{i-\sigma}$. The area between the dashed lines is limited by $t_{i+0.5}$ and $t_{i-0.5}$. For further explanation, see text.

but more than three times worse for the smallest particles.

(2) Moreover, the resolution in the chromatographic sense, the separation resolution, has to be considered, *i.e.*, the resolution of two different size populations in *one* sol. Strongly monodisperse colloids were hardly available. Therefore, the peak half-width of potassium iodide was used for this estimation, although as a small ionic compound it had the longest possible elution time and therefore the broadest peak of any monodisperse species. Hence it is the worst case. Its peak width $b_{0.5} = 0.19$ min was transformed into size values in a similar way as before, both for selected elution times t_i and for the times $t_{i+0.5} = t_i + 0.5b_{0.5}$ and $t_{i-0.5} = t_i - 0.5b_{0.5}$ the corresponding diameters $d_{i+0.5}$ and $d_{i-0.5}$ were calculated. In Fig. 7 (bottom), these resulting sizes are plotted against the measured diameters. The area between the full lines represents the uncertainty due to the standard deviation of the elution time. The area between the dashed lines is equivalent to all sizes between the peak half-width. This looks worse than it is for two reasons. First, in practice sols with a size distribution of a few per cent standard deviation do not exist, nor do they occur in one sol with a very close mean size. The typical CdS samples in Fig. 1 have standard deviations in the range 14–23% according to the ELMI results. Second, the earlier a peak eluted the smaller was its peak width, whereas the calculation was carried out with the broadest possible peak width. Theoretically, ELMI should be superior in this respect. However, actually the high energy of the electron beam can lead to radiation damage of the sample itself, so an artificial size distribution is generated and the resolution is decreased, though it is difficult to quantify this effect depending on the material [15].

Statistics and other factors

SEC gives an integral picture of the size distribution with perfect statistics as long as all components elute, whereas the number of counted particles in ELMI is limited. It happened also in ELMI that small particles were completely hidden under larger particles or a

minor population was not observed, at all as in Fig. 1, sample IV, or smaller particles were concentrated in one part of the ELMI support and larger particles in another. All of these effects would deteriorate the statistics for an ELMI size result. Another advantage of SEC is the measurement in solution. The colloids do not lose their solvent, which could cause particle growth.

3.5. Limitations of the method

There are two limitations to the SEC of colloids: too large and too active particles. CdS particles with diameters larger than 20 nm are filtered off by the column. Colloids with very high surface activity such as lead sulphide or silver iodide are irreversibly adsorbed. In such cases it is sometimes successful to work with less fine stationary phases, e.g., 15–25 μm instead of 7 μm material, where the adsorption power and pore volume are more favourable.

4. Conclusions

SEC is a powerful method for the size determination of nanometre-sized colloidal particles. Even unstable colloids can be analysed fairly accurately when the eluent contains a suitable stabilizer. SEC needs electron microscopy once for a calibration. The result is statistically optimum. However, it should be stressed that as for organic polymers, each kind of colloid has its own calibration and optimum conditions including eluent composition. Connection of various detectors will allow easy measurements of various kinds of size-dependent properties. Preparative separations yield very oligodisperse colloids from polydisperse colloids. A paper on this topic is in preparation. Finally, one of the main

benefits of the technique is the speed, which allows the elucidation of growth mechanisms even in cases of very rapidly growing particles.

5. Acknowledgements

The authors thank Ms. U. Michalczyk for helpful assistance with the laboratory work and Ms. L. Katsikas for the preparation and evaluation of the CdS sols used on Nucleosil 500 C₄ and Nucleosil 1000 C₄ for the calibration. The support of Dr. E. Orlova and Ms. U Bloeck with the electron microscopy is gratefully acknowledged.

6. References

- [1] Ch.-H. Fischer, J. Lilie, H. Weller, L. Katsikas and A. Henglein, *Ber. Bunsenges. Phys. Chem.*, 93 (1989) 61.
- [2] Ch.-H. Fischer, H. Weller, L. Katsikas and A. Henglein, *Langmuir*, 5 (1989) 429.
- [3] Ch.-H. Fischer and M. Giersig, *Langmuir*, 8 (1992) 1475.
- [4] T. Siebrands, M. Giersig, P. Mulvaney and Ch.-H. Fischer, *Langmuir*, 9 (1993) 2297.
- [5] A. Henglein, *Top. Curr. Chem.*, 143 (1988) 115.
- [6] H. Weller, *Angew. Chem.*, 105 (1993) 43.
- [7] Ch.-H. Fischer and A. Henglein, *J. Phys. Chem.*, 93 (1989) 5578.
- [8] A.I. Kirkland, D.A. Jefferson, D. Tang and P.P. Edwards, *Proc. R. Soc. London, Ser. A*, 423 (1991) 279.
- [9] K.F. Krebs and W. Wunderlick, *Angew. Makromol. Chem.*, 20 (1971) 203.
- [10] T. Tarutani, *J. Chromatogr.*, 50 (1970) 523.
- [11] J.J. Kirkland, *J. Chromatogr.*, 185 (1979) 273.
- [12] M. Holtzhauer and M. Rudolph, *J. Chromatogr.*, 605 (1992) 193.
- [13] A. Fojtik, H. Weller, U. Koch and A. Henglein, *Ber. Bunsenges. Phys. Chem.*, 88 (1984) 969.
- [14] P.C. Hiemenz, *Principles of Colloid and Surface Chemistry*, Marcel Dekker, New York, 2nd ed., 1986.
- [15] E. Zeitler (Editor), *Cryoscopy and Radiation Damage*, North-Holland, Amsterdam, 1982.

Ion chromatographic separation of alkali metal and ammonium cations on a C₁₈ reversed-phase column

Kazuaki Ito^{*,a}, Haruki Shimazu^a, Eiji Shoto^a, Mitsumasa Okada^a,
Takeshi Hirokawa^b, Hiroshi Sunahara^{a,☆}

^aDepartment of Environmental Science, Faculty of Engineering, Hiroshima University, 1-4-1 Kagamiyama,
Higashi-Hiroshima 724, Japan

^bDepartment of Applied Physics and Chemistry, Faculty of Engineering, Hiroshima University, 1-4-1 Kagamiyama,
Higashi-Hiroshima 724, Japan

(First received October 18th, 1993; revised manuscript received February 1st, 1994)

Abstract

The separation of alkali metal (Li⁺, Na⁺, K⁺, Rb⁺ and Cs⁺) and ammonium cations on a C₁₈ reversed-phase column using three anionic surfactants [sodium 1-icosyl sulphate, sodium dodecyl benzenesulphonate and sodium dodecyl sulphate (SDS)] is described. Two methods were examined: (a) “permanent” coating, with the use of a C₁₈ reversed-phase column previously coated with the surfactants; and (b) dynamic coating, with addition of the surfactants to the mobile phase. With method (a) the separation of the six cations was achieved with SDS. However, the retention times gradually decreased owing to dissolution of the SDS coating. Good separation was obtained with method (b), where 10 mM HNO₃ containing 0.1 mM SDS was used as the mobile phase with conductivity detection, and it was applied satisfactorily to real samples. The effect of system peaks on determination is also discussed.

1. Introduction

Ion chromatography (IC) is a useful technique for the separation and detection of alkali metal and ammonium cations. Low-capacity cation-exchange columns are used for the separation, and various systems of eluents and detection methods have been studied to optimize both separation and detection [1–4]. The elution order is in general Li⁺ < Na⁺ < NH₄⁺ < K⁺ < Rb⁺ < Cs⁺ and it almost follows the order of ionic size (Li⁺ < Na⁺ < K⁺ < NH₄⁺, Rb⁺ < Cs⁺).

On the other hand, reversed-phase columns may be used to separate these cations if cation-exchange groups can be introduced on the surface of the packing material or an electrical double layer can be obtained for cation retention. For anion separation, the use of such columns has been extensively studied and successfully applied to many real samples [5–7]. However, it has hardly been examined for the above cations. If reversed-phase columns can also be used, such columns would have greater flexibility.

The above approach was examined by Molnar *et al.* [8] and Smith and Pietrzyk [9] for the separation of alkali metal and ammonium cations. However, separation of the six cations was

* Corresponding author.

☆ Present address: Faculty of Engineering, Kinki University,
1-Umenobe, Takaya, Higashi-Hiroshima 729-17, Japan.

not successful. Molnar *et al.*'s method [8] used three long octadecylsilica (ODS) columns (of each 250×4.6 mm I.D.) with 5 mM *n*-heptanesulphonate [$\text{CH}_3(\text{CH}_2)_6\text{SO}_3^-$] solution (pH 2) as a mobile phase. Although the chromatographic peaks of Na^+ , K^+ and NH_4^+ appeared at retention times around 9–12 min (flow-rate 2 ml/min), the peaks of Li^+ and Na^+ and those of NH_4^+ and Rb^+ overlapped. Smith and Pietrzyk [9] also examined the separation of Na^+ , K^+ , NH_4^+ and Cs^+ using mobile phases containing alkanesulphonate salts [$\text{CH}_3(\text{CH}_2)_6\text{SO}_3^-\text{Li}^+$ and $\text{CH}_3(\text{CH}_2)_7\text{SO}_3^-\text{Li}^+$] as additives in H_2O –MeOH mixed solvents on a poly(styrene–divinylbenzene) column (150×4.1 mm I.D.). MeOH was added to adjust the exchange capacity in the range 20–40 μM per column. However, even under the best conditions tested the peaks appeared around retention times of 8–11 min and the peak of NH_4^+ almost overlapped that of Cs^+ . The low separability may be mainly due to the small amounts of chemicals sorbed, *viz.*, a lower cation-exchange capacity. Schwedt *et al.* [10] examined the separation of alkali metal cations on an ODS column (250×4 mm I.D.) with a pre-column (50×4 mm I.D.) using various kinds of weak acids and applied the method to wine and mineral water samples. The retention times of Li^+ , Na^+ and K^+ were around 7–10 min using 2 mM *n*-hexylsuccinic acid–1 mM oxalic acid (pH 2.92).

Another method using reversed-phase columns for cation separations is to use neutral ligands such as crown ethers. Crown ether moieties are immobilized on the column surface through covalent bonding, or lipophilic crown ethers are coated by hydrophobic interaction [11,12]. The retention behaviour of crown ether stationary phases depends strongly on the type of crown ether used. For an ODS column coated with dodecyl-18-crown-6, for example, the elution order is $\text{Li}^+ < \text{Na}^+ < \text{Cs}^+ < \text{Rb}^+ < \text{K}^+$. The elution of K^+ is retarded, indicating that K^+ ion is suitably captured in the cavity of the crown compound. This suggests that good separations may be obtained by using crown compounds designed for the retention of individual analytes. However, such modified ODS columns have the drawback that the retention times change with

the counter anions, because anions with higher polarizability generally enhance the cation complexation of the crown ether.

The purpose of this study was to find the optimum conditions for the mutual separation of alkali metal and NH_4^+ cations by using a bonded silica (C_{18}) reversed-phase column. The separation was examined on a column using three anionic surfactants with long alkyl chains [sodium 1-icosyl sulphate (SES), sodium dodecyl benzenesulphonate (SDBS) and sodium dodecyl sulphate (SDS)]. These surfactants were used for the preparation of previously coated columns and as additives to the mobile phase. Nitric acid was employed as the mobile phase because of its wide use in IC for the separation of alkali metal and ammonium cations [1,3] and the low solubility of the surfactants in acidic solutions. Further, the chromatographic method obtained was compared with conventional IC and was applied to real samples.

2. Experimental

2.1. Chemicals

All inorganic salts were of analytical-reagent grade and used as received. Working standard solutions of alkali metal and ammonium cations were prepared from stock standard solutions (10 g/l) of the chloride and perchlorate salts, prepared using deionized water. SES, SDBS and SDS of analytical-reagent grade, HPLC-grade acetonitrile (AN) and ultra-pure nitric acid were used.

2.2. Ion chromatographic system

The ion chromatograph consisted of a CCPM pump (Tosoh, Tokyo, Japan), a Rheodyne (Cotati, CA, USA) Model 7125 injection valve equipped with a 100- μl sample loop, a CM-8010 conductivity detector (Tosoh) and an SC-8010 chromato-processor (Tosoh). The C_{18} reversed-phase column employed was Capcellpak C_{18} (Shiseido, Tokyo, Japan) of $150 \text{ mm} \times 4.6 \text{ mm}$ I.D., packed with 5- μm spherical particles of octadecyl-bonded silica gel coated with silicone

polymer. The silicone coating permits the use of the column over a wide pH range (2–10), suppressing the undesirable peak tailing of compounds in reversed-phased LC [13,14]. The temperature of the column and the injection valve was maintained at $20 \pm 1^\circ\text{C}$.

2.3. Preparation of coated columns and mobile phases

“Permanent” coating system of columns with surfactants

The columns coated with surfactants were obtained by pumping 1 mM aqueous solutions of SDS and SDBS at a flow-rate of 0.5 ml/min until adsorption equilibrium was accomplished. For SES, a 0.2 mM solution in H_2O –AN (75:25, v/v) was employed owing to its low solubility in water. Completion of the column equilibrium was determined by the rapid increase in the conductivity of the effluent from the columns up to a level equal to that of the individual surfactant solution. It was also determined by measuring the total organic carbon (TOC-500 instrument; Shimadzu, Kyoto, Japan) for SDBS and SDS, and by the retention times of cations with SES. The coating solutions were pumped for a further 2–3 h and then switched to 5 mM HNO_3 in order to examine the chromatographic efficiencies. The times taken were *ca.* 17 h for SDS, 23 h for SDBS and 30 h for SES.

Dynamic coating system of columns with SDS

The mobile phases used were 10 mM HNO_3 containing 0.01–0.04 mM SDS, which were prepared from stock standard solutions of 10 mM SDS and 1 M HNO_3 . The solutions were filtered through a membrane filter (pore size 0.45 μm) and degassed under reduced pressure prior to use.

2.4. Samples

Tap and pond water were sampled and analysed immediately with the proposed IC system with a C_{18} reversed-phase column, 0.1 mM SDS–10 mM HNO_3 as the mobile phase and conductivity detection. For comparison, the samples were further analysed by a conventional IC

system with conductivity detection (Model IC-100; Yokogawa, Tokyo, Japan) using CX-1 columns $(50 + 250) \times 4.6$ mm I.D. and 5 mM nitric acid as the mobile phase.

3. Results and discussion

3.1. “Permanent” coating system of columns with surfactants

The amounts of surfactant sorbed per column are given in Table 1 for each coating solution, together with that of $\text{CH}_3(\text{CH}_2)_7\text{SO}_3\text{Li}$ [9]. The amounts were determined by two methods. One is the determination of Na^+ eluted by 5 mM nitric acid, which was directly switched from the individual coating solution. The amount was determined with a conventional IC system. The other is the difference in the TOC content for the surfactants between the influent and the effluent. The amount of sorbed SES with a long alkyl chain (C_{20}) is very small, in spite of its high hydrophobicity. This is probably due to the addition of acetonitrile to increase the solubility of SES. For SDBS and SDS, the values are relatively large, being comparable to the results from breakthrough volumes.

Fig. 1 shows the separation of alkali metal and ammonium cations on a C_{18} reversed-phase column coated with three anionic surfactants.

Table 1
Amounts of anionic surfactants sorbed

Surfactant	Structure	Amount sorbed ^a (mmol per column)	
		Na^+	TOC
SES	$\text{CH}_3(\text{CH}_2)_{19}\text{OSO}_3\text{Na}$	0.06	—
SDBS	$\text{CH}_3(\text{CH}_2)_{11}\text{C}_6\text{H}_4\text{SO}_3\text{Na}$	0.32	0.36
SDS	$\text{CH}_3(\text{CH}_2)_{11}\text{OSO}_3\text{Na}$	0.25	0.24
	$\text{CH}_3(\text{CH}_2)_7\text{SO}_3\text{Li}$	0.02 ^b	—

^a C_{18} reversed-phase column (150×4.6 mm I.D.) was equilibrated with 0.1 mM SES in AN– H_2O (25:75, v/v) and 1 mM DBS and SDS in H_2O , respectively.

^b Ref. 9. Poly(styrene–divinylbenzene) copolymeric reversed-phase column (150×4.1 mm I.D.) was equilibrated with a 2.5 mM solution in MeOH– H_2O (20:80, v/v).

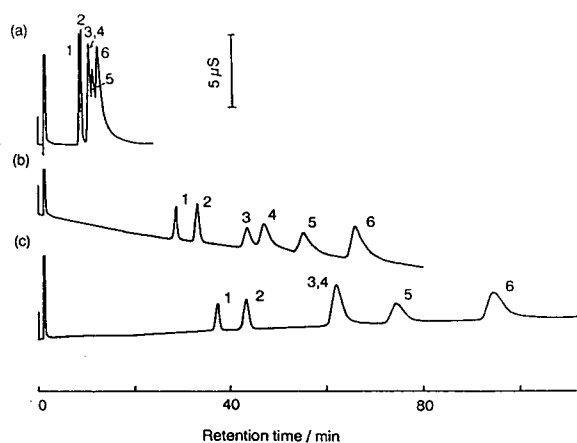


Fig. 1. Ion chromatograms of alkali metal and ammonium cations. C_{18} reversed-phase column coated with anionic surfactants: (a) 0.2 mM SES in H_2O -AN (75:25, v/v); (b) 1 mM SDS; (c) 1 mM SDBS. Mobile phase, 5 mM HNO_3 ; conductivity detection; flow-rate, 1.0 ml/min; sample, chloride salts, 100 μ l. Peaks: 1 = Li^+ (0.45 mg/l); 2 = Na^+ (2 mg/l); 3 = NH_4^+ (2 mg/l); 4 = K^+ (7.5 mg/l); 5 = Rb^+ (20 mg/l); 6 = Cs^+ (50 mg/l).

The mobile phase used was 5 mM nitric acid and the flow rate was 1 ml/min. Fig. 1a shows the chromatogram obtained with the column coated with SES: the order of retention times ($Li^+ < Na^+ < NH_4^+$, $K^+ < Rb^+ < Cs^+$) was the same as the order obtained by conventional IC with nitric acid [1,3]. No dissolution of the SES coating was observed. However, the volumes were small and the separability was poor, mainly owing to low ion-exchange capacity. For SDBS (Fig. 1c), the separation of K^+ and NH_4^+ could not be achieved in spite of the large retention time. The retention volumes of the six cations were almost constant up to pumping *ca.* 2.2 l of 5 mM HNO_3 (37 h), although the SDBS coating level decreased from 0.32 to 0.18 mmol per column. This suggests that the effective ion-exchange capacity was almost constant until that concentration of SDBS. When SDS was used, the six cations were separated as shown in Fig. 1b. However, the retention times decreased rapidly owing to the dissolution of SDS with weak hydrophobicity. For example, pumping 400 ml of 5 mM HNO_3 resulted in a *ca.* 50% decrease in the amount of SDS sorbed. This suggests that SDS should be

present in the mobile phases to obtain constant retention times.

3.2. Dynamic coating system of column with SDS

Fig. 2 shows typical ion chromatograms of the six cations using three mobile phases containing SDS at different concentrations (Fig. 2a, 0.1 mM; b, 0.2 mM; c, 0.4 mM). A 10 mM HNO_3 concentration was adopted for the mobile phase for faster elution of the cations. There were no differences in the retention times of the cations between chloride and perchlorate salts, unlike the results with crown compounds [11,12]. Smith and Pietrzyk [9] suggested that the retention of analyte cations was directly proportional to the hydrophobic ion concentration. However, under the conditions they used [$CH_3(CH_2)_6SO_3^-Li^+$ and $CH_3(CH_2)_7SO_3^-Li^+$ in H_2O -MeOH mixtures], the amount of hydrophobic ions sorbed on the poly(styrene-divinylbenzene) resin was not sufficient to separate four cations (Na^+ , K^+ , NH_4^+ and Cs^+). The retention times increased with concentration of SDS in the mobile phases and were stable, suggesting that the retention times in this system were controllable. The 0.1

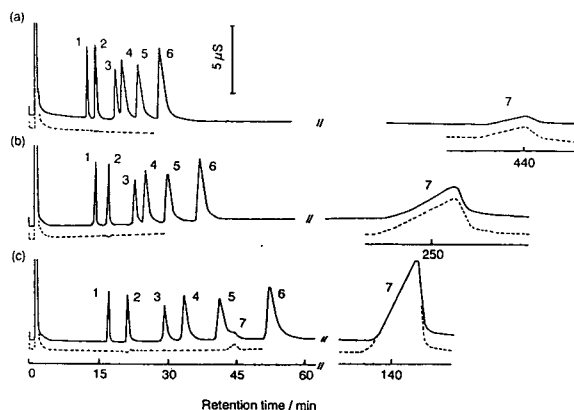


Fig. 2. Ion chromatograms of alkali metal and ammonium cations using a C_{18} reversed-phase column. Mobile phase: (a) 0.1 mM SDS; (b) 0.2 mM SDS; (c) 0.4 mM SDS; each mobile phase contained 10 mM HNO_3 . Conductivity detection; flow-rate, 1.0 ml/min; sample, 100 μ l. Solid lines, as in Fig. 1; dashed lines, pure water. Peaks: 1 = Li^+ ; 2 = Na^+ ; 3 = NH_4^+ ; 4 = K^+ ; 5 = Rb^+ ; 6 = Cs^+ ; 7 = system peak.

mM SDS–10 mM HNO₃ system was effective with respect to separation efficiency and the shorter retention times.

The appearance of system peaks, as shown in Fig. 2, was as follows. (1) The system peak increased in intensity with increase in SDS concentration but with decreased retention times. For 0.4 mM SDS, a small system peak was observed around 45 min (Fig. 2c). (2) The peak intensity of a standard solution was smaller than that of pure water but they gave the same retention times. (3) The system peaks were not observed when using both a standard solution and pure water containing SDS and HNO₃ at the same concentration as that in the mobile phase.

From the above results, the following conclusions can be drawn. In acidic condition (10 mM HNO₃), added SDS exists mainly as dodecylsulphuric acid (DSA) in both the mobile and solid phases. The injection of standard solutions or H₂O causes the elution of sorbed DSA. Hence the system peak may be attributed to the desorption and adsorption of DSA (neutral eluent molecules) from the column surface, taking account of the results for anions [15]. Accordingly, the disturbance from the desorption–adsorption equilibrium increases with increasing concentration of SDS, but on the other hand the retention times decreases. The retention of DSA in a standard solution will be larger than that of pure water, owing to the salting-out effect [16]. The small system peak for a 0.4 mM concentration may be attributed to SDS. From the viewpoint of determination, a 0.1 mM SDS system is better because of the low intensity of the system peak and the long retention time, as shown in Fig. 2a.

The detection limits with the 0.1 mM SDS–10 mM HNO₃ system were 0.004 (Li⁺), 0.1 (Na⁺), 0.02 (NH₄⁺), 0.08 (K⁺), 0.2 (Rb⁺) and 0.4 mg/l (Cs⁺) for a signal-to-noise ratio of 2. These values are larger than those with indirect UV and fluorimetric detection [0.01 mM Ce(III) mobile phase and a IC column] [2] and with conductivity detection (2 mM HNO₃ mobile phase) [3]. This is mainly due to both the larger retention times and background conductivity with 10 mM HNO₃. The lower detection limit of Na⁺ is due

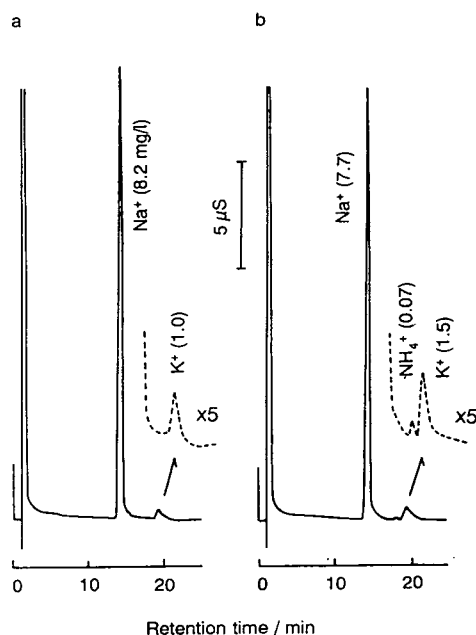


Fig. 3. Ion chromatograms of (a) tap water and (b) pond water. Mobile phase, 0.1 mM SDS–10 mM HNO₃. Other conditions as in Fig. 2.

to the addition of SDS and is improved (0.02 mg/l) by using lithium dodecyl sulphate as an additive.

3.3. Analysis of samples

Fig. 3 shows ion chromatograms of tap and pond water and Table 2 gives the results obtained by both the present and conventional IC methods. The results obtained by the peak-height method correspond well with those ob-

Table 2
Analytical results (mg/l) obtained by the present method and a conventional IC method

Sample	Method	Na ⁺	NH ₄ ⁺	K ⁺
Tap water	Present	8.2	N.D.	1.0
	IC	7.8	N.D.	1.1
Pond water	Present	7.7	0.07	1.5
	IC	7.5	0.08	1.8

tained by a conventional IC system, suggesting that the present SDS addition system is useful for the determination of alkali metal and ammonium cations.

In conclusion, the separation of alkali metal and ammonium cations could be achieved by the addition of SDS to the mobile phase. Although the system obtained has larger retention times compared with conventional IC, the use of a C₁₈ reversed-phase column, which has several advantages compared with “fixed-site” ion-exchange columns, may have various applications because of the wide flexibility in the choice of mobile phases.

4. References

- [1] D.T. Gjerde and J.S. Fritz, *Ion Chromatography*, Hüthig, New York, 2nd edn., 1987.
- [2] J.H. Sherman and N.D. Danielson, *Anal. Chem.*, 59 (1987) 1483.
- [3] P.R. Haddad and R.C. Foley, *Anal. Chem.*, 61 (1989) 1435, and references cited therein.
- [4] P. Pastore, A. Boaretto, I. Lavagnini and A. Diop, *J. Chromatogr.*, 591 (1992) 219.
- [5] P.K. Dasgupta, in J.G. Tarter (Editor), *Ion Chromatography*, Marcel Dekker, New York, 1987, pp. 253–272; and references cited therein.
- [6] K. Ito, Y. Ariyoshi, F. Tanabiki and H. Sunahara, *Anal. Chem.*, 63 (1991) 273.
- [7] K. Ito, Y. Ariyoshi and H. Sunahara, *J. Chromatogr.*, 598 (1992) 237.
- [8] I. Molnar, H. Knauer and D. Wilk, *J. Chromatogr.*, 201 (1980) 225.
- [9] R.L. Smith and D.J. Pietrzyk, *Anal. Chem.*, 56 (1984) 1572.
- [10] G. Schwedt and H.-H. Schaper, *Fresenius' J. Anal. Chem.*, 336 (1990) 415.
- [11] K. Kimura, H. Harino, E. Hayata and T. Shono, *Anal. Chem.*, 58 (1986) 2233.
- [12] T. Iwachido, H. Naito, F. Samukawa, K. Ishimaru and K. Tôei, *Bull. Chem. Soc. Jpn.*, 59 (1986) 1475.
- [13] J. Koyama, T. Kanda, Y. Ohtsu, K. Nakamura, H. Fukui and O. Nakata, *Nippon Kagaku Kaishi*, (1989) 45.
- [14] Y. Ohtsu, Y. Shiojima, T. Okumura, J. Koyama, K. Nakamura, O. Nakata, K. Kimata and N. Tanaka, *J. Chromatogr.*, 481 (1989) 147.
- [15] P.E. Jackson and P.R. Haddad, *J. Chromatogr.*, 346 (1985) 125.
- [16] A. Berthod, I. Girard and C. Gonnet, *Anal. Chem.*, 58 (1986) 1362.

Extra-thermodynamic relationships in chromatography Enthalpy–entropy compensation in gas chromatography

Jianjun Li[☆], Peter W. Carr^{*}

Department of Chemistry, University of Minnesota, 207 Pleasant Street SE, Minneapolis, MN 55455, USA

(First received October 25th, 1993; revised manuscript received January 18th, 1994)

Abstract

The phenomenon of enthalpy–entropy compensation in gas chromatography is examined. Using 53 probe solutes that span a wide range in size (dispersive interaction), dipolarity, hydrogen-bond-donor and hydrogen-bond-acceptor strength, enthalpy–entropy compensation is not observed, while for probe solutes within a homologous series enthalpy–entropy compensation is observed as predicted by the linear solvation energy relationship methodology.

1. Introduction

The issue of “enthalpy–entropy compensation” is closely related to the effect of temperature on retention in chromatography. Enthalpy–entropy compensation is also called the isokinetic relationship (IKR), the “compensation effect”, the “ θ ” rule, the isoselectivity relationship, etc. It has been found in a wide variety of processes and reaction equilibria including: heterogeneous catalysis; diffusion in metals, ionic crystals, and amorphous polymers; conduction in amorphous semiconductors; and phase equilibria between hydrophobic and hydrophilic phases and between multicomponent fluid phases [1–10]. Despite its utility it has also led to a great deal of misunderstanding and controversy [1–9]. In essence, enthalpy–entropy compensation refers to the experimental observation of a linear

relationship between enthalpy (H) and entropy (S) for a series of related processes as, for example, when a series of similar reactants are subjected to the same reaction:

$$\Delta H = \beta \Delta S + \alpha \quad (1)$$

Clearly the constant of proportionality (β) in Eq. 1 must have units of absolute temperature. β is called the compensation temperature (see below).

This phenomenon is often called “enthalpy–entropy compensation” because when Eq. 1 is inserted into the fundamental relationship between free energy (G), enthalpy and entropy, the change in ΔG upon change in reactant is always smaller than the change in either ΔH or $T\Delta S$. Thus part of ΔH and ΔS cancel or compensate when ΔH and $T\Delta S$ are combined to give ΔG .

$$\begin{aligned} \Delta G &= \Delta H - T\Delta S \\ &= \Delta H[1 - (\beta/T)] + \alpha T/\beta = \Delta S(\beta - T) + \alpha \end{aligned} \quad (2)$$

Eq. 2 predicts that when T is equal to β , ΔG

^{*} Corresponding author.

[☆] Present address: The Procter & Gamble Company, Miami Valley Laboratories, P.O. Box 398707, Cincinnati, OH 45239-8707, USA.

becomes the same for *all* reactants thus β represents the temperature at which ΔH and ΔS are completely compensated.

It is an axiom of extra-thermodynamic relationships that all sets of reactions (processes) which exhibit enthalpy–entropy compensation are governed by a single mechanism and all related reactions that have the same compensation temperature proceed via the same mechanism [10]. What this means is that only a single characteristic of the solute is needed to describe both ΔH and ΔS and therefore ΔH and ΔS must be linearly correlated. This principle is very important in chromatography. If enthalpy–entropy compensation is observed for a set of solutes then we can conclude that the differences in retention between the solutes are governed by a *single* type of parameter which governs their intermolecular interactions. This conclusion is in accord with the very general model of enthalpy–entropy compensation developed by Boots and de Bokx [11,12]. In their model they describe a suitably defined Gibbs free energy change (similar to our $\Delta G'$, see below) as the product of a temperature-dependent, system-independent factor $y(T)$ and a temperature-independent, system-dependent factor $\sigma(\{f\})$

$$\Delta G = y(T)\sigma(\{f\}) \quad (3)$$

Here the system dependence is described by a collection of parameters $\{f\}$ [similar to our linear solvation energy relationship (LSER) parameters, see below]. They conclude that only when G depends on one parameter, compensation can and must occur. If G depends on more than one parameter, compensation is not guaranteed.

When considered in detail (see below) it becomes clear that the above concepts are at odds with the fundamental basis for the use of LSERs [13] and other models of chromatographic retention such as multicomponent solubility parameter [14] which fundamentally represent solute–solvent interactions as a suite of parameters (dispersive, dipolar, hydrogen bonding). Furthermore it is difficult to imagine how a system governed by a single interaction mecha-

nism could display the very large variations in relative retention and even retention sequences commonly observed in specific forms of chromatography. It is therefore very important to understand the phenomenon of enthalpy–entropy compensation in detail and to assess its limits.

The enthalpies and entropies of solvation processes have been studied by many workers [10,15–20]. Barclay and Butler [16], and Frank and Evans [17,18] extensively studied the enthalpies and entropies of vaporization of pure liquids at 25°C and found that Eq. 4 adequately represented the behavior of most pure liquids. They proposed that it be regarded as a standard relationship representing “normal” behavior.

$$\begin{aligned} \Delta H_{\text{vap}}^0 (\text{J mol}^{-1}) = & -43\,012 \\ & + 3372\Delta S_{\text{vap}}^0 (\text{J mol}^{-1} \text{K}^{-1}) \end{aligned} \quad (4)$$

This is clearly an enthalpy–entropy compensation relationship. The reference or standard states are the pure liquid and pure gas at 1 atm (10^5 Pa) and 25°C. Eq. 4 also applies to the vaporization of a series of dilute solutes from a variety of non-hydroxylic solvents [18]. Although Eq. 4 applies to many series of compounds as a whole [17], better fits are obtained by using separate lines for different types of solutes. The latter procedure is equivalent to assuming that each class of compound has a second interaction mechanism whose magnitude is constant within the class [10]. Appreciable deviations from the standard relationship (Eq. 4) may be taken as evidence for the presence of strong additional interactions [10].

The study of enthalpy–entropy relationships has been of considerable interest in chromatography. For RPLC, Melander *et al.* [21], obtained a linear correlation between the logarithm of the capacity factor, and the corresponding enthalpies for a particular chromatographic process. Since the compensation temperatures were indistinguishable, they concluded that the mechanism of interaction of various solutes with the stationary phase was invariant under the chromatographic conditions examined, even though the nature

and concentration of organic modifier was varied substantially. Subsequently, the same authors developed a simple three-parameter relationship to express retention as a function of mobile phase composition and temperature [22–26].

Following Melander *et al.*'s work [21], Jinno and co-workers [27,28] investigated the effect of low temperatures (temperature range -50°C to 45°C) in RP-HPLC. Based on their observation that the compensation temperature was within the same range as the other systems, Jinno and co-workers concluded that the retention mechanism at low temperatures is similar to that at higher temperatures. Similar conclusions were drawn by Vigh and Varga-Puchony [29] in a study of retention of members of a homologous series in RPLC.

The influence of intramolecular interactions on the chromatographic behavior of arylaliphatic acids, aryloalkanoic acids and arylhydroxylalkanoic acids in RPLC have been explored by means of enthalpy–entropy compensation by Kuchar and co-workers [30,31]. For the three different homologous series of acids, they observed three different slopes for plots of $\log k'$ vs. ΔH^0 (*i.e.* enthalpy–entropy compensation). It appears that enthalpy–entropy compensation occurs only within a single homologous series. Riley *et al.* [32] have observed the same phenomenon in ion-pair RPLC.

Although temperature has a much greater effect on retention in GC than in LC, there are only a few reports on the use of temperature to explore retention mechanisms in GLC [33,34]. Kuchar *et al.* [34] used the enthalpy–entropy compensation concept to explore differences in the mechanism of separation of alkyl and arylalkyl esters of benzoic acids on two capillary columns (SE-30 and OV-351).

It is unfortunately true that it is entirely possible to observe correlations between ΔH and ΔS even though such correlations are adventitious and due only to spurious statistical effects that relate to least squares data fitting. This can happen when ΔH and ΔS are both measured via the temperature dependence of the free energy. That is, when ΔH is taken from the slope of a Van 't Hoff plot [4–7]. This problem cannot

occur when ΔH is obtained by calorimetric methods and ΔS is computed from the measured ΔG . Krug and co-workers [4–7] have shown that due purely to statistical effects apparently high correlations between ΔH and ΔS can be observed when the Van 't Hoff slope is used to obtain ΔH even when in fact no such physical phenomenon is actually taking place. In a recent paper, Reddy *et al.* [35] also showed that they obtained an excellent correlation between enthalpy and entropy in spite of the lack of good correlations between ΔG and ΔH (*i.e.*, the lack of enthalpy–entropy compensation, see below). Krug [5] has outlined three methods to avoid the observation of false correlations. Unfortunately these methods have been seldom used in chromatographic studies of enthalpy–entropy compensation. All three methods were used in this work.

Krug [5] has pointed out that when ΔH and ΔS compensation is real then plots of ΔG (or an equivalent parameter such as the logarithm of a capacity factor) vs. $1/T$ must intersect at a single temperature for all compounds. Second, when enthalpy–entropy compensation is real then plots of ΔG_{Th} vs. ΔH must form a straight line. ΔG_{Th} is defined as the measured free energy change at the harmonic mean temperature given below:

$$1/T_h = \left(\sum_{i=1}^n 1/T_i \right) / n \quad (5)$$

Purely statistical effects cannot cause correlation in such a plot. Furthermore, the slope of such a plot (denoted γ) is related to the compensation temperature (β)

$$\Delta H = \gamma \Delta G + (1 - \gamma) \Delta G_{\beta} \quad (6)$$

where

$$\Delta G = \Delta G_{\text{Th}} = \Delta H - T_h \Delta S$$

$$\Delta G_{\beta} = \Delta H - \beta \Delta S$$

$$\gamma = 1 / (1 - T_h / \beta) \quad (7)$$

or

$$\beta = T_h / (1 - 1/\gamma) \quad (8)$$

Third, Krug has devised a detailed statistical analysis method based on the analysis of variance method (ANOVA) which allows dissection of the data set, that is the measurements of ΔG for p compounds at q temperatures, into real effects and measurement error. Only when there is a high probability that the variance due to true enthalpy–entropy correlation exceeds random error can one say that enthalpy–entropy compensation is physically real. The reader is referred to refs. 5 and 36 for computational details.

In this work we examined the enthalpy–entropy compensation phenomenon in capillary gas chromatography according to the Krug's procedures and the results were compared with predictions of solvatochromic linear solvation energy relationships.

2. Experimental

The retention data studied here include a set of capacity factors ($\log k'$) for 53 highly varied compounds that span an extremely wide range in chemical characteristics on eight common capillary columns ranging from a methyl silicone oil to polyethylene glycol. The details of this data base have been published [37].

3. Results and discussion

3.1. Enthalpy–entropy compensation in gas chromatography

To examine whether enthalpy–entropy compensation took place in our data sets, we followed the procedures of Krug [5] for detection of such effects. We examined our retention data on all eight columns but will only present data on one column (DB-1701) as a typical example.

First, we show the result of plotting the values of ΔH^0 and $\Delta S'$ as obtained from a Van 't Hoff plot (Fig. 1). The relationship between ΔH^0 and $\Delta S'$ is shown in Eq. 9. It might be concluded that there is enthalpy–entropy compensation (correlation coefficient > 0.95).

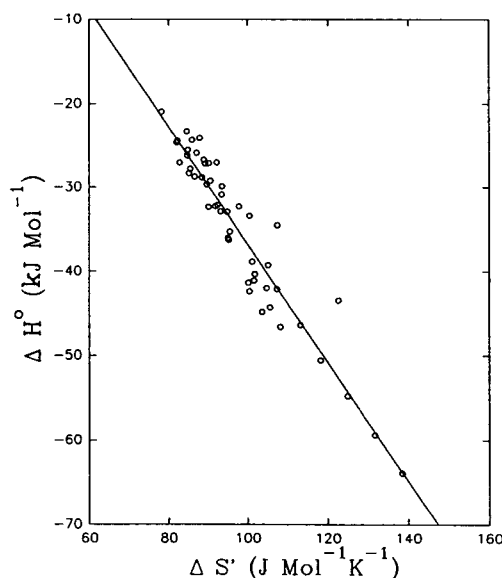


Fig. 1. Plot of ΔH^0 vs. $\Delta S'$ for all compounds on the DB-1701 column.

$$\Delta H^0 (\text{kJ mol}^{-1}) = (33.20 \pm 3.11) + (0.70 \pm 0.03)\Delta S' \quad (9)$$

$$\text{S.D.} = 2.9, r = 0.95, n = 50$$

We now test to see if there is a common intersection point in plots of $\log k'$ vs. $1/T$ for all compounds (see Fig. 2). Clearly the lines intersect but they do so over a fairly wide range

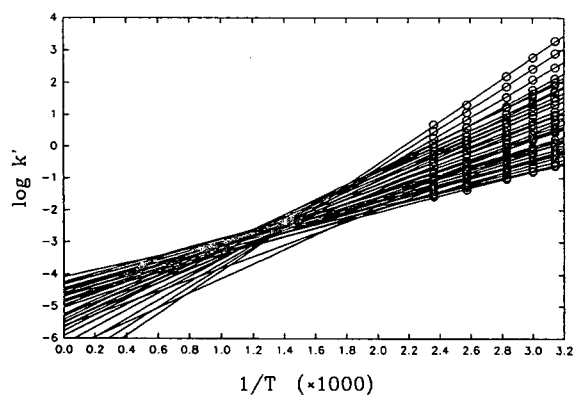


Fig. 2. Plot of $\log k'$ vs. $1/T$ (K) for all compounds on the DB-1701 column.

of temperatures not at a single temperature. A detailed examination suggests the possibility of enthalpy–entropy compensation for some compounds. When we restricted the data set to just the *n*-alkanes, a single intersection point was observed suggesting real enthalpy–entropy compensation for these solutes (Fig. 3). Similar plots were obtained for other homologous series. From Fig. 3, the compensation temperature for the alkanes determined from the common intersecting point is about 712 K.

Second, $\Delta G'_{Th}$ was calculated ($\Delta G'_{Th} = \Delta H^0 - T_h \Delta S'$, see Table 1). The ΔH^0 vs. $\Delta G'_{Th}$ plot is shown in Fig. 4. We see a similar linear relationship as that observed in Fig. 1 (the solid line represents the least squares line for all solutes). The regression results for all solutes are shown in Eq. 10. We point out that there was no deterioration in the quality of fit compared with Eq. 9. This is not expected since the ΔH^0 vs. $\Delta G'_{Th}$ correlation should remove any statistic effects existing in the ΔH^0 vs. $\Delta S'$ correlation, therefore result in a worse correlation. This might be due to the different coordinates in the two correlations. Again, if we examine only the *n*-alkanes, a much tighter relationship is obtained (the dashed line in Fig. 4 and Eq. 11).

$$\Delta H^0 = (-34.95 \pm 0.37) + (1.74 \pm 0.07) \Delta G'_{Th} \quad (10)$$

$$\text{S.D.} = 2.58, r = 0.96, n = 50$$

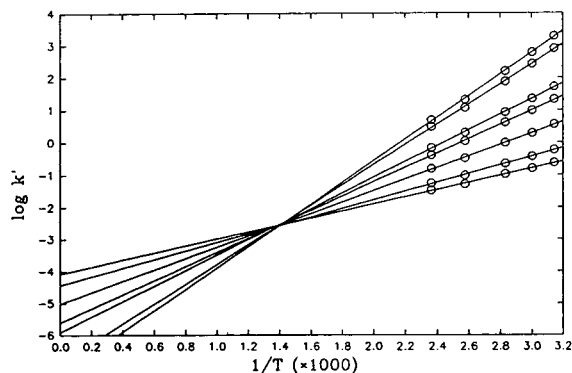


Fig. 3. Plot of $\log k'$ vs. $1/T$ (K) for *n*-alkane solutes on the DB-1701 column.

$$\Delta H^0 = (-35.01 \pm 0.22) + (2.02 \pm 0.03) \Delta G'_{Th} \quad (11)$$

$$\text{S.D.} = 0.54, r = 1.00, n = 7$$

The same compensation temperature (712 K) was obtained for the alkanes by use of Eq. 7. Additional homologous series were examined as shown in Fig. 5. We see that all are straight lines and that they are almost parallel. This strongly suggests that there is more than one interaction mechanism contributing to retention [10].

Similar plots of ΔH^0 vs. $\Delta G'_{Th}$ are obtained for all other phases studied in this work. The compensation temperatures for all solutes and just the *n*-alkanes are summarized in Table 2. These are based on regression results for ΔH^0 vs. $\Delta G'_{Th}$. Compensation was never observed when all solutes were included. Compensation was observed for the *n*-alkanes on all columns. Moreover, the compensation temperature for the *n*-alkanes on all columns are very similar. By and large the compensation temperature for the full solute set does not agree with those for the *n*-alkanes and vary greatly from phase to phase.

By using Krug's ANOVA method [5], we tested for the existence of enthalpy–entropy compensation for all compounds and for each homologous series. Similar results were obtained (Table 3). That is, there was no compensation for all compounds as a whole, but there was compensation for solutes within a homologous series. Each homologous series has its own compensation temperature. Enthalpy–entropy compensation was not observed for the three aliphatic alcohols. This is not surprising because we only examined retention data for methanol, ethanol and propanol, and usually the first few members of a homologous series behave differently from the higher homologues.

3.2. LSER, the Martin equation and enthalpy–entropy compensation

In a previous study [38], we showed that the following equations describe retention on a wide variety of GC stationary phases.

Table 1
Apparent Gibbs free energy ($\Delta G'$, kJ/mol) at the harmonic temperature

No.	Compound	DB-1	DB-5	DB-1301	DB-1701	DB-17	DB-210	DB-225	DB-WAX
		93°C ^a	93°C	73°C	86°C	93°C	73°C	93°C	73°C
1	Cyclohexane	1.78	2.23	^b	^b	4.00	^b	5.28	^b
2	1-Hexene	3.39	3.87	3.53	4.79	6.41	5.92	7.47	6.28
3	Pentane	5.34	6.04	5.73	7.11	8.95	7.97	10.14	9.45
4	Hexane	3.27	3.87	3.39	4.93	6.77	6.06	8.11	7.34
5	Octane	-1.02	-0.27	-1.07	0.56	2.57	2.32	4.07	3.43
6	Decane	-5.14	-4.51	-5.52	-3.55	-1.47	-1.23	0.48	-0.35
7	Undecane	-7.20	-6.53	-7.71	-5.71	-3.60	-3.08	-1.48	-2.30
8	Tetradecane	-13.43	-12.71	-14.20	-12.05	-9.85	-8.43	-7.06	-7.99
9	Pentadecane	-15.49	-14.75	-16.36	-14.15	-11.93	-10.20	-8.88	-9.86
10	Ethyl acetate	3.46	3.83	2.43	3.29	4.35	1.72	3.61	1.42
11	Propyl acetate	1.31	1.49	0.12	1.12	2.33	-0.19	1.72	-0.27
12	Ethylether	5.39	5.96	5.24	6.55	7.70	6.71	8.15	6.69
13	Propylether	1.52	2.03	1.14	2.66	3.93	3.57	4.87	3.70
14	Butylether	-2.51	-2.03	-3.16	-1.47	0.02	0.05	1.04	0.14
15	Acetonitrile	^b	6.28	4.23	4.22	5.24	1.35	2.49	-0.91
16	Propionitrile	4.45	4.32	2.39	2.37	3.65	-0.28	0.97	-1.36
17	Acetone	5.89	6.15	5.01	5.09	6.56	^b	4.49	2.71
18	2-Butanone	3.82	3.90	2.68	2.92	4.32	0.71	2.68	1.05
19	2-Pentanone	1.84	1.99	0.40	1.03	2.44	-0.96	0.98	-0.42
20	Dimethylformamide	0.23	-0.10	-2.56	-2.54	-1.46	-5.87	-4.67	-7.05
21	Dimethylacetamide	-1.68	-1.74	-4.48	-4.36	-3.24	-7.46	-6.25	-8.52
22	Dimethylsulfoxide	-0.84	-1.02	-4.31	-4.61	-3.50	-8.25	-7.66	-11.29
23	Propionaldehyde	6.26	6.03	^b	5.39	6.47	3.43	5.00	3.22
24	Tetrahydrofuran	3.11	3.10	^b	2.87	3.78	2.13	3.10	1.67
25	Triethylamine	1.77	2.22	1.08	2.67	4.14	2.77	4.79	^b
26	Nitromethane	5.08	5.01	2.42	2.51	3.67	0.01	0.64	^b
27	Nitroethane	2.96	2.68	0.64	0.73	1.90	-1.66	-0.90	-3.78
28	Nitropropane	1.03	1.00	-1.23	-0.99	0.23	-3.18	-2.34	-4.71
29	Methanol	8.50	9.21	7.34	7.42	^b	7.74	6.32	1.25
30	Ethanol	^b	7.80	^b	6.03	8.03	6.13	5.03	0.49
31	1-Propanol	4.45	5.32	3.08	3.65	5.73	4.05	^b	-1.50
32	2-Propanol	5.94	6.55	^b	5.23	7.15	5.29	4.71	0.69
33	2-Methyl-2-propanol	5.26	5.61	4.07	4.83	7.01	4.62	4.51	1.30
34	Trifluoroethanol	8.53	7.95	4.02	4.07	9.15	5.63	2.54	-4.16
35	Hexafluoroisopropanol	2.28	6.82	0.47	0.60	^b	^b	^b	^b
36	Acetic acid	^b	5.14	1.85	^b	^b	^b	^b	^b
37	Aniline	-4.03	-4.06	-6.61	-6.32	-5.64	-5.70	-8.44	^b
38	N-Methylaniline	-5.80	-5.69	-8.27	-7.75	-7.14	-7.02	-9.18	^b
39	Phenol	-3.96	-3.98	-8.15	-8.09	-4.83	-4.38	-10.52	^b
40	Benzyl alcohol	-5.09	-5.00	-8.08	^b	-6.44	-6.16	-9.88	^b
41	<i>m</i> -Cresol	-5.95	^b	-10.09	-9.93	-6.77	-6.35	-12.09	^b
42	Ethylamine	6.90	7.76	^b	7.05	8.45	5.96	7.68	^b
43	Propylamine	5.23	5.36	^b	5.17	6.29	3.82	5.60	^b
44	Butylamine	2.87	2.94	1.46	2.81	4.33	1.62	3.21	^b
45	Benzene	1.92	2.21	1.28	2.21	2.67	2.52	2.50	0.16
46	Toluene	-0.24	0.08	-1.01	0.01	0.59	0.55	0.55	-1.69
47	Ethylbenzene	-2.15	-1.81	-3.05	-1.92	-1.37	-1.02	-1.18	-3.28
48	Propylbenzene	-4.01	-3.66	-5.00	-3.77	-3.10	-2.62	-2.75	-4.77
49	<i>p</i> -Xylene	-2.32	-2.01	-3.21	-2.08	-1.38	-1.13	-1.12	-3.42
50	Benzaldehyde	-3.66	-3.82	-5.81	-5.34	-4.94	-6.22	-6.53	-10.26
51	Benzonitrile	-4.13	-4.26	-6.60	-6.26	-5.62	-7.65	-7.77	^b
52	NN-Dimethylaniline	-6.52	^b	-8.25	-7.57	-7.15	-7.04	-7.78	^b
53	Carbontetrachloride	1.94	2.29	1.49	2.68	3.23	^b	3.72	1.56

^a Harmonic mean temperature calculated from Eq. 5.

^b No data due to missing ΔH values.

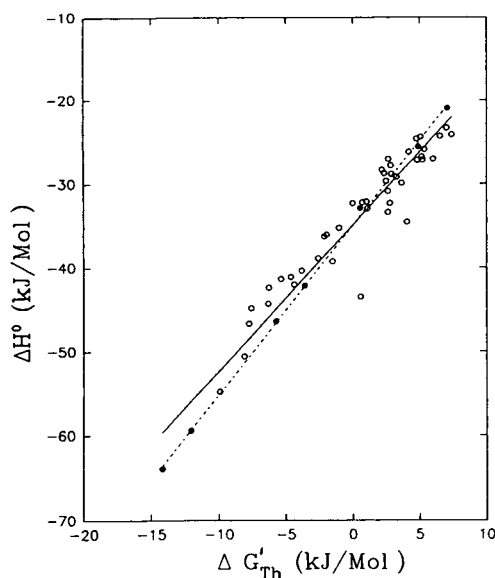


Fig. 4. Plot of ΔH^0 vs. $\Delta G'_{Th}$ for all solutes on the DB-1701 column. The solid line represents the least squares line for all solutes (\circ). The dashed line represents the least squares line for the *n*-alkanes (\bullet) only.

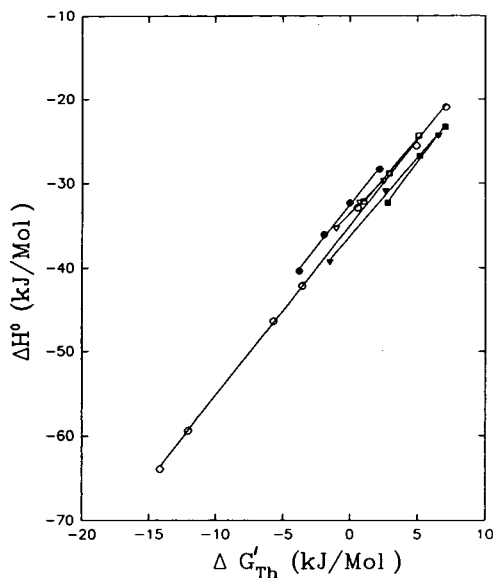


Fig. 5. Plot of ΔH^0 vs. $\Delta G'_{Th}$ for 6 homologous series on the DB-1701 column. \circ = *n*-Alkanes, \bullet = alkylbenzenes, ∇ = nitroalkanes, \blacktriangledown = alkylethers, \square = 2-ketones, \blacksquare = amines.

$$\Delta G'(T) = SP_{o,G} + l_G \log L^{16} + s_G \pi_2^{*,C} + d_G \delta_2 + a_G \alpha_2^C + b_G \beta_2^C \quad (12)$$

$$\Delta H^0 = SP_{o,H} + l_H \log L^{16} + s_H \pi_2^{*,C} + d_H \delta_2 + a_H \alpha_2^C + b_H \beta_2^C \quad (13)$$

$$\Delta S' = SP_{o,S} + l_S \log L^{16} + s_S \pi_2^{*,C} + d_S \delta_2 + a_S \alpha_2^C + b_S \beta_2^C \quad (14)$$

In Eqs. 12–14, the characteristic constants have the same meaning as before but they now have their respective units. In order for enthalpy–entropy compensation to take place for all compounds, the free energies for all compounds must become equal at $T = \beta$. That is, for all solutes:

$$\begin{aligned} \Delta G' &= \Delta H^0 - \beta \Delta S' = \text{constant} \\ &= SP_{o,H} - \beta SP_{o,S} + (l_H - \beta l_S) \log L^{16} \\ &\quad + (s_H - \beta s_S) \pi_2^{*,C} + (d_H - \beta d_S) \delta_2 \\ &\quad + (a_H - \beta a_S) \alpha_2^C + (b_H - \beta b_S) \beta_2^C \end{aligned} \quad (15)$$

Note that for a given column, $SP_{o,H}$ and $SP_{o,S}$ are independent of solutes, thus evidently:

$$\begin{aligned} &(l_H - \beta l_S) \log L^{16} + (s_H - \beta s_S) \pi_2^{*,C} \\ &\quad + (d_H - \beta d_S) \delta_2 + (a_H - \beta a_S) \alpha_2^C \\ &\quad + (b_H - \beta b_S) \beta_2^C = \text{constant}' \end{aligned} \quad (16)$$

Given that the sets of solutes used in this work were highly variegated it is most unlikely, if not impossible, for Eqs. 15 and 16 to be true for more than a limited set of solutes. If we assume that the solute parameters are essentially uncorrelated that is $\log L^{16}$, $\pi_2^{*,C}$, α_2^C , β_2^C and δ_2 do not covary, which is true, then exact compensation for all solutes can only take place if each coefficient of each parameter in Eq. 16 individually compensates. Thus:

$$l_H = l_S \beta$$

$$s_H = s_S \beta$$

etc.

This is evidently an exceedingly stringent condition for compensation. It is most unreasonable to believe that this can take place *exactly* when

Table 2

Compensation temperatures based on ΔH^0 vs. $\Delta G'_{Th}$ regression for all solutes and for *n*-alkanes only on all columns^a

Column	All solutes ^b		<i>n</i> -Alkanes only ^c	
	β^d	Compensation ^e	β	Compensation
DB-1	842 38 ^f	No 28	712	Yes
DB-5	922 44	No 11	719	Yes
DB-1301	808 42	No 16	749	Yes
DB-1701	845 34	No 11	712	Yes
DB-17	855 20	No 12	765	Yes
DB-210	802 27	No 10	673	Yes
DB-225	1009 45	No 18	729	Yes
DB-WAX	855 31	No 16	744	Yes

^a ΔH^0 and $\Delta G'_{Th}$ are in units of kJ/mol.^b All solutes are included in the regression.^c Only *n*-alkane solutes are included in the regression.^d Compensation temperature (K) calculated from Eq. 8 as if compensation occurs.^e Compensation effect detected by ANOVA (see text).^f Standard deviation of the compensation temperature calculated by $S.D.(\beta) = [T_h / (\text{slope} - 1)] \cdot S.D.(\text{slope})$.

Table 3

ANOVA results for detection of the compensation effect

Solutes	Compensation effect ^a	T_c (K) ^b	S.D. ^c
All ^d	No		
Alkanes ^e	Yes	712	10
Ethers ^f	Yes	777	39
2-Ketones ^g	Yes	757	31
Nitroaliphatics ^h	Yes	961	55
Alcohols ⁱ	No		
Alkylbenzenes ^j	Yes	722	30

^a Compensation is declared real only when there is a high probability that the variance due to true enthalpy–entropy correlation exceeds the random error.^b Compensation temperature calculated using Eq. 8.^c Standard deviation of the compensation temperature.^d All solutes, *n* (number of compounds) = 50.^e All *n*-alkane solutes, *n* = 7.^f Ethylether, propylether and butylether.^g Acetone, 2-butanone and 2-pentanone.^h Nitromethane, nitroethane and nitropropane.ⁱ Methanol, ethanol and 1-propanol.^j Benzene, toluene, ethylbenzene and propylbenzene.

one considers the very different processes that are involved in each of the individual terms in the LSER. However, we previously showed that approximately linear relationships for the LSER coefficients for $\Delta G'$ and ΔH^0 did exist but the slopes are different for each coefficient. Thus it is impossible to find a single temperature at which each coefficient of each parameter in Eq. 16 will individually compensate.

Compensation can take place *approximately* at least to the extent indicated by the scatter shown in Fig. 4 provided that one term in Eq. 16 dominates and thereby provides most of the variation in the $\Delta G'$ and ΔH^0 (other terms being small or largely compensated). We believe that the dispersive interactions that dominate retention in gas chromatography and are reflected in the $\log L^{16}$ parameter provide the basis for the approximate compensation seen in Fig. 4. A plot of $\Delta G'_{Th}$ vs. $\log L^{16}$ (see Fig. 6) is very similar to Fig. 4.

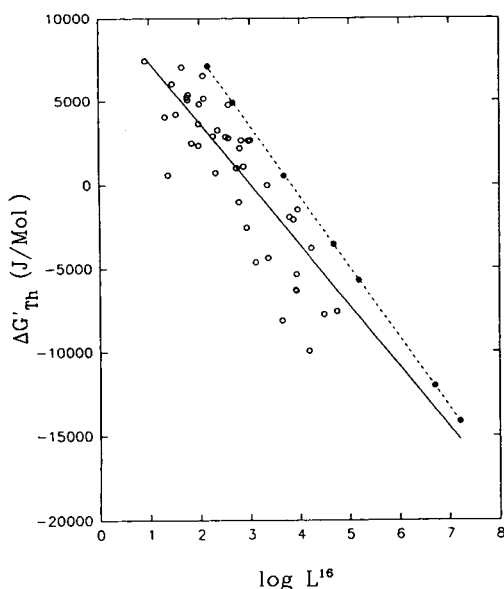


Fig. 6. Plot of $\Delta G'_{Th}$ vs. $\log L^{16}$ for all solutes on the DB-1701 column. The solid line represents the least squares line for all solutes (○). The dash line represents the least squares line for the *n*-alkanes (●) only.

Compensation can take place much more precisely within a homologous series of solutes. Previously we showed [39] that $\log L^{16}$ is a linear function of homologue number (HN) (Eq. 17), $\pi_2^{*,C}$ is a constant or an approximately linear function of the homologue number (Eq. 18).

$$\log L^{16} = A_1 + B_1 \text{HN} \quad (17)$$

$$\pi_2^{*,C} = A_2 + B_2 \text{HN} \quad (18)$$

δ_2 is a constant within a homologous series, α_2^C and β_2^C are almost constant within a homologous series [39–41]. Upon substitution of Eqs. 17 and 18 into Eq. 16, we get

$$\begin{aligned} (l_H - \beta l_S)(A_1 + B_1 \text{HN}) + (s_H - \beta s_S)(A_2 + B_2 \text{HN}) \\ + (d_H - \beta d_S)\delta_2 + (a_H - \beta a_S)\alpha_2^C \\ + (b_H - \beta b_S)\beta_2^C = \text{constant} \end{aligned} \quad (19)$$

Upon rearranging this equation and setting the coefficients of HN to zero, we can calculate a temperature at which all homologues will have

the same free energy, that temperature should be the compensation temperature.

$$\begin{aligned} \beta &= (B_1 l_H + B_2 s_H)/(B_1 l_S + B_2 s_S) \\ &= (l_H + \theta s_H)/(l_S + \theta s_S) \end{aligned} \quad (20)$$

$$\theta = B_2/B_1$$

Alternatively, the compensation temperature can be predicted directly from the equations for $\log k'(T)$ [38].

$$\begin{aligned} \log k'(T) &= SP_{o,A} + SP_{o,B}/T \\ &\quad + (l_A + l_B/T) \log L^{16} \\ &\quad + (s_A + s_B/T) \pi_2^{*,C} + (d_A + d_B/T) \delta_2 \\ &\quad + (a_A + a_B/T) \alpha_2^C + (b_A + b_B/T) \beta_2^C \end{aligned} \quad (21)$$

Upon substituting Eqs. 17 and 18 into Eq. 21, and setting the coefficient of HN to zero, we get

$$\begin{aligned} \beta &= (l_B B_1 + s_B B_2)/(l_A B_1 + s_A B_2) \\ &= (l_B + \theta s_B)/(l_A + \theta s_A) \end{aligned} \quad (22)$$

$$\theta = B_2/B_1$$

From Eqs. 20 and 22, we can see that within a homologous series, enthalpy–entropy compensation will be observed at the temperature β . However, we must point out that Eqs. 13, 14 and 18 are approximate results, that is to say, the compensation temperature predicted by Eq. 20 or 22 are only qualitative. The most efficient and accurate way to calculate a compensation temperature is by using Eq. 7. For compounds of different homologous series, judging from Eq. 16 or 21, it is not clear at all that there is such a temperature which satisfies either equation.

Previously, we have shown [39] that our LSER equation and parameters are, within any reasonable expectations of the experimental precision, in accord with the Martin equation. That is, our LSER equation and parameters predict that within a homologous series the free energy of retention ($\Delta G'$, Eq. 15) is a linear function of the homologue number. Similarly, from Eq. 16 and 17, one can conclude that within a homologous series the enthalpy and entropy of retention are also approximately linear functions of the homo-

logue number. If the free energy and enthalpy of retention are both linear functions of only the homologue number, then the free energy must be linearly related to the enthalpy of retention, and enthalpy–entropy compensation must then result (see Fig. 5). The above derivation agrees with the much more general model of enthalpy–entropy compensation developed by Boots and de Bokx [11,12].

The fact that a set of LSER parameters ($\log L^{16}$, $\pi^{*,C}$, α_2^C and β_2^C) are needed to describe retention in GC (and in RPLC, octanol–water partitioning, water solubility, etc.) stands in fundamental contradiction to the observation of enthalpy–entropy compensation in view of the Boots–de Bokx rule. We conclude that when such approximate compensation is observed it means nothing more or less than there is only a single dominant variable among the specific set of solutes under study. Thus one can “force” enthalpy–entropy compensation to be observed in chromatography by deliberately or inadvertently choosing a set of solutes in which only dispersive or only dipolar or only hydrogen bond acceptor or acceptor strength are varied.

However, more importantly, when a highly variegated set of solutes is chosen and enthalpy–entropy is still observed then one can usually infer that a single contribution to the retention process is dominant. One must be wary of some special instances as is the case in reversed-phase chromatography where there are very strong correlations between different factors such as the effect of the size of a molecule which simultaneously controls both cavity formation processes and dispersive interactions. In such instance one can observe enthalpy–entropy compensation when there is more than a single major retention process and thus be seriously misled.

3.3. Overview of extra-thermodynamic relationships in chromatography

Elsewhere we considered the phenomena of “ $S - \ln k'_w$ compensation” in RPLC [42]. This refers to the observation that the intercepts (\ln

k'_w) and slopes (S) of plots of $\ln k'$ versus mobile phase composition in RPLC are often strongly correlated. We showed that such a relationship is actually a specific form of the well known Colander equation [43,44] which specifies that plots of logarithmic capacity factors or logarithmic partition coefficients for a series of solutes in two different stationary phases with a fixed mobile phase are often quite linear. In both these situations and in the case of enthalpy–entropy compensation such must be observed when the variation in retention from solute to solute is governed by a *single* solute-dependent intermolecular parameter. We find it convenient to refer to such a chromatographic system and set of solutes as being “*iso-retentive*”. It is evident that a homologous series of solutes represents a trivial case of “*iso-retentive*” set of solutes.

As shown in Eqs. 15 and 16 it is possible for enthalpy–entropy compensation to take place when the same compensation temperature is observed for each retention controlling process. In this case it will appear as if there is a single solute-dependent retention governing parameter when there is not. We have referred to this situation as being “*pseudo iso-retentive*”.

Whether a chromatographic system behaves “*iso-retentively*” or not depends both on the nature of the system and the nature of the set of solutes. Consider first a chromatographic system, e.g. GC on a totally non-polar phase such as hexadecane. Differences in a solute’s ability to donate or accept a hydrogen bond will have no effect on its retention on such a phase. Thus a set of solutes might appear to be *iso-retentive* in fact they are capable of additional interactions given the right phase system. Conversely suppose we consider the case of RPLC where it has been shown that along with its size the solute’s hydrogen bond basicity is very important. If one examines a set of congeners or homologues or molecules that differ only in size but not hydrogen bond basicity one could fallaciously conclude that RPLC is an “*iso-retentive*” system when in fact it is not. It therefore of utmost importance in all fields of chromatography that one choose a set of probe molecules that truly do explore a wide range in types of molecular interaction

parameters before coming to any general conclusions.

4. Conclusions

Based on several statistically unbiased procedures, we examined the phenomenon of enthalpy–entropy compensation in capillary gas chromatographic retention. For all compounds as a whole, enthalpy–entropy compensation was not observed. For solutes within a homologous series, enthalpy–entropy compensation was observed. Our LSER equation and parameters predict that within a homologous series the free energy, enthalpy and entropy are linear functions of the homologue number and thus enthalpy–entropy compensation will occur within a homologous series but it is most unlikely to occur across a non-homologous sets of solutes of different polarity, hydrogen bond donor and acceptor strength.

5. Acknowledgements

This work was supported in part by grants to the University of Minnesota from the National Science Foundation and the Petroleum Research Foundation.

6. References

- [1] W. Linert and R.F. Jameson, *Chem. Soc. Rev.*, 18 (1989) 477.
- [2] W. Linert, L. Han and I. Lukovits, *Chem. Phys.*, 139 (1989) 441.
- [3] W. Linert and V.N. Sapunov, *Chem. Phys.*, 119 (1988) 265.
- [4] R.R. Krug, W.G. Hunter and R.A. Grieger-Block, *Chemometrics: Theory Appl., Symp.*, (ACS Symposium Series, No. 52), American Chemical Society, Washington, DC, 1977, p. 192.
- [5] R.R. Krug, *Ind. Eng. Chem. Fundam.*, 19 (1980) 50.
- [6] R.R. Krug, W.G. Hunter and R.A. Grieger, *J. Phys. Chem.*, 80 (1976) 2335.
- [7] R.R. Krug, W.G. Hunter and R.A. Grieger, *J. Phys. Chem.*, 80 (1976) 2341.
- [8] O. Exner, *Collect. Czech. Chem. Commun.*, 40 (1975) 2762.
- [9] C.G. Swain, M.S. Swain, A.L. Powell and S. Aluni, *J. Am. Chem. Soc.*, 105 (1983) 502.
- [10] J.E. Leffler and E. Grunwald, *Rates and Equilibria of Organic Reactions*, John Wiley and Sons, New York, 1963.
- [11] H.M.J. Boots and P.K. de Bokx, *J. Phys. Chem.*, 93 (1989) 8240.
- [12] P.K. de Bokx and H.M.J. Boots, *J. Phys. Chem.*, 93 (1989) 8243.
- [13] P.W. Carr, *Microchem. J.*, 48 (1993) 4.
- [14] B.L. Karger, L.R. Snyder and C. Eon, *Anal. Chem.*, 50 (1978) 2126.
- [15] F. Trouton, *Phil. Mag.*, 18 (1884) 54.
- [16] I.M. Barclay and J.A.V. Butler, *Trans. Faraday Soc.*, 34 (1938) 1445.
- [17] H.S. Frank, *J. Chem. Phys.*, 13 (1945) 493.
- [18] H.S. Frank and M.W. Evans, *J. Chem. Phys.*, 13 (1945) 507.
- [19] D.H. Everett, *J. Chem. Soc.*, (1960) 2566.
- [20] L. Nash, *J. Chem. Educ.*, 61 (1984) 981.
- [21] W. Melander, D.E. Campbell and C. Horvath, *J. Chromatogr.*, 158 (1978) 215.
- [22] W.R. Melander, B.-K. Chen and C. Horvath, *J. Chromatogr.*, 185 (1979) 99.
- [23] W. Melander, J. Stoveken and C. Horvath, *J. Chromatogr.*, 199 (1980) 35.
- [24] W.R. Melander, C.A. Mannan and C. Horvath, *Chromatographia*, 15 (1982) 611.
- [25] W.R. Melander and C. Horvath, *Chromatographia*, 19 (1984) 353.
- [26] W.R. Melander, B.-K. Chen and C. Horvath, *J. Chromatogr.*, 318 (1985) 1.
- [27] K. Jinno, T. Ohshima and Y. Hirata, *J. High Resolut. Chromatogr. Chromatogr. Commun.*, 5 (1982) 621.
- [28] K. Jinno and Y. Hirata, *J. High Resolut. Chromatogr. Chromatogr. Commun.*, 4 (1981) 466.
- [29] G. Vigh and Z. Varga-Puchony, *J. Chromatogr.*, 196 (1980) 1.
- [30] M. Kuchar, E. Kraus, V. Rejholec and V. Miller, *J. Chromatogr.*, 449 (1988) 391.
- [31] M. Kuchar, V. Rejholec, V. Miller and E. Kraus, *J. Chromatogr.*, 280 (1983) 289.
- [32] C.M. Riley, E. Tomlinson and T.L. Hafkenscheid, *J. Chromatogr.*, 218 (1981) 427.
- [33] J.-C. Huang, *J. Chromatogr.*, 321 (1985) 458.
- [34] M. Kuchar, H. Tomkova, V. Rejholec and I.O.O. Korhonen, *J. Chromatogr.*, 398 (1987) 43.
- [35] K.S. Reddy, J.-Cl. Dutoit and E. sz. Kovats, *J. Chromatogr.*, 609 (1992) 229.
- [36] J. Li, *Ph.D. Thesis*, University of Minnesota, Minneapolis, 1992.
- [37] J. Li, A.J. Dallas and P.W. Carr, *J. Chromatogr.*, 517 (1990) 103.
- [38] J. Li and P.W. Carr, *J. Chromatogr. A*, 659 (1994) 367.
- [39] J. Li, Y. Zhang, A.J. Dallas and P.W. Carr, *J. Chromatogr.*, 550 (1991) 101.
- [40] J. Li, Y. Zhang and P.W. Carr, *Anal. Chem.*, 64 (1992) 210.

- [41] J. Li, Y. Zhang, H. Ouyang and P.W. Carr, *J. Am. Chem. Soc.*, 114 (1992) 9813.
- [42] L.C. Tan and P.W. Carr, *J. Chromatogr. A*, 656 (1993) 521.
- [43] R. Collander, *Acta Chem. Scand.*, 5 (1951) 774.
- [44] D.J.W. Grant and T. Higuchi, *Solubility Behavior of Organic Compounds*, John Wiley and Sons, New York, 1990.

Selective chemiluminescence detection of sulfur-containing compounds coupled with nitrogen–phosphorus detection for gas chromatography

Thomas B. Ryerson, Robert M. Barkley, Robert E. Sievers*

Department of Chemistry and Biochemistry, Cooperative Institute for Research in Environmental Sciences, and Global Change and Environmental Quality Program, University of Colorado, Boulder, CO 80309-0216, USA

(First received December 24th, 1993; revised manuscript received February 23rd, 1994)

Abstract

A new sulfur and nitrogen–phosphorus detector for gas chromatography is described. The detector is an integrated thermionic ionization–chemiluminescence device permitting simultaneous detection of sulfur-containing and nitrogen- or phosphorus-containing compounds. This new flameless detector utilizes a heated rubidium-doped ceramic bead in a thermionic ionization chamber to produce sulfur monoxide from sulfur compounds. The SO is mixed with O₃ and the resulting chemiluminescence is monitored with a photomultiplier tube, providing sulfur-selective detection. The thermionic ionization detector signal serves as an independent second response channel, affording simultaneous selective and sensitive nitrogen–phosphorus detection. Two chromatograms are obtained, one in which selectivity is exhibited for nitrogen and phosphorus compounds, and the other for sulfur compounds present in the sample.

1. Introduction

Gas chromatographic (GC) separation, combined with selective detection, is often used in the analysis of volatile S, N and P compounds in the complex matrices characteristic of environmental samples. Selective detection methods for GC determination of S, N and/or P compounds are flame photometric (FPD) [1–3], atomic emission (AED) [2,4,5], Hall electrolytic conductivity (ELCD) [2,6], thermionic ionization (TID) [2,7–9], and several chemiluminescence (CL) detec-

tion methods [2,10–13]. With the exception of AED, combined S, N and P detection requires the use of some combination of these detectors, repeat analyses, or splitting of the sample.

FPD is the most widely used GC detection method for sulfur and phosphorus; selective S and P detection is achieved by monitoring, in part, S₂^{*} emission at 394 nm and HPO^{*} emission at 526 nm. However, the FPD response to sulfur compounds is highly compound-dependent, varies non-linearly with sulfur concentration, and is affected by quenching and substantial interferences by co-eluting species. AED can detect S, N and P compounds simultaneously and is not as greatly affected by quenching and interferences, but this method is expensive and requires a skilled operator. ELCD can detect S and N

* Corresponding author. Address for correspondence: Department of Chemistry and Biochemistry, University of Colorado, Campus Box 215, Boulder, CO 80309-0215, USA.

compounds but is not widely used because it is difficult to set up and maintain and also exhibits quenching and interference problems from compounds that do not contain sulfur or nitrogen.

TID (also called nitrogen–phosphorus detection, NPD) is selective for N and P compounds [9]. Widespread use of TID has been hindered in part due to the poorly understood chemistry by which it operates and a perceived reproducibility problem as detector elements age. Nonetheless, TID designs offer sensitive detection for N and P compounds for GC, with detection limits in the picogram range.

A flame-based sulfur chemiluminescence detection (flame-SCD^a) system has been developed [12]. Flame-SCD monitors the chemiluminescence produced when SO, formed from S compounds combusted in a flame, is oxidized by added ozone. Flame-SCD exhibits a linear response to sulfur independent of sulfur atom functionality, is not affected by co-eluting hydrocarbons, and is sensitive to ppb concentrations of sulfur compounds in complex matrices.

The instrument described here integrates a unique form of a sulfur CL detector with a thermionic detector. While this new detector uses no flame to generate SO, it is similar in some respects to the SCD system; thus, a brief review of sulfur CL and TID will be presented in the Results and discussion section.

2. Experimental

2.1. Materials

Helium was used as the GC carrier gas and was purified by passing it through a molecular sieve and then a reducing catalyst trap. Molecular sieve (5 Å) from Fisher Scientific (Pittsburgh, PA, USA) was conditioned under vacuum at >400°C for 12 h prior to use. R3-11 Copper catalyst was obtained from Chemical Dynamics (South Plainfield, NJ, USA) and was conditioned under hydrogen gas at 160°C for 24 h

prior to use. Hopcalite (6–14 mesh, 1.41–3.36 mm), supplied by Mine Safety Appliances (Pittsburgh, PA, USA), was used to trap excess ozone upstream of the vacuum pump. Reagent-grade hexanes (*ca.* 50% *n*-hexane), acetone and dimethyl sulfoxide (DMSO) were purchased from Mallinckrodt Specialty Chemicals (Chesterfield, MO, USA). Malathion (95%), 3-methylpyridine and dimethyldisulfide (DMDS) were purchased from Pfalz & Bauer (Waterbury, CT, USA). The 1,4-thioxane, thiophene, 2,5-dimethylthiophene, dimethyl sulfate, tetramethylene sulfone, 4-*tert.*-butylpyridine and 2-bromochlorobenzene used to make standards were supplied by Aldrich. N-Dodecane and 1-tridecene standards were obtained from Polyscience (Niles, IL, USA). A test mixture of various mercaptans, sulfides and disulfides was supplied by Sievers Instruments (Boulder, CO, USA). The SO₂, SF₆ and H₂S gas standards were from Matheson (Secaucus, NJ, USA). All commercially supplied reagents were used as received without further purification. Thiirane-1-oxide was synthesized in our laboratory by the method of Hartzell and Paige [14].

2.2. Apparatus

A Hewlett-Packard Model 5730A gas chromatograph was modified with a Grob-type split/splitless injection port. Chromatographic separation was accomplished by use of a Hewlett-Packard HP-1 25 m × 0.2 mm I.D. fused-silica capillary column with a 0.33-μm layer of cross-linked poly(dimethylsiloxane) stationary phase. GC conditions were 20 p.s.i.g. (1 p.s.i. = 6894.76 Pa) of helium head pressure (18 cm/s linear velocity) and a split ratio of 1:40. Helium was used as the carrier gas and was purified by passing it through molecular sieve and copper catalyst traps to remove carbon dioxide, water and oxygen. The gas chromatograph was equipped with unmodified flame ionization (FID) and TID detection systems. A digital multimeter (Fluke, Model 77) was used to measure the TID bead heating voltage. A Sievers Instruments Model 350A SCD system was used to measure sulfur monoxide CL; the new flame-

^a SCD is a registered trademark of Sievers Instrument Co., Boulder, CO, USA.

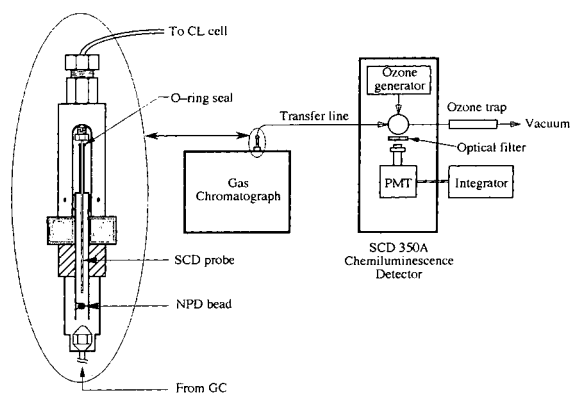


Fig. 1. Schematic of SNPD.

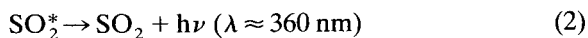
less method of SO generation was the only modification to the SCD design. The SCD ozone generator was supplied with pure industrial-grade air passed through a Drierite trap to remove water. Two Hewlett-Packard Model 3390A integrators were used to simultaneously monitor TID and SCD signals.

The sulfur and nitrogen–phosphorus detection (SNPD) system is shown schematically in Fig. 1. It consists of the following components: a gas chromatograph, a thermionic ionization detector and a sulfur chemiluminescence detector (without the flame interface) consisting of an alumina probe and transfer line, an ozone source, a CL reaction chamber, a photomultiplier tube (PMT) and a vacuum pump. An adapter was machined from an aluminum block to position the SCD probe (ordinarily located above a hydrogen-rich hydrogen–air flame) and was threaded to allow variable probe tip positioning from 1 to 35 mm above the thermionic ionization bead. Flow was maintained through the probe and CL chamber by the SCD vacuum pump, which served to maintain operating pressures in the chamber below 25 Torr (1 Torr = 133.322 Pa). A trap filled with Hopcalite catalyst on the vacuum pump inlet destroyed excess ozone before the pump exhaust was vented to a fume hood.

3. Results and discussion

Flame-SCD has been used for GC [10,12,15–23] supercritical fluid chromatography [19,24,25]

and capillary liquid chromatography [19,26]. It has been compared with FPD [15,17], with AED [5] and has been recently reviewed [18,22,27–29]. Briefly, flame-SCD is based on a two-step process described by Benner and Stedman [12]. Sulfur-containing compounds are combusted in a hydrogen-rich hydrogen–air flame to form SO. The SO is withdrawn under vacuum to a reaction chamber and O₃ is added. SO is oxidized to sulfur dioxide (SO₂^{*}) in an excited electronic state [30]. The SO₂^{*} decays by chemiluminescent emission of a photon, which is counted by a photomultiplier tube (reaction 2).



This chemiluminescence is highly selective for S compounds and affords excellent sensitivity due to the low background. Detection limits for the SCD are on the order of 0.5 pg S/s, or low ppb concentrations of sulfur. Detector response is linear over five orders of magnitude. The response to sulfur is independent of the configuration of sulfur atoms in the parent molecule. When gas flows are adjusted correctly, co-eluting hydrocarbons, including the large solvent peak, do not quench the sulfur CL signal. A patent has been granted for coupling flame-SCD with FID, the use of which permits simultaneous general and sulfur-selective chromatograms to be obtained [31].

Although generation of SO in a flame is a widely used sensitive and selective method of sulfur detection, there are several possible advantages to be realized by using other ways to produce SO from sulfur-containing compounds. Although the absolute conversion efficiency of sulfur compounds to SO in the flame is unknown, this efficiency has been estimated to be quite low, below 1% [20]. An increase in conversion efficiency has the potential to dramatically increase the sensitivity offered by SCD. Flame-SCD response to sulfur is dependent on a number of operating factors, especially those involving sampling of a flame for SO generated from S compounds.

Alternative methods to generate SO for sub-

sequent CL detection have been sought to avoid the use of an open flame. A flameless combustion chamber has been recently reported to convert sulfur compounds to SO for subsequent CL detection [32,33]. Our choice of the heated catalyst bead in a TID system was based on two reasons. First, coupling the two detectors in this manner offers the possibility of simultaneous S, N and P detection. Second, this technology was readily available from several manufacturers and was accessible to virtually any laboratory equipped with a GC system. Replacing the flame as the SO source has the potential to offer some operational advantages over flame-SCD. Less gas is consumed during SNPD operation, and less water is formed. The positioning of the sample probe is not as critical in SNPD as it is in flame-SCD.

The Hewlett-Packard TID system used in the present report collects positive ions, unlike most other commercial designs which collect negative ions. A recent theory, based on bead surface chemistry, proposes an explanation for the selective production of positive N and P ions in TID [34]. This theory describes the TID mechanism as one of purely surface decomposition and ionization. N and P analytes are first adsorbed onto the bead via lone pair interaction with a surface site. Analyte decomposition proceeds by loss of H or CH₃; ionization follows for those radicals with low ionization potentials, *i.e.*, those containing a N or P heteroatom. Mass spectral studies suggest that formation of reactive species residing on the bead surface, presumably H atoms, can account for the observed formation of both positive and negative N- and P-containing ions [34]. Thus, all steps involved in the production of charge carriers may occur on the bead surface. Subsequent discussion of the SO formation in the new SNPD system will be in terms of this surface decomposition and ionization theory. The TID system used in this study differs from other TID systems only in ion collection, not in fundamental ion formation chemistry. We expect that other TID systems may be successfully coupled to SCD, subject to the physical constraints of probe positioning inside the thermionic ionization source.

Sulfur CL detection can be coupled very easily to conventional TID; this coupling allows simultaneous selective measurement of S and N or P compounds in GC (see Fig. 1). A custom adapter was designed and fabricated to hold the SCD probe in the TID collector chimney. A 1/16-in. (1 in. = 2.54 cm) O.D. alumina SCD probe was inserted to within 2 mm of the TID bead. A solution of 50 ppm (w/w) DMSO in hexanes was injected into the GC system to determine whether any SO was produced by the reactive species on the surface of the heated TID bead. The resulting chromatogram is shown in Fig. 2a, with a comparison to the response obtained with a cool, inactive bead shown in Fig. 2b. There was no detectable response when the bead was not electrically heated, which demonstrated that the conversion depends upon processes that occur when TID is being operated. This rules out the possibility of cold catalytic formation of SO by the TID bead.

Fig. 2b also indicates DMSO does not exhibit reduced sulfur CL [13,35] upon direct ozone oxidation. Thus, S response is shown to be via production of SO by the heated TID bead. This novel method of S compound conversion to SO is highly selective. No response for solvent is

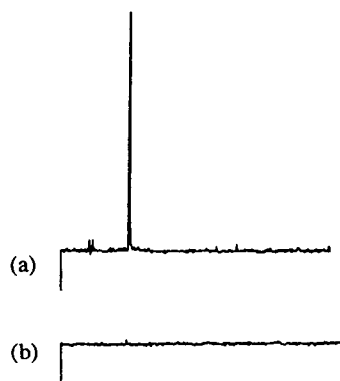


Fig. 2. Sulfur-selective detection by SNPD. (a) DMSO is converted to SO by a heated TID bead and detected by O₃-induced chemiluminescence. (b) This conversion is not accomplished until a minimum heating voltage is applied to the bead. GC conditions: 1.0 μ l of a 50 ppm DMSO in hexanes solution was injected, split 1:40; column and stationary phase as noted in the text. GC oven temperature 80°C, bead heating voltages (a) 26.00 V d.c.; (b) 0.00 V d.c.

noted under these conditions, indicating a SNPD S-channel selectivity over carbon-, hydrogen- and oxygen-containing compounds of $>10^6$.

Further experiments showed that SCD probe insertion does not disrupt normal TID processes. Chromatograms exhibiting selective, two-channel S and NP detection by the new SNPD system is shown in Fig. 3b and c. Neither S nor NP channel of the SNPD system exhibited detectable response to the non-S or -NP compounds, respectively, present at comparable or higher concentration levels. Examination of the NP trace in Fig. 3c reveals this SNPD channel behaves similarly to unmodified TID. A slight negative response for the large amount of solvent is noted and is characteristic of properly functioning TID. The large hydrocarbon plug

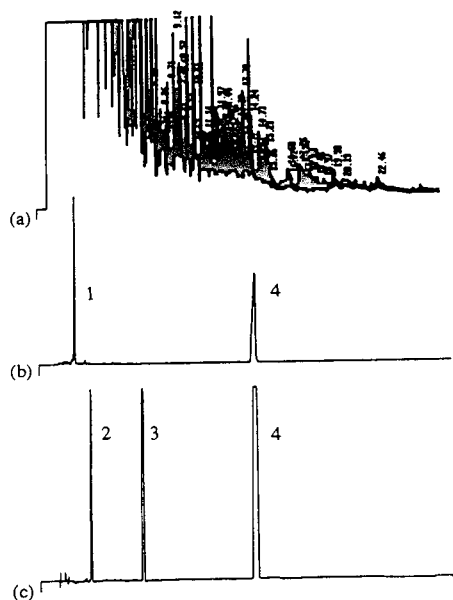


Fig. 3. Selective two-channel SNPD operation (b = S channel, c = NP channel), with comparison to FID (a). Only those compounds containing S, N or P are detected. These two chromatograms result from a single injection of a mixture of S/N/P compounds diluted in a complex mixture of hydrocarbons. Conditions were as follows: 1.0 μ l of a solution of ca. 100 ppm of each S, N and P compound and 10% (v/v) gasoline in hexanes was injected, split 1:40; column and stationary phase as noted in the text. GC oven temperature program: 80°C for 2 min, increased at 8°C/min to 160°C and held at 160°C for 2 min. Bead heating voltage 22.45 V d.c. Peaks: 1 = dimethyl sulfoxide; 2 = trimethylphosphate; 3 = 4-tert.-butylpyridine; 4 = dimethylthiourea.

tends to interfere with radical processes on the bead surface and thereby “cool” the bead. These processes are rapidly reestablished by continual external heating of the bead after passage of solvent.

SNPD response dependence on a number of operating parameters has been determined, and is presented below with a comparison to normal TID and SCD operation. In most cases, the NP channel response dependence is identical to that in normal TID. However, there are several differences between the S channel of the new SNPD and flame-SCD operation. These differences will be discussed in detail in section 3.1.

3.1. Detector optimization: bead heating voltage

Both the S and NP channel response dependence on TID bead heating voltage were investigated. DMSO and 3-methylpyridine were diluted in hexanes to form a stock solution containing 50 ng/ μ l of each compound. Repetitive injections of this solution were made while varying the heating voltage to the bead from 0 to 25.50 V. The results are shown graphically in Fig. 4. No response was seen in either channel until the voltage exceeded ca. 22 V. Above this threshold, response increased rapidly with increased heating voltage. This is similar to normal TID behavior [9]. As with TID, the SNPD bead heating voltage was chosen to give a baseline deflection of 10% of full scale at attenuation 8 on the NP channel. This deflection signals the initiation of the radical processes at the surface of the bead. Increasing the voltage above this setting enhanced the S-channel response, but degraded reproducibility in both channels, increased NP-channel noise, and reduced the long-term stability of the SNPD system.

3.2. Probe positioning

Upon initial insertion of a flame-conditioned alumina SCD probe into the thermionic ionization chamber, an increased bead heating voltage (relative to conventional TID operation) was required to initiate and sustain TID chemical processes leading to selective N- and P-com-

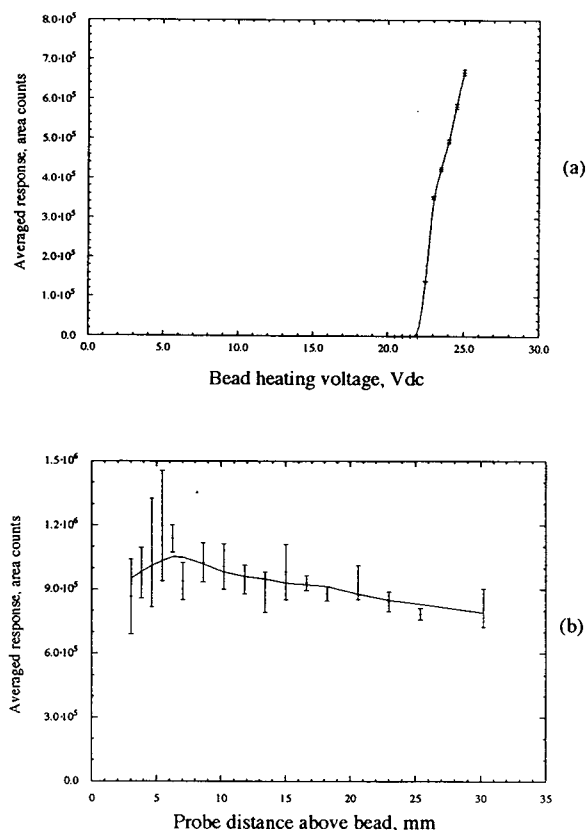


Fig. 4. SNPD Sulfur channel response dependence on (a) TID bead heating voltage and (b) SCD probe height above the bead. Plotted values represent average responses for five 1.0- μ l injections, of 50 ng/ μ l DMSO in hexanes, at each voltage/probe height; split ratio measured at 1:40. Error bars represent ± 1 standard deviation.

pound detection. The SCD vacuum pump creates a positive flow of over 600 ml/min through the probe, while TID gas flows total less than 100 ml/min into the chamber. A partial vacuum is created in the chamber, necessitating higher heating voltages to sustain the chemical processes leading to analyte decomposition and ionization [36].

Once the thermionic surface processes were initiated, injections of a solution of DMSO in hexanes were made while varying the probe height above the bead to ascertain the effect of probe positioning on the magnitude of the S channel response. The axial probe tip position was varied from 3 to 30 mm above the heated

bead. The results are shown in Fig. 4. A broad maximum is seen in the response, with the optimum at roughly 6 mm. Therefore, the S-channel response in SNPD is relatively independent of axial probe position.

This broad, forgiving maximum in SNPD S-channel dependence on axial probe position is markedly different than for flame-SCD. A sharply peaked maximum is exhibited when a flame is used to generate SO from S compounds [12]. Sulfur chemistry in flames is characterized by complex and rapid reactions between many different S species. These competing equilibria, and the relatively short lifetime in air of the SO diradical [37], give rise to a highly localized region within the flame in which the SO concentration is maximized. Thus, in flame-SCD, optimum sensitivity is highly dependent on the probe position. In practice, probe positioning has been a time-consuming step in the flame-SCD optimization process; recently, a new probe interface design has greatly reduced fluctuations arising from variations in the probe position.

The lessened dependence on probe position in the SNPD design does, however, facilitate S response optimization. The lessened dependence may be due to the lower pressures obtained in the thermionic ionization chamber. The lifetime of SO at reduced pressure is much longer than at atmospheric pressure [38,39]; therefore, SNPD may preserve SO longer than flame-SCD. At probe distances closer to the bead than optimum, the decreased sensitivity in the SNPD design may be due to interferences in bead surface chemistry. At short distances, the probe disturbs gas flows in the thermionic ionization chamber, thereby decreasing the S-channel sensitivity by interfering with radical processes at the bead surface. However, this decrease at short distances is still not as great as in conventional SCD.

3.3. Probe conditioning

The first alumina probe used in this study had been conditioned by heating for 12 h in a flame, as the manufacturer has suggested for flame-SCD operation. However, in SNPD, new, un-

conditioned probes used as replacements gave equivalent or slightly increased S-channel sensitivity. Therefore, the data in the present study were all obtained using an unconditioned probe.

3.4. Gas flows

Initial success in selective SNPD was achieved at detector gas flow settings appropriate to unmodified TID, *i.e.*, 4 ml/min hydrogen, 50 ml/min air and 30 ml/min nitrogen makeup gas. The effects of changing both the absolute and relative amounts of these detector gases on both the S- and the NP-channel responses were investigated. A solution of DMDS and 3-methylpyridine in hexanes was repeatedly injected while simultaneously varying both hydro-

gen and air flows into the SNPD thermionic ionization chamber. Optima for S- and NP-channel response were located by using a Simplex method. Data are presented as response surfaces in three dimensions in Fig. 5.

Examination of these surfaces indicates that S and NP responses are maximized under roughly similar conditions. However, two other criteria must be included in a determination of optimum gas flows. One is solvent response in the S channel, which becomes a significant factor at high total gas flow-rates. Another is the bead heating voltage required to sustain a given background signal in the NP channel. NP background is indicative of the “robustness” of the surface processes of the bead. The heating voltage required to sustain the reactions at the bead

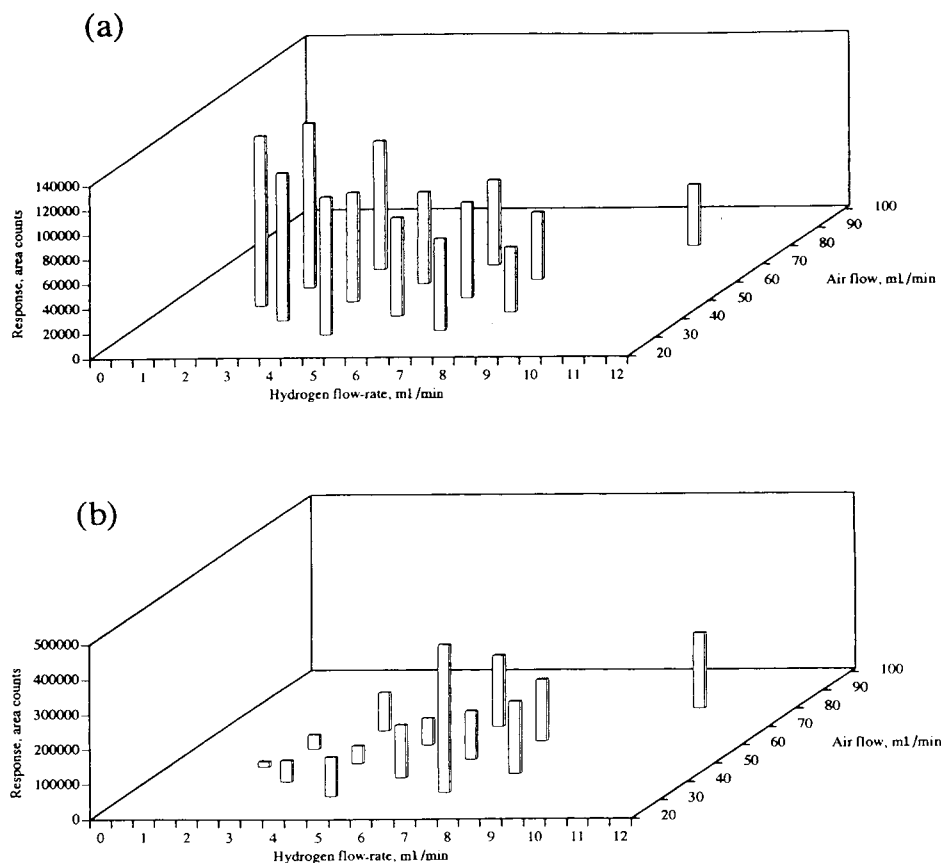


Fig. 5. Response surfaces in three dimensions obtained by varying hydrogen and air flows in SNPD. (a) S-Channel response surface; (b) NP-channel response surface. Values are averages of five 1.0- μ l injections, split 1:40, of a 100 ppm solution of dimethyldisulfide (S channel) or 3-methylpyridine (NP channel) in hexanes.

Table 1

Comparison of detection limits of SNPD with other detection methods

	Sulfur, pg S/s (2,5-dimethylthiophene)	Nitrogen, pg N/s (4- <i>tert.</i> -butylpyridine)
NPD	N.D. ^a	0.23
SCD	0.73	N.D.
SNPD	1.5	1.1

Detection limits calculated based on $S/N_{pp} = 3.29$ (95% confidence), N_{pp} = peak-to-peak noise.^a N.D. = Not detectable by this method.

surface increases rapidly at high gas flows. Therefore, the optimum gas mixture and the flow-rates must allow sensitive S and NP detection, with no response from the solvent in the S channel, at a reasonable heating voltage. These criteria are met at 4 ml/min hydrogen, 50 ml/min air and 30 ml/min of nitrogen makeup, which happen to be the flows recommended by the manufacturer for traditional TID operation. Apparently the conditions needed for effective NP detection also generate SO with virtually optimum efficiency.

Once the maximum SNPD response for simultaneous, selective two-channel S and NP detection was obtained, detector sensitivity, selectivity and linearity were determined. The detector response is linear over three orders of magnitude in concentration, from 0.3 to 375 ng/ μ l; the linear least-squares regression equation, detector response = $(18598 \pm 730) \times$ con-

centration + (15409 ± 15932) , yielded a correlation coefficient $r = 0.9996$ for the compound malathion. Malathion is an insecticide commonly used in formulations for pest control, and contains both S and P.

Detection limits were determined for this new detector and are presented in Table 1 and compared with unmodified TID and SCD operation. SNPD, when operated in the combined mode, is a factor of 5 less sensitive than TID for a test N compound, and a factor of 2 less sensitive than SCD for a test S compound. However, SNPD can selectively detect S and NP compounds at low ppm concentrations, and can do so virtually simultaneously without splitting of the sample.

A wide range of S and NP compounds has been detected by SNPD (see Table 2). The NP-channel response is equivalent in this respect to that of conventional TID [8,9]. The S-channel

Table 2

S-Containing compounds detected by SNPD

Sulfides	Carbon disulfide, hydrogen sulfide, methyl ethyl sulfide, dimethyl sulfide, diethyl sulfide, dimethyl disulfide, diethyl disulfide, dimethyl trisulfide, 1,4-thioxane, thiazole, thiourea, dimethylthiourea, diethylthiorea, 2-chloroethyl ethyl sulfide (half-mustard)
Mercaptans	Methyl, ethyl, 1-propyl, 2-propyl, 2-methylpropyl, 1-butyl, 2-butyl and <i>tert.</i> -butyl mercaptan
Aromatics	Thiophene, 2-methylthiophene, 2,5-dimethylthiophene
Oxides	Thiirane-1-oxide, dimethyl sulfoxide
Pesticides	Malathion, aldicarb, chlorpyrifos

response characteristics, however, are different than in flame-SCD. The flame-SCD design exhibits nearly equimolar responses to sulfur compounds regardless of the environment of the S atom in the analyte [12,23]. Although SNPD is sensitive to a wide range of sulfur compounds, the response is dependent on the S atom functionality. The chemiluminescence intensity decreased in the order sulfide > aromatic > mercaptan > sulfoxide; sensitivities of detection of these representative compounds are in the ratio 5.3:2.6:1.7:1.

While all reduced sulfur compounds tested were detected by SNPD, of those tested, only two of the oxidized sulfur compounds examined, DMSO and thiirane-1-oxide, gave a response. SO₂, SF₆, dimethyl sulfate and tetramethylene sulfone were not detected; the reason for this is not clear. We surmise that oxidizing conditions sufficient to convert reduced sulfur compounds to SO obtain at the surface of the bead. Oxidized sulfur compounds, with the two exceptions noted, do not appear to be reduced to SO under these conditions. Oxidized sulfur compounds are converted to SO by combustion in a hydrogen-rich flame in the conventional SCD design.

4. Conclusions

The new SNPD design offers the following advantages.

(a) *Simultaneous S and NP detection.* Information on S and NP compounds can now be obtained without duplicate analyses or splitting of sample. Many pharmaceuticals, pesticides and herbicides contain different combinations of S, N and P; therefore, a selective two-channel detector simplifies compound identification by providing an extra dimension of information. Detector response ratioing can assist in confirmation of the identities of unknown peaks.

(b) *High selectivity.* No solvent response is observed in the SNPD S channel under a wide range of operating conditions. In contrast, the SCD flame gas flows must be carefully adjusted to eliminate either positive or negative response from solvent.

(c) *Easy optimization.* The SNPD S channel can tolerate a wide range of variation in gas flows, probe positioning and bead heating voltage and still give sensitive, selective S and NP detection.

(d) *Low gas consumption.* Gas flows are identical to those in TID, and a tenth of that required for SCD. In contrast to conventional SCD, very little water is produced as a byproduct of SNPD operation. This prolongs pump oil and ozone trap lifetimes and permits more efficient pumping.

Applications for SNPD involve detection of S and NP compounds in complex matrices, especially those in which the constituents are so numerous that the resolving power of capillary GC is insufficient. These matrices include hydrocarbon feedstocks, petrochemical products and environmental samples. SNPD may also be useful for determining trace levels of drugs, medications and metabolites in complex biological matrices such as plasma and other bodily fluids. Many pesticides and almost all chemical warfare agents should be sensitively detected by this detector, since they contain sulfur, nitrogen and/or phosphorus.

5. Acknowledgements

Support from the NSF under grant ATM-9115295 is gratefully acknowledged. We would also like to thank Sievers Instruments Co. for the generous gift of a sulfur chemiluminescence detector, and Dr. R. Hutte for his insightful comments throughout the course of this research.

6. References

- [1] S.O. Farwell and C.J. Barinaga, *J. Chromatogr. Sci.*, **24** (1986) 483.
- [2] M. Dressler, *Selective Gas Chromatographic Detectors*, Elsevier, Amsterdam, New York, 1986.
- [3] S.S. Brody and J.E. Chaney, *J. Gas Chromatogr.*, **4** (1966) 44.
- [4] P.C. Uden, Y. Yoo, T. Wang and Z. Cheng, *J. Chromatogr.*, **468** (1989) 319.

- [5] S.E. Eckert-Tilotta, S.B. Hawthorne and D.J. Miller, *J. Chromatogr.*, 591 (1992) 313.
- [6] R.C. Hall, *J. Chromatogr. Sci.*, 12 (1974) 152.
- [7] B. Kolb and J. Bischoff, *J. Chromatogr. Sci.*, 12 (1974) 625.
- [8] C.A. Burgett, D.H. Smith and H.B. Bente, *J. Chromatogr.*, 134 (1977) 57.
- [9] P.L. Patterson, *DET Report 17*, DETector Engineering and Technology, Walnut Creek, CA, 1989.
- [10] J.K. Nelson, R.L. Getty and J.W. Birks, *Anal. Chem.*, 55 (1983) 1767.
- [11] S.A. Nyarady, R.M. Barkley and R.E. Sievers, *Anal. Chem.*, 57 (1985) 2074.
- [12] R.L. Benner and D.H. Stedman, *Anal. Chem.*, 61 (1989) 1268.
- [13] J.S. Gaffney, D.J. Spandau, T.J. Kelly and R.L. Tanner, *J. Chromatogr.*, 347 (1985) 121.
- [14] G.E. Hartzell and J.N. Paige, *J. Am. Chem. Soc.*, 88 (1966) 2616.
- [15] R.L. Benner and D.H. Stedman, *Environ. Sci. Technol.*, 24 (1990) 1592.
- [16] R.S. Hutte, N.G. Johansen and M.F. Legier, *J. High Resolut. Chromatogr.*, 13 (1990) 421.
- [17] K.K. Gaines, W.H. Chatham and S.O. Farwell, *J. High Resolut. Chromatogr.*, 13 (1990) 489.
- [18] A.L. Howard and L.T. Taylor, *J. High Resolut. Chromatogr.*, 14 (1991) 785.
- [19] N.G. Johansen and J.W. Birks, *Am. Lab.*, 23 (1991) 112.
- [20] R.L. Benner, *Ph. D. Thesis*, University of Denver, Denver, CO, 1991.
- [21] B. Chawla and F. Di Sanzo, *J. Chromatogr.*, 589 (1992) 271.
- [22] R.S. Hutte, R.E. Sievers and J.W. Birks, *J. Chromatogr. Sci.*, 24 (1986) 499.
- [23] R.L. Shearer, D.L. O'Neal, R. Rios and M.D. Baker, *J. Chromatogr. Sci.*, 28 (1990) 24.
- [24] H.-C.K. Chang and L.T. Taylor, *J. Chromatogr.*, 517 (1990) 491.
- [25] W.T. Foreman, C.L. Shellum, J.W. Birks and R.E. Sievers, *J. Chromatogr.*, 465 (1989) 23.
- [26] H.-C.K. Chang and L.T. Taylor, *Anal. Chem.*, 63 (1991) 486.
- [27] R.S. Hutte and J.D. Ray, in H.H. Hill and D.G. McMinn (Editors), *Detectors for Capillary Chromatography*, Wiley, New York, 1992, p. 193.
- [28] W. Wardencki and B. Zygmunt, *Anal. Chim. Acta*, 255 (1991) 1.
- [29] M. Dyson, *Anal. Proc.*, 30 (1993) 79.
- [30] C.J. Halstead and B.A. Thrush, *Photochem. Photobiol.*, 4 (1965) 1007.
- [31] R. Godec, N. Johansen and D.H. Stedman, *US Pat.*, 5 227 135 (July 13, 1993).
- [32] R.L. Shearer, *Anal. Chem.*, 64 (1992) 2192.
- [33] R.L. Shearer, E.B. Poole and J.B. Nowalk, *J. Chromatogr. Sci.*, 31 (1993) 82.
- [34] D.D. Bombick and J. Allison, *J. Chromatogr. Sci.*, 27 (1989) 612.
- [35] T.J. Kelly, J.S. Gaffney, M.F. Phillips and R.L. Tanner, *Anal. Chem.*, 55 (1983) 135.
- [36] L. Trelly and D. Bombick, presented at the 43rd Pittsburgh Conference on Analytical Spectroscopy, New Orleans, LA, 1992, poster 148P.
- [37] J.O. Sullivan and P. Warneck, *Ber. Bunsenges. Phys. Chem.*, 69 (1965) 7.
- [38] C.J. Halstead and B.A. Thrush, *Proc. Roy. Soc. A*, 295 (1966) 380.
- [39] M.A.A. Clyne, C.J. Halstead and B.A. Thrush, *Proc. Roy. Soc. A*, 295 (1966) 355.

Capillary column gas chromatographic–tandem mass spectrometric analysis of phosphate esters in the presence of interfering hydrocarbons

Paul A. D'Agostino *, Lionel R. Provost

Defence Research Establishment Suffield, P.O. Box 4000, Medicine Hat, Alberta T1A 8K6, Canada

(First received December 6th, 1993; revised manuscript received February 15th, 1994)

Abstract

Daughter, parent and constant neutral loss spectra, and multiple reaction ion monitoring data were all evaluated for the detection and confirmation of phosphate esters during capillary column GC–MS–MS analysis with a hybrid tandem mass spectrometer. Constant neutral loss and parent modes involve scanning of the sector, thus reducing the benefits of higher sector resolution, while daughter and multiple reaction ion monitoring data may be acquired with higher sector resolution. The benefit of higher sector resolution was demonstrated for the detection and confirmation of phosphate esters in the presence of diesel exhaust extract components at levels several orders of magnitude above that of the phosphate esters. Detection limits for daughter operation were approximately the same as those obtained during capillary column GC–MS analysis of standards under electron impact ionization, and S/N ratios in excess of 100:1 were observed during multiple reaction ion monitoring of the diesel exhaust extract spiked at the 200 pg level with phosphate esters.

1. Introduction

The widespread agricultural and industrial use of organophosphorus compounds as pesticides, fertilizers and fire retardants has led to the development of numerous instrumental methods for the detection and confirmation of these compounds in environmental samples. Some organophosphorus compounds, including pesticides and chemical warfare agents or their decomposition products, are toxic and for this reason highly specific methods are required for

the trace detection of these compounds in the environment. Mass spectrometry (MS) and in particular, capillary column gas chromatography (GC)–MS, while generally accepted as the technique of choice for the confirmation of many organophosphorus compounds, has limitations in the presence of chemical interferences. The selectivity of tandem mass spectrometry (MS–MS), particularly when interfaced to a chromatographic separation technique, may overcome difficulties associated with the confirmation of target compounds in the presence of chemical interferences.

This drive for increased specificity for the trace analysis of toxic organophosphorus compounds

* Corresponding author.

in environmental and other samples has resulted in a number of applications involving the use of MS–MS. Recent pesticide studies include a paper detailing the MS–MS data for 26 organophosphorus pesticides [1], the use of MS–MS for the determination of pesticide residues in foods [2,3] and the demonstration of high-performance liquid chromatography–MS–MS with thermospray ionization for the analysis of organophosphorus pesticides [4]. Similar investigations have been conducted with organophosphorus chemical warfare agents to support the detection and confirmation of these compounds under the United Nations Chemical Weapons Convention. The ammonia chemical ionization (CI) daughter spectra of four organophosphorus chemical warfare agents have been reported [5] and the specificity of capillary column GC–MS–MS has recently been demonstrated for the confirmation of organophosphorus chemical warfare agents in matrices similar to those expected during battlefield sampling [6,7]. In the latter two cases the MS–MS analyses were performed under low-resolution conditions with a hybrid instrument. Higher sector resolution with a hybrid instrument should decrease chemical interferences over those observed during analysis under low-resolution hybrid or triple quadrupole operation. The potential advantages of higher resolution during daughter and multiple reaction ion monitoring (RIM) operation and the relative merits of parent and constant neutral loss operation have not been previously investigated for the capillary column GC–MS–MS confirmation of organophosphorus compounds.

Mass-analysed ion kinetic energy mass spectra have been acquired for dimethyl methylphosphonate and trimethyl phosphite [8] and the daughter spectra of m/z 110 for trimethyl phosphate and m/z 110 and 138 for triethyl phosphate have been published [9,10]. The MS⁵ spectra for triethyl phosphate was obtained during multiple-stage MS analysis [11] and a number of other organophosphorus compounds, including phosphate esters, have been characterized during atmospheric-pressure ionization MS–MS [12–14]. Most recently a homologous series of n -C₁

to n -C₄ phosphate esters (trimethyl phosphate, triethyl phosphate, tri- n -propyl phosphate and tri- n -butyl phosphate), often employed as chemical simulants for chemical warfare agents, were characterized by MS–MS. Daughter spectra were obtained for all the principal electron impact ionization (EI) ions of each phosphate ester and optimal collisional-activated dissociation (CAD) cell conditions were established by stepping the CAD cell energy from 1 to 100 eV (laboratory scale) in 1-eV increments with residual air and argon target gases [15].

Previous CAD cell conditions [15], were incorporated in the present study designed to evaluate the capabilities of a hybrid tandem mass spectrometer for the confirmation of organophosphorus compounds. A complex hydrocarbon matrix, similar to that expected during battlefield sampling, was used to evaluate the relative merits of daughter, parent, constant neutral loss and RIM for the confirmation of organophosphorus compounds in the presence of significant chemical interferences.

2. Experimental

2.1. Standards

Trimethyl phosphate, triethyl phosphate, tri- n -propyl phosphate and tri- n -butyl phosphate were provided by the Defence Research Establishment Suffield Organic Chemistry Laboratory. Standard solutions used for capillary column GC–MS–MS analysis were prepared in dichloromethane (BDH, Omnisolv).

The phosphate esters were added to a complex extract of diesel exhaust emissions collected on a Canadian C2 respirator canister. Two aliquots of this diesel extract were spiked with the phosphate esters such that 1- μ l GC injections of the spiked extracts resulted in the loading of either 2.5 ng or 200 pg of phosphate ester. This matrix, described previously [6], contains numerous hydrocarbons at high concentrations and was selected to evaluate the sensitivity and selectivity

of GC–MS–MS for the analysis of phosphate esters.

2.2. Instrumental

Capillary column GC–MS–MS analyses were performed with a VG AUTOSPEC-Q (EBEQQ geometry) hybrid tandem mass spectrometer equipped with a Hewlett-Packard Model 5890 gas chromatograph. A 15 m \times 0.32 mm I.D. DB-1701 J & W capillary column (0.25 μ m film thickness) was used for all GC–MS and GC–MS–MS analyses with the following temperature program: 40°C (2 min hold) 10°C/min to 280°C (5 min hold). All GC injections were cool on-column using an injector of our own design [16].

The EI-MS operating conditions were as follows: source pressure, $3 \cdot 10^{-6}$ Torr (1 Torr = 133.322 Pa); source temperature, 200°C; electron energy, 70 eV; and electron emission, 100 μ A. EI mass spectra were obtained using a VG EI/CI source at a resolution of 1000 (10% valley definition) and an accelerating voltage of 8 kV. Mass spectral data were collected from 250 to 50 u at a scan rate of 1 s/decade.

In an initial study, all four phosphate esters were introduced through the heated septum reservoir and breakdown curves were obtained for all the principal ions at three different CAD cell pressures over 1 to 100 eV [15]. The best compromise between sensitivity and spectral content were obtained with a CAD cell argon pressure of $8 \cdot 10^{-7}$ – $9 \cdot 10^{-7}$ Torr and an energy of 25 eV (laboratory scale). This argon pressure reduced the intensity of the perfluorokerosene (PFK) ion at m/z 219 to 50% of its original intensity under residual air CAD cell pressures. A typical daughter spectrum for m/z 219 at 30 eV (with no detectable signal below 12 eV) under this CAD cell condition gave the following ion ratios: m/z 219: m/z 131: m/z 69 = 1:0.25:0.15. Daughter spectra were obtained under these CAD cell conditions for the molecular ion or a high-mass EI fragmentation ion for each of the four phosphate esters during capillary column GC–MS–MS analysis. The quadrupole was operated at unit resolution and scanned from 250 to

50 u at 1 s/scan and the sector resolution was set at a value in the 1000 to 3400 (10% valley definition) range.

Multiple reaction ion monitoring GC–MS–MS data were obtained for tripropyl phosphate by monitoring the m/z 183 to m/z 141 and m/z 183 to m/z 99 transitions under the chromatographic and CAD cell conditions described above. Each transition was monitored for 80 ms with a 40-ms delay. Resolution of the sector was either 1000 or 2500 (10% valley definition).

Parent spectra for diagnostic phosphate ester EI fragmentation ions were obtained under identical chromatographic and CAD cell conditions used for daughter spectra acquisition. Spectra were obtained by scanning the sector from 250 to 50 u at 0.7 s/decade.

Constant neutral loss spectra were obtained for the loss of 30 u (corresponds to the loss of CH₂O; trimethyl phosphate detection), 28 u (corresponds to loss of C₂H₄; triethyl phosphate monitoring), 42 u (corresponds to loss of C₃H₆; tripropyl phosphate monitoring) and 56 u (corresponds to loss of C₄H₈; tributyl phosphate monitoring) by scanning the sector and quadrupole over 250 to 50 u at 1.5 s/scan. Chromatographic and CAD cell conditions were identical to those used during daughter spectra acquisition.

Daughter, parent or constant neutral loss spectra for all four phosphate esters were obtained in a single chromatographic analysis by monitoring for trimethyl phosphate during the first 6 min and each of the remaining phosphate esters over subsequent 3-min intervals (triethyl phosphate followed by tripropyl phosphate and tributyl phosphate).

3. Results and discussion

3.1. General

Hybrid tandem mass spectrometers are typically operated in one of the following four modes during capillary column GC–MS–MS analysis:

Scan mode	Sector operation	Quadrupole operation
(a) Daughter scan	Transmit specified ion (parent ion)	Scan over a mass range
(b) Parent scan	Scan over a mass range	Transmit specified ion (daughter ion)
(c) Constant neutral loss	Scan over a mass range	Quadrupole scanning linked to the sector scanning such that at any point in time the quadrupole transmits lower mass ions equal to the neutral loss mass
(d) Reaction ion monitoring (RIM)	Transmit specified ion (parent ion)	Transmit specified ion (daughter ion)

The first three modes result in the acquisition of MS data over a given mass range and as such provide a high level of confirmation, particularly if the acquired mass spectra contain three or more ions. The fourth mode, RIM, like selected ion monitoring during capillary column GC–MS, results in the acquisition of single (or multiple) ion data. This results in an increase in sensitivity, generally at the expense of identification certainty.

Two modes, daughter and RIM, require transmission of ions of a selected mass through the sector of the hybrid instrument. By increasing the resolution of the sector it is possible to resolve a target ion from other ions of the same nominal mass. This advantage of the hybrid geometry, which generally leads to a reduction in chemical interferences, is not possible with triple quadrupole tandem mass spectrometers and may be advantageous for the analysis of target compound(s) in complex matrices.

Parent operation, a technique often used for the detection of compounds that fragment to form a specific daughter ion (*e.g.*, compounds with a certain functional group), generally does not have equivalent utility for target compound analyses in complex samples. The nominal (daughter) mass transmitted through the quadrupole could easily be formed from ions, other than those of interest, in a complex sample matrix. This would result in the acquisition of numerous parent spectra, making it difficult to resolve the target compound unless the daughter mass was unique to the compound and was not common to the matrix.

Constant neutral loss can be quite specific provided the neutral loss is unique to the target compound(s) and not to extraneous sample com-

ponents. However, both parent and constant neutral loss operation gain little from increased resolution as the sector is scanned as opposed to being locked on a particular mass (where the resolution of the sector determines the width of the mass window).

3.2. Phosphate ester applications

A concern of the United Nations Organization for the Prohibition of Chemical Weapons is the ability to retrospectively detect and positively identify the presence of organophosphorus chemical warfare agents and related compounds in samples collected in support of peacekeeping or peacemaking operations. Under these scenarios the likelihood of collecting extraneous compounds increases, particularly where diesel powered vehicles would be in use. Collected airborne samples would contain a large amount of hydrocarbon material similar to the diesel exhaust samples collected previously [6,7]. This complex matrix was therefore selected to evaluate the suitability of capillary column GC–MS–MS with a hybrid instrument for the detection and confirmation of phosphate esters.

Fig. 1 illustrates the capillary column GC–MS total-ion-current chromatogram obtained for the diesel exhaust extract spiked with 2.5 ng of each phosphate ester under full scanning EI conditions, the most commonly employed mode of operation for the analysis of environmental samples. The four phosphate esters were effectively masked by the presence of high levels of chemical interferences and EI ions characteristic of hydrocarbons were acquired at the retention times of the phosphate esters. Only tributyl phosphate, which elutes following the bulk of the

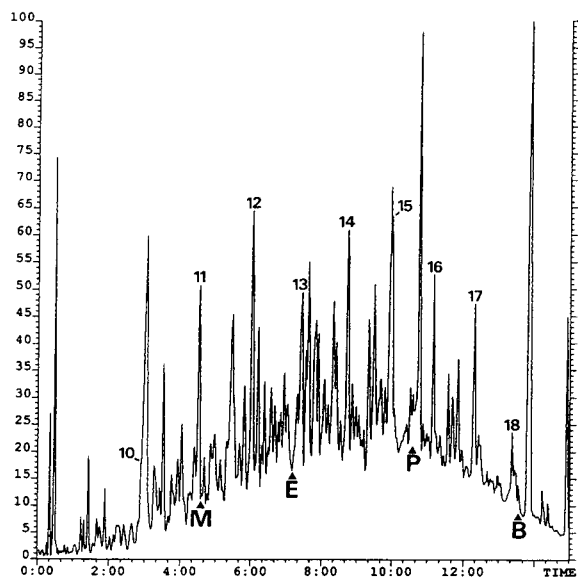


Fig. 1. Capillary column GC-MS (EI) total-ion-current (250 to 50 u) chromatogram obtained for the diesel exhaust extract spiked with 2.5 ng of trimethyl phosphate (M), triethyl phosphate (E), tripropyl phosphate (P) and tributyl phosphate (B). *n*-Alkane carbon numbers are indicated above the appropriate sample component and the retention time of phosphate esters are indicated by letter. Time in min.

hydrocarbon envelope, exhibited characteristic ions in approximately the same ratio as observed during standard analysis. However, background ions were equivalent to or greater than the signal of m/z 155 and m/z 211, which would suggest a sample detection limit of approximately 25 ng ($S/N = 10$). Sample detection limits for the other phosphate esters would be much higher.

As in conventional MS analyses, the monitoring of higher-mass ions during MS-MS analyses is preferred as chemical background decreases with mass. For this reason, the daughters of the molecular ion or highest-mass EI fragmentation ion (in the absence of molecular ion data) were evaluated for the detection and confirmation of phosphate esters spiked into the diesel exhaust extract at the 2.5-ng level (Fig. 2). Monitoring of the daughters of the molecular ions (even mass) of trimethyl phosphate and triethyl phosphate resulted in the detection of both compounds with minimal chemical interference. Considerably more chemical interference

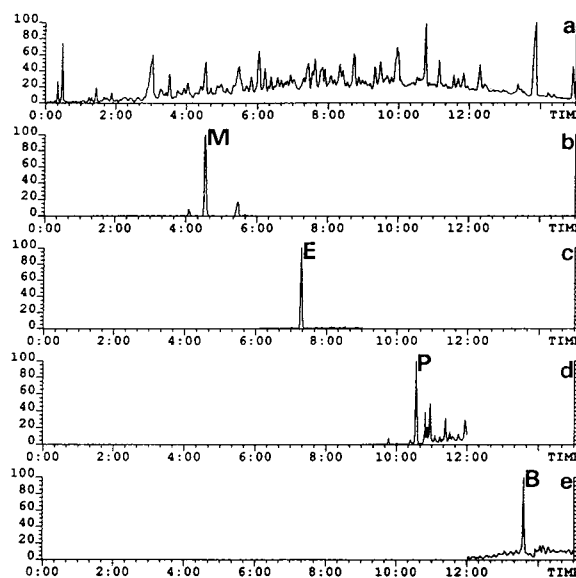


Fig. 2. (a) Capillary column GC-MS (EI) total-ion-current (250 to 50 u) chromatogram obtained for the diesel extract exhaust spiked at the 2.5-ng level with each phosphate ester. CAD chromatograms for daughters of (b) m/z 140 [$M^{+\bullet}$ for trimethyl phosphate (M)], (c) m/z 182 [$M^{+\bullet}$ for triethyl phosphate (E)], (d) m/z 183 [$[M - C_3H_5]^+$ for tripropyl phosphate (P)] and (e) m/z 211 [$[M - C_4H_7]^+$ for tributyl phosphate (B)] obtained with a sector resolution of 1000. Time in min.

was noted during the acquisition of daughter data for the higher-mass fragmentation ions (odd mass) of tripropyl phosphate and tributyl phosphate. The observed reduction in chemical interference during monitoring of even mass ions (generally odd electron species) and the reduction of chemical interferences with increased mass were consistent with generally accepted MS ion abundances. Fig. 3 illustrates the CAD spectra obtained for the daughters of m/z 140 ($M^{+\bullet}$ for trimethyl phosphate), m/z 182 ($M^{+\bullet}$ for triethyl phosphate), m/z 183 ($[M - C_3H_5]^+$ for tripropyl phosphate) and m/z 211 ($[M - C_4H_7]^+$ for tributyl phosphate) obtained with a sector resolution of 1000. The daughter spectra obtained were identical to those obtained with standards, even in the presence of numerous chemical interferences, and contained the minimum of three ions, considered essential for target compound confirmation.

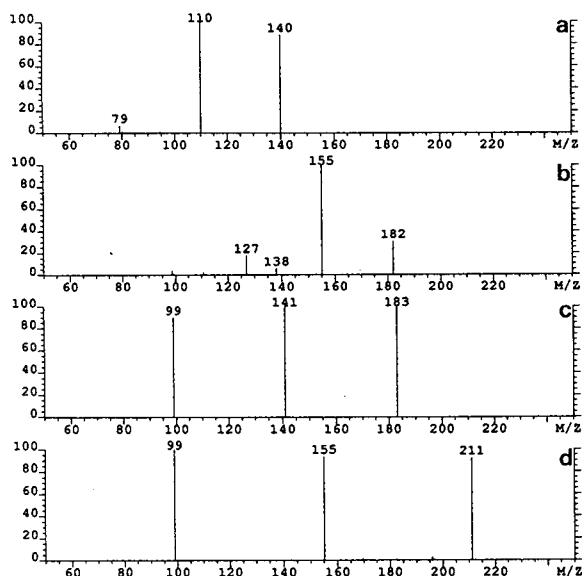


Fig. 3. Daughter spectra of (a) m/z 140 for trimethyl phosphate, (b) m/z 182 for triethyl phosphate, (c) m/z 183 for tripropyl phosphate and (d) m/z 211 for tributyl phosphate obtained during capillary column GC–MS–MS analysis of diesel exhaust extract spiked at the 2.5-ng level with each phosphate ester (see Fig. 2).

The highest level of chemical interferences were noted during acquisition of the daughters of m/z 183.08 ($[M - C_3H_5]^+$ for tripropyl phosphate). The bulk of the chemical interferences were likely due to hydrocarbon or amine (from amines on the charcoal bed material used for diesel exhaust sampling) ions with the following general formulae, $[C_xH_y]^+$ or $[C_xH_yN]^+$. By increasing the sector resolution to 2400 (10% valley definition), a significant reduction in chemical interference was observed for the daughters of m/z 183.08 (Fig. 4). Similar reductions in chemical interference were observed for the other three phosphate esters upon increasing the sector resolution to 2400, the practical upper limit for reliable automated operation. Above this resolution (e.g., 3400) manual operation was required to ensure transmission of the desired mass.

The sensitivity of daughter operation, based on 2.5-ng injections of phosphate ester standards, was found to approach typical EI full

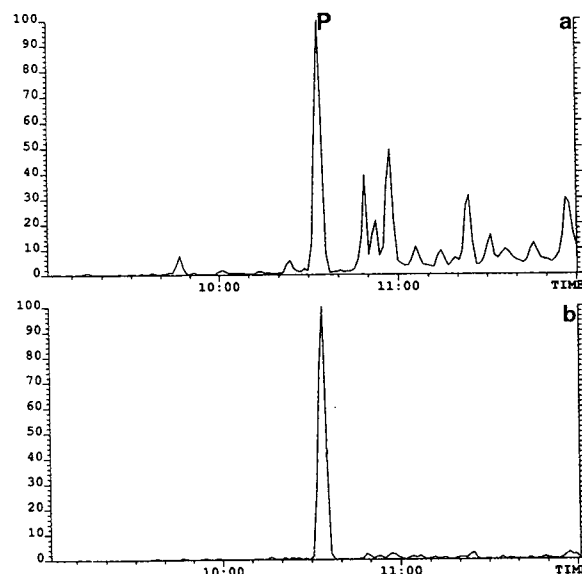


Fig. 4. CAD chromatograms for daughters of m/z 183.08 ($[M - C_3H_5]^+$ for tripropyl phosphate (P)) obtained with a sector resolution of (a) 1000 and (b) 2400. Time in min.

scanning detection limits (e.g., 100 to 500 pg). Lower levels of phosphate esters may be confirmed by multiple RIM (minimum of two transitions) in a mode analogous to selected ion monitoring (SIM). However, RIM sensitivity suffers over that routinely quoted for SIM due to quadrupole transmission of some neutrals formed in the CAD cell.

Multiple RIM was evaluated for the diesel exhaust extract spiked with 200 pg of tripropyl phosphate, as chemical interference was greatest for this phosphate ester (see Fig. 2). Fig. 5 illustrates the RIM chromatograms for the m/z 183 to m/z 141 transition (loss of C_3H_6) with a sector resolution of 1000 and 2400. Chemical interferences eluting after tripropyl phosphate were reduced with increased resolution and similar S/N ratios in excess of 100 were observed for tripropyl phosphate at both sector resolutions. During the same analysis the m/z 183 to m/z 99 transition, due to sequential losses of C_3H_6 , was also monitored to meet confirmation requirements (monitoring of a minimum of three ions). Increased resolution was of little benefit as

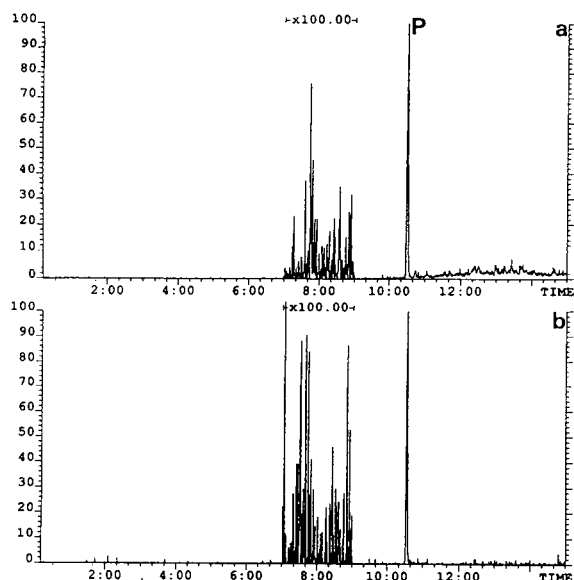


Fig. 5. Reaction ion monitoring chromatograms obtained for m/z 183 to m/z 141 transition during analysis of diesel exhaust extract spiked with 200 pg of tripropyl phosphate with a sector resolution of (a) 1000 and (b) 2500. Time in min.

this transition was not observed in the daughter spectra of typical extract sample components.

Constant neutral loss can be specific if the neutral loss monitored is not common to the chemical background. Neutral losses of CH_2O (for trimethyl phosphate) and C_xH_{2x} (where $x = 2, 3$ or 4 for the remaining phosphate esters) were selected for evaluation as they were commonly observed during characterization of these compounds. Fig. 6 illustrates the constant neutral loss spectra obtained during GC–MS–MS analysis of a 5-ng standard. The spectra obtained were consistent with the acquired daughter data, with the observed ions being those that would fragment in the CAD cell to give rise to a lower mass ion due to loss of a CH_2O or C_xH_{2x} .

The specificity of constant neutral loss for phosphate esters was evaluated by spiking the diesel exhaust extract at the 2.5-ng level. While the spiked components appeared to be resolved from chemical interferences, this was not the case. All the acquired constant neutral loss spectra were heavily influenced by coeluting

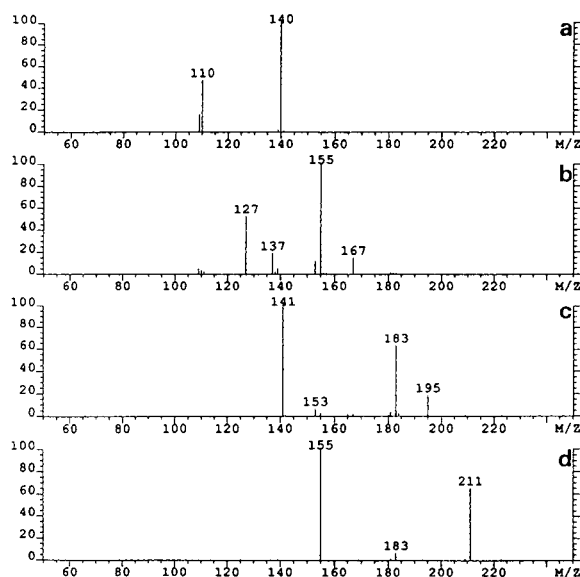


Fig. 6. Constant neutral loss spectra for (a) trimethyl phosphate (loss of 30 u), (b) triethyl phosphate (loss of 28 u), (c) tripropyl phosphate (loss of 42 u) and (d) tributyl phosphate (loss of 56 u) obtained during capillary column GC–MS–MS analysis of a standard containing 5 ng of each phosphate ester.

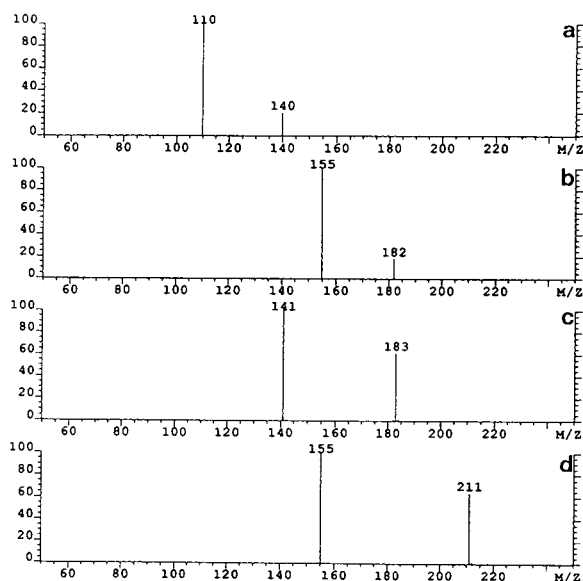


Fig. 7. Parent spectra of (a) m/z 110 for trimethyl phosphate, (b) m/z 155 for triethyl phosphate, (c) m/z 141 for tripropyl phosphate and (d) m/z 155 for tributyl phosphate obtained during capillary column GC–MS–MS analysis of a standard containing 4 ng of each phosphate ester.

hydrocarbon(s). The spectra closest to that obtained with a standard was that at the retention time of trimethyl phosphate. The loss of CH_2O would be less likely than C_xH_{2x} for a hydrocarbon matrix, but the possibility of constant neutral loss of C_2H_6 remains and likely contributed to the chemical background in the acquired spectra.

Parent spectra of higher-mass EI fragmentation ions at m/z 110 ($[\text{M} - \text{CH}_2\text{O}]^+$ for trimethyl phosphate), m/z 155 ($[\text{M} - \text{C}_2\text{H}_3]^+$ for triethyl phosphate), m/z 141 ($[(\text{PrO})\text{P}(\text{OH})_3]^+$ for tripropyl phosphate) and m/z 155 ($[(\text{BuO})\text{P}(\text{OH})_3]^+$ for tributyl phosphate) were obtained during GC–MS–MS analysis of a 4-ng standard (Fig. 7). However, the parent data obtained following spiking of the diesel exhaust extract with 5 ng of each phosphate ester were heavily influenced by coeluting interferences and were not interpretable.

4. Conclusions

Daughter, parent and constant neutral loss spectra, and multiple reaction ion monitoring data were all evaluated for the detection and confirmation of phosphate esters during capillary column GC–MS–MS with a hybrid tandem mass spectrometer. Constant neutral loss and parent modes involve scanning of the sector, thus negating the potential benefits of higher sector resolution. Both parent and constant neutral loss were evaluated as possible techniques for the detection and confirmation of phosphate esters in the presence of chemical interferences, similar to those expected during battlefield sampling. Neither technique was specific to the phosphate esters and resulted in the detection of considerable chemical hydrocarbon content.

Daughter and multiple reaction ion monitoring data may be acquired while operating with higher sector resolution. This benefit was demonstrated for the detection and confirmation of phosphate esters in the presence of hydrocarbon interferences at levels several orders of magnitude above that of the phosphate esters. De-

tection limits for daughter operation were approximately the same as those obtained during capillary column GC–MS analysis of standards under electron impact ionization, and S/N ratios in excess of 100 were observed during multiple reaction ion monitoring of the same diesel exhaust extracts spiked at the 200 pg level. Both of these modes of operation were highly specific for the detection and confirmation of these chemical warfare agent simulants in presence of numerous chemical interferences.

5. References

- [1] S.V. Hummel and R.A. Yost, *Org. Mass Spectrom.*, 21 (1986) 785–791.
- [2] J.A.G. Roach and L.J. Carson, *J. Assoc. Off. Anal. Chem.*, 70 (1987) 439–442.
- [3] T. Cairns and E.M. Siegmund, *J. Assoc. Off. Anal. Chem.*, 70 (1987) 858–862.
- [4] L.D. Betowski and T.L. Jones, *Environ. Sci. Technol.*, 22 (1988) 1430–1433.
- [5] A. Hesso and R. Kostianen, *Proceedings of the 2nd International Symposium on Protection Against Chemical Warfare Agents, Stockholm, June 15–19, 1986*, National Defence Research Institute, Umeå, 1986, pp. 257–260.
- [6] P.A. D'Agostino, L.R. Provost, J.F. Anacleto and P.W. Brooks, *J. Chromatogr.*, 504 (1990) 259–268.
- [7] P.A. D'Agostino, L.R. Provost and P.W. Brooks, *J. Chromatogr.*, 541 (1991) 121–130.
- [8] J.R. Holtzclaw, J.R. Wyatt and J.E. Campana, *Org. Mass Spectrom.*, 20 (1985) 90–97.
- [9] H.I. Kenttamaa and R.G. Cooks, *J. Am. Chem. Soc.*, 107 (1985) 1881–1886.
- [10] J.S. Brodbelt, H.I. Kenttamaa and R.G. Cooks, *Org. Mass Spectrom.*, 23 (1988) 6–9.
- [11] L.C. Zeller, J.T. Farrell, Jr., H.I. Kenttamaa and T. Kuivalainen, *J. Am. Soc. Mass Spectrom.*, 4 (1993) 125–134.
- [12] A.P. Snyder and C.S. Harden, *Org. Mass Spectrom.*, 25 (1990) 53–60.
- [13] A.P. Snyder and C.S. Harden, *Org. Mass Spectrom.*, 25 (1990) 301–308.
- [14] C.S. Harden, P.A. Snyder and G.A. Eiceman, *Org. Mass Spectrom.*, 28 (1993) 585–592.
- [15] P.A. D'Agostino and L.R. Provost, presented at the 41st ASMS Conference on Mass Spectrometry and Allied Topics, San Francisco, CA, May 30–June 4, 1993.
- [16] P.A. D'Agostino and L.R. Provost, *J. Chromatogr.*, 331 (1985) 47–54.



ELSEVIER

Journal of Chromatography A, 670 (1994) 135–144

JOURNAL OF
CHROMATOGRAPHY A

Determination of various pesticides using membrane extraction discs and gas chromatography–mass spectrometry[☆]

C. Crespo, R.M. Marcé*, F. Borrull

Department of Chemistry, Universitat Rovira i Virgili, Imperial Tarraco 1, 43005 Tarragona, Spain

(First received December 6th, 1993; revised manuscript received January 20th, 1994)

Abstract

A method for the determination of a group of pesticides in water by gas chromatography–mass spectrometry with electron impact ionization was developed. The preconcentration of 500 ml of water with C₁₈ and styrene–divinylbenzene (SDB) allowed the determination of pesticides at low- $\mu\text{g/l}$ levels. The use of SDB membrane extraction discs gave a large increase in the recovery of aldrin compared with the value obtained with C₁₈ discs. With SDB discs the recoveries were >85% for most compounds. The limits of detection were between 0.06 and 0.2 $\mu\text{g/l}$ in the full-scan mode. The mass spectra under positive and negative chemical ionization conditions with methane were also obtained and higher sensitivity with negative chemical ionization was obtained for most compounds.

1. Introduction

The identification and determination of pesticides in different water matrices is an analytical problem of increasing importance. Different techniques have been applied to the determination of pesticides, mainly employing GC [1–6] and HPLC [6–8] with a variety of detectors. In practice, capillary GC with electron-capture and nitrogen–phosphorus detection is the preferred separation technique for the determination of most pesticides, but HPLC is widely used for most polar compounds.

The advantage of the high sensitivity of these detectors contrasts with the lack of identification power of these techniques. The combination of

GC with mass spectrometry (GC–MS) is the most specific method for the analysis of complex matrices and it has been widely applied to the determination of pesticides [6,9–14]. In addition to the electron impact (EI) mode, which is the most routine confirmatory method, the use of GC–MS with positive-ion (PCI) and/or negative-ion chemical ionization (NCI) increases the already high identification power of mass spectrometry [5,11,15], in addition to an increase in sensitivity in some instances [10,13].

On the other hand, GC–MS shows low sensitivity even with selected-ion monitoring (SIM) and, in addition to the low levels of these compounds allowed in drinking water, the use of a preconcentration system is always required.

Various preconcentration methods based on different physico-chemical principles are commonly used, such as liquid–liquid extraction (LLE) and solid-phase extraction (SPE). Al-

* Corresponding author.

[☆] Presented at the 22nd Annual Meeting of the Spanish Chromatography Group, Barcelona, October 20–22, 1993.

though most official methods for the determination of pesticides in water still use LLE, SPE is becoming more popular because it has some advantages over LLE [16,17]. SPE has already been used in some standard methods of the US Environmental Protection Agency (EPA) [18]. The most often used SPE approach utilizes short columns or cartridges containing sorbent particles [2,14], but the use of membrane extraction discs, originally described by Hagen *et al.* [19], is increasing because of the advantages of a higher sampling flow-rate and the elimination of some impurities such as plasticizers and oligomers extracted from the polymeric column and frit components [20,21]. PTFE filter discs containing octadecyl or octyl groups chemically bonded to silica are the most commonly used discs [19,22], but higher breakthrough volumes for some more polar compounds when styrene-divinylbenzene copolymer is used were demonstrated with cartridges [17,23].

In addition to the off-line methods of SPE, on-line systems have also been developed for LC [24,25] and also for GC [26–28]. In on-line LC–GC, precolumns containing the sorbent [27] are the most often used, but membrane extraction discs have also been applied [29]. Owing to the simplicity of the instrument required when off-line methods are used, these are actually preferred.

In this paper, the determination of a group of organochlorine, organophosphorus and chlorotriazine pesticides by GC–MS and off-line SPE with C_{18} and styrene-divinylbenzene discs is presented. In addition to EI mass spectra, CI mass spectra were also obtained to confirm the presence of these pesticides in real water samples.

2. Experimental

2.1. Chemicals

Standards of pesticides were obtained from Riedel-de-Häen (Seelze-Hannover, Germany). Stock standard solutions of each pesticide of

2000 $\mu\text{g/ml}$ were prepared by weighing and dissolving them in ethyl acetate and stored at 4°C in amber screw-capped vials with solid PTFE-lined cap. Working standard solutions were prepared by dilution and mixing of these solutions with ethyl acetate and stored in the same way as the stock standard solutions. The internal standard 1-chlorooctadecane was supplied by Aldrich (Steinheim, Germany).

Ethyl acetate was of Pesticide quality (Riedel-de-Häen) and methanol of HPLC quality (Scharlau, Germany). Water was prepared by purifying demineralized water in a Milli-Q filtration system (Millipore, Bedford, MA, USA).

Helium carrier gas and the reagent gas methane (both of 99.99% quality) were supplied by Carburos Metalicos (Tarragona, Spain).

2.2. Gas chromatography–mass spectrometry

A Hewlett-Packard (Palo Alto, CA, USA) model 5989 A MS Engine equipped with a dual EI–CI source in conjunction with an HP 5890 (Series GCII) and an HP-UX 59944C data system was used. The analytical column was an HP-1 (cross-linked methyl silicone gum, 0.33 μm film thickness) 12 m \times 0.2 mm I.D. fused-silica capillary column, which was inserted directly into the ion source.

The initial column temperature was 75°C, maintained for 1 min and then programmed at 20°C/min to 200°C, then at 2.5°C/min to 210°C and at 3°C/min to 225°C, and maintained at 225°C for 3 min. The total run time between injections was 19.25 min. The injector temperature was set at 250°C. A 1- μl volume of sample was injected in the splitless mode. The temperature of the transfer line was 250°C and the ion source and quadrupole temperatures were 200 and 100°C, respectively.

Helium was used as the carrier gas and methane as the reagent gas in the PCI and NCI modes at 1.8 and 1.7 Torr, respectively (1 Torr = 133.322 Pa). EI mass spectra were obtained at 70 eV. The mass range that was scanned was m/z 60–500.

The MS Engine was tuned to m/z 69, 219 and

502 for EI, m/z 219, 414 and 652 for PCI and m/z 264, 414 and 633 for NCI, corresponding to perfluorobutylamine (PFTBA).

The area of the base peak ion for each compound was used in the quantification procedure using the base peak of the internal standard, 1-chlorooctadecane.

2.3. Sample preparation

A standard Millipore 47-mm filtration apparatus was used. The membrane extraction discs were Empore discs manufactured by 3M (St. Paul, MN, USA), obtained from J.T. Baker (Deventer, Netherlands). The discs were 47 mm in diameter and 0.5 mm thick and each disc contained about 500 mg of C_{18} -bonded silica or styrene–divinylbenzene copolymer (SDB).

Prior to the extraction procedure, the discs were conditioned with about 20 ml of ethyl acetate as this was the final eluting solvent. After ethyl acetate had been left undisturbed on the disc for 1 min, vacuum was applied to draw ethyl acetate through the disc. A 20-ml volume of methanol was added and eluted under vacuum, 20 ml of Milli-Q-purified water were added and vacuum was applied, avoiding allowing the disc to dry completely.

The sample with 1% of NaCl added was passed through the disc under an adjusted vacuum at a speed about 10 ml/min. The disc was not allowed to dry completely during the extraction. After the sample had been processed, air was drawn through the disc for about 5 min to remove residual water.

After this operation, the pesticides trapped in the disc were collected using 2×15 ml of ethyl acetate. Ethyl acetate was left undisturbed on the disc for 1 min, then vacuum was applied to draw the ethyl acetate through. The ethyl acetate was transferred to a concentration tube marked at 100 μ l and, after the addition of the internal standard, the ethyl acetate solution was evaporated under vacuum to 100 μ l. A 1- μ l volume was injected into the GC–MS system.

River water samples were filtered through a 0.45- μ m PTFE filter prior to extraction.

3. Results and discussion

Fig. 1 shows the chromatogram of 22 pesticides and the internal standard 1-chlorooctadecane obtained under full-scan conditions and EI ionization. In Table 1 the retention time, the main ions and the relative abundance of each compound are included. Although 4,4'-DDE and dieldrin eluted almost at the same time, they could be quantified using selected ions, m/z 246 for 4,4'-DDE and m/z 79 for dieldrin.

The full-scan mode was used for the acquisition of the chromatogram as this allows the identification of the compounds, although better sensitivity under selected-ion monitoring (SIM) conditions was obtained.

The linearity of the response was checked at levels ranging from 2 to 100 μ g/ml and good linearity was obtained with correlations coefficients (r^2) from 0.990 to 0.9998 for all the compounds studied. The repeatability of the response for four injections was between 4.2 and 7.2% and the limit of detection (signal-to-noise ratio = 3) was between 0.3 and 0.8 μ g/ml.

For the chromatograms obtained with positive and negative chemical ionization, the main ions of each compound are given in Table 2. For triazines, under PCI conditions the base peaks corresponded to $[M - Cl]^+$ and two other important peaks corresponded to $[M + H]^+$ and $[M + C_2H_5]^+$. Some papers [11,13] have reported $[M + H]^+$ as a base peak whereas other workers [5] obtained $[M - Cl]^+$ as the base peak. In the NCI mode, the two triazines showed $[M - H]^-$ as the base peak according to some workers [11], instead of the low relative abundance (13%) obtained by others [13]. The sensitivity was better in the EI mode, which is in agreement with other workers [5,11,13].

In the PCI mode, all organophosphorus compounds exhibited a peak corresponding to $[M + 1]^+$ as one of the most abundant and in the NCI mode the major peaks corresponded to $[M]^-$ or $[M - 1]^-$. The sensitivity in the PCI mode was similar to that obtained under EI conditions but NCI increased the sensitivity.

The molecular peak, $[M + 1]^+$ or $[M - 1]^-$, of the organochlorine pesticides could be obtained

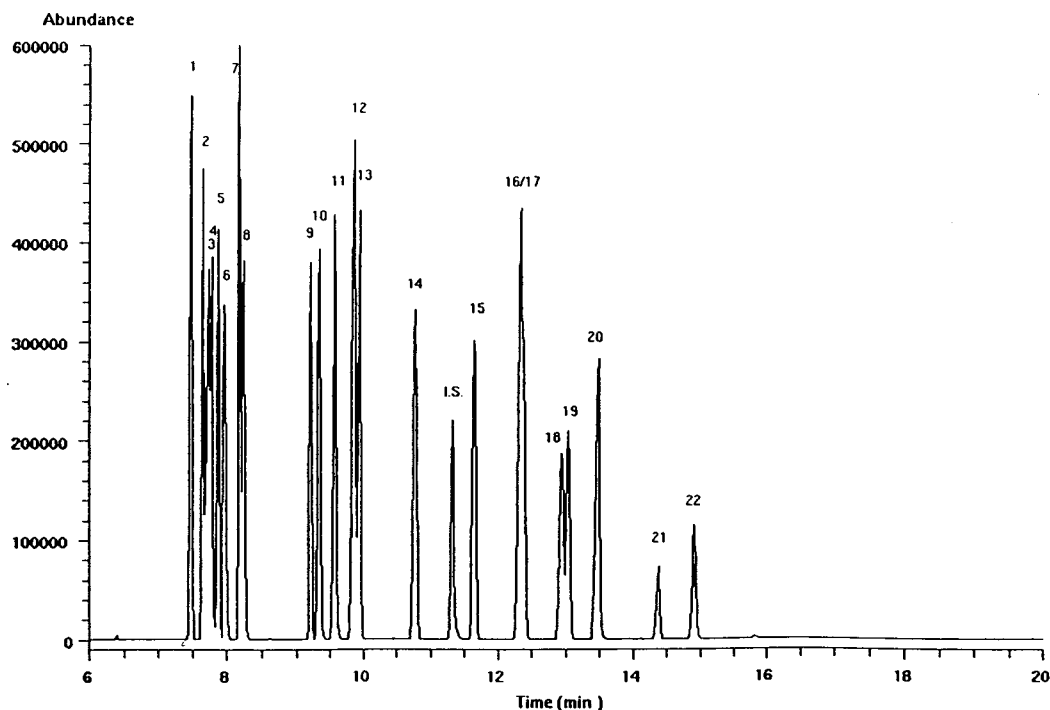


Fig. 1. Total ion chromatogram of the 22 pesticides and the internal standard. An amount of 100 ng of each pesticide was injected. Peaks: 1 = α -HCH; 2 = β -HCH; 3 = simazine; 4 = atrazine; 5 = lindane; 6 = δ -HCH; 7 = diazinon; 8 = disulfoton; 9 = heptachlor; 10 = fenitrothion; 11 = malathion; 12 = parathion; 13 = aldrin; 14 = epoxyheptachlor; 15 = α -endosulfan; 16 = 4,4'-DDE; 17 = dieldrin; 18 = endrin; 19 = β -endosulfan; 20 = 4,4'-DDD; 21 = endosulfan sulphate; 22 = 4,4'-DDT; I.S. = internal standard, 1-chlorooctadecane. For GC conditions, see text.

for most compounds under PCI or NCI conditions, but much higher sensitivity was obtained in the latter mode. The increase in sensitivity was in some instances three orders of magnitude, *e.g.*, the limit of detection of both endosulfan and endosulfan sulphate was about 1 pg.

From these results, it can be deduced that NCI allowed the confirmation of most of the compounds studied and higher m/z values were obtained compared with EI which implied an increase in selectivity. For some compounds an increase in sensitivity was also observed.

Owing to the low sensitivity of GC-MS, an extraction process is necessary in order to determine the pesticides at low ng/ml levels, taking into account that the standard level of tolerance in the European Community of these pollutants in drinking water is 0.1 ng/ml.

The extraction process was carried out using membrane extraction discs, and two different

sorbents, the commonly C_{18} and the newer SDB, were compared. The blank of these membrane extraction discs was initially checked and some peaks of low abundance were found, but only one eluted at the same time as one of the pesticides and was found with both types of discs, and was a phthalate co-eluting with malathion. However, this was not a drawback as the pesticide could be determined by its major ion, which was not present in the mass spectrum of the phthalate.

When an SPE method is developed, two important features are the capacity of the cartridges, column or disc and the maximum volume of the sample that can be preconcentrated without elution of the compound, known as the breakthrough volume. Before the study of these two steps, the addition of NaCl, recommended by some workers [30,31], was initially tested, and an improvement in the recovery of some com-

Table 1

Retention times (t_R) recorded under the experimental conditions, major ions and relative abundances in EI mass spectra of the pesticides studied

Pesticide	t_R (min)	Class ^a	Main ions, m/z (relative abundance, %)		
α -HCH	7.483	OC	219 (100)	181 (95)	183 (92)
β -HCH	7.654	OC	219 (100)	181 (98)	183 (92)
Simazine	7.739	TR	201 (100)	173 (70)	68 (65)
Atrazine	7.783	TR	200 (100)	215 (55)	173 (40)
Lindane	7.876	OC	181 (100)	183 (97)	219 (85)
δ -HCH	7.972	OC	183 (100)	109 (90)	219 (90)
Diazinon	8.188	OP	179 (100)	137 (70)	304 (60)
Disulfoton	8.245	OP	88 (100)	97 (35)	61 (20)
Heptachlor	9.220	OC	100 (100)	272 (55)	274 (42)
Fenitrothion	9.353	OP	125 (100)	109 (98)	277 (50)
Malathion	9.579	OP	127 (100)	173 (90)	125 (65)
Parathion	9.876	OP	109 (100)	97 (95)	137 (55)
Aldrin	9.954	OC	66 (100)	101 (42)	263 (40)
Epoxyheptachlor	10.786	OC	183 (100)	81 (85)	135 (80)
α -Endosulfan	11.659	OC	195 (100)	159 (80)	197 (75)
4,4'-DDE	12.350	OC	246 (100)	318 (80)	248 (60)
Dieldrin	12.350	OC	79 (100)	108 (25)	263 (12)
Endrin	12.943	OC	81 (100)	65 (75)	263 (40)
β -Endosulfan	13.045	OC	63 (100)	195 (90)	160 (80)
4,4'-DDD	13.489	OC	235 (100)	165 (60)	199 (20)
Endosulfan sulphate	14.374	OC	272 (100)	229 (80)	273 (75)
4,4'-DDT	14.912	OC	235 (100)	165 (60)	199 (20)

^a OC = Organochlorines, OP = organophosphorus, TR = triazines.

Table 2

Molecular masses (M_r), major ions and relative abundances obtained under PCI and NCI conditions

Pesticide	M_r	Ions, m/z (relative abundance, %)				
		PCI		NCI		
α -HCH	288	219 (100)	217 (80)	221 (50)	71 (100)	255 (50)
β -HCH	288	219 (100)	166 (75)	221 (50)	71 (100)	325 (60)
Simazine	201	166 (100)	202 (87)	230 (25)	200 (100)	165 (20)
Atrazine	215	180 (100)	216 (80)	244 (20)	214 (100)	179 (30)
Lindane	288	219 (100)	217 (80)	221 (50)	71 (100)	255 (50)
δ -HCH	288	219 (100)	217 (80)	221 (50)	71 (100)	255 (50)
Diazinon	304	305 (100)	333 (21)	346 (5)	169 (100)	303 (10)
Heptachlor	370	337 (100)	339 (90)	335 (70)	300 (100)	266 (98)
Fenitrothion	277	248 (100)	278 (80)		277 (100)	168 (86)
Malathion	330	285 (100)	331 (50)	359 (27)	157 (100)	330 (20)
Parathion	291	292 (100)	262 (99)	332 (10)	291 (100)	154 (50)
Aldrin	362	329 (100)	263 (70)	293 (62)	—	—
Epoxyheptachlor	386	81 (100)	325 (37)		280 (100)	237 (98)
α -Endosulfan	404	71 (100)	277 (80)	407 (85)	406 (100)	404 (90)
4,4'-DDE	316	319 (100)	317 (75)	283 (65)	316 (100)	236 (40)
Dieldrin	380	279 (100)	345 (99)		237 (100)	380 (20)
Endrin	380	281 (100)	279 (93)	345 (92)	308 (100)	380 (50)
β -Endosulfan	404	277 (100)	325 (50)	405 (48)	406 (100)	404 (62)
4,4'-DDD	318	209 (100)	283 (44)	319 (24)	272 (100)	308 (50)
Endosulfan sulphate	423	325 (100)	423 (75)		386 (100)	97 (55)
4,4'-DDT	352	243 (100)	319 (40)	353 (15)	71 (100)	281 (40)

pounds was observed. Different amounts of NaCl were added and when more than 4 g were added, some NaCl appeared in the concentrated sample, which implied a decrease in repeatability.

In order to determine the capacity of the discs, different concentrations between 1 and 10 ng/ml of the pesticides were studied by preconcentrating a volume of 200 ml of Milli-Q-purified water. No significant differences in the recoveries were obtained, so it could be deduced that the capacity of the discs was high enough at the concentration levels studied, as had already been demonstrated by other workers [3,19].

The recoveries of each compound with different volumes of samples were also studied and recoveries of each compound were determined for a concentration of 5 ng/ml. In Table 3 the

Table 3

Mean recoveries and relative standard deviations ($n = 3$) of pesticides in reagent water using a C_{18} membrane extraction disc

Pesticide	Volume (ml)			
	500		1000	
	Recovery (%)	R.D.S. (%)	Recovery (%)	R.D.S. (%)
α -HCH	98	5.3	78	7.8
β -HCH	97	4.5	100	5.7
Simazine	80	4.3	65	6.4
Atrazine	95	3.4	92	2.8
Lindane	90	6.5	80	4.5
δ -HCH	94	6.2	95	5.3
Diazinon	84	5.6	76	5.8
Heptachlor	94	6.2	59	8.2
Fenitrothion	102	4.5	81	6.5
Malathion	89	6.3	96	5.7
Parathion	85	5.8	78	5.3
Aldrin	52	8.9	40	9.3
Epoxyheptachlor	75	7.5	70	7.2
α -Endosulfan	85	5.3	72	6.4
4,4'-DDE	80	8.3	60	7.8
Dieldrin	85	4.3	80	5.6
Endrin	89	5.8	80	8.3
β -Endosulfan	70	6.8	60	9.8
4,4'-DDD	60	9.7	51	9.2
Endosulfan sulphate	72	8.5	60	9.3
4,4'-DDT	70	5.9	62	8.0

Spiking level: 5 ng/ml.

recoveries and relative standard deviations obtained for the C_{18} disc are shown; recoveries $>85\%$ were obtained for most compounds when 500 ml of the sample were preconcentrated. Higher volumes were also tested but good recoveries were obtained only for some compounds. The organophosphorus compound disulfoton was not recovered and further attempts to increase the recovery were not successful. A low recovery of aldrin was also observed even at 500 ml, as reported previously [3,19].

The results of recovery as a function of sample volume for the SDB disc are given in Table 4. The recovery of disulfoton was not improved but a substantial increase in the recovery of aldrin was observed compared with the results obtained with the C_{18} disc. Triazines showed high recoveries even at a volume of 1000 ml. It has

Table 4

Mean recoveries and relative standard deviations ($n = 3$) of pesticides in reagent water using an SDB membrane extraction discs

Pesticide	Volume (ml)			
	500		1000	
	Recovery (%)	R.D.S. (%)	Recovery (%)	R.D.S. (%)
α -HCH	96	4.3	90	5.3
β -HCH	110	5.8	92	6.8
Simazine	105	6.2	87	9.8
Atrazine	91	5.6	101	6.3
Lindane	85	4.5	87	5.8
δ -HCH	105	6.3	95	7.3
Diazinon	86	6.2	54	8.9
Heptachlor	97	5.9	49	9.2
Fenitrothion	84	7.3	18	12.3
Malathion	85	6.8	20	13.3
Parathion	87	6.3	47	10.2
Aldrin	95	5.4	99	7.2
Epoxyheptachlor	79	5.3	66	6.3
α -Endosulfan	82	6.3	58	9.2
4,4'-DDE	66	8.3	43	7.5
Dieldrin	92	4.5	97	6.8
Endrin	85	6.3	88	4.2
β -Endosulfan	108	3.2	78	7.3
4,4'-DDD	75	5.0	63	10.2
Endosulfan sulphate	89	6.0	58	6.2
4,4'-DDT	72	6.8	62	12.3

Spiking level: 5 ng/ml.

already been reported [23] that the breakthrough volume for triazines is much higher with SDB than C_{18} . A considerable decrease in the recovery of organophosphorus compounds was observed when 1000 ml of sample were pre-concentrated.

From these results it can be deduced that for the determination of the pesticides a volume of 500 ml gave a good recovery of most compounds. When some specific pesticides must be determined, *e.g.*, triazines, volumes of 1000 ml or even higher can be pre-concentrated. When only confirmation of the peaks is required, volumes of 1 l or higher can be pre-concentrated.

The application of the method to real samples was tested with different samples of Ebre river water. Special attention was given to samples from the location where water is used as a water supply for many cities and after treatment used as tap water. This location is before the Ebre

delta, which is an important agricultural zone and where the presence of some pesticides has been found [6].

The chromatogram obtained for 500 ml of Ebre river water pre-concentrated using a C_{18} membrane extraction disc is depicted in Fig. 2. No pesticides studied were found in the sample and some of the peaks could be assigned to different phthalates.

The same sample was pre-concentrated using an SDB disc and the chromatogram obtained is shown in Fig. 3. Although some of the peaks are the same as those obtained when the C_{18} disc was used, different selectivities of the discs was observed and no pesticides could be found.

In order to study the recovery of the method for real samples, the same sample was spiked with different amounts of a standard solution and the recoveries and repeatability ($n = 3$) obtained for a concentration of 5 ng/ml are given

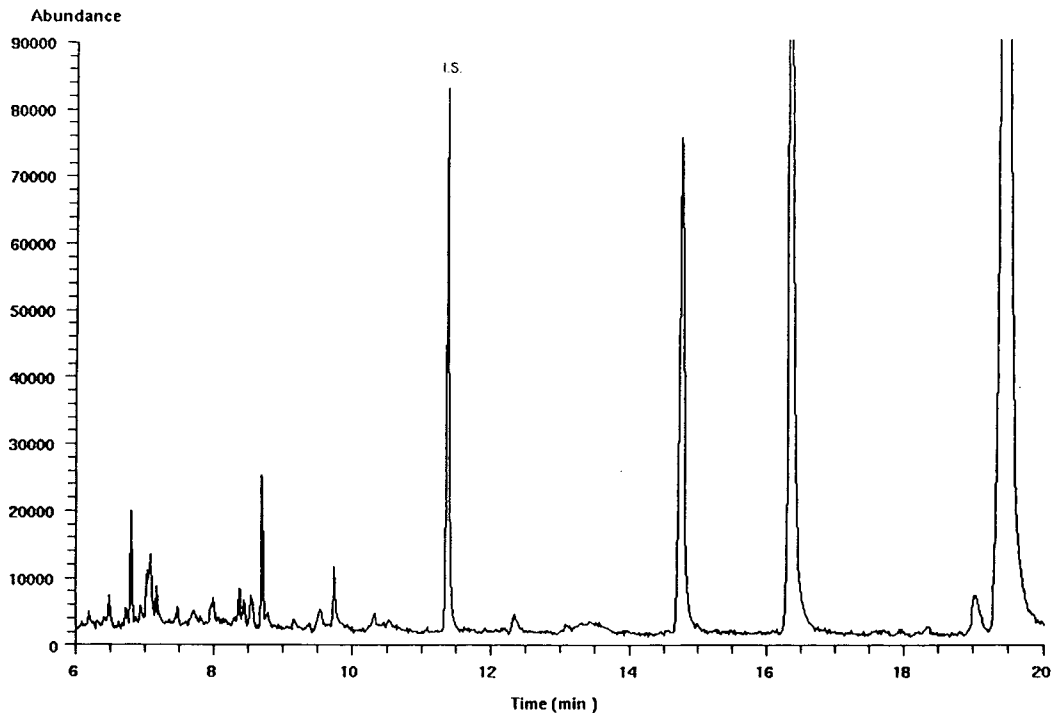


Fig. 2. Total ion chromatogram of a sample of 500 ml of Ebre river water after extraction with a C_{18} disc. For conditions, see text.

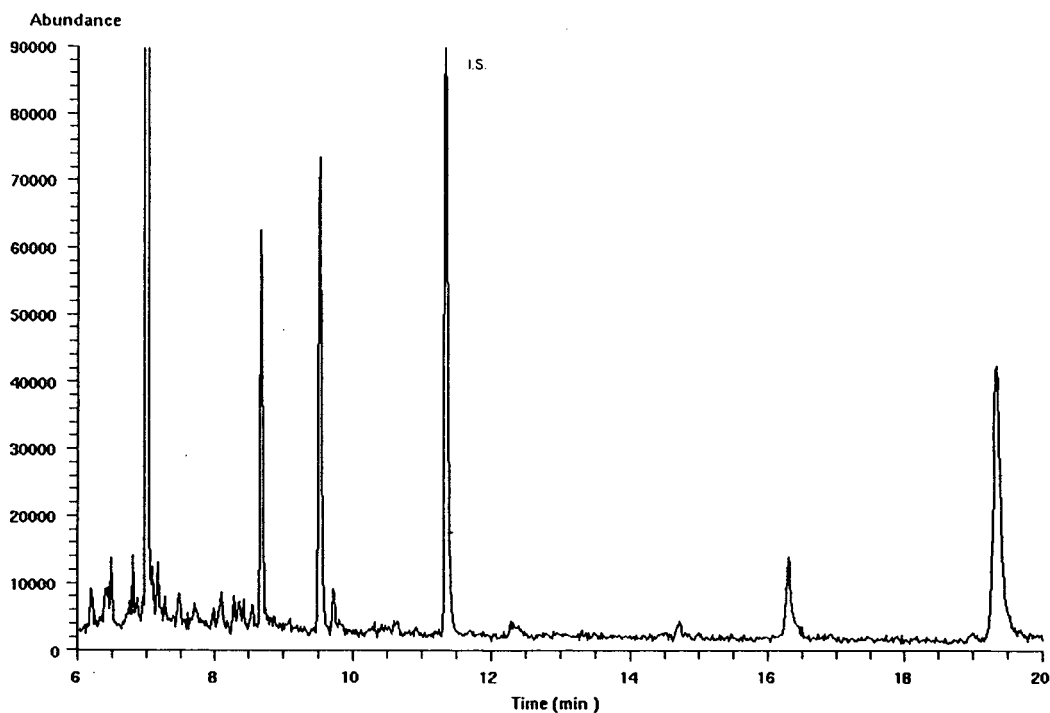


Fig. 3. Total ion chromatogram of a sample of 500 ml of Ebre river water extraction with an SDB disc. For conditions, see text.

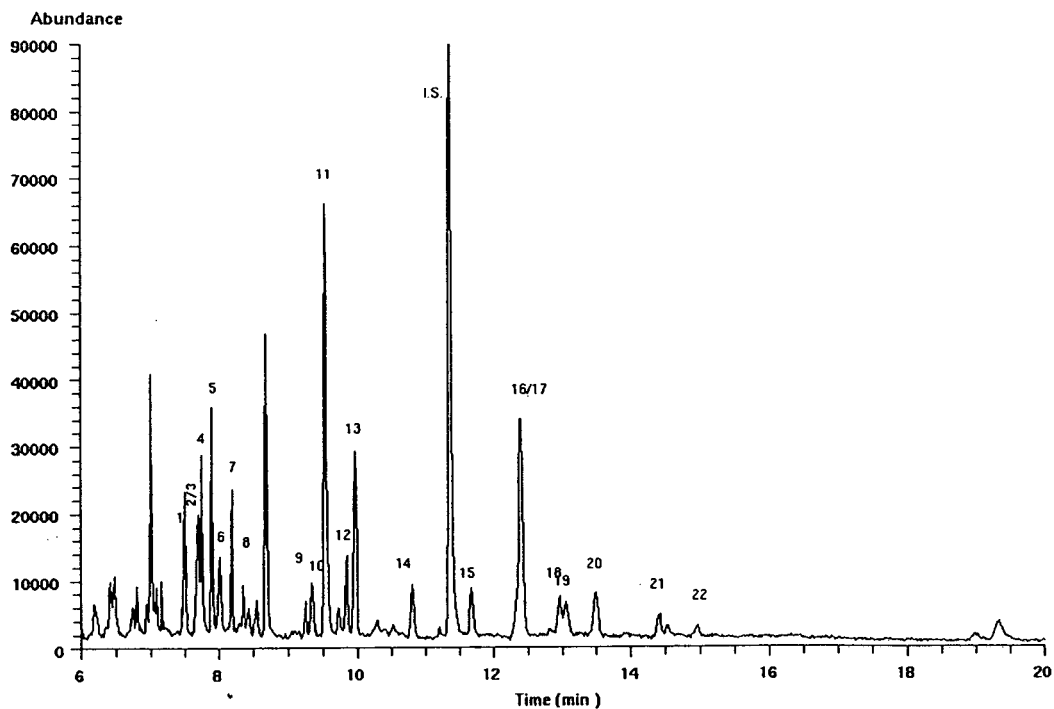


Fig. 4. Total ion chromatogram of a sample of 500 ml of Ebre river water spiked with each pesticide at a concentration of 0.8 ng/ml. For conditions, see text. Peak numbers as in Fig. 1.

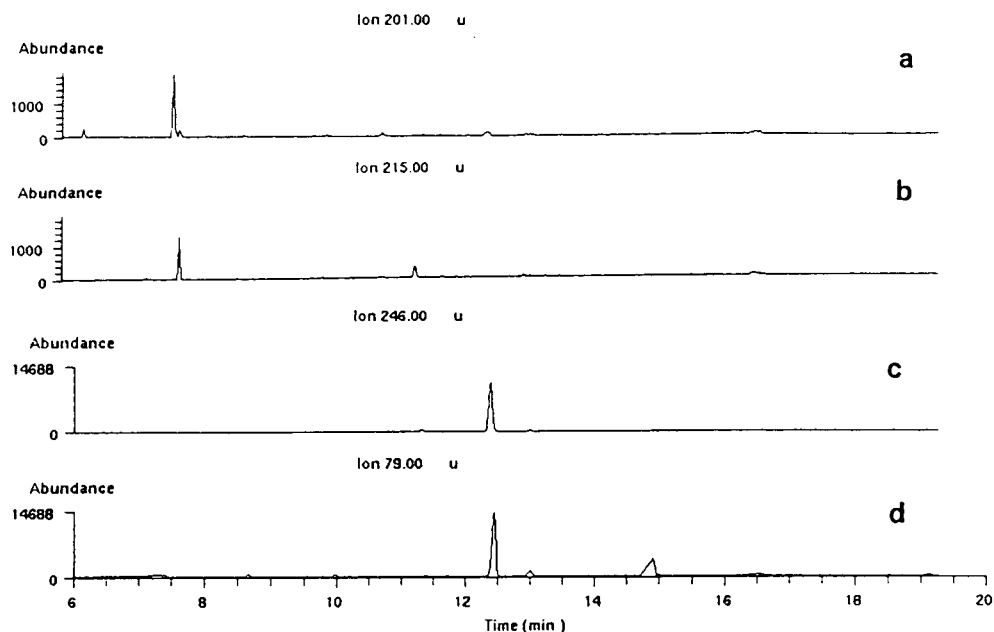


Fig. 5. Ion chromatogram obtained using EI ionization of different pesticides after preconcentration in an SDB membrane extraction disc of 500 ml of river water spiked at 0.2 ng/ml. Pesticide: (a) simazine; (b) atrazine; (c) 4,4'-DDE; (d) dieldrin.

Table 5

Mean recoveries and relative standard deviations ($n = 3$) of pesticides at 5 ng/ml in 500 ml of Ebre river water using C_{18} and SDB membrane extraction discs

Pesticide	C_{18}		SDB	
	Recovery (%)	R.D.S. (%)	Recovery (%)	R.D.S. (%)
α -HCH	94	5.3	93	5.8
β -HCH	98	4.6	97	6.2
Simazine	82	6.5	98	5.8
Atrazine	89	3.6	96	4.7
Lindane	96	5.6	87	4.3
δ -HCH	90	4.8	93	6.4
Diazinon	86	5.2	85	6.7
Heptachlor	89	4.9	95	5.2
Fenitrothion	98	6.3	86	4.3
Malathion	92	5.8	88	7.2
Parathion	91	6.3	85	5.0
Aldrin	54	8.4	93	4.3
Epoxyheptachlor	80	5.3	82	4.6
α -Endosulfan	86	6.5	78	9.2
4,4'-DDE	72	7.3	73	7.5
Dieldrin	91	5.4	93	4.8
Endrin	86	6.3	92	7.2
β -Endosulfan	73	7.3	96	5.3
4,4'-DDD	78	8.0	73	7.8
Endosulfan sulphate	79	6.2	92	6.2
4,4'-DDT	66	7.8	73	6.8

in Table 5. It can be seen that the results are very similar to those obtained with Milli-Q-purified water.

The total ion chromatogram of the same Ebre river sample spiked with each pesticide at a concentration of about 0.8 ng/ml is shown in Fig. 4.

The limit of detection of the method in the full-scan mode with quantification from the ion chromatogram for real samples, determined for a signal-to-noise ratio of 3, was between 0.06 and 0.2 ng/ml when a volume of 500 ml was pre-concentrated. In Fig. 5, the ion chromatogram of different compounds in a river water spiked at 0.2 ng/ml is depicted.

4. Conclusions

The use of membrane extraction discs and GC-MS with EI ionization allowed the determination of a group of pesticides at levels of 0.06–0.2 $\mu\text{g/l}$ in the full-scan mode. SDB extraction discs gave better recoveries than C_{18} extraction discs for some compounds. A volume of sample of 500 ml gave good recoveries for most pesticides with the SDB disc. Mass spectra were

obtained with PCI and NCI with methane and higher sensitivity was achieved in general for organophosphorus and organochlorine compounds in the NCI mode and limits of detection as low as 1 pg were reached for some compounds.

5. References

- [1] J. Hajslova, L. Ryparova, I. Viden and J. Davidek, *Int. J. Environ. Anal. Chem.*, 38 (1990) 105.
- [2] G.H. Tan, *Analyst*, 117 (1992) 1129.
- [3] B.A. Tomkins, R. Merriweather, R.A. Jenkins and C.K. Bayne, *J. Assoc. Off. Anal. Chem. Int.*, 75 (1992) 1091.
- [4] P.J.M. Kwakman, J.J. Vreuls, U.A.Th. Brinkman and R.T. Ghijsen, *Chromatographia*, 34 (1992) 41.
- [5] G. Durand and D. Barceló, *Anal. Chim. Acta*, 243 (1991) 259.
- [6] G. Durand, V. Bouvot and D. Barceló, *J. Chromatogr.*, 607 (1992) 319.
- [7] I. Liska, E.R. Brouwer, A.G.L. Ostheimer, H. Lingeman, U.A. Th. Brinkman, R.B. Geerdink and W.H. Mulder, *Int. J. Environ. Anal. Chem.*, 47 (1992) 267.
- [8] V. Coquart and M.C. Hennion, *J. Chromatogr.*, 600 (1992) 195.
- [9] H.-J. Stan, *J. Chromatogr.*, 467 (1989) 85.
- [10] D. Barceló, *Anal. Chim. Acta*, 263 (1992) 1.
- [11] H. Bagheri, J.J. Vreuls, R.T. Ghijsen and U.A. Th. Brinkman, *Chromatographia*, 34 (1992) 5.
- [12] M.T. Meyer, M.S. Mills and E.M. Thurman, *J. Chromatogr.*, 629 (1993) 55.
- [13] H.-J. Stan and A. Bockhorn, *Fresenius' J. Anal. Chem.*, 339 (1991) 158.
- [14] E. Benefati, P. Tremolada, L. Chiappetta, R. Frasanito, G. Bassi, N. Di Toro, R. Fanelli and G. Stella, *Chemosphere*, 21 (1990) 1411.
- [15] D. Barceló, *Trends Anal. Chem.*, 10 (1991) 323.
- [16] W.E. Johnson, N.J. Fendinger and J.R. Plimmer, *Anal. Chem.*, 63 (1991) 1510.
- [17] I. Liska, J. Krupcik and P.A. Leclercq, *J. High Resolut. Chromatogr.*, 12 (1989) 577.
- [18] J.W. Eichelberger, T.D. Behymer and W.L. Budde, *EPA Method 525*, Environmental Monitoring Systems Laboratory, U.S. Environmental Protection Agency, Cincinnati, OH, 1988.
- [19] D.F. Hagen, C.G. Markell, G.A. Schmitt and D.D. Blevins, *Anal. Chim. Acta*, 236 (1990) 157.
- [20] G.A. Junk, M.J. Avery and J.J. Richard, *Anal. Chem.*, 60 (1988) 1347.
- [21] T. McDonnell, J. Rosenfeld and A. Rais-Firouz, *J. Chromatogr.*, 629 (1993) 41.
- [22] J.C. Moltó, Y. Picó, G. Font and J. Mañes, *J. Chromatogr.*, 555 (1991) 137.
- [23] M.C. Hennion, P. Subra, R. Rosset, M. Grimaud and M. Callibotte, *J. Water SRT-Aqua*, 40 (1991) 35.
- [24] E.R. Brouwer, H. Lingeman and U.A.Th. Brinkman, *Chromatographia*, 25 (1990) 415.
- [25] H. Bagheri, J. Slobodnik, R.M. Marcé, R.T. Ghijsen and U.A.Th. Brinkman, *Chromatographia*, 37 (1993) 159.
- [26] K. Grob, in W. Bertsch, W.G. Jennings and P. Sandra (Editors), *On-Line Coupled LC-GC*, Hüthig, Heidelberg, 1987.
- [27] J.J. Vreuls, G.J. de Jong and U.A.Th. Brinkman, *Chromatographia*, 31 (1991) 113.
- [28] J.J. Vreuls, R.T. Ghijsen, G.J. de Jong and U.A.Th. Brinkman, *J. Chromatogr.*, 625 (1992) 237.
- [29] P.J.M. Kwakman, J.J. Vreuls, U.A.Th. Brinkman and R.T. Ghijsen, *Chromatographia*, 34 (1992) 41.
- [30] F. Hernández, J. Beltrán and J.V. Sancho, *Sci. Total Environ.*, 132 (1993) 297.
- [31] T.A. Bellar and W.L. Budde, *Anal. Chem.*, 60 (1988) 2076.



ELSEVIER

Journal of Chromatography A, 670 (1994) 145–152

JOURNAL OF
CHROMATOGRAPHY A

Detection of alcohols in gas chromatographic effluent by laser-light scattering

Brian L. Wittkamp, David C. Tilotta *

Department of Chemistry, University of North Dakota, University Station, Box 7185, Grand Forks, ND 58202, USA

(First received November 11th, 1993; revised manuscript received February 14th, 1994)

Abstract

A laser-light-scattering detector that is sensitive to alcohols has been developed for gas chromatography. The detector consists of a miniature concentric nebulizer that uses a cold atomization gas and an Ar^+ laser. Calibration curves for the alcohols exhibit characteristic sigmoidal shapes. Signal-to-noise ratios were optimized by examining the photomultiplier tube temperature, collection wavelength and detection scheme (*i.e.*, photon counting *vs.* direct current detection). Limits of detection for five test alcohols were in the 2–8 $\mu\text{g/s}$ range.

1. Introduction

Evaporative laser-light-scattering detection (ELSD) has been shown to be useful for detecting analytes in liquid chromatographic effluent [1–6]. The basic operational principles of ELSD involve the generation of an analyte aerosol free of the mobile phase and the detection of the aerosol by light scattering. To these ends, nebulizers coupled with heated drift tubes are necessary in order to produce the analyte aerosol and minimize or eliminate the mobile phase. Of course, a laser beam and an adequate detection system are required in order to detect the aerosol.

Since its inception, ELSD has been applied exclusively to liquid chromatographic techniques, *e.g.*, high-performance liquid chromatography [1–4], gel permeation chromatography [5], supercritical fluid chromatography [6], etc. Surprisingly, there is no published report of an

application of laser-light-scattering detection (LSD) to gas chromatography (GC). In theory, the principle of LSD should be equally applicable to GC. In fact, a heated drift tube would not be required to remove the mobile phase since it is a permanent gas. Therefore, cooling the chromatographic effluent before or during nebulization should allow the detection of the aerosols of the separated analytes by laser-light scattering.

This paper is a preliminary report on the development of a LSD system for GC. The detector described in this paper has shown sensitivity to alcohols. Other compounds, such as benzene, toluene, pentane and chloroform, produce no response from this detector in its current configuration. In order to understand, and ultimately expand, the selectivity of LSD, several optimization studies were conducted. These studies included: the selection of detection wavelength, detector temperature and nebulizer gas temperature. Application of LSD to GC is advantageous from the standpoint of species-

* Corresponding author.

specific (*i.e.*, alcohol) detection. Specifically, the ability to selectively detect alcoholic compounds in complex matrices (*e.g.*, alcohols in fuel hydrocarbons) would greatly simplify the chromatography since no interference from the hydrocarbons would exist. The applications of LSD to GC will be the subject of a future communication.

2. Experimental

2.1. Apparatus

Fig. 1 shows a schematic diagram of the GC-LSD system. A Coherent Innova Series 70 argon ion laser (Palo Alto, CA, USA) lasing at 514.5 nm with a maximum operating output power of 450 mW served as the excitation source. A Continental Optical (Hauppauge, NY, USA) Pellin-Broca prism was installed near the front of the laser head, which serves as a plasma line filter. At the location where the sample exits the nebulizer, the measured laser power was 80 mW due to scattering losses from the prism and mirrors.

The scattered radiation from the analytes in the GC effluent is collected via a Nikon camera lens (collection throughput of $f/3.9$) and focused onto the entrance slit of a scanning 1/4-m

Digikrom DK 242 double monochromator (CVI, Albuquerque, NM, USA). The double monochromator is fitted with two 1800-g/mm holographic diffraction gratings and employs unilaterally adjustable slits. Unless otherwise noted, the monochromator slits were fixed at widths of 10 μm and the monochromator detection wavelength was fixed at 514.73 nm.

The detection system consisted of a red-sensitive Hamamatsu (Hamamatsu City, Japan) R928 photomultiplier tube (PMT) operating at -1000 V and held 40°C below ambient temperature (final temperature -17°C) by a Thorn/EMI (Fairfield, NJ, USA) Model WCTS-02 thermoelectric cooler. A Thorn/EMI C10 photon counter was employed for the photon-counting measurements. Although the integration time of the photon counter was fixed at 0.1 s for all data acquisitions, its analog output employs a 1-s integration time. The direct current (d.c.) experiments utilized an Analog Modules Model 341-3 current-voltage converter (Longwood, FL, USA) with an adjustable gain of 10–10000 V/A and an output time constant of 1 s. For all the data presented in this paper, the gain of the current-voltage converter was fixed at 10000 V/A. The data from either experiment (*i.e.*, photon counting or d.c. detection) was displayed on an analog strip-chart recorder (Omni-Scribe, Model 5211-12, Bellaire, TX, USA).

A Varian Aerograph Model 90P-3 gas chromatograph (Walnut Creek, CA, USA) was used for all experiments and was fitted with a 0.2% Carbowax 1500 column (180×0.20 cm I.D.), 150–175 μm Carbowax C) (Supelco, Bellefonte, CA, USA). The outlet of the column was connected to the nebulizer input capillary (see above) with the use of a 24 cm \times 0.20 cm O.D. stainless-steel transfer tube fed through a hole in the side of the GC oven. The transfer tube was then reduced with the use of a voidless reducing fitting to a 0.16 cm O.D. stainless-steel capillary which served as the nebulizer input tube. Thermal tape (Model L-03105-40; Cole-Parmer, Chicago, IL, USA), set at 160°C , was wrapped around the transfer tube in order to prevent effluent condensation. Helium was used as the carrier gas and was held at a constant flow-rate of 30 ml/min.

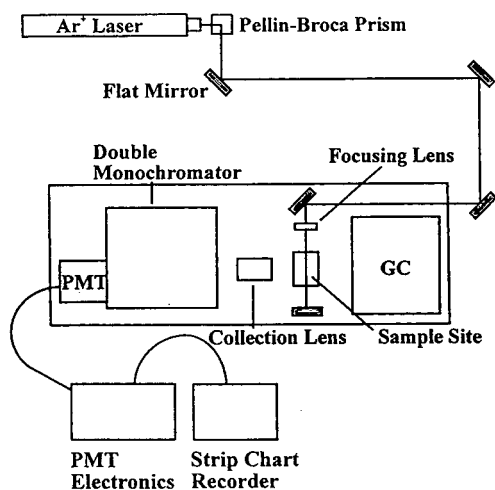


Fig. 1. Schematic diagram of the LSD system.

A miniature concentric nebulizer was constructed in this laboratory and evaluated for its ability to form aerosols from the analytes in the GC effluent. The nebulizer consists of two sections, the head and the body, and is shown schematically in Fig. 2. The nebulizer body was made from a solid block of aluminum $3\frac{3}{4}$ in. (1 in. = 2.54 cm) on each side. The nebulizer head was machined from a 1 in. long \times 1 in. diameter aluminum rod and a 0.094-cm hole was drilled through the center. As shown in Fig. 2, the nebulizer head was mounted on the body by boring a 1.85-cm diameter hole at one end of the aluminum block. A 0.094-cm diameter hole was drilled through the center of the aluminum block to accommodate the capillary transfer tube which passes the GC effluent to the nebulizer head. The capillary tube was admitted into the bottom of the body through a standard 1/4-in. nominal pipe thread (NPT)-to-Swagelok connector. A septum, placed into the Swage end of the connector and tightened with a 1/4-in. nut, prevented leaking of the nebulizer air.

The nebulizer capillary tubing was placed into the center of the 0.094-cm hole (2 mm from the outlet), and the head inserted into the body and sealed via an O-ring. The orifice where the capillary tube enters the nebulizer head is sealed with silicon sealant (part 64-2314B; Archer, Fort

Worth, TX, USA) in order to restrict the nebulizer gas from passing into the cavity of the nebulizer body. Air was used as the nebulizer gas and was introduced into the head through a standard 1/4-in. NPT fitting tapped into its side. Standard 1/16-in. copper tubing connected the air-tank regulator output and the 1/4-in. NPT fitting. A type K thermocouple purchased from Omega (Stamford, CT, USA) was used to monitor both the temperature of the capillary transfer tube and the temperature of the nebulizer gas.

2.2. Reagents

All chemicals were of reagent grade and were obtained from Fisher Scientific (Itasca, IL, USA) and were used as purchased. Helium as the carrier gas for the GC system and compressed air for the nebulizer were obtained from local sources and were used as purchased.

2.3. Procedure

Prior to data acquisition, the GC and spectrometer system were allowed to warm up for 1 h. The GC column temperature was fixed at 130°C, the injector temperature was held at 150°C and the temperature of the heat tape surrounding the transfer tubing was held at 160°C. Calibration curves for the alcohol test compounds were obtained by plotting the average peak area (triplicate measurements) vs. concentration. Limits of detection were obtained by injecting successively smaller amounts of a compound until its corresponding signal measured $2N_{\text{peak-to-peak}}$ (where N = noise) of the GC system.

3. Results and discussion

3.1. Instrumental considerations

The optical design of this GC detector, shown in Fig. 1, is modeled from a conventional fluorescence spectrometer with a 90° scattering geometry. Analytes exiting the chromatographic column pass through the heated transfer tube and

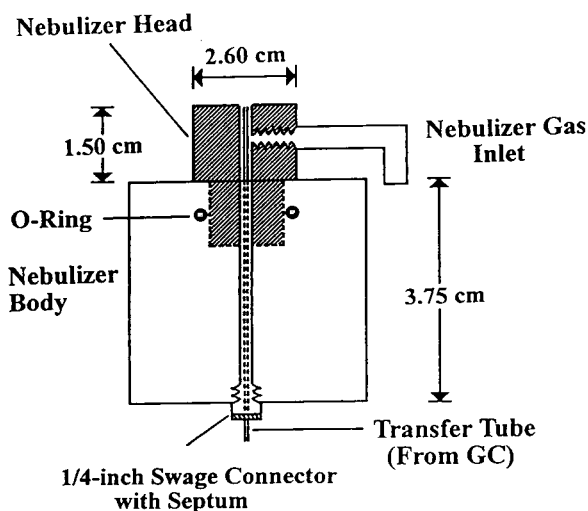


Fig. 2. Schematic diagram of the miniature cross-flow nebulizer.

are aspirated into the path of the laser beam by a miniature concentric nebulizer. The aerosol of the separated analytes is generated simultaneously with nebulization by employing a cold nebulizer gas (see below). The resulting scattered radiation from the aerosol of the eluting species is collected by the lens and focused onto the entrance slit of the double monochromator. The signal generated by the PMT is measured via the photon counter and displayed on the chart recorder.

The nebulizer assembly is mounted on a three-direction translation stage and is shown schematically in Fig. 3. The x - y - z translation stage provides sufficient flexibility for aligning the outlet of the transfer tube directly over the path of the laser beam. The inverted geometrical arrangement of the nebulizer (as opposed to upright) was found to be useful in facilitating the generation of the aerosol.

The GC system used in these experiments, because of its age, did not have temperature-programming features. In addition, capillary columns were incompatible with the oven due to size and plumbing requirements. Thus, a packed column with a fairly polar stationary phase was

recommended by its manufacturer (Supelco) for the separation of alcohols.

3.2. Gas chromatograph interface

The essential design consideration of the ELSD system is in the generation of an aerosol with a high concentration of analyte and a relatively low concentration of mobile phase. In contrast, the major concern in the application of LSD to GC is in the generation of an aerosol from the gas-phase analyte. Since the mobile phase is a gas with an extremely low boiling point, separation of the analyte from the mobile phase is unnecessary. However, the formation of the analyte aerosol is of primary concern because the analytes exiting the chromatographic column must be cooled before or during nebulization in order to provide the nebulizer with a liquid. In this detector, cooling is accomplished simultaneously with nebulization by employing a cold nebulizer gas. As the analytes exit the transfer tube they come in contact with the cooled stream of air and condense to form an aerosol.

The nebulizer gas is cooled by submersing a portion of the nebulizer supply tubing (180×0.62 cm I.D. copper tubing wound into a coil) into either a solution of dry ice–acetone or liquid nitrogen. The cooling solution lowers the temperature of the nebulizer gas by an amount corresponding to the length (*i.e.*, the number of copper coils) submersed in the cooling solution and the flow-rate of the nebulizer gas. With a nebulizer-gas flow-rate of 19.4 l/min (the maximum flow-rate examined in this study), the dry ice–acetone bath and liquid nitrogen bath allowed temperatures as low as $+10^{\circ}\text{C}$ and -10°C to be attained, respectively. It should be pointed out that temperatures higher than about 0°C could not be obtained with the liquid nitrogen bath. In addition, temperatures below -10°C could not be obtained with either bath due to the freezing of trace amounts of water in the nebulizer supply gas.

Since the formation of the analyte aerosol depends on the temperature of the nebulizer gas, the effect of cooling the nebulizer gas on the

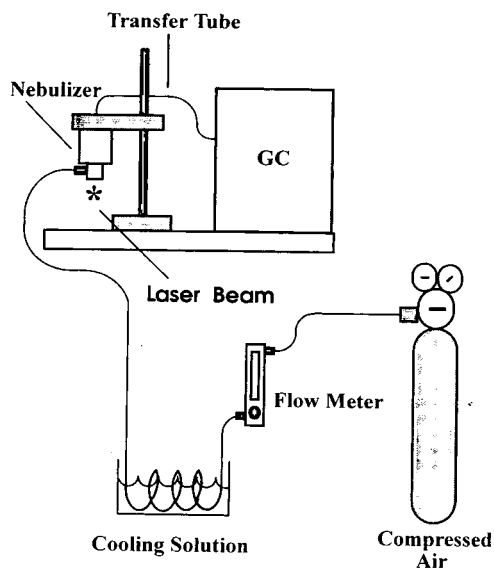


Fig. 3. Diagram of the nebulizer geometry relative to the outlet of the GC system.

signal-to-noise ratio (S/N) was examined. Ethanol was chosen as a representative analyte, and the temperature of the coolant gas was adjusted in the range of -10 to $+25^{\circ}\text{C}$ using either the dry ice–acetone mixture or the liquid nitrogen. The critical parameter in cooling the nebulizer gas was maintaining the nebulizer flow-rate at 19.4 l/min (see below). To achieve both cooling and proper nebulizer gas flow-rate, individual coils of the copper tubing were submersed in the cooling solution. This approach allowed different temperatures to be obtained while maintaining the flow at a desired rate.

The results from this temperature study show that the optimum S/N for ethanol is found at a cooling temperature of $+10^{\circ}\text{C}$. As the temperature of the nebulizer gas is decreased from $+25^{\circ}\text{C}$ to -10°C , the S/N for ethanol begins to increase and reaches a maximum at $+10^{\circ}\text{C}$. At temperatures below $+10^{\circ}\text{C}$, the ethanol freezes at the tip of the transfer tube and causes the nebulizer to sputter. Thus, the gaseous ethanol eluting from the gas chromatograph is not converted into the liquid phase until the nebulizer gas is sufficiently cooled below ambient temperature. Therefore, all the data discussed in the proceeding sections were obtained by maintaining the nebulizer gas at a temperature of $+10^{\circ}\text{C}$.

The optimum flow-rate of the nebulizer gas for this capillary nebulizer was determined to be 19.4 l/min. This flow-rate is needed to ensure complete expulsion of small sample quantities from the transfer tube. As the flow-rate is decreased, the ability to properly aspirate the separated analytes begins to decrease until the flow-rate is so slow that essentially no aerosol is generated. On the other hand, if the flow-rate of the nebulizer gas is too high, the droplet size becomes too small and decreases the amount of scattered radiation. It should be noted that previous work by Stolyhwo *et al.* [7] showed that ELSD in liquid chromatography require significant flow-rates of nebulizer gas as well. Of course, the high nebulizer flow-rate may be minimized by decreasing the diameter of the nebulizer tip. A smaller diameter would effectively give rise to the same nebulization effect but at a lower nebulizer gas flow-rate.

3.3. Detection wavelength

Although several studies have examined the effect of the excitation wavelength on the detection signal, little work has been undertaken in examining the effect of the choice of detection wavelength [8,9]. A collection wavelength study was performed over the wavelength interval of 514.14–514.90 nm. Triplicate 0.5- μl aliquots of ethanol were injected onto the column, and the corresponding baseline noise and signal of each injection was recorded at each of the specified wavelengths. The average values of the signals and the peak-to-peak noises were tabulated, and plots of wavelength vs. relative signal and wavelength vs. relative noise are shown in Fig. 4. It should be noted that the magnitudes of the noises and signals shown in Fig. 4 are in relative logarithmic intensity units.

It can be concluded from Fig. 4 that the signal begins to rise appreciably near 514.25 nm. The signal then plateaus from 514.40–514.75 nm and then drastically decreases. The noise recorded at each wavelength appears to follow the same general trend as the signal except in the range of 514.60–514.90 nm. Within this range, the magnitude of the noise is significantly low and is due to the dark-current noise of the PMT. At 514.73 nm, the optimum collection wavelength, the

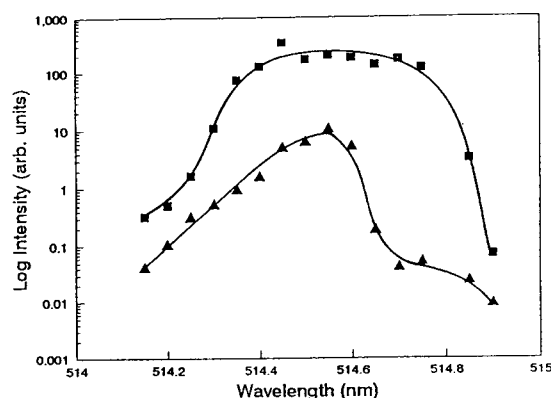


Fig. 4. Logarithmic intensity (arbitrary units) of the signal and the noise from triplicate 0.5- μl injections of ethanol as a function of collection wavelength (nm). The squares represent the signal and the triangles represent the noise at each of the wavelength intervals.

noise is 200-fold lower than observed at the Rayleigh line (514.54 nm).

This experimental result may have direct application in the ELSD systems more commonly used in high-performance liquid chromatography. These systems detect radiation at the wavelength of the excitation source (in fact, wavelength selection devices are not generally employed). The increase in the noise at the Rayleigh line is attributed to extraneous scattering from the mirrors and atmospheric particles (*i.e.*, dust). A spectrum of the Rayleigh line, a scan from 514.30–514.90 nm, shows that the intensity of scattering due to the atmosphere and the mirrors is approximately 5-fold greater at the Rayleigh line than at 514.73 nm. Thus, the collection wavelength throughout this study was fixed at 514.73 nm, which yielded an S/N for ethanol that was 200-fold greater than that observed at the Rayleigh line.

3.4. Photon counting vs. d.c. detection

To date, all LSD systems employ PMT circuits that utilize d.c. detection. Specifically, the current output of the PMT detectors is converted to a voltage signal with the use of a suitable pre-amplifier. It is well-known that under some circumstances, *e.g.*, detector-noise limited measurements, photon counting can improve S/N by factors of 3–10 [10]. These improvements are made possible with the use of discrimination electronics to effectively reduce dark-current counts.

Photon-counting detection was compared to d.c. detection by injecting triplicate 0.5- μ l aliquots of ethanol onto the packed column. In order to compare the results obtained by photon counting, the same experiment was conducted with the exception of the replacement of the photon-counting electronics with a current-to-voltage converter. The average S/N obtained from the 0.5- μ l injections for photon-counting detection and d.c. detection were 567 and 20, respectively, at a sample laser power of 80 mW. This result shows that there is a significant improvement in the S/N (28-fold) when utilizing photon-counting vs. d.c. detection.

In d.c. detection, the signal and noise of the PMT are measured simultaneously. If the observed signal is quite intense, then the dark current noise of the PMT becomes insignificant. However, the signals observed in this detector are very weak (on the order of Raman scattering signals). Therefore, the noise of the PMT becomes more predominant as the strength of the signal decreases, which results in the poor S/N values observed for d.c. detection. Photon counting discriminates between the signal and the noise, therefore making photon counting more useful in low-light-level detection.

3.5. Detector cooling

It is a common practice in many “low”-light-level techniques, such as Raman and fluorescence spectroscopies, to cool the detector below ambient temperature in order to improve the S/N by reducing the dark-current noise [11]. Consequently, an experiment was conducted to determine if a significant difference exists in the S/N values of chromatograms obtained with a non-cooled PMT (ambient temperature, 23°C) vs. that obtained using a cooled PMT (–17°C). Triplicate 1.0- μ l injections of ethanol were introduced onto the column and the corresponding average S/N values were calculated for both the cooled and non-cooled PMT.

It was found that the S/N obtained for the cooled PMT was twofold greater than the S/N for the ambient-temperature PMT. The principal reason for the decrease in the S/N for the ambient-temperature PMT was the increase in the dark current. The dark current increased from 350–400 counts/s (cooled tube) to 700–800 counts/s (ambient tube). Since the dark-current noise in a PMT is proportional to the square root of the dark current, an improvement in the S/N on the order of 50% would be expected. Therefore, all chromatographic data presented in this paper utilized the cooled PMT.

3.6. Analytical calibration data

Fig. 5 shows calibration curves for methanol, ethanol, isopropanol, propanol and butanol.

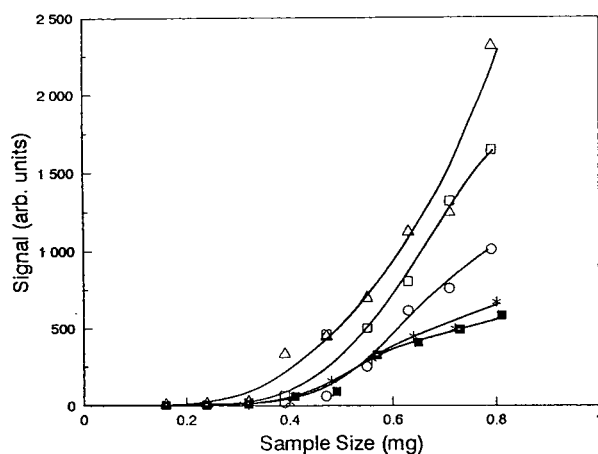


Fig. 5. Calibration curves for methanol (\square), ethanol (Δ), isopropanol (*), propanol (\circ) and butanol (\blacksquare).

Each calibration curve was obtained by injecting successively larger amounts of the pure compound onto the column. As can be seen in this figure, the calibration curves are sigmoidal-shaped over the entire concentration range.

It has been well demonstrated that sigmoidal calibration curves are obtained from light-scattering detectors employed in liquid chromatographic methods [5,7,9,12–14]. These sigmoidal curves have been determined to arise from the change of the average aerosol-particle diameter as the amount of the analyte is varied. Since the concentrations of the analytes in this gas chromatographic experiment are less than $2 \cdot 10^{-4}$ g/ml (assuming an average retention volume of 4.0 ml at a carrier gas flow-rate of 30 ml/min), exponential/sigmoidal-shaped calibration curves would be predicted [5]. Thus, the shapes of these calibration curves (the lower portions of the sigmoids) are in agreement with the prior work on the application of LSD to liquid chromatography.

It should be noted that the deviation from linearity of the calibration curves is attributed to particle size effects and not to non-linearity of the photon counter. The upper limit of linearity for the photon counter employed in these experiments is 10^6 – 10^7 , according to the manufacturer's specifications [15]. Typically, the highest photon counts observed in 1.0 s was $6 \cdot 10^5$ for a

1.0- μ l injection of ethanol, which is well within the linearity range of the photon counter.

After characterization of the operating parameters of the LSD system with respect to the five alcohols, the LSD responses to various compounds were examined. It was immediately observed that compounds such as toluene, benzene, pentane, tetrahydrofuran, ethylene glycol and 1,2-dichloroethane yielded no appreciable signal. However, all alcohols used in the study yielded significant signals. The apparent sensitivity of this system to alcohols has been tentatively appointed to the surface tension of the nebulized droplets. Hydrogen bonding in the alcohols is much greater than that for the other compounds tested. This hydrogen bonding is thought to enhance the formation of droplets when the liquid effluent is nebulized. Further work is underway in this laboratory to gain insight into this phenomenon.

The limits of detection of the five test alcohols were determined by making triplicate injections at decreasing injection sizes until the signals were buried within the noise of the system. Table 1 presents a compilation of the limits of detection for the five test alcohols obtained under identical operating conditions. In addition, Table 1 lists the reproducibilities of each of the triplicate injections. As can be seen from Table 1, the limits of detection range from 7.54 to 2.46 μ g/s and increase approximately as the boiling points of the alcohols decrease. However, the series of the five examples is interrupted by ethanol exhibiting a limit of detection similar to that obtained for butanol.

Table 1
LSD calibration data for five alcohols

Alcohol	Limit of detection ^a (μ g/s)	R.S.D. ^b (%)
Methanol	7.54	7.0
Ethanol	2.65	7.4
Isopropanol	4.49	7.4
Propanol	4.06	7.1
Butanol	2.46	6.5

^a Measured at a signal intensity equal to $2N_{\text{peak-to-peak}}$.

^b Determined from quadruplicate 1.0- μ l injections.

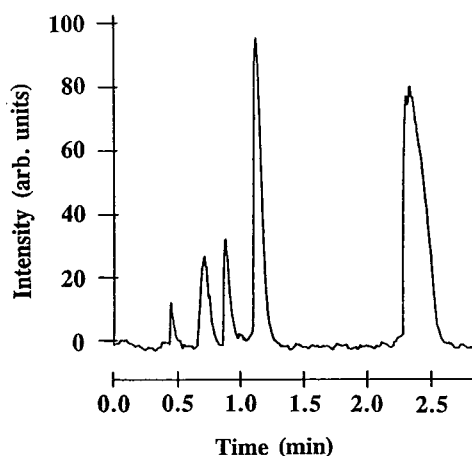


Fig. 6. A chromatogram of a 3.0- μ l injection of methanol, ethanol, isopropanol, propanol and butanol (in order of elution). Operating parameters: injector temperature 150°C, column temperature 130°C, carrier gas flow-rate 30 ml/min, nebulizer flow-rate 19.4 l/min, nebulizer gas temperature 10°C.

3.7. Chromatographic application

A typical chromatogram obtained with this LSD system is shown in Fig. 6. Although all the peaks in the chromatogram of Fig. 6 are baseline resolved, they are somewhat asymmetrical and exhibit tailing in their trailing edges. This slight asymmetry is most likely due to poor chromatography. It should be noted that butanol, which is the last compound to elute from the column, appears in the chromatogram as slightly "split". This splitting is presumably due to a slight sputtering of the cold butanol as its aerosol is being generated. Sputtering can be eliminated by warming the nebulizer gas slightly, but at the expense of a poorer detection limit.

4. Conclusions

LSD can be applied to GC provided the analytes in the GC effluent can be sufficiently converted to the liquid state and nebulized. However, the LSD selectivity is apparently limited to alcohols. The results of various S/N

studies show that the S/N ratio is increased 200-fold by detecting the scattered light at 514.73 nm rather than at the Rayleigh line, increased twofold by cooling the PMT to -17°C , and increased 28-fold by using photon counting instead of d.c. detection. These improvements result in an overall S/N enhancement greater than four orders of magnitude.

5. Acknowledgement

The authors would like to thank the 3M Corporation for providing financial support in the form of a fellowship for B.L.W.

6. References

- [1] Y. Mengerink, H.C.J. de Man and S.J. van der Wal, *J. Chromatogr.*, 552 (1991) 593–604.
- [2] S. Hoffmann, G.R. Norli and T. Greibrokk, *J. High Resolut. Chromatogr.*, 12 (1989) 260–264.
- [3] A.M. Davila, R. Marchal, N. Monin and J.P. Vandecasteele, *J. Chromatogr.*, 648 (1993) 139–149.
- [4] K. Rissler, H.P. Kunzi and H.J. Grether, *J. Chromatogr.*, 635 (1993) 89–101.
- [5] J.M. Charlesworth, *Anal. Chem.*, 50 (1978) 1414–1420.
- [6] M. Demirbaker, P.E. Anderson and L.G. Blomberg, *J. Microcol. Sep.*, 5 (1993) 141–147.
- [7] A. Stolyhwo, H. Colin, M. Martin and G. Guiochon, *J. Chromatogr.*, 288 (1984) 253–275.
- [8] M. Righezza and G. Guiochon, *J. Liq. Chromatogr.*, 11 (1988) 2709–2729.
- [9] P. Van der Merren, J. Vanderdeelen and L. Baert, *Anal. Chem.*, 64 (1992) 1056–1062.
- [10] J.D. Ingle Jr. and S.R. Crouch, *Spectrochemical Analysis*, Prentice Hall, Englewood Cliffs, NJ, 1988, Ch. 5, pp. 155–156.
- [11] J.D. Ingle, Jr. and S.R. Crouch, *Spectrochemical Analysis*, Prentice Hall, Englewood Cliffs, NJ, 1988, Ch. 16, p. 505.
- [12] T.H. Mourey and L.E. Oppenheimer, *Anal. Chem.*, 56 (1984) 2427–2434.
- [13] L.E. Oppenheimer and T.H. Mourey, *J. Chromatogr.*, 323 (1985) 297–304.
- [14] G. Guiochon, A. Moysan and C. Holley, *J. Liq. Chromatogr.*, 11 (1988) 2547–2570.
- [15] *Photon Counter Manual C-10/C-604*, Thorn/EMI Electron Tubes, Fairfield, NJ, 1990, Ch. 1, p. 2.

Toxic aldehydes formed by lipid peroxidation

I. Sensitive, gas chromatography-based stereoanalysis of 4-hydroxyalkenals, toxic products of lipid peroxidation

Gerhard Bringmann *, Michael Gassen, Silvia Schneider

Institute of Organic Chemistry, University of Würzburg, Am Hubland, D-97074 Würzburg, Germany

(First received November 4th, 1993; revised manuscript received February 8th, 1994)

Abstract

An efficient analytical method is presented that does not only allow to detect and quantify 4-hydroxyalkenals, but for the first time provides a tool to look at the enantiomeric ratio of these interesting lipid peroxidation products. It involves acetylation as the only derivatization step, which can be carried out under mild conditions with acetic anhydride and gas chromatography on a chiral permethyl cyclodextrin phase. All biologically important homologues (C_5 – C_9) can be selectively observed in a single chromatographic run. The resolution allows a reliable quantification of the enantiomers. The method was successfully applied in the stereoanalysis of 4-hydroxynonenal formed in rat liver microsomes after treatment with ADP/ Fe^{2+} .

1. Introduction

Lipid peroxidation (LPO) has been suggested to play an important role in the pathogenesis of several diseases [1,2]. This free radical mediated process was studied *in vivo* [3] as well as in

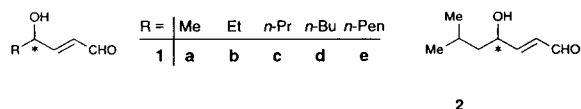


Fig. 1. Structures of naturally occurring 4-hydroxyalkenals **1a–e** and of the novel internal standard **2**.

model systems like liver microsomes [4], isolated hepatocytes [5], lipid vesicles [6] and isolated unsaturated fatty acids [7]. Although the whole process is far from being completely understood, it is generally accepted that LPO involves formation of unstable lipid hydroperoxides as a first step [1]. These intermediates rapidly decompose to form a vast variety of mostly aldehydic secondary products. The most prominent representatives are malonic dialdehyde, *n*-hexanal and 4-hydroxynonenal (**1e**) [4,7] (see Fig. 1).

Compound **1e** and the other hydroxyalkenals **1a–d** have been observed first in rat liver microsomes after initiation of LPO with ADP/ Fe^{2+} or CCl_4 [4]. They exhibit numerous toxic effects, which have been associated with their ability to react as cross-linkers of proteins [8] or DNA [9]. Hydroxyalkenals are known to covalently modify

* Corresponding author.

low-density lipoprotein [10] and glucose-6-phosphatase [8] and to show chemotactic activity towards rat neutrophils [11].

Many analytical procedures have been developed for a sensitive and selective detection of hydroxyalkenals. Modern methods are mostly based on gas chromatography (GC), which is a powerful tool for the efficient analysis of volatile LPO products, such as **1a–e**, especially if modern capillary columns are used. Derivatization at the carbonyl function or at the hydroxy group of these reactive compounds has been employed and serves three purposes simultaneously: it protects the sensitive analytes during the workup of biological samples, increases their volatility and enhances the sensitivity of detection. The so far most successful GC-based method employs a “tandem derivatization” including conversion of the carbonyl function into an O-pentafluorobenzyl oxime and trimethylsilylation of the hydroxy group [12]. If combined with sensitive mass-selective or electron-capture detection, it allows the analysis of hydroxyalkenals down to the picomolar concentration range.

The stereochemistry at C-4 of the chiral hydroxyalkenals is an interesting aspect, which has been completely neglected so far, even in studies concerning the biological activity of these toxic lipid peroxidation products, as well as their formation and metabolism. An *in vivo* occurrence of hydroxyalkenals in an optically active form would be a strong hint that enzymes are involved in the biological pathway of these compounds. Still, the established analytical methods do not permit to detect and separately quantify the enantiomers. In this paper we present a procedure for a sensitive and enantioselective analysis, which is based on resolution of *R*- and *S*-hydroxyalkenals on a chiral β -cyclodextrin stationary phase. The enantiomers were identified by comparison with material obtained by stereoselective total synthesis. Our analysis can be applied to determine the enantiomeric excess of 4-hydroxyalkenals in biological samples. For the reliable quantification of the analytes, a novel internal standard, the branched-chain hydroxyalkenal **2**, has been developed.

2. Experimental

2.1. Chemicals

All reagents were of commercial quality. Organic solvents were dried and distilled prior to use. Deionized water was prepared with a Milli-Q appliance (Millipore, Bedford, MA, USA). Trimethylsilyltrifluoroacetamide (MSTFA) was obtained from Machery–Nagel (Düren, Germany), heptafluorobutyric anhydride (HBFA), trifluoroacetic anhydride (TFA) and acetic anhydride were obtained from Aldrich (Milwaukee, WI, USA). Buffer salts were supplied by Merck (Darmstadt, Germany), biochemicals by Fluka (Buchs, Switzerland).

2.2. Synthesis

Hydroxyalkenals were prepared from commercially available 1,1-diethoxypropyne and the corresponding aliphatic aldehydes (ethanal–*n*-hexanal) (Aldrich), as published by Esterbauer and Wegner [13]. The new internal standard 4-hydroxy-6-methylhept-2-enal (**2**) was synthesized from 3-methylbutyric aldehyde analogously and was characterized spectroscopically. NMR spectra have been recorded on an AC 200 system from Bruker (Karlsruhe, Germany), IR spectra on a Perkin-Elmer 1420 IR spectrometer (Perkin-Elmer, Norwalk, CT, USA).

IR (film): $\nu = 3600\text{--}3100\text{ cm}^{-1}$, 3020–2700, 1680, 1620, 1460, 1380, 1360, 1260, 1120, 970, 730. ^1H NMR (C^2HCl_3 , 200 MHz): $\delta = 0.93$ (d, $^3J = 6.6\text{ Hz}$, 3 H, CH_3), 0.98 (d, $^3J = 6.7\text{ Hz}$, 3 H, CH_3), 1.48 (t, $^3J = 7.1\text{ Hz}$, 2 H, 5-H), 1.61 [s(b), 1 H, OH], 1.70–2.02 (m, 1 H, 6-H), 4.51 (m_c , 1 H, 4-H), 6.33 (dd, $^3J_{2-3} = 15.5\text{ Hz}$, $^3J_{1-2} = 7.7\text{ Hz}$, 1 H, 2-H), 6.83 (dd, $^3J_{3-2} = 15.7\text{ Hz}$, $^3J_{3-4} = 4.7\text{ Hz}$, 1 H, 2-H), 9.59 (d, $^3J = 7.9\text{ Hz}$, 1 H, CHO).

Optically active 4*S*-**1a** and 4*S*-**1e** were obtained after reduction of a ketone precursor with *S*-BINAL-H, a chiral aluminum hydride [14]. The absolute configuration of the synthetic material has been elucidated by oxidative degradation to

the known corresponding α -hydroxycarboxylic acids [14].

2.3. Derivatization and calibration

For calibration, samples of the aldehydes **1a–e** (10, 5, 1, 0.5 and 0.1 mg) were dissolved in 300 ml of toluene–0.1 M triethylamine. Acetic anhydride (100 μ l) was added and the solutions were kept in a sealed vial at 100°C for 3 h. After cooling to room temperature, the samples were extracted with phosphate buffer (pH 6.0, 0.5 M, 100 μ l) and analyzed by GC. The other anhydrides were used analogously for derivatization. MSTFA was added neat, the samples were heated to 60°C for 30 min and analyzed without further purification.

2.4. Gas chromatography

GC was performed on a GC 2000 Vega Series 2 (Carlo Erba, Milan, Italy), equipped with a flame ionization detector, and on a 5890 Series II, equipped with a 5971 A mass-selective detector (Hewlett-Packard, Palo Alto, CA, USA). Data acquisition and processing were carried out with a Hewlett-Packard ChemStation software (1989 release). Separations were accomplished on a C-Dex-B fused-silica capillary column (30 m \times 0.25 mm I.D., film thickness 0.25 μ m) (J & W Scientific, Folsom, CA, USA), guarded with a retention gap consisting of uncoated fused silica (1 m \times 0.52 mm). Helium was used as carrier gas at 100 kPa. Samples of 1 μ l were injected on column. Temperature: 100°C (5 min), 2°C/min at 170°C (5 min).

2.5. GC–MS

The mass-selective detector was automatically tuned before processing sample analysis with perfluorotributylamine (PFTBA) as a standard. Electron impact ionization with 70 eV energy was used. Total ion chromatograms were recorded from 50 to 250 u, dwell time 100 ms. The characteristic fragments chosen for selected ion

Table 1

Characteristic fragments of acetylated hydroxyalkenals employed for MS–SIM detection

Compound	Fragments
1a	100, 71, 81
1b	114, 85, 81
1c	128, 99, 81
1d	142, 113, 81
1e	156, 127, 81

monitoring (SIM) of the aldehydes **1a–e** are given in Table 1.

2.6. Preparation and workup of liver microsomes

Liver microsomes were prepared from male Wistar rats according to literature procedures [15] and diluted in a buffered solution of 50 mM Tris–HCl, 5 mM MgCl₂ and 25 mM KCl (adjusted to pH 7.5). For calibration 100, 50, 10, 5 and 1 μ g of **1e** and 25 μ g of the internal standard **2** were added to 2.5 ml microsome suspension (equivalent to 1 g liver wet mass). The samples were diluted with water (17.5 ml), poured on a column charged with 10 g Chemtube hydromatrix (Varian, Harbor City, CA, USA) and extracted with dichloromethane (40 ml). The eluate was collected in a flask containing 0.1 M acetate buffer (pH 3.0, 2 ml). Dichloromethane was removed under reduced pressure. The residue was applied to a conditioned 200 mg RP-18 extraction column (J.T. Baker, Phillipsburg, PA, USA). The column was washed with cyclohexane (1 ml) and methanol (2 ml). The methanol fraction was evaporated to dryness and derivatized as described.

2.7. LPO experiments

For LPO experiments, 2.5 ml of microsome suspension were diluted with 17.5 ml of a NADPH-generating solution [16] (0.174 mM Na₂NADP, 37.2 mM nicotinamide, 4.3 mM glucose-6-phosphate, 6 U/ml glucose-6-phosphate dehydrogenase (EC 1.1.1.49)). LPO was

initiated by the addition of ADP (1.61 mM) and FeSO_4 (18 μM). The samples were incubated at 37°C for 30 min. Internal standard **2** (25 mg) was added prior to workup. Preparation, acetylation and analysis by GC–SIM was performed as described above.

3. Results and discussion

3.1. GC on chiral stationary phases

During the last years, a wide variety of chiral polysiloxane derivatives have become commercially available for use in GC. Amide and metal complex phases have been successfully employed to separate several chiral natural products like flavours or pheromones [17]. A third class of growing importance are cyclodextrin phases. Cyclodextrins are cyclic α -D-glucose oligomers, the hexa-, hepta- and octamers (α -, β - and γ -cyclodextrins) are of importance for GC applications. They can be employed as different derivatives (*e.g.* alkylated, acylated), either pure or dissolved in polysiloxanes, such as DB-1701 (7% phenylmethyl-, 7% cyanopropylmethyl-, 86% dimethylpolysiloxane). These composites combine the high stability and chemoselectivity of polysiloxanes with the stereoselectivity of cyclodextrins.

As we aimed at the simultaneous enantiomer separation of all the relevant hydroxyalkenals in one single chromatographic run, we had to find a stationary phase that was sufficiently selective for analytes of different polarity and volatility. The influence of the stereocentre on the overall physical properties of the 4-hydroxyalkenals decreases with increasing chain length, therefore the separation of *R*- and *S*-4-hydroxynonenal (**1a**) is especially challenging. Our first choice was a C-Dex-B capillary column, which is coated with a 10% solution of permethyl- β -cyclodextrin in DB-1701. This composite has been used for numerous applications in the literature [18], for analytes with different functional groups and a wide range of polarity.

3.2. Chromatography of 4-hydroxyalkenals **1**

Nearly all of the published procedures for a chromatographic analysis of 4-hydroxyalkenals include one or two derivatization steps. Most successful so far has been a “tandem derivatization” of the carbonyl function as a pentafluorobenzyl oxime and of the hydroxy group as a trimethylsilyl ether, which renders the analytes more volatile, more sensitive to detect and more stable during the workup procedure [12]. The non-derivatized hydroxyalkenals can rapidly react with nucleophiles like $-\text{NH}$ and $-\text{SH}$ groups in peptides and amino acids, which may cause a severe loss during the analysis in biological samples.

3.3. GC of 4-hydroxyalkenals **1** on a chiral phase without derivatization

The hydroxyalkenals **1a–e** are sufficiently volatile to be examined without derivatization on a permethylcyclodextrin stationary phase. We found, however, that their resolution is significantly influenced by the chain length. While hydroxypentenal (**1a**) could be separated easily, resolution of the non-derivatized longer-chain homologues could not be accomplished (see Table 2).

3.4. GC of 4-hydroxyalkenals on chiral column with derivatization

Derivatization of the carbonyl function was also found to be disadvantageous for a separation of the enantiomers. So we finally opted for transformation only of the polar OH group to obtain more volatile derivatives. These could be analyzed at lower temperatures when the cyclodextrins are less flexible and when their separation properties are consequently better. Furthermore, O-derivatization enabled us to modify the close neighbourhood of the stereocentre. Reagents of different steric bulk were examined to optimize chiral discrimination in the interaction between stationary phase and the analytes. For a first approach we focussed on

Table 2
Chromatography of derivatized 4-hydroxyalkenals on a chiral C-Dex-B stationary phase

Compound	Derivatization				
	(H ₃ C) ₃ Si–	F ₇ C ₃ C(O)–	F ₃ CC(O)–	H ₃ CC(O)–	H
1a	–	–	–	+	+
1b	n.d.	n.d.	–	+	(+)
1c	n.d.	n.d.	–	+	–
1d	n.d.	n.d.	–	+	–
1e	–	–	–	+	–

+ = Separation; (+) = partial separation; – = no separation; n.d. = not determined.

well established methods like trimethylsilylation with MSTFA and O-acylations with HFBA, TFA and acetic anhydride. The results of our chromatographic experiments are summarized in Table 2.

Only acetylation of the five hydroxyalkenals **1**, which could be accomplished selectively under

mild conditions, led to derivatives that could be separated in one single chromatographic run (see Fig. 2). The resolution factors R_s even of the long-chain homologues are well above the limit (0.8–1) that is generally regarded as critical for secure quantification of the resolved peaks (see Table 3). The samples are stable for several days, if they are stored at -18°C and water is carefully removed.

The peaks were identified by their mass spectra and by comparison with synthetic material. Racemic derivatized **1a** and **1e** were mixed with synthetic optically active material to establish their sequence of elution. It could be demonstrated that the early peaks correspond to the *R* isomers (Fig. 3).

Interestingly the resolution R_s of the acetylated hydroxyalkenals decreases with increasing chain length only for hydroxypentenal (**1a**), hydroxyhexenal (**1b**) and hydroxyheptenal (**1c**). For the longer-chain homologues, no more significant changes were observed. Peak widths

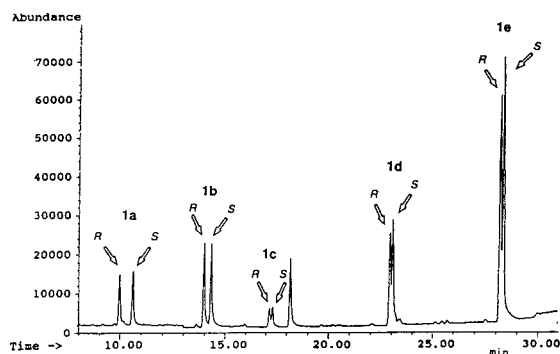


Fig. 2. Separation of derivatized *R*- and *S*-4-hydroxyalkenals by GC on permethyl cyclodextrin stationary phase.

Table 3
Separation data of acetylated *R*- and *S*-hydroxyalkenals **1**

Compound	$t_R(S) - t_R(R)$ (min)	$\bar{\omega}$ (min)	α	R_s
1a	0.674 ± 0.083	$0.0626 \pm 6.80 \cdot 10^{-3}$	$1074 \pm 9.29 \cdot 10^{-3}$	10.8 ± 1.22
1b	0.348 ± 0.013	$0.0738 \pm 6.34 \cdot 10^{-3}$	$1027 \pm 8.54 \cdot 10^{-4}$	4.75 ± 0.54
1c	0.146 ± 0.009	$0.0788 \pm 1.05 \cdot 10^{-2}$	$1009 \pm 4.79 \cdot 10^{-4}$	1.88 ± 0.31
1d	0.136 ± 0.005	$0.0814 \pm 9.61 \cdot 10^{-3}$	$1006 \pm 2.78 \cdot 10^{-4}$	1.70 ± 0.26
1e	0.152 ± 0.015	$0.0790 \pm 1.89 \cdot 10^{-2}$	$1006 \pm 4.06 \cdot 10^{-4}$	2.06 ± 0.70

Mean \pm R.S.D. ($n = 5$).

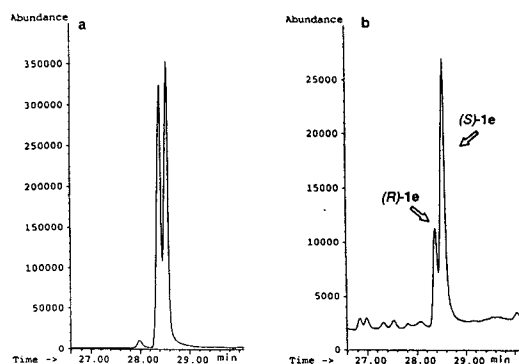


Fig. 3. (a) GC of racemic derivatized **1e**. (b) GC after addition of the *S*-enantiomer.

show no correlation to configuration or chain length of the analytes.

3.5. GC–flame ionization detection experiments

With flame ionization detection, 250 ng of the acetylated aldehydes **1a–e** could still be identified and quantified. The analysis functions $m = f(R)$ (m = mass of the analyte, R = detector response) were linear (Table 4).

3.6. GC–MS experiments

Mass-selective detection was used to obtain total ion chromatograms and the mass spectra of acetylated **1a–e**. The mass spectra show three

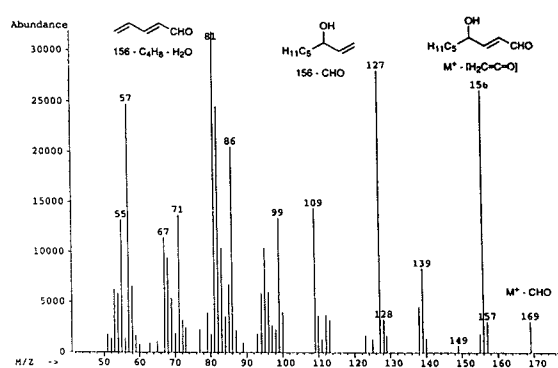


Fig. 4. Mass spectrum of acetylated 4-hydroxynonenal (**1e**) with typical fragmentation pattern.

typical fragmentations: loss of the acetyl group, β -cleavage of the alcohol and α -cleavage of the carbonyl group (Fig. 4). The most characteristic fragments have been chosen for SIM.

3.7. Analysis of 4-hydroxyalkenals **1** in biological samples

First experiments have been carried out to apply the described method to the analysis of biological samples. For calibration, aliquots between 100 and 1 μ g **1e** were added to an amount of rat liver microsomes equivalent to 1 g liver wet mass. The aldehydes were reextracted with dichloromethane, purified on RP-18 material, derivatized with acetic anhydride and finally

Table 4
Analysis functions for the quantitative analysis of derivatized **1a–e**

Equation	r	n
<i>Flame-ionization detection</i>		
1a $R = 714.2 (\pm 26.62)m - 138.1 (\pm 58.92)$	0.994	3
1b $R = 457.3 (\pm 13.91)m + 187.0 (\pm 25.47)$	0.927	3
1c $R = 888.2 (\pm 4.55)m + 122.5 (\pm 54.28)$	0.998	3
1d $R = 1233.7 (\pm 142.24)m - 538.2 (\pm 204.12)$	0.993	3
1e $R = 1118 (\pm 73.64)m - 260.3 (\pm 38.17)$	0.974	3
<i>Mass-selective detection</i>		
1e $R = 41117 (\pm 5119)m - 52\,683 (\pm 21\,206)$	0.993	6
<i>Mass-selective detection + I.S. 2</i>		
1e $R/R_{I.S.} = 0.771 (\pm 0.038)m/m_{I.S.} + 0.772 (\pm 0.431)$	0.996	4

m = Mass of the analyte; R = detector response.

subjected to chromatography. For selective detection of **1e** in rat liver microsomes, the fragment at m/z 156 was the target ion and those at 127 and 81 the qualifier ions. After extraction and purification, 75% of the free aldehyde **1e** could be recovered in the samples. The detection limit for derivatized **1e** was 660 pg. The analysis function (Table 4) was linear for the whole concentration range, even near the detection limit. In blank samples no peaks with the retention time of derivatized **1e** were observed.

3.8. Use of 4-hydroxy-6-methylhept-2-enal (**2**) as an internal standard

To improve the precision of quantification even in complex biological samples we decided to use the synthetic branched-chain 4-hydroxy-6-methylhept-2-enal (**2**) as an internal standard. Compound **2** was added to the samples before workup. It could be assumed that **2** would exhibit the same chemical properties as the hydroxyalkenals **1a–e**, especially with regard to solubility or binding to biological matrix components. Calibration data shows a linear correlation between the response ratio and the mass ratio of **1e** vs. **2** (Table 4). Deuterated internal standards like 2,3-dideutero-4-hydroxynon-2-enal [19] or 9,9,9-trideutero-4-hydroxynon-2-enal [20] cannot be used in difficult enantiomer separations because they may not coelute with the unlabelled compound. This may affect the quality of separation as even a slight shift of retention times causes peak broadening.

3.9. Detection and stereochemical analysis of 4-hydroxynon-2-enal (**1e**) in liver microsomes after treatment with ADP/Fe²⁺

As a first test for the applicability of our method, we investigated rat liver microsomal fractions that had been freshly prepared from male Wistar rats and stored in a NADPH-generating solution. After LPO initiation by treatment with ADP/Fe²⁺, the samples were analyzed for 4-hydroxynon-2-enal (**1e**) by GC–SIM. We have been able to detect **1e** and to demonstrate that it is formed as a racemate (see

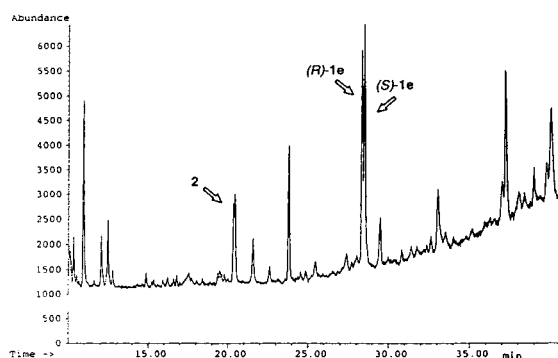


Fig. 5. Formation of racemic **1e** in ADP/FeSO₄-treated rat liver microsomes, as demonstrated by GC–SIM after acetylation of the free aldehyde.

Fig. 5), the first concrete experimental evidence on the non-stereoselective formation of this metabolite. This finding strongly supports the generally accepted concept [1] that hydroxyalkenals are formed, at least in liver tissue, without any enzymatic stereocontrol by a free radical mechanism.

4. Discussion and outlook

With our novel sensitive enantiomer analysis, the ratio of *R*- and *S*-hydroxyalkenals in biological model systems can be determined. For the first time it is possible to study the implications of stereochemistry on the generation and metabolism of these toxic LPO products.

However, the scope of our method is still limited, as the sensitivity of detection is considerably lower, compared with established non-selective methods. This is due in part to the simple effect of peak splitting, but more importantly to constraints imposed by the chromatographic system. We had to find a compromise for the choice of the derivatization procedure since the hydroxyalkenal analysis had to be optimized with respect to enantiomer separation. With perfluorinated agents, which improve the detection especially for GC–MS, unfortunately the racemate could not be resolved. We further had to leave the reactive carbonyl group unprotected. As a consequence, loss of hydroxy-

alkenals during the isolation from biological material cannot be ruled out.

Further work will be directed at solutions of these problems. Hopefully, we will be able to expand the scope of this encouraging method to the investigation of animal or human serum and tissue. So far, we have been able to provide a tool to examine the hitherto unexplored field of hydroxyalkenal stereochemistry and thus contribute to a more complete understanding of the complex processes involved in LPO.

5. Acknowledgements

The authors wish to thank Dr. Michael Horn (Department of Cardiology, Würzburg University Hospitals) for providing rat liver samples. Financial support by the “Fonds der Chemischen Industrie” is gratefully acknowledged.

6. References

- [1] H. Esterbauer, in D.C.H. McBrien and T.F. Slater (Editors), *Free Radicals, Peroxidation and Cancer*, Academic Press, London, 1982, p. 101.
- [2] H. Kappus, in H. Sies (Editor), *Oxidative Stress*, Academic Press, London, 1985, p. 273.
- [3] A. Benedetti, A. Pompella, R. Fulceri, A. Romani and M. Comporti, *Biochim. Biophys. Acta*, 876 (1986) 658.
- [4] A. Benedetti, M. Comporti and H. Esterbauer, *Biochim. Biophys. Acta*, 620 (1980) 281.
- [5] G. Poli, M.U. Dianzani, K.H. Cheeseman, T.F. Slater, J. Lang and H. Esterbauer, *Biochem. J.*, 227 (1985) 619.
- [6] K. Fukuzawa, T. Seko, K. Minami and J. Terao, *Lipids*, 28 (1993) 497.
- [7] E.N. Frankel, *J. Am. Oil Chem. Soc.*, 61 (1984) 1908.
- [8] M. Comporti, A. Benedetti, M. Ferrali and R. Fulceri, *Front. Gastrointest. Res.*, 8 (1984) 46.
- [9] H. F. Hoff, J. O'Neil, G.M. Chisolm III, T.B. Cole, O. Quehenberger, H. Esterbauer and G. Jürgens, *Arteriosclerosis*, 9 (1989) 538.
- [10] B. Halliwell and J.M.C. Gutteridge, *FEBS Lett.*, 128 (1981) 347.
- [11] M. Curzio, H. Esterbauer, C. Di Mauro, G. Cecchini and M.U. Dianzani, *Biol. Chem. Hoppe-Seyler*, 367 (1986) 321.
- [12] F.J.G.M. van Kuijk, D.W. Thomas, R.J. Stephens and E.A. Dratz, *Methods Enzymol.*, 186 (1990) 399.
- [13] H. Esterbauer and W. Wegner, *Monatsh. Chem.*, 98 (1967) 1994.
- [14] G. Bringmann, M. Gassen and R. Lardy, unpublished results.
- [15] S. A. Kamath, F. A. Kummerow and K. Narayan, *FEBS Lett.*, 17 (1971) 90.
- [16] T.F. Slater and B.C. Sawyer, *Biochem. J.*, 123 (1971) 805.
- [17] W.A. König, *The Practice of Enantiomer Separation by Capillary Gas Chromatography*, Hüthig, Heidelberg, 1987.
- [18] Z. Juvancz, G. Alexander and J. Szejtli, *J. High Resolut. Chromatogr. Chromatogr. Commun.*, 10 (1987) 105.
- [19] H. Esterbauer, *Monatsh. Chem.*, 102 (1971) 824.
- [20] M.S. Rees, F.J.G.M. van Kuijk, R.J. Stephens and B.P. Mundy, *Synth. Comm.*, 23 (1993) 757.

Effect of the sample solvent and instrument design on the reproducibility of retention times and peak shapes in packed-column supercritical fluid chromatography

Roger M. Smith *, David A. Briggs

Department of Chemistry, Loughborough University of Technology, Loughborough, Leics. LE11 3TU, UK

(First received November 30th, 1993; revised manuscript received February 18th, 1994)

Abstract

Factors affecting the reproducibility of retention times and peak shapes in supercritical fluid chromatography on a cyano-bonded silica packed column have been studied. These included the inclusion of low proportions of modifier in the eluent and the solvent used to inject the analyte. With carbon dioxide as the eluent, polar sample solvents were found to cause residual effects, which changed subsequent separations. These effects were lost when an eluent modifier was present suggesting that they resulted from temporary masking of silanol groups on the silica surface. If the mobile phase was cooled to near the critical point between the oven and a spectroscopic detector, small changes in conditions caused baseline fluctuations, which was considered to be due to changes in the refractive index of the solution.

1. Introduction

Supercritical fluid chromatography (SFC) is now generally accepted as a viable complementary technique to gas-liquid chromatography or high-performance liquid chromatography (HPLC). However, relatively few studies have been reported which examine the reproducibility of retention times or the effect of experimental factors, such as sample preparation, sample solvent or instrument design. This is probably because with a few exceptions, such as the stability control of antipruritic preparations reported by Anton *et al.* [1], SFC methods have not yet been adopted within routine operational or quality control laboratories. Instead they have

found their greatest application in research areas or as a sample introduction system for mass spectrometry. One likely reason is that most SFC systems currently in use have been based on existing HPLC or gas chromatography instruments, rather than having been designed specifically for SFC. The resulting methods have not been robust and have proved difficult to adapt for operation with unskilled personnel.

The aim of the present study was to investigate some of the operating parameters and sample preparation practices that might effect the reproducibility of retention times of a typical packed-column system, with particular interest in separations using low proportions of modifier. During an earlier study of the separation of homologous series of phenylalkanols and phenylalkanoic acids [2], although retention times were re-

* Corresponding author.

producibile during a single day, it was difficult to obtain reproducible day-to-day results. It was also noted that there was a considerable change in the retention of phenylalkanols on changing the solvent used for the preparation of the samples.

Packed-column SFC systems, both commercial and laboratory-made are typically derived from dual-pump HPLC instruments by the addition of a cooler to the pump head of the reciprocating pump used for carbon dioxide and of a back-pressure regulation device [3–6]. Early studies by Greibrokk *et al.* [3] reported that over a short term, a packed-column system could give a retention time reproducibility of 1.3% (relative standard deviation, R.S.D.). However, in a later paper [4] they reported some problems at low flow-rates with check valves. Simpson *et al.* [5] reported that the temperature of the cooled pump head was important and that above 1°C the flow-rate was considerably reduced. To avoid the problem of cooling the pump heads, helium head pressures can be employed to deliver the carbon dioxide to the pump as a liquid. However, this method has been reported to result in different retention times to non-pressurised systems and Rosselli *et al.* [7] observed that the changes appeared to depend on the instrument being used. Subsequently, Görner *et al.* [8] suggested that the differences could be caused because helium was soluble in the carbon dioxide and could reduce its density and hence its elution strength.

Another potential source of variation in retention time is the reliability of the composition of the mobile phase. In previous work, we have noted that at low levels of a modifier the selectivity of a separation would be highly sensitive to small changes in concentration [9]. Because of the very low modifier flow-rates that are often needed it might be difficult to maintain a sufficiently high reproducibility of eluent composition with reciprocating pumps. However, in a recent study Morissey *et al.* [10] reported good reproducibility of retention times (0.3–1.75%) during eluent programming up to 10% modifier for the separation of polymer additives. Although it has been reported that cylinders of premixed sol-

vents can be employed to avoid mixing problems, Schweighardt and Mathias [11] found that the composition delivered to the column changes with the extent of usage because of the different volatilities of the carbon dioxide and modifier.

The solvent used to inject the analyte onto the column may be a further potential source of retention variation. In a recent review of injection techniques, Kirschner and Taylor [12] reported that considerable effort had gone into the study of injection methods for capillary SFC because it is relatively easy to overload the column. Large volumes of polar solvents can have a significant effect on retention and solvent elimination methods, such as the work of Brosard *et al.* [13] for waxes, or peak focussing, as described by Bouissel *et al.* [14] for aqueous samples, have been needed to obtain good results. The review also noted that apart from preparative-scale samples, the injection solvent was usually considered to have little effect in packed-column separations [12]. However, Schoenmakers *et al.* [15] found that for a number of liquid crystal components, the retention time was dependent on the sample size suggesting a self-deactivation effect. However, the results were independent of the sample solvent and the effect was not observed with modified eluents.

2. Experimental

2.1. Chemicals and samples

The samples of the phenylalkanols and decanophenone were of laboratory grade from a range of suppliers. Carbon dioxide was of laboratory grade from British Oxygen Company and solvents were of HPLC grade from Fisons Scientific Equipment.

2.2. Equipment

The supercritical fluid separations were carried out using a JASCO (Tokyo, Japan) system, consisting of a 880 PU pump with cooled pump head for the delivery of carbon dioxide at 2 ml

min⁻¹ and a PU-980 pump for the delivery of modifier. For low levels of modifier (<1%), a customised Acurate microflow processor (LC Packings, Amsterdam, Netherlands) [16] was used to split the flow from the modifier pump. The eluent was mixed in a SP8500 dynamic mixer (Spectra-Physics) and passed to a cyano Capcell SG120 column (150 mm × 4.6 mm; Shiseido, Yokohama, Japan) in a 860-CO column oven. The peaks were detected using a 875-UV ultraviolet detector fitted with a high-pressure flow cell and a 880-81 back-pressure regulator. The chromatograms were recorded using a Jones JCL6000 chromatographic data system software on an Elonex 386SX computer. Samples (5 µl) were injected using a 7125 valve (Rheodyne, Cotati, CA, USA) fitted with a 20-µl loop.

3. Results and discussion

In a recent study of the separation of phenylalkanol and phenylalkanoic acids [2], there was concern that the results showed poor reproducibility. Although for a packed-column system it might be assumed that similar precision to a HPLC separation should be achievable, SFC may be regarded as inherently less robust because of the high sensitivity of the eluent strength to temperature and pressure as well as composition. The need for a restrictor or back-pressure regulator introduces an additional component, which might cause problems as it can suffer from blocking or icing-up on decompression of the eluent. The diversity of SFC designs, different pumps, different back pressure systems, and restrictors or pressure vent valves, could cause a particular system to differ to a greater or lesser extent than another so that previous claims may not be a useful guide to expected results.

3.1. Retention reproducibility

To determine the reproducibility for typical analytes with supercritical carbon dioxide as the eluent, the retentions of benzyl alcohol, 3-phenylpropanol, 5-phenylpentanol and de-

canophenone in isooctane were determined on a cyano-bonded silica column over a 7-day period. The experiment ran continuously for two days (six injections) then was turned off for a weekend and restarted for three further days (twelve injections) (Fig. 1). The same instrument settings, carbon dioxide flow-rate of 2 ml min⁻¹, back-pressure regulator at 150 bar and column temperature of 60°C, were used in both runs. The exit gas flow-rate, pump-head coolant temperature and ambient temperature were monitored throughout the runs.

The retention times of the analytes (Table 1) showed significant variations with R.S.D.s of 4.8–6.6%. The relative retention times compared to decanophenone as an internal standard were much better with a R.S.D. of 1.1–1.5%. This suggested that the principal variations were in the retentive capacity of the system rather than in the selectivity of the separation. However, the mean retention times for decanophenone (mean t_R = 8.85 min, S.D. 0.15) from the first two days were markedly different from the results for the second period (mean t_R = 9.52 min, S.D. 0.65). The corresponding

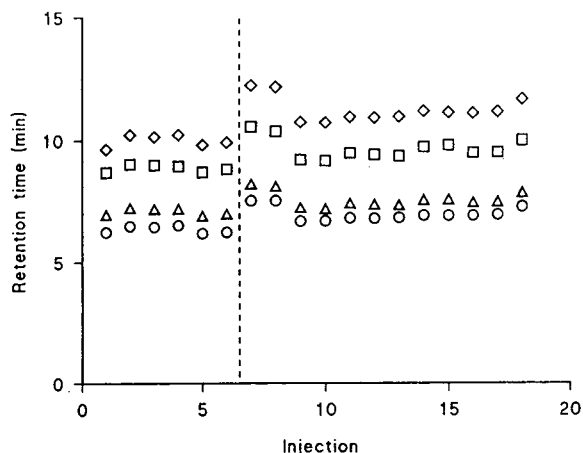


Fig. 1. Reproducibility of retention times using SFC over a 7-day period. Conditions: column, cyano Capcell; eluent, carbon dioxide; temperature, 60°C; pressure, 150 bar. Analytes: ○ = benzyl alcohol; △ = 3-phenylpropanol; □ = decanophenone; ◇ = 5-phenylpentanol. The system was run for six assays over two days, turned off for two days (marked by the dotted line), and then run for a further twelve assays over three days.

Table 1
Reproducibility of retention in packed-column SFC

Compound	Retention time (min)			Relative retention time		
	Mean	S.D.	R.S.D. (%)	Mean	S.D.	R.S.D. (%)
Benzyl alcohol	6.77	0.39	5.81	0.721	0.009	1.25
3-Phenylpropanol	7.32	0.35	4.85	0.780	0.009	1.15
Decanophenone	9.38	0.53	5.67	1.000		
5-Phenylpentanol	10.81	0.72	6.63	1.152	0.018	1.54

Conditions: column, cyano Capcell SG120; eluent, carbon dioxide; flow-rate, 2 ml min⁻¹; pressure, 150 bar; temperature, 60°C; detection, 254 nm. Retentions, relative retentions compared to decanophenone, standard deviations (S.D.) and relative standard deviations (R.S.D.) were based on 18 measurements over 7 days.

mean relative retention times for 5-phenylpentanol changed from 1.13 to 1.16. It therefore appeared that both the selectivity and the absolute retentions were changing and the effects of a number of potential variables in the system were examined.

There was concern that the flow-rate delivered by the pump, and hence the flow through the column, might be affected by density changes in the liquid carbon dioxide in the pump head. The coolant temperature of the pump head was therefore deliberately altered between -12°C to +1°C. Apart from a large increase in retention at the highest temperature when the carbon dioxide might not be completely condensed [5], there was only a small increase in retention times with increasing temperature. Over the range of temperatures observed in the reproducibility test, from -10.5 to -12.1°C, this effect would have a negligible effect. This study does identify a potential source of variation between systems as often the pump head temperature is not controlled as carefully as the column temperature. The eluent gas flow-rate exiting the column, pressure drop across the column and ambient temperature were also recorded but no systematic correlations could be obtained with changes in retention times. It was concluded that there were no obvious instrumental causes for the poor reproducibility.

3.2. Low modifier flow-rates

In capillary SFC the addition of a modifier to the eluent primarily alters the properties of the

mobile phase and thus a significant proportion is required for the effect to be apparent. In contrast, in packed-column SFC, a marked change occurs with even very small amounts of modifier suggesting a surface effect on the stationary phase [17,18]. The present study had initially set out to examine separations with low percentages of modifier. However, in order to introduce 1.0% modifier into a carbon dioxide rate of 1 ml min⁻¹ a flow-rate of 10 µl min⁻¹ of modifier is required, which is at or smaller than the specification of many reciprocating pumps. In previous work, an attempt to prepare a eluent of 2% methanol in carbon dioxide eluent for supercritical fluid extraction had been made using a pump, which was claimed to have the capability of 10 µl min⁻¹. When the eluent flow was examined using an ultraviolet spectroscopic detector at 254 nm it gave a flat baseline. However, if the detection wavelength was changed to 205 nm, it was clear that modifier flow was only occurring during the final part of each piston stroke. The pump was therefore delivering regular but discrete pulses of modifier to the carbon dioxide. Even the introduction of a stirred mixing chamber with a volume of 2.5 ml was unable to even out the variation in the composition. It was felt that this problem was probably being accentuated by the compressibility of the carbon dioxide eluent and relatively high pressures being used. As soon as the flow-rate from the modifier pump diminished slightly, the pressurised carbon dioxide backed up the modifier inlet tube, effectively stopping the flow. Similar problems probably also occur in dual-pump HPLC separations, although it is rare

for such low proportions of a minor component to be employed in reversed-phase separations, except in the early stages of a gradient. In normal-phase chromatography, the much easier approach of a premixed eluent is usually adopted as there is rarely a requirement for gradient elution.

To determine if this was a general problem, four further commercial HPLC pumps were tested for the addition of modifier to an SFC system, two dual-head pumps and two master/slave systems, each with a specified minimum flow-rate capability of 10 or 1 $\mu\text{l min}^{-1}$. Acetone was used as the test modifier and its concentration in the column eluent was monitored using a spectroscopic detector set at 260 nm. The pumps were assessed using a packed column at 50°C, a carbon dioxide flow-rate of 4 ml min^{-1} and a back-pressure regulator setting of 200 or 100 bar. All the pumps gave a pulsating signal for the modifier (for example see Fig. 2). The magnitude of the pulsation was dependent on the volume of the pump head. As the specified modifier flow-rates decreased the signal for the acetone decreased in each case. However, the

magnitude of the signals was not proportional to the nominal flow-rates suggesting that the eluent composition differed from the value that had been set. Although one pump stood out as giving a particularly low pulsation, its flow stopped completely below 15 $\mu\text{l min}^{-1}$.

Clearly none of these pumps could be used at the 0.1% level with any confidence and these results must raise questions about published work, which has claimed to use similar levels without confirmation of the eluent composition. Two alternatives can be used, either syringe pumps or flow splitting. The former was ruled out because of the cost (4–5 times greater than a reciprocating pump). Studies were therefore carried out using a commercial capillary flow splitter [16]. As these are normally intended for work against a relatively low back-pressure in a liquid chromatography system, a specially modified version was provided by the manufacturer, which was designed to work against the higher pressure in SFC. To achieve a split with this system it is necessary to have a certain pressure drop across the splitter and thus the inlet pressure must be raised significantly about the column head pressure.

The principal problem with the splitter was that it was difficult to calibrate the system *in situ*. The outlet flow for a given inlet flow could be easily measured when the unit was not connected to the SFC system but in use the flow would differ because of the high back-pressure of the eluent in the SFC system, which might typically range from 100 to 400 bar. As methanol lacks a chromophore, it could not easily be measured directly at these low levels in the carbon dioxide eluent. Because the split ratio is dependent on the viscosity of the modifier, methanol cannot be replaced by an alternative solvent with a chromophore. Instead the flow-rates with no back-pressure were measured and these were used as nominal maximum flow-rates. At an input flow of methanol of 0.3 ml min^{-1} and an inlet pump pressure of 160 bar the splitter delivered 4.3 $\mu\text{l min}^{-1}$ and at 0.7 ml min^{-1} and 375 bar, it delivered 8.6 $\mu\text{l min}^{-1}$.

When the splitter was employed in a SFC system, for the same modifier inlet flow a higher pressure was recorded suggesting that there was

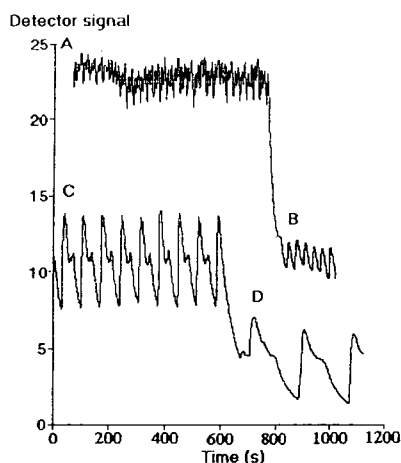


Fig. 2. Test of reciprocating pumps for the addition of modifier to carbon dioxide. Conditions; carbon dioxide flow-rate, 4 ml min^{-1} ; modifier, acetone; back-pressure, 200 bar; spectroscopic detection, 260 nm. Pumping systems: A, modifier pump with 10 μl pump head volume set at 50 $\mu\text{l min}^{-1}$ of modifier; B, as A set at 20 $\mu\text{l min}^{-1}$; C, modifier pump with 100 μl pump head volume set at 50 $\mu\text{l min}^{-1}$ modifier; D, as C set at 20 $\mu\text{l min}^{-1}$.

increased resistance to flow. There was no evidence of fluctuations in composition in the outlet flow. As well as being unable to determine the exact flow-rate, two further problems were encountered with this system. Firstly only a narrow nominal outlet range of 4.3 to 10.2 $\mu\text{l min}^{-1}$ modifier could be obtained before the maximum pressure setting of the input pumping system was exceeded. Secondly the range of modifiers which could be used was limited by their viscosity. Solvents such as isopropanol gave no outlet flow even when used without a back-pressure.

This system was used in the subsequent work in the paper but modifier proportions of less than 0.5% must be regarded as nominal maximum values.

3.3. Solvent effects

In many cases, with alkyl-bonded silica-based packed columns, the primary mode of retention in SFC is normal-phase interaction with the underlying silanols so that the column behaves in very much a normal-phase mode [19,20]. Under these conditions, the separations can potentially be influenced by the solvent used to prepare the sample if it can interact strongly with the stationary phase. These interactions might also alter the retention of subsequent analytes if the solvent remained on the silica and masked active groups on the surface.

Preliminary experiments using a cyano-bonded silica had suggested that solvent effects were occurring with the phenylalkanols as there were considerable differences in the retentions of 3-phenylpropanol, 4-phenylbutanol and 5-phenylpentanol, when injected as samples in isooctane ($t_R = 4.8, 5.8$ and 7.1 min, respectively) or in methanol ($t_R = 3.5, 3.7$ and 3.9 min, respectively) into carbon dioxide at 60°C and 160 bar. The peak shapes were also markedly different, which suggested that when the samples were injected as solutions in isooctane they were interacting strongly with the stationary phase (Fig. 3). Although the cyano-bonded column material used in this study is reported to be prepared by coating the silica surface with a polymer [21], it has previously been found to

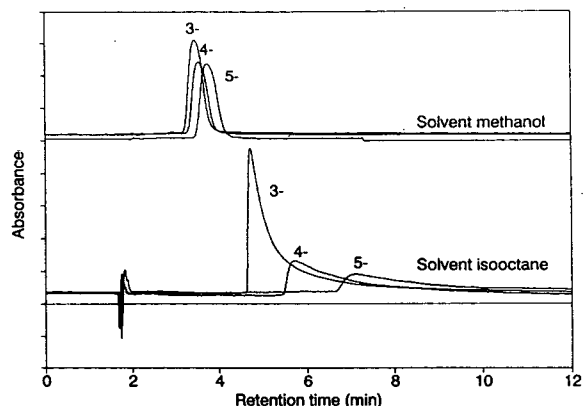


Fig. 3. Separations of 3-phenylpropanol, 4-phenylbutanol and 5-phenylpentanol injected as solution in isooctane and methanol. Conditions: column, cyano Capcell; eluent, carbon dioxide; temperature, 60°C ; pressure, 160 bar; detection, 254 nm.

shown strong interactions with analytes in SFC [19].

The experiment was then repeated with a series of phenylalkanols from benzyl alcohol to 5-phenylpentanol using both carbon dioxide and 0.2% methanol modified carbon dioxide as the eluent (Table 2). The retentions generally increased with the molecular mass, as in the earlier study [2], but in each case the samples injected in isooctane were more highly retained than those injected in methanol. The difference between the solvents was reduced in the methanol-modified eluent. The retention of the phenylalkanols appeared to be more effected by the sample solvent than by the proportion of modifier in the mobile phase. When the chromatograms were examined, isooctane was found to cause a solvent disturbance peak but the methanolic solutions showed no signal suggesting that the methanol might have been adsorbed onto the column.

To determine the effect of different solvents, samples of 2-phenylethanol and 4-phenylbutanol as solutions in methanol, isopropanol, tetrahydrofuran (THF) and hexane were chromatographed using an increasing proportion of methanol as a modifier in carbon dioxide (Table 3 and 2-phenylethanol, Fig. 4). At low levels of modifier there were marked differences between

Table 2

Effect of sample solvent on phenylalkanols in the presence and absence of modifier

	Capacity factor			
	0% Methanol		0.21% Methanol	
	Sample solvent		Sample solvent	
	Isooctane	Methanol	Isooctane	Methanol
Benzyl alcohol	—	1.12	1.35	0.85
2-Phenylethanol	1.40	0.84	1.56	0.85
3-Phenylpropanol	1.81	1.24	1.60	1.17
4-Phenylbutanol	2.31	1.22	1.84	1.30
5-Phenylpentanol	3.50	1.31	2.25	1.64

Conditions: column, cyano Capcell SG120; eluent, carbon dioxide; flow-rate, 2 ml min⁻¹; column outlet pressure, 160 bar; temperature, 60°C; detection, 254 nm.

the solvents in each case. Generally the retentions decreased with increasing polarity of the solvent. The differences were reduced as the proportion of modifier in the eluent increased and above 0.5% modifier each of the solvents gave the same retention times suggesting that all the silanols were effectively masked. These results suggested that the more polar solvents were contributing to the deactivation of the stationary

phase. The extents of the interactions can be related to the effectiveness of the solvents as modifiers in SFC. Blilie and Greibrokk [22] found that hexane had little effect on retention but the alcohols and THF reduced the interaction with the stationary phase. Berger and Deye [18] reported that on cyano and other polar columns, less polar modifiers such as THF and acetonitrile gave poorer peak shapes than

Table 3

Effect of different sample solvents on retention times with different proportions of methanol as modifier in the eluent

Compound	Solvent	Retention time (min)				
		Methanol (%)				
		0.0	0.21	0.43	1.0	2.0
2-Phenylethanol	Methanol	2.39	2.49	2.41	2.25	2.01
	Isopropanol	2.97	2.93	2.49	2.21	2.04
	THF	2.99	3.14	2.50	2.21	2.05
	Hexane	3.16	3.31	2.47	2.21	2.04
4-Phenylbutanol	Methanol	3.06	3.11	2.99	2.65	2.30
	Isopropanol	4.20	3.69	3.06	2.62	2.36
	THF	4.10	4.57	3.05	2.61	2.35
	Hexane	4.12	3.31	3.13	2.63	2.35

Conditions: column, cyano Capcell SG120; eluent, carbon dioxide with methanol modifier; flow-rate, 2 ml min⁻¹; column outlet pressure, 151 bar; temperature, 60°C; detection, 254 nm.

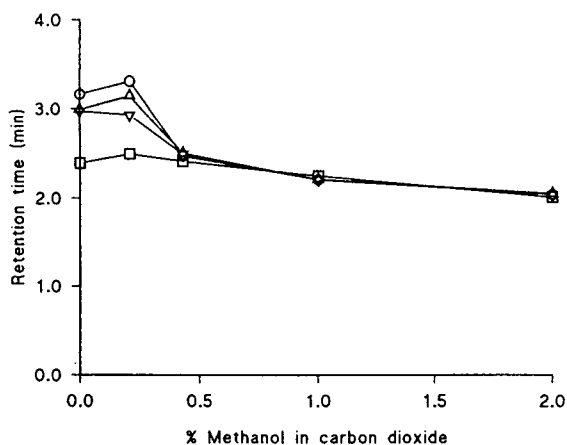


Fig. 4. Effect of sample solvent on retention time of 2-phenylethanol. Conditions as in Fig. 3: eluent, carbon dioxide containing different proportions of methanol as modifier. Sample solvents: \circ = hexane; \triangle = THF; ∇ = isopropanol; \square = methanol.

polar additives, such as methanol. This reflected results by Levy and Ritchey [23] who found that the effect of modifiers and level of effective complete deactivation depended on the nature of the analyte and stationary phase.

There was concern that the interaction of the sample solvent would effectively represent a temporary but uncontrolled modification of the stationary phase activity, which might influence subsequent samples even if these were in a low-polarity solvent. A series of studies was carried out to determine the persistence of the solvent effect on retention. When the injection of a sample of 5-phenylpentanol in methanol was directly followed by a sample in isooctane, the retention time of the analyte from the second solution was slightly longer but the peak shape was much better (Fig. 5). Further injections in isooctane showed a steady reversion to the typical isooctane sample retention time and peak shape. These results suggested that two effects were occurring. Firstly, the initial methanol injection had deactivated the silica surface and this reduced tailing in subsequent injections. This effect continued until sufficient carbon dioxide had passed through the column to wash out the methanol and regenerate the active sites. Secondly, because the first isooctane injection

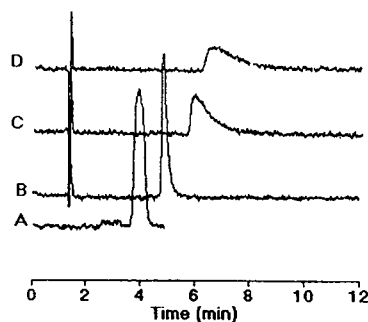


Fig. 5. Separation of 5-phenylpentanol injected successively in different solvents. Solvents: A = methanol; B, C and D = sequential injections in isooctane. Conditions as in Fig. 3.

gave a sharper peak for 5-phenylpentanol than the peak from the methanol injection, the sample solvent appeared to be having a direct effect on the band broadening. The methanol solvent was acting as a strong eluent causing rapid elution and hence band broadening until significant mixing occurred with the carbon dioxide mobile phase. The less polar isooctane solvent acted as a weak eluent on the deactivated column giving sharp peaks. Similar band broadening caused by a sample solvent, which is a stronger eluent than the mobile phase, is well recognised as a problem in HPLC [24] but does not appear to have been reported previously in packed-column SFC.

In a more extensive study, five 5- μ l samples of 5-phenylpentanol in methanol were injected at 1-min intervals onto the column with carbon dioxide as the mobile phase. These injections were used to calculate the peak height on a methanol-deactivated column. After a delay of 10 min, a 5- μ l sample of 5-phenylpentanol in isooctane was injected. As the 5-phenylpentanol was eluted, a further sample in isooctane was injected to monitor the continuing changes with time. These injections were repeated until the peak heights were nearly constant. The full experiment was then repeated using delays of 15, 20 and 30 min between the methanol solutions and the first isooctane solution. The heights of the peaks for 5-phenylpentanol were monitored as they were a good guide to the peak shapes. For each series of injections there was a sys-

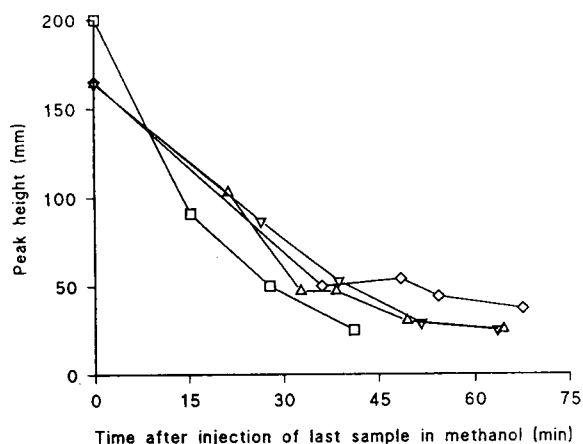


Fig. 6. Change in peak heights for 5-phenylpentanol with time. Peak height at 0 min is the mean of five injections of a solution in methanol. These were followed after: (□) 10 min; (Δ) 15 min; (∇) 20 min and (◇) 30 min by a series of sequential injections of a solution of 5-phenylpentanol in isooctane. Conditions as in Fig. 3.

tematic and nearly exponential decrease in peak height with time after the methanolic samples (Fig. 6), which continued for over 45 min. Although the broadening occurred most rapidly for the set of runs that started after only 15 min, the results were variable and there did not appear to be a significant correlation between the waiting time before injecting the first isooctane sample and the peak shape after a particular time. This suggested that the reactivation of the column occurred at a similar rate irrespective of the number of isooctane samples that had been examined. Thus the primary mode of reactivation appeared to be the slow elimination of the methanol from the column by the carbon dioxide.

The effect of an injection of a sample as a solution in methanol can therefore persist for a considerable time even after that particular sample has eluted. Importantly, the residual methanol on the column can have a significant effect on any subsequent polar samples injected in a less polar solvent altering both their peak shapes and retention times. A related prolonged retention of a polar additive was exploited by Berger and Deye [25] for the separation of phenols. They loaded a diol-bonded silica col-

umn with trifluoroacetic acid and found that it still behaved as a deactivated column even after washing with methanol. Other researchers [26] have found that SFC columns can be conditioned by the repeated injection of basic analytes to deliberately coat the active sites. The observation that the retention times of some analytes can vary with injection size can be considered to be a form of self deactivation [15].

Despite these observations, the deactivation effect of a polar sample solvent does not appear to have been widely reported in SFC and the preparation of samples for packed-column SFC is rarely mentioned. However, the effect is not new in chromatography and frequently occurs in normal-phase HPLC using non-polar mobile phases. In that case, traces of a polar solvent can disrupt the separation and change selectivity and resolution [27]. It can also take a considerable time to reactivate the column. Consequently, low proportions of a polar modifier are frequently included in the mobile phase to improve the stability of the system [27,28].

Steuer *et al.* [29] have reported that, if the mobile phase composition was altered in SFC, the system stabilised much more rapidly than in HPLC (10–20 column volumes compared to over 300 volumes). However, the present study suggests that subsequent samples can still be affected and this effect could be a contributor to poor reproducibility in some SFC separations. For example, samples containing traces of moisture even in apparently low-polarity solvent could also have an effect on subsequent retentions although this was not tested.

3.4. Baseline noise

During this work, an attempt was made to work at lower pressures so that a less dense mobile phase could be examined. However, at 100 bar the baseline of the detector response became very unstable and acceptable results could not be recorded (Fig. 7, part A). Careful investigation suggested that the noise was caused by the detector rather than the pumping or column system. Surprisingly, the baseline stabil-

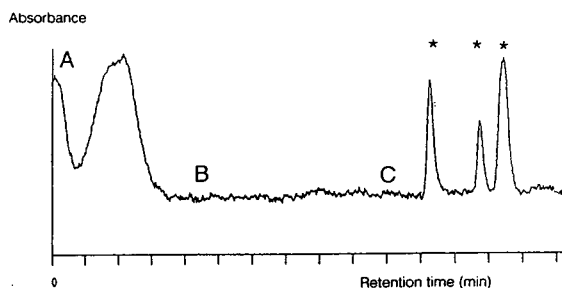


Fig. 7. Effect of temperature fluctuations in the connecting tubing on the baseline of spectroscopic detector at low eluent pressures. Conditions: column, cyano Capcell; eluent, carbon dioxide; temperature, 60°C; pressure, 100 bar. Detector response at 260 nm: A, background signal with no precautions; B, background signal with cooling to 0°C between oven and detector; C, effect of holding the connecting tubing between two fingers at *.

ised on increasing the pressure even though this would put more mechanical strain on the system.

As in many converted HPLC systems, the detector flow cell in the present chromatograph was external to the column oven and was effectively at ambient temperature. Heat loss from the connecting tubing carrying the eluent to the detector would cause the eluent to cool from the oven temperature of 60°C. As a result, the eluent in the detector flow cell would probably be near to the critical point particularly at low pressures. Under these circumstances the refractive index of carbon dioxide is very susceptible to even small changes in the temperature {typical values at 1500 p.s.i. (ca. 103 bar), $n = 1.1580$ at 37°C and 1.0587 at 71°C [30]}. Thus even small changes in the temperature, such as those caused by sunlight or drafts near the connecting tubing, would cause significant changes in the refractive index. This would result in changes in the path of the light through the detector flow cell and baseline noise. The present system was so sensitive at 100 bar that significant changes in the baseline could be produced by holding the connecting tubing between two fingers (Fig. 7, part C). Once the problem was identified, the noise could be almost eliminated by cooling the eluent between the oven and detector in an icebath so that it was subcritical and was therefore not as sensitive to small changes in the conditions (Fig.

7, part B). This approach was more successful than attempting to maintain the connecting tubing at the oven temperature. Although there was a heat-exchanger coil built into the detector prior to the flow cell, it appeared that this was insufficient to stabilise the temperature. However, the detector was originally designed for HPLC use, where large temperature changes or such a high sensitivity of the refractive index of the eluent to the conditions in the flow cell are rarely found.

4. Conclusions

Although there have been a number of claims of high reproducibility for SFC separations, these are not always easy to replicate. Many of the problems observed in the present study can be attributed to deactivation effects of the active surface of the stationary phase. These will be more serious for polar analytes which are being retained partly by a normal-phase mechanism and will be worsened if polar solvents are used to prepare the sample solutions. Although the reactivation of the column will be faster in SFC than in normal-phase HPLC, the retention and peak shapes of subsequent injections may still be affected for a significant time. The effects can be reduced by the introduction of a modifier into the eluent to mask the silanol sites but a consequence can be the loss of retention and possibly of selectivity from the column, although the peak shapes will often improve. These studies emphasise that a normal-phase type of interaction is often a significant contributor to packed-column SFC retentions.

The importance of the solvent used to prepare sample for SFC, experimental limitations in the preparation of eluents containing low proportions of modifier, and of sensitivity of the refractive index of the eluent to conditions in the detector flow cell near the critical point were also identified as problems in packed-column SFC. Some of these effects have been recognised by manufacturers and equipment specifically designed to work with supercritical fluids is now becoming available.

5. Acknowledgements

The authors thank the Science and Engineering Research Council for a research grant, Shiseido Ltd. for column materials and LC Packings for the loan of equipment.

6. References

- [1] K. Anton, M. Bach and A. Geiser, *J. Chromatogr.*, 553 (1991) 71.
- [2] R.M. Smith and D.A. Briggs, *J. Chromatogr.*, submitted for publication.
- [3] T. Greibrokk, A.B. Blilie E.J. Johansen and E. Lundanes, *Anal. Chem.*, 56 (1984) 2681.
- [4] T. Greibrokk, J. Doebl, A. Farbrod and B. Iversen, *J. Chromatogr.*, 371 (1986) 145.
- [5] R.C. Simpson, J.R. Gant and P.R. Brown, *J. Chromatogr.*, 371 (1986) 109.
- [6] R.M. Smith and M.M. Sanagi, in R.M. Smith (Editor), *Supercritical Fluid Chromatography*, Royal Society of Chemistry, London, 1988, Ch. 2.
- [7] A.C. Rosselli, D.S. Boyer and R.K. Houck, *J. Chromatogr.*, 465 (1989) 11.
- [8] T. Görner, J. Dellacherie and M. Perrut, *J. Chromatogr.*, 514 (1990) 309.
- [9] R.M. Smith and M.M. Sanagi, *Chromatographia*, 26 (1988) 77.
- [10] M.A. Morissey, A. Giorgetti, M. Polasek, N. Pericles and H.M. Widmer, *J. Chromatogr. Sci.*, 29 (1991) 237.
- [11] F.K. Schweighardt and P.M. Mathias, *J. Chromatogr. Sci.*, 31 (1993) 207.
- [12] C.H. Kirschner and L.T. Taylor, *J. High Resolut. Chromatogr.*, 16 (1993) 73.
- [13] S. Brossard, M. Lafosse, M. Dreux, and J. Becart, *Chromatographia*, 36 (1993) 268.
- [14] S. Bouissel, F. Erni and R. Link, *J. Chromatogr.*, 630 (1993) 307.
- [15] P.J. Schoenmakers, L.G.M. Uunk and P.K. Bokx, *J. Chromatogr.*, 459 (1988) 201.
- [16] J.P. Chervet, C.J. Meijvogel, M. Ursem and J.P. Salzmann, *LC·GC Int.*, 4 (1991) 32.
- [17] J.G.M. Janssen, P.J. Schoenmakers and C.A. Cramers, *J. High Resolut. Chromatogr.*, 12 (1989) 645.
- [18] T.A. Berger and J.F. Deye, *J. Chromatogr. Sci.*, 29 (1991) 280.
- [19] R.M. Smith, S. Cocks, M.M. Sanagi, D.A. Briggs and V.G. Evans, *Analyst*, 116 (1991) 1281.
- [20] P.J. Schoenmakers, L.G.M. Uunk and H.-G. Janssen, *J. Chromatogr.*, 506 (1990) 563.
- [21] O. Shiota, Y. Ohtsu and O. Nakata, *J. Chromatogr. Sci.*, 28 (1990) 553.
- [22] A.L. Blilie and T. Greibrokk, *Anal. Chem.*, 57 (1985) 2239.
- [23] J.M. Levy and W.M. Ritchey, *J. Chromatogr. Sci.*, 24 (1986) 242.
- [24] L.R. Snyder and J.J. Kirkland, *Introduction to Modern Liquid Chromatography*, Wiley, New York, 2nd ed., 1979, p. 298.
- [25] T.A. Berger and J.F. Deye, *J. Chromatogr. Sci.*, 29 (1991) 54.
- [26] M. Ashraf-Khorassani and L.T. Taylor, in C.M. White (Editor), *Modern Supercritical Fluid Chromatography*, Hüthig, Heidelberg, 1988, p. 115.
- [27] L.R. Snyder and J.J. Kirkland, *Introduction to Modern Liquid Chromatography*, Wiley, New York, 2nd ed., 1979, p. 374.
- [28] J.J. Kirkland, C.H. Dilks and J.J. DeStefano, *J. Chromatogr.*, 635 (1993) 19.
- [29] W. Steuer, M. Schindler and F. Erni, *J. Chromatogr.*, 454 (1988) 253.
- [30] G.J. Besserer and D.B. Robinson, *J. Chem. Eng. Data*, 18 (1973) 137.

Experimental study of band broadening and solute interferences in preparative supercritical fluid chromatography

G. Cretier*, J. Neffati, J.L. Rocca

Laboratoire des Sciences Analytiques, Université Claude Bernard Lyon I, 43 Boulevard du 11 Novembre 1918, F-69622 Villeurbanne Cedex, France

(First received July 21st, 1993; revised manuscript received February 3rd, 1994)

Abstract

The effect of the amount injected on the elution profile of a single solute was used to investigate the shape of the distribution isotherm in overloaded supercritical fluid chromatography. Subsequently, the role of competition between solutes when the column is overloaded with a binary mixture was studied. The band broadening pattern is explained by the difference between the solubilities of the solutes in the supercritical fluid mobile phase.

1. Introduction

The main interest in preparative supercritical fluid chromatography (PSFC) is that the separation of the collected substance from the mobile phase is theoretically easy as a decrease in solvating power of the supercritical fluid mobile phase can be obtained simply by pressure reduction. Although the application of PSFC on a small scale was suggested as early as 1962 [1] and the feasibility of large-scale PSFC was demonstrated in 1982 [2], the technique is not yet widely accepted and used. Its development has been limited by some technological difficulties, more particularly the design of efficient devices for sample injection and solute collection (for a complete bibliography, see the reviews by Berger and Perrut [3] and Kirschner and Taylor [4]). Today, the technological problems seem to have been solved and the establishment of PSFC as an optimized purification tool requires a

better understanding of the band broadening mechanism under column overload conditions and in the case of multi-component samples. Such fundamental studies were the origin of the recent and spectacular developments in preparative liquid chromatography (PLC).

This paper presents some results of an experimental study of the competitive adsorption phenomena when the column is overloaded with a binary mixture. The objective was to exhibit the solute elution profiles when the column is heavily overloaded and the eluted bands considerably overlap. For this purpose, the chosen test solutes have large spectral differences so that a judicious adjustment of the detection wavelength in each experiment allowed only one of the two injected solutes to be detected. It was also necessary to eliminate any source of extraneous band broadening and, in order to avoid peak distortion resulting from partial flooding of the column by the liquid solvent of the sample [5], we used the sample solvent evaporation injection technique investigated previously [6,7]:

* Corresponding author.

the sample solution is first loaded in a pre-column, then the sample solvent is removed by using a flow of warm helium in a similar manner to gas chromatography and finally the supercritical fluid mobile phase is introduced into the precolumn to sweep the sample on to the separation column.

2. Experimental

2.1. Supercritical fluid chromatograph

Fig. 1 shows the system used for the experiments. The liquid CO_2 pump (4) was a Shimadzu (Kyoto, Japan) LC-6A equipped with a cooling jacket kept at 5°C by means of a Julabo F30-HC circulation bath (Julabo Labortechnik, Seelback, Germany). The modifier pump (5) was a Waters Model 6000A (Waters–Millipore, Milford, MA, USA) modified for delivering micro flow-rates. The mixing between liquid CO_2 and the organic modifier is achieved by placing downstream of the tee-piece a 150×4.6 mm I.D.

column (6) packed with $100\text{-}\mu\text{m}$ glass beads. The column inlet pressure is monitored with a Chromatem 944 pressure gauge (7) (Touzart et Matignon, Vitry sur Seine, France). The injection device is composed of two Rheodyne (Cotati, CA, USA) sampling valves, Model 7010 (8) and Model 7125 (9), and a 50×4.6 mm I.D. loading precolumn (10). The injection device, the 250×4 mm I.D. separation column (11) and the back-pressure regulator (14) (Model 26-1724-24; Tescom, Elk River, MN, USA) are immersed in a thermostated water-bath (15) (Polystat 86602; Bioblock Scientific, Illkirch, France). The Shimadzu SPD-6A UV spectrophotometer (12) equipped with a high-pressure cell of volume $3\text{ }\mu\text{l}$ and optical path 6 mm is connected to an integrator (C-R5A; Shimadzu). For collecting a small amount of component, the Tescom back-pressure regulator is by-passed and the solute is trapped in a collection solvent (17) by using a $34\text{ mm} \times 50\text{ }\mu\text{m}$ I.D. fused-silica restrictor (16). The collection flask (18) is topped by a condenser (19) in order to avoid any loss of solute resulting from formation of an

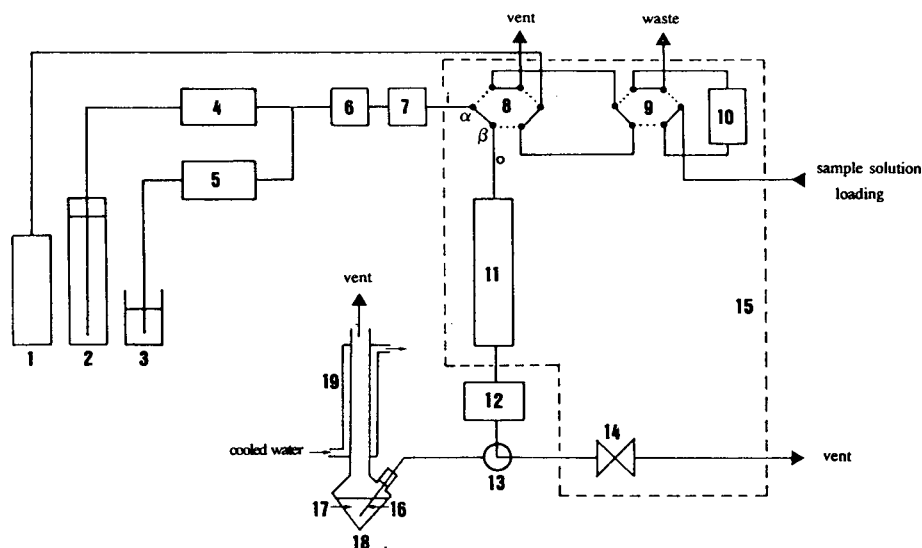


Fig. 1. Schematic diagram of the supercritical fluid chromatograph. 1 = Helium cylinder; 2 = liquid CO_2 cylinder; 3 = modifier solvent tank; 4 = CO_2 pump; 5 = modifier pump; 6 = mixer; 7 = column inlet pressure gauge; 8 and 9 = six-way valves (— load position; --- inject position); 10 = precolumn; 11 = column; 12 = UV detector; 13 = three-way valve; 14 = back-pressure regulator; 15 = thermostated bath; 16 = linear fused-silica restrictor; 17 = trapping solvent; 18 = cone-shaped flask; 19 = condenser; i and o = tubings connected to positions α and β of sampling valve 8.

aerosol by decompression of the supercritical fluid inside the trapping solvent.

2.2. Procedures

For evaporating the sample solvent prior to injection, first both valves 8 and 9 are in the load position (see Fig. 1) and the sample solution is introduced directly into the precolumn by means of a syringe (Model 702 or 725; Hamilton, Bonaduz, Switzerland) while the supercritical fluid mobile phase is flowing through the separation column. Second, valve 9 is rotated to the inject position and a regulated flow of helium is delivered through the precolumn to remove the sample solvent. Third, valve 8 is switched to the inject position, the supercritical fluid mobile phase flows through the precolumn in the reverse direction and the solventless sample is swept on to the column with minimum band broadening.

For determination of the purity of the collected solute, the contents of the collection flask were quantitatively analysed with a Shimadzu LC-6A liquid chromatograph using the external standardization method.

2.3. Chemicals and experimental conditions

Liquid CO₂ (99.99% pure) and HP-grade helium were supplied by Carboxyque Française (Venissieux, France). All solvents (methanol, heptane and ethyl acetate) were of HPLC grade (Carlo Erba, Milan, Italy). Acetic acid, orthophosphoric acid and all solutes (benzyl alcohol, methylparaben and vanillin) were of RP grade (Prolabo, Paris, France). The loading precolumn and the separation column were laboratory-packed with Kromasil C₁₈, 5 µm (Eka Nobel, Surte, Sweden).

For supercritical fluid chromatographic experiments, the elution conditions were as follows: the temperatures of the helium flow, precolumn, column and back-pressure regulator were 60°C; the organic modifier was a 0.01 mol l⁻¹ methanolic solution of orthophosphoric acid at a flow-rate of 75 µl min⁻¹; the liquid CO₂ flow-rate was 1.7 ml min⁻¹, which corresponded to a mobile phase composition of CO₂–methanolic modifier

(95.8:4.2); the opening of the back-pressure regulator and the length of the linear restrictor were adjusted so that the column inlet pressure was maintained at 112 bar; the detection wavelength was chosen for each experiment; and samples were dissolved in methanol.

For liquid chromatographic analysis of the collected fractions, the elution conditions were as follows: the stationary phase was LiChroprep Si 60, 5–20 µm (Merck, Darmstadt, Germany), laboratory-packed in a 150 × 4.6 mm I.D. column; the mobile phase was heptane–ethyl acetate–acetic acid (85:15:1), which was also used as a trapping solvent in supercritical fluid experiments; the elution flow-rate was 1 ml min⁻¹; and the detection wavelength was 254 nm.

3. Results and discussion

3.1. Elution profile of a single solute

Because there is no interference between the migrating solutes, the behaviour of a single solute yields little information on the separation in preparative chromatography. However, in order to gain an insight into the mechanisms that govern the distribution of the solute between the mobile and stationary phases, it is instructive to investigate the variation of the concentration profile of a single solute under overload conditions.

Fig. 2 shows how an increase in the amount injected influences both the dispersion of the peak front and the sharpening of the peak rear. First, it was checked that these fronting peaks were not the result of the combined effects of partial saturation of the stationary phase during the introduction of the sample solution into the precolumn and reversal of the flow through the precolumn during the transfer of the solventless sample from the precolumn to the column. If so, tailing peaks should be obtained with no reversal of the flow direction. Consequently, the same experiments were carried out after connection of tubings (i) and (o) to positions β and α, respectively, of the sampling valve (8) (Fig. 1); with

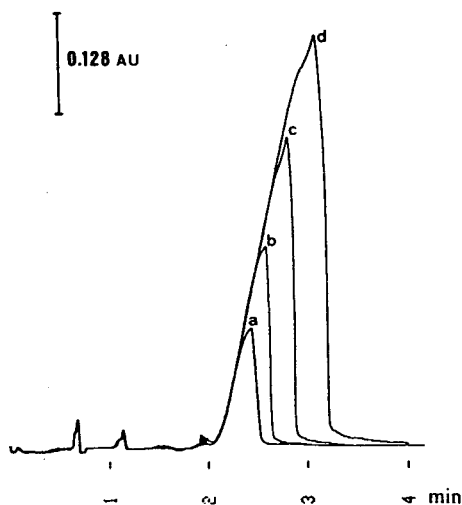


Fig. 2. Effect of amount injected on the peak shape of a single solute. Solute, vanillin; volume injected, 20 μ l; amount injected, (a) 1.6, (b) 3.2, (c) 6.4 and (d) 12.8 μ mol; detection wavelength, 338 nm.

this configuration, the flow through the precolumn was no longer reversed and the sample was forced to migrate along the whole length of the precolumn before being transferred to the column. Fig. 3 shows that the peaks obtained under these conditions are slightly delayed and distorted, but with a band broadening pattern that is identical with that observed during the previous experiments: as the injected amount is increased, the elution time of the peak front

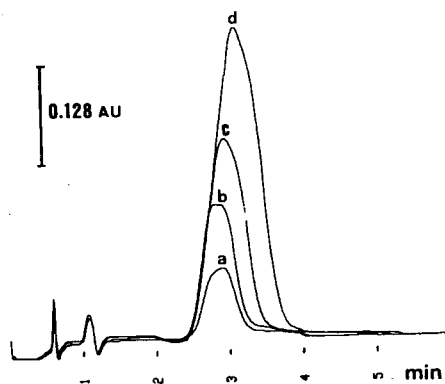


Fig. 3. Same as Fig. 2, except tubings (i) and (o) were connected to positions β and α , respectively, of the sampling valve (8) (see text).

remains constant while the peak rear elutes progressively later. This result confirms that the overload effects observed in Fig. 2 do not depend on some band broadening phenomenon associated with the injection process on the precolumn.

However, two other types of phenomena can explain the change in peak profile with increasing amount of solute. The fronting peak can result from either a concave distribution isotherm due to limited solubility of the solute in the supercritical fluid mobile phase or competition between the solute and the organic modifier of the supercritical fluid mobile phase for the stationary phase surface. Indeed, fronting peaks have been observed in PLC with binary eluents containing a strongly sorbed additive [8,9]. In the latter instance, the peak front should move to earlier retention times when the amount of solute is increased [8], which is not observed in Figs. 2 and 3. Hence the solute follows a true concave distribution isotherm and the overload effects observed in Figs. 2 and 3 only arise from the low solvating power of the supercritical fluid mobile phase.

3.2. Elution profile of the second-eluted component of a binary mixture

The chromatograms in Fig. 4a correspond to the separation of benzyl alcohol and vanillin when increasing amounts of benzyl alcohol are co-injected with a constant amount of vanillin. Comparison with the peak obtained when the same amount of vanillin is injected alone (Fig. 4b) indicates clearly that the vanillin peak shifts to higher retention times as the benzyl alcohol load is increased. This phenomenon, known as the restriction effect [10] or the retainment effect [11], is related to limited solubility of the solutes in the supercritical fluid mobile phase: when the load of the more soluble solute 1 is increased, the minor and less soluble solute 2 is forced out of the supercritical fluid mobile phase and, consequently, is more retained than it would be if it was injected as a pure component.

Identical with the displacement effect occurring with convex isotherms in PLC [12], this

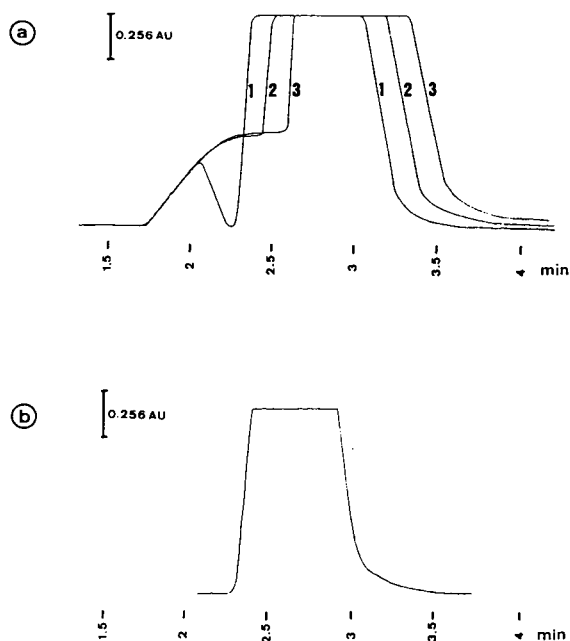


Fig. 4. Effect of amount of the first-eluted component (benzyl alcohol) injected on the elution profile of the second-eluted component (vanillin). Detection wavelength, 243 nm; volume injected, 20 μ l; amount of vanillin injected, 10 μ mol. (a) Chromatograms of binary mixture with increasing injected amounts of benzyl alcohol: 1 = 10; 2 = 30; 3 = 50 μ mol. (b) For comparison, peak corresponding to 10 μ mol of vanillin injected alone.

restriction effect occurring with concave isotherms in PSFC is beneficial and contributes to facilitate the separation. Fig 5a and b illustrate the effect of increasing sample load on chromatograms and elution profiles of the second-eluted component, respectively, for a 25:1 benzyl alcohol–vanillin mixture. The less soluble solute 2 (vanillin) seems to form a zone at the rear of the elution profile of solute 1 (benzyl alcohol) that is clearly driven back as the sample size is increased and the peak rear of solute 1 moves to longer retention times. However, it is difficult to visualize the relative overlapping of the two elution profiles because, on the one hand, the benzyl alcohol elution profile cannot be monitored selectively, and on the other, whatever the detection wavelength chosen, the UV absorptivity of vanillin is so large that it is impossible to have a close representation of the 25:1 sample

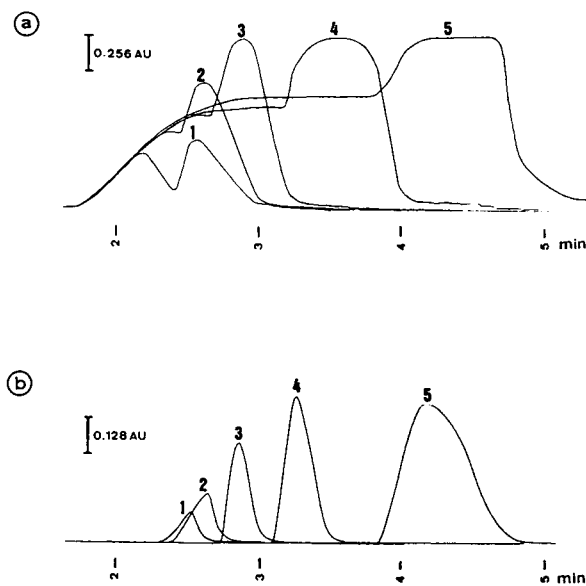


Fig. 5. Effect of sample size on separation of a 25:1 benzyl alcohol–vanillin mixture. (a) Chromatograms monitored at 243 nm; (b) elution profiles of vanillin monitored at 330 nm where benzyl alcohol has no UV absorption. Volume injected and sample concentration: 1 = 20 μ l, 0.65 mol l⁻¹; 2 = 20 μ l, 1.3 mol l⁻¹; 3 = 20 μ l, 2.6 mol l⁻¹; 4 = 40 μ l, 2.6 mol l⁻¹; 5 = 80 μ l, 2.6 mol l⁻¹.

composition. Therefore, in order to qualify the separation obtained in the different experiments in Fig. 5, solute 2 was totally recovered (detection at 330 nm where solute 1 does not absorb, as in Fig. 5b, allowed the collection of solute 2 as soon as it began to elute) and its purity was determined by quantitative liquid chromatographic analysis of the collected fraction (Table 1). Although the sample size is increased, the purity of solute 2 remains approximately constant, which means that the restriction effect prevents band overlapping even if band broadening is occurring.

3.3. Elution profile of the first-eluted component of a binary mixture

The separation of vanillin (solute 1) and methylparaben (solute 2) is used as a model system for the study of the interaction between solutes on the first-eluted component of a binary mixture. Fig. 6 shows the chromatograms and

Table 1

Effect of sample size on purity of vanillin totally recovered from the 25:1 benzyl alcohol–vanillin mixture

Volume injected (μl)	Sample concentration (mol l^{-1})	Sample load (μmol)	Corresponding chromatogram in Fig. 5	Purity of vanillin (%)
20	0.65	13	1	94.9
20	1.3	26	2	94.0
20	2.6	52	3	94.9
40	2.6	104	4	95.3
80	2.6	208	5	95.4

For experimental conditions, see Fig. 5.

the vanillin elution profiles observed for 0.4 μmol of vanillin injected with various larger loads of methylparaben. The vanillin peak shape undergoes broadening and the separation deteriorates as the proportion of methylparaben is increased. This phenomenon, termed the pull-back effect [11], mirrors the tag-along effect

encountered in PLC for convex isotherms [12], but its origin is different. The pull-back effect is related to the limited solvating power of the supercritical fluid mobile phase: although the less retained component, solute 1, is more soluble in the mobile phase than is solute 2, the high concentration of solute 2 results in a shift of the distribution equilibrium of solute 1 away from the mobile phase, leading to a higher retention for solute 1 and increased overlapping between solutes 1 and 2.

Fig. 7a illustrates the overload effect on the elution profile of vanillin for the 1:25 vanillin–methylparaben mixture. Comparison with peaks obtained on injection of the equivalent amounts of vanillin alone (Fig. 7b) indicates clearly that, at high column loading, the pull-back effect can become very detrimental for the separation and recovery of pure solute 2.

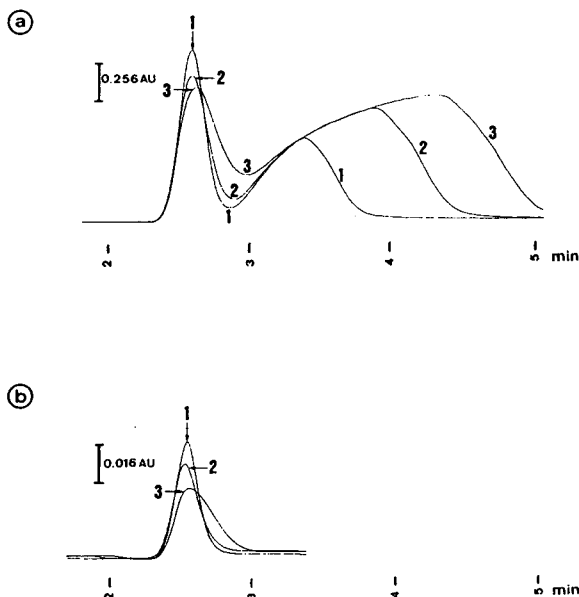


Fig. 6. Effect of amount of the second-eluted component (methylparaben) injected on elution profile of the first-eluted component (vanillin). Volume injected, 20 μl ; amount of vanillin injected, 0.4 μmol ; amount of methylparaben injected, 1 = 2; 2 = 6 and 3 = 10 μmol . (a) Chromatograms monitored at 285 nm; (b) elution profiles of vanillin monitored at 330 nm (wavelength at which methylparaben has no UV absorption).

4. Conclusions

In supercritical fluid chromatography with the sample solvent evaporation injection technique, the fronting behaviour of peaks observed for a single solute under overload conditions results from the concave isotherm, explained by the limited solubility of solute in the supercritical fluid mobile phase. Investigation of solute interferences when peaks overlap has revealed two effects, the restriction effect and the pull-back effect, which are both related to the limited solvating power of the supercritical fluid mobile phase. Hence band broadening in PSFC is gov-

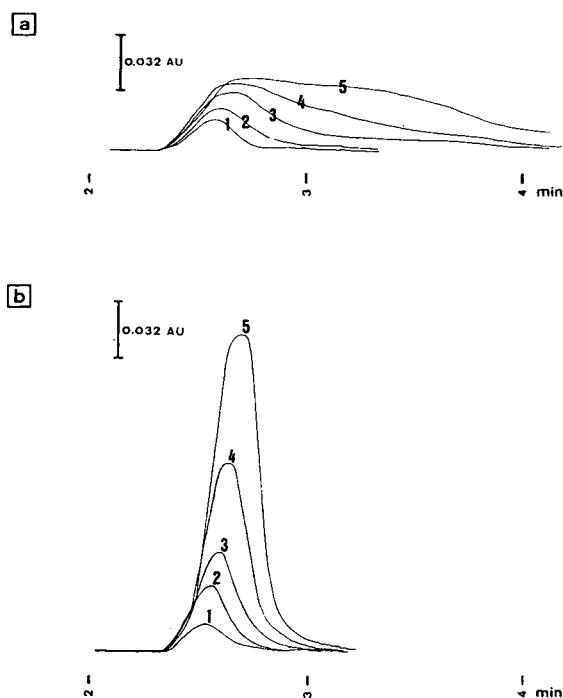


Fig. 7. Effect of sample size on behaviour of the first-eluted component of the 1:25 vanillin–methylparaben mixture. (a) Elution profiles of vanillin monitored at 330 nm (wavelength at which methylparaben has no UV absorption); (b) for comparison, peaks corresponding to the same amounts of vanillin injected alone. Volume injected and sample concentration: 1 = 20 μl , 0.13 mol l^{-1} ; 2 = 20 μl , 0.26 mol l^{-1} ; 3 = 20 μl , 0.52 mol l^{-1} ; 4 = 40 μl , 0.52 mol l^{-1} ; 5 = 80 μl , 0.52 mol l^{-1} .

erned by saturation of the mobile phase and a knowledge of the phase diagram for supercritical eluent–solute 1–solute 2 ternary mixture would make it easier to understand the phenomena and optimization of preparative separations.

PLC references in the literature clearly indicate that, owing to the beneficial displacement effect and the detrimental tag-along effect, a separation is easier when the minor solute is less retained than the major solute. In PSFC, the opposite situation seems to apply: owing to the beneficial restriction (or retainment) effect and the detrimental pull-back effect, a separation is easier when the minor solute is more retained than the major solute.

5. References

- [1] K. Klesper, A.H. Corwin and D.A. Turner, *J. Org. Chem.*, 27 (1962) 700.
- [2] M. Perrut, *Fr. Pat.*, 82 09 649 (1982).
- [3] C. Berger and M. Perrut, *J. Chromatogr.*, 505 (1990) 37.
- [4] C.H. Kirschner and L.T. Taylor, *J. High Resolut. Chromatogr.*, 16 (1993) 73.
- [5] Y. Yamauchi, M. Kuwajima and M. Saito, *J. Chromatogr.*, 515 (1990) 285.
- [6] G. Cretier, R. Majdalani and J.L. Rocca, *Chromatographia*, 30 (1990) 645.
- [7] G. Cretier, R. Majdalani, J. Neffati and J.L. Rocca, *Chromatographia*, in press.
- [8] S. Golshan-Shirazi and G. Guiochon, *J. Chromatogr.*, 461 (1988) 1.
- [9] S. Golshan-Shirazi and G. Guiochon, *J. Chromatogr.*, 461 (1988) 19.
- [10] E.B. Guglya and A.A. Zhukhovitskii, *J. Chromatogr.*, 509 (1990) 157.
- [11] C.A. Lucy, T.L. Luong and S. Elchuk, *J. Chromatogr.*, 546 (1991) 27.
- [12] G. Guiochon and S. Ghodbane, *J. Phys. Chem.*, 92 (1988) 3682.

Chromatographic behaviour of diastereoisomers XII[☆]. Effects of alumina on separations of esters of maleic and fumaric acids

M. Palamareva*, I. Kozekov, I. Jurova

Department of Chemistry, University of Sofia, 1 James Bourchier Avenue, Sofia 1126, Bulgaria

(First received December 20th, 1993; revised manuscript received February 1st, 1994)

Abstract

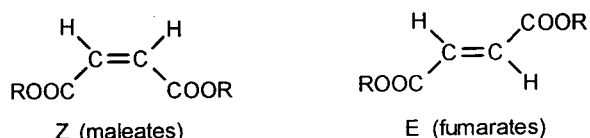
The thin-layer chromatographic separations on three different aluminas of twenty diastereoisomeric 1,2-disubstituted ethenes, ROOCCH=CHCOOR, were studied with 24 mobile phases having strength, ϵ , in the range 0.210–0.250 and a wide variety of solvent selectivity effects. The relative retention of the diastereoisomers was always $Z > E$ independently of the type of the alumina and the increase in the selectivity of the mobile phases and the effective volume of the group R as a result of an expected site chelation via the two ester groups in Z isomers only. A comparison shows that the separations of these diastereoisomers are similar with both alumina and silica using a given mobile phase. However, the overall separation obtained on any alumina is better than that found for silica.

1. Introduction

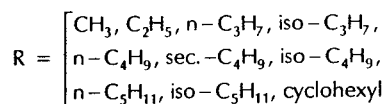
A series of papers (see, *e.g.*, refs. 1–6) have reported the thin-layer chromatographic (TLC) separation and relative retentions of more than 150 conformational flexible and rigid diastereoisomers. The role of steric effects, the adsorption of two adjacent solute groups on one adsorbent site or the so-called site chelation [7] and mobile phase selectivity effects [7–11] have been discussed in detail.

Recently, we reported [1] that the diastereoisomeric 1,2-dialkoxycarbonylethenes of type 1 show on silica a stronger retention of the Z

isomer than that of the corresponding E isomer as a result of site chelation via the two ester groups only in the former isomer. The above-mentioned importance of steric effects, site chelation and solvent selectivity effects on silica makes it interesting to study similar separations on alumina, the other widely used adsorbent



type 1



* Corresponding author.

[☆] For Part XI, see ref. 1.

in normal-phase liquid–solid chromatography (LSC). This paper deals with the TLC behaviour on alumina of the twenty diastereoisomers of type 1 studied previously [1] having two equal adsorbing groups COOR with an increasing volume of R. The choice of mobile phases was made by a microcomputer program [12] based on Snyder's theory [7–10] as an easier alternative [1,2,13,14] to the trial-and-error approach used in LSC separations of other *Z*–*E* diastereoisomers [15–45].

2. Experimental

Details of the synthesis and ^1H NMR spectra of compounds 1–20 in Table 2 are given in ref. 1.

TLC was done as in ref. 5 using three different aluminas, namely (1) aluminium oxide (Riedel-de Haën, Hannover, Germany), (2) acidic alu-

minium oxide (Merck, Darmstadt, Germany) and (3) neutral aluminium oxide (Merck). The adsorbent number corresponds to the adsorption activity (see below). A slurry of 60 g of adsorbent and 90 ml of distilled water was spread on four 20×20 cm plates by means of an apparatus according to Stahl. The samples were $2 \mu\text{l}$ of a solution prepared from 60 mg of each solute and 1.4 ml of toluene. The reproducibility of the R_F values was ± 0.03 unit, which is worse than that in ref. 1 because of some tailing in the most instances. R_F values in Table 2 are arithmetic means of four to eight measurements.

3. Results and discussion

Table 1 lists the mobile phases used together with values of strength, ϵ , localization, m , and polarity, P' . The values were calculated by

Table 1

Mobile phases studied and the corresponding computer-calculated [12] values of strength, ϵ , localization, m , and polarity P'

No.	Components	Composition (vol.-%)	ϵ	m	P'
1	Hexane–diethyl ether	84.8:15.2	0.210	0.57	0.51
2	Hexane–toluene	63.24:36.76	0.220	–0.16	0.95
3	Hexane–diethyl ether	82.3:17.7	0.220	0.58	0.58
4	Hexane–acetone	99.03:0.97	0.220	0.90	0.15
5	Hexane–ethyl acetate	97.9:2.1	0.220	0.72	0.19
6	Hexane–tetrahydrofuran	97.0:3.0	0.220	0.77	0.22
7	Hexane–tetrachloromethane–methylene chloride	82.1:10.0:7.9	0.220	0.30	0.74
8	Hexane–toluene–diethyl ether	82.5:10.0:7.5	0.220	0.43	0.53
9	Hexane–chloroform–diethyl ether	84.8:10.0:5.2	0.220	0.42	0.64
10	Hexane–tetrachloromethane–diethyl ether	76.5:10.0:13.5	0.220	0.54	0.62
11	Hexane–tetrachloromethane–diethyl ether	69.0:20.0:11.0	0.220	0.50	0.70
12	Hexane–tetrachloromethane–diethyl ether	60.55:30.0:9.45	0.220	0.43	0.81
13	Hexane–tetrachloromethane–diethyl ether	51.65:40.0:8.35	0.220	0.35	0.93
14	Hexane–tetrachloromethane–diethyl ether	42.5:50.0:7.5	0.220	0.29	1.05
15	Hexane–tetrachloromethane–diethyl ether	14.3:80.0:5.7	0.220	0.13	1.45
16	Hexane–tetrachloromethane–diethyl ether	4.84:90.0:5.16	0.220	0.10	1.59
17	Hexane–diisopropyl ether–1,2-dichloroethane	74.9:20.0:5.1	0.220	–	0.73
18	Hexane–chloroform–ethyl acetate	89.5:10.0:0.5	0.220	0.46	0.52
19	Hexane–toluene–chloroform–diethyl ether	83.93:5.0:5.0:6.07	0.220	0.43	0.58
20	Hexane–tetrachloromethane–toluene–methylene chloride–ethyl acetate	89.3:3.33:3.33:3.33:0.7	0.220	0.47	0.36
21	Hexane–tetrachloromethane–diisopropyl ether–toluene–methylene chloride–diethyl ether	80.87:2.5:2.5:2.5:2.5:9.14	0.220	–	0.59
22	Hexane–diethyl ether	79.4:20.6	0.230	0.59	0.66
23	Hexane–diethyl ether	76.24:23.76	0.240	0.60	0.74
24	Hexane–diethyl ether	72.74:27.26	0.250	0.60	0.84

means of the above-mentioned microcomputer program [12]. The mobile phases are arranged in terms of increasing ϵ and increasing number of solvents when ϵ is constant. Ten different non-localizing and localizing solvents were used for the preparation of the mobile phases. The non-localizing or weakly localizing solvents were hexane, toluene, methylene chloride, chloroform, tetrachloromethane and 1,2-dichloroethane [9]. The mobile phases were composed of two to six solvents showing a limited variation in ϵ (0.210–0.250) and greater variations in m and P' , *i.e.*, in solvent selectivity effects. Mobile phases 1, 3 and 22–24 are composed of hexane and diethyl ether in different ratios and have increasing ϵ . Mobile phases 2–21 have constant ϵ (0.220).

Table 2 summarizes the structure and the configuration of the compounds studied, their R_F values obtained on the three aluminas and the derived values of the separation factor, α , of the diastereoisomeric pairs which were calculated by the following equation:

$$\log \alpha = R_{M(Z)} - R_{M(E)} \quad (1)$$

where the subscripts E and Z specify the isomer (see ref. 1 for the R_F – R_M conversion). Fig. 1 shows the separations established.

According to Table 2, $\log \alpha$ is positive in all cases studied, which corresponds to a stronger retention of the Z isomer than that of the corresponding E isomer taking into account Eq. 1. This relative retention, being the same as that found on silica [1], did not depend on the structure of the compounds, type of alumina or mobile phase used.

The discussions required some data about the adsorption of groups available in solute molecules. According to Snyder's theory, a group i is adsorbed if the mobile phase used has ϵ less than a critical value, ϵ_c , which is calculated on the basis of the free energy of adsorption of the group, Q_i^0 , and its effective area under adsorption, a_i (see the contribution of Snyder in ref. 46 and also ref. 47). Table 3 summarizes the values according to Snyder [7] of the three parameters mentioned above for different groups of interest.

It also includes values of net free energy of adsorption ($Q_i^0 - \epsilon a_i$) when $\epsilon > 0$. The values shown concern mobile phases 2–21 with $\epsilon = 0.220$.

3.1. Microcomputer-aided choice of the mobile phases used

LSC separations by means of TLC and high-performance liquid chromatography (HPLC) of diastereoisomeric substituted ethenes have been widely reported [7 (p. 315), 15–45] because of the importance of such compounds including vitamin A and terpenes. Most of the separations uses the normal-phase LSC on predominantly silica or alumina (*cf.*, ref. 10, p. 92). The selection of the mobile phases in these separations have been done only by the trial-and-error approach.

Recently [1,2,13,14], we chose the mobile phases for TLC separations on the basis of Snyder's theory [7–10] and the microcomputer program [12] which was applied also in this study. Thus, the choice of the mobile phases for alumina 1 began with mobile phase 6 showing R_F values of compounds 1–20 in a favourable range, 0.13–0.46. Using the microcomputer program, we calculated the strength $\epsilon = 0.220$ of the mobile phase and selected the remaining mobile phases of the same or close ϵ . Greater variation of ϵ was not tried because some compounds could remain at the start line and other compounds could move to the front. Details of the microcomputer choice of the mobile phases are given in refs. 1, 2, 13 and 14.

A comparison of the R_F values of a given compound obtained with a given adsorbent and all mobile phases with $\epsilon = 0.220$ showed a mean standard deviation (S.D.) for the three aluminas of 0.11. Consequently, Snyder's theory and the microcomputer program used permitted an easier choice of similar mobile phases.

3.2. Role of the alumina type on retention

The adsorbents used were of two types: neutral (aluminas 1 and 3) and acidic (alumina 2). Mobile phase 3 is the only mobile phase used

Table 2
Experimental R_F values and derived values of $\log \alpha$ for the diastereoisomeric compounds 1–20 of type 1

R	Solute	R_F on alumina 1 for indicated mobile phase									
		Configuration	No.	2	3	4	5	6	7	8	19
CH ₃	Z	1	1	0.07	0.23	0.08	0.15	0.13	0.15	0.12	0.17
				0.14	0.45	0.15	0.29	0.30	0.24	0.24	0.29
CH ₂ CH ₃	E	2	2	0.08	0.31	0.09	0.15	0.18	0.16	0.14	0.20
				0.17	0.58	0.20	0.36	0.36	0.26	0.34	0.37
CH ₂ CH ₂ CH ₃	Z	4	4	0.09	0.34	0.09	0.20	0.20	0.15	0.16	0.20
				0.18	0.58	0.19	0.39	0.38	0.25	0.35	0.38
CH(CH ₃) ₂	E	6	6	0.08	0.39	0.09	0.22	0.22	0.16	0.17	0.21
				0.18	0.64	0.21	0.39	0.42	0.26	0.39	0.41
CH ₂ CH ₂ CH ₂ CH ₃	Z	8	8	0.10	0.41	0.09	0.18	0.22	0.15	0.17	0.21
				0.20	0.66	0.21	0.40	0.44	0.25	0.40	0.40
CH(CH ₃)CH ₂ CH ₃	E	10	10	0.09	0.44	0.09	0.21	0.23	0.16	0.19	0.23
				0.20	0.70	0.22	0.38	0.44	0.27	0.42	0.43
CH ₂ CH(CH ₃) ₂	Z	12	12	0.09	0.42	0.08	0.21	0.23	0.18	0.19	0.23
				0.19	0.68	0.22	0.38	0.43	0.28	0.42	0.43
CH ₂ CH ₂ CH ₂ CH ₂ CH ₃	E	14	14	0.09	0.43	0.08	0.20	0.21	0.15	0.18	0.22
				0.20	0.68	0.20	0.37	0.44	0.24	0.40	0.44
CH ₂ CH ₂ CH(CH ₃) ₂	Z	16	16	0.08	0.44	0.08	0.21	0.38	0.46	0.25	0.42
				0.07	0.44	0.07	0.18	0.23	0.16	0.17	0.21
Cyclohexyl	E	20	20	0.17	0.69	0.18	0.34	0.44	0.21	0.40	0.43

Log α for indicated mobile phase											
1–2	0.33	0.43	0.31	0.36	0.46	0.25	0.37	0.30			
3–4	0.37	0.49	0.40	0.50	0.41	0.27	0.50	0.37			
5–6	0.34	0.43	0.37	0.41	0.39	0.27	0.45	0.39			
7–8	0.40	0.44	0.42	0.36	0.41	0.27	0.50	0.42			
9–10	0.35	0.45	0.42	0.48	0.45	0.27	0.51	0.40			
11–12	0.40	0.47	0.45	0.37	0.42	0.31	0.49	0.40			
13–14	0.37	0.47	0.51	0.37	0.40	0.25	0.49	0.40			
15–16	0.40	0.45	0.46	0.37	0.48	0.25	0.48	0.45			
17–18	0.46	0.47	0.48	0.39	0.45	0.21	0.49	0.43			
19–20	0.43	0.45	0.46	0.37	0.42	0.14	0.51	0.46			

R_f on alumina 2 for indicated mobile phase		3	9	10	11	12	13	14	15	16	17	18	20	21	22	23	24
1	Z	0.27	0.26	0.30	0.22	0.31	0.25	0.30	0.29	0.37	0.32	0.20	0.08	0.16	0.35	0.40	0.45
2	E	0.50	0.43	0.52	0.42	0.58	0.46	0.54	0.54	0.61	0.59	0.36	0.22	0.40	0.58	0.65	0.69
3	Z	0.36	0.29	0.37	0.29	0.39	0.31	0.34	0.33	0.42	0.43	0.22	0.12	0.23	0.45	0.51	0.56
4	E	0.63	0.58	0.71	0.57	0.72	0.60	0.65	0.65	0.73	0.71	0.45	0.25	0.50	0.74	0.80	0.83
5	Z	0.39	0.28	0.42	0.34	0.43	0.31	0.37	0.36	0.45	0.43	0.22	0.13	0.29	0.53	0.61	0.65
6	E	0.66	0.54	0.73	0.63	0.73	0.61	0.66	0.64	0.74	0.79	0.39	0.30	0.55	0.79	0.86	0.88
7	Z	0.41	0.30	0.44	0.36	0.45	0.33	0.37	0.38	0.47	0.53	0.22	0.13	0.31	0.56	0.63	0.68
8	E	0.70	0.57	0.76	0.66	0.74	0.63	0.67	0.64	0.75	0.81	0.40	0.31	0.57	0.80	0.88	0.90
9	Z	0.42	0.31	0.44	0.36	0.46	0.35	0.37	0.38	0.49	0.57	0.23	0.14	0.32	0.57	0.66	0.69
10	E	0.69	0.61	0.77	0.70	0.79	0.64	0.68	0.66	0.75	0.85	0.40	0.34	0.62	0.82	0.90	0.91
11	Z	0.43	0.35	0.50	0.39	0.49	0.34	0.40	0.48	0.53	0.61	0.23	0.14	0.34	0.62	0.67	0.70
12	E	0.69	0.63	0.82	0.72	0.79	0.64	0.69	0.75	0.83	0.85	0.44	0.31	0.60	0.87	0.90	0.91
13	Z	0.43	0.35	0.50	0.39	0.49	0.34	0.40	0.48	0.53	0.61	0.23	0.14	0.34	0.62	0.67	0.70
14	E	0.69	0.63	0.81	0.71	0.78	0.64	0.69	0.75	0.83	0.85	0.44	0.31	0.60	0.87	0.90	0.90
15	Z	0.42	0.33	0.48	0.37	0.49	0.35	0.38	0.49	0.53	0.60	0.23	0.13	0.33	0.62	0.68	0.70
16	E	0.69	0.63	0.81	0.66	0.80	0.63	0.69	0.75	0.80	0.88	0.42	0.30	0.60	0.88	0.90	0.91
17	Z	0.44	0.34	0.50	0.37	0.50	0.36	0.39	0.49	0.53	0.61	0.23	0.13	0.35	0.62	0.68	0.71
18	E	0.71	0.63	0.82	0.68	0.78	0.66	0.69	0.75	0.82	0.88	0.44	0.29	0.62	0.88	0.90	0.90
19	Z	0.41	0.33	0.47	0.38	0.48	0.38	0.33	0.48	0.55	0.59	0.23	0.10	0.30	0.58	0.64	0.67
20	E	0.68	0.57	0.76	0.60	0.77	0.63	0.56	0.74	0.81	0.85	0.40	0.23	0.55	0.84	0.90	0.89
Log α for indicated mobile phase																	
1–2		0.43	0.33	0.40	0.41	0.49	0.41	0.44	0.46	0.42	0.49	0.35	0.51	0.54	0.41	0.45	0.44
3–4		0.48	0.53	0.62	0.51	0.60	0.53	0.56	0.58	0.57	0.51	0.46	0.39	0.52	0.54	0.58	0.59
5–6		0.48	0.48	0.57	0.52	0.55	0.54	0.52	0.50	0.54	0.56	0.36	0.46	0.48	0.53	0.60	0.60
7–8		0.53	0.49	0.60	0.54	0.54	0.54	0.54	0.46	0.53	0.58	0.37	0.47	0.47	0.50	0.64	0.62
9–10		0.49	0.54	0.62	0.62	0.62	0.52	0.56	0.50	0.50	0.63	0.34	0.50	0.54	0.54	0.66	0.65
11–12		0.47	0.50	0.66	0.60	0.60	0.54	0.53	0.51	0.55	0.56	0.42	0.44	0.47	0.62	0.64	0.63
13–14		0.47	0.50	0.63	0.58	0.57	0.54	0.53	0.51	0.55	0.56	0.42	0.44	0.47	0.62	0.64	0.58
15–16		0.49	0.54	0.66	0.52	0.62	0.50	0.56	0.50	0.55	0.69	0.38	0.46	0.49	0.66	0.62	0.63
17–18		0.49	0.52	0.66	0.56	0.55	0.54	0.54	0.50	0.61	0.68	0.42	0.44	0.48	0.66	0.62	0.56
19–20		0.49	0.43	0.55	0.39	0.55	0.44	0.41	0.48	0.54	0.59	0.34	0.43	0.46	0.58	0.70	0.60

(Continued on p. 186)

Table 2 (continued)

R	Solute	R_F on alumina 3 for indicated mobile phase									
		Configuration	No.	1	3	19	22	23	24		
CH_3	Z	1	0.26	0.26	0.21	0.31	0.40	0.40			
	E	2	0.52	0.51	0.41	0.57	0.63	0.66			
CH_2CH_3	Z	3	0.35	0.35	0.27	0.41	0.49	0.51			
	E	4	0.64	0.65	0.52	0.71	0.77	0.78			
$\text{CH}_2\text{CH}_2\text{CH}_3$	Z	5	0.44	0.43	0.31	0.49	0.54	0.60			
	E	6	0.73	0.73	0.59	0.77	0.83	0.85			
$\text{CH}(\text{CH}_3)_2$	Z	7	0.45	0.46	0.33	0.50	0.57	0.63			
	E	8	0.74	0.76	0.61	0.79	0.85	0.87			
$\text{CH}_2\text{CH}_2\text{CH}_2\text{CH}_3$	Z	9	0.46	0.47	0.34	0.51	0.58	0.64			
	E	10	0.77	0.76	0.63	0.80	0.85	0.89			
$\text{CH}(\text{CH}_3)\text{CH}_2\text{CH}_3$	Z	11	0.46	0.48	0.34	0.52	0.62	0.66			
	E	12	0.79	0.79	0.62	0.82	0.88	0.91			
$\text{CH}_2\text{CH}(\text{CH}_3)_2$	Z	13	0.47	0.48	0.34	0.52	0.62	0.66			
	E	14	0.78	0.78	0.62	0.81	0.88	0.91			
$\text{CH}_2\text{CH}_2\text{CH}_2\text{CH}_2\text{CH}_3$	Z	15	0.48	0.48	0.34	0.54	0.62	0.67			
	E	16	0.79	0.77	0.64	0.79	0.88	0.91			
$\text{CH}_2\text{CH}_2\text{CH}(\text{CH}_3)_2$	Z	17	0.47	0.47	0.34	0.52	0.62	0.66			
	E	18	0.77	0.78	0.65	0.80	0.89	0.92			
Cyclohexyl	Z	19	0.45	0.45	0.34	0.49	0.59	0.65			
	E	20	0.75	0.74	0.61	0.74	0.85	0.91			
Log α for indicated mobile phase											
		1-2	0.48	0.47	0.42	0.47	0.41	0.47			
		3-4	0.52	0.54	0.46	0.55	0.54	0.53			
		5-6	0.53	0.55	0.51	0.54	0.62	0.57			
		7-8	0.54	0.57	0.50	0.58	0.63	0.60			
		9-10	0.59	0.55	0.52	0.58	0.61	0.66			
		11-12	0.65	0.61	0.50	0.63	0.66	0.71			
		13-14	0.60	0.58	0.54	0.60	0.66	0.71			
		15-16	0.61	0.55	0.54	0.51	0.66	0.69			
		17-18	0.57	0.60	0.56	0.57	0.70	0.77			
		19-20	0.57	0.54	0.48	0.47	0.59	0.73			

For composition of mobile phases, see Table 1. The values of log α were calculated from R_M values of the corresponding Z-E pair using Eq. 1.

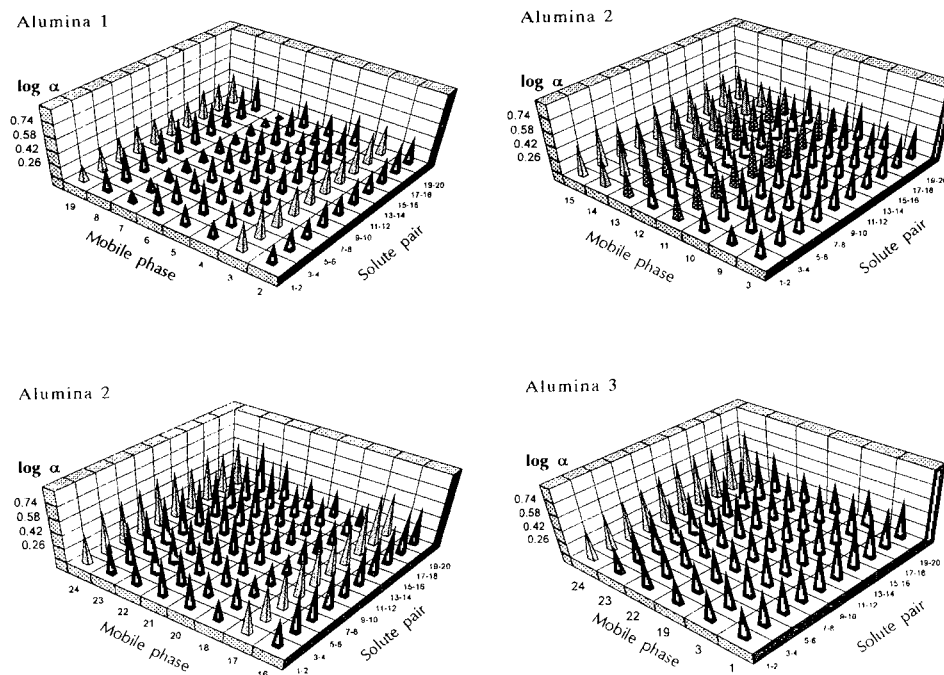


Fig. 1. Three-dimensional representation of all separations α of diastereoisomeric pairs 1–20 obtained on aluminas 1–3 with mobile phases 1–24.

Table 3

Values of Q_i^0 , a_i and derived values of ϵ_{ci} and $Q_i^0 - \epsilon a_i$ on alumina for groups i available in the compounds studied according to Snyder [7]

Group i	Q_i^0	a_i	$\epsilon_{ci} = Q_i^0/a_i$	$Q_i^0 - \epsilon a_i$ ($\epsilon = 0.220$)
C=C	0.31	2.0	0.16	−0.13
CO ₂ CH ₃	4.02	3.0	1.34	3.36
CO ₂ C ₂ H ₅	4.04	3.4	1.19	3.29
CO ₂ C ₃ H ₇ - <i>n</i>	4.06	3.7	1.10	3.25
CO ₂ C ₃ H ₇ - <i>iso</i>	4.01	4.4	0.91	3.04
CO ₂ C ₄ H ₉ - <i>n</i>	4.08	4.1	1.00	3.18
CO ₂ C ₄ H ₉ - <i>sec.</i>	4.03	4.7	0.86	3.00
CO ₂ C ₄ H ₉ - <i>iso</i>	4.03	4.7	0.86	3.00
CO ₂ C ₅ H ₁₁ - <i>n</i>	4.10	—	—	—
CO ₂ C ₅ H ₁₁ - <i>iso</i>	4.05	—	—	—
CO ₂ cyclohexyl	4.12	4.6	0.90	3.11

The values of free energy of adsorption of group i , Q_i^0 , and its effective area under adsorption, a_i , are additive and are calculated on the bases of ref. 7, Tables 8-4 and 10-2. The values for Ar-CO₂CH₃ are taken into account because the ester groups in compounds 1–20 are next to a double bond. ϵ_{ci} is the critical value of ϵ and $Q_i^0 - \epsilon a_i$ is the net free energy of adsorption when $\epsilon > 0$.

with all three aluminas. The corresponding mean R_F values for compounds 1–20 were calculated, namely 0.51, 0.53 and 0.58 for adsorbent 1, 2 and 3, respectively. Consequently, the adsorption activities of the neutral alumina 1 and the acidic alumina 2 are virtually identical and that of the neutral alumina 3 is the lowest.

The retention of compounds 1–20 on any alumina depends on the size of the alkyl group R. Thus, the compounds with *Z* or *E* configuration show increasing R_F values (decreasing retention) with any mobile phase. The increase is distinct when R increases from methyl to *sec.*-butyl and for larger groups the R_F values remain almost constant. This behaviour is in agreement with the decreasing values of net free energy of adsorption for the ester groups shown in Table 3.

Mobile phases 10–16 used with alumina 2 are composed of hexane, tetrachloromethane and diethyl ether in different ratios. All mobile phases have $\epsilon = 0.220$, decreasing m and increasing P' . However, the R_F values of a given

compound obtained with these mobile phases do not vary regularly with m or P' .

Mobile phases 1, 3 and 22–24 of increasing ϵ (0.210–0.250) used with aluminas 2 and 3 give the expected increase in R_F values of compounds 1–20 having a given configuration. Thus, the corresponding R_F values of compound 6 increase from 0.73 to 0.85 on alumina 3.

3.3. Role of the alumina type on separation and comparisons with silica

The mobile phases used with alumina 1 have $\epsilon = 0.220$ and the greatest variation of m from -0.2 to 0.9 . However, the mean values of $\log \alpha$ for compounds 1–20 and a given mobile phase except mobile phase 7 varied in the range 0.39 – 0.48 , *i.e.*, the separations in this instance do not depend significantly on m .

Let us discuss the effect of the adsorbent on the separation $\log \alpha$ of diastereoisomeric pairs studied. Fig. 1 shows that $\log \alpha$ varies from 0.14 to 0.77 , *i.e.*, fair to excellent separations were obtained. The separations of the diastereoisomers on aluminas 2 and 3 are better than those on alumina 1. Relatively poorer but still good separations with $\log \alpha \approx 0.3$ were obtained with mobile phases 2 and 7 composed of non-localizing and weakly localizing solvents. The same is valid for mobile phase 18, which contains the localizing solvent ethyl acetate in a very small amount (0.5 vol.-%). Very good separations having $\log \alpha \approx 0.5$ were obtained with mobile phases 20 and 21, composed of five and six solvents, respectively.

In general, the best separation of diastereoisomers 1–20 ($\log \alpha = 0.6$ – 0.7) was obtained with alumina 2 using mobile phases 10, 12, 17 and 22–24 and alumina 3 using mobile phases 1, 3, 22–24, with both constant and increasing ϵ .

As also seen from Fig. 1, the diastereoisomeric pairs with greater size of the group R and smaller retention usually show better separations. Thus, the diastereoisomeric pairs 17–18 and 19–20 with $R = n - C_5H_{11}$ and cyclohexyl,

respectively, give the best separations with mobile phase 24 on alumina 3.

Concerning a comparison with silica, TLC of compounds 1–20 with hexane–ethyl acetate (98:2) (mobile phase 5 in this study and mobile phase 17 in ref. 1) shows mean values of $\log \alpha$ of 0.40 and 0.38 for alumina 1 and silica, respectively, or virtually identical separations on the two adsorbents with this mobile phase.

The overall separation of a given adsorbent of the diastereoisomeric pairs can be expressed by the mean value of the individual $\log \alpha$ found for this adsorbent. Calculated on the basis of ref. 1 and Table 2 in this paper, the corresponding values are 0.34 (silica), 0.41 (alumina 1), 0.53 (alumina 2) and 0.57 (alumina 3), taking into account that the mobile phases are very different in each instance. Consequently, alumina 3 shows the best overall separation of the diastereoisomeric pairs studied, irrespective of the fact that it has the lowest adsorption activity.

3.4. Expected model of adsorption

The values of ϵ calculated permit a discussion of the model of adsorption for the cases studied. All mobile phases used have ϵ greater than ϵ_c for the double bond (see Table 3) and adsorption of this group is not expected. In contrast, all ester groups should adsorb because $\epsilon < \epsilon_c$. Complicating effects are not assumed because compounds 1–20 do not possess intramolecular hydrogen bonds and are conformational rigid compounds.

The retention of the *Z* isomer is favoured by the site chelation of the two close ester groups on an adsorbent site and hindered by their mutual steric hindrance. The site chelation on alumina is known to predominate over steric hindrance to adsorption (see ref. 7, p. 316). This appears to be true in the cases studied irrespective of the wide variation in the size of group R, explaining the greater retention of any *Z* isomer than that of the corresponding *E* isomer. Site chelation in the last isomer is not possible because of the significantly greater distance between the two ester groups than in the *Z* isomer.

This explains the relative retention $Z > E$ found in all instances studied (cf., ref. 1).

4. Conclusions

The separations achieved showed the following unexpected features: (1) the best separations of the diastereoisomeric pairs studied were obtained on the neutral alumina 3 having the lowest adsorption activity; and (2) better separations were usually obtained for the diastereoisomeric pairs having lower retentions.

5. Acknowledgements

On the occasion of his 75th birthday, we thank Academician B. Kurtev for his participation and interest in the studies in this series. We thank Dr. L.R. Snyder for the very helpful comments on the manuscript. This study was supported by the National Research Fund, Bulgaria.

6. References

- [1] M. Palamareva and I. Kozekov, *J. Chromatogr.*, 606 (1992) 113.
- [2] M.D. Palamareva, B.J. Kurtev and I. Kavrakova, *J. Chromatogr.*, 545 (1991) 161; and references cited therein.
- [3] M.D. Palamareva, B. Kurtev, M. Mladenova and B. Blagoev, *J. Chromatogr.*, 235 (1982) 299; and references cited therein.
- [4] M. Palamareva and L.R. Snyder, *Chromatographia*, 19 (1984) 352.
- [5] L.R. Snyder, M.D. Palamareva, B.J. Kurtev, L.Z. Viteva and J.N. Stefanovsky, *J. Chromatogr.*, 354 (1986) 107.
- [6] M. Palamareva, B. Kurtev and L. Viteva, *God. Sofii. Univ., Khim. Fak.*, 79 (1985) 258.
- [7] L.R. Snyder, *Principles of Adsorption Chromatography*, Marcel Dekker, New York, 1968.
- [8] L.R. Snyder and J.J. Kirkland, *Introduction to Modern Liquid Chromatography*, Wiley-Interscience, New York, 2nd edn., 1979.
- [9] L.R. Snyder, in Cs. Horváth (Editor), *High-performance Liquid Chromatography*, Vol. 3, Academic Press, New York, 1983, p. 157.
- [10] L.R. Snyder, J.L. Glajch and J.J. Kirkland, *Practical HPLC Method Development*, Wiley, New York, 1988.
- [11] E. Soczewiński, *J. Chromatogr.*, 388 (1987) 91; and references cited therein.
- [12] M.D. Palamareva and H.E. Palamarev, *J. Chromatogr.*, 477 (1989) 235.
- [13] M.D. Palamareva, *J. Chromatogr.*, 438 (1988) 219.
- [14] M. Palamareva and I. Kavrakova, *Commun. Dept. Chem., Bulg. Acad. Sci.*, 21 (1988) 218.
- [15] E. Knappe and D. Peteri, *Fresenius' Z. Anal. Chem.*, 190 (1962) 380.
- [16] G. Pastuska and H.J. Petrowitz, *J. Chromatogr.*, 10 (1963) 517.
- [17] L.D. Bergelson, E.V. Dyatlovitskaya and V.V. Voronkova, *J. Chromatogr.*, 15 (1964) 191.
- [18] L.J. Morris, D.M. Wharry and E.W. Hammond, *J. Chromatogr.*, 31 (1967) 69.
- [19] Z. Kwapniewski and K. Szota, *Czas. Tech., M* (1971) 32.
- [20] P. Cooper, *J. Chromatogr.*, 67 (1972) 184.
- [21] H. Thielemann, *Mikrochim. Acta*, (1973) 521.
- [22] E. Fuggerth, *J. Chromatogr.*, 169 (1979) 469.
- [23] R.P. Evershed, E.D. Morgan and L.D. Thompson, *J. Chromatogr.*, 237 (1982) 350.
- [24] Z. Grodzińska-Zachwieja, *J. Chromatogr.*, 241 (1982) 217.
- [25] S. Tammilehto, M. Sysmalainen and P. Makinen, *J. Chromatogr.*, 285 (1984) 235.
- [26] M.C. Monje, A. Lattes and M. Riviere, *J. Chromatogr.*, 521 (1990) 148.
- [27] F. Mikes, V. Schurig and E. Gil-Av, *J. Chromatogr.*, 83 (1973) 91.
- [28] G. Schomburg and K. Zegarski, *J. Chromatogr.*, 114 (1975) 174.
- [29] H. Morrison, D. Avnir and T. Zarrella, *J. Chromatogr.*, 183 (1980) 83.
- [30] R.R. Heath and P.E. Sonnet, *J. Liq. Chromatogr.*, 3 (1980) 1129.
- [31] K. Šlais and J. Šubert, *J. Chromatogr.*, 191 (1980) 137.
- [32] K. Tsukida, R. Masahara and M. Ito, *J. Chromatogr.*, 192 (1980) 395.
- [33] H. Steuerle, *J. Chromatogr.*, 206 (1981) 319.
- [34] S.M. McKay, D. Mallen, P. Shrubsall, J. Smith, S. Baker, W. Jamieson and W. Ross, *J. Chromatogr.*, 214 (1981) 249.
- [35] R. Westwood and P. Hairsine, *J. Chromatogr.*, 219 (1981) 140.
- [36] E.J. Conkerton and D.C. Chapital, *J. Chromatogr.*, 281 (1983) 326.
- [37] B. Buglio and V.S. Venturella, *J. Chromatogr. Sci.*, 22 (1984) 276.
- [38] T. Vaněk, I. Valterová and L. Streinz, *J. Chromatogr.*, 347 (1985) 188.
- [39] Y. Tanaka, H. Sato, A. Kageyu and T. Tomita, *J. Chromatogr.*, 347 (1985) 275.
- [40] B.G. Snider, *J. Chromatogr.*, 351 (1986) 548.

- [41] S.G. Levine, K.D. Barboriak and H.S. Cho, *J. Chem. Educ.*, 65 (1988) 79.
- [42] W.W. Christie and G.H. Breckenridge, *J. Chromatogr.*, 469 (1989) 261.
- [43] N.G. Levis, M. Inciong, K. Dhara and E. Yamamoto, *J. Chromatogr.*, 479 (1989) 345.
- [44] G. Vigh, G. Farkas and G. Quintero, *J. Chromatogr.*, 484 (1989) 251.
- [45] A.P. Leenheer, W. Lambert, J. Bersaques and H. Andre, *J. Chromatogr.*, 500 (1990) 637.
- [46] E. Soczewiński, *Anal. Chem.*, 41 (1969) 179.
- [47] M.D. Palamareva, B.J. Kurtev and M.A. Haimova, *J. Chromatogr.*, 132 (1977) 73.



ELSEVIER

Journal of Chromatography A, 670 (1994) 191–198

JOURNAL OF
CHROMATOGRAPHY A

Overpressured layer chromatography in comparison with thin-layer and high-performance liquid chromatography for the determination of coumarins with reference to the composition of the mobile phase

Pia Vuorela*, Eeva-Liisa Rahko, Raimo Hiltunen, Heikki Vuorela

Pharmacognosy Division, Department of Pharmacy, P.O. Box 15, FIN-00014 University of Helsinki, Helsinki, Finland

(First received September 10th, 1993; revised manuscript received February 9th, 1994)

Abstract

The retention behaviour of fifteen closely related coumarins in normal-phase overpressured layer chromatography (OPLC) was studied with the aim of comparing the retentions with those in normal-phase thin-layer chromatography (TLC) and high-performance liquid chromatography (HPLC) when optimization of the mobile phase was carried out according to the PRISMA system. The mobile phase optimization was carried out on TLC plates in unsaturated chambers. The resulting mobile phases were transposed to off-line, non-equilibrated OPLC and further to HPLC. The retention in TLC was measured at 37 selectivity points and in OPLC and HPLC at 13 points. Capacity factors (k') and separation factors (α) were calculated in order to study the retention behaviour in the different systems. Two- and three-dimensional evaluations of k' against selectivity points showed similar retention behaviours for the coumarins in TLC, OPLC and HPLC. The α values for TLC, OPLC and HPLC showed similar patterns in the three-dimensional evaluations. The retention behaviour at different solvent strengths was also examined. According to quadratic regression, k' showed a dependence on the change in solvent strength. OPLC, which can be considered as a “planar column” technique, and TLC are closely related methods, whereas HPLC shows a different behaviour in the elution process with regard to solvent strength.

1. Introduction

Based on the paper by Kirkland and Glajch [1] and the solvent classification of Snyder [2], the PRISMA optimization model was developed for thin-layer chromatography (TLC) and for high-performance liquid chromatography (HPLC) [3,4]. The model has since been applied to overpressured layer chromatography (OPLC) [5]

and the different types of rotational planar chromatography (RPC) [6,7].

The basic concept of the PRISMA system [4] is first to optimize the solvent strength and subsequently the selectivity in a triangular mixture solvent diagram. The three selectivity-adjusting solvents are selected from ten solvents used in preliminary experiments and diluted, if necessary, by the solvent strength-adjusting solvent. The optimum solvent mixture is found by testing appropriate solvent mixtures located at “selectivity points”. Transfer of the optimized

* Corresponding author.

mobile phase between various planar and column chromatographic methods is one of the concepts used in the PRISMA system [8,9].

To assess the possibilities of transfer between methods, their specific features have to be taken into account. In conventional TLC, the mobile phase moves by means of capillary forces through the porous thin layer always as an unsaturated flow, and the mobile phase content (and correspondingly the phase ratio) varies with the distance from the source to the front [10]. OPLC is a planar chromatographic technique in which the vapour space is eliminated above the sorbent layer by means of overpressure, and the mobile phase must be forced through the stationary phase using pressure [11,12]. The separation time in this kind of forced-flow technique is usually short, the diffusion effects can be reduced and the bands of compounds are small and compact. Because OPLC can be used as an equilibrated or non-equilibrated "planar column" technique, it may be employed as a pilot technique for the transfer of the optimized TLC mobile phase to the various column chromatographic (CLC) methods [13]. CLC is a closed system in which no vapour phase is present and the eluent is forced through by external pressure. HPLC, which is the most established form of CLC nowadays, is used equilibrated with the mobile phase.

In this work, the retention behaviours of fifteen closely related coumarins was studied using three different methods (TLC, OPLC and HPLC) in order to investigate the transfer of the optimized mobile phase from one method to another according to the PRISMA system. Transferring data from the TLC separation to HPLC has been discussed earlier [14]. The retention measurements were performed at 37 selectivity points for TLC and 13 points for OPLC and HPLC, and also at the middle selectivity point 333 using different solvent strengths of the optimized mobile phase. The aim of the study was to determine if the dependences between the capacity factors and/or separation factors at the selectivity points show similar behaviours in the methods when the same mobile phase solvent composition is transferred from one system to another. Therefore, two- and

three-dimensional evaluations were carried out. The solvent strength behaviour of the retentions of the investigated coumarins was also described mathematically and compared between methods. As OPLC is considered as a "column separation in plane" owing to the forced flow of solvent, it was also of interest to discuss which system is actually closer to OPLC.

2. Experimental

2.1. Apparatus

A Linomat IV TLC spotter (Camag, Muttentz, Switzerland) was used to apply the samples on TLC and OPLC plates, and a CS-9000 dual-wavelength flying-spot scanner (Shimadzu, Kyoto, Japan) for the densitometric evaluations. OPLC separations were performed on a Chrompres-25 chromatograph (Factory of Laboratory Instruments, Budapest, Hungary) using a 20-bar external pressure. A pump from Haenni (Switzerland) was used for solvent delivery. Each development was preceded by a prerun with *n*-hexane.

A model 425 HPLC gradient former and a model 420 pump (Kontron Instruments, Rotkreuz, Switzerland), equipped with an ERC-7210 UV detector (ERMA Optical Works, Tokyo, Japan) and a Shimadzu C-R1B integrator were used. The HPLC system was connected to an Olivetti (Ivrea, Italy) model M24 personal computer.

2.2. Chemicals

The coumarins (umbelliferone, herniarin, psoralen, osthol, 2'-angeloyl-3'-isovaleryl vanillin, angelicin, bergapten, oxypeucedanin, osthrol, isobergapten, sphondin, xanthotoxin, imperatorin, pimpinellin and isopimpinellin) and solvents were obtained as described previously ([15]; see also molecular structures).

2.3. Chromatographic conditions

The coumarins were applied in the form of spots (1 μ l of solute in chloroform) in four

groups on the TLC and OPLC plates. The TLC separations were performed on 4×10 cm plates in the ascending one-dimensional mode in 6×22 cm unsaturated N-chambers (Camag) at ambient temperature. The OPLC separations were performed on 10×20 cm plates. The plates were prepared by impregnating all sides with a polymer suspension (Factory of Laboratory Instruments). For the development two channels were scraped in the silica coating, one for the solvent inlet and the other, at a distance of 18 cm, for the solvent outlet. The assays were carried out on alufoil TLC plates coated with silica gel 60 F₂₅₄ (average particle size 10 μ m) (Merck, Darmstadt, Germany). The migration distance and the solvent front were measured with a densitometer at 320 nm.

The column for the HPLC separations was LiChrosorb Si 60 (average particle size 10 μ m) (250×4 mm I.D.) (Merck) at ambient temperature. The flow-rate was 1.0 ml/min and detection was effected at 320 nm. The solvent peak was treated as the dead volume.

2.4. Calculation of retardation data obtained from the analysis

The capacity factors for HPLC (k'_c) were calculated from the equation $k'_c = (t_R - t_0)/t_0$, where t_R is the retention time of the compound and t_0 is the dead time. The retardation values obtained from the TLC plate without correction [$(R_F)_{\text{obs}}$] were converted into capacity factor values (k'_p) using the equation $(1/(R_F)_{\text{obs}}) - 1$ [10,14].

Calculations and statistical evaluations were performed with a StatView II v1.03 program on a Macintosh IIsi computer. For three-dimensional evaluation of the retardation data, Systat v5.1 software was used.

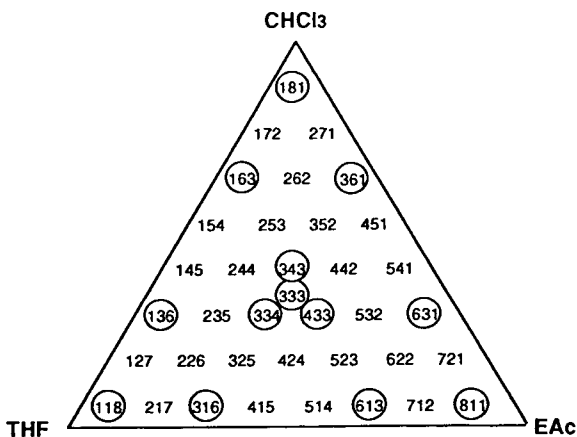
3. Results and discussion

In preliminary experiments, optimization of the mobile phase was performed using the PRISMA model on normal-phase TLC plates in unsaturated chambers as described [14]. Ethyl acetate (solvent strength $S_i = 4.4$), chloroform

($S_i = 4.1$) and tetrahydrofuran ($S_i = 4.0$) in *n*-hexane ($S_i = 0.0$) were found to give the best separation of these coumarins. Retention measurements were performed by TLC at 37 selectivity points (P_s ; see Fig. 1). The solvent strength was adjusted to $S_T = 2.0$ to give retardation factor (R_F) values between 0.2 and 0.8 for the solutes in the TLC assays at the middle selectivity point 333.

OPLC retention measurements were performed at thirteen selectivity points (Fig. 1) using the same solvents and *n*-hexane as the S_T regulator as in the TLC runs. Air and/or gas possibly adsorbed on the surface of the stationary phase was eliminated by a prerun with *n*-hexane. In this case, the application distance from the solvent inlet was adjusted to 5 mm to avoid a decisive influence on the separation of the multi-front formations [16]. S_T was adjusted to 2.2 and the flow-rate to 0.65 at $P_s = 333$ in order to keep the spots of the analysed coumarins as sharp bands. The R_F values for the solutes were also kept between 0.2 and 0.8, when the runs were made in the non-equilibrated mode.

HPLC retention measurements were performed at the same selectivity points as for the OPLC runs. The chosen S_T of 1.2 at $P_s = 333$ gave for the last-eluting compound a capacity factor (k'_c) of less than 20.



3.1. Dependence of capacity factors and selectivity points

Regression functions of different order for the measured two-dimensional retention data were compared at constant solvent strength (for S_T s, see above). The capacity factors of the coumarins at selectivity points along one edge, *i.e.*, 118–811, 811–181 or 181–118, of the PRISMA showed dependences as quadratic regressions of the type $k' = A(P_S)^2 + B(P_S) + C$ ($r^2 = 0.98$ – 0.83 for TLC, $r^2 = 1.00$ – 0.79 for OPLC and $r^2 = 1.00$ – 0.90 for HPLC). The k' value with this mobile phase system was highest at $P_S = 181$, as can be seen in Fig. 2. The three representative

compounds were chosen according to the elution order, *i.e.*, one from the beginning (angelicin), one from the middle (2'-angeloyl-3'-isovaleryl vagnate) and one from the end (ostruthol). The mobile phase composition had a similar effect on the elution of all the coumarins in TLC, OPLC and HPLC. In reversed-phase (RP) HPLC, similar findings for retention were obtained by Nyiredy *et al.* [17]. Outinen *et al.* [18] found that the linear and quadratic functions were insufficient to describe the retention of dansylamides in RP-HPLC. They selected cubic regression functions to describe the dependence.

The three numerical values in P_S were plotted on x - y coordinates against a fourth parameter

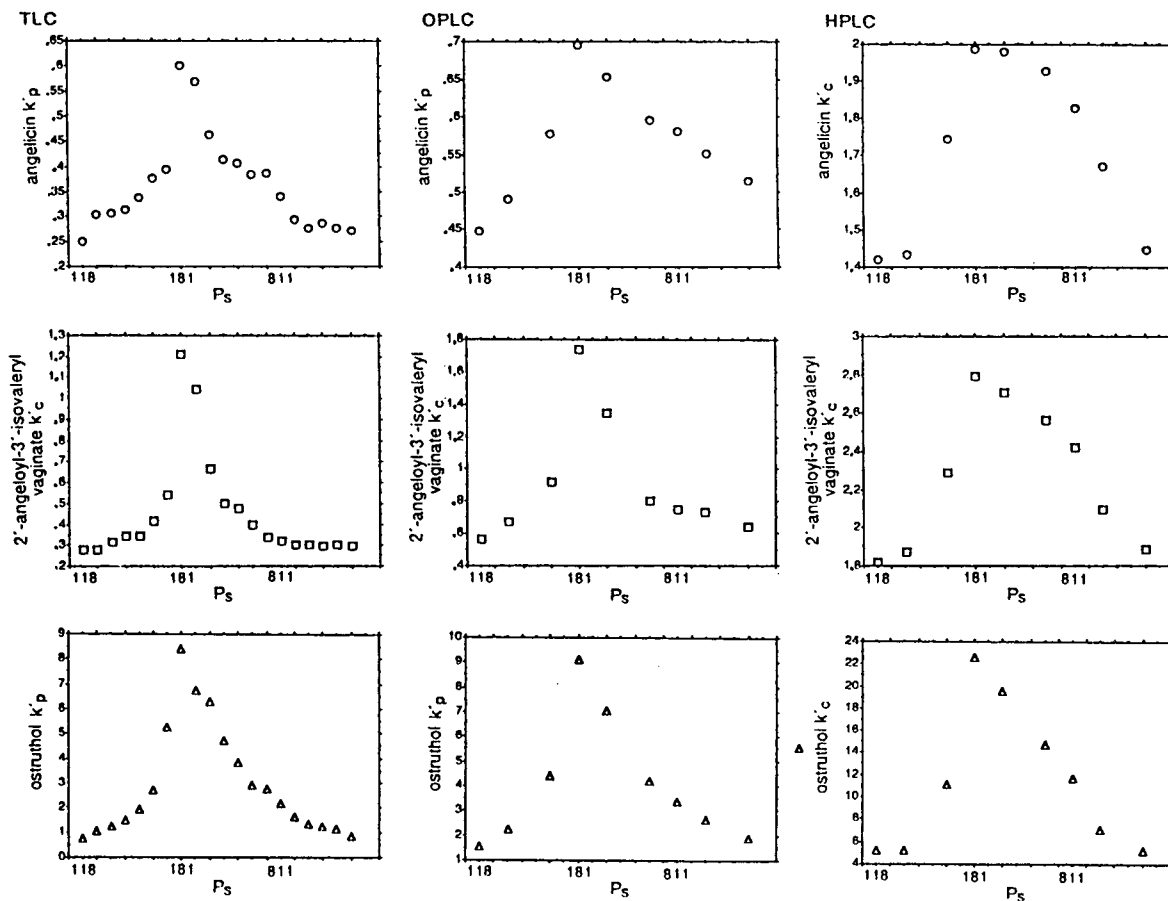


Fig. 2. Dependences between the k' values of angelicin, 2'-angeloyl-3'-isovaleryl vagnate and ostruthol and selectivity points (P_S) between 118–811–181–118.

(z-coordinate: k') in order to obtain three-dimensional figures of the P_s in the prism. Coumarins have similar three-dimensional surfaces in TLC, OPLC and HPLC, as demonstrated by the three representative compounds in Fig. 3. Selectivity point 181 gives the highest capacity factor values, falling to the corner of

118 with the lowest k' values and the surface follows this decreasing trend fairly smoothly. The corner 811 k' values are about half of the maximum values for each compound in TLC and HPLC. OPLC shows a different trend for the middle selectivity compared with the other two methods.

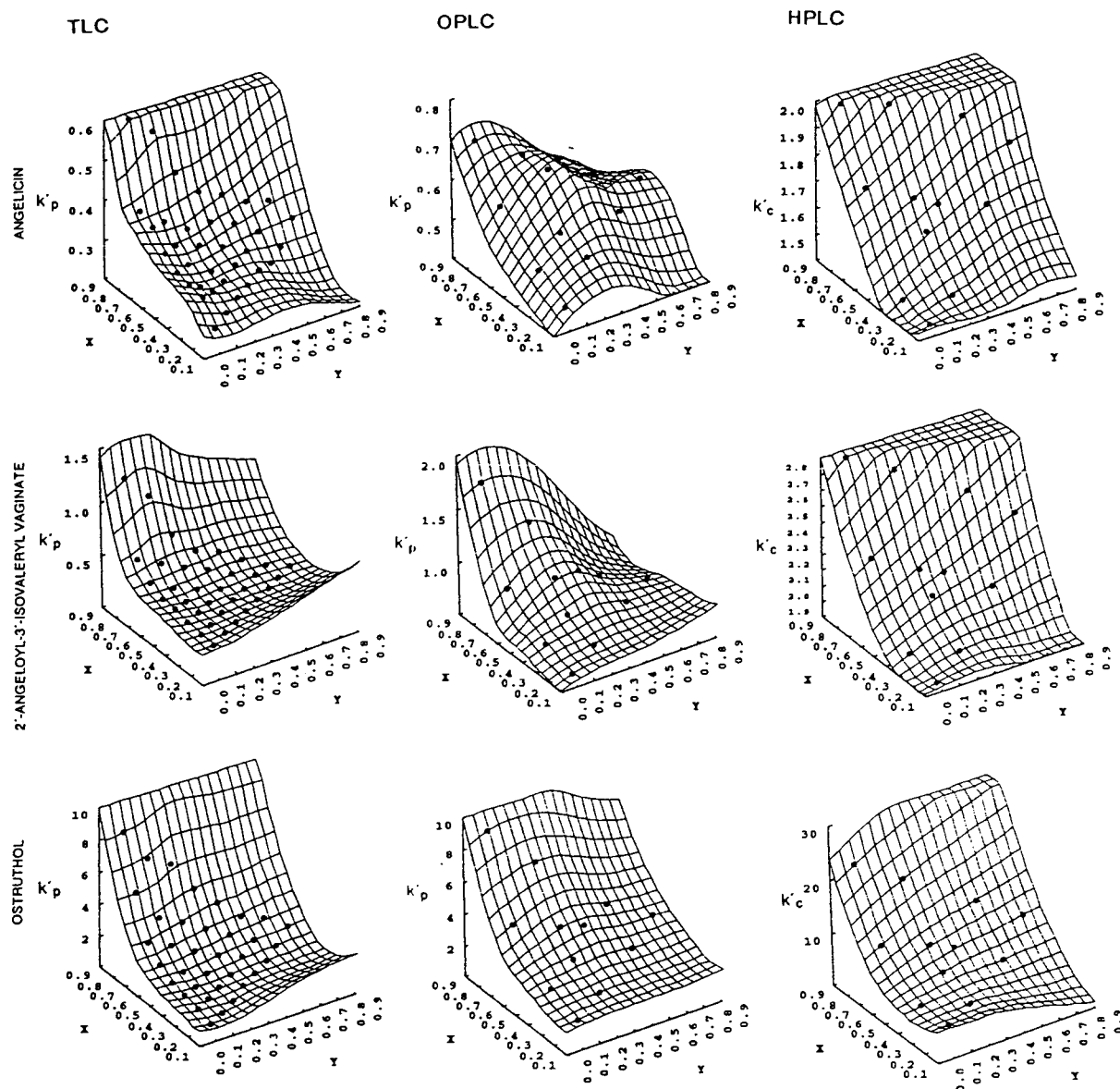


Fig. 3. Three-dimensional k' surfaces of the three representative compounds. $P_s = 118$ (front), 181 (top) and 811 (right).

3.2. Dependence of separation factors and selectivity points

The three-dimensional α (separation factor, $\alpha = k'_2/k'_1$, where k'_1 and k'_2 are the capacity factors of the last- and first-eluted compounds, respectively) surfaces were constructed for the fifteen coumarins at all selectivity points. The behaviour of α is shown in ref. 14 for TLC and HPLC for the first two and last two eluting coumarins, and an average value for seven coumarins eluting in the middle of the run. In OPLC the same kind of behaviour was obtained, *i.e.*, for the first ($1.0 < \alpha < 1.5$) and last ($1.0 < \alpha < 1.8$) α values the surfaces decreased fairly smoothly from P_s 181 down to the corner of 118, and for the compounds eluting in the middle ($1.0 < \alpha < 1.15$) the surface started to rise along the side of P_s 118–811. The range of α values also remained fairly constant in the methods. This indicates that the separation of the coumarins would be similar if the conditions for the analysis are the same in these methods.

3.3. Influence of solvent strength

Solvent strength values of 1.4–2.2 in TLC, 1.4–2.6 in OPLC and 0.8–1.6 in HPLC (S_T steps of 0.2 in all methods) were examined at selectivity point 333. The capacity factors of the coumarins were calculated and are plotted against the solvent strengths demonstrated by angelicin, 2'-angeloyl-3'-isovaleryl valinate and ostruthol in Fig. 4. The capacity factors of the fifteen coumarins showed dependences in all three methods as a quadratic regression of the type $k' = A(S_T)^2 + B(S_T) + C$ ($r^2 = 1.00$ –0.96). This result is in accordance with that of Vuorela *et al.* [19] for six investigated coumarins in TLC ($0.45 < S_T < 1.15$). Outinen *et al.* [20] also demonstrated that the dependence between the k' values of seventeen dansyl amides and the rate of change in the gradients at solvent strength $S_T = 0.5 \rightarrow 2.6$ in RP-HPLC followed a quadratic regression function ($r^2 = 1.00$ –0.98). The dependences for the coumarins were not linear over the investigated k' range and the solvent strengths used for OPLC in this study.

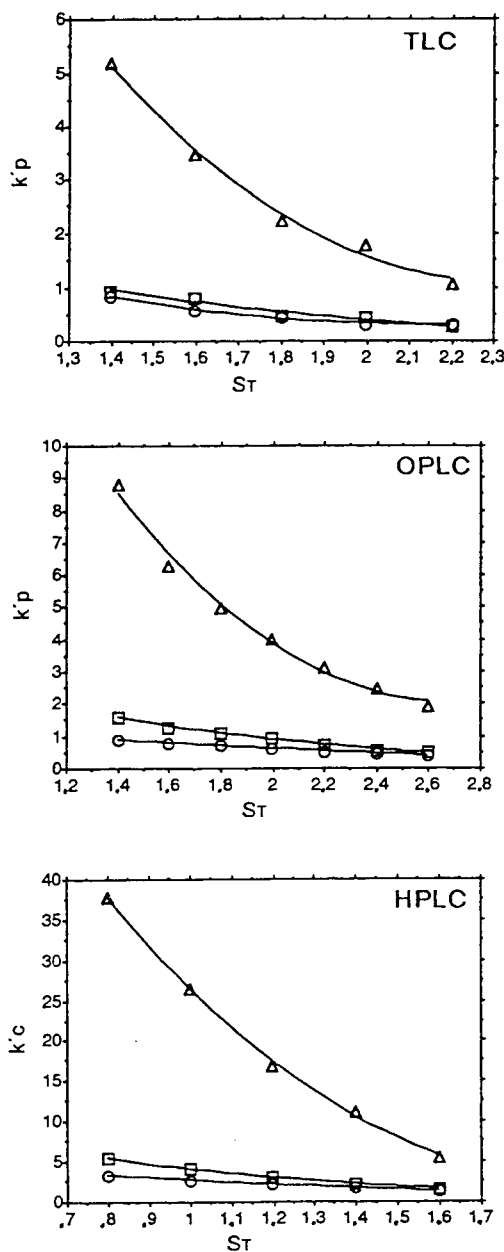


Fig. 4. Dependences between the k' values of (\circ) angelicin, (\square) 2'-angeloyl-3'-isovaleryl valinate and (\triangle) ostruthol and the solvent strengths (S_T) tested in TLC, OPLC and HPLC at $P_s = 333$.

The behaviour of S_T was investigated further. In order to compare the changes in retention with different S_T values in these methods, the k'_p

and k'_c values at the joint S_T value of 1.4 were plotted against k'_p and k'_c values at the other S_T , and regression analysis was carried out (Table 1). The slopes of the curves (A in Table 1) were further plotted against various S_T (Fig. 5). The curves obtained for TLC and OPLC compared with HPLC had clearly different slope values, whereas the functions for TLC and OPLC showed similar S_T behaviour. Changing S_T in HPLC causes a much larger change in the retention behaviour of the coumarins. This indicates that, for unsaturated TLC and off-line, non-equilibrated OPLC, a change in S_T causes a similar change in the retention behaviour of the compounds and these methods are therefore more closely related to each other than to HPLC.

When a multi-component mobile phase is used, a mobile phase gradient might arise along the migration distance due to mobile phase demixing. Moreover, precoating the stationary phase with molecules of the mobile phase can modify the surface properties, a phenomenon that might affect the separation. Petrović and Acanski [21] have shown that small changes of the silica surface affect only the phase ratio of the TLC system, whereas adsorption of acetic acid vapour by the silica surface has a significant influence on both the equilibrium constant of a solute and the phase ratio. A short "equilibration" of a few minutes can, but need not, lead to

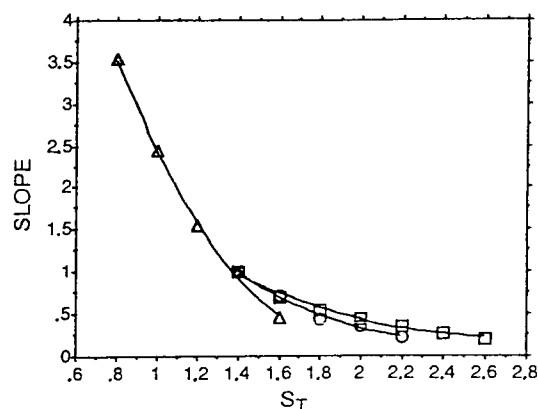


Fig. 5. Plot of slope values against various S_T . ○ = TLC; □ = OPLC; △ = HPLC.

sorptive saturation [22]. Further, there are differences in the evaporation of the different solvents from the adsorbent layer. For instance, chloroform, which has a high solvent strength value (4.1) in normal-phase systems, evaporates more readily from the normal-phase adsorbent layer than, *e.g.*, *n*-hexane ($S_i = 0.0$) [23], making the separation process complex. This causes changes in the solvent strength and the selectivity of the mobile phase in use. OPLC pre-equilibrated with the mobile phase might be considered closer to equilibrated CLC, because the selectivity of the mobile phase is considered to be the same all over the adsorbent [13]. These phenomena might be responsible for the differ-

Table 1

Slopes (A), intercepts (B) and correlation coefficients (r) for equations obtained from $k'_{S_Tx} = Ak'_{S_{T1.4}} + B$ for TLC, OPLC and HPLC from fifteen coumarins

S_T	TLC			OPLC			HPLC		
	A	B	r	A	B	r	A	B	r
0.8							3.53	-3.53	0.99
1.0							2.46	-1.86	0.99
1.2							1.54	-0.54	1.00
1.4	1.00	0	1.00	1.00	0	1.00	1.00	0	1.00
1.6	0.72	-0.01	0.98	0.71	0.22	1.00	0.46	0.77	0.97
1.8	0.45	0.10	0.99	0.55	0.31	0.99			
2.0	0.35	0.06	0.99	0.44	0.35	0.99			
2.2	0.22	0.13	0.94	0.34	0.32	0.98			
2.4				0.27	0.31	0.97			
2.6				0.20	0.28	0.96			

ences in the separation of compounds between TLC, OPLC and HPLC.

4. Conclusions

Using a multi-component eluent results in the same kind of behaviour with regard to the capacity factors of the fifteen coumarins. In the two- and three-dimensional evaluations of the capacity factors in TLC, OPLC and HPLC, similar behaviour of the coumarins occurred when the mobile phase selectivity was changed, *i.e.*, retention of the compounds is similarly dependent on the mobile phase composition. A similar, three-dimensional figure for the α values is obtained with the three methods, which indicates similar separations of compounds when transferring analytical conditions between the methods. The selectivity of the mobile phase seems to remain the same in the methods, whereas a change in solvent strength in TLC and OPLC has a different effect on the retention behaviour of the compounds to that for a change in S_T in HPLC. This should be taken into consideration when transferring the mobile phase composition from TLC via OPLC to HPLC.

5. Acknowledgement

Financial support from the Finnish Cultural Foundation is gratefully acknowledged.

6. References

- [1] J.J. Kirkland and J.L. Glajch, *J. Chromatogr.*, 255 (1983) 27.
- [2] L.R. Snyder, *J. Chromatogr. Sci.*, 16 (1978) 223.
- [3] S. Nyiredy, C.A.J. Erdelmeier, B. Meier and O. Stichler, *Planta Med.*, 51 (1985) 241.
- [4] S. Nyiredy, B. Meier, C.A.J. Erdelmeier and O. Stichler, *J. High Resolut. Chromatogr. Chromatogr. Commun.*, 8 (1985) 186.
- [5] K. Dallenbach-Tölke, S. Nyiredy, B. Meier and O. Stichler, *J. Chromatogr.*, 365 (1986) 63.
- [6] S. Nyiredy, C.A.J. Erdelmeier, B. Meier and O. Stichler, *GIT Suppl. Chromatogr.*, 4/85 (1985) 24.
- [7] S. Nyiredy, K. Dallenbach-Tölke and O. Stichler, in: F.A.A., Dallas, H. Read, R.J. Ruane and I. Wilson (Editors), *Recent Advances in Thin Layer Chromatography*, Plenum Press, New York, 1988, pp. 45–54.
- [8] S. Nyiredy, K. Dallenbach-Tölke and O. Stichler, *J. Planar Chromatogr.*, 1 (1988) 336.
- [9] G.C. Zogg, *Thesis*, No. 8780, ETH Zurich, Zurich, 1989.
- [10] F. Geiss, *Fundamentals of Thin Layer Chromatography (Planar Chromatography)*, Hüthig, Heidelberg, 1987.
- [11] E. Tyihák, E. Mincsovics and H. Kalász, *J. Chromatogr.*, 174 (1979) 75.
- [12] S. Nyiredy, *Application of the "PRISMA" Model for the Selection of Eluent Systems in Over-Pressure Layer Chromatography (OPLC)*, Labor MIM, Budapest, 1987.
- [13] S. Nyiredy, K. Dallenbach-Tölke, G.C. Zogg and O. Stichler, *J. Chromatogr.*, 499 (1990) 453.
- [14] P. Härmälä, H. Vuorela, E.-L. Rahko and R. Hiltunen, *J. Chromatogr.*, 593 (1992) 329.
- [15] P. Härmälä, *J. Planar Chromatogr.*, 6 (1991) 460.
- [16] S. Nyiredy, C.A.J. Erdelmeier and O. Stichler, in E. Tyihák (Editor), *Proceedings of the International Symposium on TLC with Special Emphasis on Overpressured Layer Chromatography (OPLC)*, Szeged, Hungary, Labor MIM, Budapest, 1986, pp. 222–231.
- [17] S. Nyiredy, K. Dallenbach-Tölke and O. Stichler, *J. Liq. Chromatogr.*, 12 (1989) 95.
- [18] K. Outinen, H. Vuorela and R. Hiltunen, *Acta Pharm. Fenn.*, 101 (1992) 11.
- [19] H. Vuorela, K. Dallenbach-Tölke, R. Hiltunen and O. Stichler, *J. Planar Chromatogr.*, 1 (1988) 123.
- [20] K. Outinen, V.-M. Lehtonen, R. Hiltunen and H. Vuorela, *XII Helsinki University Course in Drug Research, Abstract Book*, The Finnish Pharmaceutical Society, Helsinki, 1993, p. 43.
- [21] S.M. Petrović and M. Acanski, *J. Planar Chromatogr.*, 6 (1991) 439.
- [22] F. Geiss, *J. Planar Chromatogr.*, 2 (1988) 102.
- [23] P. Merkkü, J. Yliruusi, H. Vuorela and R. Hiltunen, *J. Planar Chromatogr.*, submitted for publication.



ELSEVIER

Journal of Chromatography A, 670 (1994) 199–208

JOURNAL OF
CHROMATOGRAPHY A

Factors affecting the capillary electrophoresis of ricin, a toxic glycoprotein

Harry B. Hines*, Ernst E. Brueggemann

Toxinology Division, United States Army Medical Research Institute For Infectious Diseases, Fort Detrick, Frederick, MD 21702-5011, USA

(First received November 1st, 1993; revised manuscript received January 25th, 1994)

Abstract

Conditions for the analysis of ricin with capillary electrophoresis were investigated. Uncoated and coated columns were tested with a variety of different buffer combinations which included different principal components, pH, ionic strength, and additives. Of the combinations tested, uncoated columns used with either zwitterionic salts or putrescine gave the best results. Multiple peaks were resolved with these conditions. Coated columns generally yielded between 1000 and 5000 plates with several buffer combinations. Ricin may be analyzed faster and with greater resolution with capillary electrophoresis employing untreated fused-silica columns than by using other chromatographic techniques.

1. Introduction

Ricin (RCA 60) is a heterodimeric, glycoprotein phytoxin with a molecular mass of approximately 66 000 and a *pI* of 7.1. The two protein chains, A and B, that comprise ricin are linked by a single disulfide bond. This toxin is produced by the castor bean plant, *Ricinus communis*, which grows in temperate climates, including California and the southern United States. Although ricin is found throughout the castor bean plant, it is concentrated in the seeds [1]. Up to 1.2 mg of ricin can be isolated from 100 g of seeds with lactamyl–Sephareose affinity chroma-

tography [2]. Two basic forms of seeds and ricin are produced by castor bean plants from different regions of the world. The D form of ricin is found in large grain seeds, whereas small grain seeds contain the D and E forms. The two variants are distinguished by different *pI* values which reflect differences in amino acid composition of the B chain [3,4]. Regardless of form, ricin is highly toxic to eukaryotes with a reported mouse LD₅₀ as low as 0.1 µg per 25 g mouse [5]. Ricin's toxicity is based upon the ability of the A chain to inhibit cellular protein synthesis [6,7], which has prompted the incorporation of ricin or its individual chains into immunotoxins to treat different clinical conditions such as cancer [8–10]. The capability to separate and quantify ricin, or its subunits rapidly, is very important for monitoring the production and stability of

* Corresponding author.

ricin immunotoxins and for monitoring the potential health hazard posed by the plant within its indigenous areas.

In the past, ricin was purified for animal and cell toxicity studies. Generally, purification relied upon column chromatography [11–13]. Because the extracts were chemically complex, chromatographic techniques such as gel filtration, ion-exchange, and affinity chromatography had to be combined to obtain the required pure product. However, none of these preparative techniques provides the appropriate combination of speed, resolution, and simplicity needed for accurately screening many samples for ricin analytically. One analytical study on ricin included detection by capillary electrophoresis [14]. That report indicated that ricin eluted within 7 min as broad peaks, that the detection limit was 50 mg/ml, and that ricin was detectable in crude, acidic extracts of castor bean meal. A more complete study of the factors affecting ricin behavior in capillary electrophoresis columns was not conducted.

The previous study that included ricin detection emphasized one of the most attractive features of capillary electrophoresis (CE) for ricin analysis: its ability to resolve complex protein mixtures relatively rapidly. Ideally, ricin analysis by CE would be possible in one, relatively short step with the proper analysis conditions. However, discovering these conditions may require extensive investigation, as most protein separations require modifications to buffers or columns or both to suppress protein–column interactions. Reducing or preventing these interactions is essential for proper peak shape(s) and the required resolution. Many CE column and buffer variations have been developed to reduce protein–capillary interactions [15–27]. When planning a protein separation strategy for CE, it may be necessary to consider carefully many different approaches.

In this study, we evaluated the feasibility of using capillary electrophoretic analysis for ricin analyses, primarily as a function of column efficiency. We studied a number of different solutions and operating parameters to ascertain which would be optimal for efficiently screening samples for ricin.

2. Experimental

2.1. Materials and instrumentation

Affinity-purified ricin was purchased from Vector Laboratories (Burlingame, CA, USA) and was used without additional purification. Some ricin aliquots were desalted with 30 000 molecular mass-limit centrifuge filters (PGC Scientifics, Gaithersburg, MD, USA). Acidic extracts of castor bean meal were prepared according to the procedure described by Wannemacher *et al.* [14]. A modular CE unit from Spectrovision (Chelmsford, MA, USA) equipped with an ISCO CV⁴ UV detector (Lincoln, NE, USA) and a Beckman P/ACE 2000 (Beckman Instruments, Palo Alto, CA, USA) CE unit were employed in this study. Untreated, fused-silica capillary columns were purchased from Polymicro Technologies (Phoenix, AZ, USA) and Beckman Instruments. Coated, fused-silica capillary columns were purchased from Supelco (Bellefonte, PA, USA). An aminopropyl-coated column was prepared according to the method of Mosely *et al.* [21]. All inner column dimensions were either 75 μm or 50 μm diameter. When listed, total column lengths are given in this report. The distance from the injection end to the detector is the total column length minus 7 cm. Buffer components were purchased from Sigma (St. Louis, MO, USA) and were the highest purity available. Accupure Z-1-methyl reagent (trimethylammoniumpropanesulfonic acid) was purchased from Waters Division of Millipore (Milford, MA, USA). Mesityl oxide, lysozyme, chymotrypsinogen A, and cytochrome c were purchased from Sigma. Phosphoric acid, glacial acetic acid, hydrochloric acid, sodium hydroxide, and putrescine were purchased from Aldrich (Milwaukee, WI, USA). Urea was purchased from Mallinkrodt (St. Louis, MO, USA). Deionized water (18 M Ω) was used in all experiments. All solutions were filtered with 0.22- μm filters (Gelman Science, Ann Arbor, MI, USA).

2.2. Column preparation and sample analysis

Uncoated columns were initially pretreated with the pressure feature of the Beckman P/ACE

2000 unit in the following manner: a water wash for 1 min, a 1.0 *M* NaOH wash for 5 min, a 0.1 *M* NaOH wash for 1 min, a 5-min water wash, and a 5-min wash with the running buffer, which varied depending upon the experiment. Between analyses, untreated columns were washed with 0.1 *M* NaOH for 0.5 min followed by a 2-min wash with running buffer. Before the first use, coated columns were cleaned with water for 1 min followed by a wash with 0.1 *M* NaOH for 1 min. Base treatment was followed by a 5-min water wash. Activation was concluded with a 5-min wash with running buffer. Between analyses, coated columns were cleansed with 0.1 *M* NaOH for 0.5 min followed by a 2-min wash with running buffer.

General operating parameters for the Beckman P/ACE 2000 CE unit included the following: 1 or 2 s hydrostatic, anodic sample injection; 20–30 kV applied voltage; 20°C coolant temperature; and either 200 or 214 nm detection wavelength.

Column efficiency was calculated using the following formula: $N = 5.54(t/t_{0.5})^2$, where N represents the theoretical plate number, t is the migration time of the peak and $t_{0.5}$ represents the peak width in time at half height. This formula did not compensate for various interactions, but it was adequate for assessing the variables we studied.

3. Results

Many variables were screened to determine which combination(s) would be optimal for analyzing ricin. A partial listing of buffers, additives, and column coatings is presented in Table 1. Variables fell into two general categories: (1) untreated columns with buffer modifications/additives, and (2) treated columns. Theoretical plate number values were used to evaluate the effectiveness of the analytical conditions. Of the variables tested, few combinations yielded satisfactory results.

Borate buffer was one of the first buffers tried due to its previous successful utility reported for other difficult proteins and glycoproteins [28,29]. By using alkaline 0.03 *M* borate buffer (pH 9) and a short, untreated column (35 cm × 50 μm), a single peak was obtained for ricin (injection from a 0.5 mg/ml solution). Fig. 1 depicts a representative electropherogram for that sample. These conditions provided reasonable results when theoretical plate number was considered ($N = 1550$; $N/m = 4429$). The presence of a broad, tailing peak indicated that either protein-column interaction occurred, that additional components were present, or both. To test for the presence of additional compounds, standard ricin was analyzed with a smaller inner diameter column. Two peaks were observed, although

Table 1
Representative selection of important buffers, additives, and inorganic salts used in this study

Organic buffers	Organic additives	Inorganic salts
CHES ^a	Ethylene glycol	Potassium chloride
Tricine ^b	Hexanesulfonic acid	Potassium sulfate
Tris ^c	Methanol	Potassium phosphate
	Putrescine ^d	Sodium acetate
	Sodium dodecylsulfate	Sodium borate
	Triethylamine	
	Trimethylammonium-propanesulfonic acid ^e	
	Urea	

^a 2-[N-Cyclohexylamino]ethanesulfonic acid.

^b N-Tris(hydroxymethyl)methylglycine.

^c Tris(hydroxymethyl)aminoethane.

^d 1,4-Diaminobutane.

^e Accupure Z-1-methyl reagent (Millipore).

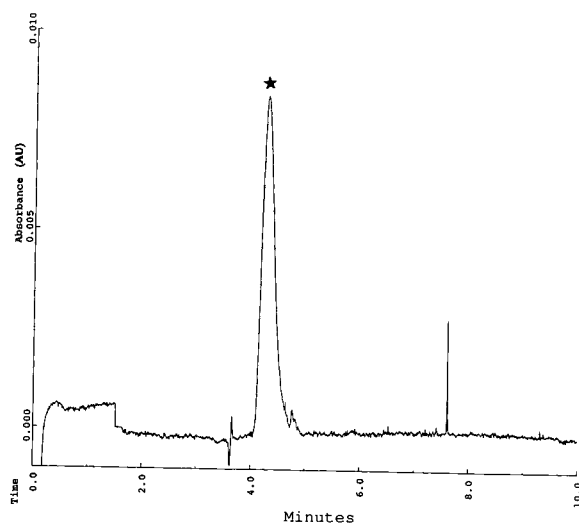


Fig. 1. Representative electropherogram of ricin (*) using an untreated 35 cm \times 50 μ m fused-silica capillary column. The running buffer was 0.03 M sodium borate, pH 8.5. A 3-s pressure injection (3447.4 Pa) of a 0.5 mg/ml solution of standard ricin was made. The applied voltage was 20 kV (571 V/cm). UV detection was accomplished at 200 nm.

resolution was poor (data not shown). This finding indicated that more than one component was present. To check for contaminants, ricin was analyzed by non-denaturing polyacrylamide gel electrophoresis (PAGE). Results showed that standard ricin contained only one component. Results acquired with sodium dodecylsulfate (SDS)-PAGE (data not shown) demonstrated that the A chain was heterogeneous, which may explain the appearance of at least two components in the borate electropherogram. Additional attempts with borate buffer to separate possible ricin components were unsuccessful. Other inorganic buffers such as potassium sulfate, potassium chloride, and potassium phosphate also had no utility. Additives such as ethylene glycol, hexanesulfonic acid, and triethylamine had little or no effect upon either column efficiency or resolution. No improvement was obtained when organic buffers such as 2-(N-cyclohexylamino)ethanesulfonic acid (CHES) and Tris were used alone or combined with inorganic salts. Altering the pH of inorganic,

organic, and mixed buffers had no marked effect upon peak shape.

Zwitterionic and bifunctional buffers (or additives) were tested for their effect upon ricin's peak shape. These compounds do not increase Joule heating while providing pH stability and ionic strength [18]. Furthermore, zwitterionic buffers such as N-tris(hydroxymethyl)methylglycine (Tricine) may interact with column silanol groups, as well as protein amine groups [18], which would enhance column efficiency and peak shape. When Tricine was used alone, there was no distinct improvement in theoretical plate number compared to borate buffer. However, by combining Tris and Tricine buffers and varying Tris–Tricine concentration ratios, more components of the ricin sample were resolved. Fig. 2 shows that, by holding the Tris concentration constant and increasing the quantity of Tricine, several additional peaks were detected (compare Fig. 2A to Fig. 2B). In Fig. 2A, we calculated the plate number to be 19 284 ($N/m = 38\,568$), but this number could increase or decrease dramatically depending upon which peak was chosen. Tris concentration had little effect when it was increased and the Tricine level was held constant (data not shown). Doubling Tris–Tricine concentrations while maintaining a constant ratio compromised resolution, resulting from poor peak shape. The same was also true when Tris–Tricine concentrations were dropped to 0.005 M while maintaining a constant ratio. Altering the pH of the optimal Tris–Tricine buffer did not affect column efficiency and peak shape. SDS combined with methanol did not improve separations when added to the optimal Tris–Tricine buffer. Another zwitterionic compound, trimethylammoniumpropanesulfonate (Accupure Z-1-methyl reagent) was used as an additive to 0.1 M potassium phosphate buffer (pH 9.0). This additive reduced resolution, but improved overall peak shape, relative to the optimum Tris–Tricine buffer (Fig. 3). We calculated the plate number to be 42 405 ($N/m = 74\,395$), but, again, the value was variable due to the double peak. This compromise between peak shape and resolution combined with a detection limit of approximately

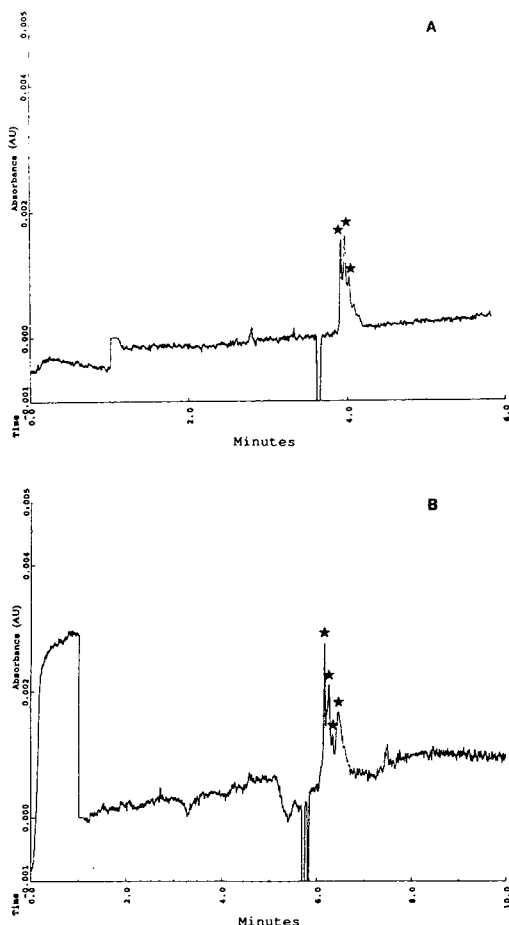


Fig. 2. Electropherogram of standard ricin (*) showing increased resolution of sample components when changes were made in buffer composition. (A) 0.01 *M* Tris, 0.01 *M* Tricine, pH 9.0. (B) 0.01 *M* Tris, 0.04 *M* Tricine, pH 9.0. An untreated 50 cm \times 75 μ m fused-silica column was used. Samples consisted of 0.5 mg/ml solutions of ricin and were injected for 1 s with pressure (3447.4 Pa). A voltage of 20 kV (400 V/cm) was applied to the column. UV detection was at 200 nm.

10 mg/ml indicated that it may be possible to analyze a complex sample containing ricin under these conditions. Fig. 4 depicts a sample electropherogram. It was possible to tentatively identify ricin in this crude, acidic extract of castor bean meal. Ricin peaks were tentatively identified by comparing migration times to standard ricin.

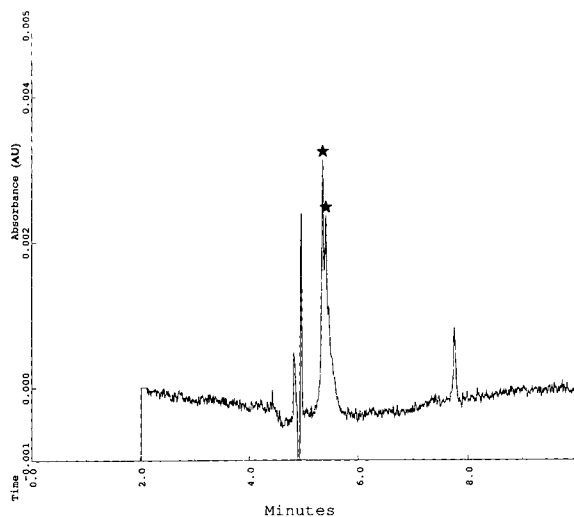


Fig. 3. Electropherogram of standard ricin (*) analyzed with 1 *M* trimethylammoniumpropanesulfonic acid (Accupure Z-1-methyl reagent) in 0.1 *M* KH_2PO_4 (pH 9.0). An untreated 57 cm \times 50 μ m fused-silica column was used. Pressure injections (3447.4 Pa) of 1 s were made for 0.5 mg/ml solutions of ricin. After injection, 25 kV were applied to the column (439 V/cm). A UV wavelength of 200 nm was used for detection.

We also used a bifunctional compound as an additive. Putrescine (1,4-diaminobutane), added to potassium sulfate buffer [20], gave very good results for a standard mixture of three proteins: lysozyme, cytochrome *c*, and chymotrypsinogen A [theoretical plate numbers of 138 282 ($N/m = 242\,600$), 32 000 ($N/m = 56\,140$), and 170 717 ($N/m = 299\,504$), respectively]. Each of these proteins is usually difficult to analyze with untreated columns. Fig. 5A is an electropherogram depicting the result of that analysis with putrescine. When ricin was analyzed under the same conditions, excellent resolution and peak shape were obtained ($N = 64\,300$ for the largest peak; $N/m = 112\,807$). More components were observed compared to the number of peaks obtained with Tris–Tricine (Fig. 2B).

To determine if the multiple peaks were aggregates, 0.03 *M* potassium phosphate buffer (pH 8.5) containing 6 *M* urea was used to analyze standard ricin. There was no evidence of aggre-

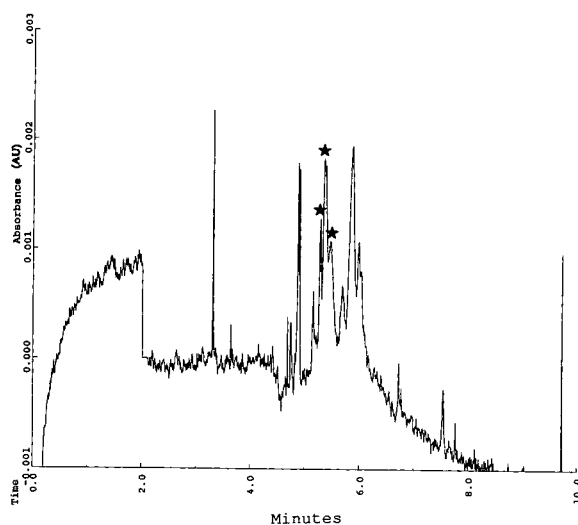


Fig. 4. Electropherogram of a crude, acidic extract of castor bean meal containing ricin (*). A 1 M Accupure Z-1-methyl reagent in 0.1 M KH_2PO_4 , pH 9.0, buffer was used. The column was untreated, 57 cm \times 50 μm fused-silica tubing. A 3-s pressure (3447.4 Pa) injection was used to load the solution. An applied voltage of 25 kV (439 V/cm) was used for analysis. The UV wavelength at 200 nm was used for detection.

gation (data not shown). Impurities or microheterogeneity seemed to be the best logical origin of the multiple peaks in the ricin samples.

We investigated four coated columns in this study. As seen in Fig. 6, a column coated with a proprietary hydrophilic phase (Supelco P150) performed only slightly better than an untreated column with a borate buffer system. Plate numbers were 4546 ($N/m = 7975$) and 1550 ($N/m = 4429$) for the coated and uncoated columns, respectively. Attempts to enhance performance by changing buffers were unsuccessful. A C_{18} column also performed poorly for ricin (Fig. 7; $N = 494$; $N/m = 867$). A C_1 column gave a relatively sharp peak ($N = 12436$; $N/m = 21\,878$) with a 0.005 M disodium phosphate buffer (pH 6.0) containing 0.005 M SDS. A representative electropherogram is shown in Fig. 8. Equilibration times before analysis were typically 12 h or longer, which made it difficult to use this buffer routinely. Furthermore, the column was unable to resolve components of the ricin sample. Adequate results were obtained for peak charac-

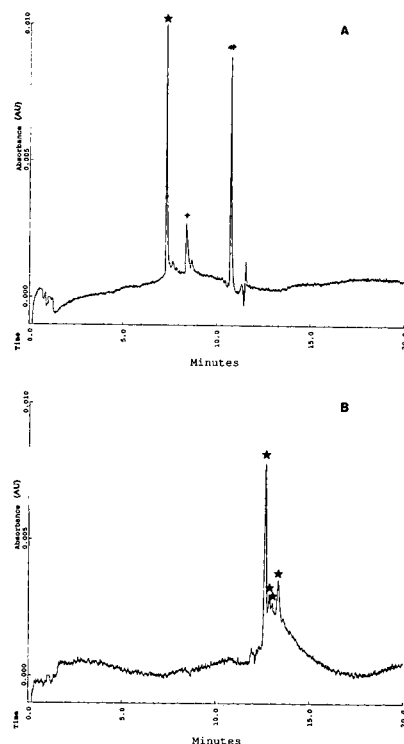


Fig. 5. Electropherograms of (A) standard protein mixture containing 1 mg/ml each of chymotrypsinogen A (*), cytochrome c (+), and lysozyme (#); and (B) 0.5 mg/ml ricin (*) solution analyzed under the same conditions. The electrophoresis buffer contained 0.02 M K_2SO_4 and 0.03 M putrescine at pH 7.0. An untreated, 57 cm \times 50 μm fused-silica column was used for both analyses. An applied voltage of 20 kV (351 V/cm) was used for analysis. The UV wavelength at 200 nm was used for detection.

teristics with an aminopropyl column ($N = 3638$; $N/m = 6382$) prepared in this laboratory. However, the coating was unstable (Fig. 9), which ultimately rendered the column unusable after 3 days. The coating could be regenerated and used again satisfactorily, but the time required for regeneration made the coating an unlikely candidate for routine use.

4. Discussion

The results of this study indicated that relatively complex ricin samples may be rapidly analyzed in a single step with capillary electro-

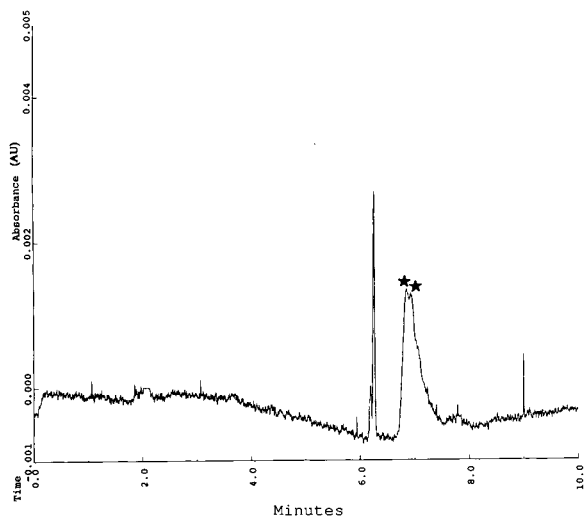


Fig. 6. A representative electropherogram of ricin (*) on a Supelco P150 column. A 1-s pressure injection (3447.4 Pa) of a 0.5 mg/ml ricin solution was made to load the sample. The electrophoresis buffer consisted of 0.01 M KH_2PO_4 at pH 8.6. The column dimensions were 57 cm \times 50 μm . The applied voltage was 20 kV (351 V/cm). The UV wavelength at 200 nm was used for detection.

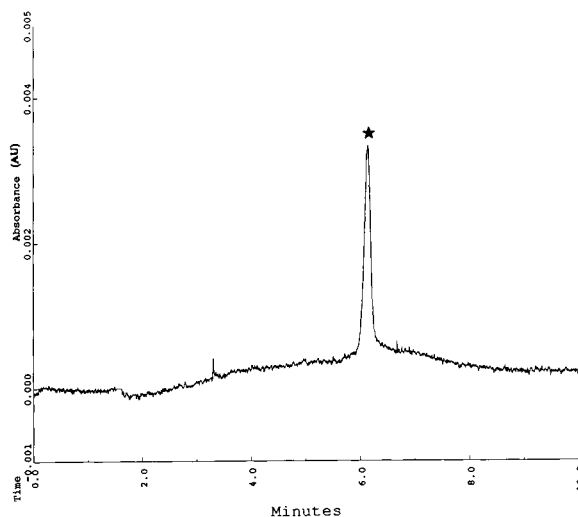


Fig. 8. Electropherogram of ricin analyzed on a Supelco C_1 column (57 cm \times 50 μm). Pressure injections (3447.4 Pa) of 1 s were made to load the ricin sample (0.5 mg/ml). The electrophoresis buffer contained 0.005 M Na_2HPO_4 and 0.005 M SDS at pH 6.0. A voltage of 30 kV (526 V/cm) was applied to the column. UV detection was at 200 nm.

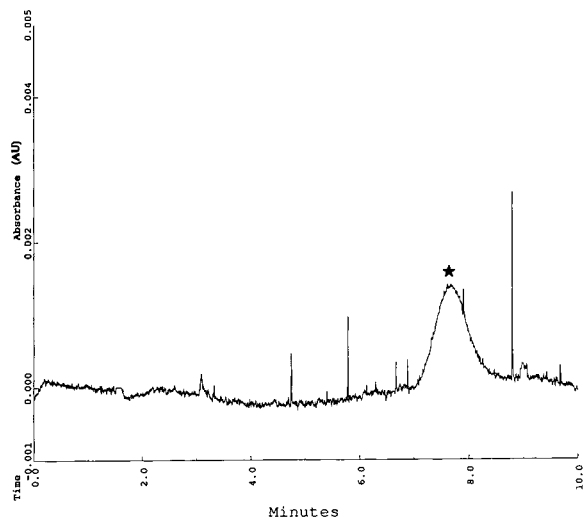


Fig. 7. Electropherogram of ricin using a 57 cm \times 50 μm Supelco C_8 column. Injections of a 0.5 mg/ml solution of ricin were made with pressure (3447.4 Pa) for 1 s. The electrophoresis buffer consisted of 0.005 M Na_2HPO_4 and 0.005 M SDS at pH 6.0. The applied voltage was 30 kV (526 V/cm). UV detection was at 200 nm.

phoresis. Column efficiency, which influences resolution and sensitivity, was greatly affected by protein interactions. To compensate for protein-column binding, it was necessary to investigate several approaches. One of the first approaches utilized alkaline borate buffer. Several investigators report good separations with this buffer for difficult proteins, such as lysozyme and glycoproteins, for the following reasons: (1) induction of Coulombic repulsion among proteins and negatively charged silanol groups with alkaline conditions [15]; and (2) possible carbohydrate complexation by borate molecules [28,29]. Ricin appears to be an excellent candidate for this analysis profile as it is a glycoprotein with a pI of 7.1. While these conditions produced reasonable column efficiency for ricin, they were disappointing overall. It was necessary to shorten the column length from 50 to 35 cm to achieve a reasonable peak shape and efficiency ($N = 1550$). Attempts to improve these results with a 50 cm \times 25 μm column yielded peak splitting, which indicated that peak shape was being influenced by the presence of unresolved components, as

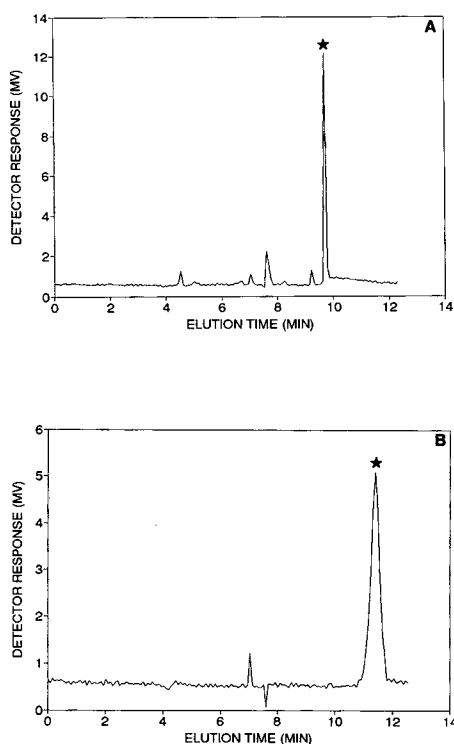


Fig. 9. Electropherograms of standard ricin analyzed on an aminopropyl-coated column (57 cm \times 50 μ m). (A) Freshly prepared column. (B) Same column after 3 days of use. For both analyses, 1-s pressure injections (3447.4 Pa) of a 0.5 mg/ml ricin solution were made to load the sample onto the column. The electrophoresis buffer consisted of 0.01 M sodium acetate at pH 3.5. A voltage of 20 kV (351 V/cm) was applied to the column. UV detection was at 200 nm.

well as protein interactions. We believed that protein interactions were the primary influence. Therefore, by using conditions to reduce protein interactions, we enhanced resolution by using other inorganic salts such as potassium sulfate, which revealed additional peaks. Alkali metal salts have been used to establish a neutral inner capillary surface through ion exchange with silanolate groups on the capillary's inner surface [17]. In the present study, this approach failed to improve the results obtained with alkaline borate buffer. We used insufficient ionic strength (0.02 to 0.03 M), compared to reported concentrations [17], for the potassium salt buffers to compete effectively against ricin for the cation-exchange

sites on the capillary surface. When the concentration was increased to the recommended 0.3 M potassium salt [17], the capillary current maximized, and poor peak shapes resulted, possibly due, in part, to lack of adequate capillary cooling. Decreasing the voltage did not markedly improve peak shape. Increasing pH of the lower ionic strength buffers did not positively influence the results, when compared to results with borate buffer. Most common organic buffers, used either singly or in combination with inorganic salts, failed to improve upon the results obtained with borate buffer.

Acidic buffers were ineffective for untreated, fused-silica columns. Generally, irreversible protein adsorption or loss occurred with most acidic buffers. It is reported that conformational changes occur in ricin at low pH [30,31]. Specifically, the ricin's hydrophobicity increases as the pH is lowered. This was determined with 1-anilino-8-naphthalene sulfonate binding [30,31]. An increase in hydrophobicity would increase the possibility for aggregation and protein loss, although we did not observe any precipitation in ricin solutions.

We used zwitterionic buffers and bifunctional additives because they are reported to compete for silanol groups on the inner surface of untreated capillary columns and active groups on the proteins, especially basic proteins [18,20]. For ricin, zwitterionic buffers enhanced peak shape, increased resolution, and resolved several peaks. Zwitterionic buffers and putrescine complicated analyses, however, due to the appearance of additional peaks in the electropherogram. Analyzing castor bean extracts demonstrated that the presence of additional ricin peaks may not prevent its identification in a complex matrix. Successful ricin analysis will depend upon the number of possible interfering substances in the sample, however. Nevertheless, ricin in a complex matrix would be difficult to quantify unless a peak was chosen to represent the ricin fraction. At best, only semi-quantitative results would be possible with such a restriction. In addition, the modest detection limit obtained with UV detection restricts application to samples containing relatively large

amounts of ricin. Because, ideally, a single, sharp peak is required for ricin analysis, we evaluated coated columns.

Coated columns tested in this study did not perform as well as the uncoated columns with the appropriate buffer or additives. Generally, a single peak was obtained for ricin for each of the columns tested, but, in each case, the peak was inadequate for analytical purposes due to its width. Attempts to optimize column performance by varying buffer characteristics were unsuccessful. Other coated columns must be explored for ricin analyses. It is especially important that columns and buffers be compatible with mass spectrometric detection. Acidic buffers, which are commonly used with coated columns, are also required for interfacing CE with electrospray ionization mass spectrometry. Molecular mass information on ricin samples could then be provided by electrospray ionization mass spectrometry. Of the coated columns we studied, the stability of the aminopropyl column requires improvement. Other investigators have been more successful using this type of column, even when it was interfaced with mass spectrometry [21]. Acrylamide-coated and gel-filled columns should also be studied.

There were several possible explanations for the appearance of multiple peaks in the ricin samples. First, contamination of the sample by individual A and B chains or other proteins may have occurred during the isolation/purification process. This possibility was eliminated because there were no individual chains or proteins detected by SDS-PAGE [14]. In addition, individual chains and extraneous proteins should have been resolved by CE due to differences in charge-to-mass ratios between ricin, its components, and, perhaps, other proteins. Second, possible aggregation of ricin presented another alternative, but analysis with 6 *M* urea did not reveal a change in the ricin's elution pattern. This indicated that no aggregation had occurred. A third possibility involved scrambling the A and B chains by dissociation then reassociating them at alkaline pH to give AA, AB, and BB recombinations. This seemed unlikely as no sulfhydryl compound was present to act as a proton donor

to cleave the disulfide bond that links the two chains; however, it cannot be totally eliminated.

Of the several possibilities, sample heterogeneity appears to represent the most likely explanation. Classical denaturing electrophoresis displayed the presence of a heterogeneous A chain, as has been previously reported [32–34]. In addition, there are subvariants of ricin [2]. One variation known to occur in ricin is glycosylation [35–37]. Glycoside microheterogeneity is restricted to neutral sugars, as charged sugars are not found in carbohydrates attached to ricin [37]. Consequently, glycoside variation has the greatest influence upon ricin's mass, not its charge. Other typical protein modifications such as phosphorylation, sulfation, methylation, and acetylation that could influence ricin's charge state have not been found [38–41]. On the other hand, the presence of small, but critical, differences in amino acid composition or sequence cannot be eliminated as a potential source of variation, which would affect the charge state of ricin. Such differences were reported for abrin, a related toxic glycoprotein [42]. Variations in amino acid composition could arise from post-translational processing of ricin precursors. Amino acid differences may also cause conformational changes in ricin which may be detectable with CE.

The present study demonstrated that it is possible to analyze ricin with CE. Our results indicated that untreated, fused-silica capillary columns and zwitterionic buffers produce the best peak shapes and column efficiencies for ricin. Analysis times were short and were accomplished in a single step. While detection limits were not evaluated in detail, 10 mg/ml (*S/N* = 3; optimal buffers) was the approximate detection limit when the largest peak was followed. This is less than the 50 mg/ml value reported previously for CE [14], which reflects improved analytical conditions. Nevertheless, the 10 mg/ml value for CE (UV detection) was much greater than the low ng/ml values reported for immunoassays [14] and will be a restriction for sample-limited analyses. In addition, it may be possible to resolve ricin variants and/or subvariants with capillary electrophoresis and buffers containing zwitterionic salts or diamino compounds. Addi-

tional studies to identify the extra peaks as ricin variants will be required in the future.

5. Acknowledgements

The authors thank Mr. Richard Dinterman for performing the polyacrylamide gel electrophoresis analyses of ricin; Drs. Frank Lebeda, Robert W. Wannemacher, and Robert Wellner for reviewing the manuscript; and Ms. K.F. Kenyon for her editorial assistance. The views of the authors do not purport to reflect the position of the Department of the Army or the Department of Defense.

6. References

- [1] G.A. Balint, *Toxicology*, 2 (1974) 77.
- [2] R. Hegde and S.K. Podder, *Eur. J. Biochem.*, 204 (1992) 155.
- [3] M. Ishiguro, G. Funatsu and M. Funatsu, *Agric. Biol. Chem.*, 35 (1974) 724.
- [4] T. Mise, G. Funatsu, M. Ishiguro and M. Funatsu, *Agric. Biol. Chem.*, 41 (1977) 2040.
- [5] J.Y. Lin and S.Y. Liu, *Toxicon*, 24 (1989) 757.
- [6] L. Montanaro, S. Sperti and F. Stirpe, *Biochem. J.*, 136 (1973) 677.
- [7] S. Olsnes, *Nature*, 328 (1987) 474.
- [8] W. Mi, T. Si-Lun, Z. Ren-Jie and Y. He, *Int. J. Immunopharmacol.*, 12 (1990) 235.
- [9] A.A. Hertler and A.E. Frankel, *Cancer Res.*, 9 (1991) 211.
- [10] H. Schmidberger, L. King, L.C. Lasky and D.A. Valleria, *Cancer Res.*, 50 (1990) 3249.
- [11] B.M. Simmons and J.H. Russell, *Anal. Biochem.*, 146 (1985) 206.
- [12] G. Nicholson and J. Blaustein, *Biochem. Biophys. Acta*, 266 (1972) 543.
- [13] S. Olsnes and A. Pihl, *Biochemistry*, 12 (1973) 3121.
- [14] R.W. Wannemacher, Jr., J.F. Hewetson, P.V. Lemley, M.A. Poli, R.E. Dinterman, W.L. Thompson and D.R. Franz, in P. Gopalakrishnakone and C.K. Tan (Editors), *Recent Advances in Toxinology Research*, Vol. 3, Venom and Toxin Research Group, National University of Singapore, Singapore, 1992, p. 108.
- [15] H.H. Lauer and D. McManigill, *Anal. Chem.*, 58 (1986) 166.
- [16] M. Zhu, R. Rodriguez, D. Hansen and T. Wehr, *J. Chromatogr.*, 516 (1990) 123.
- [17] J.S. Green and J.W. Jorgenson, *J. Chromatogr.*, 478 (1989) 63.
- [18] M.M. Bushey and J.W. Jorgenson, *J. Chromatogr.*, 480 (1989) 301.
- [19] M.J. Gordon, K. Lee, A.A. Arias and R.N. Zare, *Anal. Chem.*, 63 (1991) 69.
- [20] J.A. Bullock and L. Yuan, *J. Microcolumn Sep.*, 3 (1991) 241.
- [21] M.A. Mosely, L.J. Deterding and K.B. Tomer, *Anal. Chem.*, 63 (1991) 109.
- [22] S. Hjerten, *J. Chromatogr.*, 347 (1985) 191.
- [23] G.J.M. Bruin, J.P. Chang, R.H. Kuhlman, K. Zegers, J.C. Kraak and H. Poppe, *J. Chromatogr.*, 471 (1989) 429.
- [24] K.A. Cobb, V. Dolnik and M. Novotny, *Anal. Chem.*, 62 (1990) 2478.
- [25] S.A. Swedberg, *Anal. Biochem.*, 185 (1990) 51.
- [26] J.K. Towns and F.E. Regnier, *J. Chromatogr.*, 516 (1990) 69.
- [27] M. Zhu, R. Rodriguez, D. Hansen and T. Wehr, *J. Chromatogr.*, 516 (1990) 123.
- [28] J. Liu, O. Shiota, D. Wiesler and M. Novotny, *Proc. Natl. Acad. Sci. USA*, 88 (1991) 2302.
- [29] J. Liu, O. Shiota and M. Novotny, *Anal. Chem.*, 63 (1991) 413.
- [30] L.L. Houston, *Biochem. Biophys. Res. Chem.*, 92 (1980) 319.
- [31] R. Hegde and S.K. Podder, in S.C. Sanyal (Editor), *Proceedings 2nd Asia-Pacific Congress of Animal, Plant, and Microbial Toxins, Banaras Hindu University, Varanasi, February 19–22, 1990*, Institute of Medical Sciences, Banaras Hindu University, Varanasi, India, 1990, p. C3.
- [32] R.J. Fulton, D.C. Blakey, P.P. Knowles, J.W. Uhr, P.E. Thorpe and E.S. Vitetta, *J. Biol. Chem.*, 261 (1986) 5314.
- [33] M. Ono, M. Kuwano, K. Watanabe and G. Funatsu, *Mol. Cell. Biol.*, 2 (1982) 599.
- [34] S. Ramakrishnan, M.R. Eagle and L.L. Houston, *Biochim. Biophys. Acta*, 719 (1982) 341.
- [35] Y. Kimura, H. Kusuoku, J. Tada, S. Takagi and G. Funatsu, *Agric. Biol. Chem.*, 54 (1990) 157.
- [36] Y. Kimura, S. Hase, Y. Kobayashi, Y. Kyogoku, T. Ikenaka and G. Funatsu, *J. Biochem.*, 103 (1988) 944.
- [37] S. Olsnes, K. Refsnes, T.B. Christensen and A. Pihl, *Biochim. Biophys. Acta*, 405 (1975) 1.
- [38] G. Funatsu, Y. Taguchi, M. Kamenosono and M. Yanaka, *Agric. Biol. Chem.*, 52 (1988) 1095.
- [39] G. Funatsu, S. Ueno and M. Funatsu, *Agric. Biol. Chem.*, 41 (1977) 1737.
- [40] G. Funatsu, S. Yoshitake and M. Funatsu, *Agric. Biol. Chem.*, 42 (1979) 501.
- [41] G. Funatsu, M. Kimura and M. Funatsu, *Agric. Biol. Chem.*, 42 (1979) 2221.
- [42] C.-H. Hung, M.-C. Lee, T.-C. Lee and J.-Y. Lin, *J. Mol. Biol.*, 229 (1993) 263.

Use of capillary electrophoresis for the determination of vitamins of the B group in pharmaceutical preparations

S. Boonkerd, M.R. Detaevernier, Y. Michotte*

Department of Pharmaceutical Chemistry and Drug Analysis, Pharmaceutical Institute, Vrije Universiteit Brussel, Laarbeeklaan 103, 1090 Jette, Belgium

(Received December 15th, 1993)

Abstract

The separation of four water-soluble vitamins, *i.e.*, thiamine, riboflavine, pyridoxine and nicotinamide, was investigated by capillary zone electrophoresis and micellar electrokinetic chromatography. The usefulness of the internal standard technique in order to improve the precision of peak area when either the migration time or the injection volume varied was demonstrated. Quantitative analyses of different pharmaceutical formulations were compared with the LC method of the US Pharmacopeia. A good correlation was obtained.

1. Introduction

Vitamins are structurally heterogenous substances which need elaborate chromatographic techniques for their separation and determination. Amin and Reusch [1] published a liquid chromatographic (LC) method for the simultaneous determination of vitamins B₁, B₂, B₆ and B₁₂ in pharmaceutical preparations. Recently, the USP XXII [2] introduced a monograph for the LC determination of thiamine (B₁), riboflavine (B₂), pyridoxine (B₆) and nicotinamide (PP) in tablets and capsules. As these so-called water-soluble vitamin compounds are readily ionizable, except PP, capillary electrophoresis (CE) has been shown a valuable alternative technique for their separation. Micellar electrokinetic chromatography (MEKC) was proposed by Fujiwara *et al.* [3] and Nishi *et al.* [4] for the separation of water-soluble vitamins and Ong *et*

al. [5] proposed the separation of water- and oil-soluble vitamins. However, only limited attention was paid to pharmaceutical analysis. In this work, a capillary zone electrophoresis (CZE) method and an MEKC method were developed for the determination of B₁, B₂, B₆ and PP in some commercial preparations. The results were compared with those obtained by the LC method given in the USP.

2. Experimental

2.1. Equipment

Electrophoresis was carried out on a Beckman (Palo Alto, USA) P/ACE 2100 system fitted with a UV detector. Separations were performed in a 570 mm × 0.075 mm I.D. fused-silica capillary tube (Beckman). Integration of the electropherograms was achieved by System Gold V.711 software (Beckman).

* Corresponding author.

The LC system consisted of an L-6000 LC pump, an L-400 variable-wavelength UV detector and a D-2000 integrator, all from Merck–Hitachi. A 250 mm \times 4 mm I.D. LiChroCART column containing LiChrospher 100 RP-18 (5 μ m) packing from Merck was used. Injections were made with a 20- μ l loop valve.

2.2. Chemicals and reagents

Thiamine hydrochloride (B_1) and pyridoxine hydrochloride (B_6) were obtained from Merck (Darmstadt, Germany) and riboflavine (B_2) and nicotinamide (PP) from Bios (Belgium). All the reagents were of analytical-reagent grade. The solvent used in all CE experiments for dissolving and diluting the vitamin solutions consisted of 0.01 M hydrochloric acid containing 20% (v/v) acetonitrile. The addition of acetonitrile was necessary to ensure complete dissolution of B_2 . Throughout all experiments paracetamol was used as an internal standard. The separation buffer of pH 9 was 0.02 M sodium tetraborate solution and the separation buffer of pH 7 was prepared by mixing an appropriate volume of 0.02 M borate solution with 0.02 M sodium dihydrogenphosphate solution. All solutions were prepared with water obtained from a Seralpur Pro $_{90}$ CN purification system (Seral, Germany). For MEKC, sodium dodecyl sulphate (SDS) was added to the buffer solutions at a concentration of 0.1 M. All buffer solutions were filtered through a 0.2- μ m membrane filter before use.

For the LC analyses according to the USP XXII [2], the solvent was dilute acetic acid containing 5% (v/v) acetonitrile; the vitamin solution was kept on a water-bath at 65–70°C for 10 min and cooled before injection.

2.3. Procedures

For CZE and MEKC, injections were made hydrodynamically by pressure for 3 s. The applied voltage was 20 kV, which provided a current of *ca.* 50 μ A in CZE and 100 μ A in MEKC. The temperature was kept constant at 25°C. Detection was performed at 214 nm. Before each injection, separating buffer was passed through the capillary for 4 min.

According to the LC method of the USP [2], separations were performed in the reversed-phase mode on a 5- μ m C_{18} column. The mobile phase was water–methanol–glacial acetic acid (73:26:1) to which sodium hexanesulphonate was added. Detection was performed at 280 nm.

2.4. Sample preparation

For tablets, ten tablets were ground to a homogeneous powder and an aliquot was suspended in 50.0 ml of solvent, sonicated and centrifuged. Appropriate volumes were taken, internal standard solution was added and the volumes were adjusted with the same solvent so as to obtain concentrations of each vitamin up to 500 μ g/ml.

For soft gelatin capsules, ten capsules were immediately dissolved in 500.0 ml of solvent, sonicated and further treated as for tablets.

For syrups, an aliquot volume was weighed, the internal standard solution was added and the volume was adjusted with the solvent.

3. Results and discussion

Under the conditions used in the CZE mode, a mixture of the four vitamins was completely resolved within 6 min. The migration sequence of the vitamins observed in borate buffer (pH 9) was the same as that found by Nishi *et al.* [4], *i.e.*, B_1 , PP, B_2 and B_6 , and paracetamol eluted between PP and B_2 . Thiamine elutes first owing to its positive charge, followed by PP, which is neutral. Paracetamol, B_2 and B_6 are negatively charged at pH 9 and their migration velocity depends largely upon their degree of ionization and molecular size. The fact that B_2 elutes after paracetamol is the result of the complexation of the ribose moiety of riboflavine with borate ions. By this reaction B_2 becomes more negatively charged than expected from its pK_a value of 10.2, corresponding to only 6% ionization, in contrast with paracetamol (pK_a = 9.5), which provides about 25% ionization.

In MEKC, a concentration of 100 mM SDS in the borate buffer (pH 9) was found to provide the separation of PP from acetonitrile, both neutral compounds eluting together with the

electroosmotic flow (EOF) in the CZE mode. The addition of acetonitrile to this buffer improved the peak efficiency, especially for PP. On the other hand, it can be seen from Fig. 1A that, as a function of the acetonitrile concentration of the buffer, the migration times are prolonged except for B_1 , resulting from the decrease in the EOF as indicated by the EOF marker formamide.

In contrast to CZE, in MEKC B_1 elutes with the slowest velocity owing to the electrostatic interaction of the positively charged compound with the negatively charged micelles. However, when the separating buffer contained larger amounts of acetonitrile, a second peak of B_1 appeared between the peaks of B_2 and B_6 . This peak was found to originate from the degradation of B_1 in alkaline medium, which might be

enhanced by the addition of acetonitrile. This degradation was not observed in the aqueous buffer of pH 9 in CZE.

On lowering the pH of the running buffer from 9 to 7, the degradation peak disappeared in the mixed aqueous–acetonitrile solution (see Fig. 1B). At this pH thiamine is completely ionized whereas the other vitamins are no longer ionized. It can also be noted from Fig. 1B that at pH 7 the migration of thiamine and, to a lesser extent, riboflavin becomes progressively faster in buffers with a higher acetonitrile content. However, the overall longer migration times of these two compounds is due to their stronger interaction with the micelles: ionic interaction for thiamine and hydrophobic interaction for riboflavin. In the presence of acetonitrile these interactions become weaker and result in smaller capacity factors.

A concentration of 13% of acetonitrile in the separating buffer at pH 7 containing 0.1 M SDS was chosen to perform the MEKC analyses. Under these conditions the separations were completed within 13 min. The order of elution was PP, paracetamol, B_6 , B_2 and B_1 .

For quantification purposes, some workers report the necessity to correct the raw peak area by dividing by the corresponding migration time, [6,7] whereas others [8–11] stress the use of the internal standard technique to obtain precise results.

Before starting quantitative analyses of the vitamins we investigated the problem of peak area precision under two different experimental conditions, first such that the migration times were not altered, and second when the migration times exhibited large differences. A 0.01 M HCl solution containing 600 $\mu\text{g}/\text{ml}$ of B_1 , 100 $\mu\text{g}/\text{ml}$ of paracetamol and 150 $\mu\text{g}/\text{ml}$ of B_6 was analysed in the CZE mode at 10, 15 and 20 kV, performing six replicate injections at each voltage. B_1 and B_6 were considered as test substances: B_1 eluted before and B_6 behind the internal standard paracetamol. The results are given in Table 1.

It can be seen that at any voltage, correcting the peak area by the migration time does not improve the precision (R.S.D. 7–10%) which in fact is expected from the low R.S.D. values of

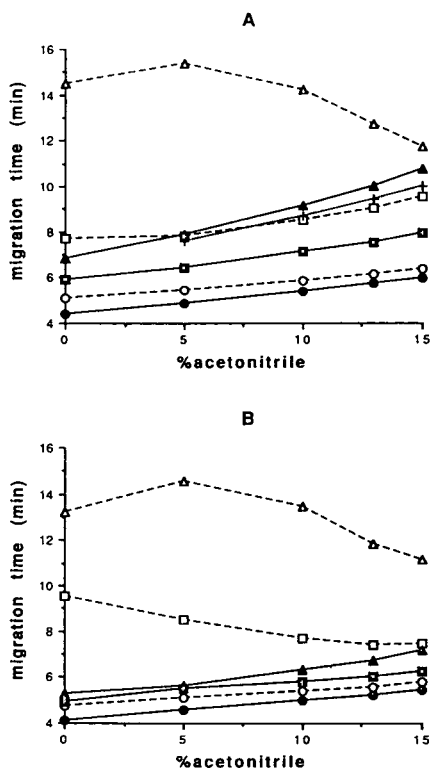


Fig. 1. Effect of acetonitrile on the migration time in MEKC. Buffer, 0.1 M SDS in 0.02 M sodium borate, (A) pH 9 and (B) pH 7; capillary, fused silica, 0.075 mm I.D., length to detector 500 mm, total length 570 mm; injection time, 3 s; voltage, 20 kV; temperature, 25°C. ● = Formamide; ○ = PP; ■ = paracetamol; □ = B_2 ; ▲ = B_6 ; △ = B_1 ; + = B_1 (peak 2).

Table 1

Influence of using corrected area and/or internal standard technique on the precision of peak area

Voltage (kV)	Parameter	t_m (min)			A			$A/A_{1.s.}$		A_c			$A_c/A_{q.s.}$	
		B_1	I.S.	B_6	B_1	I.S.	B_6	B_1	B_6	B_1	I.S.	B_6	B_1	B_6
20	\bar{x}_{20}	2.98	4.49	5.94	0.628	1.140	0.982	0.551	0.862	0.211	0.254	0.165	0.831	0.651
	R.S.D. (%)	0.18	0.44	0.33	7.30	7.64	7.981	1.14	0.72	7.34	7.55	7.94	0.95	0.68
15	\bar{x}_{15}	4.02	6.04	8.04	0.882	1.529	1.409	0.577	0.922	0.219	0.253	0.175	0.867	0.692
	R.S.D. (%)	0.16	0.20	0.15	6.80	6.99	6.82	0.52	0.42	6.94	6.93	6.86	0.48	0.39
10	\bar{x}_{10}	6.15	9.31	12.44	1.103	2.049	1.839	0.538	0.898	0.179	0.220	0.148	0.815	0.672
	R.S.D. (%)	0.15	0.14	0.10	9.76	10.20	9.59	0.76	1.18	9.87	10.18	9.68	0.59	1.03
	$\bar{x}_{10}/\bar{x}_{20}$	2.06	2.07	2.08	1.79	1.87	2.09	0.97	1.04	0.85	0.86	0.89	0.98	1.03
	$\bar{x}_{15}/\bar{x}_{20}$	1.34	1.34	1.35	1.40	1.34	1.43	1.04	1.06	1.03	0.99	1.05	1.04	1.06
	$\bar{x}_{10}/\bar{x}_{15}$	1.52	1.54	1.54	1.25	1.34	1.30	0.93	0.97	0.81	0.87	0.84	0.94	0.97

Capillary, fused silica, 0.075 mm I.D., length to detector 500 mm, total length 570 mm; sample, B_1 600 $\mu\text{g/ml}$, paracetamol (I.S.) 100 $\mu\text{g/ml}$ and B_6 150 $\mu\text{g/ml}$ in 0.01 M HCl; injection time, 3 s; running buffer, 0.02 M sodium borate (pH 9); voltage, 20, 15 and 10 kV; temperature, 25°C. t_m = migration time; A = peak area; $A_c = A/t_m$ = corrected area; \bar{x} = mean of six replicate analyses.

the migration times. The precision is greatly improved, however, by the use of an internal standard (R.S.D. 1%).

Moreover, in situations where a variation in migration times was induced by injecting the same solution at different voltages, it can be seen from Table 1 that the ratios of the mean areas calculated from the results obtained at 10, 15 and 20 kV nearly attain unity when the internal standard is taken into account.

3.1. Calibration

For CZE and MEKC, calibration lines were

constructed with concentrations up to 600 $\mu\text{g/ml}$ for B_1 , 1200 $\mu\text{g/ml}$ for PP and 120 $\mu\text{g/ml}$ for B_2 and B_6 . Linear regression lines of the ratios of the peak areas to that of the internal standard as a function of the concentration were calculated using the least-squares method. Good linearity was obtained for all components in the range studied.

3.2. Precision and accuracy

The accuracy and the within-day precision (repeatability) were evaluated by determining the four vitamins in an artificially prepared

Table 2

Recovery (\bar{x}), repeatability (R.S.D.) and accuracy [95% confidence interval (C.I.)] for spiked powder samples ($n = 6$)

Method	Parameter	PP	B_6	B_2	B_1
CZE	\bar{x}	143.6	100.5	99.7	101.2
	R.S.D. (%)	1.7	1.3	2.2	2.2
	C.I.	141.3–145.8	99.3–101.7	97.6–101.7	99.1–103.2
MEKC	\bar{x}	100.4	99.8	99.7	100.9
	R.S.D. (%)	0.8	1.2	1.8	2.8
	C.I.	99.1–101.7	98.7–101.0	97.8–101.6	98.4–103.6

Sample, B_1 and B_2 120 $\mu\text{g/ml}$, B_6 85 $\mu\text{g/ml}$ and PP 400 $\mu\text{g/ml}$ in 20% acetonitrile in 0.01 M HCl; running buffer, CZE 0.02 M sodium borate (pH 9), MEKC 13% acetonitrile in 0.02 M borate-phosphate (pH 7) containing 0.1 M SDS; voltage, 20 kV; other conditions as in Table 1.

mixture composed of 3.3% B₁, 11.0% PP, 3.3% B₂ and 2.2% B₆, added to a mixture of tablet excipients composed of lactose, starch, polyvinylpyrrolidone (PVP), talc and magnesium stearate. Samples were treated as described in the procedure for sample preparation for tablets and the final concentrations of vitamins were 120 µg/ml of B₁, 400 µg/ml of PP, 120 µg/ml of B₂ and 85 µg/ml of B₆, using 2.0 ml of 50 µg/ml paracetamol solution as the internal standard. Six replicate samples were analysed by comparison with an external reference solution of the vitamins. Mean recoveries are given in Table 2, together with the relative standard deviations and 95% confidence intervals (C.I.) of the mean. Acceptable repeatability (R.S.D. 3%) and good accuracy were obtained for all vitamins. However, a high recovery was observed in the CZE analysis of PP, which is attributed to PVP, which was present in a high concentration (6% of the total mass) in the excipient mixture. PVP is an uncharged compound and interferes with nicotinamide, both migrating at the velocity of the EOF. Such interferences could be resolved in the MEKC mode.

3.3. Analyses of commercial vitamin preparations

Three commercial tablet formulations, one syrup and one soft gelatin capsule preparation were analysed by CZE and MEKC. For comparison, the LC method of the USP XXII [2] for the analysis of vitamin tablets was also applied to the same samples. Fig. 2 shows typical CZE and MEKC results and the LC results for tablet 1. For most of the preparations investigated, each vitamin could be determined without interference by both CE and LC methods. It can be noted from Fig. 2 that calcium pantothenate could also be determined with the CE systems used. In tablets that contained PVP, the result for PP by CZE was not different from those given by LC and MEKC; probably the amount of PVP present in the tablets was lower than the detectable concentration. However, with soft gelatin capsules LC could not be used owing to the presence of oily droplets in the sample solution. In CZE, these droplets were

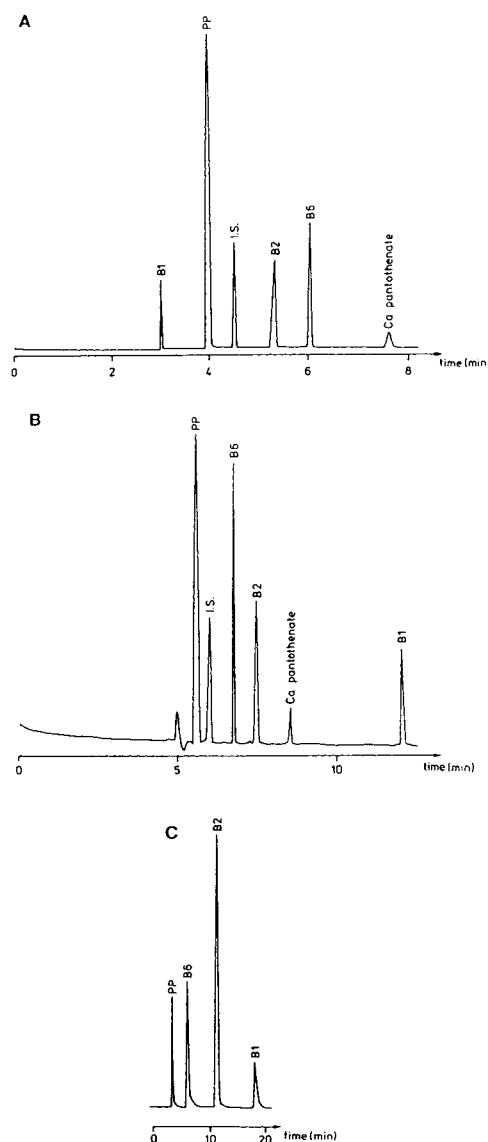


Fig. 2. Comparison of CE separations and LC separation of tablet 1. (A) CZE separation, 0.02 M borate buffer (pH 9), 214 nm, 20 kV; (B) MEKC separation, 13% acetonitrile in 0.02 M borate-phosphate buffer (pH 7) containing 0.1 M SDS, 214 nm, 20 kV; (C) LC separation, USP method [2].

probably adsorbed on the capillary surface and caused broadening of the zones and increased migration times resulting from a decrease in the EOF [12]. This was not a problem in MEKC as the surfactant SDS probably dissolves the oily droplets. The results of the analyses of the commercial preparation are given in Table 3.

Table 3
Determination of vitamins B₁, B₂, B₆ and PP in commercial preparations

Sample	Analyte	$\bar{x} \pm \text{S.D.} (\%)$		
		CZE	MEKC	LC
Tablet 1	B ₁ (15 mg)	118.7 \pm 1.7	123.6 \pm 2.6	123.8 \pm 3.6
	PP (50 mg)	110.8 \pm 3.1	108.0 \pm 1.2	108.7 \pm 2.1
	B ₂ (15 mg)	99.0 \pm 2.2	99.4 \pm 2.1	103.9 \pm 0.7
	B ₆ (10 mg)	110.9 \pm 3.3	113.7 \pm 1.7	112.4 \pm 3.2
Tablet 2	B ₁ (10 mg)	130.3 \pm 1.3	132.3 \pm 2.1	129.0 \pm 4.6
	PP (25 mg)	107.7 \pm 0.7	105.2 \pm 2.1	109.0 \pm 1.8
	B ₂ (5 mg)	106.9 \pm 3.5	102.1 \pm 2.3	101.1 \pm 4.4
	B ₆ (5 mg)	108.4 \pm 1.6	108.2 \pm 5.3	102.7 \pm 3.1
Tablet 3	B ₁ (50 mg)	104.4 \pm 2.0	103.7 \pm 1.3	106.4 \pm 3.7
	PP (100 mg)	99.8 \pm 0.7	98.2 \pm 1.3	100.2 \pm 1.4
	B ₂ (10 mg)	104.1 \pm 1.6	109.6 \pm 3.1	108.0 \pm 3.0
	B ₆ (10 mg)	96.3 \pm 1.5	95.0 \pm 1.6	95.7 \pm 3.0
Syrup (5 ml)	B ₁ (10 mg)	117.2 \pm 4.0	112.4 \pm 1.7	111.6 \pm 1.6
	PP (20 mg)	111.2 \pm 1.4	109.4 \pm 0.9	111.5 \pm 3.4
	B ₂ (1 mg)	115.4 \pm 1.5	119.3 \pm 2.9	117.2 \pm 2.2
	B ₆ (5 mg)	109.9 \pm 1.4	106.2 \pm 3.1	113.2 \pm 3.9
Soft capsule	B ₁ (10 mg)	122.0 \pm 2.2	126.6 \pm 1.7	
	PP (30 mg)	111.3 \pm 1.8	108.6 \pm 1.7	
	B ₂ (7 mg)	112.1 \pm 3.1	114.9 \pm 1.6	
	B ₆ (5 mg)	108.6 \pm 1.8	108.2 \pm 1.6	

Results from five determinations are given as mean percentages of the labelled amount (values in parentheses) \pm S.D.

4. Conclusions

The analysis of water-soluble vitamins by capillary electrophoresis (both CZE and MEKC) can be considered as a valuable alternative to LC. Short analysis times and low running costs are the dominant features in CE. It was found that the use of the internal standard technique is necessary in order to obtain good precision with either constant or varying migration times.

5. Acknowledgement

The authors thank Dr. J. Vindevogel for helpful discussions and advice.

6. References

- [1] M. Amin and J. Reusch, *J. Chromatogr.*, 390 (1987) 448.
- [2] *The United States Pharmacopoeia XXII Revision*, Suppl. 8, 1990, p. 3343.
- [3] S. Fujiwara, S. Iwase and S. Honda, *J. Chromatogr.*, 447 (1988) 133.
- [4] H. Nishi, N. Tsumagari, T. Kakimoto and S. Terabe, *J. Chromatogr.*, 465 (1989) 331.
- [5] C.P. Ong, C.L. Ng, H.K. Lee and S.F.Y. Li, *J. Chromatogr.*, 547 (1991) 419.
- [6] T. Ackermans, F.M. Everaets and J.L. Beckers, *J. Chromatogr.*, 549 (1991) 345.
- [7] K.D. Altria, *Chromatographia*, 35 (1993) 177.
- [8] A.M. Hoyt, Jr., and M.J. Sepaniak, *Anal. Lett.*, 22 (1989) 861.
- [9] M.E. Swartz, *J. Liq. Chromatogr.*, 14 (1991) 923.
- [10] E.V. Dose and G.A. Guiochon, *Anal. Chem.*, 63 (1991) 1154.
- [11] E.W. Tsai, M.H. Singh, H.H. Lu, D.P. Ip and M.A. Brooks, *J. Chromatogr.*, 626 (1992) 245.
- [12] J.W. Jorgenson and K.D. Lukacs, *Science*, 222 (1983) 266.

Capillary electrophoresis of nicotinamide–adenine dinucleotide and nicotinamide–adenine dinucleotide phosphate derivatives in coated tubular columns

Marina Nesi, Marcella Chiari*

Istituto di Chimica degli Ormoni, CNR, Via Mario Bianco 9, Milan 20131, Italy, and Faculty of Pharmacy and Department of Biomedical Sciences and Technologies, University of Milan, Via Celoria 2, 20133 Milan, Italy

Giacomo Carrea, Gianluca Ottolina

Istituto di Chimica degli Ormoni, CNR, Via Mario Bianco 9, Milan 20131, Italy

Pier Giorgio Righetti

Faculty of Pharmacy and Department of Biomedical Sciences and Technologies, University of Milan, Via Celoria 2, 20133 Milan, Italy

(First received November 2nd, 1993; revised manuscript received January 28th, 1994)

Abstract

HPCE was shown to be an effective and convenient method for the determination of nicotinamide–adenine dinucleotide (oxidized, NAD^+ ; reduced, NADH), nicotinamide–adenine dinucleotide phosphate (oxidized, NADP^+ ; reduced, NADPH) and their synthetic derivatives. The coenzymes were easily separated among themselves and from their degradation products, which are inhibitors of dehydrogenases, in 15 min in a coated capillary. Several coenzyme derivatives such as N^6 -(2-aminoethyl)- NAD(P)^+ and $\text{N}(1)$ -(2-aminoethyl)- NAD(P)^+ were separated by zone electrophoresis in uncoated or coated capillaries using 50 mM 3-(N-morpholino)propane-sulphonic acid (pH 7.0) or Tris–HCl (pH 8.0) as buffer systems. Capillary zone electrophoresis and micellar electrokinetic capillary chromatography can also be used to monitor continuously coenzyme chemical modifications.

1. Introduction*

The pyridine coenzymes play a central role in the metabolic activities of plants, animals and

microorganisms. The availability of NAD^+ , NADP^+ , NADH and NADPH to investigators has improved dramatically since the introduction of ion-exchange chromatography, which allowed the production of nearly pure NAD^+ in gram amounts. The Dowex chromatography developed by Kornberg [1] was the basis for the commercial preparation of NAD^+ from baker's yeast. NADP^+ , first isolated from red blood cells and then from yeast, in turn obtained from NAD^+ through the NAD -kinase [2] catalysed phosphorylation.

* Corresponding author. Address for correspondence: Istituto di Chimica degli Ormoni, CNR, Via Mario Bianco 9, Milan 20131, Italy.

* Abbreviations: NAD^+ = nicotinamide–adenine dinucleotide, oxidized; NADH = nicotinamide–adenine dinucleotide, reduced; NADP^+ = nicotinamide–adenine dinucleotide phosphate, oxidized; NADPH = nicotinamide–adenine dinucleotide phosphate, reduced.

The chemical stability of pyridine coenzymes has been the subject of extensive investigations since the coenzymes were first isolated [3]. Their reactivity towards acidic or basic pH is remarkably complementary, with both oxidized and reduced coenzymes fortuitously stable in a narrow range of pH, centred on physiological conditions.

A considerable number of NAD(P)⁺ analogues with simple or multiple structural alterations have been synthesized for a variety of experimental needs [4–11]. Analogues have been prepared containing fluorescent bases, reactive groups for covalent modifications of enzymes or, more generally, derivatives designed to investigate structure–function relationships. During the last 15 years, interest has focused on the development of methods for synthesizing macromolecular NAD(H) and NADP(H) derivatives to be used in continuous-flow membrane reactors [12]. Modification of coenzymes outside the active centre generally does not cause a marked loss of enzymatic activity and the analogues can bind to the enzyme and participate in the hydrogen transfer similarly to native coenzymes [13].

Chromatographic methods have been widely applied for the determination of the purity of the pyridine coenzymes and for the determination of the analogues. These methods include chromatography on DEAE-cellulose [14], DEAE-Sephadex [15,16], benzoylated DEAE-cellulose [17], AG MP-1 [18] and reversed-phase high-performance liquid chromatography [19,20].

Capillary zone electrophoresis (CZE) and micellar electrokinetic capillary chromatography (MECC) appear to be attractive tools for the determination of pyridine coenzymes, because of their high separation efficiency, easy operation and low running costs.

In this paper we describe the separation of NAD⁺, NADH, NADP⁺ and NADPH among themselves and from their degradation products and analogues by CZE and MECC. Separations were obtained by CZE in coated or uncoated capillaries according to the electrophoretic mobility of the compounds, or by MECC on the basis of their hydrophobicity or ionic character.

2. Experimental

2.1. Materials

Nicotinamide–adenine dinucleotide (NAD⁺), nicotinamide–adenine dinucleotide reduced form (NADH), nicotinamide–adenine dinucleotide phosphate (NADP⁺), nicotinamide–adenine dinucleotide phosphate reduced form (NADPH), adenosine 5'-diphosphoribose (ADPR), adenosine 5'-monophosphate (AMP), adenosine 5'-diphosphate (ADP), 3-(N-morpholino)propane-sulphonic acid (MOPS), sodium dodecyl sulphate (SDS) and Tris were purchased from Sigma (St. Louis, MO, USA). N-Acryloylaminoethoxy-ethanol was synthesized as described by Chiari *et al.* [21]. Ammonium peroxodisulphate and N,N,N',N'-tetramethylethylenediamine (TEMED) were obtained from Bio-Rad Labs. (Richmond, CA, USA). N(1)-Carboxymethyl-NAD⁺, N⁶-(2-aminoethyl)-NAD⁺, N(1)-(2-aminoethyl)-NADP, N⁶-(2-aminoethyl)-NADP⁺ and N⁶-(2-hydroxy-3-trimethylammoniumpropyl)-NAD⁺ were synthesized as already described [12].

2.2. Methods

CZE was performed in a Waters Quanta 4000 capillary electrophoresis system (Millipore, Milford, MA, USA). For the experiments, uncoated and coated (modified Hjertén procedure [22]) fused-silica capillaries (Polymicro Technologies, Phoenix, AZ, USA) 40 cm (35 cm to the detector) long were used. The separations in uncoated capillaries were carried out using 50 mM Tris–HCl buffer (pH 8.0) or 50 mM MOPS buffer (pH 7.0) in the presence of 50 mM SDS and 10% methanol. The separations in coated capillaries were performed in 50 mM MOPS buffer (pH 7.0). The samples were loaded by hydrostatic pressure and the separations were carried out at room temperature. The detector was set at 254 nm.

2.3. Coating the capillary wall

The following procedure gave the best results. The capillary was first treated with 100 µl of 1 M

NaOH for 5 h, then rinsed and flushed with 100 μ l of 0.1 M HCl followed by 100 μ l of 0.1 M NaOH. After 1 h it was rinsed with water and acetone, filled with a 1:1 solution of Bind Silane [3-(trimethoxysilyl)propyl methacrylate] in acetone and then incubated overnight. After this treatment, the capillary was flushed with air for 5 min and then washed with 20 mM phosphate

buffer (pH 7.0). The capillary was filled with 6% N-acryloylaminoethoxyethanol solution in the same degassed buffer containing the appropriate amount of catalyst (0.5 μ l of TEMED and 0.5 μ l of 40% ammonium peroxodisulphate per ml of gelling solution). Polymerization was allowed to proceed overnight at room temperature and then the capillary was emptied by means of a syringe.

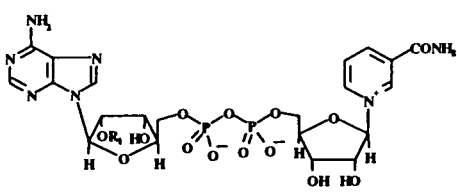
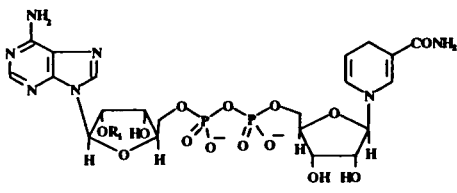
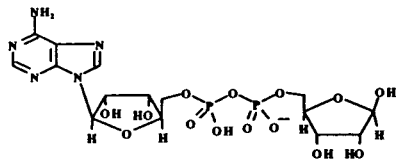
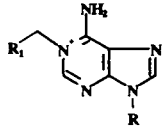
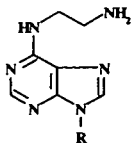
NAD^+ $\text{R}_1 = \text{H}$ (1) NADP^+ $\text{R}_1 = \text{PO}_3^-$ (2)	
NADH $\text{R}_1 = \text{H}$ (3) NADPH $\text{R}_1 = \text{PO}_3^-$ (4)	
Adenosine 5'-diphosphoribose (5)	
$\text{N}(1)-(2\text{-aminoethyl})\text{-NAD}^+/\text{NADP}^+$ $\text{R}_1 = \text{CH}_2\text{NH}_2$ (6) $\text{N}(1)\text{-carboxymethyl-NAD}^+$ $\text{R}_1 = \text{COOH}$ (7)	
$\text{N}^6\text{-(2-aminoethyl)-NAD}^+/\text{NADP}^+$ (8)	

Fig. 1. Structures of $\text{NAD(P)}^+/\text{NAD(P)H}$ derivatives.

3. Results and discussion

The structures of the coenzymes and of their degradation products and analogues are shown in Fig. 1. A mixture of NAD^+ , NADP^+ , NADH , NADPH , AMP , ADP and adenosine 5'-diphosphoribose was resolved into seven well separated peaks by HPCE (Fig. 2). Identification was achieved by injecting either the mixture of products or a sample of each component. The CE separation reported was performed using different buffers in a coated capillary: 50 mM Tris-HCl (pH 8.0) or 50 mM MOPS (pH 7.0). Satisfactory resolution was achieved in both instances but MOPS is preferable as it allows a high voltage to be used as its conductivity is lower. The use of a coated capillary is essential

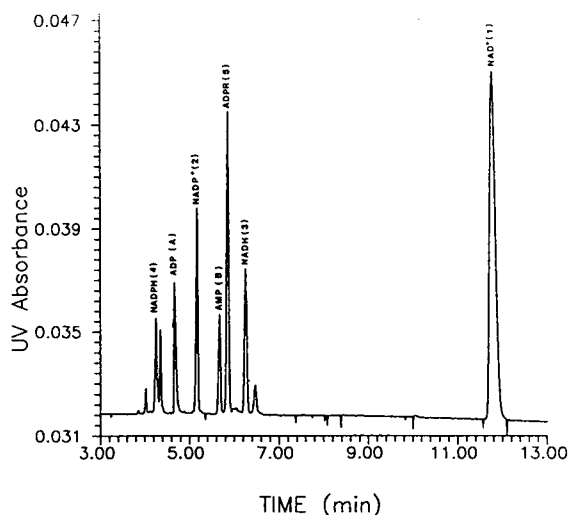


Fig. 2. CZE profile of a mixture of seven NAD(P)^+ and NAD(P)H derivatives. Conditions: Waters Quanta 4000 unit, fitted with a coated capillary of 45 cm \times 100 μm I.D. with 50 mM MOPS (pH 7.0), run at 15 kV and 39 μA ; sample concentration, 0.1 mM in 50 mM MOPS buffer; sample injection, 5 s by hydrostatic pressure; detection at 254 nm; anodic migration (reverse polarity). Peaks: 4 = nicotinamide-adenine dinucleotide phosphate (NADP^+), A = adenosine 5'-diphosphate (ADP); 2 = nicotinamide-adenine dinucleotide phosphate (NADP^+); B = adenosine 5'-monophosphate (AMP); 5 = adenosine 5'-diphosphoribose (ADPR); 3 = nicotinamide-adenine dinucleotide reduced form (NADH); 1 = nicotinamide-adenine dinucleotide (NAD^+).

in order to obtain sharp peaks and reproducible results.

Fig. 3A and B depict the electropherograms of

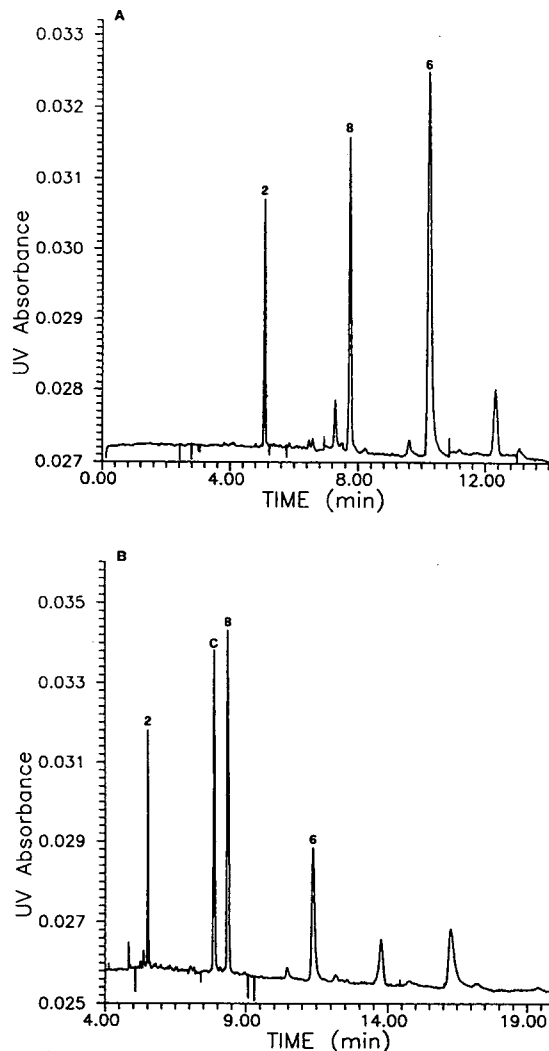


Fig. 3. (A) CZE separation of a mixture of NADP^+ derivatives. Conditions as in Fig. 1. Sample concentration, 0.03 mg/ml in 50 mM MOPS buffer; sample injection, 5 s by hydrostatic pressure; detection at 254 nm. Peaks: 2 = NADP^+ ; 8 = N^6 -(2-aminoethyl)- NADP^+ ; 6 = $\text{N}(1)$ -(2-aminoethyl)- NADP^+ . (B) Analysis of Dimroth rearrangement products. Conditions as in Fig. 1. Sample concentration, 0.03 mg/ml in 50 mM MOPS buffer; sample injection, 5 s by hydrostatic pressure. Peaks: 2 = NADP^+ ; C = tricyclic 1, N^6 -ethanoadenine- NADP^+ ; 8 = N^6 -(2-aminoethyl)- NADP^+ ; 6 = $\text{N}(1)$ -(2-aminoethyl)- NADP^+ .

some NADP⁺ derivatives. It can be seen that NADP⁺ was easily and rapidly separated from N(1)-(2-aminoethyl)-NADP⁺ and from N⁶-(2-aminoethyl)-NADP⁺ (Fig. 3A). The incubation of N(1)-(2-aminoethyl)-NADP⁺ at pH 6.0–6.5 and 40–50°C yields, through a Dimroth rearrangement, N⁶-(2-aminoethyl)-NADP⁺ [12], which is the coenzymatically active form to be used for the covalent linking to soluble polymers [12,13]. In the rearrangement a low conversion of the N(1)- to the N⁶-derivative occurs, as a parallel transformation to the tricyclic 1,N⁶-ethanoadenine-NADP⁺ takes place. Fig. 3B shows that the separation of the three reaction components is fast and complete, which facilitates the continuous monitoring of the reaction course. The detection limit for the coenzyme assay (at a signal-to-noise ratio of 3) was 2.0 μ M and the response was linear in the concentration range 0.0025–5 mM. The unidentified peaks are probably degradation and secondary products of the reaction.

In Fig. 4 it can be seen that NAD⁺, N(1)-(2-aminoethyl)-NAD⁺ and N⁶-(2-aminoethyl)-NAD⁺ are resolved in an uncoated capillary in 5 min using Tris–HCl as buffer. Analogous conditions have been used for resolving NAD⁺ from N⁶-(2-hydroxy-3-trimethylammoniumpropyl)-NAD⁺, as shown in Fig. 5. The electropherogram in Fig. 6 depicts a MECC separation of NAD⁺ from the N(1)-carboxymethyl derivative. The running conditions chosen were 50 mM MOPS (pH 7.0)–50 mM SDS–10% methanol in an uncoated capillary. With the experimental conditions used the N(1)-carboxymethyl derivative was found to elute after 4 min.

Both commercial and enzymatically generated preparations of pyridine nucleotides, in particular the reduced forms, contain impurities. Some of these, such as adenosine 5'-diphosphoribose, are inhibitors of a number of dehydrogenases. The speed and the resolving capability of HPCE provide a valid method for the analysis of NAD(P)⁺ and NAD(P)H impurities which are clearly separated in a single run. Most of the currently used purification and analytical procedures rely on anion-exchange chromatography on DEAE columns. These methods suffer from

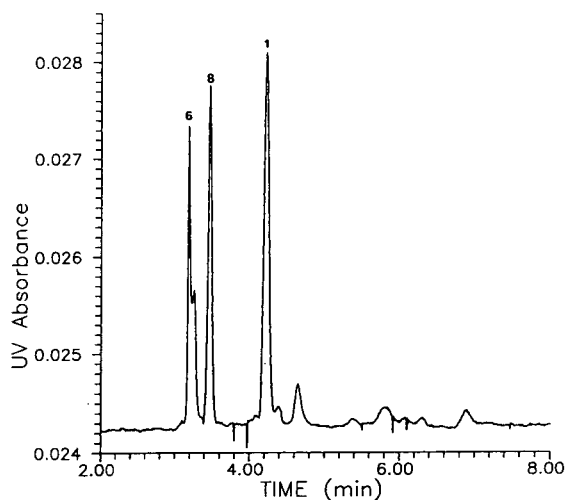


Fig. 4. CZE profile of a mixture of NAD⁺ derivatives. Conditions: Waters Quanta 4000 unit, fitted with an uncoated capillary of 40 cm \times 75 μ m I.D. with 50 mM Tris–HCl (pH 8.0), run at 12 kV and 42 μ A; sample concentration, 0.3 mg/ml in 50 mM Tris–HCl buffer; sample injection, 5 s by hydrostatic pressure; detection at 254 nm; cathodic migration. Peaks: 6 = N(1)-(2-aminoethyl)-NAD⁺; 8 = N⁶-(2-aminoethyl)-NAD⁺; 1 = NAD⁺.

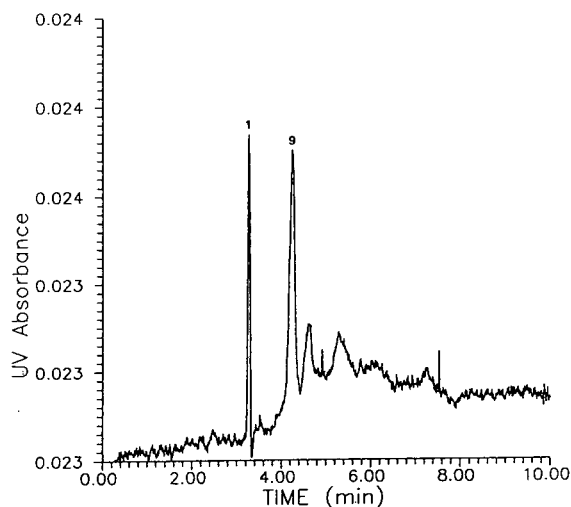


Fig. 5. CZE separation of NAD⁺ (peak 1) from N⁶-(2-hydroxy-3-trimethylammoniumpropyl)-NAD⁺ (peak 9). Conditions as in Fig. 3. Sample concentration, 0.3 mg/ml in 50 mM Tris–HCl buffer; sample injection, 5 s by hydrostatic pressure; detection at 254 nm.

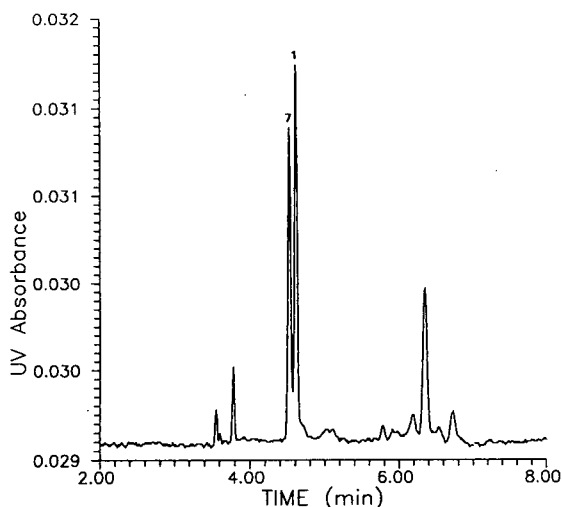


Fig. 6. MECC separation of N(1)-carboxymethyl-NAD⁺ (peak 7) from NAD⁺ (peak 1). Conditions: uncoated capillary of 40 cm × 75 μm I.D. with 50 mM MOPS (pH 7.0)–50 mM SDS–10% methanol, run at 12 kV and 35 μA; sample concentration, 0.15 mM in 50 mM MOPS buffer; sample injection, 5 s by hydrostatic pressure; detection at 254 nm; cathodic migration.

several disadvantages over that described here; for instance, NADH and NADP⁺ are not resolved and ADPR is not separated from NADH [14–18]. Reversed-phase HPLC [18] easily separates NAD⁺ from NADH but does not resolve very well NADP⁺ from NADPH, which are eluted very close to the column void volume [23].

CE and MECC appear to be effective tools also for the determination of pyridine coenzyme derivatives. Some analogues are important probes for studying the structure–activity relationships and mapping the coenzyme binding sites of dehydrogenases, and others are used for various immobilization procedures, but in all instances a high level of purity of the synthetic derivatives is required for obtaining reproducible results. Among the low-molecular-mass precursors N⁶-(2-aminoethyl)-NAD(P)⁺ and N(1)-(2-aminoethyl)-NAD(P)⁺ are of direct interest for use in dehydrogenase-based membrane reactors and for the preparation of affinity matrices.

In conclusion, the results described in this paper demonstrate the great effectiveness and

convenience of HPCE for the determination of NAD(P)⁺ and NAD(P)H and their synthetic derivatives. Because of the high analysis speed, HPCE can also be used to monitor continuously the course of coenzyme chemical modifications.

4. Acknowledgement

This work was supported in part by a grant from CNR, Progetto Finalizzato Chimica Fine II SP. 3 Prodotti con Attività Biologica, to P.G.R.

5. References

- [1] A. Kornberg, *Methods Enzymol.*, 3 (1957) 876–882.
- [2] T.P. Wang, N.O. Kaplan and F.E. Stolzenbach, *J. Biol. Chem.*, 211 (1954) 465–472.
- [3] O. Warburg, W. Christian and A. Griesse, *Biochem. Z.*, 282 (1935) 157–205.
- [4] B.M. Anderson, in B.M. Anderson and K. You (Editors), *The Pyridine Nucleotide Coenzymes*, Academic Press, New York, 1982, pp. 91–133.
- [5] H. Vutz, R. Koob, R. Jeck and C. Woenckhaus, *Liebigs Ann. Chem.*, (1980) 1259–1270.
- [6] H.N. Jayaram, G.S. Ahluwalia, R.L. Dion, G. Gebeyehu, V.E. Marquez, J.A. Kelley, R.K. Robins, D.A. Cooney and D.G. Johns, *Biochem. Pharmacol.*, 32 (1983) 2633–2636.
- [7] Y. Yamazaki and H. Maeda, *Agric. Biol. Chem.*, 45 (1981) 2277–2288.
- [8] S. Chen and R.J. Guillory, *J. Biol. Chem.*, 256 (1981) 8318–8323.
- [9] J. Marchand, J. Torrelles, M.C. Guerin, B. Descomps, A. Crastes de Paulet, M. Gabriel and D. Larcher, *Biochimie*, 64 (1982) 203–209.
- [10] K.G. Glogger, K. Balasubramanian, A. Beth, T.M. Fritzche, J.H. Park, D.E. Pearson, W.E. Trommer and S.D. Venkataramu, *Biochim. Biophys. Acta*, 701 (1982) 224–228.
- [11] G. Gebeyehu, V.E. Marquez, J.A. Kelley, D.A. Cooney, H.N. Jayaram and D.G. Johns, *J. Med. Chem.*, 26 (1983) 922–925.
- [12] A.F. Buckmann and G. Carrea, *Adv. Biochem. Eng. Biotechnol.*, 39 (1989) 97–151; and references cited therein.
- [13] C. Wandrey and R. Wichmann, in A. Laskin (Editor), *Application of Isolated Enzymes and Immobilized Cells to Biotechnology*, Addison-Wesley, NJ, 1985, pp. 177–208.
- [14] E.J. Pastore and M. Friedkin, *J. Biol. Chem.*, 236 (1961) 2314–2316.

- [15] I. Wenz, W. Loesche, U. Till, H. Petermann and A. Horn, *J. Chromatogr.*, 120 (1980) 187–196.
- [16] W. Loesche, I. Wenz, U. Till, H. Petermann and A. Horn, *Methods Enzymol.*, 66 (1980) 11–23.
- [17] L. Kurz and C. Frieden, *Biochemistry*, 16 (1977) 5207–5216.
- [18] R.E. Viola, P.F. Cook and W.W. Cleland, *Anal. Biochem.*, 96 (1979) 334.
- [19] S.A. Margolis, B.F. Howell and R. Shaffer, *Clin. Chem.*, 22 (1976) 1322.
- [20] M. Pace, P.L. Mauri, C. Gardana and P.G. Pietta, *J. Chromatogr.*, 476 (1989) 487–490.
- [21] M. Chiari, C. Micheletti, M. Nesi, M. Fazio and P.G. Righetti, *Electrophoresis*, in press.
- [22] S. Hjertén, *J. Chromatogr.*, 347 (1985) 191–198.
- [23] G. Ottolina, S. Riva, G. Carrea, B. Danieli and A. Buckmann, *Biochim. Biophys. Acta*, 998 (1989) 173–178.

Determination of fluoride in feed mixtures by capillary isotachopheresis

Pavel Blatný*, František Kvasnička

Department of Carbohydrate Chemistry and Technology, Institute of Chemical Technology Prague, Technická 5, CZ-166 28 Prague 6, Czech Republic

(First received August 19th, 1993; revised manuscript received January 24th, 1994)

Abstract

An isotachopheretic (ITP) method for the determination of fluoride in feed mixtures was developed. A sample of feed mixture, after extraction with 1 M HCl, was analysed using a ZKI 02 column-coupling isotachopherograph. Leading electrolytes for presentation and analytical capillaries consisted of 0.008 M HCl–0.022 M ϵ -aminocaproic acid (EACA)–0.001 M CaCl_2 –0.05% hydroxypropylmethyl cellulose (HPMC) and 0.002 M HCl–0.005 M EACA–0.05% HPMC, respectively. The terminating electrolyte was 0.01 M tartaric acid. The fluoride released from samples by microdiffusion in 25% perchloric acid was determined using an Ionosep 900.1 single capillary isotachopherograph with 0.002 M HCl–0.005 M EACA–0.05% HPMC as the leading electrolyte and 0.002 M tartaric acid as the terminating electrolyte. The detection limit, depending on the sample treatment, was as low as 4 $\mu\text{g/g}$ as fluoride. A comparison of the developed ITP method with ion-selective electrode method was carried out.

1. Introduction

Fluoride is included in the category of harmful substances and its content in feeds is limited (150 ppm in the Czech Republic [1]). Fluoride levels in feeds should not exceed the authorised limits, and therefore it is necessary to have a suitable method available for its determination. Spectrophotometric determination with xylenol orange can be used [2], where an ashed sample is analysed after isolation of fluoride by steam distillation from perchloric acid. Another method involves microdiffusion from perchloric acid and spectrophotometric determination with

lanthanum alizarin complexone [2]. Tušl [3] developed a method for the determination of fluoride in phosphates with a fluoride ion-selective electrode. Torma [4] used a fluoride ion-selective electrode to determine fluoride released from an animal feed by extraction with 1 M hydrochloric acid. He compared this method with the official AOAC method (ashing the sample followed by steam distillation and titration) and reported good agreement of the results. Singer and Ophaug [5] determined fluoride in some foods with a fluoride ion-selective electrode. Fluoride was isolated from ashed and unashed sample by heat- or silicone-facilitated diffusion. Higher levels of fluorine were found in ashed samples (total fluorine) than in unashed samples (ionic acid-labile fluorine).

* Corresponding author.

2. Experimental

2.1. Chemicals

Analytical-reagent grade chemicals were used unless indicated otherwise.

Hydrochloric acid (Normanal), 0.1 mol/l, acetic acid (99%), hydrochloric acid (35–37%), and perchloric acid (70%), were obtained from Lachema (Brno, Czech Republic), β -alanine (BALA) (99%+), and ϵ -aminocaproic acid (EACA), from Janssen Chimica (Beerse, Belgium), hydroxypropylmethylcellulose (HPMC) 4000 from Aldrich (Milwaukee, WI, USA), and tartaric acid, disodium phosphate, sodium hydroxide and calcium chloride from Lachema.

2.2. Samples

Animal feed mixtures were as follows: sample A = feed mixture for pigs of up to 35 kg of live mass; sample B = feed mixture for broilers; sample C = feed mixture for calves; and sample D = feed mixture prepared by mixing of phosphate B (see below) with sample A.

The phosphate samples were (A) dicalcium phosphate exported from The Netherlands and (B) dicalcium phosphate purchased from Fosfa Poštorná (Czech Republic).

2.3. Instrumentation

A ZKI 02 column-coupling isotachopherograph; a PTFE preseparation capillary (170 \times 0.8 mm I.D.) and a PTFE analytical capillary (170 \times 0.3 mm I.D.) were obtained from Villa (Slovak Republic). An Ionosep 900.1 volume-coupling single-capillary isotachopherograph (preseparation part 50 \times 1 mm I.D., separation part 150 \times 0.45 mm I.D. and detection part 70 \times 0.40 mm I.D.) was obtained from Recman-Laboratorní Technika (Czech Republic).

A TZ 4200 chart recorder (Laboratorní přístroje, Prague, Czech Republic), a QP-205/1 pH meter (Radelkis, Budapest, Hungary), a Crytur fluoride ion-selective electrode (Monokrystaly Turnov, Czech Republic) and a Model AT/286 IBM-compatible microcomputer were used.

2.4. Conditions of analysis

The electrolyte systems and running parameters are presented in Table 1.

2.5. Calibration

An external standard calibration method was used with sodium fluoride as the standard. For the determination of fluoride on ZKI 02, four

Table 1
Electrolyte systems and running parameters

Electrolyte system ^a	Capillary	Current (μ A)
(I) LE ₁ : 8 mM HCl–22 mM EACA–1 mM CaCl ₂ –0.05% HPMC, pH 4.45	Preseparation	Initial 300 Detection 250
LE ₂ : 2 mM HCl–5 mM EACA–0.05% HPMC, pH 4.25	Analytical	Initial 30 Detection 5
TE: 10 mM tartaric acid (for determination of fluoride in phosphates, 10 mM sodium hydrogenphosphate)		
(II) LE: 2 mM HCl–5 mM EACA–0.05% HPMC		Initial 40 Detection 5
TE: 2 mM tartaric acid		

^a I = Electrolyte system for the determination of fluoride released by extraction with 1 M HCl using the ZKI 02 (analysis time 22–27 min depending on sample dilution). II = Electrolyte system for determination of fluoride released by heat-facilitated diffusion from 25% perchloric acid on the Ionosep 900.1 (analysis time 10 min). LE = Leading electrolyte; TE = terminating electrolyte.

concentration levels were measured (0.2–1 $\mu\text{g/ml}$). The standard solution was injected into the isotachopherograph by a sample valve (40 ml) and by a 100-ml Hamilton syringe. For the determination of fluoride on the Ionosep 900.1, four calibration points were measured (0.2–1 $\mu\text{g/ml}$). Standard solutions were injected by a sample valve (20 μl).

2.6. Sample preparation

Determination of fluoride released by extraction of 1 M HCl on the ZKI 02

Into a 200-ml volumetric flask, 2–5 g of an animal feed mixture were weighed and extracted with 20 ml of 1 M HCl with magnetic stirring for 30 min at ambient temperature. The volume was then made up to 200 ml with distilled water. After filtration and dilution (tenfold with deionized water), the solution obtained was injected into the isotachopherograph. For the determination of fluoride in dicalcium phosphates, 500 mg of sample were weighed into a 100-ml volumetric flask and extracted with 20 ml of 1 M HCl with magnetic stirring under the above-mentioned conditions. The volume was made up to 100 ml with distilled water. After dilution (20–50-fold with deionized water), the solution obtained was analysed using the ZKI 02 isotachopherograph.

Determination of fluoride released by heat-facilitated diffusion from 25% perchloric acid on the Ionosep 900.1

On the bottom of a polyethylene Petri dish, 1–2 g of feed mixture or 150 mg of dicalcium phosphate were placed and 25% perchloric acid (8 ml) was added. The diffused fluoride was trapped in 1 ml of 0.5 M NaOH that was placed in a smaller dish at the bottom of the Petri dish. The rims of both parts of the Petri dishes were coated with silicone grease. The dishes were placed in a thermostat at 60°C for 16 h. After heat-facilitated diffusion, the contents of the smaller dish were transferred into a 25-ml volumetric flask (stock solution). A 1–2 ml volume of the stock solution was pipetted into a 10-ml volumetric flask, 1 ml of 0.01 M acetic acid was

added and the volume was made up with deionized water. The solution was then analysed using the Ionosep 900.1 isotachopherograph.

3. Results and discussion

For the determination of fluoride released by the extraction with 1 M HCl, an isotachopherograph with a column-coupling system (ZKI 02) is necessary because of the high concentration of chloride. In addition, various feed samples can have different qualitative compositions, causing difficulties in the selection of an electrolyte system for the determination of fluoride released by extraction with HCl. First leading electrolytes without co-counter ions were tested. These electrolytes were chosen with the support of computer steady-state simulation in order to prevent mixed zones of fluoride with anions, which are present in feed mixtures (oxalate, tartrate, formate, pyrophosphate).

Leading electrolytes with BALA, EACA and histidine counter ions were tested. As the sample contains a very low concentration of fluoride it is necessary to apply a driving current that is as low as possible (5 μA), allowing quantitative analysis. Therefore, it was also necessary to use a leading electrolyte with a lower concentration of the leading anion to ensure sufficiently sharp boundaries between the zones. We tested leading electrolytes with concentrations 2 mM of leading anion (HCl) and 5 mM of counter ion (the same counter ion as in the pre-separation capillary). However, it was found that fluoride created a mixed zone with unknown anions in all these systems. Therefore, these leading electrolytes were optimized through the addition of a co-counter ion (Ca) to the leading electrolyte in the pre-separation capillary. The best results were obtained with the system presented in Table 1. In this system the separation of fluoride from interfering ionic compounds due to a complex-forming equilibrium with Ca was achieved.

For the determination of fluoride in feed mixtures, 10 mM tartaric acid served as the terminating electrolyte. The choice of this terminator is very important, because some anions

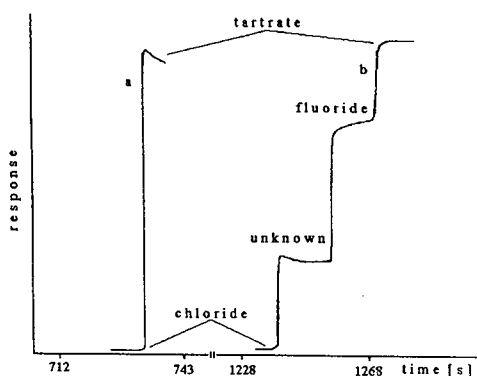


Fig. 1. Isotachopherogram of animal feed mixture (sample C), measured with the ZKI 02 column-coupling isotachopherograph: (a) pre-separation capillary; (b) analytical capillary. The isotachopherograms were measured with a contact conductivity detector. It is clear from the analytical conditions (see Table 1) that a 1 mm step length of fluoride in the pre-separation capillary gives a 50 mm step length in the analytical capillary. The optimum timing of the column switching was found to be 3 s before the fluoride zone reached the bifurcation block.

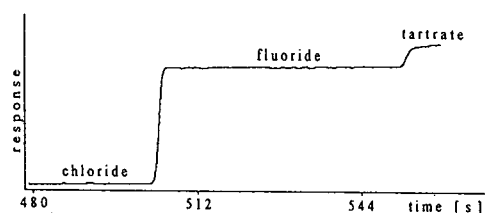


Fig. 2. Isotachopherogram of a model mixture of the 2 mg/ml of fluoride acquired with the Ionosep 900.1 single-capillary isotachopherograph. As microdiffusion represents purification process, the isotachopherogram of the real sample analysis also contains only one step, fluoride. For details, see text (Table 1).

that form complexes with Ca have an effective mobility lower than that of the terminator. Hence these anions remain the pre-separation capillary and do not load the very low separation capacity in the analytical capillary.

For the determination of fluoride released by heat-facilitated diffusion from 25% perchloric acid, a single-capillary isotachopherograph can be used. In this instance the selection of the electrolyte system is easier, because only fluoride and some volatile acids are trapped in the solution of NaOH. With regard to the concentration of fluoride in the alkali solution (see Section 2.6), the same leading electrolyte as for the analytical capillary of the ZKI 02 analyser was chosen (see Table 1). Although the dilution of the leading electrolytes also decreases its separation capacity, it was confirmed by the standard addition technique that the fluoride from the sample is separated and determined correctly using the above-mentioned leading electrolyte. The terminating electrolyte was 2 mM tartaric acid. Although the step height of fluoride is close to that of the tartrate, we verified that fluoride migrates correctly even at a concentration exceeding our calibration range twofold. Calibration results are given in Table 2.

The ITP method developed for the determination of fluoride was tested on a series of phosphate samples and animal feed mixtures. The results obtained are summarized in Table 3. An isotachopherogram of animal feed mixture (sample C) analysed on the ZKI 02 column-coupling isotachopherograph is shown in Fig. 1. Fig. 2 shows an isotachopherogram of a model mix-

Table 2
Results of calibration analyses

Isotachopherograph	RSH ^a	Calibration equation	R_{xy} ^b	Sample loading
ZKI 02	0.74	$y = 51.2x - 0.5^c$	0.999	Via sample valve
ZKI 02	0.74	$y = 1.37x + 1.27^d$	0.999	Via syringe
Ionosep 900.1	0.81	$y = 603.2x - 5.3^e$	0.999	Via sample valve

^a RSH = Relative step height.

^b R_{xy} = Correlation coefficient.

^c y = Step length in mm; x = concentration of fluoride in $\mu\text{g/ml}$; chart speed 6 cm/min.

^d y = Step length in mm; x = amount of fluoride in ng; chart speed 6 cm/min.

^e y = Step length in sample; x = concentration of fluoride in $\mu\text{g/ml}$; sample rate 20/s.

Table 3

Results of fluoride determination (extraction with 1 M HCl, analysis on ZKI 02 column-coupling isotachopherograph and heat-facilitated diffusion from 25% HClO₄ with analysis on Ionosep 900.1 single-capillary isotachopherograph) in phosphate and animal feed mixture samples

Sample	Fluoride content (mg/kg)	
	ZKI 02 ^a	Ionosep ^b
Animal feed A	16	10
Animal feed B	8	8
Animal feed C	53	45
Animal feed D	171	117
Phosphate A	920	890
Phosphate B	1510	1740

For detailed conditions of analysis, see text.

^a Average of three replicate analyses; R.S.D. = 1.9% (*n* = 10, sample C).

^b Average of two replicate analyses; R.S.D. = 4% (*n* = 10, sample C).

ture (2 µg of fluoride/ml) analysed on IONOSEP 900.1.

The technique based on extraction of a sample with hydrochloric acid gives recoveries between 80 and 100% (determined with the ZKI 02 analyser) and the method based on heat-facilitated diffusion from perchloric acid gives recoveries between 60 and 120% (determined with the Ionosep analyser). The poorer recoveries and higher R.S.D. values (see Table 3) obtained with the latter technique are probably due to the low sample mass (1–2 g) with respect to heterogeneity of feed mixtures. This disadvantage could be eliminated by the use of a device for heat-facilitated diffusion, enabling larger amounts of sample to be used. The different contents of fluoride found by the two isotachophoretic methods (171 ppm with the ZKI 02 and 117 ppm with the Ionosep 900.1) are probably caused by imperfect homogenization of sample. Sample D was prepared in our laboratory by addition of phosphate sample B to animal feed sample A obtain a sample with a higher fluoride content (150 ppm). The heat-facilitated diffusion from perchloric acid seems to be a more advantageous technique than the extraction method, especially for the determi-

nation of fluoride in phosphate samples. The sample amount of dicalcium phosphate (150 mg) ensures perfect solubility under the conditions of microdiffusion and provides a sufficient step length of fluoride on the isotachopherogram. For example, the sample phosphate B was diluted 50-fold after extraction in 1 M HCl and the step length of fluoride on the isotachopherogram was therefore only 5 s (ZKI 02) whereas the step length of fluoride for this sample treated by the heat-facilitated diffusion method was over 30 s (Ionosep 900.1).

Analyses of ashed samples were carried out. Fluoride was released from the ashed sample by heat-facilitated diffusion. It was found that during the ashing of a sample part of the fluoride escaped (for detailed conditions of ashing, see ref. 5), because the ashed sample contained less fluoride than the unashed sample. The escape of fluoride could be suppressed by the addition of NaOH or Na₂CO₃ before ashing, but we did not try this. It was also found that it is not possible to dissolve the ashed sample by the classical method [6], because all the fluoride escaped as hydrogen fluoride owing to the action of concentrated hydrochloric acid and therefore no fluoride was found in the sample. Partial fluoride escape was also observed during the extraction by a sample with 1 M HCl. Therefore, distilled water, 1 M phosphoric acid and more dilute hydrochloric acid (0.01, 0.1 and 0.5 M) were tested as extractants. We found that if the content of fluoride in the feed mixture does not exceed 20 ppm (determined after extraction with 1 M HCl), all of these solvents are suitable. When the content of fluoride exceeds 20 ppm, extraction with 1 M HCl gave the best results, probably owing to better solubilization of phosphates containing fluoride.

Comparative analyses using an ion-selective electrode (ISE) were carried out. On the basis of the results obtained it is concluded that the ITP method is more suitable than the ISE method for the determination of fluoride in feed mixtures and/or in phosphate samples. The ISE method gave recoveries of up to 180%, *i.e.*, only semi-quantitative results for fluoride content. The only advantage of the ISE method is the rela-

tively short analysis time. However, the rate of voltage stabilization between the ISE and the reference electrode is dependent on the condition of the ISE. The experiments described lasted 6 months. At the beginning of this period the voltage stabilization took 2 min and this time had increased to 10 min by the end of experimental work. A daily decrease of the ISE sensitivity was observed and a calibration analysis had to be carried out every day. Although the ISE method is highly recommended in some papers for the determination of fluoride in feed mixtures, our experience showed that the use of this technique is questionable. In addition, a large consumption of chemicals, *i.e.*, 16 g of sodium citrate and *ca.* 8 g of sodium acetate per analysis, is necessary. In contrast, the ITP calibration graph did not change with time. Nevertheless, we recommend that the calibration is verified every time a new leading electrolyte is prepared.

The detection limits for feed mixtures analysis under the experimental conditions adopted using the ZKI-02 and Ionosep isotachopherographs were 6 and 4 mg/kg as fluoride, respectively, and those for fluoride determination in phosphate samples were 120 and 50 mg/kg, respectively. These values are much lower than the admissible

fluoride content in phosphate samples (2000 mg/kg) or in feed mixtures (150 mg/kg).

On the basis of the results obtained and the fact that there are few methods for fluoride determination, we recommend ITP as suitable technique for this purpose. With advantages such as the relatively simple sample preparation and very low consumption of chemicals per analysis, resulting in low running costs, the ITP technique presented could find practical use in this field.

4. References

- [1] *Výroba a Složení Krmných Směsí*, Supplement to the Notice No. 362/1992 Sb., Ministry of Agriculture of the Czech Republic, 1992, p. 98.
- [2] J. Davídek, J. Hrdlička, M. Karvánek, J. Pokorný, J. Seifert and J. Velíšek, *Laboratorní Příručka Analýzy Potravin*, SNTL, Prague, 1977, pp. 150–153.
- [3] J. Tušl, *J. Assoc. Off. Anal. Chem.*, 53 (1970) 267–269.
- [4] L. Torma, *J. Assoc. Off. Anal. Chem.*, 58 (1975) 477–481.
- [5] L. Singer and R.H. Ophaug, *J. Agric. Food Chem.*, 34 (1986) 510–513.
- [6] O. Kacerovský, L. Babička, D. Biro, J. Heger, Z. Jedlička, J. Lohninsky, Z. Mudřík, P. Roubal, M. Svobodá, B. Vencel, P. Vrátný and J. Zelenka, *Zkoušení a Posuzování Krmiv*, SZN, Prague, 1990, pp. 61–62.



ELSEVIER

Journal of Chromatography A, 670 (1994) 229–233

JOURNAL OF
CHROMATOGRAPHY A

Short Communication

Purification of bacilli ribonucleases by reversed-phase high-performance liquid chromatography

Konstantin I. Panov[☆]

Engelgardt Institute of Molecular Biology, Russian Academy of Science, 32 Vavilov Street, 1179884 Moscow, Russian Federation

(First received July 19th, 1993; revised manuscript received February 15th, 1994)

Abstract

A two-step purification method is presented that utilizes the specific chromatographic properties of bacilli extracellular cycling ribonucleases. A double gradient system of elution is used. Initial concentration of the sample followed by reversed-phase HPLC gives high yields (90–95%) of homogeneous, active protein on both analytical and preparative scales. The procedure may be applied to the isolation of ribonucleases from different sources without significant modifications

1. Introduction

The extracellular cycling ribonucleases from bacilli provide a convenient model for structure–function studies of enzymes [1–5]. This is primarily due to their small size (M_r 11 000–12 000), the absence of disulphide bonds, easy assay and resistance to denaturation over a wide pH range (3–7.5) [1]. Cloning of the genes coding for ribonucleases from *Bacillus intermedius* (binase, Bi) and *Bacillus amyloliquefaciens* (barnase, Ba) [6,7] has made it possible to apply protein engineering methods to detailed structure–functional analysis of these enzymes [2,4]. To date, a variety of multi-step procedures have been described for the purification of homogeneous binase, barnase, their mutants and other similar extracellular ribonucleases from bacilli, with yields ranging from 20% to 60%

[2,8–11]. The present procedure consists of only two steps: the sample is first concentrated, and then subjected to reversed-phase HPLC. This method gives consistently high yields (85–90%) of homogeneous native protein in both analytical and preparative amounts.

2. Experimental

2.1. Materials

Analytical reagent grade salts (Reakhim, Moscow, Russian Federation) were used throughout. isopropyl-6-D-thiogalactopyranoside (IPTG) was obtained from Biopol (Moscow, Russian Federation). Mobile phases were prepared with HPLC-grade acetonitrile (Fluka, Buchs, Switzerland) as the stronger solvent. The aqueous portions of the mobile phase were prepared using water purified with a Milli-Q system (Millipore, Bedford, MA, USA) with 0.1% trifluoro-

[☆] Present address: Department of Chemistry, University of Groningen, Nijenborgh 4, 9741 AG Groningen, Netherlands.

acetic acid (TFA), 0.1 M ammonium phosphate (pH 2.2), 0.1 M ammonium phosphate (pH 3.0), 0.1 M ammonium phosphate (pH 3.5), 0.1 M ammonium phosphate (pH 4.0), 0.1 M ammonium acetate (pH 5.0), 0.1 M ammonium phosphate (pH 6.0) and 0.1 M ammonium acetate (pH 7.5). All components for growth media purchased from Difco Labs. (Detroit, MI, USA). All buffers and samples for HPLC were filtered through membrane filters (Dia-M, Moscow, Russian Federation) with a pore size of 0.2 μm . The ammonium sulphate fraction of *Bacillus pumilus* culture medium, containing RNase (Bp), was obtained from Dr. A.A. Dementiev (IMB, Russian Academy of Science). Binase was purified as described by Golubenko *et al.* [10].

2.2. RNase activity assay

RNase activity was assayed at pH 7.5 in 120- μl mixtures containing 0.1 M Tris-HCl, 0.1 M NaCl and 1.6 mg/ml of ribonucleic acid from yeast (Serva). After incubation at 37°C for 15 min, 300 μl of 2-propanol were added with vigorous mixing. After the mixtures had stood for 20 min at -20°C, they were centrifuged for 10 min at 14 000 g. The supernatant was diluted (1:100) in water and the absorbance at 260 nm was measured. The absorbance at 260 nm of the supernatant was a linear function of added enzyme up to an absorbance of at least 1.5.

2.3. Strains and cultivation conditions

The *B. intermedius* 7P strain, a binase producer, was obtained from the Russian National Collection of Industrial Microorganisms (Institute for Genetics of Microorganisms, Moscow, Russian Federation), and cultivation was carried out according to Golubenko *et al.* [10]. The *Escherichia coli* strain JM105, containing the pMT416 plasmid, also a barnase producer, was provided by courtesy of Professor R.W. Hartley (NIH, Bethesda, MD, USA). Cultivation was according to the scheme of Hartley [7], with the exception that cells were induced immediately upon inoculation. In this step, IPTG was added to a final concentration of 4 $\mu\text{g/ml}$.

2.4. Preparation of binase ammonium sulphate fractions

Cells (from 5 l) were pelleted and the supernatant was chilled to 4°C. Ammonium sulphate was then added to the supernatant to a final concentration of 95% saturation while stirring. After overnight stirring (at 4°C), centrifugation (3000 g, 30 min) yielded the protein predominantly in the pellet. The pellet was dissolved in 50 ml of 0.1 M ammonium acetate (pH 7.5), centrifuged and filtered through a 0.2- μm membrane filter prior to loading on the column. The protein yield (according to the RNase activity) at this stage was 99%.

2.5. Preparation of concentrated barnase

Cell culture was grown overnight at 37°C. Cell growth was halted by chilling followed by the addition of acetic acid to 5%, in order to release that part of the barnase still located in the bacterial periplasm (about 50%). Stirring was continued for a further 15 min. Cells were pelleted by centrifugation for 10 min at 10 000 g. SP-Trisacryl cation-exchange resin (5 ml of settled volume per litre of culture medium), previously equilibrated with 50 mM sodium acetate (pH 4.5), was added to the supernatant whilst gently stirring. After stirring for 1 h, the resin was allowed to settle and the supernatant decanted. The sorbent was transferred to a glass filter and washed with 2 M ammonium acetate (pH 8.0) until the absorbance of the eluate at 280 nm became negligible [12]. The protein yield (according to the activity) at this stage was 91%.

2.6. High-performance liquid chromatography

The HPLC apparatus (Gilson Medical Electronics, Middleton, WI, USA) consisted of Model 305 pumps, a Model 803C manometric module, Model 811B mixer with a 1.5-ml chamber, UV112 detector (set at 280 nm) and Model 7125 injector (Reodyne, Cotati, CA, USA) with 20- and 100- μl and 1- and 2-ml loops. A Model 714 HPLC system controller (Gilson) was used to regulate chromatographic processes

and register results. The following columns were used for analytical separations: Silasorb SPH C₈, $d_p = 9 \mu\text{m}$ ($150 \times 4 \text{ mm I.D.}$) and Silasorb SPH C₁₈, $d_p = 9 \mu\text{m}$ ($150 \times 4 \text{ mm I.D.}$). For preparative purification we used a Silasorb SPH C₁₈ column, $d_p = 13 \mu\text{m}$ ($250 \times 10 \text{ mm I.D.}$). All columns were manufactured by Elsico (Moscow, Russian Federation). Elution was performed with a 0–70% linear gradient of buffer B (acetonitrile) in the aqueous buffer at a flow-rate of 1 ml/min for analytical separations and 3 ml/min for preparative separations.

3. Results and discussion

The intention behind this work was to devise a rapid, simple and efficient purification method applicable to the ribonucleases barnase, binase and other similar extracellular RNases of bacilli. The investigation of the behaviour of barnase on the modified silica gels (C₈ and C₁₈) showed a strong dependence of its recovery on the pH of eluent. At acid pH values (2–2.5) the protein is eluted from the column in 80–98% yield, where-

as at neutral pH (6–7.5) its yield falls almost to zero (Table 1). Reiteration of the elution cycle without changing the conditions (pH of the eluent) does not increase the yield of barnase. However, with repeated elution with acidic buffer barnase elutes from the column in high yield. In contrast, the retention time of barnase at different pH values is virtually constant.

The pH of the chromatographic elution buffer was found to influence strongly the protein yield. At an eluent pH of 5 or above, RNase was strongly retained on the column; even repeated cycles with C₁₈ phase were unsuccessful in eluting significant amounts of RNase and only a 20% yield could be reached using a C₈ phase. This also applies to the other bacilli RNases, such as binase, RNase of *Bacillus thuringiensis* and RNase of *Bacillus pumilus*, for which retention times were determined to be close to those of barnase itself.

More detailed studies are being carried out to determine the basis for these observations. The purification method now described is based on these chromatographic properties of barnase. A sample containing barnase was applied to a

Table 1
Dependence of binase yield and capacity of the sorbents on the type of buffer used

Buffer	Protein yield (%)		Sorbent capacity (mg protein/ml sorbent)	
	C ₈ phase	C ₁₈ phase	C ₈ phase	C ₁₈ phase
0.1% TFA (pH 2.2)	98.9	97.8	5.3	6.1
0.1 M ammonium phosphate (pH 2.2)	98.9	86.8	5.2	6.2
0.1 M ammonium phosphate (pH 3.5)	68.7	61.7	5.1	6.0
0.1 M ammonium phosphate (pH 4.0)	49.3	19.7	5.1	6.0
0.1 M ammonium acetate (pH 5.0)	6.2	5.6	5.2	6.1
0.1 M ammonium acetate (pH 6.0)	5.6	2.3	6.3	6.3
0.1 M ammonium acetate (pH 7.5)	2.8	1.5	5.5	6.7

Chromatographic conditions: columns, Silasorb C₈ and Silasorb C₁₈ ($150 \times 4 \text{ mm I.D.}$). Mobile phase, linear gradient of acetonitrile, 0–70%; flow-rate, 1 ml/min.

reversed-phase column equilibrated with buffer A1 (pH >7). Contaminants were eluted with an acetonitrile gradient. The column was then washed with buffer A1 and re-equilibrated with buffer A2 (pH 2.2–2.5). A second elution yielded homogeneous RNase (Fig. 1a).

Although the conditions used failed to achieve a 100% protein yield, the sorption of RNase proteins is not irreversible, and it is possible to remove the remainder of the protein from the column by a method described by Henderson *et al.* [13]. The best results were obtained using C_{18} as the stationary phase and buffers A1 (0.1 M ammonium acetate, pH 7.5) and A2 (0.1% TFA) as mobile phases. TFA-containing solu-

tions are widely used as RP-HPLC buffers [14,15] owing to their useful properties. Their volatility, in particular, allows desalting of enzyme preparations immediately after lyophilization.

Fig. 1b shows an elution profile with an acetonitrile gradient in 0.1% TFA and Fig. 1a an elution profile with a double gradient of acetonitrile in 0.1 M ammonium acetate (pH 7.5) and then 0.1% TFA. Despite having identical separation times, the peaks in Fig. 1b contained contaminants. When a double gradient was used (Fig. 1a), barnase eluted in a homogeneous peak with the second gradient.

A chromatogram of a preparative separation is shown in Fig. 2; the amount of protein in the peak is 100 mg. It demonstrates that even when a large volume of sample is injected, peaks are well resolved.

The method by which the protein is concentrated prior to chromatographic separation was found not to affect significantly the chromatographic efficiency. Therefore, any convenient method may be used for this purpose.

The method described here can provide protein of sufficient purity for amino acid analysis and sequence determination [16]. The method was used to purify RNases Ba, Bi, Bt and Bp (Table 2) and some other barnase and binase mutant forms.

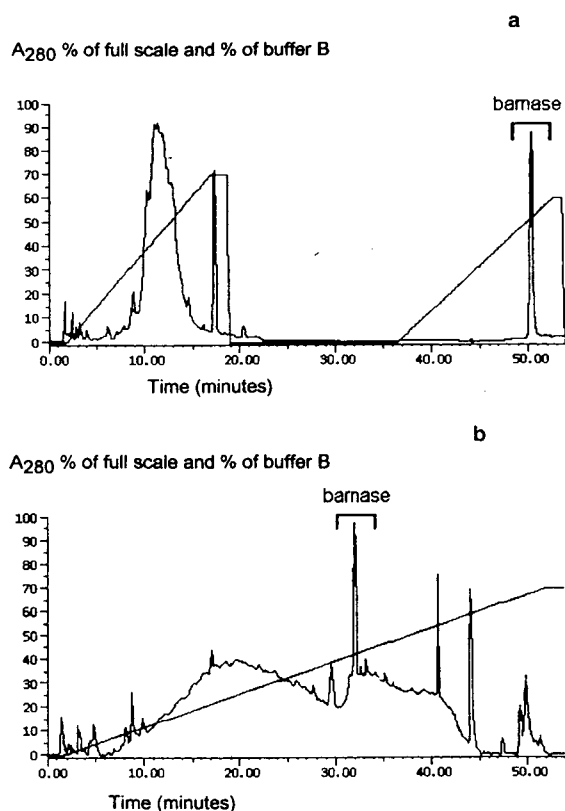


Fig. 1. Analytical separation of 20 μ l of ammonium sulphate fraction from cultural liquid of JM105 (pMT416) strain. Column, Silasorb C_{18} SPH (150 \times 4 mm I.D.). Mobile phase, (a) 0.1 M ammonium acetate (pH 7.5)-acetonitrile (first gradient) and 0.1% TFA-acetonitrile (second gradient). (b) 0.1% TFA-acetonitrile. Flow-rate, 1 ml/min. A_{280} = 0.1 AUFS.

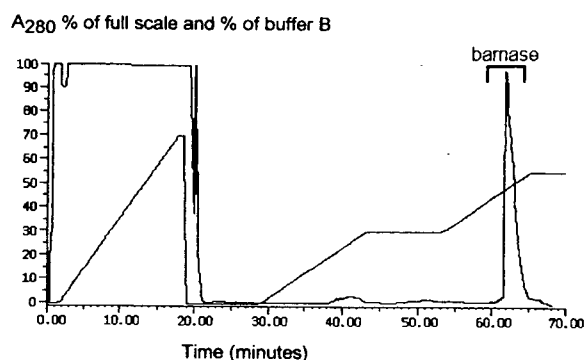


Fig. 2. Preparative separation of ammonium sulphate fraction from JM105 (pMT416) strain cultural liquid, 100 mg Ba in peak. Column, Silasorb C_{18} SPH (250 \times 10 mm I.D.). Mobile phase, 0.1 M ammonium acetate (pH 7.5)-acetonitrile (first gradient) and 0.1% TFA-acetonitrile (second gradient). Flow-rate, 3 ml/min. A_{280} = 3 AUFS.

Table 2

Purification scheme for RNases Ba, Bi and Bp

Stage of purification	Volume (ml)	Total protein (A_{280})	Total activity ^a (units per ml of 1 A_{280})		Yield (%)
Culture liquid, JM105 (pMT416)	2000	16 000	55 000	6875	100
After SP-Trisacryl chromatography	40	7500	$2.5 \cdot 10^6$	$1.3 \cdot 10^4$	91
After RP-HPLC	8	102	$1.2 \cdot 10^6$	$9.5 \cdot 10^5$	89
Culture liquid, <i>B. intermedius</i>	2000	18 000	$4 \cdot 10^5$	$4.4 \cdot 10^4$	100
After ammonium sulphate precipitation	15	1375	$5.3 \cdot 10^7$	$5.8 \cdot 10^5$	99
After RP-HPLC	10	648	$7.2 \cdot 10^7$	$1.1 \cdot 10^6$	90
Ammonium sulphate fraction RNase Bp	15	210	$6.3 \cdot 10^5$	$4.5 \cdot 10^4$	100
After RP-HPLC	10	9.1	$8.5 \cdot 10^5$	$9.4 \cdot 10^5$	95

^a One unit will produce alcohol-soluble oligonucleotides equivalent to a ΔA_{260} of 1.0 in 30 min at pH 7.5, 37°C, in a 120- μ l reaction volume.

4. Acknowledgements

The author thanks Dr. Robert W. Hartley for his generous gift of the plasmid pMT416 and valuable unpublished information. He also thanks Dr. Alexei A. Dementiev for his experimental support of this work and Professor Marat Ya. Karpeisky and Dr. Andrei L. Okorokov for useful discussions of the experimental results. This work was supported by a grant from the Protein Engineering of RNases N103 from the Ministry of Science, Russian Federation.

5. References

- [1] I.B. Grishina, I.A. Bolotina, N.G. Esipova, A.G. Pavlovsky and A.A. Makarov, *Mol. Biol. (Moscow)*, 23 (1989) 455–457.
- [2] A. Horovitz, L. Serrano and A.R. Fersht, *J. Mol. Biol.*, 219 (1991) 5–9.
- [3] S. Baudet and J. Janin, *J. Mol. Biol.*, 219 (1991) 123–132.
- [4] M. Bycroft, A. Matouschek, J.T. Kellis, L. Serrano and A.R. Fersht, *Nature*, 346 (1990) 488–490.
- [5] J. Sevcik, R.G. Sanishvili, A.G. Pavlovsky and K.M. Polyakov, *Trends Biochem. Sci.* 15 (1990) 158–162.
- [6] K.M. Nurkijanov, V.M. Sachariev, M.P. Kirpichnikov, K.G. Skryabin and A.A. Shulga, *Dokl. Akad. Nauk SSSR*, 309 (1989) 1476–1479.
- [7] R.W. Hartley, *J. Mol. Biol.*, 202 (1988) 913–915.
- [8] G. Hill, G. Dodson, U. Heinemann, W. Saenger, Y. Mitsui, K. Nakamura, V. Borisov, G. Tichenko, K. Polyakov and A. Pavlovsky, *Trends Biochem. Sci.*, 8 (1983) 364–371.
- [9] R.W. Hartley and D.L. Rogerson, *Prep. Biochem.*, 2 (1972) 229–242.
- [10] I.A. Golubenko, N.P. Balaban, O.K. Leschinskaya, T.I. Volkova, G.I. Kleiner, N.K. Chepurnova, G.A. Afanasenko and S.M. Dudkin, *Biokhimiya*, 44 (1979) 640–648.
- [11] N.K. Chepurnova, D.L. Lyakhov, V.O. Rechinsky and M.Ya. Karpeisky, *Biochemistry (USSR)*, 53 (1988) 609–612.
- [12] R.W. Hartley, National Institutes of Health, Bethesda, MD, personal communication.
- [13] L.E. Henderson, R. Solver and S. Orozlan, in R. Liu, N. Schechter, L. Heirikson and J. Condlife (Editors), *Chemical Synthesis and Sequencing of Peptides and Proteins*, North-Holland, Amsterdam, 1981, pp. 251–259.
- [14] J.D. Pearson, N.T. Lin and F.E. Regnier, *Anal. Biochem.*, 124 (1982) 217–221.
- [15] F.E. Regnier, *Methods Enzymol.*, 91 (1983) 137–140.
- [16] A.A. Dementiev, Engelhardt Institute of Molecular Biology, Russian Academy of Science, Moscow, unpublished results.



ELSEVIER

Journal of Chromatography A, 670 (1994) 234–238

JOURNAL OF
CHROMATOGRAPHY A

Short Communication

High-performance liquid chromatographic determination of mitoxantrone in liposome preparations using solid-phase extraction and its application in stability studies

Sai-Lung Law*, Tsuei-Fen Jang

Pharmaceutics Research Laboratory, Department of Medical Research, Veterans General Hospital, Taipei 112, Taiwan

(First received September 23rd, 1993; revised manuscript received February 17th, 1994)

Abstract

A method for the determination of the entrapped mitoxantrone in liposome preparations was developed. The method consists of a solid-phase extraction procedure followed by HPLC analysis. A C_{18} cartridge was used for solid-phase extraction and 0.5 M methanolic HCl was used for elution. The extraction demonstrated a good separation of the mitoxantrone from the phospholipid. A C_{18} column and a mobile phase containing acetonitrile–0.01 M monopotassium phosphate (40:60) with the pH adjusted to 3.0 with orthophosphoric acid were employed. The detection wavelength was 242 nm. The HPLC method was stability indicating and was applied to determine the degradation of the entrapped mitoxantrone in liposomes. A pseudo-first-order reaction was found for the degradation of the entrapped mitoxantrone. The half-life of the mitoxantrone decreased with increasing pH of the medium. The results demonstrate that the proposed method is satisfactory for the determination of the stability of mitoxantrone in liposome preparations.

1. Introduction

Liposomes are widely used as carriers for anticancer drugs [1]. Mitoxantrone, an anthracene derivative, shows significant antitumour activity in advanced breast cancer, leukaemia and lymphoma [2]. Mitoxantrone-containing liposomes have been developed [3] and are expected to increase the antitumour activity for some modestly active or inactive cancer systems. HPLC methods together with various sample clean-up procedures for the determination of mitoxantrone in solutions or biological fluids have been introduced [4–16]. However, there appears to be no HPLC method available for the

determination of the entrapped mitoxantrone in liposome preparations.

This study was conducted to develop a method for the determination of the entrapped mitoxantrone in liposomes by HPLC using solid-phase extraction. The application of this method in stability tests for the entrapped mitoxantrone in liposome preparations was also studied. The use of solid-phase extraction as a sample clean-up procedure for the liposome preparations offers the advantage of avoiding emulsification of the sample during extraction. As the main component of liposome is phospholipid, which is a good emulsifying agent, the liposome preparation may easily form an emulsion when liquid–liquid extraction is used in the sample clean-up procedure.

* Corresponding author.

2. Experimental

2.1. Materials

Mitoxantrone was obtained from Kingdom Pharmaceutical (Taipei, Taiwan). Phosphatidylcholine (from fresh egg yolk, Type XI E) and cholesterol were purchased from Sigma (St. Louis, MO, USA). Dicetyl phosphate was obtained from Pharmacia (Uppsala, Sweden). Water-soluble siliconizing fluid (AquaSil) was purchased from Pierce (Rockford, IL, USA). Propyl paraben (internal standard) was obtained from Fluka (Buchs, Switzerland). All chemicals were of analytical-reagent grade and all solvents were of HPLC grade.

2.2. Preparation of liposomes

Multilamellar liposomes were prepared by a method described previously [3]. Phosphatidylcholine, cholesterol and dicetyl phosphate at a molar ratio of 1.6:1.0:0.15 were dissolved in chloroform in a 50-ml round-bottomed flask and dried in a rotary evaporator under reduced pressure at 37°C to form a thin film on the flask. The desired concentration of mitoxantrone in 0.9% sodium chloride solution was added to the film. Multilamellar liposomes were formed by constant vortex mixing for 5 min on a vortex mixer (Thermolyne, Dubuque, IA, USA). The mitoxantrone-containing liposomes were separated from the untrapped mitoxantrone by dialysis (Spectra/Por 2, molecular mass cut-off 12 000–14 000; Spectrum, Los Angeles, CA, USA) for 24 h until the dialysate was free from mitoxantrone.

2.3. Extraction procedure

An Aspec system (Gilson, Villiers le Bel, France) equipped with 3-ml Supelclean LC-18 cartridges (Supelco, Bellefonte, PA, USA) was used for sample extraction. The cartridge was preconditioned by washing with 1 ml of methanol and 1 ml of water. One volume of mitoxantrone-containing liposomes was dissolved in three volumes of absolute ethanol and 0.5 ml of the sample was applied to the cartridge. After

the sample had passed through the cartridge followed by washing with 1 ml of water, the drug was eluted with 1.0 ml of 0.5 M methanolic HCl. The eluate was stored at –70°C for HPLC analysis.

2.4. Recovery study

One volume of a mixture of a known amount of mitoxantrone standard solution and empty liposomes was added to three volumes of absolute ethanol and mixed well to dissolve the liposomes to give a phospholipid solution. The resultant concentration of the solution was 10 µg/ml for both mitoxantrone and phospholipid. A 0.5-ml volume of this solution was used for extraction immediately and chromatographed in triplicate. Recoveries were calculated by comparing the peak heights of the spiked samples with those for the standards.

In order to test for the presence of phospholipids in the eluate, the method of Schiefer and Neuhoﬀ was used [17]. This method involved fluorimetric determination of phospholipids by means of rhodamine complexation. This method is fairly sensitive, allowing the measurement of phospholipid in the range 0.1–100 µg.

2.5. High-performance liquid chromatography

The HPLC apparatus consisted of two solvent-delivery pumps (Model 880-PU; Jasco, Tokyo, Japan), a solvent-mixing module (Model 880-30 Jasco), a variable-wavelength UV–Vis detector (Model 870-UV; Jasco), an on-line degasser (ERC-3511; Erma, Tokyo, Japan), an autosampler (Model 851-AS; Jasco), a system controller (Model 801-SC; Jasco) and an integrator (Chromatocorder 12; SIC, Tokyo, Japan). The column employed for analysis was reversed-phase column (25 cm × 4.6 mm I.D.) packed with LiChrospher RP-18, 5 µm (Merck, Darmstadt, Germany). The mobile phase was acetonitrile–0.01 M monopotassium phosphate (40:60, v/v) with the pH adjusted to 3.0 with orthophosphoric acid. The detector was operated at 242 nm with a sensitivity range of 0.005 AUFS. The attenuation of the integrator was set

at 4. The flow-rate was 1.0 ml/min and the temperature was ambient. The internal standard was propyl paraben.

2.6. Stability study

The buffers used for the stability measurements were pH 3.7 acetate buffer (0.1 M acetic acid and sodium acetate), pH 5.8 phosphate buffer (0.5 M monopotassium phosphate and disodium phosphate), pH 7.4 phosphate buffer (0.5 M monopotassium phosphate and disodium phosphate) and pH 9.6 carbonate buffer (1.0 M sodium hydrogencarbonate and sodium carbonate). The ionic strength of the buffers was adjusted with sodium chloride to a value equivalent to that of 0.9% sodium chloride.

The liposome preparations were dispensed and sealed into the AquaSil-treated glass vials. The samples were stored at 37°C and removed at designated times for the measurement of mitoxantrone concentration. To ensure that the method was stability indicating, the intact mitoxantrone in solution was heated at 80°C for 36, 6 and 0.5 h at pH 3.6, 7.4 and 9.6, respectively, to accelerate degradation of the drug [18,19].

2.7. Calibration graph

Accurately weighed mitoxantrone was dissolved in water to make a stock standard solution. Suitable dilutions of the stock standard solution to the concentration range 12.5–200 ng/ml and triplicate injections into the HPLC system were made. The calibration graph was constructed by plotting the mean peak-height ratios of mitoxantrone to propyl paraben against mitoxantrone concentration. Each run with the samples, which involved about 24 injections, was carried out with a new calibration graph constructed using the stock standard solution.

3. Results and discussion

Fig. 1 shows the chromatograms of mitoxantrone after heating at 80°C for 36, 6 and 0.5 h at pH 3.6, 7.4 and 9.6, respectively. The retention time was 4.2 min for mitoxantrone, 8.4

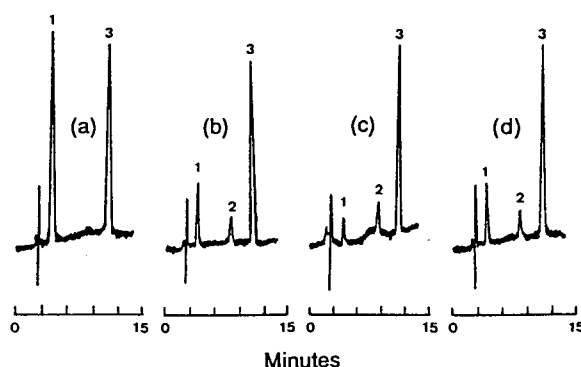


Fig. 1. HPLC of (1) mitoxantrone, (2) mitoxantrone degradation product and (3) propyl paraben. (a) Standard mitoxantrone (100 ng/ml) and propyl paraben (150 ng/ml); mitoxantrone (b) at pH 3.6 heated at 80°C for 36; (c) at pH 7.4 heated at 80°C for 6 h; (d) at pH 9.6 heated at 80°C for 30 min.

min for the degradation product of mitoxantrone and 11.4 min for propyl paraben. No degradation of propyl paraben was observed in this study. It is clear that the eluted peaks of the mitoxantrone, its degradation product and propyl paraben were well separated, demonstrating that the HPLC method is stability indicating.

Nine standard solutions of mitoxantrone in the concentration range 12.5–200 ng/ml were analysed. The calibration graphs were analysed by linear least-squares regression and showed a correlation coefficient of 0.999. The relative standard deviations in within-day and between-day ($n = 10$) assays were 0.51 and 1.22%, respectively, at a concentration of 100 ng/ml.

The recovery of mitoxantrone from phospholipid solution using the solid-phase extraction method for five preparations showed an average of 83.5–88.0%. No trace of phospholipid was found in the eluate after solid-phase extraction. This indicated that the mitoxantrone was well separated from the phospholipid.

For the stability study, the logarithm of the concentration of residual mitoxantrone was plotted against time for the entrapped mitoxantrone in liposomes at pH 3.6, 5.8, 7.4 and 9.6 when stored at 37°C as shown in Fig. 2. It is clear that the degradation of mitoxantrone followed a pseudo-first-order reaction. The degradation rate of the mitoxantrone increased with increasing

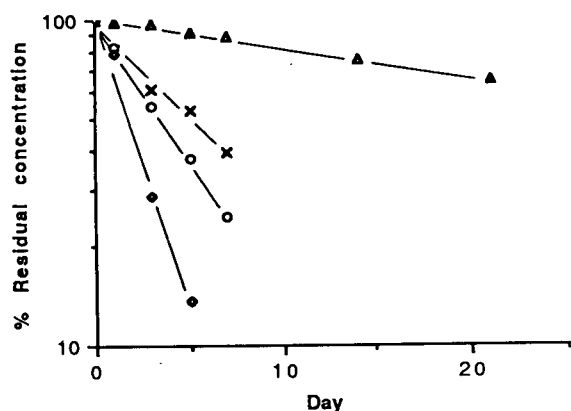


Fig. 2. Concentration–time plots of entrapped mitoxantrone in liposomes at pH (Δ) 3.6, (\times) 5.8, (\circ) 7.4 and (\diamond) 9.6 stored at 37°C.

pH of the medium. The possible reaction for the degradation of mitoxantrone may be due to the oxidation of the phenylenediamine moiety of mitoxantrone to form a quinone diimine and then cyclization to yield the degradation product [20,21]. This reaction is significant at higher pH. Fig. 3 shows the half-life of the entrapped mitoxantrone at pH 3.6, 5.8, 7.4 and 9.6 when stored at 37°C. The most stable liposome preparation showed a half-life of 75 days at pH 3.6. In contrast, it was only 3.9 days for the less stable preparation at pH 9.6.

In conclusion, the method described here is accurate and precise for the determination of the

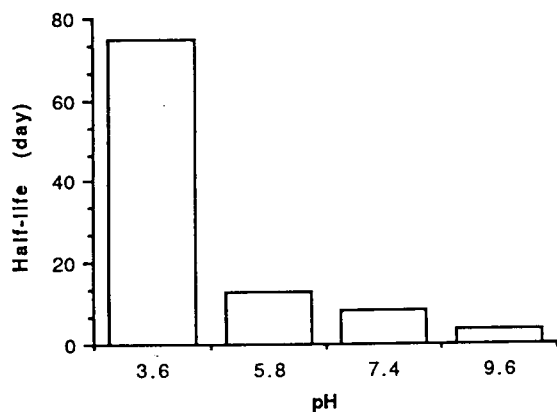


Fig. 3. Half-lives of entrapped mitoxantrone in liposomes at pH 3.6, 5.8, 7.4 and 9.6 stored at 37°C.

entrapped mitoxantrone in liposome preparations, and the solid-phase extraction procedure is capable of separating mitoxantrone from liposomes. This method was successfully applied to a stability study of the entrapped mitoxantrone in liposomes.

Acknowledgements

This study was supported by the National Science Council (NSC 81-0412-B-075-03). The authors thank Dr. P. Chang for helpful discussions.

References

- [1] G.V. Betageri, S.A. Jenkins and D.L. Parsons, *Liposome Drug Delivery Systems*, Technomic, Basle, 1993.
- [2] J. Koeller and M. Eble, *Clin. Pharm.*, 7 (1988) 574.
- [3] S.L. Law, P. Chang and C.H. Lin, *Int. J. Pharm.*, 70 (1991) 1.
- [4] L. Boros, T. Cacek, R.B. Pine and A.C. Battaglia, *Cancer Chemother. Pharmacol.*, 31 (1992) 57.
- [5] G. Micelli, A. Lozupone, M. Quaranta, A. Donadeo, M. Coviello and V. Lorusso, *Biomed. Chromatogr.*, 6 (1992) 168.
- [6] P. Chang, K.C. Chen and M.L. King, *Chin. Pharm. J.*, 42 (1990) 129.
- [7] O.Y.P. Hu, S.P. Chang, Y.B. Song, K.Y. Chen and C.K. Law, *J. Chromatogr.*, 532 (1990) 337.
- [8] A. El-Yazigi and A. Yusuf, *J. Pharm. Biomed. Anal.*, 7 (1989) 877.
- [9] K.T. Lin, G.E. Rivard and J.M. Leclerc, *J. Chromatogr.*, 233 (1982) 235.
- [10] M.J. Czejka and A. Georgopoulos, *J. Chromatogr.*, 425 (1988) 429.
- [11] B. Payet, Ph. Arnonx, J. Catalin and J.P. Cano, *J. Chromatogr.*, 424 (1988) 337.
- [12] E.K. Choi, J.A. Sinkule, D.S. Han, S.C. McGrath, K.M. Daly and R.A. Larson, *J. Chromatogr.*, 420 (1987) 81.
- [13] F.S. Chiccarelli, J.A. Morrison, D.B. Cosulich, N.A. Perkinson, D.N. Ridge, F.W. Sum, K.C. Murdock, D.L. Woodward and E.T. Arnold, *Cancer Res.*, 46 (1986) 4858.
- [14] G. Ehninger, B. Proksch and E. Schiller, *J. Chromatogr.*, 324 (1985) 119.
- [15] Y.M. Peng, D. Ormberg, D.S. Alberts and T.P. Davis, *J. Chromatogr.*, 233 (1982) 235.
- [16] R.F. Taylor and L.A. Guadio, *J. Chromatogr.*, 187 (1980) 212.

- [17] H.G. Shiefer and V. Neuhoﬀ, *Hoppe-Seyler's Z. Physiol. Chem.*, 352 (1971) 913.
- [18] P. Chang, *Chin. Pharm. J.*, 42 (1990) 341.
- [19] K.A. Connors, G.L. Amidon and L. Kennon (Editors), *Chemical Stability of Pharmaceuticals: a Handbook for Pharmacists*, Wiley, New York, 1979, p. 44.
- [20] J. Blanz, K. Mewes, G. Ehninger, B. Proksch, D. Waidelich, B. Greger and K.P. Zeller, *Drug Metab. Dispos.*, 19 (1991) 871.
- [21] P. Chang, *Proc. Natl. Sci. Counc. ROC*, 16 (1992) 304.

Short Communication

Determination of enantiomeric purity of (*S*)-carboranylalanine using capillary column supercritical fluid chromatography

P. Petersson^a, J. Malmquist^b, K.E. Markides^a, S. Sjöberg^{b,*}

^aDepartment of Analytical Chemistry, Uppsala University, P.O. Box 531, S-751 21 Uppsala, Sweden

^bDepartment of Organic Chemistry, Uppsala University, P.O. Box 531, S-751 21 Uppsala, Sweden

(First received December 28th, 1993; revised manuscript received March 4th, 1994)

Abstract

Carboranylalanine, the *o*-carborane analogue of phenylalanine, is a potential candidate for boron neutron capture therapy of cancer. In this paper a method is described for the determination of enantiomeric purity of (*S*)-carboranylalanine as the (*N*-trifluoroacetyl)propylester using open tubular column supercritical fluid chromatography with a chiral stationary phase consisting of permethyl- β -cyclodextrin methyloctylsiloxane.

1. Introduction

Currently, much interest is being paid to the synthesis of compounds which could be used for boron neutron capture therapy (BNCT) of cancer [1–3]. α -Amino acids containing the boron-rich *closo*-1,2- $C_2B_{10}H_{11}$ -carborane cage are potential candidates for this purpose [4,5]. (*S*)-Carboranylalanine (Fig. 1), the *o*-carborane analogue of phenylalanine, first reported in 1976 [6], was early shown to be able to replace phenylalanine in biological systems [7–9] and has recently attracted renewed interest for BNCT [5,10–12]. As the (*R*)- and (*S*)-form have different biological activity it is essential to find an accurate method for the determination of enantiomeric purity when working with biological applications [13].

In 1988 Harada and Takahashi [14] showed that the *closo*-1,2- $C_2B_{10}H_{12}$ -carborane cage form strong inclusion complexes with cyclodextrins, a

result indicating that cyclodextrins could be useful as chiral stationary phases (CSPs) for this type of compounds. Later Plešek *et al.* [15] managed to separate several enantiomers of zwitterionic deltahedral *nido*-carboranes and metallaboranes using liquid chromatography (LC) and CSPs based on cyclodextrins. These compounds owe their chirality to the dissymmetry of the cage. It was therefore tempting

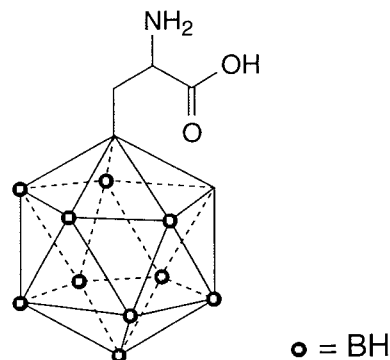


Fig. 1. (\pm)-Carboranylalanine.

* Corresponding author.

to examine if a CSP based on permethylated β -cyclodextrin, which we have developed for open tubular column chromatography [16], is applicable to the separation of the enantiomers of carboranylalanine with a stereogenic centre in a side-arm of the carborane cage.

Unfortunately carboranylalanine is too polar to be eluted in gas chromatography (GC) or supercritical fluid chromatography (SFC) using carbon dioxide as mobile phase. It is also not readily analysed by LC or capillary electrophoresis since it only absorbs light at short wavelengths. An achiral derivatization is therefore motivated. As GC would give the highest efficiency it was decided to prepare the (N-trifluoroacetyl)propyl ester, however, no chiral selectivity was obtained by GC and a relatively high temperature was required to elute the enantiomers. The efforts were therefore focused on open tubular column SFC, a technique in which mainly the density of the mobile phase is used to control the retention of solutes and the temperature can therefore be kept at a favourably low level in order to improve the chiral selectivity as well as decrease the risk of thermal decomposition and racemization.

In the present work open tubular column SFC is used to investigate the enantiomeric purity of (S)-carboranylalanine obtained by asymmetric synthesis.

2. Experimental

The (N-trifluoroacetyl)propyl esters^a of racemic [5] and (S)-carboranylalanine (obtained via alkylation of the Oppolzer's sultame-derived glycine equivalent [17] with propargylbromide, followed by reaction with decaborane and subsequent hydrolysis [18]) were prepared from the corresponding hydrochlorides by adapting the

general procedure by Abe *et al.* [19]. A stock solution of hydrogen chloride in propanol was prepared by dropwise addition of 6 ml of acetyl chloride in propanol at 0°C and brought to room temperature after 10 min. The hydrogen chloride of the amino acid was dissolved in the acidic propanol solution (9 mg ml⁻¹) and heated at 100°C for 1 h. The solution was then evaporated to dryness and the residue pumped (*ca.* 0.1 mmHg, 13.3 Pa) for 4 h. Trifluoroacetic anhydride and dichloromethane (0.2 ml and 0.9 ml respectively, per 9 mg of amino acid hydrogen chloride) was added to the residue at 0°C. The mixture was heated to reflux for 15 min and then cooled to room temperature. The solution was evaporated to dryness, pumped at room temperature over night and the crystalline residue was homogenised.

In the preparation of sample and standard solutions dichloromethane was used as solvent. In order to minimize the evaporation of the solvent crimp-sealed vials were employed.

Chromatography was performed with a series 600-D supercritical fluid chromatograph (Dionex, Salt Lake City, UT, USA) equipped with a flame ionisation detector (350°C). The injector consisted of a C14W.5 high-pressure four-port valve injector with a 0.5- μ l sample loop (Valco Instruments, Houston, TX, USA) in combination with a splitter (split ratio *ca.* 1:10, 300 μ m I.D.) (SGE, Austin, TX, USA). SFC grade CO₂ (Scott Speciality Gases, Plumsteadville, PA, USA) was used as mobile phase. The density of the mobile phase was kept constant along the column using a deactivated integral restrictor [20]. A 5 m \times 50 μ m I.D. deactivated open tubular column coated with a 53% (w/w) permethyl- β -cyclodextrin methyl octylsiloxane (film thickness *ca.* 0.25 μ m) [16] was used for this study. Chromatograms were recorded with a SP4290 integrator (Spectra Physics, San Jose, CA, USA). The chromatograms were transferred from the integrator to a Macintosh IIfx computer (Apple Computer, Cupertino, CA, USA) and subsequently decoded with an in-house written routine in Microsoft QuickBasic (Microsoft, Redmond, WA, USA). A program for general graphing and data analysis, Igor

^a ¹H-NMR data for the (N-trifluoroacetyl)propyl ester of carboranylalanine (CDCl₃): δ 7.06 (d, 1H, NH), 4.56 (dd, 1H, α -H), 4.16 (m, 2H, CH₂-O), 3.79 (bs, 1H, cage-H), 3.04 (dd, 1H, CH₂-CH), 2.77 (dd, 1H, CH₂-CH), 1.70 (m, 2H, CH₂-CH₃), 0.96 (t, 3H, CH₂-CH₃).

(Wave Metrics, Lake Oswego, OR, USA), was used for determination of peak areas.

3. Results and discussion

The separation was optimized to obtain baseline resolution, *i.e.* $R_s = 1.5$, within the shortest possible time (Fig. 2) [21]. As both the racemate and the sample containing the (*S*)-form and an unknown impurity of the (*R*)-form contained a small amount of impurities from the derivatization it was, unfortunately, not possible to utilize spiking to evaluate quantitatively the determination of enantiomeric purity without recrystallization.

In order to distinguish the peak corresponding to the (*R*)-form from the noise the column had to be overloaded and thus complete baseline resolution was no longer obtainable (the peak corresponding to the (*S*)-form becomes somewhat fronting) (Fig. 3). To decrease the influence of this partial overlapping and noise it

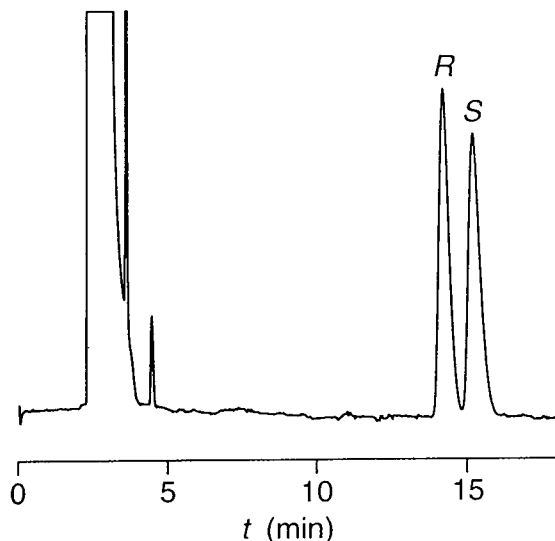


Fig. 2. SFC–FID chromatogram, the optimized separation of the (*N*-trifluoroacetyl)propyl ester of (\pm)-carboranylalanine (10.0 mg ml^{-1}). Conditions: 60°C , density programmed from 0.20 to 0.485 g ml^{-1} at $0.20 \text{ g ml}^{-1} \text{ min}^{-1}$ after a 2-min isopycnic period.

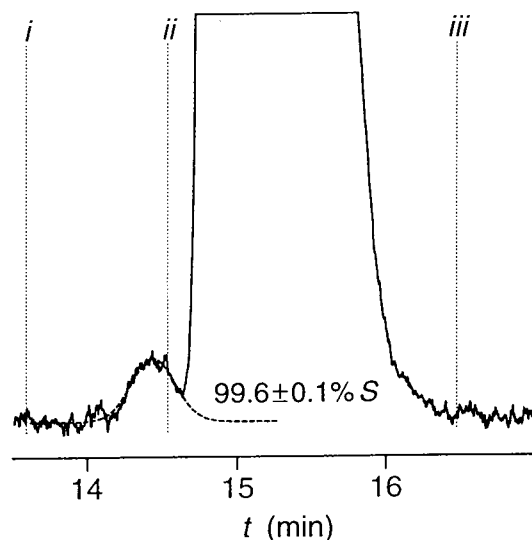


Fig. 3. SFC–FID chromatogram of the (*S*)-carboranylalanine sample (19.3 mg ml^{-1}). The dashed curve represents the fitted peak used for the area estimation of the minor peak. Enantiomeric purity of the (*S*)-form is given with a 95% confidence interval based on five measurements. Conditions: see Fig. 2.

was decided to determine the area of the minor peak by fitting a Gaussian function [22,23] to the data points between *i* and *ii* in Fig. 3 after baseline subtraction. This should ensure a better area estimation than the more commonly used tangent skim or perpendicular drop. The total area of both peaks was subsequently estimated by trapezoidal integration between *i* and *iii* in Fig. 3.

Having repeated measurements of these areas it is then possible to estimate the enantiomeric purity of the sample. However, these calculations are only valid if the linearity of the detection system is ensured and the detector response to the different enantiomers is identical or known. Even though the flame ionization detector is known to be one of the most linear detectors available and it is not likely that the flame ionization detector should have different responses to the enantiomers it was decided to verify this. Five racemic standard solutions with concentrations covering the smallest and largest concentrations of the analytes in the sample were

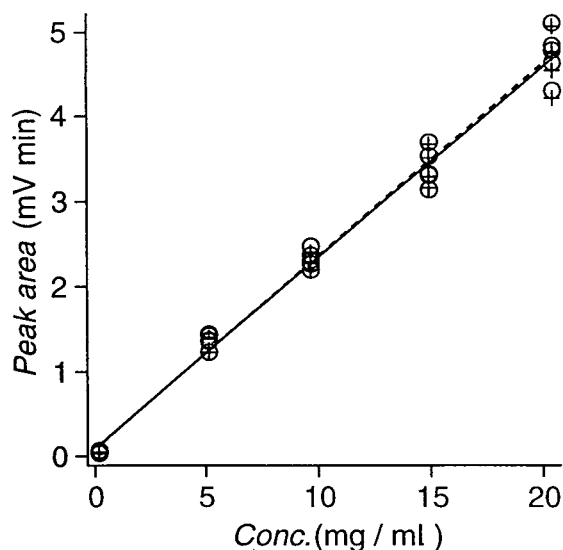


Fig. 4. Detector linearity and response, peak area vs. concentration for each enantiomer. The dashed line represents the (*R*)-form (○) and the solid line the (*S*)-form (⊕). The regression coefficient was 0.996 for both forms.

each injected five times. As shown in Fig. 4 the linearity is good and there is no significant difference in detector response, in other words, the method should be valid. The increasing standard deviation of peak area with increasing concentration is related to the injection technique which is expected to give a relative standard deviation in the order of 5%.

The enantiomeric purity of the (*S*)-form, defined as the percentage of the ratio between the area of the peak corresponding to the (*S*)-form and the sum of peak areas of both forms, was found to be $99.6 \pm 0.1\%$ (95% confidence interval based on five measurements). This result supports the suggested method for quantification as well as the method for asymmetric synthesis of (*S*)-carboranylalanine [18].

References

- [1] J. Carlsson, S. Sjöberg and B.S. Larsson, *Acta Oncologica*, 31 (1992) 803.
- [2] M.F. Hawthorne, *Angew. Chem. Int. Ed. Engl.*, 32 (1993) 950.
- [3] R.F. Barth, A.H. Soloway, R.G. Fairchild and M. Brugger, *Cancer*, 70 (1992) 2995.
- [4] A. Varadarajan and M.F. Hawthorne, *Bioconjugate Chem.*, 2 (1991) 242.
- [5] S. Sjöberg, M.F. Hawthorne, P. Lindström, J. Malmquist, J. Carlsson, A. Andersson and O. Pettersson, in R.F. Barth, D.E. Carpenter and A.H. Soloway (Editors), *Advances in Neutron Capture Therapy*, Plenum, New York, 1993, p. 269.
- [6] O. Leukart, M. Caviezel, A. Eberle, E. Escher, A. Tun-Kyi. and R. Schwyzler, *Helv. Chim. Acta*, 59 (1976) 2184.
- [7] W. Fischli, O. Leukart, and R. Schwyzler, *Helv. Chim. Acta*, 60 (1977) 959.
- [8] O. Leukart, E. Escher, and D. Regioli, *Helv. Chim. Acta*, 62 (1979) 546.
- [9] J.L. Fauchère, O. Leukart, A. Eberle and R. Schwyzler, *Helv. Chim. Acta*, 62 (1979) 1385.
- [10] I.M. Wyzlic and A.H. Soloway, *Tetrahedron Lett.*, 33 (1992) 7489.
- [11] A. Andersson, J. Andersson, J.-O. Burgman, J. Capala, J. Carlsson, H. Condé, J. Crawford, S. Graffman, E. Grusell, A. Holmberg, E. Johansson, B.S. Larsson, B. Larsson, T. Liljefors, P. Lindström, J. Malmquist, L. Pellettieri, O. Pettersson, J. Pontén, A. Roberti, K. Russel, H. Reist, L. Salford, S. Sjöberg, B. Stenerlöw, P. Strömberg, B. Westermarck, in B.J. Allen, J.B. Moore and B.V. Harrington (Editors), *Progress in Neutron Capture Therapy for Cancer*, Plenum, New York, 1992, p. 41.
- [12] P.A. Radel and S.B. Kahl, *Fifth International Symposium on Neutron Capture Therapy of Cancer, Columbus, Ohio, September 13–17, 1992*, Abstracts, p. 5.
- [13] O.A. Pettersson, P. Olsson, S. Sjöberg and J. Carlsson, *Melanoma research*, 3 (1993) 369.
- [14] A. Harada and S. Takahashi, *J. Chem. Soc. Chem. Commun.*, (1988) 1352.
- [15] J. Plešek, B. Grüner and P. Maloň, *J. Chromatogr.*, 626 (1992) 197.
- [16] P. Petersson, S.L. Reese, G. Yi, H. Yun, A. Malik, J.S. Bradshaw, B.E. Rossiter, M.L. Lee and K.E. Markides, *J. Chromatogr.*, submitted for publication.
- [17] W. Oppolzer, R. Moretti and S. Thomi, *Tetrahedron Lett.*, 30 (1989) 6009.
- [18] P. Lindström and S. Sjöberg, unpublished results.
- [19] I. Abe, S. Kuramoto and S. Musha, *J. High Resolut. Chromatogr. Chromatogr. Commun.*, 6 (1983) 366.
- [20] M.L. Lee and K.E. Markides (Editors), *Analytical Supercritical Fluid Chromatography and Extraction*, Chromatography Conferences, Provo, UT, p. 172.
- [21] P. Petersson, N. Lundell and K.E. Markides, Proceedings of the 15th International Symposium On Capillary Chromatography, Riva del Garda, Italy, May 1993, Hüthig, Heidelberg, Germany, 1993, p. 1566.
- [22] A.N. Papas, *CRC Crit. Rev. Anal. Chem.*, 20 (1989) 359.
- [23] M.O. Koskinen and L.K. Koskinen, *J. Liquid Chromatogr.*, 16 (1993) 3171.



ELSEVIER

Journal of Chromatography A, 670 (1994) 243–244

JOURNAL OF
CHROMATOGRAPHY A

Book Review

Environmental analysis —Techniques, applications and quality assurance (Techniques and Instrumentation in Analytical Chemistry, Vol. 13), edited by D. Barceló, Elsevier, Amsterdam, 1993, 658 pp., price Dfl. 465.00, US\$ 265.75, ISBN 0-444-89648-1.

This is a well written and presented book which fulfills a much needed requirement within the ever growing and increasingly complex field of environmental analyses. As scientific research continues to demonstrate that environmental damage can be caused by a diverse array of organic and inorganic compounds at very low concentrations, and radioactive materials, the emphasis has continued to grow around the development of sensitive, soundly-based and cost-effective methods which yield unequivocally accurate and precise data. To date, the environmental scientist has not been afforded the choice of a broad variety of texts which competently pay attention to all of these requirements within a single book and Barcelo's contribution does much to right this state of affairs.

The book is divided into four sections covering, in turn, field sampling techniques and sample preparation, the application of analytical techniques to the characterisation of key compounds of environmental interest, validation of methods and analytical quality assurance, and finally a section on some new and emerging techniques which are (or will be) directly relevant to the environmental scientist's "toolkit". Covered over seventeen chapters (and 646 pages of text, including the subject index), the material is methodically written, clearly illustrated with appropriate figures and tables and supported by a comprehensive set of literature references. No

single subject area is allowed to dominate at the others' expense, which invites the interested reader to at least "scan" each chapter for new and relevant information without becoming overcome by the complexity of the subject matter. In that sense, the book is as likely to be picked up and read by the "industrial" environmental chemist (or technician) with limited time on his/her hands as well as the academically-based chemist focusing on certain key aspects of environmental methodological research. The book therefore has a relevant "applied" as well as "theoretical" dimension.

As a training tool for persons entering the field of environmental analyses, the book has much to commend it. Not only does it provide an excellent introductory text spanning a broad range of techniques ranging from gas chromatography to capillary electrophoresis, the authors have also made the effort to explain what the techniques are, why they are chosen, and why they work. This is extremely important, as many new workers often fail to recognise the significance and pitfalls of analytical techniques *before* they attempt to carry out the work, making mistakes which are punitively expensive in terms of time and money. For example, in Chapter 3, D.E. Wells begins the section on extraction, clean-up and recoveries of persistent trace organic contaminants in sediment and biota samples by comprehensively and competently explaining

most of the essential factors which the newcomer must bear in mind before starting work. He then goes on to present the subject matter theoretically and pragmatically, covering key areas ranging from the *practical* approach to making recovery measurements, to the comparative performance of a suite of extraction technique options. This information is of unquestionable value to the practising environmental chemist.

The section on quality assurance and reference materials is particularly welcome in a text of this type. As environmental samples are, in many cases, more prone to problems with quality assurance than “process”-based samples, major environmental laboratories have had to invest significantly in programmes to attain, understand, document and maintain high levels of quality assurance. To this day, many laboratories working within this field compromise their data through inadequate attention to quality assurance, or through ignorance of the basic requirements of quality control. Without safeguards against poor quality, environmental analyses suffer significantly from problems associated with improper or inadequate calibration, inconsistent handling techniques, and poor reproducibility both between and within groups of laboratories. All of these problems serve to diminish confidence in the quality and value of data and forestalls the ability of environmental scientists to reliably assess the *status quo*. By dedicating three chapters to the subject of quality assurance, certified reference materials and standard reference materials, the book clearly acknowledges the importance of analytical quality and provides detailed and highly useful information and references to the prospective analyst, efficiently condensed into a section which would be worthy as an independent text in its own right.

Although this book aims to be as comprehensive in its coverage as possible, particularly in its treatment of quality assurance and emerging environmental techniques, it nonetheless excludes some potentially valid and useful material. For example, in Chapter 1, the section(s) on

air sampling by suction could have been extended to cover the general use of systems which employ adsorbent tubes and evacuated vessels in more detail. These techniques currently rank amongst the most commonly used by environmental control and environmental health scientists and yet the majority of readily available literature concerning their use and applications appears to be commercially, rather than independently produced, and thus relatively uncritical in its assessment. Similarly, in Chapter 2, the section on headspace analyses might have been clearer and the discussion of stripping-purging techniques could have been more explicit in differentiating between closed-loop and open-loop stripping methods. Some of the references were older than ten years and did not acknowledge much of the new work on open-loop stripping published within the last five years. Information on approaches towards the stripping of volatile organic compounds from sediments would also have been highly useful as interest in this area has increased tremendously. These are not major criticisms however, as the authors have done well to cover so much ground in relatively few pages.

Overall, the book achieves what it sets out to do. It is, as the editor claims, novel in many ways, with its broad and comprehensive coverage of so many techniques both established and new. Although it might be argued in some quarters that any book on environmental analyses should incorporate some idea of the cost of such analyses, in terms of equipment and manpower costs, such a discussion should perhaps be covered by a parallel text subject to a more regular update and review. As a reference text or as an instructional tool the book succeeds. It is on one hand interesting, educational and informative and on the other it represents a high quality update on developments within an increasingly complex and intellectually challenging discipline.

Southampton, UK Alexander P. Bianchi

Book Review

Statistical methods in analytical chemistry (Chemical Analysis Series, Vol. 123), by P.C. Meier and R.E. Zünd, Wiley, New York, Chichester, 1993, XIV + 321 pp. (+diskette), price £49.50, ISBN 0-471-58454-1.

In general, the quality of measurements is increasingly important. This is certainly the case in analytical chemistry, because of the far-reaching consequences of decisions taken on the basis of analytical chemical information. Therefore, statistics are or, better, have to be of crucial significance in chemical analysis; statistical evaluation of the measurement results is part and parcel of the analytical procedure. However, analysts are not statisticians, which can be a disadvantage because of their relatively limited theoretical statistical knowledge. On the other hand, an analyst knows the real world, knows the practical problems and speaks the language of the chemist.

Many books on statistics have been published, including books particularly intended for analysts. The book under consideration is written typically from the point of view of the practical analyst and the mentioned advantages and disadvantages are clearly visible. It contains four chapters, supplemented with a chapter with Appendices, treating univariate data, bi- and multivariate data, ancillary techniques and complex examples, respectively.

In Chapter 1 the basic statistics of one-dimensional data are clearly explained and illustrated with some relevant examples. A few pages are dedicated to control charts. Only a very elementary treatment of Shewhart and cumsum charts (also known as cusum charts) is given, although

the (quality) control of chemical processes is becoming more and more important. The opinion of the authors that the combination of intuition, experience and insider's knowledge is more revealing than a statistical approach (aiming at the application of V-masks in cumsum control charts) is remarkable in a book on statistical methods. More advanced quality control methods are hardly or not mentioned.

In general, the statistical processing of bivariate data (Chapter 2) is, like the univariate data, treated in a clear way, particularly in the case of linear relationships between the variables; linear regression is extensively explained. In the same chapter, analytical method validation is only indicated by the verbal definition of key terms, where one can remark that linearity is not characterized only by a linear signal-to-concentration relationship, as is suggested by the authors. Non-linear regression is hardly discussed; linearization by transformations is mentioned, but almost no attention is given to more advanced non-linear regression. Very well known algorithms such as Levenberg–Marquardt and in general Gauss–Newton methods are not discussed at all. Only some attention is paid to a sequential simplex method to find the optimum in a response surface. Also, the treatment of multi-dimensional data is concise; obviously this book is not intended to be a reference in the field of chemometrics.

In Chapter 3 a number of diverging techniques and subjects, but with little coherence, are briefly discussed: optimization technique, exploratory data analysis, error propagation and numerical artefacts, ruggedness and suitability of a method, smoothing and filtering data, Monte Carlo techniques, computer simulation and computer programs. The explanation is, again, mainly verbal.

Chapter 4, describing complex examples, is very instructive from a practical point of view. Many examples are worked out. However, there is some doubt concerning the statistical justification of some example; the choice of a model, for instance parabolic or exponential, to fit the data is rather arbitrary in certain cases (non-linear fitting).

Finally, some remarks about the SMAC software included in the book are appropriate. The most suitable application of the package is probably to illustrate the statistical concepts in the book. For daily practical applications, several shortcomings can be noticed compared with professional statistical software. The programs

are slow (written in Q-Basic) and rather user unfriendly. For instance, they do not have protection against illegal input and crash when large data sets are used. Maybe the package can be used as toolbox usable for those wanting to write their own statistical programs.

The final conclusion is that this book is certainly an asset to the practical analyst, but it contains shortcomings. The authors demonstrate an ambiguous attitude with respect to statistics. On the one hand they are promoting and using a theoretical statistically justified approach, but on the other a considerable controversy between (analytical) practice and statistical theory is assumed. Obviously there is, according to them, a large difference between statistics and statistics in analytical chemistry; a questionable opinion. The references are almost exclusively from the analytical chemical literature, and extensively used professional statistical software packages are not mentioned at all.

Amsterdam, Netherlands

H.C. Smit

Author Index

- Abidi, S.L. and Mounts, T.L.
Separations of tocopherols and methylated tocopherols on cyclodextrin-bonded silica 670(1994)67
- Barkley, R.M., see Ryerson, T.B. 670(1994)117
- Bianchi, A.P.
Environmental analysis —Techniques, applications and quality assurance (edited by D. Barceló) (Book Review) 670(1994)243
- Blatný, P. and Kvasnička, F.
Determination of fluoride in feed mixtures by capillary isotachopheresis 670(1994)223
- Boonkerd, S., Detaevernier, M.R. and Michotte, Y.
Use of capillary electrophoresis for the determination of vitamins of the B group in pharmaceutical preparations 670(1994)209
- Borrull, F., see Crespo, C. 670(1994)135
- Briggs, D.A., see Smith, R.M. 670(1994)161
- Bringmann, G., Gassen, M. and Schneider, S.
Toxic aldehydes formed by lipid peroxidation. I. Sensitive, gas chromatography-based stereoanalysis of 4-hydroxyalkenals, toxic products of lipid peroxidation 670(1994)153
- Brueggemann, E.E., see Hines, H.B. 670(1994)199
- Carr, P.W., see Li, J. 670(1994)105
- Carrea, G., see Nesi, M. 670(1994)215
- Chankvetadze, B., Yashima, E. and Okamoto, Y.
Chloromethylphenylcarbamate derivatives of cellulose as chiral stationary phases for high-performance liquid chromatography 670(1994)39
- Chiari, M., see Nesi, M. 670(1994)215
- Chrétien, J.R., see Haldna, U. 670(1994)51
- Crespo, C., Marcé, R.M. and Borrull, F.
Determination of various pesticides using membrane extraction discs and gas chromatography-mass spectrometry 670(1994)135
- Cretier, G., Neffati, J. and Rocca, J.L.
Experimental study of band broadening and solute interferences in preparative supercritical fluid chromatography 670(1994)173
- D'Agostino, P.A. and Provost, L.R.
Capillary column gas chromatographic-tandem mass spectrometric analysis of phosphate esters in the presence of interfering hydrocarbons 670(1994)127
- Detaevernier, M.R., see Boonkerd, S. 670(1994)209
- Erni, F., see Yan, C. 670(1994)15
- Fischer, C.-H., Giersig, M. and Siebrands, T.
Analysis of colloidal particles. V. Size-exclusion chromatography of colloidal semiconductor particles 670(1994)89
- Gassen, M., see Bringmann, G. 670(1994)153
- Giersig, M., see Fischer, C.-H. 670(1994)89
- Golshan-Shirazi, S. and Guiochon, G.
Comparative evaluation of adsorption energy distribution functions obtained by analytical and numerical methods 670(1994)1
- Guiochon, G., see Golshan-Shirazi, S. 670(1994)1
- Haldna, U., Pentchuk, J., Righezza, M. and Chrétien, J.R.
Factor analysis in ion chromatography of carboxylate ions 670(1994)51
- Hall, S.F., see Zheng, M. 670(1994)77
- Hiltunen, R., see Vuorela, P. 670(1994)191
- Hines, H.B. and Brueggemann, E.E.
Factors affecting the capillary electrophoresis of ricin, a toxic glycoprotein 670(1994)199
- Hirokawa, T., see Ito, K. 670(1994)99
- Ito, K., Shimazu, H., Shoto, E., Okada, M., Hirokawa, T. and Sunahara, H.
Ion chromatographic separation of alkali metal and ammonium cations on a C₁₈ reversed-phase column 670(1994)99
- Jang, T.-F., see Law, S.-L. 670(1994)234
- Jurova, I., see Palamareva, M. 670(1994)181
- Kitts, D.D., see Zheng, M. 670(1994)77
- Kozekov, I., see Palamareva, M. 670(1994)181
- Kraak, J.C., see Swart, R. 670(1994)25
- Kvasnička, F., see Blatný, P. 670(1994)223
- Law, S.-L. and Jang, T.-F.
High-performance liquid chromatographic determination of mitoxantrone in liposome preparations using solid-phase extraction and its application in stability studies 670(1994)234
- Li, J. and Carr, P.W.
Extra-thermodynamic relationships in chromatography. Enthalpy-entropy compensation in gas chromatography 670(1994)105
- Liu, H.J.
Determination of amino acids by precolumn derivatization with 6-aminoquinolyl-N-hydroxysuccinimidyl carbamate and high-performance liquid chromatography with ultraviolet detection 670(1994)59
- Liu, H.-Y., see Zheng, M. 670(1994)77
- Malmquist, J., see Petersson, P. 670(1994)239
- Marcé, R.M., see Crespo, C. 670(1994)135
- Markides, K.E., see Petersson, P. 670(1994)239
- McErlane, K.M., see Zheng, M. 670(1994)77
- Michotte, Y., see Boonkerd, S. 670(1994)209
- Mounts, T.L., see Abidi, S.L. 670(1994)67
- Neffati, J., see Cretier, G. 670(1994)173
- Nesi, M., Chiari, M., Carrea, G., Ottolina, G. and Righetti, P.G.
Capillary electrophoresis of nicotinamide-adenine dinucleotide and nicotinamide-adenine dinucleotide phosphate derivatives in coated tubular columns 670(1994)215
- Okada, M., see Ito, K. 670(1994)99
- Okamoto, Y., see Chankvetadze, B. 670(1994)39
- Ottolina, G., see Nesi, M. 670(1994)215
- Palamareva, M., Kozekov, I. and Jurova, I.
Chromatographic behaviour of diastereoisomers. XII. Effects of alumina on separations of esters of maleic and fumaric acids 670(1994)181

- Panov, K.I.
Purification of bacilli ribonucleases by reversed-phase high-performance liquid chromatography 670(1994)229
- Pentchuk, J., see Haldna, U. 670(1994)51
- Petersson, P., Malmquist, J., Markides, K.E. and Sjöberg, S.
Determination of enantiomeric purity of (*S*)-carboranylalanine using capillary column supercritical fluid chromatography 670(1994)239
- Poppe, H., see Swart, R. 670(1994)25
- Provost, L.R., see D'Agostino, P.A. 670(1994)127
- Rahko, E.-L., see Vuorela, P. 670(1994)191
- Righetti, P.G., see Nesi, M. 670(1994)215
- Righezza, M., see Haldna, U. 670(1994)51
- Rocca, J.L., see Cretier, G. 670(1994)173
- Ryerson, T.B., Barkley, R.M. and Sievers, R.E.
Selective chemiluminescence detection of sulfur-containing compounds coupled with nitrogen-phosphorus detection for gas chromatography 670(1994)117
- Schaufelberger, D., see Yan, C. 670(1994)15
- Schneider, S., see Bringmann, G. 670(1994)153
- Shimazu, H., see Ito, K. 670(1994)99
- Shoto, E., see Ito, K. 670(1994)99
- Siebrands, T., see Fischer, C.-H. 670(1994)89
- Sievers, R.E., see Ryerson, T.B. 670(1994)117
- Sjöberg, S., see Petersson, P. 670(1994)239
- Smit, H.C.
Statistical methods in analytical chemistry (by P.C. Meier and R.E. Zünd) (Book Review) 670(1994)245
- Smith, R.M. and Briggs, D.A.
Effect of the sample solvent and instrument design on the reproducibility of retention times and peak shapes in packed-column supercritical fluid chromatography 670(1994)161
- Sunahara, H., see Ito, K. 670(1994)99
- Swart, R., Kraak, J.C. and Poppe, H.
Preparation and evaluation of polyacrylate-coated fused-silica capillaries for reversed-phase open-tubular liquid chromatography 670(1994)25
- Tilotta, D.C., see Wittkamp, B.L. 670(1994)145
- Vuorela, H., see Vuorela, P. 670(1994)191
- Vuorela, P., Rahko, E.-L., Hiltunen, R. and Vuorela, H.
Overpressured layer chromatography in comparison with thin-layer and high-performance liquid chromatography for the determination of coumarins with reference to the composition of the mobile phase 670(1994)191
- Wittkamp, B.L. and Tilotta, D.C.
Detection of alcohols in gas chromatographic effluent by laser-light scattering 670(1994)145
- Yan, C., Schaufelberger, D. and Erni, F.
Electrochromatography and micro high-performance liquid chromatography using 320 μm I.D. packed columns 670(1994)15
- Yashima, E., see Chankvetadze, B. 670(1994)39
- Zheng, M., Liu, H.-Y., Hall, S.F., Kitts, D.D. and McErlane, K.M.
High-performance liquid chromatographic analysis of Romet-30 in Chinook salmon (*Oncorhynchus tshawytscha*): wash-out time, tissue distribution in muscle, liver and skin, and metabolism of sulfadimethoxine 670(1994)77

Journal of Chromatography A

Request for Manuscripts

Susumu Honda will edit a special, thematic issue of the *Journal of Chromatography A* entitled

Chromatographic and Electrophoretic Analyses of Carbohydrates

Both reviews and research articles will be included.

Topics such as the following will be covered:

- Gas chromatography and gas chromatography-mass spectrometry of carbohydrates
- Supercritical fluid chromatography of carbohydrates
- Thin-layer chromatography of carbohydrates
- Liquid chromatography of carbohydrates
 - ◆ Separations based on various modes including adsorption, hydrophilic interaction, hydrophobic interaction, ion exchange, ligand exchange, size exclusion, bioaffinity, etc.
 - ◆ Derivatization
 - ◆ Preparative liquid chromatography
 - ◆ High-performance liquid chromatography-mass spectrometry
- Electrophoresis of carbohydrates
 - ◆ Gel electrophoresis
 - ◆ Capillary zone electrophoresis
 - ◆ Micellar electrokinetic capillary chromatography
 - ◆ Ultrasensitive detection
 - ◆ Derivatization
 - ◆ Capillary electrophoresis-mass spectrometry
- Chromatography and electrophoresis in glycobiology
 - ◆ Release of carbohydrates from glycoconjugates
 - ◆ Monosaccharide composition analysis
 - ◆ Oligosaccharide mapping
 - ◆ Oligosaccharide sequencing
 - ◆ Automated analysis of carbohydrates

Potential authors of reviews should contact Roger Giese, Editor, prior to any submission.

Address: Mugar Building Rm 122, Northeastern University, Boston, MA 02115, USA;

tel.: (+1-617) 373-3227; fax: (+1-617) 373-8720.

The deadline for receipt of submissions is **November 15, 1994**. Manuscripts submitted after this date can still be published in the Journal, but then there is no guarantee that an accepted article will appear in this special, thematic issue. Four copies of the manuscript, citing this issue, should be submitted to the Editorial Office, *Journal of Chromatography A*, P.O. Box 681, NL-1000 AR Amsterdam, The Netherlands. All manuscripts will be reviewed and acceptance will be based on the usual criteria for publishing in the *Journal of Chromatography A*.

Progress in Medicinal Chemistry

Volume 31

Volume edited by
**G.P. Ellis and
D.K. Luscombe**

©1994 474 pages Hardbound
Price: Dfl. 375.00 (US \$214.25)
ISBN 0-444-81807-3

This book contains six chapters, each of which is a self-contained, thorough review by an expert in the field of a particular topic in medicinal chemistry, bacteriology or pharmacology. Each topic is a currently active subject of research in either the quest for new drugs or a better understanding of the role of known biochemical phenomena. In addition, all of the chapters contain an extensive list of relevant reference books, papers and other publications. The book will be of great interest to medicinal and pharmaceutical chemists, and will serve as a valuable source of reference.

Contents:

Preface.

New hypoglycaemic agents
(B. Hulin).
Inhibition of human leukocyte
elastase
(P.R. Bernstein, P.D.
Edwards, J.C. Williams).
The medicinal chemistry of
the azido group
(R.J. Griffin).
Gastric H^+/K^+ -ATPase
inhibitors
(A.W. Herling, K. Weidmann).
Semi-synthetic derivatives of
16- membered macrolide
antibiotics

(H.A. Kirst).
B-Lactamases: targets for
drug design
(S. Coulton, I. Francois).
Silver: antibacterial action and
resistance
(A.D. Russell, B. Hugo).
Inhibition of the
pharmacological effects of
endothelin
(C. Wilson, R.B. Hargreaves).
Potassium channel activators:
pharmacological methods,
models and structure-activity
relationships
(J.M. Evans, S.G. Taylor).



ELSEVIER
An Imprint of Elsevier Science

Elsevier Science B.V.
P.O. Box 181, 1000 AD Amsterdam,
The Netherlands
Tel: +31 (20) 5803 911 Fax: +31 (20) 5803 249

Customers in the USA and Canada:
Elsevier Science B.V.
P.O. Box 945, Madison Square Station
New York, NY 10159-0945, USA
Tel: +1 (212) 633 3650 Fax: +1 (212) 633 3680

Customers resident in the European Union (EU) are liable for Value Added Tax (VAT) or, alternatively, must supply their VAT number with an order. Dutch Guider (D.G.) prices are definitive and apply worldwide, except in North America. US Dollar (\$) prices apply in North America only. Prices may be subject to change without prior notice.

PUBLICATION SCHEDULE FOR THE 1994 SUBSCRIPTION

Journal of Chromatography A and *Journal of Chromatography B: Biomedical Applications*

MONTH	1993	J	F	M	A	M	J	
Journal of Chromatography A	Vols. 652-657	658/1 658/2 659/1 659/2	660/1 + 2 661/1 + 2 662/1 662/2	663/1 663/2 664/1	664/2 665/1 665/2 666/1 + 2 667/1 + 2	668/1 668/2 669/1 + 2	670/1 + 2 671/1 + 2 672/1	The publication schedule for further issues will be published later.
Bibliography Section				681/1			681/2	
Journal of Chromatography B: Biomedical Applications		652/1	652/2 653/1	653/2 654/1	654/2 655/1	655/2	656/1 656/2	

INFORMATION FOR AUTHORS

(Detailed *Instructions to Authors* were published in *J. Chromatogr. A*, Vol. 657, pp. 463-469. A free reprint can be obtained by application to the publisher, Elsevier Science B.V., P.O. Box 330, 1000 AH Amsterdam, Netherlands.)

Types of Contributions. The following types of papers are published: Regular research papers (full-length papers), Review articles, Short Communications and Discussions. Short Communications are usually descriptions of short investigations, or they can report minor technical improvements of previously published procedures; they reflect the same quality of research as full-length papers, but should preferably not exceed five printed pages. Discussions (one or two pages) should explain, amplify, correct or otherwise comment substantively upon an article recently published in the journal. For Review articles, see inside front cover under Submission of Papers.

Submission. Every paper must be accompanied by a letter from the senior author, stating that he/she is submitting the paper for publication in the *Journal of Chromatography A* or *B*.

Manuscripts. Manuscripts should be typed in **double spacing** on consecutively numbered pages of uniform size. The manuscript should be preceded by a sheet of manuscript paper carrying the title of the paper and the name and full postal address of the person to whom the proofs are to be sent. As a rule, papers should be divided into sections, headed by a caption (e.g., Abstract, Introduction, Experimental, Results, Discussion, etc.) All illustrations, photographs, tables, etc., should be on separate sheets.

Abstract. All articles should have an abstract of 50-100 words which clearly and briefly indicates what is new, different and significant. No references should be given.

Introduction. Every paper must have a concise introduction mentioning what has been done before on the topic described, and stating clearly what is new in the paper now submitted.

Experimental conditions should preferably be given on a *separate* sheet, headed "Conditions". These conditions will, if appropriate, be printed in a block, directly following the heading "Experimental".

Illustrations. The figures should be submitted in a form suitable for reproduction, drawn in Indian ink on drawing or tracing paper. Each illustration should have a caption, all the *captions* being typed (with double spacing) together on a *separate sheet*. If structures are given in the text, the original drawings should be provided. Coloured illustrations are reproduced at the author's expense, the cost being determined by the number of pages and by the number of colours needed. The written permission of the author and publisher must be obtained for the use of any figure already published. Its source must be indicated in the legend.

References. References should be numbered in the order in which they are cited in the text, and listed in numerical sequence on a separate sheet at the end of the article. Please check a recent issue for the layout of the reference list. Abbreviations for the titles of journals should follow the system used by *Chemical Abstracts*. Articles not yet published should be given as "in press" (journal should be specified), "submitted for publication" (journal should be specified), "in preparation" or "personal communication".

Vols. 1-651 of the *Journal of Chromatography*; *Journal of Chromatography, Biomedical Applications* and *Journal of Chromatography, Symposium Volumes* should be cited as *J. Chromatogr.* From Vol. 652 on, *Journal of Chromatography A* (incl. Symposium Volumes) should be cited as *J. Chromatogr. A* and *Journal of Chromatography B: Biomedical Applications* as *J. Chromatogr. B*.

Dispatch. Before sending the manuscript to the Editor please check that the envelope contains four copies of the paper complete with references, captions and figures. One of the sets of figures must be the originals suitable for direct reproduction. Please also ensure that permission to publish has been obtained from your institute.

Proofs. One set of proofs will be sent to the author to be carefully checked for printer's errors. Corrections must be restricted to instances in which the proof is at variance with the manuscript.

Reprints. Fifty reprints will be supplied free of charge. Additional reprints can be ordered by the authors. An order form containing price quotations will be sent to the authors together with the proofs of their article.

Advertisements. The Editors of the journal accept no responsibility for the contents of the advertisements. Advertisement rates are available on request. Advertising orders and enquiries can be sent to the Advertising Manager, Elsevier Science B.V., Advertising Department, P.O. Box 211, 1000 AE Amsterdam, Netherlands; courier shipments to: Van de Sande Bakhuyzenstraat 4, 1061 AG Amsterdam, Netherlands; Tel. (+31-20) 515 3220/515 3222, Telefax (+31-20) 6833 041, Telex 16479 els vi nl. UK: T.G. Scott & Son Ltd., Tim Blake, Portland House, 21 Narborough Road, Cosby, Leics. LE9 5TA, UK; Tel. (+44-533) 753 333, Telefax (+44-533) 750 522. USA and Canada: Weston Media Associates, Daniel S. Lipner, P.O. Box 1110, Greens Farms, CT 06436-1110, USA; Tel. (+1-203) 261 2500, Telefax (+1-203) 261 0101.

Trace Element Analysis in Biological Specimens

Edited by R.F.M. Herber and M. Stoeppler

Techniques and Instrumentation in Analytical Chemistry Volume 15

The major theme of this book is analytical approaches to trace metal and speciation analysis in biological specimens. The emphasis is on the reliable determination of a number of toxicologically and environmentally important metals. It is essentially a handbook based on the practical experience of each individual author. The scope ranges from sampling and sample preparation to the application of various modern and well-documented methods, including quality assessment and control and statistical treatment of data. Practical advice on avoiding sample contamination is included.

In the first part, the reader is offered an introduction into the basic principles and methods. Quality control and all approaches to achieve reliable data are treated as well.

The chapters of the second part provide detailed information on the analysis of thirteen trace metals in the most important biological specimens.

The book will serve as a valuable aid for practical analysis in biomedical laboratories and for researchers involved with trace metal and species analysis in clinical, biochemical and environmental research.

Contents:

Part 1. Basic Principles and Methods. 1. Sampling and sample storage (A. Aitio, J. Järvisalo, M. Stoeppler). 2. Sample treatment of human biological materials (B. Sansoni, V.K. Panday). 3. Graphite furnace AAS (W. Slavin). 4. Atomic absorption spectrometry. Flame AAS (W. Slavin). 5. Atomic emission spectrometry (P. Schramel). 6. Voltammetry (J. Wang). 7. Neutron activation analysis (J. Versieck). 8. Isotope dilution mass spectrometry (IDMS) (P. de Bièvre). 9. The chemical speciation of trace elements in biomedical specimens: Analytical techniques (P.H.E. Gardiner, H.T. Delves). 10. Interlaboratory and intralaboratory surveys. Reference methods and reference materials (R.A. Braithwaite). 11. Reference materials for trace element analysis (R.M. Parr, M. Stoeppler).

12. Statistics and data evaluation (R.F.M. Herber, H.J.A. Sallé). **Part 2. Elements.** 13. Aluminium (J. Savory, R.L. Bertholf, S. Brown, M.R. Wills). 14. Arsenic (M. Stoeppler, M. Vahter). 15. Cadmium (R.F.M. Herber). 16. Chromium (R. Cornelis). 17. Copper (H.T. Delves, M. Stoeppler). 18. Lead (U. Ewers, M. Turfeld, E. Jermann). 19. Manganese (D.J. Halls). 20. Mercury (A. Schütz, G. Skarping, S. Skerfving). 21. Nickel (D. Templeton). 22. Selenium (Y. Thomassen, S.A. Lewis, C. Veillon). 23. Thallium (M. Sager). 24. Vanadium (K.-H. Schaller). 25. Zinc (G.S. Fell, T.D.B. Lyon). Subject index.

© 1994 590 pages Hardbound
Price: Dfl. 475.00 (US\$ 271.50)
ISBN 0-444-89867-0

ORDER INFORMATION ELSEVIER SCIENCE B.V.

P.O. Box 330
1000 AH Amsterdam
The Netherlands
Fax: (+31-20) 5862 845

For USA and Canada

P.O. Box 945
Madison Square Station
New York, NY 10159-0945
Fax: (212) 633 3680

US\$ prices are valid only for the USA & Canada and are subject to exchange rate fluctuations; in all other countries the Dutch guilder price (Dfl.) is definitive. Customers in the European Union should add the appropriate VAT rate applicable in their country to the price(s). Books are sent postfree if prepaid.



ELSEVIER
SCIENCE



0021-9673(19940603)670:1:2;1-Y

- 1 N.A. 2537

- 1 N.A. 2537